MINERALOGY AND GENESIS OF CRITICAL-METAL BEARING MINERALIZATION IN THE BETTS COVE AND TILT COVE VOLCANOGENIC MASSIVE SULFIDE (VMS) DEPOSITS, BAIE VERTE, NEWFOUNDLAND APPALACHIANS

By Kyra Kennedy

A Thesis submitted to the School of Graduate Studies on partial fulfillment of the requirements for the degree of

Master of Science, Department of Earth Sciences

Memorial University of Newfoundland

October 2024

ABSTRACT

The Betts Cove and Tilt Cove deposits are two Cu-Co-Ni-Zn-Te-bearing mafic-(Cyprus)-type VMS deposits hosted in the Betts Cove ophiolite, Baie Verte Peninsula, Newfoundland Appalachians. The mineralogy consists of dominantly pyrite, chalcopyrite, pyrrhotite, and sphalerite, and magnetite at Tilt Cove. Accessory minerals include cobaltite and pentlandite and trace phases include acanthite, arsenopyrite, bornite, chromite, clausthalite, electrum, galena, and hessite. These minerals contain base and precious metals (e.g., Au, Ag, Cu, Zn, Ni, Co) and other trace metals (e.g., As, Bi, Co, Hg, Sb, Se, and Te).

Mineral textures, relationships, chemistry, and paragenesis show that the deposits evolved from an early, low temperature (< 300ºC), near neutral pH, and reducing fluid, that deposited sphalerite and pyrite, to a later, high temperature (> 300ºC), acidic, and reducing fluid, that deposited chalcopyrite and pyrrhotite (+/- pyrite, cobaltite, and pentlandite). The presence of late magnetite and bornite at Tilt Cove reflects the overall cooling of the hydrothermal system and a switch to more oxidizing and sulfur poor fluid conditions. Sulfur isotope compositions range from +2.82 to +23.57‰ and indicate that reduced sulfur in the sulfides was derived from seawater sulfate mixing with leached footwall igneous sulfur; some highly positive values are best explained by the replacement of sulfate minerals by sulfide minerals.

The leaching of ophiolitic, Cu-, Co-, Ni-, As-, Au-, and Sb-bearing footwall rocks with minor potential contributions from episodic, short-lived magmatic pulses were most likely responsible for the metals found in the Betts Cove and Tilt Cove deposits.

ACKNOWLEDGMENTS

First and foremost, I would like to thank my supervisor Dr. Stephen Piercey for the opportunity to do this project. I am grateful for his time and support throughout the past two years. I would also like to thank my committee member Dr. Philippe Belley. Thank you to those who helped with the analytical aspects of this project including Wanda Aylward (SEM-EDS and EPMA), Dylan Goudie (SEM-MLA), Emma Scanlan (LA-ICP-MS), and Glenn Piercey (SIMS). Thank you to Dave Copeland and others from Signal Gold for allowing me to access their property, drill core, and databases, and for helping me with fieldwork and the 3D modelling software.

Funding for this project was provided by NSERC Discovery Grant (Piercey), SGS Fellowship (Memorial University), Mitacs, Signal Gold Inc., and the Research Affiliate Program (Government of Canada – Natural Resources Canada).

Table of Contents

List of Tables

Chapter 2

Chapter 3

List of Figures

Chapter 1

Chapter 2

Figure 3.5. Main sulfide facies at Betts Cove, including: A) chalcopyrite-dominated facies; B) chalcopyrite-pyrrhotite-dominated facies; C) sphalerite-pyrite-dominated facies; D) pyrite-dominated facies, and at Tilt Cove, including: E) pyrite-dominated facies; F) chalcopyrite +/- pyrrhotite-dominated facies; G) pyrrhotite-dominated facies; and H) magnetite-dominated facies. Here, ccp = chalcopyrite, mag = magnetite, po = pyrrhotite, py = pyrite, and sp = sphalerite.

Figure 3.6. Plane polarized reflected light and backscatter electron images of sulfide, selenide, and telluride mineral textures from Betts Cove, including: A) relic colloform pyrite being replaced by chalcopyrite; B) euhedral pyrite grains forming clusters; C) chalcopyrite forming a strain shadow around subhedral pyrite suggesting deformation; D) annealed pyrite grains suggesting deformation; E) pyrite vein following folliations in host rock; F) intergrown chalcopyrite-pyrrhotite assemblage (+ minor sphalerite and pyrite); G) chalcopyrite disease in sphalerite; H) subhedral cobalitite grains hosted in chalcopyrite; I) intergrown pentlandite and pyrrhotite within chalcopyrite; J) rounded electrum grain hosted in chalcopyrite; K) intergrown clausthalite and hessite along pyrite-chalcopyrite grain boundry; and L) intergrown galena and hessite in fracture in chalcopyrite. Here, ccp = chalcopyrite, cob = cobaltite, cth = clausthalite, el = electrum, gn = galena, hes = hessite, pnt = pentlandite, po = pyrrhotite, py = pyrite, and sp = sphalerite.

Figure 3.7. Trace element (V, Cr, Mn, Co, Ni, Cu, Zn, Se, Sn, Sb, Te, Au) variations between the main sulfide minerals (pyrite, chalcopyrite, pyrrhotite, sphalerite) composing the main sulfide facies at Betts Cove, where orange = chalcopyrite-dominated facies, red = chalcopyrite-pyrrhotite-dominated facies, green = pyrite-dominated facies, and light grey = sphalerite-pyrite-dominated facies.

Figure 3.8. Sulfur isotope analyses ($\delta^{34}S$) of pyrite textures (A), chalcopyrite (B), and pyrrhotite (C) at Betts Cove (A-C) and Tilt Cove (D-F). Here, the boxes represents the interquartile range, the lines represents the median value, the black dots represents the mean value, the whiskers represent the minimum and maximum values, and the coloured dots represent any outliers.

Figure 3.9. Plane polarized reflected light and backscatter electron images of sulfide and oxide mineral textures from Tilt Cove, including: A) relic colloform pyrite being replaced by chalcopyrite and sphalerite; B) euhedral pyrite grains; C) massive sphalerite surrounding pyrite grains; D) cataclastic pyrite with chalcopyrite infilling fracture spaces suggesting deformation; E) intergrown chalcopyrite-pyrrhotite assemblage; F) subhedral cobalitite grains hosted in pyrrhotite and chalcopyrite; G) pentlandite stringer hosted in pyrrhotite; H) arsenopyrite and chalcopyrite surrounding pyrite grains; I) bornite replacing chalcopyrite; J) magnetite surrounding pyrrhotite stringer; K) massive sulfide and magnetite showing folding as a result of deformation; L) euhedral chromite grains with magnetite rims; and M) acanthite and arsenopyrite in fracture in pyrite. Here, aca = acanthite, apy = arsenopyrite, bn = bornite, ccp = chalcopyrite, chr = chromite, cob = cobaltite, mag = magnetite, pnt = pentlandite, po = pyrrhotite, py = pyrite, and sp = sphalerite.

Figure 3.10. Trace element (V, Cr, Mn, Co, Ni, Cu, Zn, Se, Sn, Sb, Te, Au) variations between the main sulfide minerals (pyrite, chalcopyrite, pyrrhotite, sphalerite) composing

List of Abbreviations

μm	Microns
2D	Two dimensional
3D	Three dimensional
Å	Angstrom
A	Amp
AAT	Annieopsquotch accretionary tract
Aca	Acanthite
apfu	Atoms per formula unit
Apy	Arsenopyrite
AUC	Area under the curve
Bn	Bornite
BSR	Bacterial sulfate reduction
BVOT	Baie Verte oceanic tract
CA	Classification accuracy
Ccp	Chalcopyrite
Chr	Chromite
CLR	Centered log-ratio
Cob	Cobaltite
CREAIT	Core Research Equipment & Instrument Training Network
Cth	Clausthalite
Da	Dalton
e.g.	For example
El	Electrum
EPMA	Electron probe microanalyses
et al.	And others
F1	Measure of accuracy
FEG	Field emission gun
ft	Feet
Gn	Galena
g/t	Grams per tonne
Hes	Hessite
Hz	Hertz
i.e.	That is
Inc.	Incorporated
IP	Induced polarization
K	Number of clusters in K-means clustering analyses
keV	Kiloelectron volt
kg	Kilogram
km	Kilometer
kV	Kilovolt

LA-ICP-MS	Laser ablation inductively coupled plasma mass spectrometry
LBOT	Lushs Bight oceanic tract
Ltd.	Limited
LOD	Limit of detection
m	Meters
Ma	Mega annum (millions of years)
MAF	MicroAnalysis Facility
Mag	Magnetite
mm	Millimeter
MORB	Mid ocean ridge basalt
ms	Millisecond
Mt	Million tonne
n	Number
nA	Nanoamp
NI-43-101	National Instrument 43-101
PC	Principal components
PCA	Principal component analysis
Pnt	Pentlandite
Po	Pyrrhotite
ppm	Parts per million
Py	Pyrite
QA/QC	Quality assurance/quality control
QFIR	Queen's Facility for Isotope Research
ROC	Receiver-operator curve
s	Second
SEM-EDS	Scanning electron microscopy – energy dispersive spectroscopy
SEM-MLA	Scanning electron microscopy – mineral liberation analysis
SIMS	Secondary ion mass spectrometry
Sp	Sphalerite
SVM	Support vector machine
T	Temperature
TSR	Thermochemical sulfate reduction
VCDT	Vienna Canyon Diablo troilite
VMS	Volcanogenic massive sulfide
wt%	Weight percent
WD	Wavelength dispersive
yr	Year

List of Appendices

Chapter 1

An Overview of the Geology of the Baie Verte Peninsula, Newfoundland Appalachians and the Betts Cove and Tilt Cove Volcanogenic Massive Sulfide Deposits

1.1. INTRODUCTION

The mitigation of climate change and the transition to low carbon energy-delivery and transportation sectors requires the electrification of the economy and the reduced usage of hydrocarbon-sourced energy. Governments are encouraging a transition from hydrocarbon-based energy sources to green/low carbon energy sources such as batteries, solar panels, and wind turbines (Grandell et al., 2016; Sovacool et al., 2020). Developing green or low carbon energy sources is forecasted to substantially increase the demand for natural resources, some of which are of national or strategic importance and deemed critical minerals/metals. This varies with jurisdiction, but most jurisdictions (e.g., Canada, EU, USA, Australia) include Cu, Co, Ni, Zn, Te, and others (Grandell et al., 2016; Sovacool et al., 2020; Government of Canada, 2022). Critical metals are of strategic interested in part because of increased demand but also uncertainty surrounding supply chains (and national security and economic security issues; Grandell et al., 2016; Sovacool et al., 2020). Currently, there is very little known about the distribution of some critical metals in volcanogenic massive sulfide (VMS) deposits; thus, a better understanding of the setting and distribution of critical metals in VMS deposits can potentially contribute to ensuring stable supplies of said metals essential for a shift to low carbon society.

The Betts Cove and Tilt Cove deposits are mafic-(Cyprus)-type VMS deposits hosted within the Betts Cove ophiolite, Baie Verte Peninsula, Newfoundland Appalachians. Despite previous research on the deposits, the nature and styles of mineralization, critical metal distributions and controls, and metal interrelationships within these deposits is incomplete (e.g., Saunders, 1985; Strong and Saunders, 1988; Bédard et al., 2000; Sangster et al., 2007). This thesis will study the mineralogy, paragenesis, bulk ore chemistry, and major and trace element chemistry of the various sulfide mineral phases within the sulfide mineralization in these deposits. The goal of this work is to provide a better understanding of the metal distribution and residence within the mineralization, and controls on deposit formation and critical metal enrichment (e.g., Cu, Co, Ni, Zn). This work will also provide insight into the distribution and genetic controls on critical and other metals in ophiolite-hosted VMS deposits worldwide.

1.2. VOLCANOGENIC MASSIVE SULFIDE (VMS) DEPOSITS

Volcanogenic massive sulfide deposits are an important source of base, precious, and critical metals (Galley et al., 2007). They form in extensional environments through the discharge of hydrothermal fluids at or near the seafloor. These deposits are typically stratabound and polymetallic, consisting of a variably shaped massive sulfide zone underlain by a stockwork zone of sulfide stringers (Figure 1.1: Franklin et al., 2005; Galley et al., 2007).

The VMS deposit model consists of six basic elements: (1) a heat source that drives hydrothermal convection; (2) an impermeable reaction zone where metals are leached; (3) syn-volcanic faults/fractures that allow the hydrothermal fluid to discharge; (4) footwall (and to a lesser extent, hanging-wall) alteration zones that result from the interaction of the host rock and ascending hydrothermal fluid and descending seawater; (5) the massive sulfide deposit; and (6) distal hydrothermal sedimentary rocks showing the extent of plume fall out from the black smokers. This general model and its components are well accepted (Figure 1.1: Franklin et al., 2005).

Volcanogenic massive sulfide deposits have been classified based on many characteristics including base metal and Au contents, but the host rock lithology classification of Barrie and Hannington (1999), subsequently modified by Franklin et al. (2005) and Galley et al. (2007), is the most used classification system. This classification includes five sub-types of VMS deposits based on tectonostratigraphy of the VMS environment: (1) mafic, with dominantly mafic host rocks with rare or absent felsic rocks; (2) bimodal-mafic, with dominantly mafic host rocks and subordinate siliciclastic rocks; (3) mafic-siliciclastic, with equal amounts of mafic and siliciclastic rocks; (4) bimodal-felsic, with dominantly felsic rocks and lesser mafic and siliciclastic rocks; and (5) bimodal-siliciclastic, with equal amounts of felsic volcanic and basaltic rocks and siliciclastic rocks (Barrie and Hannington, 1999, Franklin et al., 2005, Galley et al., 2007). Galley et al., (2007) added the hybrid bimodal-felsic sub-type, which have deposits that contain features transitional between VMS deposits and epithermal gold deposits. Patten et al. (2022) introduced the ultramafic sub-class where mineralization is hosted within ultramafic rocks.

1.2.1. Mafic or Cyprus-type VMS Deposits

The Betts Cove and Tilt Cove deposits are mafic-(Cyprus)-type VMS deposits. These deposits have > 75% mafic rocks, rare or absent felsic rocks, and < 10% siliciclastic and/or ultramafic rocks. Mafic-type VMS deposits that are found in ophiolites and are interpreted to have formed in intra-oceanic arcs, mature back-arcs, and supra-subduction zone settings (Figure 1.2). The host mafic rocks are generally arc tholeiitic and/or boninitic (+/- mid-ocean ridge basalt/back-arc basin basalt for back-arc ophiolites) and are Cu-rich and Pb-poor compared to other VMS deposit types (Barrie and Hannington, 1999). The Betts Cove and Tilt Cove deposits are interpreted to have formed in a supra-subduction zone, forearc setting because of the presence of boninites and arc tholeiites (Bédard et al., 1998; Barrie and Hannington, 1999; Franklin et al., 2005; Galley et al., 2007).

1.3. HISTORICAL WORK

1.3.1. Betts Cove

The Betts Cove deposit was discovered in 1864, and shortly after, the Betts Cove Mining Company was established. The Betts Cove mine produced 130 682 tons of copper ore grading up to 10% Cu from 1875 to 1886; the mine closed in 1886 due to a mine collapse (Bédard et al., 2000; Anaconda Mining, 2021).

In 1955, Advocate Mines Ltd. drilled eight holes totalling 3540 ft (~ 1079 m) at Betts Cove. In 1985, Noranda Exploration Co. completed prospecting and heavy mineral concentrate sampling. In 1987, Betts Cove Minerals completed an evaluation of the mine, including sampling from historic dumps and exposed bedrock with assay results up to 28.9 g/t Au. In 1989 they completed diamond drilling, geological mapping, rock and soil sampling, and magnetic and electromagnetic surveying. From 1995 to 1999, Noveder Inc. completed a diamond drilling program, prospecting, lithogeochemical sampling, geological mapping, geophysical surveys, and channel sampling. From 2008 to 2009, Metals Creek resources completed a data compilation and undertook prospecting in the area (Anaconda Mining, 2021).

In 2020, Anaconda Mining (now Signal Gold Inc.) completed exploration work in the area including geological mapping and induced polarization (IP) geophysical surveying. Ten holes were drilled via diamond drilling totalling 1672.5 m (Anaconda Mining, 2021).

1.3.2. Tilt Cove

The Tilt Cove deposit was discovered by British surveyor, Smith McKay, in 1857. The Tilt Cove mine produced 8.2 million tons of copper ore grading on average between 4% and 12% Cu, 42 500 ounces of Au, and a small quantity of nickel grading up to 24% Ni, in two periods of operation between 1857 and 1967. In the 1950s and 1960s several companies completed diamond drilling programs, geological mapping, and geophysical surveying during deposit production (Bédard et al., 2000; Anaconda Mining, 2021).

In the 1980s, there was increased exploration at Tilt Cove. In 1982, Newmont Exploration of Canada Ltd., completed a diamond drilling program, geological mapping, rock geochemical analyses, and magnetic and electromagnetic surveys. Shortly after, IONEX Ltd. completed a diamond drilling program, geological mapping, geophysical surveys, and lithogeochemical sampling. In 1988 to 1991, Varna Gold Inc., completed a diamond drilling program, rock, soil, stream, and till sampling, airborne magnetic and electromagnetic surveys, and trenching. From 1988 to 1993, Bitech Energy Resources Ltd. completed diamond drilling, geological mapping, soil and rock sampling, and geophysical surveying. In 1994, PJAP exploration completed auger drilling of the overburden stockpile from Tilt Cove with assay results up to 4.90 g/t Au. They also determined that the stockpile contained 42 781 tonnes of material; this stockpile was later mined and processed by Metals Creek Resources and Rambler Metals and Mining in 2010. From 1995 to 2001, Noveder completed a diamond drilling program, prospecting, rock sampling, geological mapping, trenching, channel sampling, and geophysical surveying. From 2003 to 2005, Richmont Mines compiled data from previous exploration work and drilled one hole at Tilt Cove (Anaconda Mining, 2021).

Since 2017, Anaconda Mining (now Signal Gold Inc.) has been undertaking exploration work in Tilt Cove. Data was compiled and converted into digital format and ten holes were drilled via diamond drilling totalling 1641 m (Anaconda Mining, 2021).

1.4. REGIONAL GEOLOGY

1.4.1. The Newfoundland Appalachians

The Newfoundland Appalachians consist of four tectonostratigraphic zones (from west to east): Humber, Dunnage, Gander, and Avalon zones (Figure 1.3). These zones represent the opening and closure of the Iapetus and Rheic oceans that existed from the Late Precambrian to Late Paleozoic. Rocks of the Humber Zone represent the ancient Laurentian continental margin. The Dunnage Zone consists of island arcs, ophiolitic, and back-arc rocks that were accreted to the Humber zone and to one another within the Iapetus Ocean. The Gander and Avalon zones represent microcontinents that were accreted to the composite Laurentia in the Paleozoic (Williams, 1978; Williams et al., 1988; van Staal and Barr, 2012).

The Dunnage Zone consists of the Notre Dame and Exploits subzones, which are separated by the Beothuk Lake Line (=Red Indian Line in historical literature), a steep brittle fault. Betts Cove and Tilt Cove lie within the Notre Dame subzone bounded to the east by the Beothuk Lake Line and to the west by the Baie Verte Brompton Line (Figure 1.3). The Dunnage Zone is made up of mafic volcanic rocks and marine sedimentary rocks that locally overlie ophiolitic rocks, including rocks of the Lushs Bight oceanic tract (LBOT, 510-501 Ma), Baie Verte oceanic tract (BVOT, 490 Ma), Dashwoods microcontinent, Annieopsquotch accretionary tract (AAT, 480-473 Ma), and Notre Dame magmatic arc (488-435 Ma; van Staal and Barr, 2012). The LBOT consists of pillow basalts, sheeted dykes, gabbro, and rare ultramafic rocks representing a supra-subduction zone/infant arc. The BVOT consists of similar supra-subduction zone/arc rocks as the LBOT but are younger in age. The Dashwoods microcontinent in Newfoundland is a 25-50 km wide and 400 km long, peri-Laurentian microcontinent. By 493 Ma, the LBOT was obducted onto the Dashwoods forming a composite terrane (van Staal and

Barr, 2012). The AAT consists of supra-subduction zone ophiolitic rocks and lesser arc and back-arc rocks. The Notre Dame magmatic arc formed during three magmatic pulses during the Taconic and Salinic orogenies (van Staal and Barr, 2012).

The Newfoundland Appalachians were subject to several orogenies, including the Taconic (495-450 Ma), Salinic (430-422 Ma), Acadian (421-400 Ma), and Neoacadian (400-350 Ma; van Staal et al., 2009). The Taconic orogeny occurred in three stages: 1) west directed subduction initiation resulting in the LBOT and its obduction onto the Dashwoods microcontinent (Figure 1.4); 2) collision and obduction of the Notre Dame arc with the Humber margin and the closure of the Taconic Seaway, collision of the Dashwoods with the Humber margin, the formation of the supra-subduction zone that formed the BVOT, and its ultimate obduction onto the Humber margin (Figures 1.4 and 1.5); 3) arc-arc collision of the AAT and Beothuk Lake Line arc with the peri-Gondwanan Popelogan-Victoria arc that ended the Taconic orogeny (Figure 1.5). It was during the Taconic orogeny that the Betts Cove ophiolite was accreted to and thrust upon the Laurentian continental margin (van Staal et al., 2009; van Staal and Barr, 2012). Following the end of the Taconic, the Salinic orogeny occurred when a subduction zone formed beneath Laurentia, the Tetagouche-Exploits back-arc basin formed and closed, and the Gander margin collided with composite Laurentia. The Acadian orogeny occurred during the closure of the Acadian seaway and the accretion of Avalonia to composite Laurentia. The Neoacadian orogeny occurred during the collision of Meguma and composite Laurentia associated with the closure of the Rheic Ocean (Williams, 1978; Williams et al., 1988; van Staal and Barr, 2012; van Staal and Barr, 2012).

1.4.2. The Betts Cove Ophiolite

The ~ 488 Ma (e.g., Dunning and Krogh, 1985) Betts Cove ophiolite consists of a typical ophiolitic assemblage, including (from bottom to top): (1) serpentinite/talc-carbonates; (2) layered ultramafic to mafic cumulate rocks; (3) gabbroic intrusive rocks; (4) sheeted dykes; (5) a dyke to lava transition zone; and (6) pillow lavas (Figures 1.6 and 1.7). The entire ophiolite sequence is 4320 m thick (Figure 1.7; Bédard et al., 2000).

The lowermost unit is serpentinite and talc-carbonate altered rock and has a maximum thickness of 750 m. The serpentinite is dark green to black in colour and generally found within the talc-carbonate rock. The talc-carbonate rock commonly displays schistosity and is dominated by a pale blue to green talc (Hibbard, 1983; Bédard et al., 2000).

The altered ultramafic rocks are overlain by layered cumulate rocks, which have an approximate thickness of 1000 m. The layered cumulates display cyclic and rhythmic sequences that range from peridotite, pyroxenite, to gabbronorite, and rare dunite. The pyroxenite unit consists of olivine pyroxenite and orthopyroxenite that grades upwards into clinopyroxenite. Gabbronorite is feldspar and pyroxene phyric. Serpentine, talc, and chlorite are common alteration minerals in the cumulate unit, where they replace olivine and orthopyroxene (Bédard et al., 2000).

The layered cumulates are intruded by and overlain by an intrusive suite, which has an approximate thickness of 330 m. The intrusive suite includes pyroxenite, gabbro, gabbronorite, and trondhjemite dykes and sills. The intrusions are interlayered and commonly have sharp contacts with one another and vary in composition from Betts Cove to Tilt Cove. In Betts Cove, gabbronorite is dominant (with plagioclase phenocrysts altered to epidote and sericite), and quartz gabbro, diorite, and trondhjemite are subordinate. In Tilt Cove the intrusive rocks are dominated by a massive gabbro intrusion (with sericite altered plagioclase), and this grades into leucogabbro, gabbronorite, and websterite. Breccia containing clasts of all these rock types are also common in this unit (Hibbard, 1983; Bédard et al., 2000).

In sharp contact with the intrusive suite is the overlying sheeted dyke unit, which has an approximate thickness of 1600 m. This unit is prevalent in the Betts Cove area and extends 4500 m wide. These sheeted dykes are diabasic, porphyritic/picritic, and perknitic with lesser gabbroic, mafic, and ultramafic dykes. The dip of the dykes is generally vertical and nearly all have chilled margins. The diabasic dykes contain small phenocrysts of olivine, orthopyroxene, and feldspar. Porphyritic/picritic dykes contain larger olivine, orthopyroxene, and feldspar phenocrysts. Perknitic dykes are very coarse grained and consist of actinolite, chlorite, and clinopyroxene with less than 10% feldspar. The gabbroic dykes are finer grained versions of the dykes of the late intrusive suite. Dykes are pervasively altered to greenschist facies mineral assemblages in this unit (Coish and Church 1979; Hibbard, 1983; Bédard et al., 2000).

Overlying the sheeted dykes are the lavas of the Betts Head Formation, which has an approximate thickness of 1300 m. The transition zone between the sheeted dykes and overlying lavas is gradational with alternating dykes, spherulitic pillow lavas, and faults that contain abundant chlorite, which are interpreted to be reflective of a horst-and-graben system between the dykes and lavas. The Betts Head Formation consists of mostly clinopyroxene spherulitic pillow lavas and flow tubes; breccia zones are also common. These lavas can be divided into two types: (1) olivine + orthopyroxene + chromite +/- clinopyroxene-phyric or low-Ti boninites; and (2) plagioclase + clinopyroxene-phyric or intermediate-Ti boninites. In Tilt Cove, these lavas are pervasively altered to serpentine and talc-carbonate (Coish and Church 1979; Hibbard, 1983; Bédard et al., 2000).

1.4.3. The Snooks Arm Group

The cover sequence to the Betts Cove ophiolite consists of Early to Middle Ordovician sedimentary and volcanic rocks of the Snooks Arm Group. The Snooks Arm Group is comprised of six formations: (1) Mount Misery; (2) Scrape Point; (3) Bobby Cove; (4) Venam's Bight; (5) Balsam Bud Cove; and (6) Round Harbour formations (Figures 1.6 and 1.7). The lowermost formation, the Mount Misery Formation, is made up of tholeiitic lavas (Bédard et al., 2000; Skulski et al., 2010).

Overlying the rocks of the Mount Misery Formation are the rocks of the Scrape Point Formation, which includes a lower red clastic unit (the Nugget Pond Horizon), an upper green clastic unit, and volcanic rocks. The red clastic unit consists of variably magnetic red conglomerates, sandstones, siltstone, and mudstone. The overlying green clastic unit consists of green tuffaceous sandstone-siltstone-mudstone turbidites. The volcanic rocks of the Scrape Point Formation are tholeiitic, high-Ti, amygdaloidal and plagioclase-phyric pillow lavas (Bédard et al., 2000; Skulski et al., 2010).

The Bobby Cove Formation occurs stratigraphically above the Scrape Point Formation. The lower member, the East Pond member, consists of interbedded calc-alkalic lapilli and tuff, tuff breccia, volcanic conglomerate, and lava flows. The upper member consists of epiclastic turbidite interbedded with mudstone and rare tuff. The Venam's Bight Formation overlies the Bobby Cove Formation and consists of tholeiitic, high-Ti, plagioclase-phyric pillow and amygdaloidal basalts with sheet flows with local breccia, hyaloclastite, and mudstone layers. The overlying Balsam Bud Cove Formation includes a basal member of interbedded pelagic sedimentary rocks, turbidites, tuffs, and basaltic lavas and an upper member consisting of thick bedded massive flows containing a variety of large clasts. The uppermost formation, the Round

Harbour Formation, consists of tholeiitic pillow lavas, sheet flows and local thin mudstone beds. The Snooks Arm Group is overlain by the volcanic and sedimentary rocks of the Cape St. John Group (Hibbard, 1983; Bédard et al., 2000; Skulski et al., 2010).

1.5. THE BETTS COVE DEPOSIT

The Betts Cove deposit is located in the southern part of the Betts Cove ophiolite about 1.25 km southwest from Betts Cove (Figure 1.8). The largest part of the deposit is found in the transition zone between the sheeted dykes and the Betts Head Formation boninitic pillow lavas and immediately hosted within southeast striking, pervasively chlorite altered shear and fault zones. Extensions of mineralization into the pillow lavas also occur but are less extensive. The mineralized shear zones are interpreted to represent synvolcanic faults, and along with chlorite, contain quartz, anthophyllite, tremolite, calcite, and stilpnomelane (Upadhyay and Strong, 1973; Saunders, 1985; Bédard et al., 2000).

The mineralization in the Betts Cove deposit occurs as massive sulfide lenses, veins, stringers, and disseminations of pyrite, lesser chalcopyrite and sphalerite, and rare galena. The massive sulfide lenses are commonly banded, partly tectonic in origin (Sangster et al., 2007). Pyrite forms discrete crystals of similar size, whereas chalcopyrite occurs as stringers, interstitial to pyrite crystals, and between fractures in pyrite grains. Sphalerite surrounds pyrite, and galena is found interstitial to the other sulfide minerals. The mineralization at Betts Cove contains Cu, Zn, and Au (Upadhyay and Strong, 1973; Saunders, 1985; Bédard et al., 2000; Sangster et al., 2007).

1.6. THE TILT COVE DEPOSIT

The Tilt Cove deposit is located in the northern part of the Betts Cove ophiolite about 15 km from Betts Cove (Figure 1.9; Strong and Saunders, 1988). The deposit is situated between the Betts Head Formation boninitic pillow lavas and Mount Misery Formation tholeiitic lavas and immediately hosted within chlorite altered lavas and basalt breccia. At Tilt Cove, these lavas are in contact with the underlying serpentine and talc-carbonate altered ultramafic rocks. Alteration associated with the mineralization consists of chlorite, lesser carbonate, and stilpnomelane (Strong and Saunders, 1988; Bédard et al., 2000; Sangster et al., 2007).

The mineralization in the Tilt Cove deposit occurs in several zones east and west of the town of Tilt Cove. The West zone consists mostly of disseminated and stringer chalcopyrite and pyrite in a steeply dipping body, which overlies boninitic lavas and breccia. A small lens of massive sulfide occurs in the West mine but is cut off by the Valley fault. The Valley fault separates the East and West zones and consists of 50 to 75 m of serpentine and talc-carbonate altered rocks and quartz-feldspar-porphyry dykes. This fault is normal and has displaced the east side downward (Bédard et al., 2000; Sangster et al., 2007). The East zone or Main zone consists of several orebodies, including a low grade stockwork zone and further east, a zone of small, massive sulfide lenses of chalcopyrite, pyrite, and pyrrhotite; magnetite also occurs. This zone is hosted within basalt breccia. The East zone ends at the East Limit fault, which puts the deposit host rocks in contact with the rocks of the Scrape Point Formation. This fault consists of sheared quartz-feldspar-porphyry (Bédard et al., 2000; Sangster et al., 2007). The mineralization at Tilt Cove has Cu with lesser Au, Ni, and Co (Strong and Saunders, 1988; Bédard et al., 2000; Sangster et al., 2007); gold at Tilt Cove has largely been associated with Zn and massive sphalerite (Hurley and Crocket, 1985; Strong and Saunders, 1988). Papezik (1964) studied the Ni minerals present at Tilt Cove and noted that Ni mineralization contains niccolite, maucherite, chloanthite, gersdorffite, arsenopyrite, and millerite, which are concentrated in a chlorite-rich zone near the main Cu orebody and serpentinized peridotite (Papezik, 1964). Nickel has been inferred to occur at Tilt Cove because the host rocks are in contact with Ni bearing ultramafic rocks (Papezik, 1964; Bédard et al., 2000; Sangster et al., 2007).

1.7. GOALS AND OBJECTIVES

The goal of this thesis is to provide a descriptive framework and potential genetic models for both the Betts Cove and Tilt Cove VMS deposits. The descriptive work will enhance our understanding of the mineralogy, paragenesis, and chemistry of the various sulfide mineral phases to determine metal distribution and residence and controls that led to their enrichment. Further, the major and trace element chemistry and S isotope systematics will allow for more refined genetic models for the mineralization in these deposits and ophiolite-hosted VMS deposits, globally.

This thesis aims to:

1. Determine the ore and gangue minerals, mineral assemblages, mineralization styles, paragenesis, and interrelationships of the mineralization to the host rocks;
2. Develop 2D geologic cross sections and 3D assay models of the deposits;
3. Evaluate the mineralization and metals within using assay and multi-element ICP data and data obtained from (1) and (2);
4. Measure major, minor, and trace element concentrations, including critical metals (e.g., Cu, Zn, Co, Ni, and Te) in the sulfide mineral assemblages; and
5. Measure sulfur isotope compositions of the sulfide minerals.

In order to answer the following questions:

1. How did these deposits form and what controlled the metal enrichment in the mineralization (e.g., hydrothermal fluid conditions, structural controls)?
2. What are the possible sources of the metals (e.g., Cu, Zn, Ni, Co) and sulfur (e.g., leaching of metals versus hydrothermal fluids, reduced seawater sulfate versus leaching of sulfur versus magmatic sulfur), and what processes resulted in their deposition (e.g., mixing with seawater versus boiling)?
3. Why are these deposits rich in certain critical metals (e.g., Cu, Zn, Ni, Co) and how do they compare to other mafic-type VMS deposits worldwide?

This work will result in a better understanding of the mineralogy and setting of the Betts Cove and Tilt Cove deposits and the mechanisms and causes of critical metal enrichment therein. The outcomes of this study may be applicable to other mafic-type VMS deposits worldwide and may provide a broader understanding of mafic-type VMS deposits and critical metal enrichment within said deposits.

1.8. METHODS

1.8.1. Core Logging, 2D and 3D Modelling, and Machine Learning

Graphic logging, 2D and 3D modelling, and statistical modelling were used to document and evaluate the stratigraphy, mineralogy, mineralization styles, and interrelationships to host rocks within the Betts Cove and Tilt Cove deposits. Drill holes (n = 20) were graphically logged and stratigraphic sections made of each hole. This data was utilized, along with historic logs, and multi-element assay databases, to construct 2D cross sections through the mineralization, 3D assay models using the LeapFrog software, and statistical evaluations using machine learning methods using the IMDEX ioGAS software and the Orange machine learning software.

1.8.2. Petrography, SEM-EDS/MLA, Ore Mineral Chemistry, and Sulfur Isotopes

Core samples were cut at Memorial University and sent to Vancouver Petrographics for polished thin section preparation. All thin sections were analyzed by petrography using a Nikon LV100POL microscope in the Metallogeny of Orogenic Belts Laboratory at Memorial University to determine the mineralogy, mineralization styles, mineral assemblages, and paragenesis at the Betts Cove and Tilt Cove deposits. A representative subset of these samples were analyzed by SEM-EDS in the Hibernia Project Electron Beam Laboratory at Memorial University and SEM-MLA in the CREAIT SEM-MLA Facility at Memorial University to confirm the information determined from standard petrography, to identify any additional minerals and textures that are too small to be identified by standard petrographic methods, and develop mineralogy maps of key samples (SEM-MLA).

Major and trace element compositions of the ore minerals in the Betts Cove and Tilt Cove deposits were measured using electron probe micro-analysis (EPMA) at the Hibernia Project Electron Beam Laboratory at Memorial University and laser ablation inductively coupled plasma mass spectrometry (LA-ICP-MS) at Queen’s Facility for Isotope Research (QFIR), Queen’s University. These data were used to determine the chemical composition of the mineralization, metal residence, and the sources of metals in the mineralization, including critical metals, in the Betts Cove and Tilt Cove deposits. The physicochemical conditions of the hydrothermal fluids (e.g., temperature, pH, and redox) were inferred from relationships between mineral compositions and the above attributes, comparison to modern hydrothermal vent fields, and from using thermodynamic relationships of ore assemblages and compositions to physicochemical conditions of formation (e.g., Lydon, 1988; Large, 1992; Wood, 1998; Keith et al., 2014).

Sulfur isotope compositions of the sulfides (pyrite, chalcopyrite, pyrrhotite, and arsenopyrite) in the mineralization were measured using secondary ion mass spectrometry (SIMS) in the CREAIT lab at Memorial University. Sulfur isotope analyses were performed on a subset of samples that represent each mineralization style of sulfide minerals. Sulfur isotope composition of the sulfides provides insights into the source(s) of sulfur, in the mineralization within Betts Cove and Tilt Cove deposits (e.g., Sakai, 1968; Ohmoto, 1972; Shanks, 2001; Seal, 2006).

1.9. REFERENCES

Anaconda Mining, 2021. Assessment report on diamond drilling, geological mapping, and prospecting on the Tilt Cove property, Baie Verte Peninsula, Central Newfoundland. Report filed for assessment with Newfoundland and Labrador Department of Natural Resources, Mineral Lands Division., 434 p.

Barrie, C.T., Hannington, M.D., 1999. Classification of volcanic-associated massive sulfide deposits based on host rock composition. Reviews in Economic Geology, v. 8, p. 2-10.

Bédard, J.H., Lauzière, K., Tremblay, A., Douma, S.L., Dec, T., 2000. Betts Cove ophiolite and its cover rocks, Newfoundland. Natural Resources Canada, Geological Survey of Canada Bulletin, 550, p. 1-76.

Bédard, J.H., Lauzière, K., Tremblay, A., Sangster, A., 1998. Evidence for forearc seafloor-spreading from the Betts Cove ophiolite, Newfoundland: oceanic crust of boninitic affinity. Tectonophysics, v. 284, p. 233-245.

Coish, R.A., Church, W.R., 1979. Igneous geochemistry of mafic rocks in the Betts Cove ophiolite, Newfoundland. Contributions to Mineralogy and Petrology, v. 70, p. 29-39.

Dunning, G.R., Krogh, T.E., 1985. Geochronology of ophiolites of the Newfoundland Appalachians. Canadian Journal of Earth Sciences, v. 22, p. 1659-1670.

Franklin, J.M., Gibson, H.L., Jonasson, I.R., Galley, A.G., 2005. Volcanogenic massive sulfide deposits. Society of Economic Geologists, 100th Anniversary Volume, p. 523-560.

Galley, A.G., Hannington, M.D., Jonasson, I.R., 2007. Volcanogenic massive sulphide deposits, in Goodfellow, W.D., ed., Mineral Deposits of Canada: A Synthesis of Major Deposit-Types, District Metallogeny, the Evolution of Geological Provinces, and Exploration Methods: Geological Association of Canada, Mineral Deposits Division, Special Publication No. 5, p. 141-161.

Government of Canada, 2022. The Canadian critical minerals strategy. 58 p.

Grandell, L., Lehtila, A., Kivinen, M., Koljonen, T., Kihlman, S., S. Lauri, L.S., 2016. Role of critical metals in the future markets of clean energy technologies. Renewable Energy, v. 95, p. 53-62.

Hibbard, J., 1983. Geology of the Baie Verte Peninsula, Newfoundland. Newfoundland Department of Mines and Energy, Memoir 2, 279 p.

Keith, M., Haase, K.M., Schwarz-Schampera, U., Klemd, R., Petersen, S., Bach, W., 2014. Effects of temperature, sulfur, and oxygen fugacity on the composition of sphalerite from submarine hydrothermal vents. Geology, v. 42, p. 699-702.

Large, R.R, 1992. Australian volcanic-hosted massive sulfide deposits: features, styles, and genetic models. Economic Geology, v. 87, p. 471-510.

Lydon, J.W., 1988. Volcanogenic massive sulphide deposits part 2: genetic models. Geoscience Canada Reprint Series 3, v. 15, p. 155-181.

Ohmoto, H., 1972. Systematics of sulfur and carbon isotopes in hydrothermal ore deposits. Economic Geology, v. 67, p. 551-578.

Papezik, V. S., 1964. Nickel minerals at Tilt Cove, Notre Dame Bay, Newfoundland. Proceedings of the Geological Association of Canada, Part 2, v. 15, p. 27-32.

Patten, C.G.C., Coltat, R., Junge, M., Peillod, A., Ulrich, M., Manatschal, G., Kolb, J., 2022, Ultramafic-hosted volcanogenic massive sulfide deposits: an overlooked sub-class of VMS deposit forming in complex tectonic environments. Earth Science Reviews, v. 224, 30 p.

Rogers, N., van Staal, C.R., McNicoll, V., Pollock, J., Zagorevski, A., and Whalen, J., 2006. Neoproterozoic and Cambrian arc magmatism along the eastern margin of the Victoria Lake Supergroup: A remnant of Ganderian basement in central Newfoundland? Precambrian Research, v. 147, p. 320-341.

Rye, R.O., Ohmoto, H., 1974. Sulfur and carbon isotopes and ore genesis: a review. Economic Geology, v. 69, p. 826-842.

Sakai, H., 1968. Isotopic properties of sulfur compounds in hydrothermal processes. Geochemical Journal, v. 2, p. 29-49.

Sangster, A.L., Douma, S.M., Lavigne, J., 2007. Base metal and gold deposits of the Betts Cove complex, Baie Verte Peninsula, Newfoundland, in Goodfellow, W.D., ed., Mineral Deposits of Canada: A Synthesis of Major Deposit-Types, District Metallogeny, the Evolution of Geological Provinces, and Exploration Methods: Geological Association of Canada, Mineral Deposits Division, Special Publication No. 5, p. 703-721.

Saunders, C. M., 1985. Controls of mineralization in the Betts Cove ophiolite. Unpublished M.Sc. thesis, St. John's, Newfoundland, Memorial University of Newfoundland, 200 p.

Seal, R.R., 2006. Sulfur isotope geochemistry of sulfide minerals. Reviews in Mineralogy and Geochemistry, v. 61, p. 622-677.

Shanks, W.C., 2001. Stable isotopes in seafloor hydrothermal systems: vent fluids, hydrothermal deposits, hydrothermal alteration, and microbial processes. Reviews in Mineralogy and Geochemistry, v. 43, p. 469-525.

Skulski, T., Castonguay, S., McNicoll, V., van Staal, C., Kidd, W., Rogers, N., Morris, W., Ugalde, H., Slavinski, H., Spicer, W., Moussallam, Y., Kerr, I., 2010. Tectonostratigraphy of the Baie Verte oceanic tract and its ophiolite cover sequence on the Baie Verte peninsula. Current research, Newfoundland and Labrador Department of Natural Resources Geological Survey, Report 10-1, p. 315-335.

Sovacool, B.K., Ali, S.H., Bazilian, M., Radley, B., Nemery, B., Okatz, J., Mulvaney, D., 2020. Sustainable minerals and metals for a low-carbon future. Science, v. 367 , p. 30-34.

Strong, D.F., Saunders, C.M., 1988. Ophiolitic sulfide mineralization at Tilt Cove, Newfoundland: controls by upper mantle and crustal processes. Economic Geology, v. 83, p. 239-255.

Upadhyay, H.D., Strong, D.F., 1973. Geological setting of the Betts Cove copper deposits, Newfoundland: an example of ophiolite sulfide mineralization. Economic Geology, v. 68, p. 161-167.

van Staal, C.R., Barr, S.M., 2012. Lithospheric architecture and tectonic evolution of the Canadian Appalachians and associated Atlantic Margin. Chapter 2 in Tectonic Styles in Canada: the Lithoprobe Perspective, Geological Association of Canada, Special Paper 49, p. 41-95.

van Staal, C.R., Whalen, J.B., Valverde-Vaquero, P., Zagorevski, A., Rogers, N., 2009. Pre-Carboniferous, episodic accretion-related, orogenesis along the Laurentain margin of the northern Appalachians. From Murphy, J.B., Keppie, J.D. & Hynes, A.J. (eds) Ancient Orogens and Modern Analogues. Geological Society, London, Special Publications, v. 327, p. 271–316.

Williams, H., 1978. Appalachian orogen in Canada. Canadian Journal of Earth Sciences, v. 16, p. 792-807.

Williams, H., Colman-Sadd, S.P., Swinden, H.S., 1988. Tectonic-stratigraphic subdivisions of central Newfoundland. Current Research, Part B, Geological Survey of Canada, Paper 88-1B, p. 91-98.

Wood, S.A., 1998. Calculation of activity-activity and log fo2-pH diagrams. Reviews in Economic Geology, Techniques in Hydrothermal Ore Deposits Geology, v. 10, p. 81-96.

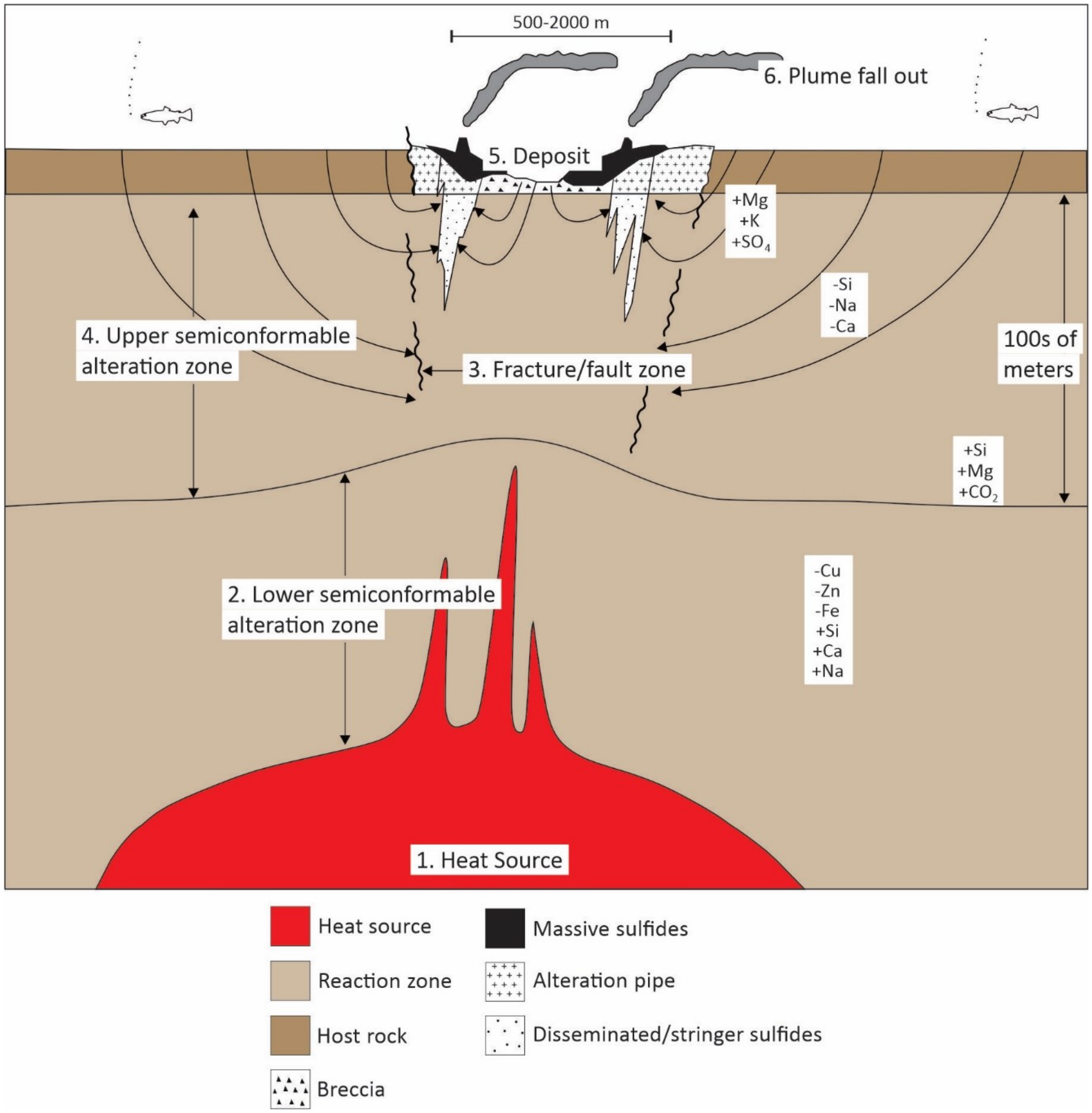

Figure 1.1. The six components of VMS deposit formation including: (1) heat source; (2) reaction zone; (3) syn-volcanic faults/fractures; (4) foot-wall (and to a lesser extent, hanging-wall) alteration zones; (5) massive sulfide deposit; and (6) distal products (from Franklin et al., 2005).

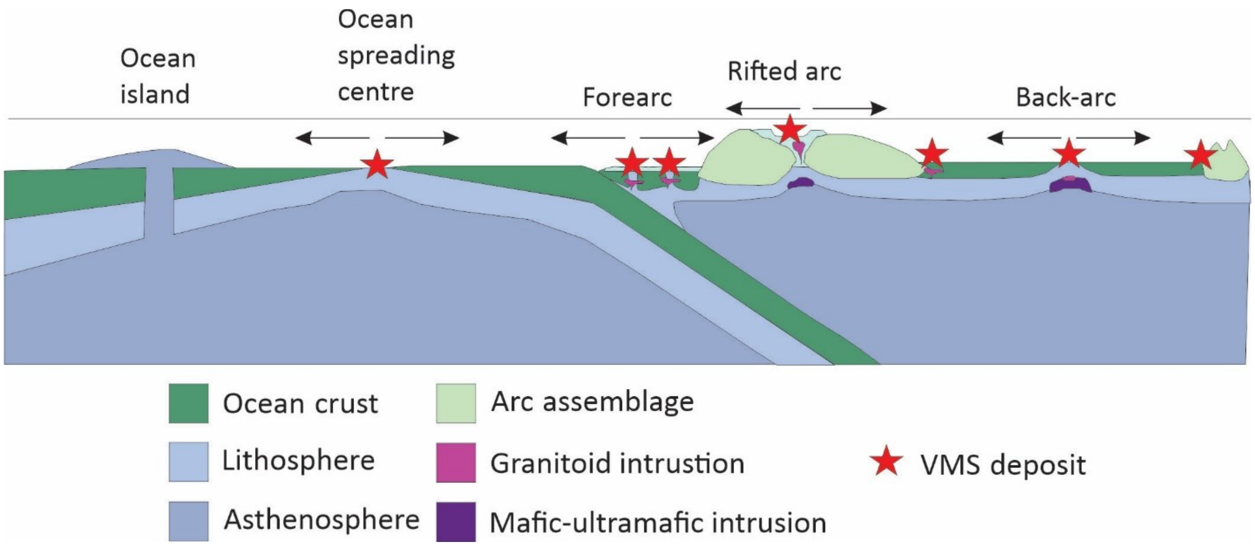

Figure 1.2. Tectonic environments where mafic-type VMS deposits may form (from Galley et al., 2007).

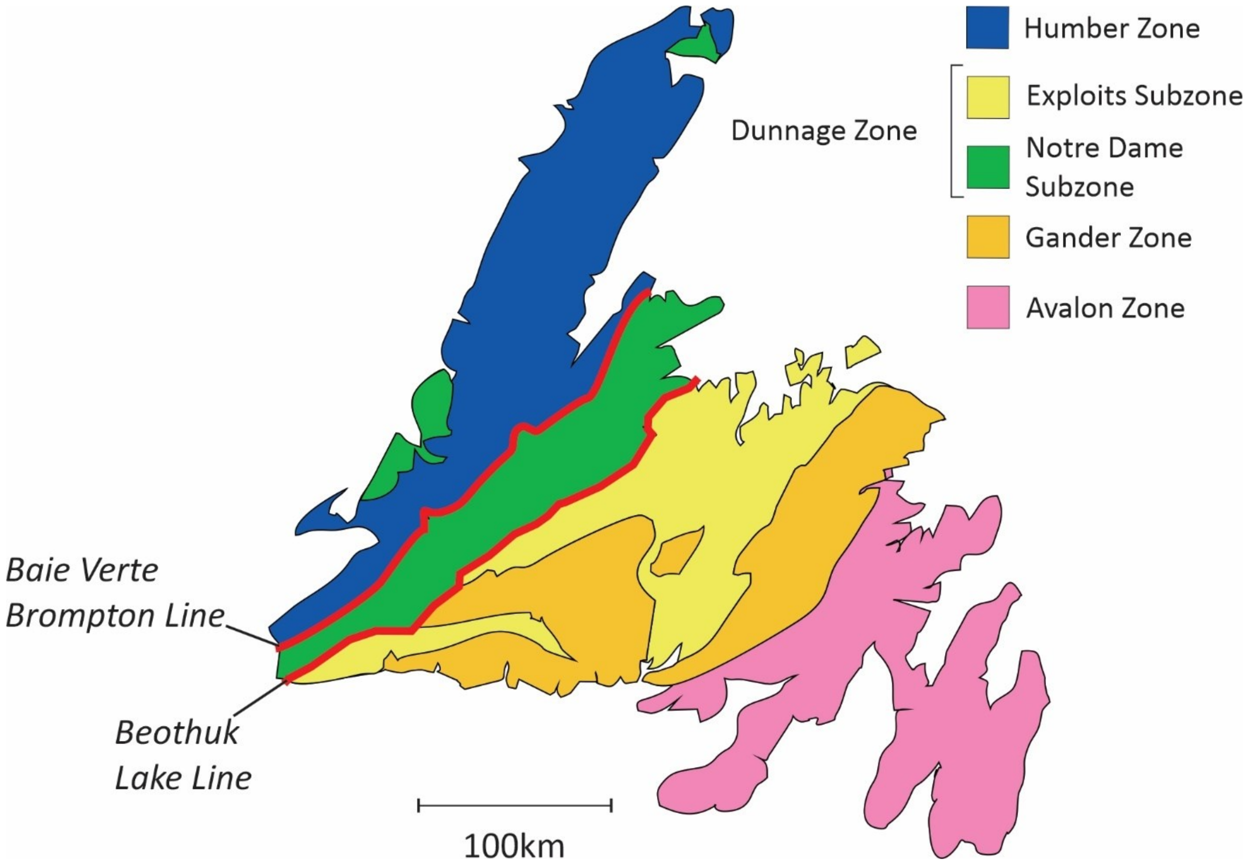

Figure 1.3. Tectono-stratigraphic zones and subzones of the Newfoundland Appalachians (from Rogers et al., 2006).

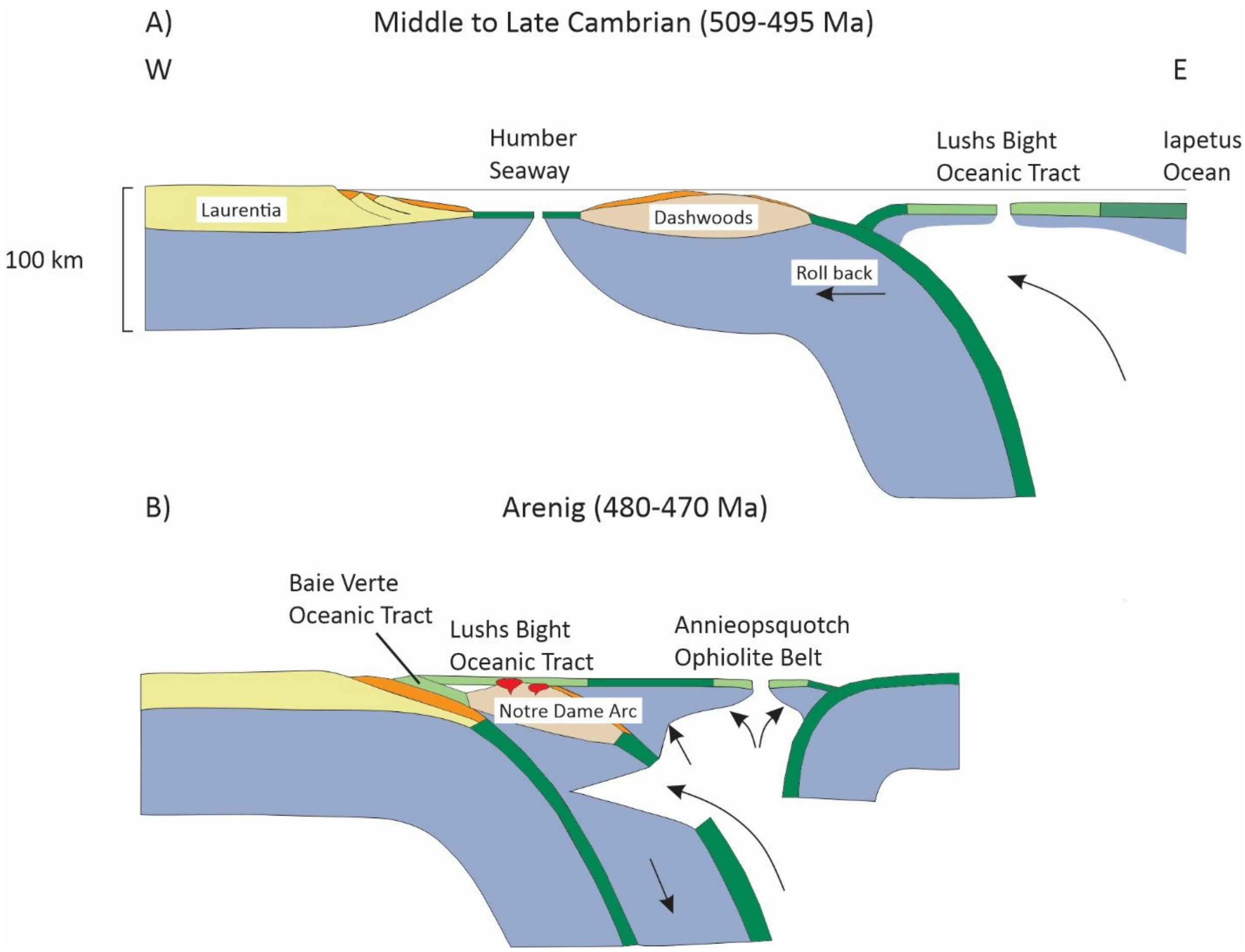

Figure 1.4. Tectonic evolution of Taconic orogeny 1 (A) and 2 (B) (from van Staal et al., 2009).

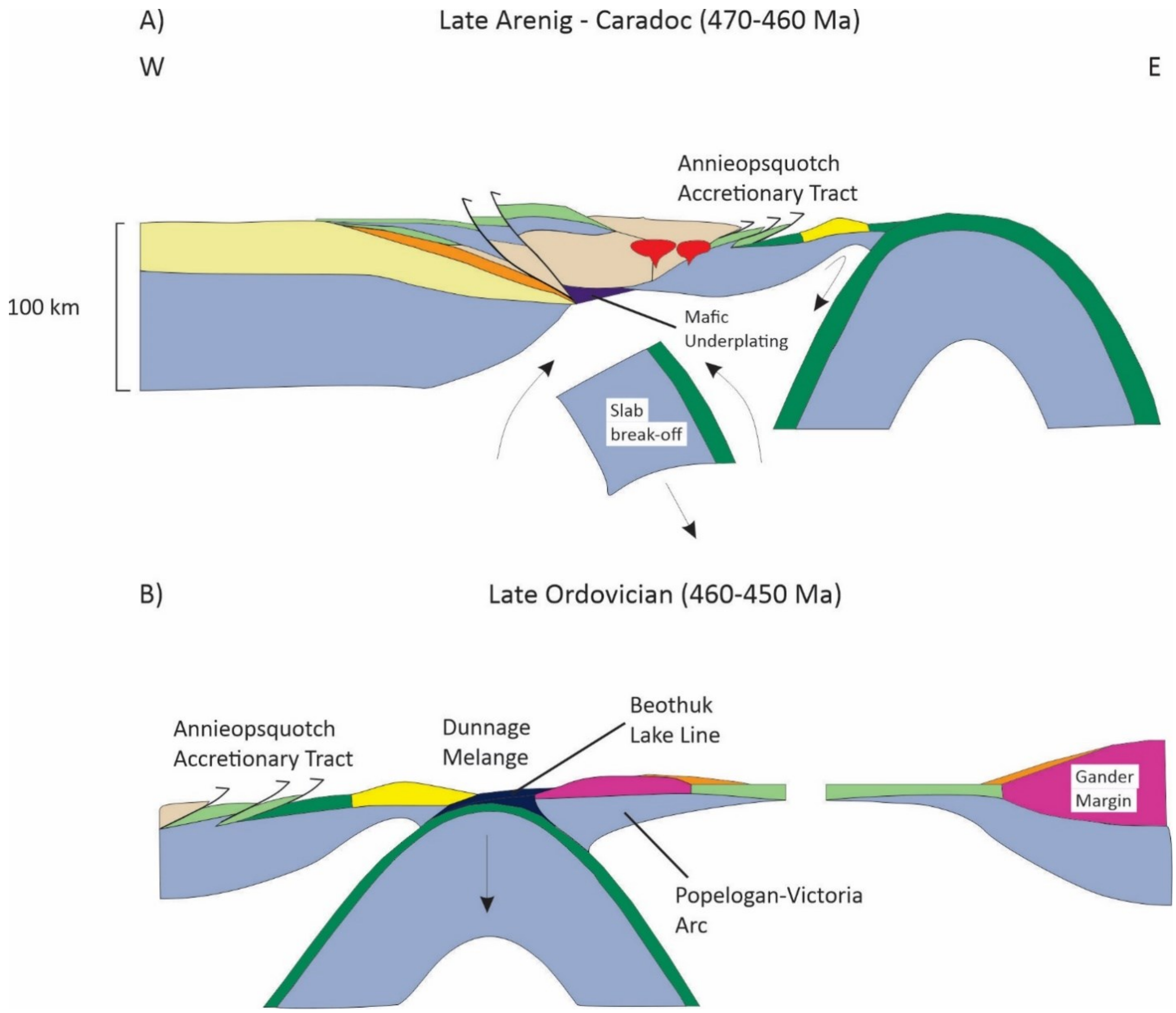

Figure 1.5. Tectonic evolution of Taconic Orogeny 2 (A) and 3 (B) (from van Staal et al., 2009).

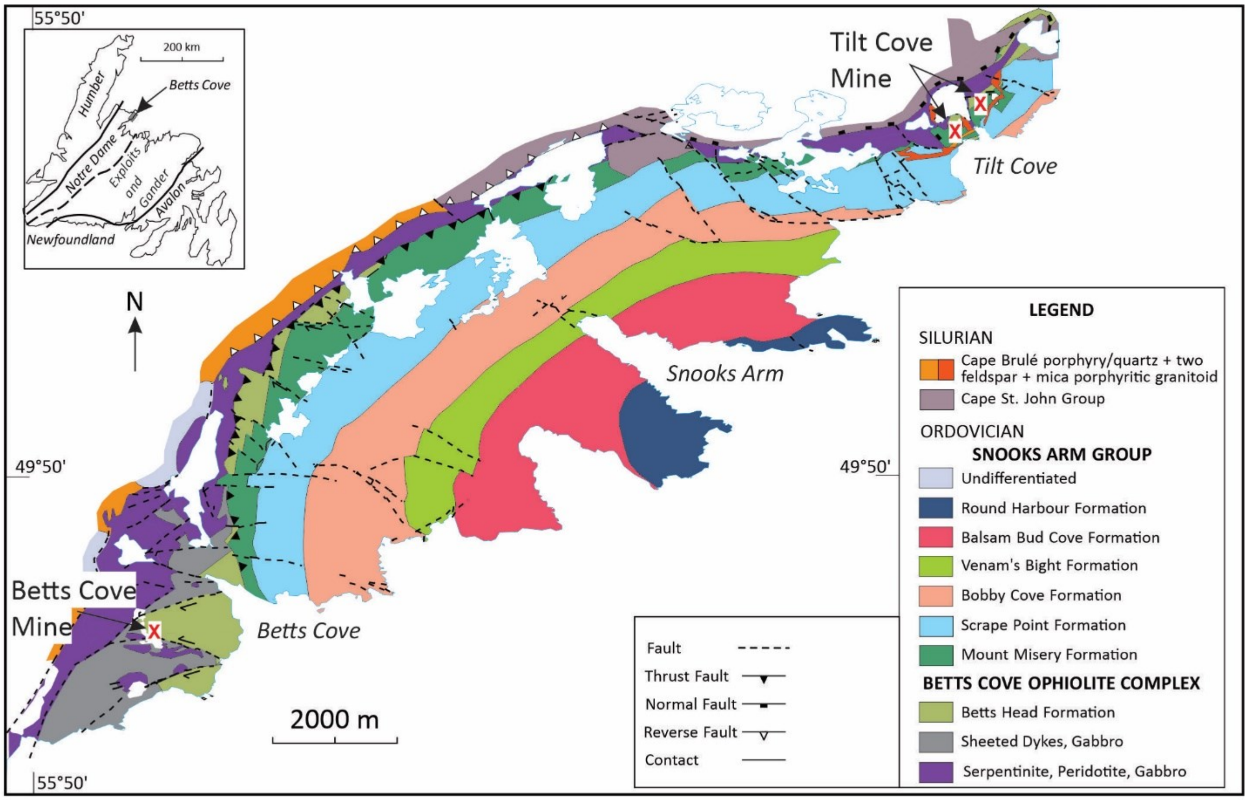

Figure 1.6. Geologic map of the Betts Cove ophiolite and Snooks Arm Group cover sequence (from Bédard et al., 2000 and Sangster et al., 2007).

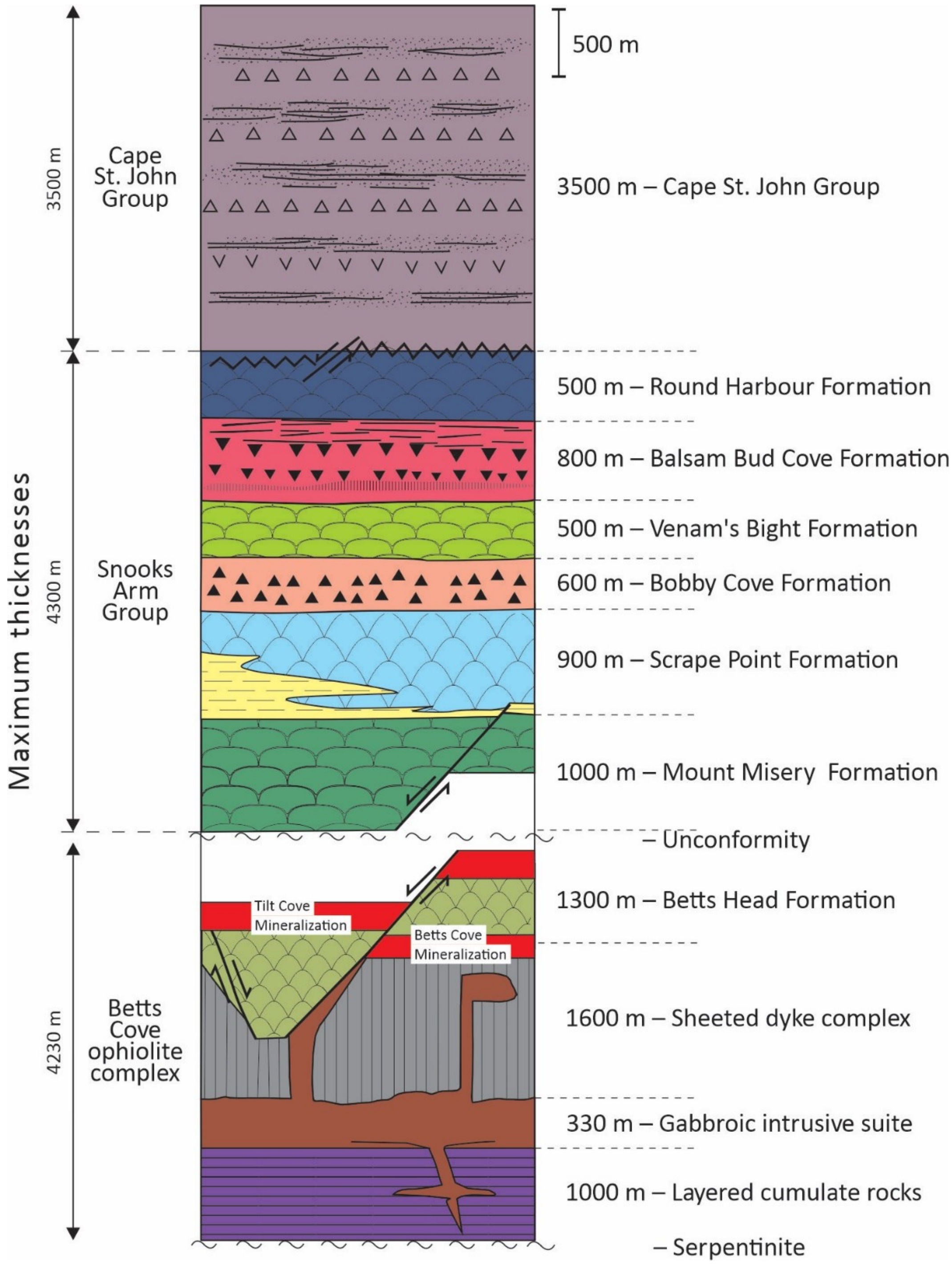

Figure 1.7. Stratigraphic section through the Betts Cove ophiolite and Snooks Arm Group cover sequence (from Bédard et al., 2000).

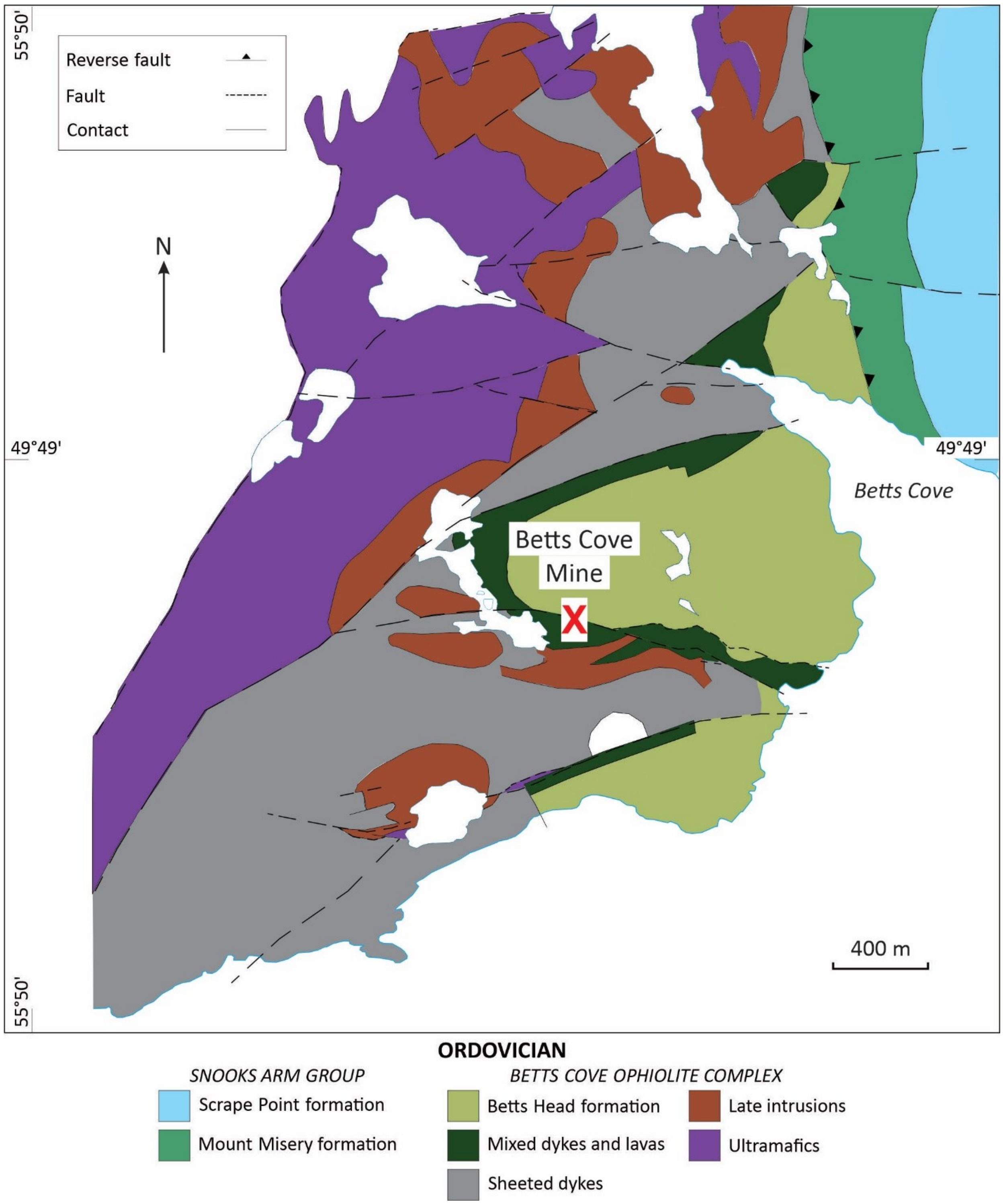

Figure 1.8. Geology of the Betts Cove deposit (from Bédard et al., 2000 and Sangster et al., 2007).

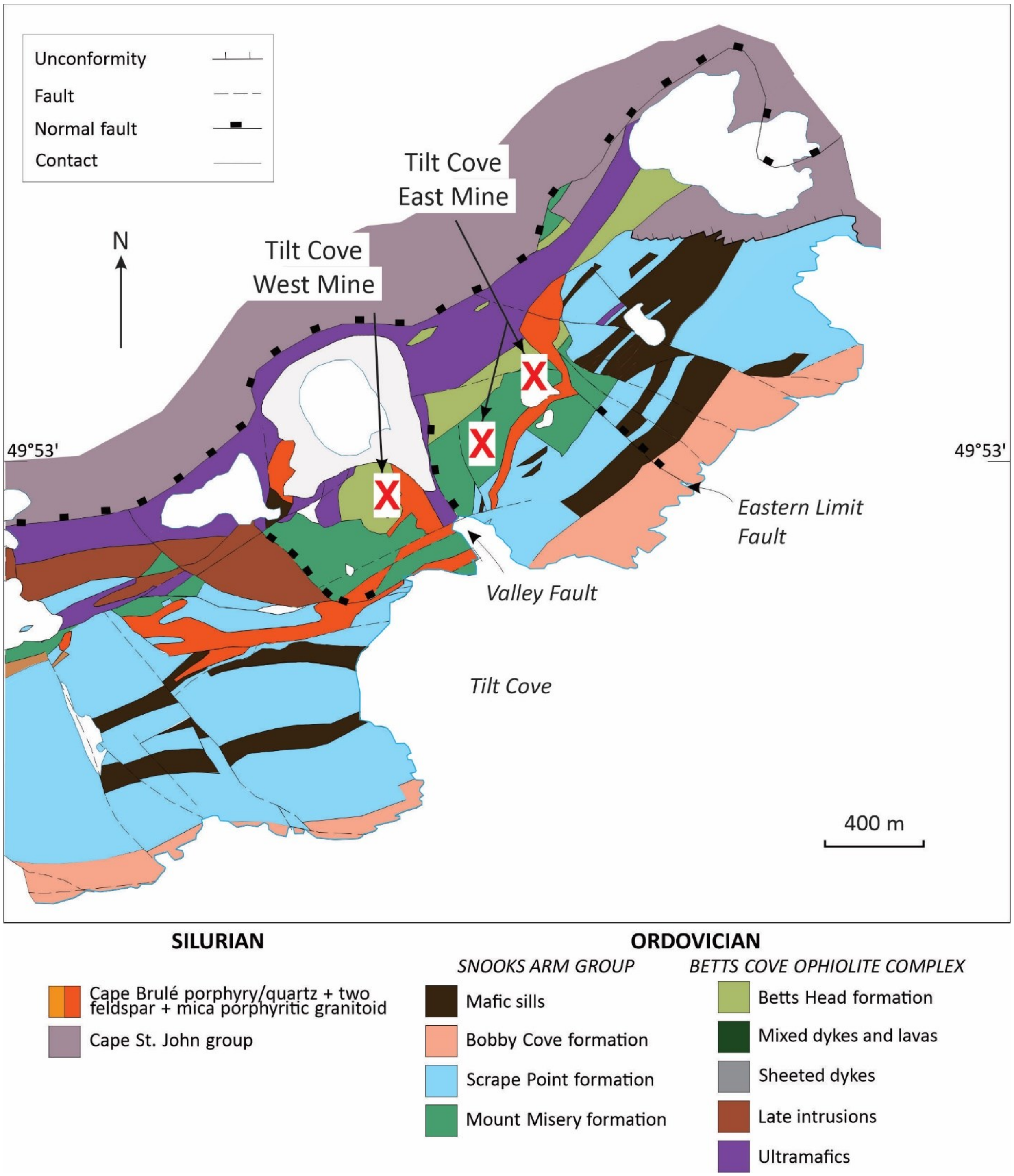

Figure 1.9. Geology of the Tilt Cove deposit (from Bédard et al., 2000 and Sangster et al., 2007).

Chapter 2

Using Machine Learning to Classify Multi-Element Assay Data in the Betts Cove and Tilt Cove Volcanogenic Massive Sulfide (VMS) Deposits and Insights into VMS Forming Processes

2.1. ABSTRACT

Unsupervised and supervised machine learning methods were utilized to evaluate multi-element assay datasets and evaluate inter-element relationships of assay data from the Betts Cove and Tilt Cove volcanogenic massive sulfide (VMS) deposits, Newfoundland Appalachians.

Principal component analysis and K-means clustering illustrate that there are specific metal associations in the Betts Cove and Tilt Cove deposits, including: Zn, Cd, and Au, Pb, S, and Ag, and Cu and Se in Betts Cove; and Zn, Cd, Au, and Ag, and Cu, S, and Pb, in Tilt Cove. These results reflect the chemistry of host rocks, and Zn-(sphalerite)-rich and Cu-(chalcopyrite)-rich sulfide mineralization. Supervised machine learning methods, including logistic regression, neural networks, support vector machine (SVM), and K-nearest neighbour, were used to test classification of the various clusters. Model success rates were > 99% for both deposits and exceptional in classifying Zn-rich and Cu-rich mineralization in Betts Cove and Tilt Cove deposits, and at predicting lithologies within the Tilt Cove deposit.

The metal associations above reflect mineralization-related processes. The Zn-Cd-Au association reflects a mineralization assemblage dominated by sphalerite and with Zn-Cd-Au that likely precipitated from a low temperature (< 300ºC), near neutral pH, and reducing hydrothermal fluid. The Cu-Se association reflects a mineralization assemblage associated with chalcopyrite that likely precipitated from high temperature (> 300ºC), acidic, and reduced fluids. The presence of Se in the Cu-Se assemblages also suggests the potential for a magmatic-hydrothermal component to the metals within the deposits. Three dimensional models of the assay data from Betts Cove and Tilt Cove show typical VMS zoning of a Cu-rich inner zone surrounded by a Zn-rich outer zone. This can be explained by the zone refining process whereby the deposits grew through multiple fluids involving early formed low temperature (< 300ºC), Zn-

rich mineralization replaced by higher temperature (< 300ºC), Cu-rich mineralization, typical of VMS deposits and consistent with field observations.

2.2. INTRODUCTION

Machine learning is increasingly being used to interpret geological, geophysical, and geochemical data (Cate et al., 2018). In geochemistry, rock classification was traditionally restricted to 2-4 variables, whereas machine learning algorithms allow us to use far more variables to find patterns and relationships in large geochemical datasets heretofore unrecognizable (Cate et al., 2018; Hood et al., 2018). Machine learning algorithms are subdivided into two types: unsupervised and supervised. Unsupervised machine learning methods recognize correlations between variables and clusters within datasets, whereas supervised machine learning models classify data using variables for samples with prescribed classifier categories (Hood et al., 2018). Supervised and unsupervised machine learning methods are commonly used in tandem. For example, the clusters determined by unsupervised machine learning can be used to define the categories for supervised machine learning classifications (Hood et al., 2018).

This paper presents both unsupervised and supervised machine learning models to cluster and classify multi-element assay data from the Betts Cove and Tilt Cove volcanogenic massive sulfide (VMS) deposits, Newfoundland Appalachians, Canada. The aim of this study was to undertake an exploratory data analysis using unsupervised methods to evaluate the assay data and determine potential data clusters. This will then be paired to utilized supervised machine learning methods to evaluate whether we can automate classifications of new assay data. Finally, results from the supervised and unsupervised machine learning approaches will be used to provide insights into VMS formation processes in the Betts Cove and Tilt Cove deposits. This work has implications for workers studying machine learning methods in ore systems and those interested in the generation of VMS deposits and their metal endowment.

2.3. GEOLOGICAL SETTING

2.3.1. Regional Geology

The Betts Cove and Tilt Cove deposits are located on the Baie Verte Peninsula of the Newfoundland Appalachians. The Newfoundland Appalachians consist of four tectonostratigraphic zones (from west to east): Humber, Dunnage, Gander, and Avalon zones which represent the opening and closure of the Iapetus and Rheic oceans that existed from the Late Precambrian to Late Paleozoic (Williams, 1978; Williams et al., 1988). Both deposits are located in the Notre Dame subzone of the Dunnage Zone, which consists of island arcs, ophiolitic, and back-arc rocks that were accreted to the Humber zone and to one another within the Iapetus Ocean. The Betts Cove ophiolite, which hosts the mineralization, formed during forearc extension during early Ordovician arc initiation in the Humber seaway, and was obducted onto the Humber margin during the Ordovician Taconic orogeny (Williams, 1978; Williams et al., 1988; Bedard et al., 2000; van Staal and Baar, 2012; Figure 2.1).

The 488 Ma ophiolitic rocks of the Betts Cove ophiolite of the Notre Dame subzone host the Betts Cove and Tilt Cove deposits (Dunning and Krogh, 1985; Bédard et al., 2000; Skulski et al., 2010). From bottom to top, these rocks consist of: (1) serpentinite/talc-carbonates; (2) layered ultramafic to mafic cumulate rocks; (3) gabbroic intrusive rocks; (4) sheeted dykes; (5) a dyke to lava transition zone; and (6) pillow lavas of the Betts Head Formation (e.g., Hibbard 1983; Bédard et al., 2000; Skulski et al., 2010). Overlying the ophiolite are the volcanic and sedimentary rocks of the Ordovician Snooks Arm Group cover sequence, which are then overlain by subaerial lavas and sedimentary rocks of the Silurian Cape St. John Group (e.g., Hibbard 1983; Bédard et al., 2000; Skulski et al., 2010).

2.3.2. The Betts Cove and Tilt Cove Deposits

The Betts Cove and Tilt Cove deposits are mafic-(Cyprus)-type VMS deposits and hosted by arc tholeiitic to boninitic rocks that and interpreted to have formed in a supra-subduction zone, forearc setting (Bédard et al., 2000). The Betts Cove deposit is located between the contact of the sheeted dyke unit and the overlying boninitic pillow lavas of the Betts Head Formation, whereas the Tilt Cove deposit is located within the boninitic pillow lavas of the Betts Head Formation and is overlain by island arc tholeiitic pillow lavas of the Mount Misery Formation of the Snooks Arm Group (Bédard et al., 2000; Sangster et al., 2007).

The immediate hosts to Betts Cove deposit mineralization are highly sheared and faulted mafic rocks that are pervasively chlorite altered. The mineralization is mostly stockwork in style and occurs as stringers and disseminations, of dominantly pyrite, chalcopyrite, sphalerite, pyrrhotite, and rare galena, and contains high Cu, Zn, Au, and low Pb concentrations (Saunders, 1985; Strong and Saunders, 1988; Bédard et al., 2000; Sangster et al., 2007). Historical reports note that the Betts Cove deposit was "crescent" or "basin" in shape and previously produced > 130 000 tons of Cu ore with grades up to 10% Cu (Saunders, 1985; Strong and Saunders, 1988; Bédard et al., 2000); however, no modern NI-43-101 compliant resources have been estimated for the deposit.

The Tilt Cove mineralization is hosted by massive and pillowed lavas and basalt breccia. The mineralization occurs in several zones and consists of chalcopyrite, pyrite, pyrrhotite, and magnetite and has high Cu with lesser Au, Ni, and Co and very low Pb concentrations. The West zone of the deposit consists of a stockwork of sulfide stringers and disseminations, whereas the East or Main zone is mostly stockwork mineralization with small lenses of massive sulfides (Strong and Saunders, 1988; Bédard et al., 2000; Sangster et al., 2007). The Tilt Cove deposit has not been sufficiently modeled due to poor surface exposure and minimal access to underground workings. The attempts made, however, suggest that the mineralized zones are lens shaped where the West zone is mostly stockwork and the East zone is more massive (Bédard et al., 2000; Sangster et al., 2007). The deposit has a historic resource data of 8.16 Mt grading 6.50% Cu (Galley et al., 2007; Piercey et al., 2023).

2.4. METHODS

2.4.1. Data Collection and Integration

Twenty diamond drill cores from the Betts Cove (n = 10, totaling 1672.5 m) and Tilt Cove (n = 10, totaling 1641 m) deposits were logged in 2022 by the author and stratigraphic sections/graphic logs were constructed to document lithology, alteration, sulfide mineralogy, and mineralization styles in each hole.

Geological data collected from drill core logging have been integrated with the assay database for both the Betts Cove (n = 1065) and Tilt Cove deposits (n = 342). Drill core samples were collected during drilling in 2021 with standard sample lengths of 0.5 to 1.0 m. Given that sampling was focused on mineralization there is an inherent bias towards mineralized samples in the database; however, shoulder samples around assay intervals provide some insight into the chemistry of the less mineralized host rocks. All samples were analyzed at Eastern Analytical Limited, Springdale, Newfoundland, and had initial crushing and pulverization prior to subsequent analysis. All samples underwent four acid digestion and subsequent analysis of solutions by inductively coupled plasma mass spectrometry (ICP-MS) for Cu, Al, Cr, Co, Mo, Mg, Mn, Ni, Sn, Ti, W, U, V, Zn, Sb, As, Ba, Be, Bi, Cd, Ca, Fe, La, Li, P, K, Na, Sr, Zr, Ag, Ce, In, Hg, Pb, S, Se, Sc, Y. Au determination was undertaken using a fire assay pre-preparation, acid dissolution, and subsequent analysis by ICP-MS. A powdered certified gold standard and a natural granite blank were inserted every 25 samples for monitoring quality assurance/quality control (QA/QC) of the assay results from the laboratory. Reference material data can be found in Appendix E. Several elements, including, Be, Bi, Ce, In, La, Li, Hg, Mo, P, Sc, Sn, U, W, and Y, were removed from the dataset because they had very little data above detection limit, and they are not geologically significant in this context (e.g., no Mo, Sn, U, or W minerals have been observed). In total, 25 elements were included in the database, integrated with field data, and used for unsupervised and supervised machine learning methods (Table 2.1).

2.4.2. Assay Models

Three dimensional models of the assay results from the Betts Cove and Tilt Cove deposits were developed using the Leapfrog Geo 2022.1.1. software. Data required to build these models included the drill hole data including collar locations, downhole surveys, assay data, and multi-element data from each hole that was drilled in 2021, as well as historic drill holes. In total, 30 drill holes from Betts Cove and 42 drill holes from Tilt Cove were used to build these models. Once the data was imported into the Leapfrog software, Zn-, Cu-, and Au-rich zones of the mineralization were manually chosen to build a combined model of the assay results. There are limitations when using few drill holes to construct this deposit model; however, these holes are considered representative as they contain all major stratigraphic units and known mineralization types for these deposits, and the resulting models correspond well with historic reports on the deposit morphologies in the Betts Cove and Tilt Cove deposits (e.g., Saunders, 1985; Bédard et al., 2000; Sangster et al., 2007).

2.4.3. Unsupervised Machine Learning

Unsupervised machine learning methods utilized included principal component analysis (PCA) and K-means clustering with all data pre-treatment and subsequent evaluation undertaken using the IMDEX ioGAS software. Prior to PCA/K-means clustering, the data were pretreated and transformed using a centered log-ratio (CLR) transformation. The CLR transformation treats all components symmetrically by dividing each element in the sample by the geometric mean of all the elemental values and then takes the logarithm of the latter (Filzmoser et al., 2009; Jansson et al., 2021). Centre log ratio transformation is important to remove the induced correlation caused by the requirement for compositional data to sum to 100% (or part per million or part per billion) - the closure problem (Aitchison, 1982; Filzmoser et al., 2009). Moreover, the resulting transformed data is approximately normally distributed, which is a requirement for statistical techniques like PCA and K-means clustering (Figure 2.2; e.g., Davis, 2003).

Principal component analysis is a multivariate statistical method that groups multivariate data (i.e., the elements) into fewer components called principal components (PC) (Filzmoser et al., 2009; Jansson et al., 2021). Scree plots were used to assess the variability in the data from both deposits (Figure 2.3). The plots shows that eight PCs for Betts Cove and seven PCs for Tilt Cove can account for the majority of the variability in the data as they have eigenvalues above 1; however, for both deposits only four PCs are truly significant and account for 60.87% and 66.16% cumulative percentage of variance for Betts Cove and Tilt Cove, respectively, as both plots flatten out significantly after PC4, and subsequent PCs explain less and less of the variability in the data.

Following PCA, which focuses on clustering elements that have correlations, K-means clustering was used to cluster samples that have similar compositions in a way that minimizes the variation within them (Jansson et al., 2021). The CLR transformed data was also used for K-means clustering. Scree plots were used to determine the number of clusters for the K-means clustering analysis (Figure 2.4). These plots show the sum of squares and delta values versus the number of clusters (K). The sum of squares is the average distance of points within a cluster to the centre of the cluster, and the delta value is the difference between the sum of squares with each increment in K (Jansson et al., 2021). The number of clusters are chosen so that additional increments in K lead to smaller decreases in the sum of squares and delta values, in this case, the plot for Betts Cove significantly flattens out after K = 4 so 4 clusters were chosen for Betts Cove. The plot for Tilt Cove significantly flattens out after K = 5 so 5 clusters were chosen for Tilt Cove.

2.4.4. Supervised Machine Learning

Supervised machine learning was undertaken using the clusters determined from unsupervised machine learning methods as the categorical values and tested using random forest, support vector machine (SVM), naïve Bayes, neural networks, logistic regression, K-nearest neighbour, and AdaBoost methods using the freeware Orange machine learning software toolkit that provides a graphical user interface for the Python-based ScikitLearn machine learning platform (Hood et al., 2018). Each of the supervised machine learning methods was evaluated using stratified random sampling, where 80% of the data was used to train the computer and the remaining 20% of the data was used to test the models. The CLR transformed data of the same 25 elements used in the unsupervised machine learning methods were used and the target (categorical) variables were the clusters obtained from PCA and K-means cluster analyses.

Random forest is a supervised machine learning method that uses numerous decision trees to classify variables for a more robust classification. When a random forest algorithm receives an input, it builds several decision trees and averages the results (e.g., Rodriguez-Galiano et al., 2015; Cate et al., 2018). Support vector machine performs classification by dividing classes using a multi-dimensional surface called the hyperplane. The hyperplane with the largest distance between the classes is chosen (e.g., Rodriguez-Galiano et al., 2015; Cate et al., 2018; Ordóñez-Calderón and Gelcich, 2018). Naïve Bayes uses Bayes theorem, which describes the probability of an event occurring, or in this case, the probability of the classifier correctly classifying data in a target group (Cate et al., 2018):

$$P (A \mid B) = (P (B \mid A) P (A)) / (P (B))$$

(Equation 2.1),

where P (A) and P (B) are the probability of A and B to occur, respectively, P (A | B) is the probability of A to occur if B is true, and P (B | A) is the probability of B to occur if A is true (Cate et al., 2018). This algorithm relies on the assumption of independence of and a normal distribution between the variables (Cate et al., 2018). Neural networks attempt to mirror how neurons in a brain process information. It interconnects information that flows unidirectionally from input to output through neurons that are connected by links (Rodriguez-Galiano et al., 2015). Logistic regression algorithms classify data by mathematically modelling the probability of something occurring between 0 (will not occur) and 1 (will occur). The logistic regression algorithm does not rely on the independence and normal distribution between variables, unlike the naïve Bayes method (Harris and Pan, 1999; Carranza and Hale, 2003; Porwal et al., 2010). K-nearest neighbour classifies data by using a selection of training samples (K) closest to the sample that is to be classified (Cate et al., 2018). The AdaBoost algorithm creates many, so called “weak”, classifiers to classify data. Data that remains unclassified gets “boosted”, in that the weight of the data is increased, and a second classifier is built. Any remaining unclassified data gets boosted once again, and this procedure will repeat and repeat, and typically 500 to 1000 classifiers are built (Freund and Schapire, 1997; Zhu et al., 2009; Lin et al., 2021). The details of the parameterization of the machine learning algorithms can be found in Table 2.2.

2.5. RESULTS

2.5.1. Betts Cove Deposit

2.5.1.1. Geology and Mineralization

The Betts Cove deposit host rocks are dominantly mafic pillowed flows with localized breccia with lesser gabbroic and mafic dykes and discontinuous mafic tuffs, (Figure 2.5A). In general, the lowermost stratigraphic unit are gabbroic dykes, which are overlain by the sheeted dyke series, and the uppermost unit is the pillowed flows (Figure 2.6A). This is consistent with the stratigraphy of the Betts Cove ophiolite in the area (e.g., Hibbard, 1983; Bédard et al., 2000; Skulski et al., 2010).

The mineralization is hosted almost exclusively within the mafic pillowed flows with less in the intrusive units. Sulfide mineralization contains predominantly chalcopyrite, pyrite, pyrrhotite, and sphalerite as stringer-type mineralization in varying amounts (Figure 2.7). Assay data from 1065 core samples from Betts Cove has Au grades up to 13.10 g/t (median = 0.01 ppm), Cu grades up to 3.98 wt% (median = 316 ppm), and Zn grades up to 2.46 wt% (median = 128 ppm). The 3D assay model of the Betts Cove deposit shows that mineralization is folded similar to the stratigraphy and has a Cu-rich inner zone surrounded by a Zn-rich +/- Au-rich outer zone (Figure 2.8A). The Au at Betts Cove is irregularly distributed; this is likely due to the gold nugget effect (e.g., Stanley, 2006).

2.5.1.2. Unsupervised Machine Learning

The results from PCA and K-means clustering are shown in Figure 2.9. Vectors distal from the origin within these plots are elements that have higher correlations and weightings, whereas those closer to the origin are less correlated, whereas colours reflect the K-means clusters. In PC1-PC2 space, key element correlations, include: (1) Zn, Cd, and Au, which have positive loadings on PC1 and PC2; (2) Pb, S, and Ag, which have positive loadings on PC1 and negative loadings on PC2; (3) Cu (+/- Se), which have positive loadings on PC1 and negative loadings on PC2; (4) Ca, Na, Sr, Ba, and K, which have negative loadings on PC1 and positive loadings on PC2; and (5) Al, V, Mg, Ni, Mn, Co, Fe, and Cr with negative loadings on both PC1 and PC2 (Figure 2.9A). PC2 and PC3 space display a new element correlation of Cr, Ni, Mg, and Mn, which have negative loadings on PC2 and positive loadings on PC3 (Figure 2.9B). Plots including PC4 do not provide any new elemental groupings not previously noted. The four element groupings above are interpreted to reflect: (1) Zn- (sphalerite) and Au-bearing mineralization, Pb- and Ag-bearing mineralization, and Cu-rich (chalcopyrite) mineralization; (2) carbonate, sericite, and albite alteration of host rocks (Ca, Na, Sr, Ba, and K); (3) non-mineralized silicate host rocks (Al, V, Mg, Ni, Mn, Co, Fe, and Cr); and (4) boninitic pillow lavas of the Betts Head Formation (Cr, Ni, Mg, and Mn).

These plots also contain the clusters from K-means clustering. Clusters 1 and 4 are interpreted to reflect sulfide mineralization, including Cu-Pb-Ag-rich samples and Zn-Au-rich samples, respectively. Samples in cluster 3 are interpreted to reflect silicate host rocks, including boninitic pillow lavas and altered rocks (i.e., samples that are not mineralized). Samples belonging to cluster 2 are hybrid and contain elements of all other clusters (e.g., weakly mineralized and altered host rocks).

2.5.1.3. Supervised Machine Learning

Evaluations of the supervised machine learning models of Betts Cove are presented in Table 2.3. Area under the curve (AUC) is a measure of the area under the receiver-operator curve (ROC), CA is the classification accuracy, F1 is the measure of accuracy, which is the ratio of correctly classified samples to all samples, precision refers to how close each measurement is to one other, and recall is the true positive rate. For every model, the closer to 1 (where 1 is perfect model performance), the better the various measures of the models are (Zaknich, 2003; Brown et al., 2003; Cate et al., 2018; Lawley et al., 2021). Results for all models have AUC, CA, F1, precision, and recall values close to 1, and therefore perform well. AdaBoost and naïve Bayes algorithms perform the worst, whereas logistic regression, neural networks, SVM, and K-nearest neighbour algorithms perform best.

Confusion matrices for the best performing Betts Cove models are show in Figure 2.10. Confusion matrices are used to evaluate how accurate a machine learning model is at classifying data relative to the user-defined classifier label (Zaknich, 2003; Brown et al., 2003; Lawley et al., 2021). All clusters are well classified with cluster predictions > 90%, with cluster 1 the best classified, cluster 2 the worst classified, and others in between cluster 1 and 2. ROC for the best performing Betts Cove models are shown in Figure 2.11. Receiver-operating characteristics curves plot the true positivity rate of classification versus the false positivity rate, where the best models should have a high true positivity rate and a low false positivity rate (i.e., area under the curve is close to 1) (Zaknich, 2003; Brown et al., 2003; Lawley et al., 2021). All clusters are well classified and have areas close to 1, with cluster 1 the best classified, cluster 2 the worst classified, and others in between cluster 1 and 2.

2.5.2. Tilt Cove Deposit

2.5.2.1. Geology and Mineralization

Tilt Cove contains predominantly talc-carbonate rocks, massive and pillowed mafic flows with lesser breccia, pyroxenite, serpentinite, and sedimentary rocks of the Betts Cove Complex and subaerial lavas of the Cape St. John Group (Figure 2.5B). Most of the drill holes intersected Cape St. John Group rocks, followed by massive and/or pillowed flows, and then by ultramafic rocks (Figure 2.6B). This is consistent with the stratigraphy of the Betts Cove ophiolite in the area (e.g., Hibbard 1983; Bédard et al., 2000; Skulski et al., 2010). The stratigraphy is locally folded and imbricated by thrust faults (Figure 2.6B).

The mineralization is hosted in rocks of the Betts Cove Complex, including talc-carbonate rocks, massive and pillowed mafic flows and volcaniclastic units. Sulfide mineralization consists of pyrite, chalcopyrite, pyrrhotite, and lesser sphalerite; magnetite is also present. The main style of mineralization is stringer-type with localized zones of semi-massive to massive sulfides and disseminations (Figure 2.7). Assay data from 342 core samples from Tilt Cove has Au grades up to 2.68 ppm (median = 0.005 ppm), Cu grades up to 7.15 wt% (median = 122 ppm), and Zn grades up to 1.61 wt% (median = 88 ppm). The 3D assay model of the Tilt Cove deposit shows that mineralization occurs as a thin lens with a Cu-rich inner zone and a Zn-rich +/- Au-rich outer zone (Figure 2.8B). The Au at Tilt Cove is cross-cutting the Zn-rich mineralization, which may suggest it was remobilized along faults or fractures.

2.5.2.2. Unsupervised Machine Learning

The results from PCA and K-means clustering are shown in Figure 2.12. The key element correlations, include: (1) Zn, Cd, Au, and Ag, which have positive loadings on PC1 and PC2; (2) Cu, S, and Pb, which have positive loadings on PC1 and PC2; (3) As, Fe, Co, Sb, Cr, Ni, Mg, Se, and Mn, which have positive loadings on PC1 and negative loadings on PC2; (4) Ca and Sr, which have negative loadings on PC1 and PC2; (5) Na, K, Al, Ba, and V, which have negative loadings on PC1 and PC2; and (6) Zr and Ti, which have negative loadings on PC1 and positive loadings on PC2. Plots including PC3 and PC4 space do not reveal any new key element suites or correlations not already identified in PC1-PC2 space. These different element groupings are interpreted to reflect: (1) Zn- (sphalerite) and Au-Ag-bearing mineralization and Cu- (chalcopyrite) and Pb-bearing mineralization; (2) non-mineralized silicate host rocks (As, Fe, Co, Sb, Cr, Ni, Mg, Se, and Mn); (3) carbonate, sericite, and albite alteration of host rocks (Ca, Sr Na, K, Al, Ba, and V); and (4) zircon-bearing rocks of the Cape St. John Group (Zr and Ti).

K-means clustering of the above data generally reflect lithological associations. Samples in cluster 1 reflect alteration as well as zircon-rich sedimentary and volcanic rocks of the Cape St. John Group. Clusters 2 and 4 reflect Cu-Pb-rich samples and Zn-Au-Ag-rich samples, respectively. Cluster 5 samples reflect ultramafic and talc-carbonate-bearing host rocks. Samples belonging to cluster 3 are hybrid and contain elements of all other clusters (e.g., weakly mineralized and altered host rocks).

2.5.2.3. Supervised Machine Learning

Evaluations of the supervised machine learning models of Tilt Cove are presented in Table 2.4. Recall that for every model, the closer to 1 (where 1 is perfect model performance), the better the various measures of the models are (Zaknich, 2003; Brown et al., 2003; Cate et al., 2018; Lawley et al., 2021). Results for all models have AUC, CA, F1, precision, and recall values close to 1, and therefore perform well. AdaBoost and naïve Bayes algorithms perform the worst, whereas logistic regression, neural networks, K-nearest neighbour, and SVM algorithms perform the best.

Confusion matrices for the best performing Tilt Cove models are shown in Figure 2.13. All clusters are well classified with cluster predictions > 83%, with cluster 1 the best classified, cluster 4 the worst classified, and clusters 2, 3, and 5 in between clusters 1 and 4. Receiver-operating characteristics curves for the best performing Tilt Cove models are shown in Figure 2.14. All clusters are well classified and have areas close to 1, with cluster 1 the best classified, cluster 4 the worst classified, and clusters 2, 3, and 5 in between clusters 1 and 4.

2.6. DISCUSSION

Integration of geological and geochemical data is important for efficient and effective mineral exploration. Utilization of machine learning methods can enhance this task and potentially automate parts of data evaluation. The results of this paper demonstrate that unsupervised and supervised clustering and classification models of data from the Betts Cove and Tilt Cove provide a rapid and reproducible approach to processing geochemical data and can aid geologic interpretations, particularly the discrimination of different host rock lithologies and metal associations and zonation within mineral deposits. The supervised machine learning algorithms, including logistic regression, neural networks, SVM, and K-nearest neighbour, were exceptional in classifying assay data in the Betts Cove and Tilt Cove deposits (Tables 2.2 and 2.3; Figures 2.10, 2.11, 2.13, and 2.14). These results demonstrate that future collected assay data could be classified, and mineralization styles, lithology, and alteration could potentially be automatically determined using supervised machine learning methods.

The unsupervised machine learning methods (PCA and K-means clustering) also illustrate that correlations and clusters in assay data have geological meaning and can be used to provide insights into deposit lithologies and genesis. Both principal component analysis and K-means cluster analysis identify elemental differences related to lithology and mineralization style. In the case of mineralization, there are Cu- and Zn-rich clusters of elements, reflecting chalcopyrite- and sphalerite-rich mineralization, respectively (Figures 2.9 and 2.12) and these are also observed spatially (Figures 2.8), where Cu-rich zones (e.g., cluster 1 in Betts Cove and cluster 2 in Tilt Cove) are surrounded by Zn-rich zones (e.g., cluster 4 from Betts Cove and Tilt Cove), typical for VMS deposits that have experienced zone refining (e.g., Eldridge et al., 1983; Ohmoto et al., 1983; Lydon, 1988; Ohmoto, 1996; Franklin et al., 2005).

VMS deposits often have protracted histories with various fluid pulses having variable temperature and composition. This variability in temperature and composition of the fluids influences the metal abundance and type in the fluids, which can result in metal zoning variations. These metal zoning patterns in many VMS deposits that involve an inner Cu-rich zone and an outer Zn-Pb-rich zone are interpreted to form as a consequence of zone refining, where earlier formed, low temperature ($T < 300^{o}C$) Zn-Pb-(Ba) rich assemblages are replaced by younger and higher temperature ($T > 300^{o}C$) Cu-rich mineral assemblages (e.g., Eldridge et al., 1983; Ohmoto et al., 1983; Ohmoto, 1996; Franklin et al., 2005). The low temperature ($< 300^{o}C$), Zn-Pb-(Ba)-rich mineral assemblages generally consist of sphalerite, galena, pyrite, and in some cases barite/anhydrite, the latter often preceding sulfide deposition. These minerals are fine grained and interpreted to have formed during rapid precipitation when hot hydrothermal fluids mixed with cold seawater (Eldridge et al., 1983; Ohmoto et al., 1983; Lydon, 1988; Ohmoto, 1996; Franklin et al., 2005). As the fluids evolved and become hotter (> 300ºC), Cu was carried in solution resulting in the dissolution of sphalerite-galena-pyrite-(barite-anhydrite) and subsequent replacement by chalcopyrite. This results in an outward displacement of sphalerite-galena-pyrite towards the edge of the VMS deposit/mound, whereas the core of the deposits becomes increasingly chalcopyrite-(pyrrhotite-pyrite) rich, resulting in the Zn-(Pb-Ba)-rich outer zone and a Cu-rich inner zone in VMS deposits (Eldridge et al., 1983; Ohmoto et al., 1983; Lydon, 1988; Ohmoto, 1996; Franklin et al., 2005). The observed Zn-Cu zoning present in the Betts Cove and Tilt Cove deposits support this hypothesis and imply the metal zoning observed likely occurred due to zone refining processes.

The clusters derived from unsupervised machine learning methods also support the spatial relationships and processes described above while also providing insight into processes that led to the formation of the Betts Cove and Tilt Cove VMS deposits, particularly the Zn-Au association in both deposits and the Cu-Se association at Betts Cove. The deposition of metals from hydrothermal fluids in VMS systems is dependent on temperature, pH, and redox state variations during the evolution of a given deposit (e.g., Huston et al., 1995; Martin et al., 2019). The Zn-Au association in both deposits implies an association of Au with sphalerite and deposition from low temperature (< 300ºC) hydrothermal fluids (e.g., Eldridge et al., 1983; Hannington and Scott, 1989; Huston and Large, 1989). Under these conditions, Au is preferentially transported as a $Au(HS)_2^-$ complex, which is stable at low temperatures (< 300ºC), near neutral pH, and reducing conditions (Huston and Large, 1989; Huston, 2000). Zn-Au associations have been observed in other VMS deposits (e.g., Rosebery; Huston and Large, 1989). In such deposits, it is interpreted that Au precipitation occurs when the $Au(HS)_2^-$ is destabilized due to the decreased activity of reduced sulfur, either from fluid mixing with seawater, co-precipitating sulfide phases, or due to fluid boiling (Huston and Large, 1989; Huston, 2000).

The Cu-Se association in the Betts Cove deposit implies an association of Se with chalcopyrite and deposition from high temperature (> 300ºC) hydrothermal fluids (e.g., Eldridge et al., 1983; Lydon, 1988; Large, 1992; Ohmoto, 1996). Under these conditions, Se may be transported as H_2Se, which is stable at temperatures > 200ºC, acidic, and reducing conditions (Huston et al., 1995; Layton-Matthews et al., 2008). Deposition can occur due to temperature increase, changing redox or pH conditions, and/or co-precipitating sulfide phases (Auclair et al., 1987; Huston et al., 1995; Layton-Matthews et al., 2008; Martin et al., 2019). Auclair et al. (1987), Huston et al. (1995), and Layton-Matthews et al. (2008) determined that Se concentrations are highest in the Cu-rich stringer zones of massive sulfide deposits and demonstrated strong Cu-Se associations (e.g., 10-200 ppm Se for Mount Chambers and Drive River South, 1100 ppm Se avg. at Wolverine, and 200 ppm Se avg. at Kudz Ze Kayah). In comparison, the Betts Cove deposit consists of stringer-type mineralization, has a similar Cu-Se association, and comparable Se concentrations ranging up to 369 ppm.

There are four sources of Se in VMS deposits: (1) seawater; (2) leached Se from sedimentary rocks; (3) leached Se from volcanic rocks; and (4) a direct input of magmatic volatiles (Huston et al., 1995; Layton-Matthews et al., 2008). Huston et al. (1995) and Layton-Matthews et al. (2008) used Se/S ratios to determine the source of Se in VMS deposits. They suggested that a $Se/S \times 10^6$ ratio > 500 indicates a magmatic or volcanic origin, whereas a $Se/S \times 10^6$ ratio < 500 indicates a seawater or sedimentary origin. The $Se/S \times 10^6$ ratios at Betts Cove have a median value of 2392, this may suggest a magmatic and/or volcanic origin of Se.

Furthermore, the presence of precious metals (i.e., Ag and Au) and the Zn-Au association along with the common epithermal element, Se, in these deposits suggests Se (and Zn-Au-Ag) may have been derived from magmatic fluids (e.g., Sillitoe et al., 1996; Hannington et al., 1997; Economou-Eliopoulos et al., 2008; Brueckner et al., 2014). Small pulses of magmatic fluids can introduce substantial amounts of epithermal elements (e.g., Ag, As, Au, Bi, Co, Hg, Sb, Se, and Te), as well as some base metals (e.g., Cu, Pb, and Zn), into a hydrothermal system (Franklin et al., 2005), and this has been observed worldwide including Ladolam, Lihir Island, Papua New Guinea (Simmons, 2008) and the Zacatecas Ag-Pb-Zn-Cu-Au district, Mexico (Wilkinson et al., 2013). While there is Se enrichment at Betts Cove and Tilt Cove, there are not enrichments in other epithermal elements, nor the distinct advanced argillic assemblages common to epithermal deposits (Sillitoe et al., 1996; Huston, 2000; Dube et al., 2007); however, there is still a possibility for a magmatic-hydrothermal contribution of metals to these deposits. In a seawater-dominated hydrothermal system, like VMS deposits, small pulses of magmatic fluids would be potentially in much lower volume compared to seawater-derived hydrothermal fluids and might have been buffered by such fluids, possibly preventing the hybrid fluid from forming these distinct ore mineral and alteration assemblages. Considering this, small, episodic magmatic pulses may have added to the metal budget to the Betts Cove and Tilt Cove deposits, such as the underlying gabbroic magma chambers (e.g., Martin, et al., 2019), but they were not the dominant metal contributor to the mineralization, and the extent of their influence is not well understood and requires further testing.

The results presented herein suggest that unsupervised approaches explain the geochemical correlations and variability in the Tilt Cove and Betts Cove VMS deposits, whereas supervised algorithms correctly classify sample and element clusters at high accuracy. The latter supervised models can be tested via new assay data from the Betts Cove and Tilt Cove deposits to determine how well these models perform with new data and/or they can be used to automate, classify, and predict the clusters and significance of future assay data. Further, the elemental clusters and correlations found in the assay data reflect VMS mineralization processes and the thermochemical evolution of VMS mineralization in the Betts Cove and Tilt Cove deposits and illustrate the potential for a magmatic-hydrothermal input in these deposits. Overall, the results of this work demonstrate that integrated fieldwork, spatial analysis, and assay database evaluation using machine learning methods can provide insights into VMS deposit forming processes and have implications for similar deposits globally.

2.7. CONCLUSIONS

The following conclusions have been made:

1. Assay and ICP data from the Betts Cove and Tilt Cove deposits were evaluated using both supervised and unsupervised machine learning methods. Principal component analysis shows specific metal associations that are related to mineralization, including: Zn, Cd, and Au; Pb, S and Ag; Cu and Se in Betts Cove and Zn, Cd, Au, and Ag; Cu, S, +/- Pb in Tilt Cove; Ni, Mg, Ca, +/- Mn, reflect boninitic host rocks at Betts Cove. K-means clustering successfully discriminates barren samples from sulfide mineralized samples and the delineation of Zn-rich (sphalerite) from Cu-rich (chalcopyrite) mineralization. It also allowed for the separation certain lithologies in the Tilt Cove deposit, including sedimentary and volcanic rocks of the Cape St. John Group, ultramafic rocks, and talc-carbonate-bearing rocks.

2. Logistic regression, neural networks, support vector machine, and K-nearest neighbour models are successful at classifying assay data clusters within the Betts Cove and Tilt Cove deposits.
3. The mineralized zones in the Betts Cove and Tilt Cove deposits have typical 3D VMS zoning patterns with Cu-rich inner zones surrounded by a Zn-rich outer zones that likely formed via zone refining during deposit evolution.
4. In both deposits, Au is associated with Zn-rich mineralization (sphalerite) suggesting Au was precipitated from a low temperature (< 300ºC), near neutral pH, and reduced hydrothermal fluid. Gold under these conditions was transported as a $Au(HS)_2^-$ complex.
5. In Betts Cove, Se is associated with Cu-rich mineralization (chalcopyrite) suggesting it was precipitated from a high temperature (> 300ºC), acidic, and reducing hydrothermal fluid. Se under these conditions is transported as H_2Se. The Cu-Se metal association as well as the presence of precious metals (i.e., Ag and Au) suggests a potential magmatic-hydrothermal contribution to the deposit.
6. Machine learning allowed clustering and automated classification of a large dataset with multiple variables quickly and for a low cost. It provides a mechanism for automatic classification and exploratory data analysis that can provide insights into ore forming processes.

2.8. REFERENCES

Aitchison, J., 1982. The statistical analysis of compositional data. Journal of the Royal Statistical Society, Series B, v. 44, p. 139-177.

Auclair, G., Fouquet, Y., Bohn, M., 1987. Distribution of selenium in high-temperature hydrothermal sulfide deposits at 13 degrees North, East Pacific Rise: The Canadian Mineralogist, v. 25, p. 577-587.

Barrie, C.T., Hannington, M.D., 1999. Classification of volcanic-associated massive sulfide deposits based on host rock composition. Reviews in Economic Geology, v. 8, p. 2-10.

Bédard, J.H., Lauzière, K., Tremblay, A., Douma, S.L., Dec, T., 2000. Betts Cove ophiolite and its cover rocks, Newfoundland. Natural Resources Canada, Geological Survey of Canada Bulletin, 550, p. 1-76.

Brown, W., Gedeon, T., Groves, D., 2003. Use of noise to augment training data: a neural network method of mineral-potential mapping in regions of limited known deposit examples. Natural Resources Research, v. 12, p. 141-152.

Brueckner, S.M., Piercey, S.J., Pilote, J., Layne, G.D., Sylvester, P.J., 2016. Mineralogy and mineral chemistry of the metamorphosed and precious metal-bearing Ming deposit, Canada. Ore Geology Reviews, v. 72, p. 914-939.

Carranza, E.J.M., Hale, M., 2003. Logistic regression for geologically constrained mapping of gold potential, Baguio District, Philippines. Exploration and Mining Geology, v. 10, p. 165-175.

Castonguay, S. van Staal, C.R., Joyce, N., Skulski, T., Hibbard, J., Taconic metamorphism preserved in the Baie Verte Peninsula, Newfoundland Appalachians: geochronological evidence for ophiolite obduction and subduction and exhumation of the leading edge of the Laurentian (Humber) margin during closure of the Taconic Seaway. Geoscience Canada, v. 41, p. 459-482.

Caté, A., Schetselaar, E., Mercier-Langevin, P., Ross, P., 2018. Classification of lithostratigraphic and alteration units from drillhole lithogeochemical data using machine learning: A case study from the Lalor volcanogenic massive sulphide deposit, Snow Lake, Manitoba, Canada. Journal of Geochemical Exploration, v. 188, p. 216-228.

Cook, D.R., Simmons, S.F., 2000. Characteristics and genesis of epithermal gold deposits. SEG Reviews, v. 13, p. 221-244.

Dunning, G.R., Krogh, T.E., 1985. Geochronology of ophiolites of the Newfoundland Appalachians. Canadian Journal of Earth Sciences, v. 22, p. 1659-1670.

Economou-Eliopoulos, M., Eliopoulos, D.G., Chryssoulis, S., 2008. A comparison of high-Au massive sulfide ores hosted in ophiolite complexes of the Balkan Peninsula with modern analogues: genetic significance. Ore Geology Reviews, v. 33, p. 81-100.

Eldridge, C.S., Barton, P.B., Ohmoto, H., 1983. Mineral textures and their bearing on formation of the Kuroko orebodies. Economic Geology, Monograph 5, p. 241-281.

Filzmoser, P., Hron, K., Reimann, C., 2009. Principal component analysis for compositional data with outliers. Environmetrics, v. 20, p. 621-632.

Franklin, J.M., Gibson, H.L., Jonasson, I.R., Galley, A.G., 2005. Volcanogenic massive sulfide deposits. Society of Economic Geologists, 100th Anniversary Volume, p. 523-560.

Freund, Y., Schapire, R.E., 1997. A decision-theoretic generalization of on-line learning and an application to boosting. Journal of Computer and System Sciences, v. 55, p. 119-139.

Galley, A.G., Hannington, M.D., Jonasson, I.R., 2007. Volcanogenic massive sulphide deposits, in Goodfellow, W.D., ed., Mineral Deposits of Canada: A Synthesis of Major Deposit-

Types, District Metallogeny, the Evolution of Geological Provinces, and Exploration Methods: Geological Association of Canada, Mineral Deposits Division, Special Publication No. 5, p. 141-161.

Hannington, M.D., Peter, J.M., Scott, S.D., 1986. Gold in sea-floor polymetallic sulfide deposits. Economic Geology, v. 81, p. 1867-1883.

Hannington, M.D., Poulsen, K.H., Thompson, J.F.H., and Sillitoe, R.H., 1997. Volcanogenic gold in the massive sulfide environment. Reviews in Economic Geology, v. 8, p. 325-356.

Hannington, M.D., Scott, S.D., 1989. Sulfidation equilibria as guides to gold mineralization in volcanogenic massive sulfides: evidence from sulfide mineralogy and the composition of sphalerite. Economic Geology, v. 84, p. 1978-1995.

Harris, D., Pan, G., 1999. Mineral favorability mapping: A comparison of artificial neural networks, logistic regression, and discriminant analysis. Natural Resources Research, v. 8, p. 93-109.

Hedenquist, J.W., Arribas R, A., Gonzalez-Urien, E., 2000. Exploration for epithermal gold deposits. SEG Reviews, v. 13, p. 245-277.

Hibbard, J., 1983. Geology of the Baie Verte Peninsula, Newfoundland. Newfoundland Department of Mines and Energy, Memoir 2, 279 p.

Hood, S.B., Crackness, M.J., Gazley, M.F., 2018. Linking protolith rocks to altered equivalents by combining unsupervised and supervised machine learning. Journal of Geochemical Exploration, v. 186, p. 270-280.

Huston, D.L., 2000. Gold in volcanic-hosted massive sulfide deposits: distribution, genesis, and exploration. Reviews in Economic Geology, v. 13, p. 401-426.

Huston, D.L., Large, R.R., 1989. A chemical model for the concentration of gold in volcanogenic massive sulphide deposits. Ore Geology Reviews, v. 4, p. 171-200.

Huston, D.L., Sie, S.H., Suter, G.F., Cooke, D.R., Both, R,A., 1995. Trace elements in sulfide minerals from Eastern Australian volcanic-hosted massive sulfide deposits: Part I. Proton microprobe analyses of pyrite, chalcopyrite, and sphalerite, and Part II. Selenium levels in pyrite: comparison with $\delta^{34}S$ values and implications for the source of sulfur in volcanogenic hydrothermal systems. Economic Geology, v. 90, p. 1167-1196.

IMDEX, 2022. ioGAS™ 8.0 Help Centre.

Jansson, N.F., Allen, R.L., Skogsmo, G., Tavakoli, S., 2022. Principal component analysis and K-means clustering as tools during exploration for Zn skarn deposits and industrial carbonates, Sala area, Sweden. Journal of Geochemical Exploration, v. 233, 26 p.

Large, R.R., 1992. Australian volcanic-hosted massive sulfide deposits: features, styles, and genetic models. Economic Geology, v. 87, p. 471-510.

Lawley, C.J.M., Tschirhart, V., Smith, J.W., Pehrsson, S.J., Schetselaar, E.M., Schaeffer, A.J., Houlé, M.G., Eglington, B.M., 2021. Prospectivity modelling of Canadian magmatic Ni (±Cu ± Co ± PGE) sulphide mineral systems. Ore Geology Reviews, v. 132, 23 p.

Layton-Matthews, D., Peter, J.M., Scott, S.D., Leybourne, M.I., 2008. Distribution, mineralogy, and geochemistry of selenium in felsic volcanic-hosted massive sulfide deposits of the Finlayson Lake District, Yukon Territory, Canada. Economic Geology, v. 103, p. 61-88.

Lin, N., Chen, Y., Liu, H., Liu, H., 2021. A comparative study of machine learning models with hyperparameter optimization algorithm for mapping mineral prospectivity. Minerals, v. 11, 28 p.

Liu, W., Etschmann, B., Mei, Y., Guan, Q., Testemale, D., Brugger, J., 2020. The role of sulfur in molybdenum transport in hydrothermal fluids: insight from in situ synchrotron XAS experiments and molecular dynamics simulations. Geochimica et Cosmochimica Acta, v. 290, p. 162-179.

Lydon, J.W., 1988. Volcanogenic massive sulphide deposits part 2: genetic models. Geoscience Canada Reprint Series 3, v. 15, p. 155-181.

Maepa, F., Smith, R.S., Tessema, A., 2021. Support vector machine and artificial neural network modelling of orogenic gold prospectivity mapping in the Swayze greenstone belt, Ontario, Canada. Ore Geology Reviews, v. 130, 27 p.

Martin, A.J., Keith, M., McDonald, I., Haase, K.M., McFall, K.A., Klemd, R., MacLeod, C.J., 2019. Trace element systematics and ore-forming processes in mafic VMS deposits: evidence from the Troodos ophiolite, Cyprus. Ore Geology Reviews, v. 106, p. 205-225.

Ohmoto, H., 1996. Formation of volcanogenic massive sulfide deposits: the Kuroko perspective. Ore Geology Reviews, v. 10, p. 135-177.

Ohmoto, H., Mizukami, M., Drummond, S.E., Eldridge, C.S., Pisutha-Arnond, V., Lenagh, T.C., 1983. Chemical processes of Kuroko formation. Economic Geology, Monograph 5, p. 570-604.

Ordóñez-Calderón, J.C., Gelcich, S., 2018. Machine learning strategies for classification and prediction of alteration facies: Examples from the Rosemont Cu-Mo-Ag skarn deposit, SE Tucson Arizona. Journal of Geochemical Exploration, v. 194, p. 167-188.

Piercey, S.J., Hinchey, J.G., Sparkes, G.W., 2023. Volcanogenic massive sulfide (VMS) deposits of the Dunnage Zone of the Newfoundland Appalachians: setting, styles, key advances, and future research. Canadian Journal of Earth Sciences, v. 60, p. 1104-1142.

Pilote, J., Piercey, S.J., 2018. Petrogenesis of the Rambler Rhyolite formation: controls on the Ming VMS deposit and geodynamic implications for the Taconic seaway, Newfoundland Appalachians, Canada. American Journal of Science, v. 318, p. 640-683.

Porwal, A., González-Álvarez, I., Markwitz, V., McCuaig, T.C., Mamuse, A., 2010. Weights-of-evidence and logistic regression modeling of magmatic nickel sulfide prospectivity in the Yilgarn Craton, Western Australia. Ore Geology Reviews, v. 38, p. 184-196.

Rodriguez-Galiano, V., Sanchez-Castillo, M., Chica-Olmo, M., Chica-Rivas, M., 2015. Machine learning predictive models for mineral prospectivity: An evaluation of neural networks, random forest, regression trees and support vector machines. Ore Geology Reviews, v. 71, p. 804-818.

Sangster, A.L., Douma, S.M., Lavigne, J., 2007. Base metal and gold deposits of the Betts Cove complex, Baie Verte Peninsula, Newfoundland, in Goodfellow, W.D., ed., Mineral Deposits of Canada: A Synthesis of Major Deposit-Types, District Metallogeny, the Evolution of Geological Provinces, and Exploration Methods: Geological Association of Canada, Mineral Deposits Division, Special Publication No. 5, p. 703-721.

Saunders, C. M., 1985. Controls of mineralization in the Betts Cove ophiolite. Unpublished M.Sc. thesis, St. John's, Newfoundland, Memorial University of Newfoundland, 200 p.

Sillitoe, R.H., Hannington, M.D., and Thompson, J.F.H., 1996. High sulfidation deposits in the volcanogenic massive sulfide environment. Economic Geology, v. 91, p. 204- 212.

Simmons, S.F., 2008. Precious metals in modern hydrothermal solutions and implications for the formation of epithermal ore deposits. SEG Newsletter, no. 72, p. 8-12.

Skulski, T., Castonguay, S., McNicoll, V., van Staal, C., Kidd, W., Rogers, N., Morris, W., Ugalde, H., Slavinski, H., Spicer, W., Moussallam, Y., Kerr, I., 2010. Tectonostratigraphy of the Baie Verte oceanic tract and its ophiolite cover sequence on the Baie Verte Peninsula. Current research, Newfoundland and Labrador Department of Natural Resources Geological Survey, Report 10-1, p. 315-335.

Stanley, C.R., 2006. On the special application of Thompson–Howarth error analysis to geochemical variables exhibiting a nugget effect. Geochemistry: Exploration, Environment, Analysis, v. 6., p. 357-368.

Strong, D.F., Saunders, C.M., 1988. Geological setting of sulphide mineralization at Tilt Cove, Betts Cove ophiolite, Newfoundland. In Volcanogenic sulfide districts of central Newfoundland, Special Publication, Mineral Deposits Division, Geological Association of Canada, p. 54-62.

Upadhyay, H.D., Strong, D.F., 1973. Geological setting of the Betts Cove copper deposits, Newfoundland: an example of ophiolite sulfide mineralization. Economic Geology, v. 68, p. 161-167.

van Staal, C.R., Barr, S.M., 2012. Lithospheric architecture and tectonic evolution of the Canadian Appalachians and associated Atlantic Margin. Chapter 2 in Tectonic Styles in Canada: the Lithoprobe Perspective, Geological Association of Canada, Special Paper 49, p. 41-95.

Wilkinson, J.J., Simmons, S.F., Stoffell, B., 2013. How metalliferous brines line Mexican epithermal veins with silver. Scientific Reports, v. 3, 2057, p. 1-7.

Williams, H., 1978. Appalachian orogen in Canada. Canadian Journal of Earth Sciences, v. 16, p. 792-807.

Williams, H., Colman-Sadd, S.P., Swinden, H.S., 1988. Tectonic-stratigraphic subdivisions of central Newfoundland. Current Research, Part B, Geological Survey of Canada, Paper 88-1B, p. 91-98.

Zaknich, A., 2003. Neural networks for intelligent signal processing, v. 4, 509 p.

Zhu, J., Zou, H., Rosset, S., Hastie, T., 2009. Multi-class AdaBoost. Statistics and its Interface, v. 2, p. 349-360.

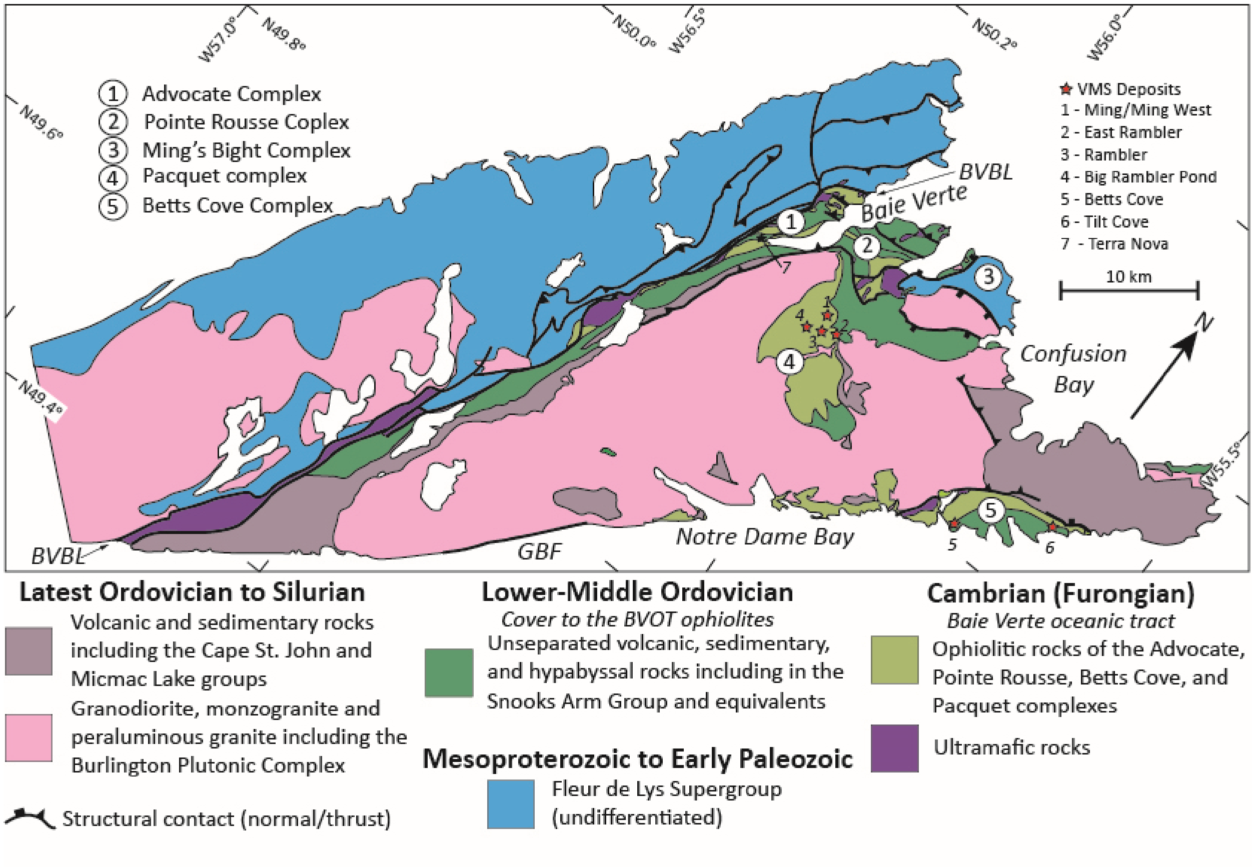

Figure 2.1. Geology of the Baie Verte Peninsula including the locations of the Betts Cove ophiolite, Snooks Arm Group, and Cape St. John Group (from Castonguay, et al., 2014; Pilote and Piercey 2018; Piercey et al., 2023).

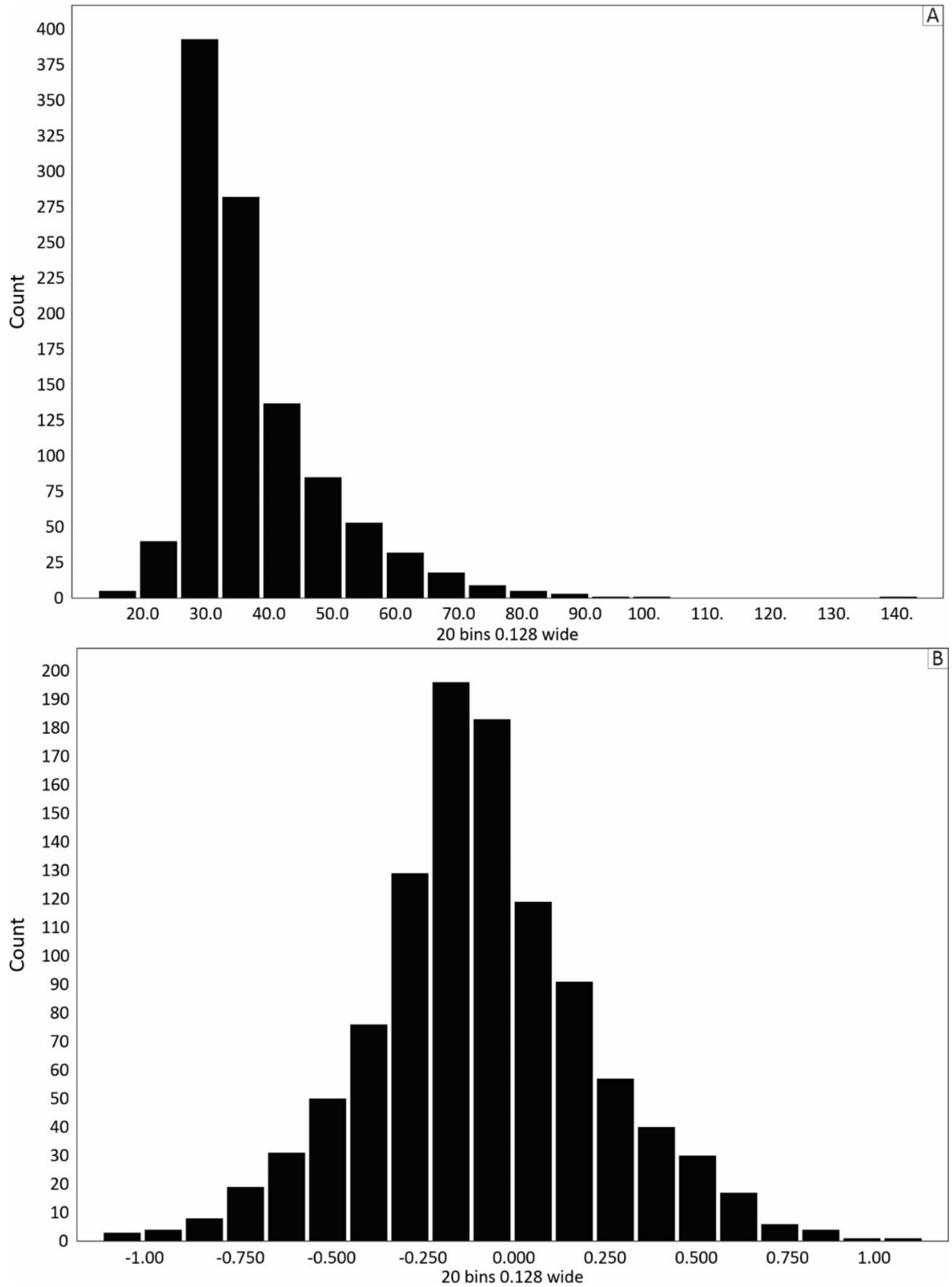

Figure 2.2. Example of the centre log ratio transformation on Co from the Betts Cove deposit showing the difference between non-transformed data (A) and CLR transformed data (B). The CLR transformed data is roughly normally distributed and the results are similar for all other elements that were transformed.

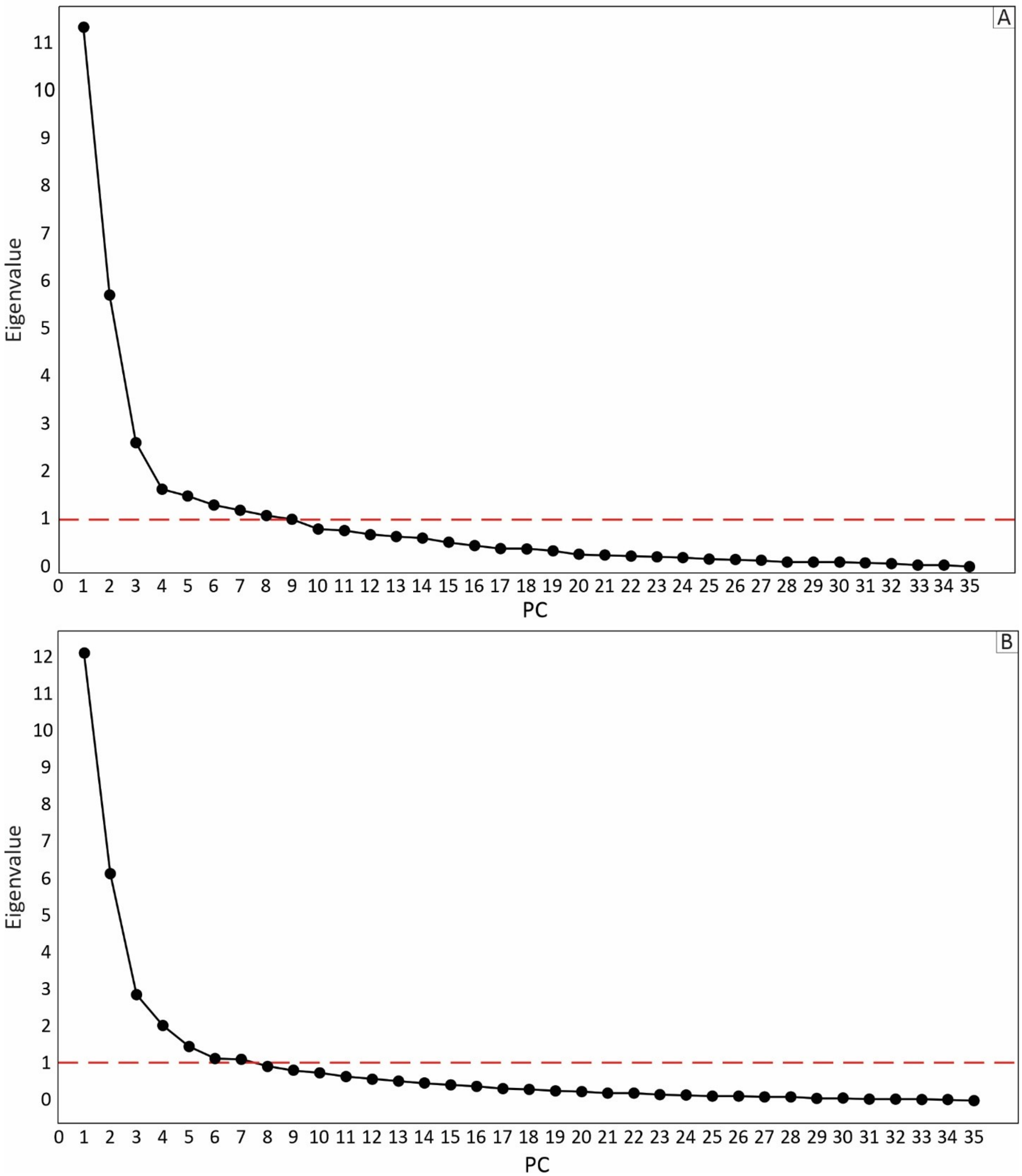

Figure 2.3. Scree plots for Betts Cove (A) and Tilt Cove (B) showing that four PCs are significant for explaining the variance in the data (i.e., the plot flattens out significantly after PC4).

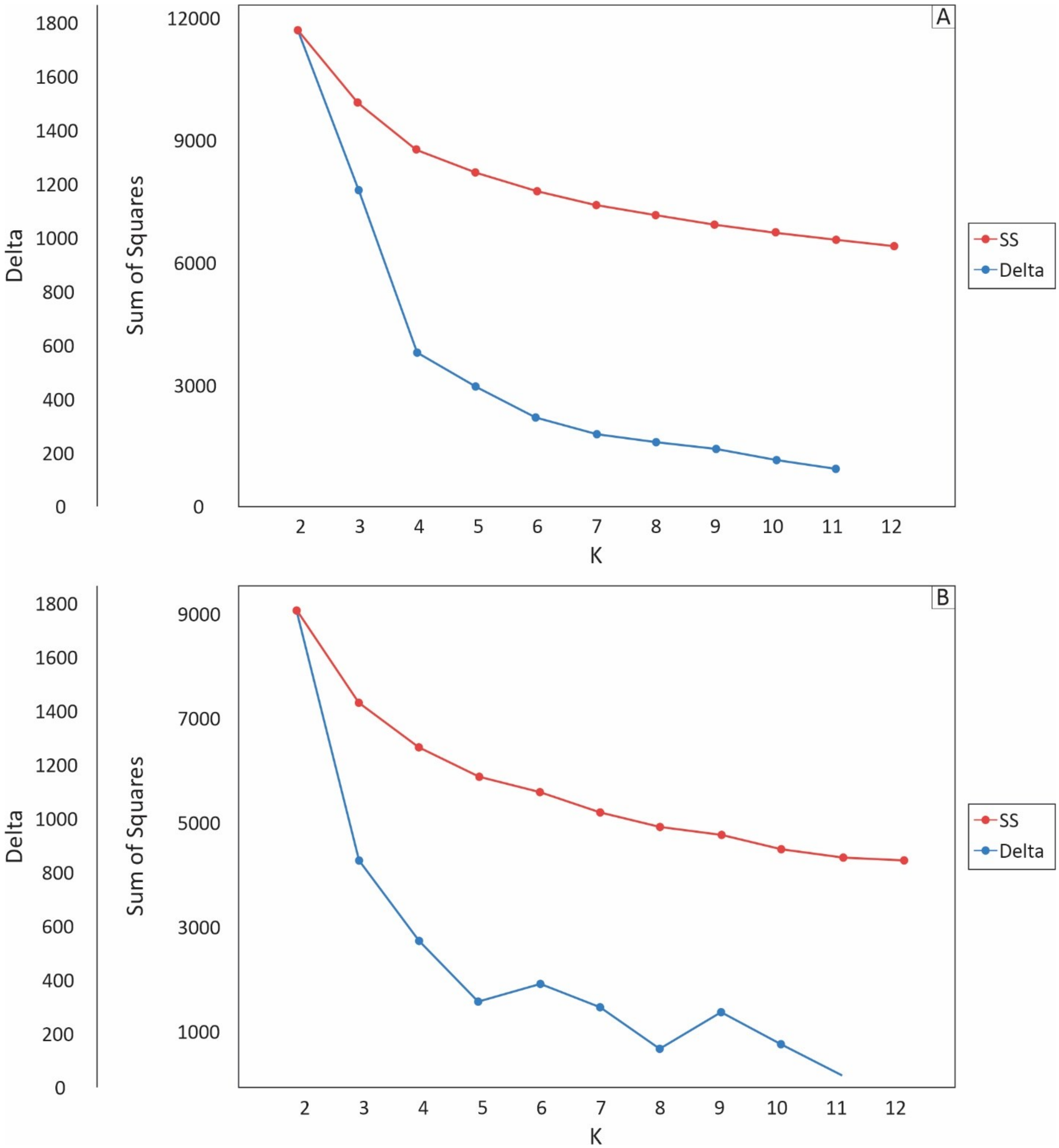

Figure 2.4. Scree plots that were used to pick the number of clusters (K) in the K-means clustering analysis for Betts Cove (A) and Tilt Cove (B).

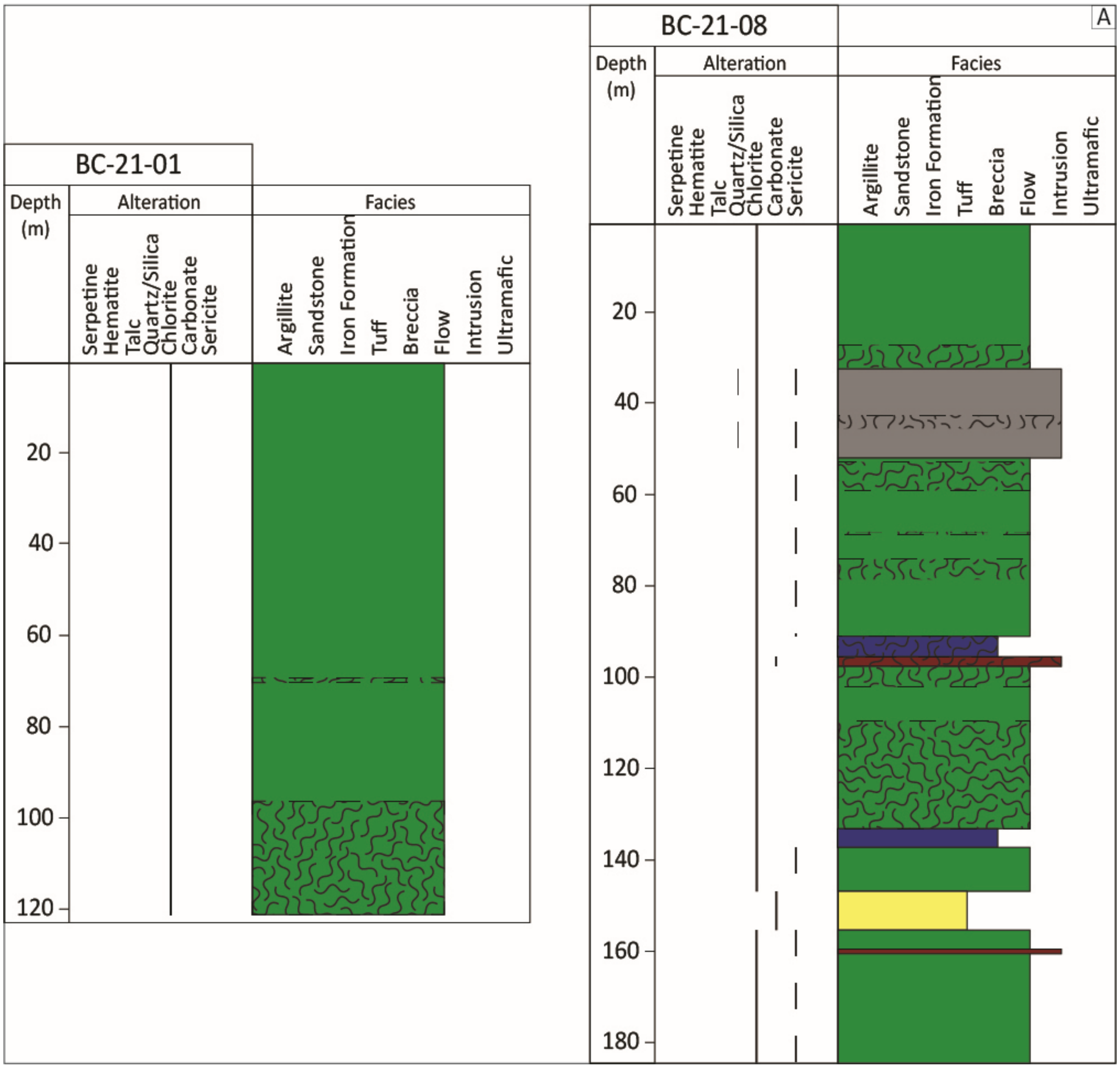
BC-21-01
Depth (m)
Alteration
Serpetine
Hematite
Talc
Quartz/Silica
Chlorite
Carbonate
Sericite
Facies
Argillite
Sandstone
Iron Formation
Tuff
Breccia
Flow
Intrusion
Ultramafic
20
40
60
80
100
120
BC-21-08
A
Depth (m)
Alteration
Serpetine
Hematite
Talc
Quartz/Silica
Chlorite
Carbonate
Sericite
Facies
Argillite
Sandstone
Iron Formation
Tuff
Breccia
Flow
Intrusion
Ultramafic
20
40
60
80
100
120
140
160
180

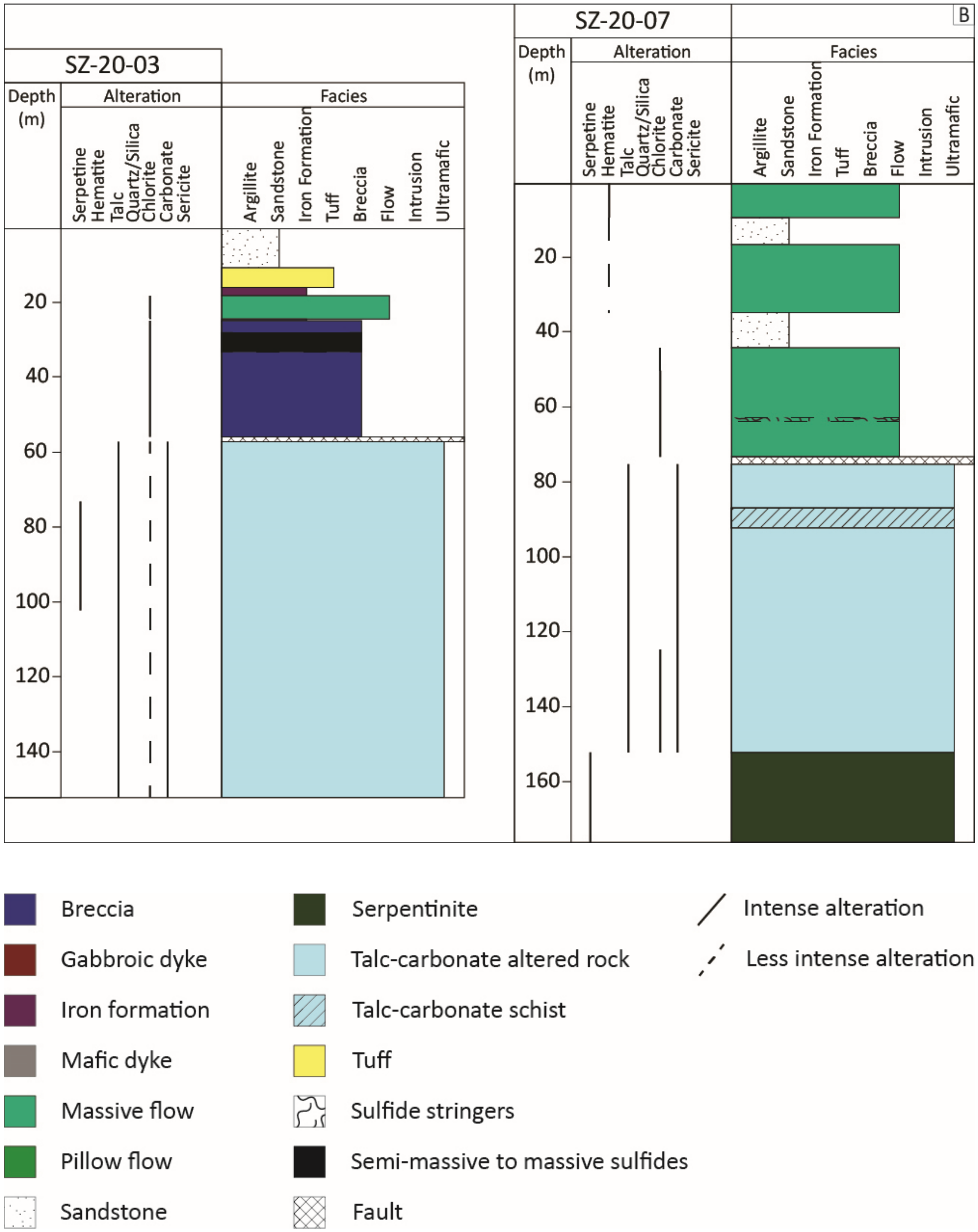

Figure 2.5. Representative graphic logs highlighting the main lithologies, alteration, and mineralization styles from: A) Betts Cove and B) Tilt Cove.

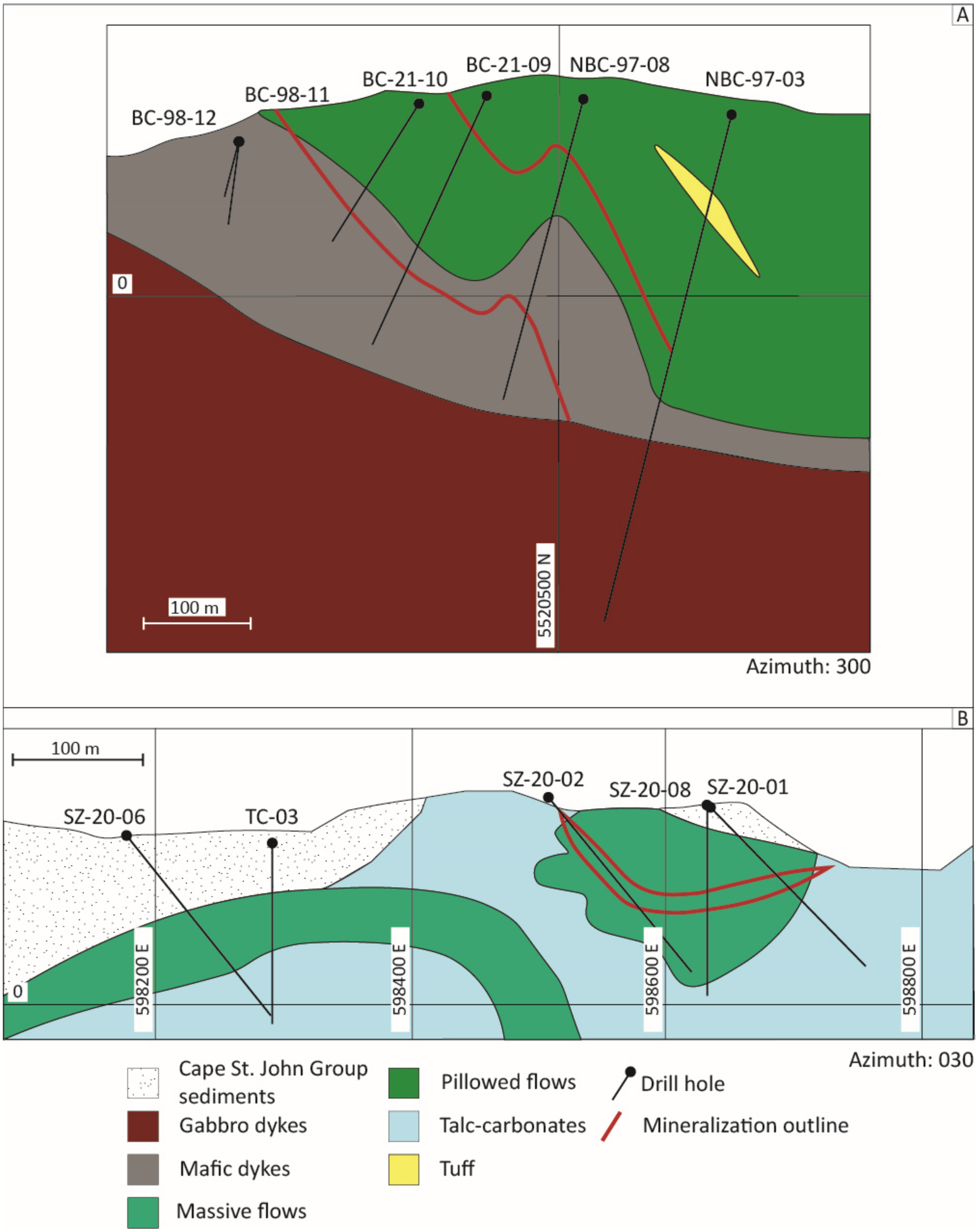

Figure 2.6. Representative cross sections from: A) Betts Cove and B) Tilt Cove.

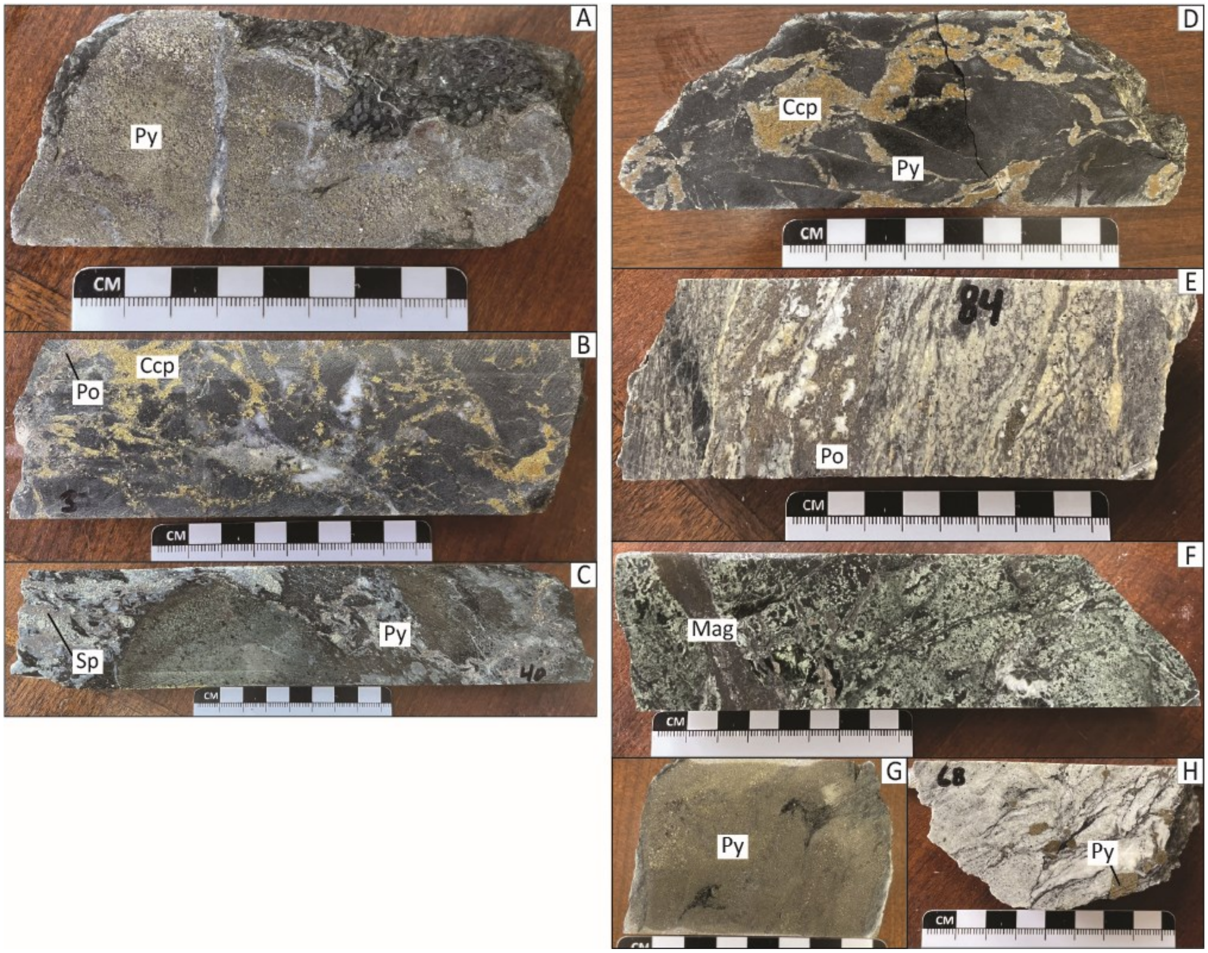

Figure 2.7. Mineralization types at Betts Cove, including: A) localized massive pyrite mineralization hosted in a pillowed flow unit; B) patchy, chalcopyrite-pyrrhotite-dominated stringer mineralization hosted in a pillowed flow unit; and C) replacement-style, sphalerite-pyrite-dominated mineralization surrounding pillows in the pillow flow unit. Mineralization at Tilt Cove, including: D) dominantly chalcopyrite with lesser pyrite stringer mineralization hosted in the pillow flow unit; E) Pyrrhotite dominated stringer mineralization hosted in the talc-carbonate schist unit; F) magnetite dominated stringer mineralization hosted in the talc-carbonate unit with pervasive chlorite alteration; G) localized area of massive pyrite mineralization hosted in a clastic unit; and H) euhedral pyrite disseminations in the talc-carbonate schist unit.

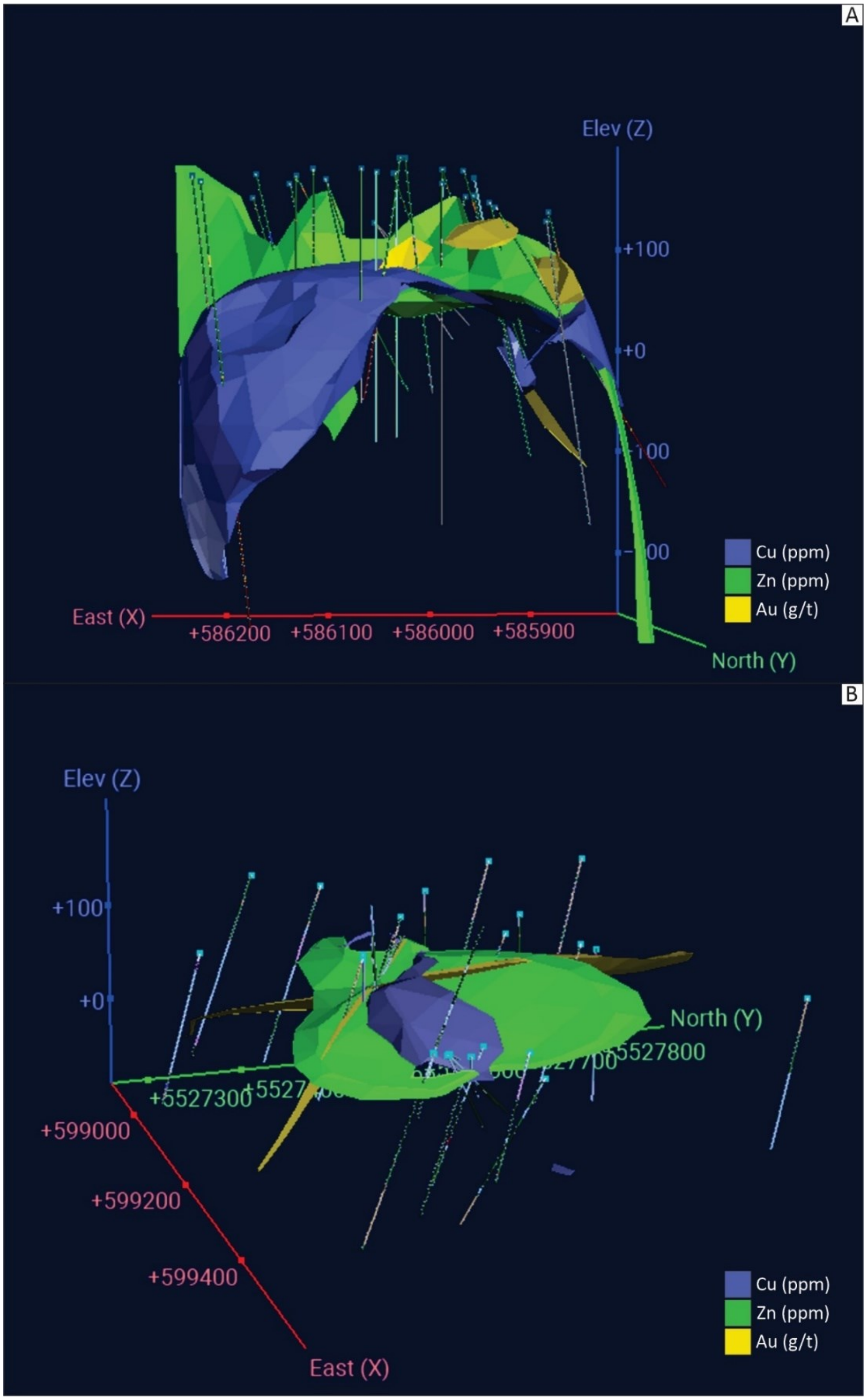

Figure 2.8. 3D models of assay data and distribution of various metals from the A) Betts Cove deposit and B) Tilt Cove deposit.

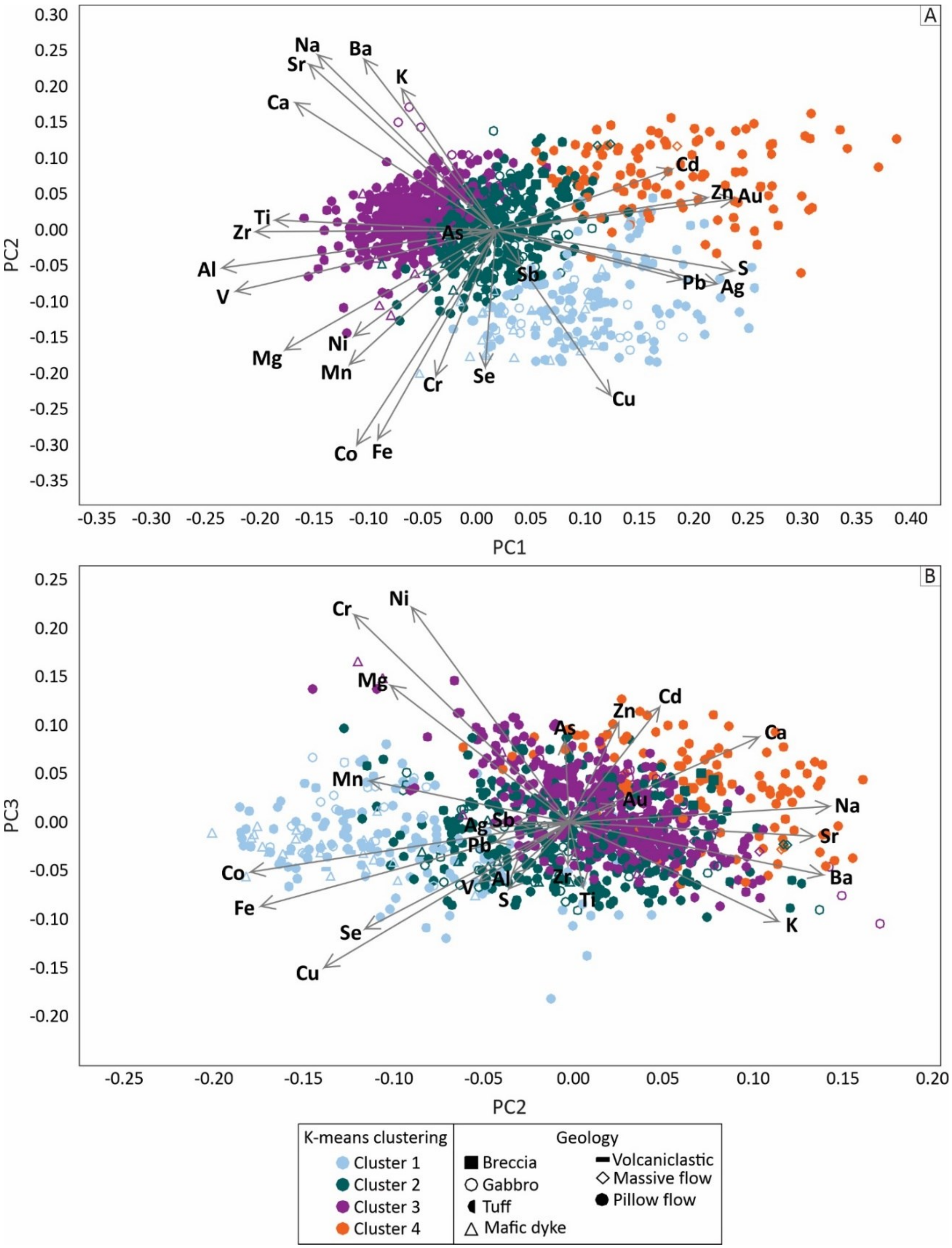

Figure 2.9. Principal component biplot for Betts Cove, showing samples colour coded by K-means clusters in PC1 and PC2 space (A) and PC2 and PC3 space (B).

Predicted

A)

Actual	Cluster 1	Cluster 2	Cluster 3	Cluster 4	Σ
Cluster 1	97.5 %	0.1 %	0.0 %	0.0 %	350
Cluster 2	1.7 %	97.6 %	1.8 %	1.9 %	730
Cluster 3	0.0 %	1.0 %	98.2 %	0.0 %	830
Cluster 4	0.8 %	1.2 %	0.0 %	98.1 %	220
Σ	358	722	838	212	2130

B)

Actual	Cluster 1	Cluster 2	Cluster 3	Cluster 4	Σ
Cluster 1	96.0 %	1.4 %	0.0 %	1.9 %	350
Cluster 2	2.9 %	92.1 %	4.1 %	4.8 %	730
Cluster 3	0.0 %	3.8 %	95.9 %	0.0 %	830
Cluster 4	1.1 %	2.7 %	0.0 %	93.3 %	220
Σ	350	734	836	210	2130

C)

Actual	Cluster 1	Cluster 2	Cluster 3	Cluster 4	Σ
Cluster 1	97.9 %	1.3 %	0.0 %	3.7 %	350
Cluster 2	1.5 %	90.8 %	4.8 %	3.7 %	730
Cluster 3	0.0 %	5.2 %	95.2 %	0.0 %	830
Cluster 4	0.6 %	2.7 %	0.0 %	92.5 %	220
Σ	339	746	831	214	2130

D)

Actual	Cluster 1	Cluster 2	Cluster 3	Cluster 4	Σ
Cluster 1	96.8 %	1.9 %	0.0 %	2.0 %	350
Cluster 2	2.6 %	89.6 %	6.8 %	1.0 %	730
Cluster 3	0.0 %	5.8 %	92.9 %	0.0 %	830
Cluster 4	0.6 %	2.7 %	0.2 %	97.0 %	220
Σ	343	738	847	202	2130

Figure 2.10. Confusion matrices for, A) logistic regression; B) neural networks; C) support vector machine; and D) K-nearest neighbour algorithms for each of the four clusters from the Betts Cove deposit.

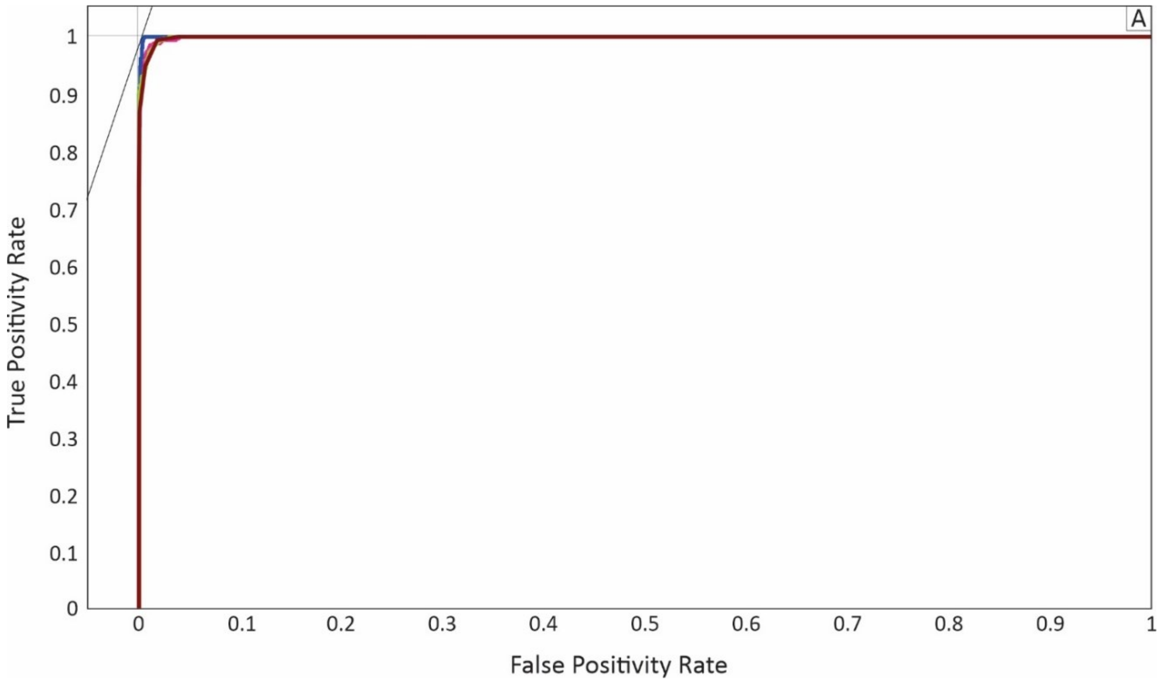
A
True Positivity Rate
False Positivity Rate
0
0.1
0.2
0.3
0.4
0.5
0.6
0.7
0.8
0.9
1

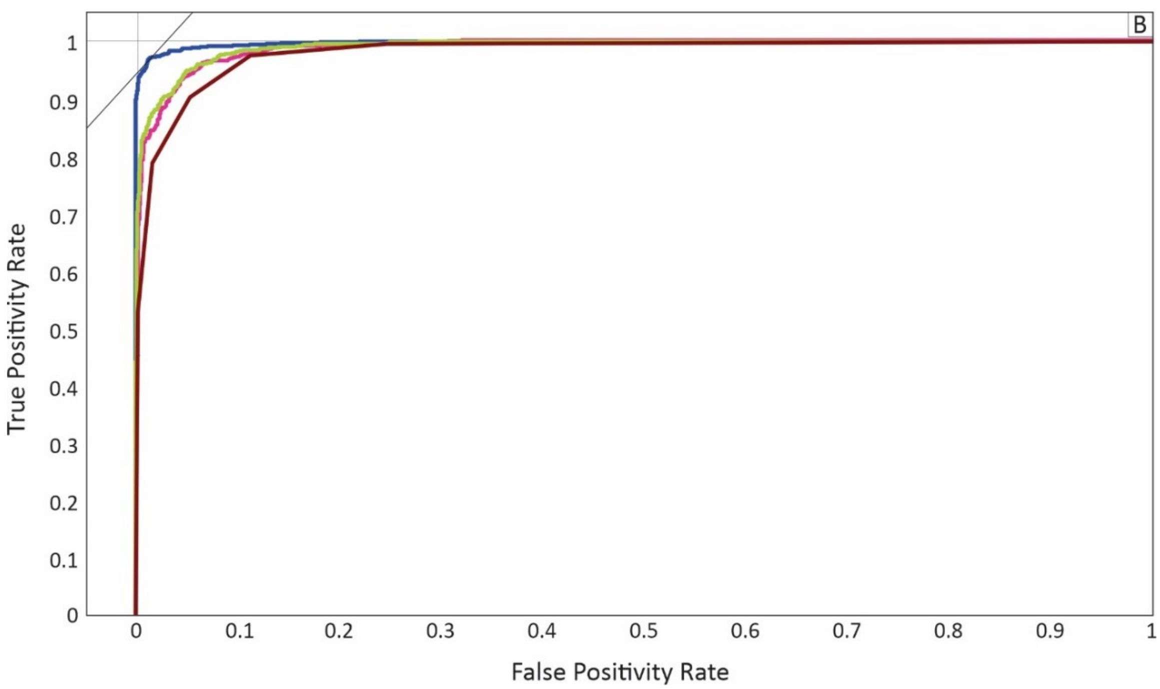
B
True Positivity Rate
False Positivity Rate
0
0.1
0.2
0.3
0.4
0.5
0.6
0.7
0.8
0.9
1

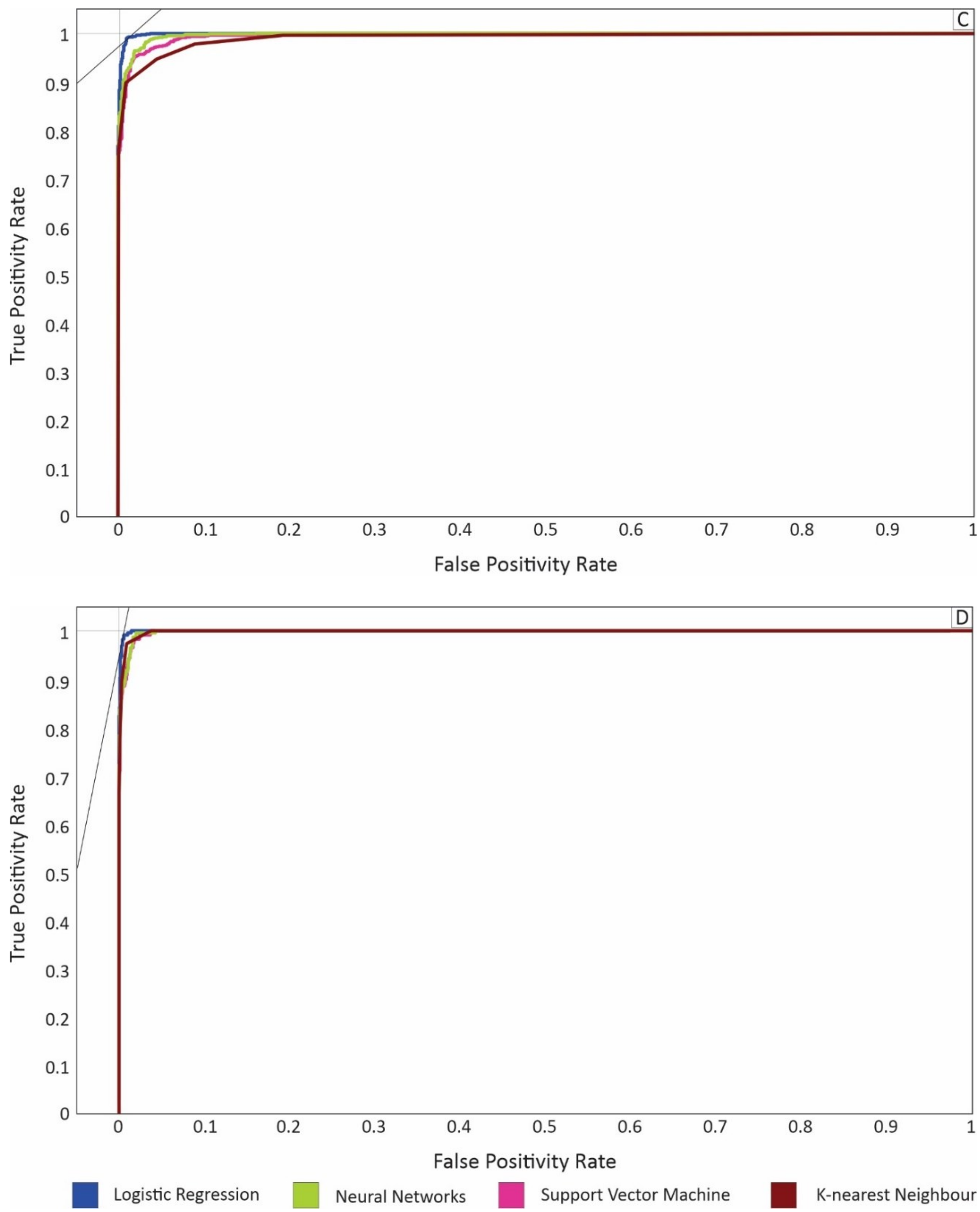

Figure 2.11. Receiver-operating characteristics curves for logistic regression, neural networks, SVM, and K-nearest neighbour for, A) cluster 1; B) cluster 2; C) cluster 3; and D) cluster 4 for Betts Cove.

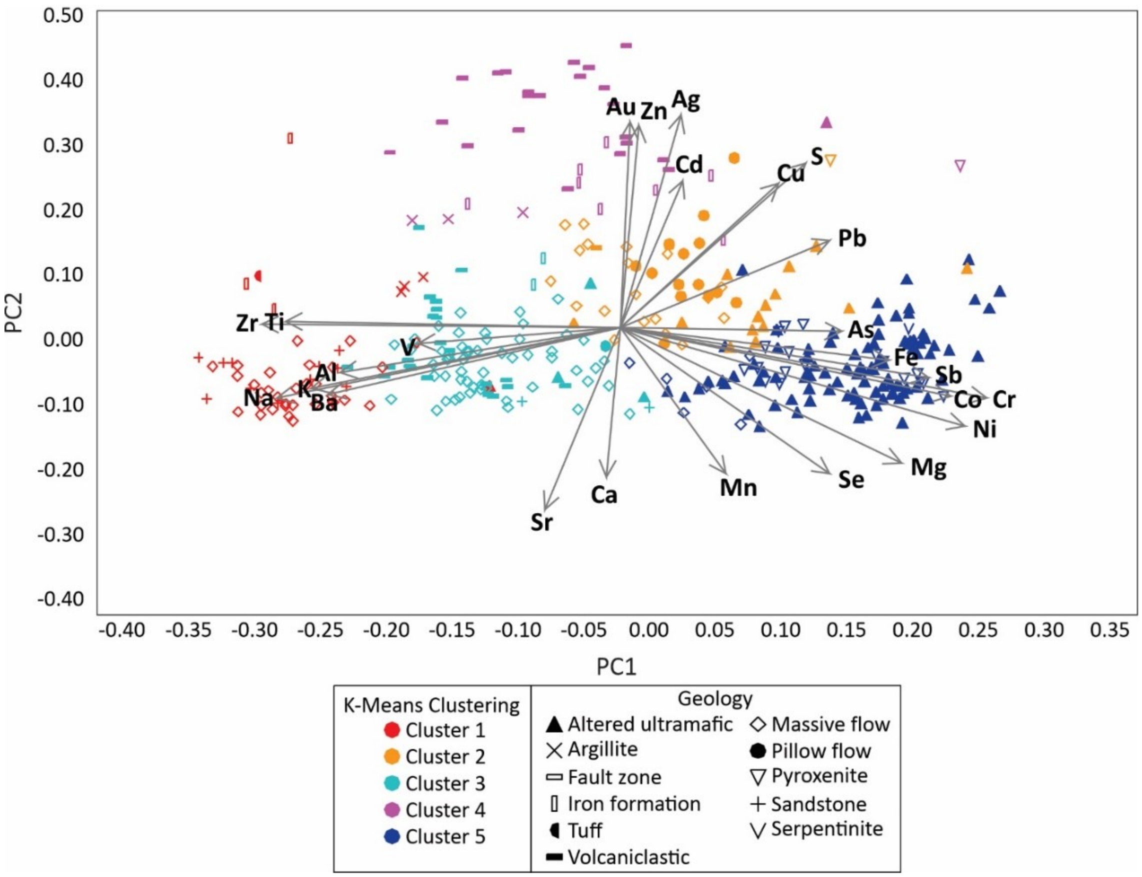

Figure 2.12. Principal component biplot for Tilt Cove, showing samples colour coded by K-means clusters in PC1 and PC2 space.

Predicted

A)

Actual	Cluster 1	Cluster 2	Cluster 3	Cluster 4	Cluster 5
Cluster 1	99.0 %	0.0 %	2.3 %	0.0 %	0.0 %
Cluster 2	0.0 %	89.6 %	0.0 %	6.2 %	1.2 %
Cluster 3	0.0 %	0.9 %	96.5 %	1.6 %	0.4 %
Cluster 4	1.0 %	8.7 %	0.0 %	92.2 %	0.0 %
Cluster 5	0.0 %	0.9 %	1.2 %	0.0 %	98.3 %
Σ	97	115	173	64	241

B)

Actual	Cluster 1	Cluster 2	Cluster 3	Cluster 4	Cluster 5	Σ
Cluster 1	99.0 %	0.0 %	2.4 %	0.0 %	0.0 %	100
Cluster 2	0.0 %	89.3 %	0.6 %	5.7 %	2.0 %	110
Cluster 3	0.0 %	1.8 %	95.8 %	4.3 %	2.0 %	170
Cluster 4	1.0 %	8.9 %	0.0 %	84.3 %	0.0 %	70
Cluster 5	0.0 %	0.0 %	1.2 %	5.7 %	95.9 %	240
Σ	97	112	167	70	244	690

C)

Actual	Cluster 1	Cluster 2	Cluster 3	Cluster 4	Cluster 5
Cluster 1	96.0 %	0.0 %	2.3 %	0.0 %	0.0 %
Cluster 2	0.0 %	92.6 %	0.6 %	9.2 %	6.2 %
Cluster 3	2.0 %	0.0 %	95.4 %	0.0 %	1.2 %
Cluster 4	2.0 %	6.4 %	1.7 %	90.8 %	0.0 %
Cluster 5	0.0 %	1.1 %	0.0 %	0.0 %	92.6 %
Σ	100	94	173	65	258

D)

Actual	Cluster 1	Cluster 2	Cluster 3	Cluster 4	Cluster 5	Σ
Cluster 1	97.9 %	0.0 %	2.4 %	2.9 %	0.0 %	100
Cluster 2	0.0 %	85.2 %	1.8 %	7.2 %	4.0 %	110
Cluster 3	1.0 %	1.9 %	94.1 %	1.4 %	2.8 %	170
Cluster 4	1.0 %	11.1 %	0.0 %	82.6%	0.0 %	70
Cluster 5	0.0 %	1.9 %	1.8 %	5.8 %	93.1 %	240
Σ	96	108	169	69	248	690

Figure 2.13. Confusion matrices for, A) logistic regression; B) neural networks; C) K-nearest neighbour; and D) support vector machine algorithms for each of the five clusters from the Tilt Cove deposit.

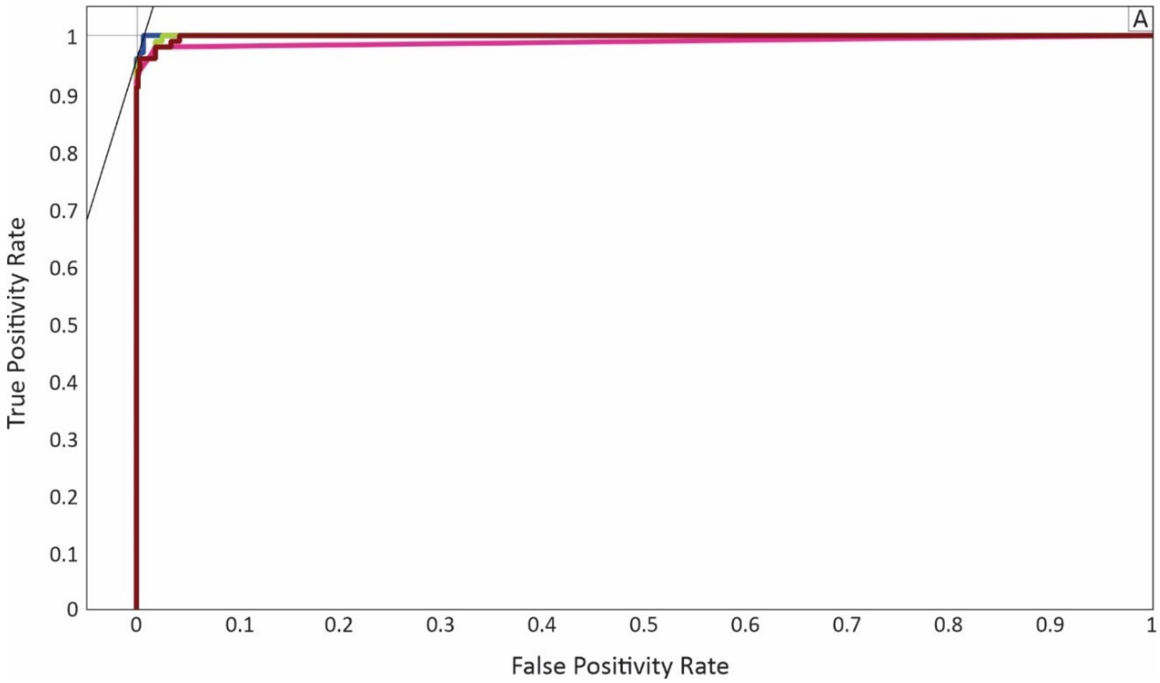

A
True Positivity Rate
False Positivity Rate
0
0.1
0.2
0.3
0.4
0.5
0.6
0.7
0.8
0.9
1

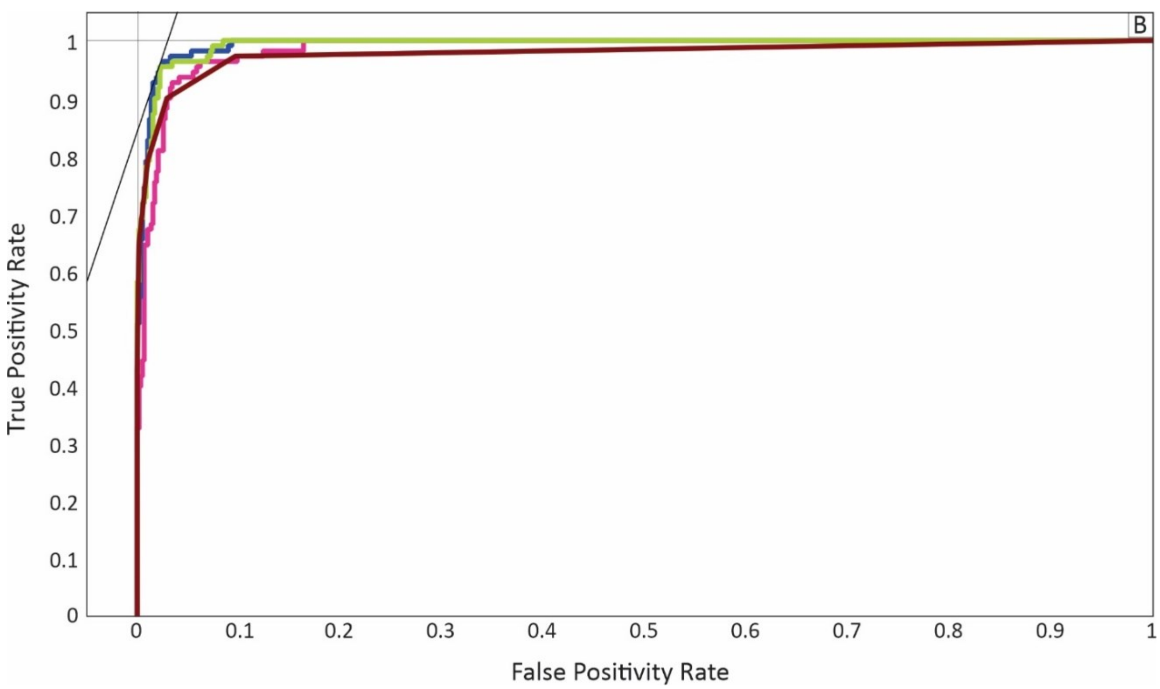

B
True Positivity Rate
False Positivity Rate
0
0.1
0.2
0.3
0.4
0.5
0.6
0.7
0.8
0.9
1

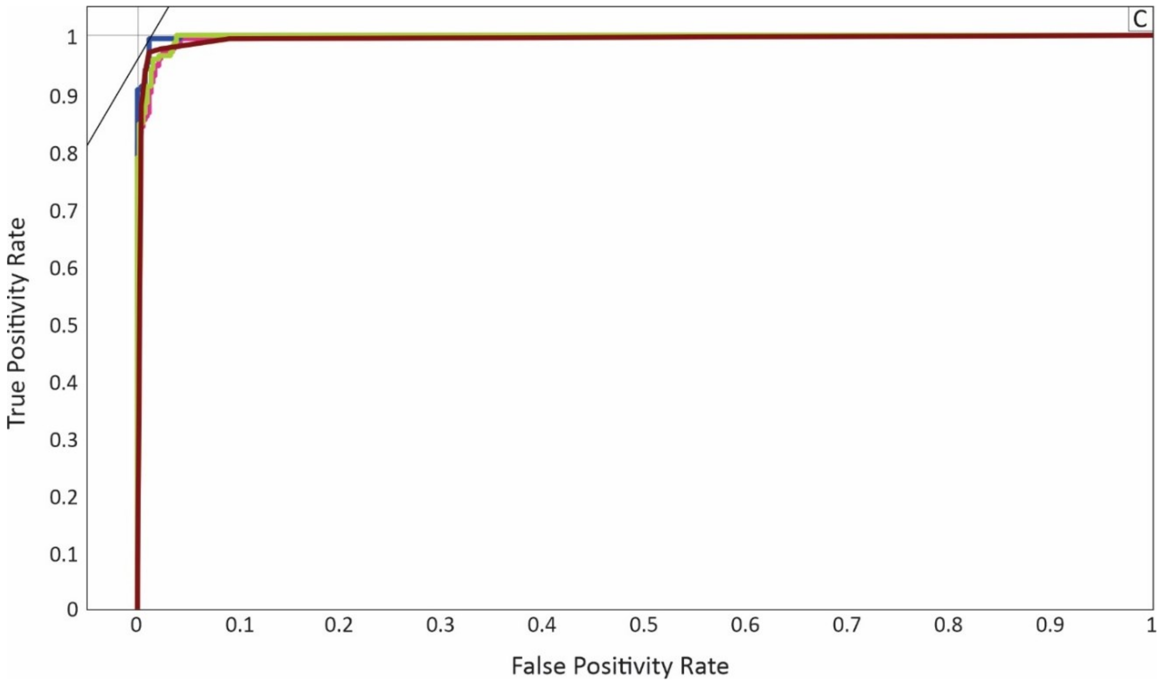
C
True Positivity Rate
False Positivity Rate
0
0.1
0.2
0.3
0.4
0.5
0.6
0.7
0.8
0.9
1

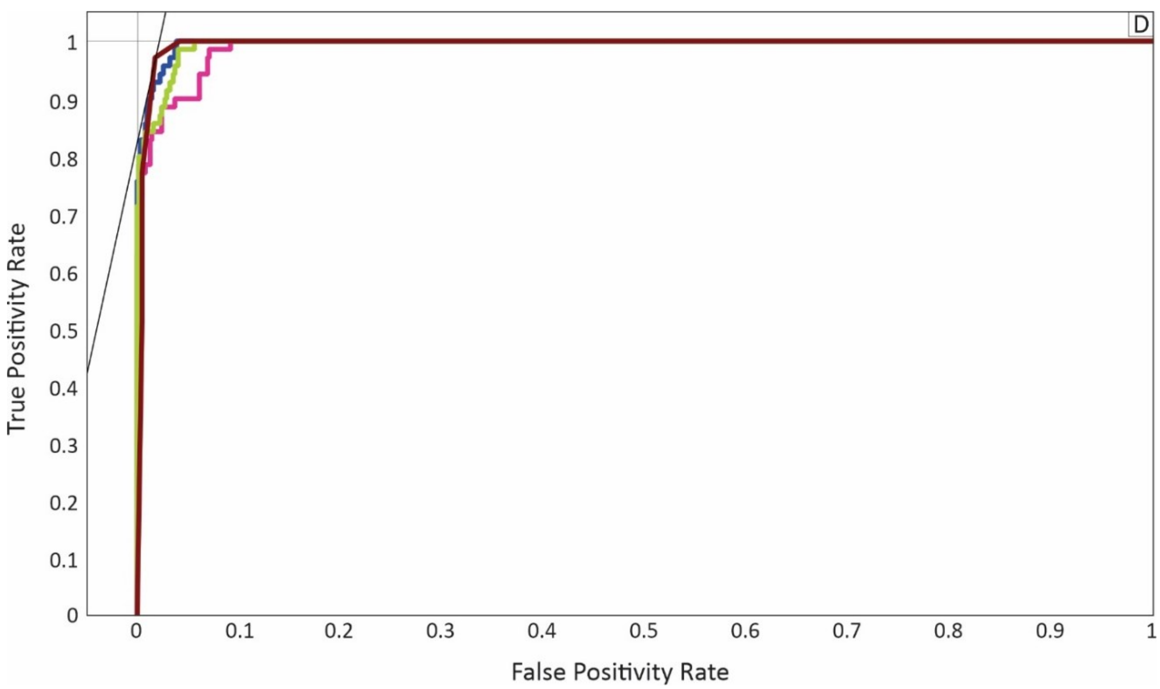
D
True Positivity Rate
False Positivity Rate
0
0.1
0.2
0.3
0.4
0.5
0.6
0.7
0.8
0.9
1

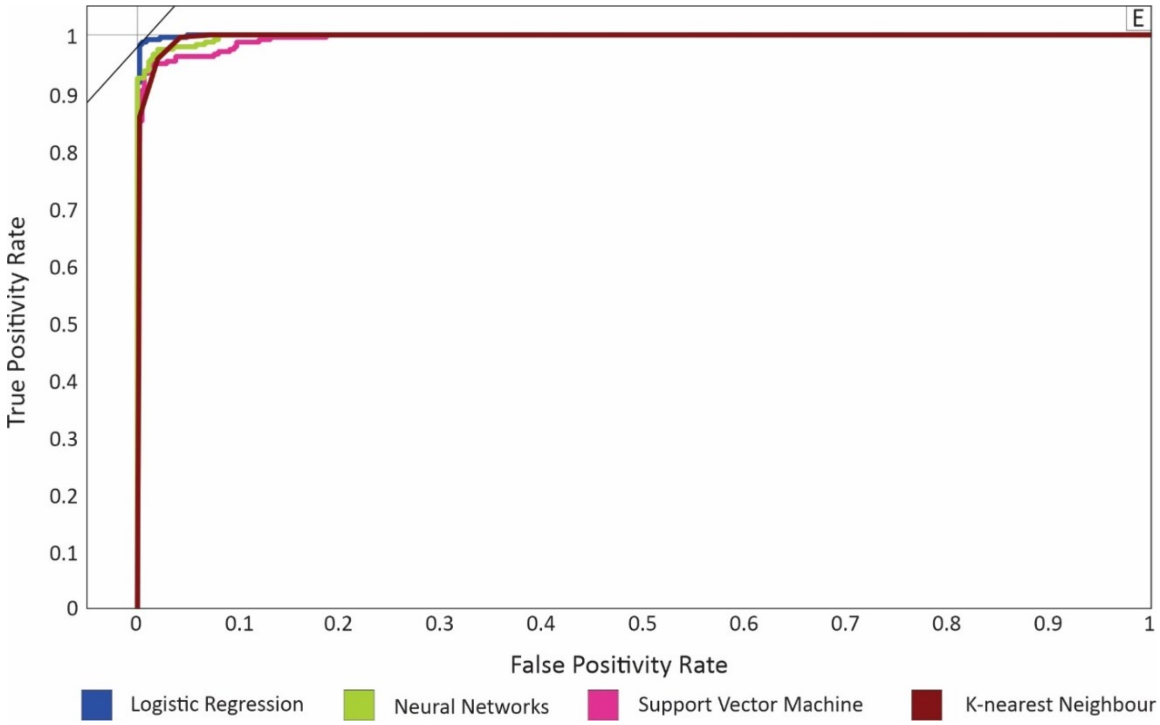

Figure 2.14. Receiver-operating characteristics curves for logistic regression, neural networks, SVM, and K-nearest neighbour for, A) cluster 1; B) cluster 2; C) cluster 3; D) cluster 4; and E) cluster 5 for Tilt Cove.

Table 2.1. Summary of assay and ICP results from Betts Cove and Tilt Cove.

Deposit	**Betts Cove**			**Tilt Cove**		
Element	Maximum (ppm)	Minimum (ppm)	Median (ppm)	Maximum (ppm)	Minimum (ppm)	Median (ppm)
Au	13	0	0	2.68	0.005	0.005
Cu	39800	3	316	71500	3	122
Al	86190	34590	66690	113490	500	54595
Cr	659	15	173	2887	27	429
Co	144	14	35	1010	5	60
Mg	95800	17500	47590	100000	3800	80845
Mn	3161	542	1409	2684	112	991
Ni	554	16	80	2200	1	275
Ti	4290	290	890	7700	50	700
V	284	119	216	326	10	163
Zn	24600	32	128	16100	32	88
Sb	26	2	8	30	2	7
As	63	3	3	203	3	5
Ba	188	3	7	10000	3	9
Cd	37	0	0	135	0	0
Ca	92100	1490	35490	131190	50	23100
Fe	100000	38700	69690	100000	21600	70400
K	19290	50	500	41900	50	100
Na	39500	100	15800	50490	50	290
Sr	442	2	56	537	2	84
Zr	58	4	13	239	1	8
Ag	16	0	0	10	0	0
Pb	516	1	8	5400	1	11
S	93300	50	2600	200000	50	2700
Se	369	5	5	67	5	5

Table 2.2. Parameters for the various machine learning algorithms in the Orange software.

Algorithm	Parameters
Support Vector Machine	Cost (C) = 1.00, ε = 0.10, Kernel = RBF, Numerical tolerance = 0.0010, Iteration limit = 100
Random Forest	100 Trees, do not split subsets smaller than 5
Neural Network	Neurons = 100, Activation = ReLu, Solver = Adam, Regularization = 0.0001, Maximum number of iterations = 200, Replicable training
Naïve Bayes	Default
Logistic Regression	Regularization type = Ridge (L2), Strength = 1
K-nearest Neighbour	Neighbours = 5, Metric = Euclidean, Weight = uniform
AdaBoost	Estimators = 50, Learning rate = 1.00, Classification algorithm = SAMME.R, Regression loss function = linear

Table 2.3. Evaluation results for each of the supervised machine learning models for Betts Cove evaluated using stratified random sampling, where 80% of the data was used to train the computer and the remaining 20% of the data was used to test the models.

Model	AUC	CA	F1	Precision	Recall
Support Vector Machine	0.994	0.938	0.938	0.938	0.938
Random Forest	0.988	0.915	0.915	0.916	0.915
Neural Network	0.996	0.944	0.944	0.944	0.944
Naïve Bayes	0.958	0.811	0.812	0.821	0.811
Logistic Regression	0.999	0.979	0.979	0.979	0.979
K-nearest Neighbour	0.990	0.928	0.928	0.928	0.928
AdaBoost	0.894	0.854	0.854	0.856	0.854

Table 2.4. Evaluation results for each of the supervised machine learning models for Tilt Cove evaluated using stratified random sampling, where 80% of the data was used to train the computer and the remaining 20% of the data was used to test the models.

Model	AUC	CA	F1	Precision	Recall
Support Vector Machine	0.994	0.917	0.917	0.917	0.917
Random Forest	0.991	0.916	0.916	0.916	0.916
Neural Network	0.997	0.941	0.941	0.941	0.941
Naïve Bayes	0.982	0.854	0.855	0.861	0.854
Logistic Regression	0.998	0.959	0.959	0.960	0.959
K-nearest Neighbour	0.991	0.936	0.935	0.936	0.936
AdaBoost	0.916	0.872	0.873	0.876	0.872

Chapter 3

Mineralogy, Mineral Chemistry, Sulfur Isotope Compositions, and Genesis of Critical-Metal Bearing Mineralization in the Betts Cove and Tilt Cove Volcanogenic Massive Sulfide (VMS) Deposits

3.1. ABSTRACT

The Betts Cove and Tilt Cove ophiolite-hosted, mafic-(Cyprus)-type volcanogenic massive sulfide (VMS) deposits in the Newfoundland Appalachians contain critical-metal, Cu-Zn-Ni-Co-Te-bearing stringer-type stockwork mineralization. The mineralization is dominated by pyrite, chalcopyrite, pyrrhotite, and sphalerite with magnetite (at Tilt Cove), and accessory cobaltite, pentlandite, and trace acanthite, arsenopyrite, bornite, chromite, clausthalite, electrum, galena, and hessite. The mineral textures, chemistry, and paragenesis reflect VMS mineralizing processes within an evolving VMS hydrothermal system. Both deposits had paragenetically early mineralization dominated by sphalerite and colloform pyrite that formed from low temperature (< 300ºC), near neutral pH, and reduced fluids, and paragenetically late mineralization dominated by chalcopyrite and pyrrhotite (+/- euhedral pyrite, cobaltite, and pentlandite), which is interpreted to have been deposited from high temperature (> 300ºC), acidic, and reduced fluids. The presence of paragenetically late magnetite at Tilt Cove reflects the cooling of the hydrothermal system and a switch to a more oxidizing and sulfur-poor fluid conditions. Metamorphism of the sulfides resulted in the micron-scale redistribution of minor and trace elements (Ag, Au, Pb, Se, and Te). These elements were likely originally dispersed amongst the major sulfide minerals and coalesced to form discrete mineral phases as inclusions in host phases.

The ophiolitic footwall rocks to the Betts Cove and Tilt Cove deposits have elevated Cu, Co, Ni, As, Au, and Sb contents and were the likely source of metals responsible for the enrichment of these metals in these deposits (i.e., they were derived from leaching of VMS-bearing fluids). Other contained metals in these deposits cannot be entirely explained by the leaching of footwall rocks alone and trace element chemistry suggests that magmatic-

hydrothermal fluids brought epithermal suite elements, including Ag, Bi, Hg, Se, and Te, into these hydrothermal systems.

The sulfur isotope compositions of the sulfides in Betts Cove and Tilt Cove indicate that thermochemical sulfate reduction (TSR) of seawater sulfate and the mixing with igneous sulfur were the primary sources of reduced sulfur (H_2S) in these deposits. Although, some highly positive sulfur isotope compositions (> 10‰) can potentially be explained by the replacement of sulfate minerals by sulfide minerals.

3.2. INTRODUCTION

There are over 850 known volcanogenic massive sulfide (VMS) deposits worldwide that are sources for Zn, Cu, Pb, Ag, Au, Co, Sn, Se, Mn, Cd, In, Bi, Te, Ga, and Ge (Galley et al., 2007). The Newfoundland Appalachians hosts over 40 VMS deposits that have made important economic contributions to Newfoundland for over a century but details about the nature and styles of mineralization, critical metal distributions and controls, and metal interrelationships within the Betts Cove and Tilt Cove VMS deposits are incomplete (e.g., Saunders, 1985; Strong and Saunders, 1988; Bédard et al., 2000; Sangster et al., 2007; Piercey et al., 2023).

The Betts Cove and Tilt Cove deposits are Cu-Co-Ni-Zn-Te-bearing mafic-(Cyprus)-type VMS deposits hosted in the Betts Cove ophiolite, Baie Verte Peninsula, Newfoundland Appalachians (Figure 3.1). Historically, Betts Cove produced 130 682 tons of Cu ore grading up to 10% Cu (Bédard et al., 2000; Sangster et al., 2007), whereas the Tilt Cove deposit has a historic resource of 8.16 Mt grading 6.50% Cu (Galley et al., 2007; Piercey et al., 2023); it also produced 42 500 ounces of Au, and a small quantity of Ni grading up to 24% Ni (Bédard et al., 2000; Sangster et al., 2007).

This paper presents the mineralogy, major, minor, and trace element chemistry, and sulfur isotope compositions of the various mineral phases within the sulfide mineralization in these deposits. The goals of this paper are to provide a better understanding of the metal distributions and residence withing these mineral phases, the causes of critical metal enrichment (e.g., Cu, Co, Ni, Zn, Te) in these deposits, and insights into the genesis of mineralization. These results also have implications for the distribution of critical and other metals in mineralization and genesis of other ophiolite-hosted VMS deposits globally.

3.3. GEOLOGICAL SETTING

3.3.1. Regional Geology

The Betts Cove and Tilt Cove deposits are located within the Notre Dame subzone of the Dunnage Zone of the Newfoundland Appalachians (van Staal et al., 2007; Rogers et al., 2007; Piercey et al., 2023). The Notre Dame subzone forms the most western portion of the Dunnage Zone. It is composed of three oceanic terranes (Lushs Bight Oceanic Tract, Baie Verte Oceanic Tract, and Annieopsquotch Accretionary Tract) and a continental magmatic arc (Notre Dame arc) (van Staal et al., 2007; Rogers et al., 2007). The Baie Verte Oceanic Tract (BVOT) is composed of supra-subduction zone ophiolite sequences, including the Betts Cove ophiolite, Lower Pacquet Harbour Group, Point Rousse Complex, and Advocate Complex, which are overlain by volcanic and sedimentary cover rocks (e.g., Hibbard 1983; van Staal et al., 2007; Rogers et al., 2007; Skulski et al., 2010; van Staal and Barr, 2012). These ophiolites host numerous Cu-Zn +/- Au-Ag-bearing VMS deposits, including the Betts Cove and Tilt Cove deposits (van Staal et al., 2007; Rogers et al., 2007; Piercey et al., 2023).

The Betts Cove ophiolite (488 Ma; Dunning and Krogh, 1985) hosts the Betts Cove and Tilt Cove deposits. The Betts Cove ophiolite is a complete ophiolite sequence consisting of serpentinite/talc-carbonates, layered ultramafic to mafic cumulate rocks, gabbroic intrusive rocks, sheeted dykes, and Betts Head Formation boninitic pillow lavas; the preserved thickness of the ophiolite is 4230 m (e.g., Hibbard 1983; Bédard et al., 2000; Skulski et al., 2010). Overlying the ophiolite is the ~ 4300 m thick Snooks Arm Group cover sequence consisting of tholeiitic to calc-alkaline lavas and sedimentary rocks (e.g., Hibbard 1983; Bédard et al., 2000; Skulski et al., 2010). The mineralization within the Betts Cove ophiolite is concentrated in the transition zone between the sheeted dyke unit and the overlying boninitic pillow lava unit (Betts Cove), as well as within the boninitic pillow lava unit and overlying tholeiitic pillow lava unit of the Snooks Arm Group (Tilt Cove). Extensions of the mineralization into the gabbros and ultramafic rocks also occur (Figures 3.2 and 3.3) (e.g., Bédard et al., 2000; Sangster et al., 2007). The ophiolite is interpreted to have formed due to forearc extension during arc initiation in the Humber (Taconic) seaway (~ 488 Ma) and was later obducted onto the Humber margin during the Taconic orogeny (~ 476-460 Ma) (Bedard et al., 2000; van Staal et al., 2007; van Staal et al., 2009; Skulski et al., 2010; van Staal and Baar, 2012).

3.3.2. The Betts Cove and Tilt Cove Deposits

The Betts Cove deposit is in the southern part of the Betts Cove ophiolite (Figure 3.1). The bulk of the mineralization is hosted within 1-3 m thick, pervasively chlorite altered and sheared mafic rocks between the sheeted dyke unit and overlying boninitic pillow lava unit of the Betts Cove ophiolite, but extensions into the sheeted dykes, gabbros, and pillow lavas occur (Figure 3.2) (e.g., Upadhyay and Strong, 1973; Saunders, 1985; Bédard et al., 2000; Sangster et al., 2007). These shear zones strike northwest-southeast (315-345º), but northeast-southwest (050-060º) striking zones also occur (Bédard et al., 2000; Sangster et al., 2007).

The mineralization at Betts Cove consists of pyrite, chalcopyrite, sphalerite, and pyrrhotite, and has Cu, Zn, and Au. The mineralization is stockwork-type consisting of sulfide stringers and disseminations (Saunders, 1985; Strong and Saunders, 1988; Bédard et al., 2000; Sangster et al., 2007). Historical reports note that the Betts Cove deposit was "crescent" or "basin" in shape and previously produced 130 682 tons of Cu ore with grades up to 10% Cu (Saunders, 1985; Strong and Saunders, 1988; Bédard et al., 2000); however, no NI-43-101 compliant resources have been defined for the deposit.

The Tilt Cove deposit is in the northern part of the Betts Cove ophiolite (Figure 3.1). Several mineralized zones (the East and West zones) are concentrated in a 400 m thick zone of massive and pillowed lavas and basalt breccia in the boninitic pillow lava unit of the Betts Cove ophiolite and the overlying tholeiitic pillow lavas of the Snooks Arm Group (Figure 3.3). The sheeted dyke unit is absent Tilt Cove and the pillow lavas are in direct contact with ultramafic rocks that include serpentinite and talc-carbonate-bearing units. The East and West zones of the deposit are separated by the Valley fault, a 50 to 75 m zone of serpentine and talc-carbonate rocks. In the West zone, the mineralization is cut off by this fault. In the East zone, another fault, the East Limit fault, cuts off the mineralization and puts it in direct contact with the sedimentary rocks of the Scrape Point Formation, including magnetite-bearing argillite and chert. This fault often contains sheared quartz-feldspar porphyry (Bédard et al., 2000; Sangster et al., 2007).

The mineralization at Tilt Cove consists of chalcopyrite, pyrite, pyrrhotite, and magnetite and has Cu, Au, Ni, and Co. The West zone mineralization is a stockwork consisting of sulfide stringers and disseminations, whereas the East or Main zone includes small lenses of massive sulfides and stockwork-type mineralization (Strong and Saunders, 1988; Bédard et al., 2000; Sangster et al., 2007). The Tilt Cove deposit has not been sufficiently modeled due to poor surface exposure and minimal access to underground workings. The attempts made, however, suggest that the mineralized zones are lens shaped where the West zone is mostly stockwork and the East zone is more massive (Bédard et al., 2000; Sangster et al., 2007). The deposit has a historic resource data of 8.16 Mt grading 6.50% Cu (Galley et al., 2007; Piercey et al., 2023).

3.4. METHODS

3.4.1. Mineralogy

The mineralization in the Betts Cove and Tilt Cove deposits were documented through core logging, reflected light microscopy, and scanning electron microscopy – energy dispersive spectroscopy (SEM-EDS) and scanning electron microscopy – mineral liberation analysis (SEM-MLA). Twenty drill holes, ten from Betts Cove and ten from Tilt Cove, were graphically logged to document mineralogy, mineral assemblages, and mineralization styles; samples were collected for petrography and further microanalytical work. Polished thin sections (n = 81) were analyzed in the Metallogeny of Orogenic Belts Laboratory at Memorial University, St. John's Newfoundland using a Nikon Eclipse LV100 POL petrographic microscope to determine mineralogy, mineral assemblages, mineral textures, mineralization styles, and paragenesis in each deposit.

A subset of samples from Betts Cove (n = 10) and Tilt Cove (n = 13) were further analyzed using SEM-EDS to expand on petrographic results and paragenetic relationships, and determine sub-microscopic mineral phases that were not identifiable by standard petrography. The SEM-EDS work was undertaken in the Hibernia Project Electron Beam Laboratory at

Memorial University. SEM-EDS analyses and imaging were preformed using the JEOL JSM – 7100F SEM with field emission gun (FEG) and a Thermo EDS system with a silicon drift detector. Operating conditions included a 15.0 kV accelerating voltage. A subset samples from Betts Cove (n = 7) and Tilt Cove (n = 5), were analyzed by SEM-MLA to supplement SEM-EDS work and to develop mineralogy maps of key samples. This work was undertaken in the CREAIT SEM-MLA Facility at Memorial University. Quantitative mineral studies were conducted using a FEI Quanta field emission gun 650 scanning electron microscope SEM equipped with Mineral Liberation Analysis (MLA) software version 3.14. Instrument conditions included a high voltage of 25 kV, working distance of 13.5 mm, and beam current of 10 nA. MLA maps were created using GXMAP mode by acquiring energy dispersive X-ray spectra in a grid every 10 pixels, with a spectral dwell time of 12 ms, and comparing these spectra against a list of known mineral reference spectra. The MLA frames were 1.5 mm by 1.5 mm with a resolution of 500 pixels × 500 pixels.

3.4.2. Mineral Chemistry

Electron probe microanalysis (EMPA) and laser ablation inductively coupled plasma mass spectrometry (LA-ICP-MS) were utilized to determine the mineral chemistry of the ore minerals (pyrite, chalcopyrite, pyrrhotite, sphalerite, cobaltite, pentlandite, arsenopyrite, acanthite, electrum, clausthalite, galena, hessite, magnetite, and chromite), to determine the residence of critical and other metals in the mineral phases. Polished thin sections from Betts Cove (n = 8) and Tilt Cove (n = 7) were analyzed at the Hibernia Project Electron Beam Laboratory at Memorial University using a JEOL JXA 8230 Superprobe with a W source, Thermo EDS imaging system, and five wavelength dispersive (WD) spectrometers. EPMA operating conditions for all minerals included a 20.0 kV accelerating voltage, beam current of 20 nA, and a beam diameter of 1 μm. The matrix correction protocol is ZAF (atomic number (Z), absorption (A), and fluorescence excitation (F) effects). The sulfides were analyzed for the following elements via the noted X-ray lines: S Kα, Fe Kα, Cu Kα, Zn Kα, Pb Mα, Co Kα, As Lα, Ni Kα, Ag Lα, Cd Lα, Sb Lα, Se Lα, and Au Mα; Te Lα was also analyzed for the selenide and telluride minerals. Oxide minerals were analyzed for Fe Kα, Ti Kα, Mn Kα, Cr Kα, V Kα, Zn Kα, Al Kα, and Co Kα; Mg Kα was also analyzed for chromite. Count times were between 20-40 seconds on peaks and 10-20 seconds on background. The samples were calibrated using natural mineral standards and metals/metal alloys (sphalerite for Zn; cuprite for Cu; pentlandite for Ni; cobalt for Co; pyrite for Fe and S; stibnite for Sb; cadmium for Cd; galena for Pb; arsenopyrite for As; selenium for Se; silver for Ag; and gold for Au). The quality control and quality assurance were monitored using secondary standards. Reference material data can be found in Appendix E. For sulfide, selenide, and telluride minerals and electrum, any analyses that had totals outside of 98-102% were rejected and not utilized further; for magnetite totals between 89-93% were considered acceptable because the instrument is unable to detect both Fe^{3+} and Fe^{2+} in magnetite, resulting in lower totals. Mineral formulae for the sulfide minerals have been calculated based on sulfur atoms per formula unit (apfu) for a given mineral phase (e.g., 2 for pyrite), whereas selenide minerals were calculated using selenium atoms per formula unit (e.g., 1 for clausthalite), and telluride minerals were calculated using tellurium atoms per formula unit (e.g., 1 for hessite). The Au proportion for electrum was calculated by comparing the Au content to the total Au and Ag content. Mineral formula for magnetite and chromite have been calculated for 32 oxygens per formula unit using Equation 1 (Droop, 1987):

$$F = 2X(1-T/S)$$

(Equation 3.1),

where F is the calculated Fe^{3+} in magnetite and chromite based on T is the ideal number of cations per formula unit and S is the observed cation total per X oxygens (X = 32) assuming that all the iron is Fe^{2+} (Droop, 1987).

The same 15 thin sections that were analyzed by EPMA were also analyzed by LA-ICP-MS at Queen's Facility for Isotope Research (QFIR) at Queen's University, Kingston, Ontario. Pyrite, chalcopyrite, pyrrhotite, sphalerite, cobaltite, pentlandite, arsenopyrite, bornite, magnetite, and chromite were spot analyzed for ^{7}Li, ^{9}Be, ^{11}B, ^{23}Na, ^{24}Mg, ^{27}Al, ^{29}Si, ^{31}P, ^{32}S, ^{39}K, ^{44}Ca, ^{45}Sc, ^{47}Ti, ^{51}V, ^{52}Cr, ^{55}Mn, ^{57}Fe, ^{59}Co, ^{60}Ni, ^{63}Cu, ^{66}Zn, ^{71}Ga, ^{73}Ge, ^{75}As, ^{77}Se, ^{85}Rb, ^{88}Sr, ^{89}Y, ^{90}Zr, ^{93}Nb, ^{95}Mo, ^{101}Ru, ^{103}Rh, ^{104}Pd, ^{105}Pd, ^{106}Pd, ^{107}Ag, ^{111}Cd, ^{115}In, ^{118}Sn, ^{121}Sb, ^{125}Te, ^{133}Cs, ^{137}Ba, ^{139}La, ^{140}Ce, ^{141}Pr, ^{146}Nd, ^{147}Sm, ^{153}Eu, ^{157}Gd, ^{159}Tb, ^{163}Dy, ^{165}Ho, ^{166}Er, ^{169}Tm, ^{172}Yb, ^{176}Lu, ^{178}Hf, ^{181}Ta, ^{182}W, ^{185}Re, ^{189}Os, ^{193}Ir, ^{195}Pt, ^{197}Au, ^{202}Hg, ^{204}Pb, ^{205}Tl, ^{206}Pb, ^{207}Pb, ^{208}Pb, ^{209}Bi, ^{232}Th, ^{238}U, and total Pb. Data was collected using the ThermoFisher triple quad ICP-MS with a ESI NWR-193nm Excimer laser that ablated 20μm spots, using 70% total energy for 5-6 mJ/cm^2 fluence, a pulse rate of 10 Hz. For each spot a gas blank was analyzed for 20 s, followed by 30 s ablation time. Between ablations a washout time of 20 s was used to ensure no material was carried over and to determine background counts. Tuning was conducted on a glass standard (NIST612) to maximize counts and minimize oxides and double charged ions to yield > 250kCPS of ^{238}U, < 1% $^{238}U^{16}O$, < 6% Ba^{++}. Every ~ 30 spots, 8 certified references materials (NIST610, NIST612, NIST614, FeS4, FeS5, PTC1b, CCu1e, and Mass-1) were used as external standards for each element and mineral and were ablated bracketing each set of sample analyses for calibration and to account for instrumentation drift and for quality control, specifically, NIST610 for ^{7}Li, ^{9}Be, ^{11}B, ^{23}Na, ^{24}Mg, ^{27}Al, ^{29}Si, ^{31}P, , ^{39}K, ^{44}Ca, ^{45}Sc, ^{85}Rb, ^{88}Sr, ^{89}Y, ^{90}Zr, ^{103}Rh, ^{133}Cs, ^{139}La, ^{140}Ce, ^{141}Pr, ^{147}Sm, ^{153}Eu, ^{157}Gd, ^{159}Tb, ^{163}Dy, ^{165}Ho, ^{169}Tm, ^{172}Yb, ^{176}Lu, ^{178}Hf,

^{181}Ta, ^{185}Re, and ^{232}Th; NIST612 for ^{73}Ge, ^{137}Ba, ^{146}Nd, ^{166}Er, ^{182}W, and ^{238}U; FeS4 for ^{57}Fe, ^{63}Cu, ^{66}Zn, ^{71}Ga, ^{101}Ru, ^{104}Pd, ^{105}Pd, ^{106}Pd, ^{125}Te, ^{189}Os, ^{204}Pb, ^{206}Pb, ^{207}Pb, ^{208}Pb, and Pb total; FeS5 for ^{47}Ti, ^{51}V, ^{59}Co, ^{60}Ni, ^{75}As, ^{93}Nb, ^{95}Mo, ^{111}Cd, ^{121}Sb, ^{193}Ir, ^{195}Pt, ^{197}Au, and ^{205}Tl; PTC1b for ^{52}Cr, and ^{107}Ag; and CCule for ^{32}S, ^{55}Mn, ^{77}Se, ^{115}In, ^{118}Sn, ^{202}Hg, and ^{209}Bi. Reference material data can be found in Appendix E. Major elements measured by EMPA were used as internal standards to correct for variability in the laser yield and included Fe for pyrite, pyrrhotite, and magnetite, Cu for chalcopyrite and bornite, Zn for sphalerite, Ni for pentlandite, Co for cobaltite, As for arsenopyrite, and Cr for chromite. The Iolite software package (v 4.8.2) was used for data normalization and drift correction (Paton et al., 2011).

3.4.3. Sulfur Isotope Compositions

Secondary ion mass spectrometry (SIMS) was utilized to determine the *in situ* sulfur isotope compositions of pyrite, chalcopyrite, pyrrhotite, and arsenopyrite following the methods of Brueckner et al. (2015). Offcuts from 8 thin sections previously analyzed by EPMA and LA-ICP-MS were epoxy mounted in aluminium ring mounts, polished down to a grit of 1 µm and sputter coated with Au (300 Å coating thickness), and analyzed at the CREAIT MicroAnalysis Facility (MAF) at Memorial University. Data was collected using the Cameca IMS 4f secondary ion mass spectrometer and $\delta^{34}S$ determinations were performed by bombarding the sample with a Cs^+ primary ion microbeam with a 0.8 – 1.0 nA current, accelerated through a 10 keV potential, and focused into a 15-20 µm diameter spot. To exclude exotic material in the polished surface from analysis, each spot was first pre-sputtered for 120s using a 10 µm raster. Signals for $^{32}S^-$, $^{34}S^-$ and a background position at 31.67 Da were obtained by cyclical magnetic peak switching. Standard counting times and peak sequence used were: 0.5 s at the background position, 2.0 s on $^{32}S^-$, and 6.0 s on $^{34}S^-$. Waiting times of 0.25 s were inserted before each peak counting position to allow for magnet settling. A typical analysis takes less than 15 min (including pre-sputtering time). Correction for instrumental mass fractionation was performed using standard reference materials UL9 for pyrite, Norilsk for chalcopyrite, PoW1 for pyrrhotite, and Arspy57 for arsenopyrite. Results are expressed as $\delta^{34}S$ relative to Vienna Canyon Diablo troilite (VCDT). Internal precisions on individual $\delta^{34}S$ determinations of better than +/- 0.3‰ (1σ) and overall reproducibility, based on replicate standard analyses, is typically better than +/- 0.35-0.45‰ (1σ).

3.5. RESULTS

3.5.1. Betts Cove Deposit

3.5.1.1. Mineralogy

The mineralization at Betts Cove is hosted in pervasively chlorite-epidote-quartz altered pillow basalts and basalt breccias (Figure 3.4). Cross-cutting calcite and ankerite are pervasive near mineralization in the eastern edge of the deposit. Betts Cove mineralization is a ~ 200 m x 200 m stockwork consisting of millimetre-scale to up to 10 cm sulfide stringers consisting of dominantly chalcopyrite, pyrite, pyrrhotite, and sphalerite with minor to trace cobaltite, pentlandite, clausthalite, galena, electrum, and hessite. The stockwork mineralization at Betts Cove has four sulfide facies: chalcopyrite-dominated, chalcopyrite-pyrrhotite-dominated, sphalerite-pyrite-dominated, and pyrite-dominated (Figure 3.5A-D). In general, the chalcopyrite-dominated and chalcopyrite-pyrrhotite-dominated facies are common in deeper sections of drill core, whereas the sphalerite-pyrite-dominated and pyrite-dominated facies are common in shallower sections of drill core.

Pyrite occurs in several different forms. Colloform pyrites occur in the chalcopyrite-dominated facies, but in general are rarely preserved (Figure 3.6A). Euhedral to subhedral pyrite grains are the most common and occur in every sulfide facies, often amalgamated to form clusters with inclusions of silicate minerals and chalcopyrite (and lesser pyrrhotite and sphalerite) (Figure 3.6B and C). Subhedral pyrite grains often have rounded and/or irregular shapes when surrounded by chalcopyrite, pyrrhotite, and/or sphalerite, whereas in pyrite-rich samples, they have annealed textures (Figure 3.6D). Elongated, pyrite veins also occur in the chalcopyrite- and chalcopyrite-pyrrhotite-dominated facies (Figure 3.6C). The pyrite veins follow foliations in the silicate host rock and are interpreted to reflect post-VMS remobilized pyrite.

Chalcopyrite, pyrrhotite, and sphalerite at Betts Cove occur as anhedral masses in all sulfide facies (Figure 3.6F). Pyrrhotite is almost always intergrown with chalcopyrite. Sphalerite is minor and typically displays chalcopyrite disease when associated with chalcopyrite and pyrrhotite (Figure 3.6G). Chalcopyrite, pyrite, and pyrrhotite either surround euhedral to subhedral pyrite grains or are found as rounded inclusions within them.

Cobaltite occurs as rounded, subhedral grains within chalcopyrite in the chalcopyrite-dominated sulfide facies (Figure 3.6H). Pentlandite occurs as inclusions within chalcopyrite and is locally intergrown with pyrrhotite along chalcopyrite grain boundaries in the chalcopyrite-dominated facies (Figure 3.6I). Electrum, clausthalite, hessite, and galena are trace phases. Electrum occurs as rounded inclusions within chalcopyrite in the chalcopyrite-dominated facies and rarely in pyrite in the sphalerite-pyrite-dominated facies (Figure 3.6J). Clausthalite occurs as rounded inclusions within chalcopyrite and pyrrhotite in the chalcopyrite- and chalcopyrite-pyrrhotite-dominated facies (Figure 3.6K). Hessite occurs as rounded inclusions within chalcopyrite and along chalcopyrite grain boundaries in the chalcopyrite- and chalcopyrite-pyrrhotite-dominated facies; hessite is commonly intergrown with clausthalite and galena (Figure

3.6K and L). Galena is found as rounded inclusions within pyrite and along pyrite grain boundaries in all sulfide facies (Figure 3.6L).

3.5.1.2. Major, Minor, and Trace Element Geochemistry

Select mineral chemical data for Betts Cove can be found in Table 3.1 and Figure 3.7.

Pyrite (FeS_2) at Betts Cove has a mineral formula that ranges from $Fe_{0.988-1.023}S_{2.000}$, with Fe and S ranging from 45.82-47.47 wt% and 51.45-54.18 wt%, respectively. Nickel concentrations range up to 1210 ppm and are highest in the chalcopyrite-pyrrhotite-dominated assemblage (median = 385 ppm). Cobalt concentrations are up to 1.92 wt% and are highest in the chalcopyrite-dominated facies (median = 1200 ppm); high Co values are likely attributed to inclusions cobaltite in pyrite. Other elements in pyrite include Ti, V, Cr, Mn, Cu, Zn, As, Se, Ag, Sb, Te, Hg, Tl, Bi, and Pb. Pyrite contains the highest V (< 255 ppm), As (< 3.96 wt%), Sb (< 120 ppm), Te (< 2650 ppm), Tl (< 321 ppm), Bi (< 174 ppm), and Pb (< 1.95 wt%) when compared to the other main sulfide minerals (chalcopyrite, pyrrhotite, and sphalerite). Pyrite from the chalcopyrite-dominated facies (n = 84) has elevated V (median = 2.51 ppm), Te (median = 140 ppm), and Bi (median = 29.8 ppm) compared to pyrite from the other sulfide facies. Pyrite from the sphalerite-pyrite-dominated facies (n = 25) has elevated As (median = 524 ppm) compared to pyrite from the other sulfide facies. Pyrite from the chalcopyrite-pyrrhotite-dominated facies (n = 12) has elevated Sb (median = 36.2 ppm) and Pb (median = 190 ppm) compared to pyrite from the other sulfide facies. Pyrite from the pyrite-dominated facies (n = 20) has elevated Tl (median = 6.74 ppm) compared to pyrite from the other sulfide facies. Other than chalcopyrite, pyrite contains the highest Cu which is highest in the chalcopyrite-dominated facies (median = 1500 ppm).

Chalcopyrite ($CuFeS_2$) has a mineral formula that ranges from $Cu_{0.801-0.972}Fe_{0.951-1.028}S_{2.000}$, with Cu, Fe, and S ranging from 29.33-33.92 wt%, 29.56-33.06 wt%, and 34.81-36.96 wt%, respectively. Nickel and Co concentrations are up to 2350 ppm and 6.75 wt%, respectively and are highest in the pyrite-dominated facies (median = 232 ppm and 1110 ppm, respectively); high Ni and Co values are likely attributed to inclusions in chalcopyrite. Other elements in chalcopyrite include V, Cr, Mn, Zn, As, Se, Ag, In, Sn, Sb, Te, Hg, Tl, and Pb. Chalcopyrite contains the highest Ti (< 5300 ppm), Cr (< 1260 ppm), Se (< 3.17 wt%), Ag (< 5750 ppm), and Sn (< 4630 ppm) when compared to the other main sulfide minerals. Chalcopyrite from the pyrite-dominated facies (n = 4) has elevated Ti (median = 6.38 ppm), Cr (median = 9.63 ppm), Se (median = 2.08 wt%), and Sn (median = 367 ppm) compared to chalcopyrite from the other sulfide facies. Chalcopyrite from the sphalerite-pyrite-dominated facies (n = 6) has elevated Ag (median = 292 ppm) compared to chalcopyrite from the other sulfide facies. Other than sphalerite, chalcopyrite contains the highest Zn which is highest in the pyrite-dominated facies (median = 4390 ppm).

Pyrrhotite ($Fe_{(1-x)}S$) has a mineral formula that ranges from $Fe_{0.822-0.871}S_{1.000}$, with Fe and S ranging from 58.66-59.71 wt% and 39.23-41.06 wt%, respectively. Pyrrhotite contains the highest Ni and Co when compared to the other main sulfide minerals. Nickel concentrations are up to 4840 ppm and are highest in the chalcopyrite-dominated facies (median = 4840 ppm). Cobalt concentrations are up to 2120 ppm and are highest in the chalcopyrite-pyrrhotite-dominated facies (median = 967 ppm). Other elements in pyrrhotite include Cr, Mn, Cu, Zn, As, Se, Ag, Sb, Te, Hg, Tl, Bi, and Pb.

Sphalerite (ZnS) has a mineral formula that ranges from $(Zn_{0.838-0.936}Fe_{0.068-0.157})S_{1.000}$, with Zn and S ranging from 56.84-62.61 wt% and 32.69-34.02 wt%, respectively. Iron concentrations in sphalerite are up to 9.11 wt%, and highest in the chalcopyrite-pyrrhotite-dominated facies (median = 7.82 wt%); high Fe concentrations are most likely due to the substitution of Fe for Zn in sphalerite. Copper concentrations are up to 1.46 wt% Cu and are highest in the chalcopyrite-dominated facies (median = 4660 ppm); high Cu concentrations are most likely due to chalcopyrite disease in sphalerite. Nickel concentrations are up to 185 ppm and highest in the pyrite-dominated facies (median = 25.9 ppm). Cobalt concentrations are up to 667 ppm and are highest in the chalcopyrite-dominated facies (median = 564 ppm). Other elements in sphalerite include V, Cr, Mn, Cu, As, Se, Ag, In, Cd, Sn, Sb, Te, Hg, Tl, and Pb. Sphalerite contains the highest Mn (< 1500 ppm), In (< 453 ppm), Cd (< 5060 ppm), and Hg (< 1.93 wt%) when compared to the other main sulfide minerals. Sphalerite from the chalcopyrite-pyrrhotite-dominated facies (n = 10) has elevated Mn (median = 969 ppm), In (median = 147 ppm), and Cd (median = 2980 ppm) compared to sphalerite from the other sulfide facies. Sphalerite from the chalcopyrite-dominated facies (n = 6) has elevated Hg (median = 498 ppm) compared to sphalerite from the other sulfide facies.

Cobaltite (CoAsS) has a mineral formula that ranges from $Co_{0.551-0.757}As_{0.545-0.768}S_{1.000}$, with Co, As, and S ranging from 28.11-31.64 wt%, 35.40-40.71 wt%, and 22.51-27.78 wt%, respectively. Iron concentrations are up to 8.07 wt% and are likely due to X-rays from surrounding minerals. Nickel concentrations are up to 6200 ppm (median = 2200 ppm). Other elements in cobaltite include Se (< 1800 ppm), Zn (< 1600 ppm), and Pb (< 1000 ppm).

Pentlandite ($(Fe,Ni)_9S_8$ has a mineral formula that ranges from from $(Fe_{3.517-4.385}Ni_{3.922-5.315})_{9.000}S_{8.000}$, with Fe, Ni, and S ranging from 25.36-32.02 wt%, 30.10-40.28 wt%, and 32.96-33.63 wt%, respectively. Cobalt concentrations are up to 3.39 wt% Co (median = 1.81 wt%).

Other elements in pentlandite include Cu (< 2.31 wt%) and Pb (< 1200 ppm); high values are likely due to X-rays from surrounding minerals.

All of the clausthalite (PbSe) and most of the galena (PbS) at Betts Cove, yielded results outside of the total cut-off for EPMA (98-102 wt%) due to their small grain sizes and because of this were challenging to polish well enough for EPMA analysis. The one acceptable galena analyses had a mineral formula of $Pb_{0.973}S_{1.000}$, with Pb and S concentrations of 85.28 wt% and 13.56 wt%, respectively. Other elements in galena include Fe (1.27 wt%), Zn (7500 ppm), and Se (3000 ppm).

Electrum (AuAg) at Betts Cove contains 77.93-88.57 wt% Au and 11.83-21.43 wt% Ag, respectively, and has minor to trace Fe (< 1.76 wt%), Cu (< 8600 ppm), Cd (< 1900 ppm), and Se (< 1300 ppm); high values are likely attributed to X-rays from surrounding minerals.

Hessite at Betts Cove has a mineral formula that ranges from $Ag_{1.7438-1.922}Te_{1.000}$, with Ag and Te ranging from 58.76-61.23 wt% and 37.27-40.03 wt%, respectively. Other elements in hessite include Cu (< 1.44 wt%), Fe (< 1.05 wt%), Cd (< 5400 ppm), Sb (< 1900 ppm), and Au (< 1700 ppm); high values are likely attributed to X-rays from surrounding minerals.

3.5.1.3. Sulfur Isotope Compositions

Sulfur isotope data for Betts Cove can be found in Figure 3.8A-C.

Pyrite at Betts Cove has $\delta^{34}S$ values that range from +4.23 to +13.30‰ (median +7.25 ± 2.01‰, n = 20). The $\delta^{34}S$ values in pyrite vary based on texture, where relic colloform pyrite has $\delta^{34}S$ = +4.23 to +7.55‰ (median +6.45 ± 1.00‰, n = 7), recrystallized pyrite has $\delta^{34}S$ = +6.16 to +9.37‰ (median +7.41 ± 0.91‰, n = 10), and remobilized pyrite veins have $\delta^{34}S$ = +10.59 to +13.30‰ (median 11.07 ± 1.18‰, n = 3).

Chalcopyrite has $\delta^{34}S$ values that range from +5.66 to +15.43‰ (median +8.27 ± 2.48‰, n = 14); all chalcopyrite was from the chalcopyrite- and chalcopyrite-pyrrhotite-dominated facies. Samples from the chalcopyrite-pyrrhotite-dominated facies, where chalcopyrite is intergrown with pyrrhotite, have the highest the highest $\delta^{34}S$ values with a median of +8.46 ± 0.65‰ (n = 8).

Pyrrhotite has $\delta^{34}S$ values that range from +6.23 to +12.63‰ (median +6.84 ± 1.70‰, n = 14); all pyrrhotite was from the chalcopyrite-pyrrhotite-dominated facies with one analysis from the chalcopyrite-dominated facies. The sample from the chalcopyrite-dominated facies, where pyrrhotite is intergrown with pentlandite and chalcopyrite, has the highest $\delta^{34}S$ value of +12.63‰ (n = 1).

3.5.2. Tilt Cove Deposit

3.5.2.1. Mineralogy

The mineralization at Tilt Cove is hosted in talc-carbonate +/- chlorite and serpentine altered ultramafic rocks and chlorite altered mafic flows and breccias (Figure 3.4). Talc and carbonates, including magnesite, ankerite, calcite, and dolomite, commonly surround and locally cross-cut the mineralization as millimetre-scale veinlets. Tilt Cove mineralization is a ~400 m x 200 m stockwork consisting of millimetre-scale to up to 10 cm sulfide stringers and disseminations, and minor up to 5.2 m thick semi-massive to massive sulfide zones consisting of dominantly pyrite, chalcopyrite, pyrrhotite, and sphalerite, with lesser cobaltite, pentlandite, arsenopyrite, acanthite, electrum, and bornite; magnetite and chromite also occur. The stockwork mineralization at Tilt Cove includes four sulfide facies: pyrite-, chalcopyrite +/- pyrrhotite-, pyrrhotite-, and magnetite-dominated (Figure 5E-H). In general, the pyrite-dominated facies is found spatially from top to bottom in every drill hole, whereas the chalcopyrite +/- pyrrhotite-dominated and pyrrhotite-dominated facies are common in deeper sections of drill core in the centre of the deposit, and the magnetite-dominated facies is common in shallower sections of drill core along the margins of the deposit.

Pyrite occurs in several forms. Colloform pyrite occurs in the pyrite-dominated facies and is replaced by chalcopyrite and sphalerite, but these are very rarely preserved (Figure 3.9A). Euhedral to subhedral pyrite grains are the most common and occur in all sulfide facies, and are often amalgamated to form pyrite clusters with inclusions of chalcopyrite, sphalerite, silicates (+/- pyrrhotite and magnetite) (Figure 3.9B). Subhedral pyrite grains are rounded and/or irregular in shape when surrounded by chalcopyrite, pyrrhotite, and/or sphalerite (Figure 3.9C). Deformed cataclastic pyrite occurs in the pyrite-dominated facies, where it is associated with chalcopyrite, which infills fracture spaces in the pyrite (Figure 3.9D).

Chalcopyrite, pyrrhotite, and sphalerite at Tilt Cove occur as anhedral masses in all sulfide facies. Pyrrhotite is almost always intergrown with chalcopyrite (Figure 3.9E). Minor sphalerite is associated with chalcopyrite and pyrrhotite and has chalcopyrite disease (Figure 3.9C). Chalcopyrite, pyrrhotite, and sphalerite surround pyrite grains or are less commonly found as rounded inclusions within large, euhedral pyrite grains.

Cobaltite at Tilt Cove is found in the chalcopyrite-, chalcopyrite-pyrrhotite-, and pyrite-dominated facies, where it occurs as euhedral to subhedral grains within chalcopyrite and pyrrhotite (Figure 3.9F). Pentlandite is found in all sulfide facies and occurs as subhedral grains within pyrrhotite and chalcopyrite and as elongated veins within pyrrhotite (Figure 3.9G). Arsenopyrite is found only in the pyrite-dominated facies where is found in spaces between pyrite grains along contacts with chalcopyrite (Figure 3.9H). Acanthite and electrum are always associated with arsenopyrite in the pyrite-dominated facies and found in fractures within arsenopyrite (Figure 3.9M). Bornite is found in the magnetite-dominated facies as disseminations with magnetite and chalcopyrite (Figure 3.9I)

Magnetite occurs in all sulfide facies. When associated with the sulfide mineralization, it is massive, and surrounds the sulfide minerals (Figure 3.9J and K), or forms discrete, euhedral to subhedral grains that are in the groundmass of the host rock groundmass and typically have chromite cores (Figure 3.9L).

3.5.2.2. Major, Minor, and Trace Element Geochemistry

Select mineral chemical data for Tilt Cove can be found in Table 3.2 and Figure 3.10.

Pyrite (FeS_2) at Tilt Cove has a mineral formula that ranges from $Fe_{0.900\text{-}1.034}S_{2.000}$, with Fe and S ranging from 42.42-46.93 wt% and 51.90-54.38 wt%, respectively. Nickel and Co concentrations are up to 2.03 wt% and 1.10 wt%, respectively and are highest in the chalcopyrite-pyrrhotite-dominated facies (median = 1.02 wt% and 5520 ppm, respectively); High Ni and Co values are likely attributed to inclusions in pyrite. Other elements in pyrite include Ti, V, Cr, Mn, Cu, Zn, As, Se, Ag, Sb, Te, Hg and Tl, Pyrite contains the highest As (< 1.30 wt%), Bi (< 7.17 ppm), and Pb (< 472 ppm) when compared to the other main sulfide minerals (chalcopyrite, pyrrhotite, and sphalerite). Pyrite from the chalcopyrite-pyrrhotite-dominated facies (n = 2) has elevated Bi (median = 4.85 ppm) and Pb (median = 467 ppm) compared to pyrite from the other sulfide facies. Pyrite from the pyrite-dominated facies (n = 45) has elevated As (median = 715 ppm) compared to pyrite from the other sulfide facies.

Chalcopyrite ($CuFeS_2$) has a mineral formula that ranges from $Cu_{0.860\text{-}0.983}Fe_{0.908\text{-}1.091}S_{2.000}$, with Cu, Fe, and S ranging from 27.27-34.43 wt%, 25.31-32.60 wt%, and 32.00-35.96

wt%, respectively. Nickel concentrations are up to 3580 ppm and are highest in the chalcopyrite-pyrrhotite-dominated facies (median = 66.6 ppm). Cobalt concentrations are up to 8.27 wt% and are highest in the chalcopyrite-dominated facies (median = 9.82 ppm); high Co values are likely attributed to inclusions in chalcopyrite. Other elements in chalcopyrite include V, Cr, Mn, Zn, As, Se, Ag, In, Sn, Sb, Te, Hg, and Tl. Chalcopyrite contains the highest V (< 1080 ppm), Cr (< 4090 ppm), Se (< 2930 ppm), In (< 1.81 wt%), Sn (< 2.26 wt%), and Tl (< 6340 ppm) when compared to the other main sulfide minerals. Chalcopyrite from the magnetite-dominated facies (n = 3) has elevated V (median = 1.06 ppm) compared to chalcopyrite from the other sulfide facies. Chalcopyrite from the chalcopyrite-dominated facies (n = 12) has elevated Cr (median = 2.63 ppm), Se (median = 164 ppm), and Tl (median = 65.2 ppm) compared to chalcopyrite from the other sulfide facies. Chalcopyrite from the pyrrhotite-dominated facies (n = 10) has elevated In (median = 38.5 ppm) compared to chalcopyrite from the other sulfide facies. Chalcopyrite from the pyrite-dominated facies (n = 29) has elevated Sn (median = 11.3 ppm) compared to chalcopyrite from the other sulfide facies. Other than sphalerite, chalcopyrite has the highest Zn which is highest in the pyrrhotite-dominated facies (median = 633 ppm)

Pyrrhotite ($Fe_{(1-x)}S$) has a mineral formula that ranges from $Fe_{0.804-0.859}S_{1.000}$, with Fe and S ranging from 56.99-59.99 wt% and 39.96-41.59 wt%, respectively. Pyrrhotite contains the highest Ni when compared to the other main sulfide minerals. Nickel concentrations are up to 4.93 wt% and are highest in the chalcopyrite-pyrrhotite-dominated facies (median = 1.81 wt%); high Ni values are likely attributed to inclusions in pyrrhotite. Cobalt concentrations are up to 5270 ppm and are highest in the pyrrhotite-dominated facies (median = 296 ppm). Other elements in pyrrhotite include Ti, Cr, Mn, Cu, Zn, As, Se, Ag, Sb, Te, Hg, Tl, Bi, and Pb. Pyrrhotite contains the highest Ti (< 24.5 ppm), Sb (< 200 ppm), Te (< 312.20 ppm) when compared to the other main sulfide minerals. Pyrrhotite from the pyrite-dominated facies has elevated Ti (median = 13.0 ppm) compared to pyrrhotite from the other sulfide facies. Pyrrhotite from the pyrrhotite-dominated facies has elevated Sb (median = 1.25 ppm) and Te (median = 1.20 ppm) compared to pyrrhotite from the other sulfide facies.

Sphalerite (ZnS) has a mineral formula that ranges from $(Zn_{0.799-0.907}Fe_{0.057-0.184})S_{1.000}$, with Zn and S ranging from 54.73-62.29 wt% and 32.91-33.75 wt%, respectively. Iron concentrations are up to 10.78 wt% Fe and are highest in the pyrrhotite-dominated facies (median = 6.49 wt%); high Fe concentrations are most likely due to the substitution of Fe for Zn in sphalerite. Copper concentrations are up to 1.10 wt% Cu and are highest in the pyrite-dominated facies (median = 1380 ppm); high Cu values are likely attributed to chalcopyrite disease in sphalerite. Nickel and Co concentrations are up to 1870 ppm and 1300 ppm, respectively and are highest in the pyrrhotite-dominated facies (median = 944 ppm and 1080 ppm, respectively). Other elements in sphalerite include V, Cr, Mn, Cu, As, Se, Ag, Cd, Sn, Sb, Te, Hg, Tl, and Pb. Sphalerite contains the highest Mn (< 148 ppm), Ag (< 2240 ppm), Cd (< 5070 ppm), and Hg (< 3.03 wt%) when compared to the other main sulfide minerals. Sphalerite from the pyrite-dominated facies (n = 8) has elevated Mn (median = 95.8 ppm), Ag (median = 1580 ppm), and Hg (median = 7210 ppm) compared to sphalerite from the other sulfide facies. Sphalerite from the pyrrhotite-dominated facies (n = 4) has elevated Cd (median = 4070 ppm) compared to sphalerite from the other sulfide facies. Other than chalcopyrite, sphalerite has the highest Cu which is highest in the pyrrhotite-dominated facies (median = 5810 ppm).

Cobaltite (CoAsS) has a mineral formula that ranges from $(Co_{0.655-0.935}Ni_{0.000-0.183})As_{0.600-0.993}S_{1.000}$, with Co, As, and S ranging from 26.08-34.34 wt%, 35.97-45.13 wt%, 19.36-25.79 wt%, respectively. Iron concentrations are up to 7.70 wt% and are likely due to X-rays from surrounding minerals. Nickel concentrations are up to 18.80 wt% and are highest in the pyrite-dominated facies (median = 6.08 wt%); high Ni values are likely due to possible solid solution with gersdorffite (NiAsS). Other trace elements in cobaltite include Sc, Ti, V, Cr, Mn, Se, Pd, Cd, Sn, Sb, Te, Pt, Au, Hg, Tl, and U.

Pentlandite ($(Fe,Ni)_9S_8$) has a mineral formula that ranges from $(Fe_{1.021-3.993}Ni_{2.647-5.262}Co_{0.022-2.364})_{9.000}S_{8.000}$, with Fe, Ni, and S ranging from 9.33-28.59 wt%, 25.41-39.77 wt%, and 32.53-42.10 wt%, respectively. Cobalt concentrations are up to 32.08 wt% (cobaltpentlandite) and are highest in the pyrrhotite-dominated facies (median = 2.28 wt%). Other trace elements in pentlandite include Mn, As, Se, Ag, Sn, Sb, Te, Hg, Tl, Bi and Pb.

Arsenopyrite (FeAsS) has a mineral formula that ranges from $Fe_{0.897-0.945}As_{0.829-0.919}S_{1.000}$, with Fe, As, and S ranging from 34.11-34.65 wt%, 42.74-44.64 wt%, and 20.75-22.07 wt%, respectively. Other trace elements in arsenopyrite include Cr, Mn, Co, Ni, Cu, Zn, Se, Rb, Nb, Pd, In, Sn, Sb, Te, Au, Hg, Tl, and U. Acanthite (Ag_2S) is closely associated with arsenopyrite and has a mineral formula that ranges from $Ag_{1.174-1.302}S_{1.000}$, with Ag and S ranging from 62.00-69.45 wt% and 15.66-16.04 wt%, respectively, as well as Sb (< 13.35 wt%) and Cd (< 5700 ppm). In one analysis, Au is 1.55 wt% but is otherwise found in trace quantities. Electrum is also closely associated with arsenopyrite, but the results were outside of the total cut-off for EPMA (98-102 wt%) possibly due to small grain size and challenges when polishing for EPMA analysis.

Bornite (Cu_5FeS_4) has a mineral formula that ranges from $Cu_{4.590-4.826}Fe_{0.996-1.081}S_{4.000}$, with Cu, Fe, and S ranging from 60.47-62.27 wt%, 11.35-12.48 wt%, and 26.05-26.58 wt%, respectively. Other trace elements in bornite include Ti, V, Cr, Mn, Zn, As, Se, Pd, Sb, Au, Hg, Tl, and U.

Magnetite (Fe_3O_4) has a mineral formula that ranges from $Fe^{2+}_{7.965-7.985}Fe^{3+}_{15.637-16.000}O_{32.000}$ and contains 90.43-92.29 wt% FeO. Nickel and Co concentrations are up to 245 ppm and 40.90 ppm, respectively. Other trace elements in magnetite include Sc, Ti, V, Cr, Cu, Zn, As, In, Sn, Tl, U, Pb. Magnetite preferentially includes Ti (< 2660 ppm), V (< 2220 ppm), and Cr (< 4.62 wt%) over the sulfide minerals. Chromite ($FeCr_2O_4$) is closely associated with magnetite contains Cr_2O_3 and FeO concentrations that range from 32.24-50.37 wt% and 18.29-26.28 wt%, respectively, and Al_2O_3 and MgO concentrations that range from 12.91-31.42 wt% and 8.93-14.52 wt%, respectively; these high values are likely due to possible solid solution with chrome spinel. Other trace elements in chromite include Sc, Ti, V, Mn, Co, Cu, and Zn.

3.5.2.3. Sulfur Isotope Compositions

Sulfur isotope data for Tilt Cove can be found in Figure 3.8D-F.

Pyrite at Tilt Cove has $\delta^{34}S$ values that range from +3.42 to +23.57‰ (median +11.9 ± 4.73‰, n = 22). The $\delta^{34}S$ values in pyrite generally overlap based on texture, where recrystallized pyrite grains have $\delta^{34}S$ values that range from +9.32 to +23.57‰ (median +12.56 ± 4.14‰, n = 10), annealed pyrite grains have $\delta^{34}S$ values that range from +9.94 to +14.10‰ (median +10.87 ± 1.56‰, n = 4), and cataclastic pyrite has $\delta^{34}S$ values that range from +3.42 to +21.62‰ (median +13.71 ± 6.08‰, n = 8).

Chalcopyrite has $\delta^{34}S$ values that range from +2.82 and +19.23‰ (median 11.13 ± 4.02‰, n = 21). Chalcopyrite was analyzed from the chalcopyrite-pyrrhotite-dominated facies, pyrrhotite-dominated facies, and pyrite-dominated facies. Samples from the chalcopyrite-pyrrhotite-dominated facies, where chalcopyrite is intergrown with pentlandite and pyrrhotite, have the highest the highest $\delta^{34}S$ values with a median of +16.30 ± 1.58‰ (n = 5), where the sample from the pyrrhotite-dominated facies, where chalcopyrite is intergrown with pentlandite stringers and massive pyrrhotite, has the overall lowest $\delta^{34}S$ values with a value of +3.42‰ (n = 1).

Pyrrhotite has $\delta^{34}S$ values that range from +5.62 to +16.38‰ (median +13.66 ± 4.04‰, n = 11). Pyrrhotite was analyzed from the chalcopyrite-pyrrhotite-dominated facies, pyrrhotite-dominated facies, and pyrite-dominated facies. Samples from the chalcopyrite-pyrrhotite-dominated facies, where pyrrhotite is intergrown with pentlandite and chalcopyrite, have the highest $\delta^{34}S$ values with a median of +15.59 ± 0.38‰ (n = 5), whereas samples from the pyrrhotite-dominated facies, where pyrrhotite massive and is intergrown with pentlandite stringers and chalcopyrite, have the lowest $\delta^{34}S$ values with a median of +5.97 ± 0.45‰ (n = 3).

Arsenopyrite has similar $\delta^{34}S$ values that range from +9.41 to +9.47‰ (median +9.47 ± 0.029‰, n = 3). Arsenopyrite was analyzed from the pyrite-dominated facies where it surrounds pyrite grains.

3.6. DISCUSSION

3.6.1. Mineral Paragenesis

A detailed diagram of the mineral paragenesis at Betts Cove and Tilt Cove are found in Figure 3.11.

Using known geochemical and thermodynamic data from VMS deposits (e.g., Ohmoto et al., 1983; Pisutha-Arnond and Ohmoto, 1983; Lydon, 1988; Large, 1992; Ohmoto, 1996), data from actively forming seafloor massive sulfide deposits (e.g., Haymon, 1983; Janecky and Seyfried, 1984), and mineral textural data (e.g., Eldridge et al., 1983), many VMS deposits show evidence of an early, low temperature (< 300ºC) mineral assemblage that is Zn-(Pb-Ba) rich, and a later, high temperature (> 300ºC) mineral assemblage that is Cu-rich, reflecting the thermal evolution of VMS hydrothermal systems (e.g., Haymon, 1983; Lydon, 1988; Large, 1992). The sulfide minerals, their textures, relationships, and mineral chemistry in the Betts Cove and Tilt Cove deposits provide evidence for a similar thermal evolution in these deposits.

Mineralogy, isotope, and fluid inclusion work (Haymon, 1983; Ohmoto et al., 1983; Pisutha-Arnond and Ohmoto, 1983; Large, 1992) showed that minerals such as sphalerite, galena, pyrite, and barite, formed during an early, “waxing stage” where temperatures were ~ 200 to 300ºC. Thermodynamic modelling on actively forming seafloor massive sulfide deposits by Janecky and Seyfried (1984) revealed similar results in that sphalerite precipitates from fluids between 180 to 255ºC. Further, mineral texture work by Eldridge et al. (1983) suggested that sphalerite with chalcopyrite disease formed by replacement of sphalerite by chalcopyrite, implying sphalerite formed before chalcopyrite. They suggested that colloform pyrite is most associated with the early sphalerite mineralization and that pyrite coarsens and becomes more euhedral to rounded as temperatures increases. Given the information above, it is interpreted that sphalerite with chalcopyrite disease (e.g., Figure 3.6G) and relict colloform pyrite (e.g., Figures 3.6A and 3.9A) in Betts Cove and Tilt Cove reflect an early, low temperature mineral assemblage that were deposited from low temperature fluids (< 300ºC).

In contrast, chalcopyrite is interpreted to have formed during a later, thermal maximum stage of deposit formation where temperatures were ~ 280 to 380ºC (e.g., Haymon,1983; Ohmoto et al., 1983; Pisutha-Arnond and Ohmoto, 1983; and Large, 1992). This is also supported by thermodynamic modelling on actively forming seafloor massive sulfide deposits where chalcopyrite has been shown to precipitate from fluids ~ 350ºC (Janecky and Seyfried, 1984). This increase in temperature of fluids also leads to the coarsening of pyrite grains and chalcopyrite abundance and the hydrothermal system gets hotter (Eldridge et al., 1983). The chalcopyrite-pyrrhotite (e.g., Figures 3.6F and 3.9E) and euhedral pyrite (e.g., Figures 3.6B and 3.9B) mineral assemblages in both deposits are consistent with deposition from high temperature fluids (> 300ºC). Further, the occurrence of cobaltite and pentlandite in chalcopyrite and pyrrhotite (e.g., Figures 3.6H-I and 3.9F-G) at Betts Cove and Tilt Cove and arsenopyrite with coarse-grained pyrite (e.g., Figure 3.9H) at Tilt Cove suggests that they formed paragenetically later with the high temperature, Cu-rich mineral assemblages. Given that Ni and Co concentrations are elevated in pyrrhotite and coarse-grained pyrite supports a high temperature origin for cobaltite and pentlandite and deposition from high temperature fluids (> 300ºC).

These temperature-assemblage associations are supported by the Fe/Zn ratios in sphalerite for the different assemblages. Fe/Zn ratios can be used for estimating the temperatures of the hydrothermal fluid that the sphalerite precipitated from using the empirical equation of Keith et al. (2014):

$$Fe/Zn_{sphalerite} = 0.0013(T) - 0.2953$$

(Equation 3.2),

where T is the temperature (in ºC) and $Fe/Zn_{sphalerite}$ is the Fe/Zn in wt% in sphalerite. Calculated temperatures from Betts Cove range from 275 to 350ºC with the highest sphalerite temperatures in the chalcopyrite- and chalcopyrite-pyrrhotite-dominated facies and the lowest temperatures are in the pyrite- and sphalerite-pyrite-dominated facies (Figure 3.12). Similarly, the calculated temperatures from Tilt Cove range from 269 to 379ºC. The highest sphalerite temperatures from the pyrite-dominated facies are problematic, however, as these sphalerite grains were small and only inclusions within pyrite; thus, the higher Fe values (and higher temperatures of deposition) are likely an artifact of X-rays from surrounding pyrite rather than Fe in the sphalerite structure. In contrast, for sphalerite that are not inclusions in other phases and large, the highest sphalerite temperatures are in the pyrrhotite-dominated facies and the lowest temperatures are in the pyrite-dominated facies (Figure 3.12).

Magnetite at the Tilt Cove deposit is associated with but surrounds sulfide minerals (e.g., Figure 3.9J-K), suggesting it formed later than the sulfides. Magnetite is also associated with bornite, which commonly replaces chalcopyrite (e.g., Figure 3.9I), also suggesting it formed later than the chalcopyrite. The presence of late magnetite and bornite at Tilt Cove suggest another stage of thermal evolution for this deposit of low temperature (< 300ºC) and oxidizing fluids that best explain the presence of magnetite being stable (Wood, 1998; Large, 1992).

Pyrite, chalcopyrite, and certain trace minerals have textural features that indicate that metamorphism and deformation affected some of the mineralization and is consistent with documented regional greenschist metamorphism (Coish, 1977; Craig and Vokes, 1992). Pyrite with annealed and cataclastic textures (e.g., Figures 3.6D and 3.9D), both of which have interstitial chalcopyrite, are interpreted to have formed during late, low to medium grade metamorphism via fluid-state remobilization. Under these conditions pyrite recrystallizes and behaves in a brittle manner and fractures, whereas chalcopyrite behaves ductility and infills fracture spaces, consistent with the textures observed above (Gilligan and Marshall, 1987; Marshall and Gilligan, 1987; Barrie et al., 2010; Lafrance et al., 2020). Chalcopyrite forms strain shadows around pyrite (e.g., Figure 3.6C), which is also consistent with ductile flow of chalcopyrite during metamorphism (Craig and Vokes, 1992). Further, acanthite, clausthalite, electrum, galena, and hessite form small, rounded inclusions in and are commonly associated with fractures and grain boundaries in other sulfide phases (e.g., Figures 3.6J-L and 3.9M). These textures suggest that these phases likely formed during post-VMS metamorphism where minor and trace elements (Ag, Au, Pb, Se, and Te) that were originally in the major sulfide minerals diffused out, coalesced, and formed discrete mineral phases (e.g., Craig and Vokes, 1992; Huston et al., 1995). Moreover, these elements (Ag, Au, Pb, Se, and Te) are elevated in many of the host phases (Figures 3.7 and 3.10); thus, they would have been available to form these discrete mineral phases during metamorphism.

3.6.2. Physiochemical Conditions of the Hydrothermal Fluids

Circulating hydrothermal fluids are essential to the formation of VMS deposits. When seawater enters the crust via faults and fractures, it heats up, reacts with wall rocks, and leaches metals and sulfur (e.g., Lydon, 1988, 1996; Ohmoto, 1996; Large, 1992). Seawater changes composition and heats up as it circulates through the crust forming a metal-rich hydrothermal fluid with H_2S and metal chlorides, which upon discharge onto the seafloor results in precipitation of sulfide and sulfate minerals (Lydon, 1988, 1996; Large, 1992). The mineral assemblages, textures, mineral chemistry, and mineral paragenesis of the mineralization at the Betts Cove and Tilt Cove deposits are consist with such origin while also providing insights into the physiochemical conditions of the hydrothermal fluids, metal transport, and metal deposition.

The paragenetically early sphalerite and colloform pyrite mineral assemblage is consistent with formation from low temperature fluids (< 300ºC) based on mineralogy, isotope, fluid inclusion studies (Haymon, 1983: Ohmoto et al., 1983; Pisutha-Arnond and Ohmoto, 1983; Large, 1992), thermodynamic modelling on actively forming seafloor massive sulfide deposits (Janecky and Seyfried, 1984), and mineral texture studies (Eldridge et al., 1983). These ideas are also supported by sphalerite deposition temperature calculations stated above (Figure 3.12). This early, lower temperature fluid is interpreted to have carried significant Zn and Fe as chloride complexes and H_2S which is consistent with fluid conditions that are near neural (pH ~ 7) and reducing (Lydon, 1988; Large, 1992; Lydon; 1996; Wood, 1996). The paragenetically early sulfide minerals were likely deposited by mixing of hydrothermal fluid with cold seawater resulted in a rapid decrease in temperature, an increase in pH, and metal saturation (Eldridge et al., 1983; Ohmoto, 1996).

The paragenetically late chalcopyrite-pyrrhotite (+/- euhedral pyrite, cobaltite, pentlandite, and arsenopyrite) mineral assemblage is consistent with formation from high temperature fluids (> 300ºC) as suggested from the literature (Haymon, 1983; Eldridge et al., 1983; Ohmoto et al., 1983; Pisutha-Arnond and Ohmoto, 1983; Janecky and Seyfried, 1984; Large, 1992) and supported by sphalerite deposition temperatures (Figure 3.12). The higher temperature fluid is also interpreted to have carried significant Cu (+/- Fe, Co, and Ni) as chloride complexes, which is consistent with fluid conditions that were acidic (pH < 6) and reducing (Lydon, 1988; Large, 1992; Lydon; 1996; Wood, 1996; Jansson and Liu, 2020). The paragenetically late sulfide minerals were likely deposited as the hydrothermal fluid moved upward and outward during zone refining and replaced the earlier formed minerals with chalcopyrite and pyrrhotite (+/- euhedral pyrite, cobaltite, and pentlandite) (Haymon, 1983; Lydon, 1988; Large, 1992; Lydon, 1996; Ohmoto, 1996).

The presence of late magnetite at the Tilt Cove deposit suggests a shift in hydrothermal fluid conditions. For magnetite to remain stable, the fluid conditions had to have been low temperature (< 300ºC), basic (pH 8-12), oxidizing, with low H_2S, and high fO_2 (Wood, 1998; Large, 1992). The bornite-magnetite association, where bornite replaces chalcopyrite, is also inferred to have been deposited from a more sulfur-poor and oxidized fluid (e.g., 32.00-35.9 wt% S for chalcopyrite to 26.05-26.58 wt% S for bornite). This is also supported by low Fe abundance in sphalerite in samples that contain magnetite, which is typically associated with a higher sulfidation state fluid where SO_4 rather than H_2S is the dominant sulfur species in the fluid (Hannington and Scott, 1989). The change in hydrothermal fluid conditions led to the precipitation of magnetite instead of pyrite, and bornite instead of chalcopyrite.

Mineral textures, chemistry, and paragenesis reflect changes in the physiochemical conditions of the hydrothermal fluids that resulted in the formation of the Betts Cove and Tilt Cove deposits. An early, low temperature (< 300ºC) phase involved a near neutral pH (pH ~7) and reduced fluid that carried Zn and Fe and resulted in the deposition of sphalerite and pyrite followed by a later, high temperature (> 300ºC) phase that involved acidic (pH < 7) and reducing fluids that carried Cu, Fe, Co, and Ni and deposited chalcopyrite and pyrrhotite (+/- pyrite, cobaltite, and pentlandite). The presence of late magnetite and bornite at the Tilt Cove deposit suggests a shift in hydrothermal fluid conditions to low temperature (< 300ºC), basic (pH > 7), oxidizing, and H_2S-poor fluids, resulting in the deposition of magnetite over pyrite and bornite over chalcopyrite. This shift may have resulted from infiltrating seawater through faults and fractures which oxidized and neutralized the reduced and acidic hydrothermal fluids but requires more testing (e.g., Franklin et al., 2005; Galley et al., 2007; Yıldırım et al., 2016).

3.6.3. Sources of Sulfur

Sources of reduced sulfur (H_2S) in VMS environments include H_2S derived from seawater sulfate (SO_4^{2-}), leached sulfur from basement rocks, and magmatic fluids that contain sulfur. These sources produce distinct $\delta^{34}S$ values in sulfide minerals within the deposits and many deposits have evidence for multiple sulfur sources (Ohmoto and Rye, 1979; Huston, 1999; Shanks, 2001; Seal, 2006; Huston et al., 2023).

Seawater sulfate can be reduced to H_2S in VMS environments through bacterial sulfate reduction (BSR). Sulfate reducing bacteria can survive in anoxic, low temperature (0 to 110ºC) environments with a pH of 5 to 9.5 (Seal, 2006). These bacteria reduce sulfate metabolically, through the reaction: $CH_2O + SO_4^{2-} = H_2S + 2\ HCO_3^-$ (Seal, 2006), which generally results in consistently negative $\delta^{34}S$ values especially when there is sufficient SO_4 supply with open system conditions (Herzig et al., 1998; Seal, 2006; Brueckner et al., 2015). Seawater sulfate may also be reduced to H_2S through thermochemical sulfate reduction (TSR) in higher temperature (250 to 350ºC) environments through reactions between seawater sulfate and ferrous minerals or other reductants (e.g., organic C). Thermochemical sulfate reduction results in variable, but positive $\delta^{34}S$ values (Shanks et al., 1981; Shanks, 2001; Seal, 2006). The leaching of sulfide-hosted sulfur from basement rocks can produce reduced sulfur, whereas magmatic fluids/vapours can produce reduced sulfur at temperatures below 400ºC by the disproportionation of SO_2, through the reaction: $4\ H_2O + 4\ SO_2 = H_2S + 3\ H^+ + 3\ HSO_4^-$ (Seal, 2006). The leaching of sulfur from igneous sources results in near zero $\delta^{34}S$ values, whereas the disproportionation of magmatic sulfur results in negative $\delta^{34}S$ values for sulfides derived from H_2S in this process (-15‰ to -5‰) (Seal, 2006; Huston et al., 2023).

Since the $\delta^{34}S$ values in the Betts Cove and Tilt Cove deposits are consistently positive, and that there is a lack of bacterial textures (e.g., framboidal pyrite), it is assumed that BSR and magmatic SO_2 did not contribute significantly to the reduced sulfur in these systems. Thermochemical sulfate reduction, however, may explain the wide range of positive $\delta^{34}S$ values in these deposits. The $\delta^{34}S$ values of sulfides formed through TSR are possible to predict as a function of temperature, using the equation (Ohmoto and Rye, 1979; Ohmoto and Goldhaber, 1997):

$$\delta^{34}S_{H_2S} - \delta^{34}S_{SO_4} = 1000\ln\alpha_{H_2S-SO_4} = A \times \frac{10^6}{T^2} + B \times \frac{10^3}{T} + C$$

(Equation 3.3),

where $\delta^{34}S_{H_2S}$ is the sulfur isotope composition of H_2S generated by TSR, $\delta^{34}S_{SO_4}$ is the sulfur isotope composition of seawater sulfate, $\alpha_{H_2S-SO_4}$ is the fractionation factor between H_2S and SO_4, T is the temperature in Kelvin, and A, B, and C are constants with A = -5.26, B = 0.00 and C = -6.00 (Ohmoto and Rye, 1979; Ohmoto and Goldhaber, 1997). The fractionation factor, $\alpha_{H_2S-SO_4}$, is calculated using the equation (Ohmoto and Rye, 1979; Ohmoto and Goldhaber, 1997):

$$\alpha_{H_2S-SO_4} = e^{\left(\frac{-5.26\times10^6}{T^2}-6\right)/1000}$$

(Equation 3.4),

where a minimum temperature (T) of 250ºC (523 K) and maximum temperature (T) of 350ºC (632 K) have been chosen based on average likely temperatures for the low temperature and high temperature assemblages found within Betts Cove and Tilt Cove and in light of ancient VMS deposit formation (e.g., Lydon, 1988; Ohmoto, 1996); these are also within the range that TSR occurs (Shanks et al., 1981). The resulting fractionation factor for T = 250ºC (523 K) is 0.975 and the fractionation factor for T = 350ºC (632 K) is 0.981.

The H_2S generated by TSR can then be calculated using the equation (Ohmoto and Rye, 1979; Ohmoto and Goldhaber, 1997):

$$\delta^{34}S_{H_2S} = \delta^{34}S_{SO_4(\text{parent},t)} + 1000(\alpha_{H_2S-SO_4} - 1)$$

(Equation 3.5),

where $\delta^{34}S_{SO_4(parent,t)}$ is the $\delta^{34}S$ value of SO_4^{2-} at some time (t) relative to the parent composition of seawater sulfate at $t = 0$ calculated from equation 6: (Ohmoto and Rye, 1979; Ohmoto and Goldhaber, 1997):

$$\delta^{34}S_{SO_4(parent,t)} = \delta^{34}S_{SO_4(parent,t=0)} + 1000 \times f^{(\alpha_{H_2S-SO_4}-1)} - 1000$$

(Equation 3. 6),

where f is the atomic fraction of the parent SO_4^{2-} reduced to H_2S relative to the originally amount of SO_4^{2-} present (when $f = 1$ no sulfate has been reduced). It can be assumed that $f = 1$ because VMS systems are generally considered to be open systems with ample sulfate supply, particularly when the ocean is oxygenated and there was abundant sulfate in the Phanerozoic oceans (Herzig et al., 1998; Seal, 2006; Brueckner et al., 2015). It is also assumed that seawater sulfate during the early Ordovician has a $\delta^{34}S_{SO_4(parent,t=0)}$ is 30.0‰ (Kampschulte and Strauss, 2004). $\delta^{34}S$ of H_2S derived from Ordovician seawater sulfate can be calculated using Equation 5. The $\delta^{34}S$ values of the main sulfide minerals (pyrite, chalcopyrite, and pyrrhotite) formed through TSR and precipitating from the derived H_2S can be calculated equation 7 (Ohmoto and Rye, 1979; Ohmoto and Goldhaber, 1997):

$$\delta^{34}S_{i(TSR)} = \frac{A \times 10^6}{T^2} + \delta^{34}S_{H_2S}$$

(Equation 3.7),

where i is the sulfide mineral in question (pyrite, chalcopyrite, and pyrrhotite) and A is a constant for each sulfide mineral, where $A_{pyrite} = 0.400$, $A_{chalcopyrite} = -0.050$, and $A_{pyrrhotite} = 0.100$, and $\delta^{34}S$ H_2S is the H_2S generated from TSR of seawater sulfate (Kajiwara and Krouse, 1971). The modelled results are presented in Table 3.3 and precited $\delta^{34}S$ values for sulfides derived from

TSR range from +6.56‰ to +10.6‰ for pyrite, +5.28‰ to +10.8‰ for chalcopyrite, and +5.46‰ to +10.9‰ for pyrrhotite.

The measured range of $\delta^{34}S$ values at Betts Cove and Tilt Cove overlap the modelled results, but many range to higher and lower $\delta^{34}S$ than modelled results; therefore, TSR alone cannot entirely explain the $\delta^{34}S$ values in sulfide minerals in these deposits and additional sulfur source(s) are required.

A possible explanation for the lower $\delta^{34}S$ values in these deposits includes the mixing of reduced sulfur from TSR with reduced sulfur leached from basement rocks. The ophiolitic basement rocks to the Betts Cove and Tilt Cove deposits have arc-like signatures and it can be assumed that these rocks have $\delta^{34}S$ values that are near MORB-like at ~ 0‰ (Sakai et al., 1984). To evaluate the potential contributions from leached igneous and TSR sulfur, mixing equations have been utilized using the equation modified from Faure and Mensing (2005):

$$\delta^{34}S_{mix} = b \times \delta^{34}S_{TSR} + (1 - b) \times \delta^{34}S_{(igneous)}$$

(Equation 3.8),

where $\delta^{34}S_{(mix)}$ is the sulfur composition of the sulfide mineral in question (*i*) and *b* is the proportion of TSR-derived sulfur (when *b* = 1, 100% of the sulfur was derived from TSR), $\delta^{34}S_{(igneous)}$ is the sulfur composition of igneous/magmatic sulfur, and $\delta^{34}S_{TSR}$ is the sulfur composition of sulfur derived from TSR. The sulfur composition of the sulfide minerals formed from igneous sulfur, $\delta^{34}S_{igneous}$ is assumed to be 0‰ (e.g., Sakai et al., 1984). The results are presented in Table 3.4 and show that at Betts Cove, 20% of the reduced sulfur could have come from the leaching of igneous rocks, and at Tilt Cove, between 40-50% of the reduced sulfur could have come from the leaching of igneous rocks. These results are consistent with the compilation of Huston (1999) where they showed the most important source of reduced sulfur in Phanerozoic VMS deposits is TSR and that leaching reduced sulfur from volcanic rocks decreases the $\delta^{34}S$ values and can explain $\delta^{34}S$ values that are between 0 and +5‰. The results herein are consistent with global compilations of sulfur for VMS that suggest mixing of igneous- and TSR-derived sulfur can explain the $\delta^{34}S$ variation in many VMS deposits, including Betts Cove and Tilt Cove.

While the lower $\delta^{34}S$ values can be explained by mixing of TSR-derived sulfur and leaching of igneous sulfur, the high $\delta^{34}S$ values found cannot be explained by mixing. A possible explanation for these higher $\delta^{34}S$ values includes the replacement of sulfate minerals by sulfide minerals. Sulfate minerals such as anhydrite and barite are precipitated during initial VMS formation and uniformly have high $\delta^{34}S$ like coeval seawater (Sangster, 1967; Huston et al., 2023), which would have been ~ 30‰ (Kampschulte and Strauss, 2004). During VMS evolution, sulfate minerals typically get replaced by sulfide minerals as hydrothermal fluid temperatures increase (Haymon, 1983; Lydon, 1988; Ohmoto, 1996). Although no textural evidence of sulfate replacement exists at Betts Cove and Tilt Cove, the sulfur isotope composition data suggests that this may have occurred and thus requires further testing, for example, using multiple sulfur isotopes (e.g., Ono et al., 2007).

To conclude, the sulfur at Betts Cove and Tilt Cove likely came predominantly from the mixing of TSR of seawater sulfate and leached igneous sulfur, whereas the lesser abundant samples with heavy $\delta^{34}S$ signatures likely inherited some sulfur from previously formed sulfate minerals.

3.6.4. Source of Metals

Sources of metals in VMS environments include footwall rocks beneath mineralization and in rarer cases magmatic fluids (Skirrow and Franklin, 1994; Lydon, 1996; Sillitoe et al., 1996; Dube et al., 2007; Jowitt et al., 2012). Basement rock compositions are important in determining what metals are available to be leached and deposited in VMS mineralization (Lydon, 1988; Ohmoto, 1996; Franklin et al., 2005). The footwall rocks to the Betts Cove and Tilt Cove deposits include boninites of the Betts Head Formation, sheeted dykes, and ultramafic rocks. The Betts Head Formation boninites, sheeted dykes, and ultramafic rocks have elevated Cu, Co, Ni and Cr concentrations compared to normal MORB (Coish and Church 1979; Bédard, 1999; Bédard et al., 2000), and given this, it is possible that the Cu, Co, and Ni in the Betts Cove and Tilt Cove deposits were leached from the footwall rocks. This idea has been proposed for the Ni by Papezik (1964) who inferred that the Ni at Tilt Cove came from peridotites, and it is reasonable to assume other metals could have been derived from this and other footwall rocks in the ophiolite.

To evaluate the role of these rocks as the potential source for metals in the Betts Cove and Tilt Cove deposits, a mass balance model for leaching of footwall rocks was undertaken using the modified equation of Beaudoin and Scott (2009):

$$V = \frac{C/(\rho \times g \times L \times P)}{1 \times 10^9}$$

(Equation 3.9),

where C = contained metals in the deposits in grams, ρ = density of rock in t/m^3, g = concentration of metals in the rock in g/t, L = % of leaching efficiency from the substrate, and P = % of precipitation efficiency. To determine C, we use the known previously produced tonnage for Betts Cove (118 530 t at 10% Cu; Bédard et al., 2000) and the historic mineral resource for Tilt Cove (8.16 Mt at 6.50% Cu; Galley et al., 2007). Unfortunately, these data are limiting and there is only resource data for Cu reported, so the calculation can only be used to determine the role of leaching footwall rocks for Cu; however, given the association of Cu with Ni and Co in the deposit, the Cu models are potential proxies for these elements, as well. The density (ρ) of rocks in the Betts Cove ophiolite include 2.87 t/m^3 for boninites, 2.84 t/m^3 for the sheeted dykes, and 2.92 t/m^3 for the ultramafic rocks (Spicer et al., 2010). The average Cu concentrations in boninites and sheeted dykes were taken as 60.0 g/t (Pearce et al., 1992; Ishizuka et al., 2014) and the Cu concentrations in ultramafic rocks were taken as 2.50 g/t (Parkinson and Pearce, 1998). Leaching efficiencies (L) for Cu are based on empirical studies of leaching of VMS substrates and were chosen as 100% based on studies by Ohmoto (1996) and Jowitt et al (2012). Precipitation efficiencies (P) are based on studies of modern hydrothermal vents. The precipitation efficiency is likely dependent on specific metal solubility and some elements (e.g., Cu) may have more efficient precipitation due to strong temperature and pH controls, thus, estimates of 10%, 38% and 99% efficiency are used to potentially account for this (Lydon, 1988; Ohmoto, 1996; Sánchez Mora, 2022).

The results of this leaching calculation for Cu are presented in Tables 3.5 and 3.6 and show the volume of boninitic and ultramafic rock needed to leach the Cu at Betts Cove and Tilt Cove. Geology maps from Skulski et al. (2010) and cross sections from Bédard et al. (2000) were used to estimate the volume of boninitic and ultramafic rock in the Betts Cove and Tilt Cove areas. In the Betts Cove ophiolite, there is ~ 3.64 km^3 of boninitic rock, ~ 5.16 km^3 of sheeted dykes, and ~ 6.41 km^3 of ultramafic rock. These volumes, however, are likely an underestimation. The areal extent and thicknesses of these units were likely much larger but have been removed and/or displaced by faulting and shearing given tectonic models of the area (e.g., van Staal et al, 2007; Spicer et al., 2010). Using a crustal thickness of 10 km (average thickness of modern oceanic crust) the volume of boninitic rock including the sheeted dykes is ~ 87.0 km^3 and the volume of ultramafic rock is ~ 37.3 km^3. Given this, the volumes of rock present in the ophiolite can easily explain the amount of Cu (+ Co and Ni) in the Betts Cove and Tilt Cove deposits via leaching of basement rocks alone.

Betts Cove and Tilt Cove sulfides also have high concentrations of trace metals, including Ag, As, Au, Bi, Co, Hg, Sb, Se, and Te. Arsenic, Au, and Sb are generally enriched in ophiolitic rocks from supra-subduction zones (e.g., the Troodos ophiolite) when compared to MORBs due to influence from the subducting slab (Hattori and Guillot, 2003; Patten at al., 2017; Patten et al., 2019). Therefore, the leaching of the ophiolitic footwall rocks may have also been the source of these metals in the deposits. In contrast, other elements cannot be easily explained by this, including Ag, Bi, Hg, Se, and Te, any of which are common magmatic-hydrothermal suite elements (e.g., Hannington and Scott, 1989; Sillitoe et al., 1996; Hannington et al., 1997; Huston, 2000; Dubé et al., 2007); thus, it is possible that the enrichments of these elements may be due to influence from small pulses of magmatic fluids. Moreover, similar deposits globally and locally in the Pacquet Complex, have enrichments in Ag, Bi, Hg, Se, and Te that have been attributed to magmatic-hydrothermal fluid input. For example, VMS deposits from the Troodos ophiolite in Cyprus show elevated Ag in sphalerite, Se in chalcopyrite, and Te in pyrite (Martin et al., 2019) and the nearby Ming deposit show elevated Ag in chalcopyrite, Bi and Te in galena, and Se enrichments in specific orebodies (Brueckner et al., 2016). In both deposits the authors argued for magmatic-hydrothermal fluids as the source of enrichment in these elements.

Magmatic-hydrothermal fluids often lead to distinctive alteration assemblages and mineralogical associations, including sulfosalt-rich ore mineral assemblages (e.g., tennantite, tetrahedrite, enargite), advanced argillic alteration assemblages (e.g., quartz, sericite, kaolinite, pyrophyllite, alunite, and barite), and negative $\delta^{34}S$ values (Sillitoe et al., 1996; Huston, 2000; Dube et al., 2007). These are notably absent in the Betts Cove and Tilt Cove deposits; however, the magmatic-hydrothermal contribution was most likely not the main source of metals in the deposits. Moreover, in a seawater-dominated hydrothermal system, like VMS deposits, small pulses of magmatic fluids would be potentially in much lower volume compared to seawater-derived hydrothermal fluids and might have been buffered by such fluids; therefore, possibly preventing the hybrid fluid from forming these distinct ore mineral and alteration assemblages, and negative $\delta^{34}S$ signatures. Considering the above, episodic, short-lived magmatic pulses may have added to the metal budget to the Betts Cove and Tilt Cove deposits, such as the underlying gabbroic magma chambers (e.g., Martin, et al., 2019), but they were not the dominant metal contributor to the mineralization, and the extent of their influence is not well understood and requires further testing.

Within the Betts Cove and Tilt Cove deposits Cu, Co, and Ni concentrations, potentially As, Au, and Sb can be best explained by the leaching of ophiolitic footwall rocks; however, other magmatic-hydrothermal trace metals (Ag, Bi, Hg, Se, and Te) may require a magmatic fluid input.

3.6.5. Genetic Models: Summary

The Betts Cove and Tilt Cove deposits formed in multiple stages, including: (1) an initial stage that involved low temperature, near neutral pH, and reduced fluids where Zn and Fe were transported and deposited as sphalerite and pyrite via mixing of hydrothermal fluids with cold seawater, and (2) a later depositional stage where high temperature, acidic, and reducing fluids carried Cu-Fe-Co-Ni and deposited chalcopyrite-pyrrhotite-(cobaltite-pentlandite)-rich assemblages; this stage also involved zone refining and replacement of earlier formed Zn-Fe-rich assemblages by the chalcopyrite-pyrrhotite-rich assemblages. At Tilt Cove, a third phase of magnetite deposition occurred and likely involved a low temperature, basic, oxidized, H_2S-poor fluid.

The enrichment of some trace metals (e.g., Ag, Bi, Hg, Se, and Te) is not entirely explained by the leaching of mafic and ultramafic footwall rocks; therefore, it is suggested that magmatic fluids potentially added some metals to the deposits during their formation. This mostly likely occurred over the entirety of the evolution of these deposits as the epithermal suite of metals occurs in varying amounts in all mineral facies, and therefore, stages of deposit formation (Figure 3.13). Both deposits show mineralogical and geochemical similarities to other deposits with known magmatic-hydrothermal contributions and suggests that magmatic fluids may be important in other mafic-(Cyprus)-type VMS deposits in the Appalachians and similar deposits globally.

3.7. CONCLUSIONS

The following conclusions have been made:

1. The mineralization at Betts Cove and Tilt Cove consists of stringer-type stockwork mineralization dominated by pyrite, chalcopyrite, pyrrhotite, and sphalerite, and magnetite at Tilt Cove. Accessory minerals include cobaltite and pentlandite and trace phases include acanthite, arsenopyrite, bornite, chromite, clausthalite, electrum, galena, and hessite.

2. Mineral textures, chemistry, and paragenesis reflect two stages of deposit formation, including, (1) low temperature (< 300ºC), near neutral pH (pH ~7), and reducing fluids, that carried Zn and Fe and deposited sphalerite and pyrite, and (2) high temperature (> 300ºC), acidic (pH < 7), and reducing fluids, that carried Cu, Fe, Co, and Ni and deposited chalcopyrite and pyrrhotite (+/- pyrite, cobaltite, and pentlandite).
3. The presence of late magnetite at the Tilt Cove deposit suggests a third stage of deposit formation in this deposit and a shift in hydrothermal fluid conditions to low temperature (< 300ºC), basic (pH > 7), oxidizing, and H_2S poor fluids, resulting in the deposition of magnetite over pyrite.
4. Leaching of ophiolitic, Cu-, Co-, Ni-, As-, Au-, and Sb-bearing footwall rocks and potentially episodic, short-lived magmatic-hydrothermal fluid pulses were most likely responsible for the metal budget of the Betts Cove and Tilt Cove deposits.
5. Variable and positive sulfur isotope compositions ($\delta^{34}S$) indicate that thermochemical sulfate reduction (TSR) of seawater sulfate and the mixing with leached igneous sulfur were the primary sources of reduced sulfur (H_2S) at Betts Cove and Tilt Cove. Some highly positive sulfur isotope compositions can be explained by the replacement of sulfate minerals by sulfide minerals.

3.8. REFERENCES

Bachinski, D.J., 1977. Sulfur isotopic composition of ophiolitic cupriferous iron sulfide deposits, Notre Dame Bay, Newfoundland. Economic Geology, v. 72, p. 243-257.

Barrie, C.D., Boyle, A.P., Cook, N.J., Prior, D.J., 2010. Pyrite deformation textures in the massive sulfide ore deposits of the Norwegian Caledonides. Tectonophysics, v. 483, p. 269-286.

Barrie, C.D., Boyce, A.J., Boyle, A.P., Williams, P.J., Blake, K., Ogawara, T., Akai, J., Prior, D.J., 2009. Growth controls in colloform pyrite. American Mineralogist, v. 94, p. 415-429.

Beaudoin, Y., Scott, S.D., 2009. Pb in the PACMANUS sea-floor hydrothermal system, eastern Manus basin: numerical modelling of a magmatic versus leached origin. Economic geology, v. 104, p. 749-758.

Bédard, J.H., 1999. Petrogenesis of boninites from the Betts Cove ophiolite, Newfoundland, Canada: identification of subducted source components. Journal of Petrography, v. 40, p. 1853-1889.

Bédard, J.H., Lauzière, K., Tremblay, A., Douma, S.L., Dec, T., 2000. Betts Cove ophiolite and its cover rocks, Newfoundland. Natural Resources Canada, Geological Survey of Canada Bulletin, 550, p. 1-76.

Bédard, J.H., Lauzière, K., Tremblay, A., Sangster, A., 1998. Evidence for forearc seafloor-spreading from the Betts Cove ophiolite, Newfoundland: oceanic crust of boninitic affinity. Tectonophysics, v. 284, p. 233-245.

Brueckner, S.M., Piercey, S.J., Layne, G.D., Piercey, G., Sylvester, P., 2015. Variations of sulphur isotope signatures in sulphides from the metamorphosed Ming Cu(−Au) volcanogenic massive sulphide deposit, Newfoundland Appalachians, Canada. Mineral Deposita, v. 50, p. 619-640.

Brueckner, S.M., Piercey, S.J., Pilote, J., Layne, G.D., Sylvester, P.J., 2016. Mineralogy and mineral chemistry of the metamorphosed and precious metal-bearing Ming deposit, Canada. Ore Geology Reviews, v. 72, p. 914-939.

Coish, R.A., 1977. Ocean floor metamorphism in the Betts Cove ophiolite, Newfoundland. Contributions to Mineralogy and Petrology, v. 60, p. 255-270.

Coish, R.A., Church, W.R., 1979. Igneous geochemistry of mafic rocks in the Betts Cove ophiolite, Newfoundland. Contributions to Mineralogy and Petrology, v. 70, p. 29-39.

Coish R.A., Hickey, R., Frey, F.A., 1982. Rare earth element geochemistry of the Betts Cove ophiolite, Newfoundland: complexities in ophiolite formation. Geochimica et Cosmochimica Acta, v. 46, p. 2117-2134.

Cook, D.R., Simmons, S.F., 2000. Characteristics and genesis of epithermal gold deposits. Reviews in Economic Geology, v. 13, p. 221-244.

Craig, J.R., and Vokes, F.M., 1992. Ore mineralogy of the Appalachian–Caledonian stratabound sulfide deposits. Ore Geology Reviews, v.7, p. 77–123.

Droop, G.T.R., 1987. A general equation for estimating Fe^{3+} concentrations in ferromagnesian silicates and oxides from microprobe analyses, using stoichiometric criteria. Mineralogical Magazine, v. 51, p. 431-435.

Dubé, B., Gosselin, P., Mercier-Langevin, P., Hannington, M., and Galley, A., 2007, Gold-rich volcanogenic massive sulphide deposits, in Goodfellow, W. D., ed., Mineral Deposits of Canada: A Synthesis of Major Deposit-types, District Metallogeny, the Evolution of

Geological Provinces, and Exploration Methods, Special Publication 5, Mineral Deposits Division, Geological Association of Canada, p. 75-94.

Dunning, G.R., Krogh, T.E., 1985. Geochronology of ophiolites of the Newfoundland Appalachians. Canadian Journal of Earth Sciences, v. 22, p. 1659-1670.

Eldridge, C.S., Barton, P.B., Ohmoto, H., 1983. Mineral textures and their bearing on formation of the Kuroko orebodies. Economic Geology Monograph, v. 5, p. 241-281.

Eldridge, C.S., Bourcier, W.L., Ohmoto, H., Barnes, H.L., 1988. Hydrothermal inoculation and incubation of the chalcopyrite disease in sphalerite. Economic Geology, v. 83, p. 987-989.

Faure, G., Mensing, T.M., 2005. Isotopes: principles and applications, third edition. Wiley, University of California, 897 p.

Franklin, J.M., Gibson, H.L., Jonasson, I.R., Galley, A.G., 2005. Volcanogenic massive sulfide deposits. Economic Geology 100th Anniversary Volume, p. 523-560.

Galley, A.G., Hannington, M.D., Jonasson, I.R., 2007. Volcanogenic massive sulphide deposits, in Goodfellow, W.D., ed., Mineral Deposits of Canada: A Synthesis of Major Deposit-Types, District Metallogeny, the Evolution of Geological Provinces, and Exploration Methods: Geological Association of Canada, Mineral Deposits Division, Special Publication No. 5, p. 141-161.

Gilligan, L.B., Marshall, B., 1987. Textural evidence for remobilization in metamorphic environments. Ore Geology Reviews, v. 2, p. 205-229.

Hannington, M.D., Poulsen, K.H., Thompson, J.F.H., Sillitoe, R.H., 1997. Volcanogenic gold in the massive sulfide environment. Reviews in Economic Geology, v. 8, p. 325-356.

Hannington, M.D., Scott, S.D., 1989. Sulfidation equilibria as guides to gold mineralization in volcanogenic massive sulfides: evidence from sulfide mineralogy and the composition of sphalerite. Economic Geology, v. 84, p. 1978-1995.

Hattori, K.H., Guillot, S., 2003. Volcanic fronts form as a consequence of serpentinite dehydration in the forearc mantle wedge. Geology, v. 31, p. 525-528.

Haymon, R.M., 1983. Growth history of hydrothermal black smoker chimneys. Nature, v. 301, p. 695-698.

Hedenquist, J.W., Arribas R, A., Gonzalez-Urien, E., 2000. Exploration for epithermal gold deposits. Reviews in Economic Geology, v. 13, p. 245-277.

Herzig, P.M., Hannington, M.D., Arribas Jr. A., 1998. Sulfur isotopic composition of hydrothermal precipitates from the Lau back-arc: implications for magmatic contributions to seafloor hydrothermal systems. Mineralium Deposita, v. 33, p. 226-237.

Hibbard, J., 1983. Geology of the Baie Verte Peninsula, Newfoundland. Newfoundland Department of Mines and Energy, Memoir 2, 279 p.

Huston, D.L., 2000. Gold in volcanic-hosted massive sulfide deposits: distribution, genesis, and exploration. SEG Reviews, v. 13, p. 401-426.

Huston, D.L., Laflamme, C., Beaudoin, G., Piercey, S.J., 2023. Light stable isotopes in volcanic-hosted massive sulfide ore systems, in D. Huston and J. Gutzmer (eds.), Isotopes in Economic Geology, Metallogenesis and Exploration, Mineral Resource Reviews, Springer, Cham, p. 245-282.

Huston, D.L., Sie, S.H., Suter, G.F., Cooke, D.R., Both, R.A., 1995. Trace elements in sulfide minerals from Eastern Australian volcanic-hosted massive sulfide deposits: Part I. Proton microprobe analyses of pyrite, chalcopyrite, and sphalerite, and Part II. Selenium levels in pyrite: comparison with δ34S values and implications for the source of sulfur in volcanogenic hydrothermal systems. Economic Geology, v. 90, p. 1167-1196.

Ishizuka, O., Tani, K., Reagan, M.K., 2014. Izu-Bonin-Mariana forearc crust as a modern ophiolite analogue. Elements, v. 10, p. 115-120.

Janecky, D.R., Seyfried Jr., W.E., 1984. Formation of massive sulfide deposits on oceanic ridge crests: incremental reaction models for mixing between hydrothermal solutions and seawater. Geochimica et Cosmochimica Acta, v. 48, p. 2723-2738.

Jansson, N.F., Liu, W., 2020. Controls on cobalt and nickel distribution in hydrothermal sulphide deposits in Bergslagen, Sweden - constraints from solubility modelling. GFF, v. 142, p. 87-95.

Jowitt, S.M., Jenkin, G.R.T., Coogan, L.A., Naden, J., 2012. Quantifying the release of base metals from source rocks for volcanogenic massive sulfide deposits: Effects of protolith composition and alteration mineralogy. Journal of Geochemical Exploration, v. 118, p. 47-59.

Kajiwara, Y., Krouuse, H.R., 1971. Sulfur isotope partitioning in metallic sulfide systems. Canadian Journal of Earth Sciences, v. 8, p. 1397-1408.

Kampschultea, A., Strauss, H., 2004. The sulfur isotopic evolution of Phanerozoic seawater based on the analysis of structurally substituted sulfate in carbonates. Chemical Geology, v. 204, p. 255-286.

Keith, M., Haase, K.M., Schwarz-Schampera, U., Klemd, R., Petersen, S., Bach, W., 2014. Effects of temperature, sulfur, and oxygen fugacity on the composition of sphalerite from submarine hydrothermal vents. Geology, v. 42, p. 699-702.

Lafrance, B., Gibson, H.L., Stewart, M.S., 2020. Internal and external deformation and modification of volcanogenic massive sulfide deposits. Reviews in Economic Geology, v. 21, p. 147-171.

Large, R.R, 1992. Australian volcanic-hosted massive sulfide deposits: features, styles, and genetic models. Economic Geology, v. 87, p. 471-510.

Lydon, J.W., 1988. Volcanogenic massive sulphide deposits part 2: genetic models. Geoscience Canada Reprint Series 3, v. 15, p. 155-181.

Lydon, J.W., 1996. Characteristics of volcanogenic massive sulphide deposits: interpretations in terms of hydrothermal convection systems and magmatic hydrothermal systems. Boletin Geologico y Minero, v. 107-3 y 4, p. 15-64.

Marshall, B., Gilligan, L.B., 1987. An introduction to remobilization: information from ore-body geometry and experimental considerations. Ore Geology Reviews, v. 2, p. 87-131.

Martin, A.J., Keith, M., McDonald, I., Haase, K.M., McFall, K.A., Klemd, R., MacLeod, C.J., 2019. Trace element systematics and ore-forming processes in mafic VMS deposits: evidence from the Troodos ophiolite, Cyprus. Ore Geology Reviews, v. 106, p. 205-225.

Müller, D., Kaminski, K., Uhlig, S., Graupner, T., Herzig, P.M., Hunt, S., 2002. The transition from porphyry- to epithermal-style gold mineralization at Ladolam, Lihir Island, Papua New Guinea: a reconnaissance study. Mineralium Deposita, v. 37, p. 61-74.

Nimis, P., Zaykov, V.V., Omenetto, P., Melekestseva, I.Yu., Tesalina, S.G., Orgeval, J.-J., 2008. Peculiarities of some mafic-ultramafic- and ultramafic-hosted massive sulfide deposits from the Main Uralian Fault Zone, southern Urals. Ore Geology Reviews, v. 33, p. 49-69.

Ohmoto, H., 1972. Systematics of sulfur and carbon isotopes in hydrothermal ore deposits. Economic Geology, v. 67, p. 551-578.

Ohmoto, H., 1996. Formation of volcanogenic massive sulfide deposits: the Kuroko perspective. Ore Geology Reviews, v. 10, p. 135-177.

Ohmoto, H., Goldhaber, M.B., 1997. Sulfur and carbon isotopes. In: Barnes HL (ed) Geochemistry of hydrothermal ore deposits, third edition. John Wiley & Sons, New York, p. 517-611.

Ohmoto, H., Mizukami, M., Drummond, S.E., Eldridge, C.S., Pisutha-Arnond, V., Lenagh, T.C., 1983. Chemical processes of Kuroko formation. Economic Geology Monograph, v. 5, p. 570-604.

Ohmoto, H., Rye, R.O., 1979. Isotopes of sulfur and carbon. In: Barnes HL (ed) Geochemistry of hydrothermal ore deposits, second edition. John Wiley & Sons, New York, p. 509-567.

Ono, S., Shanks, W.C., Rouxel, O.J., Rumble, D., 2007. S-33 constraints on the seawater sulfate contribution in modern seafloor hydrothermal vent sulfides. Geochimica et Cosmochimica Acta, v. 71, p. 1170-1182.

Papezik, V. S., 1964. Nickel minerals at Tilt Cove, Notre Dame Bay, Newfoundland. Proceedings of the Geological Association of Canada, Part 2, v. 15, p. 27-32.

Parkinson, I.J., Pearce, J.A., 1998. Peridotites from the Izu–Bonin–Mariana forearc (ODP Leg 125): evidence for mantle melting and melt–mantle interaction in a supra-subduction zone setting. Journal of Petrology, v. 39, p. 1577-1618.

Paton, C., Hellstrom, J., Paul, B., Woodhead, J., Hergt, J., 2011. Iolite: freeware for the visualisation and processing of mass spectrometric data: Journal of Analytical Atomic Spectrometry, v. 26, p. 2508-2518.

Patten, C.G.C., Pitcairn, I.K., Alt, J.C., Zack, T., Lahaye, Y., Teagle, D.A.H., Markdahl, K., 2020. Metal fluxes during magmatic degassing in the oceanic crust: sulfide mineralisation at ODP site 786B, Izu-Bonin forearc. Mineralium Deposita, v. 55, p. 469-489.

Patten, C.G.C., Pitcairn, I.K., Teagle, D.A.H., 2017. Hydrothermal mobilisation of Au and other metals in supra-subduction oceanic crust: Insights from the Troodos ophiolite. Ore Geology Reviews, v. 86, p. 487-508.

Pearce, J.A., van der Laan, S.R., Arculus, R.J., Murton, B.J., Ishii, T., Peate, D.W., Parkinson, I.J., 1992. Boninite and harzburgite from Leg 125 (Bonin-Mariana forearc): a case study of magma genesis during the initial stages of subduction. Proceedings of the Ocean Drilling Program, Scientific Results, v. 125, p. 623-659.

Piercey, S.J., Hinchey, J.G., Sparkes, G.W., 2023. Volcanogenic massive sulfide (VMS) deposits of the Dunnage Zone of the Newfoundland Appalachians: setting, styles, key advances, and future research. Canadian Journal of Earth Sciences, v. 60, p. 1104-1142.

Pisutha-Arnond, V., Ohmoto, H., 1983. Thermal history, and chemical and isotopic compositions of the ore-forming fluids responsible for the Kuroko massive sulfide deposits in the Hokuroku District of Japan. Economic Geology Monograph, v. 5, p. 523-558.

Rogers, N., van Staal, C. R., Zagorevshki, I., Skulski, T., Piercey, S.J., McNicoll, V, J., 2007. Timing and tectonic setting of volcanogenic massive sulfide bearing terranes within the Central Mobile Belt of the Canadian Appalachians, in Proceedings of Exploration 07: Fifth Decennian International Conference on Mineral Exploration, p. 1199-1205.

Rollinson, H., Pease, V., 2021. Using geochemical data to understand geological processes, second edition. Cambridge University Press, Cambridge, United Kingdom, 358 p.

Sakai, H., Des Marais, D.J., Ueda, A., Moore, J.G., 1984. Concentrations and isotope ratios of carbon, nitrogen and sulfur in ocean-floor basalts. Geochimica et Cosmochimica Acta, v. 48, p. 2433-2441.

Sánchez Mora, D., Evolution of the Lucky Strike vent field, Mid-Atlantic Ridge. Unpublished Doctor of Philosophy thesis, St. John's, Newfoundland, Memorial University of Newfoundland, 270 p.

Sangster, D. F., 1967. Relative sulphur isotope abundances in strata - bound sulphide deposits. Geological Survey of Canada, Paper, 67-1B, p. 79-91.

Sangster, A.L., Douma, S.M., Lavigne, J., 2007. Base metal and gold deposits of the Betts Cove complex, Baie Verte Peninsula, Newfoundland, in Goodfellow, W.D., ed., Mineral Deposits of Canada: A Synthesis of Major Deposit-Types, District Metallogeny, the Evolution of Geological Provinces, and Exploration Methods: Geological Association of Canada, Mineral Deposits Division, Special Publication No. 5, p. 703-721.

Saunders, C. M., 1985. Controls of mineralization in the Betts Cove ophiolite. Unpublished M.Sc. thesis, Memorial University of Newfoundland, St. John's, Newfoundland, Canada, 200 p.

Seal, R.R., 2006. Sulfur isotopes geochemistry of sulfide minerals. Reviews in Mineralogy and Geochemistry, v. 61, p. 633-677.

Shanks, W.C., 2001. Stable isotopes in seafloor hydrothermal systems: vent fluids, hydrothermal deposits, hydrothermal alteration, and microbial processes. Reviews in Mineralogy and Geochemistry, v. 43, p. 469-525.

Shanks, W.C., 2013. Stable isotope geochemistry of mineral deposits, in: Holland, H.D., Turekian, K.K. (eds.), Treatise on Geochemistry, second edition. Elsevier, Oxford. 13, p. 59– 85.

Sillitoe, R. H., Hannington, M. D., and Thompson, J. F. H., 1996, High sulfidation deposits in the volcanogenic massive sulfide environment: Economic Geology, v. 91, p. 204-212.

Simmons, S.F., 2008. Precious metals in modern hydrothermal solutions and implications for the formation of epithermal ore deposits. Society of Economic Geologists Newsletter, no. 72, p. 8-12.

Skirrow, R.G., Franklin, J.M., 1994. Silicification and metal leaching in semiconformable alteration beneath the Chisel Lake massive sulfide deposit, Snow Lake, Manitoba. Economic Geology, v. 89, p. 31-50.

Skulski, T., Castonguay, S., McNicoll, V., van Staal, C., Kidd, W., Rogers, N., Morris, W., Ugalde, H., Slavinski, H., Spicer, W., Moussallam, Y., Kerr, I., 2010. Tectonostratigraphy of the Baie Verte oceanic tract and its ophiolite cover sequence on the Baie Verte peninsula. Current research, Newfoundland and Labrador Department of Natural Resources Geological Survey, Report 10-1, p. 315-335.

Spicer, B., Morris, B., Ugalde, H., Slavinski, H., and Skulski, T., 2010. Structure of the Betts Cove ophiolite complex beneath the western margin of Notre Dame Bay, Newfoundland. Canadian Journal of Earth Sciences, v. 47, p. 181-198.

Strong, D.F., Saunders, C.M., 1988. Ophiolitic sulfide mineralization at Tilt Cove, Newfoundland: controls by upper mantle and crustal processes. Economic Geology, v. 83, p. 239-255.

Swinden, H.S., Jenner, G.A., Kean, B.F., Evans, D.T.W., 1989. Volcanic rock geochemistry as a guide for massive sulphide exploration in central Newfoundland. Current research, Newfoundland Department of Mines, Geological Survey of Newfoundland, Report 89-1, p. 201-219.

Tesalina, S.G., Nimis, P., Augé, T., Zaykov, V.V., 2003. Origin of chromite in mafic-ultramafic-hosted hydrothermal massive sulfides from the Main Uralian Fault, South Urals, Russia. Lithos, v. 70, p. 39-59.

Upadhyay, H.D., Strong, D.F., 1973. Geological setting of the Betts Cove copper deposits, Newfoundland: an example of ophiolite sulfide mineralization. Economic Geology, v. 68, p. 161-167.

van Staal, C.R., Barr, S.M., 2012. Lithospheric architecture and tectonic evolution of the Canadian Appalachians and associated Atlantic Margin. Chapter 2 in Tectonic Styles in Canada: the Lithoprobe Perspective, Geological Association of Canada, Special Paper 49, p. 41-95.

van Staal, C.R., Whalen, J.B., McNicoll, V.J., Pehrsson, S., Lissenberg, C.J., Zagorevski, A., van Breemen, O., Jenner, G.A., 2007. The Notre Dame arc and the Taconic orogeny in

Newfoundland. In Hatcher, R.D., Jr., Carlson, M.P., McBride, J.H., and Martínez Catalán, J.R., eds., 4-D Framework of Continental Crust: Geological Society of America Memoir, v. 200, p. 511–552.

van Staal, C.R., Whalen, J.B., Valverde-Vaquero, P., Zagorevski, A., Rogers, N., 2009. Pre-Carboniferous, episodic accretion-related, orogenesis along the Laurentain margin of the northern Appalachians. From Murphy, J.B., Keppie, J.D. & Hynes, A.J. (eds) Ancient Orogens and Modern Analogues. Geological Society, London, Special Publications, v. 327, p. 271–316.

Walshe, J.L., Solomon, M., 1981. An investigation into the environment of formation of the volcanic-hosted Mt. Lyell copper deposits using geology, mineralogy, stable isotopes, and a six-component chlorite solid solution model. Economic Geology, v. 76, p. 246-284.

Wilkinson, J.J., Simmons, S.F., Stoffell, B., 2013. How metalliferous brines line Mexican epithermal veins with silver. Scientific Reports, v. 3, 2057, p. 1-7.

Wood, S.A., 1998. Calculation of Activity-Activity and Log fo2-pH Diagrams. Reviews in Economic Geology, Techniques in Hydrothermal Ore Deposits Geology, v. 10, p. 81-96.

Yıldırım, N., Dönmez, C., Kang, J., Lee, I., Pirajno, F., Yıldırım, E., Günay, K.H., Seo, J., Farquhar, J., S.W., Chang, 2016. A magnetite-rich Cyprus-type VMS deposit in Ortaklar: A unique VMS style in the Tethyan metallogenic belt, Gaziantep, Turkey. Ore Geology Reviews, v. 79, p. 425-442.

Zamora-Vega, O., Richards, J.P., Spell, T., Dufrane, S.A., Williamson, J., 2018. Multiple mineralization events in the Zacatecas Ag-Pb-Zn-Cu-Au district, and their relationship to the tectonomagmatic evolution of the Mesa Central, Mexico. Ore Geology Reviews, v. 102, p. 519-561.

Zhang, P.F., Zhou, M.F., Malpas, J., Robinson, P.T., 2020. Origin of high-Cr chromite deposits in nascent mantle wedges: petrological and geochemical constraints from the Neo-Tethyan Luobusa ophiolite, Tibet. Ore Geology Reviews, v. 123, 13 p.

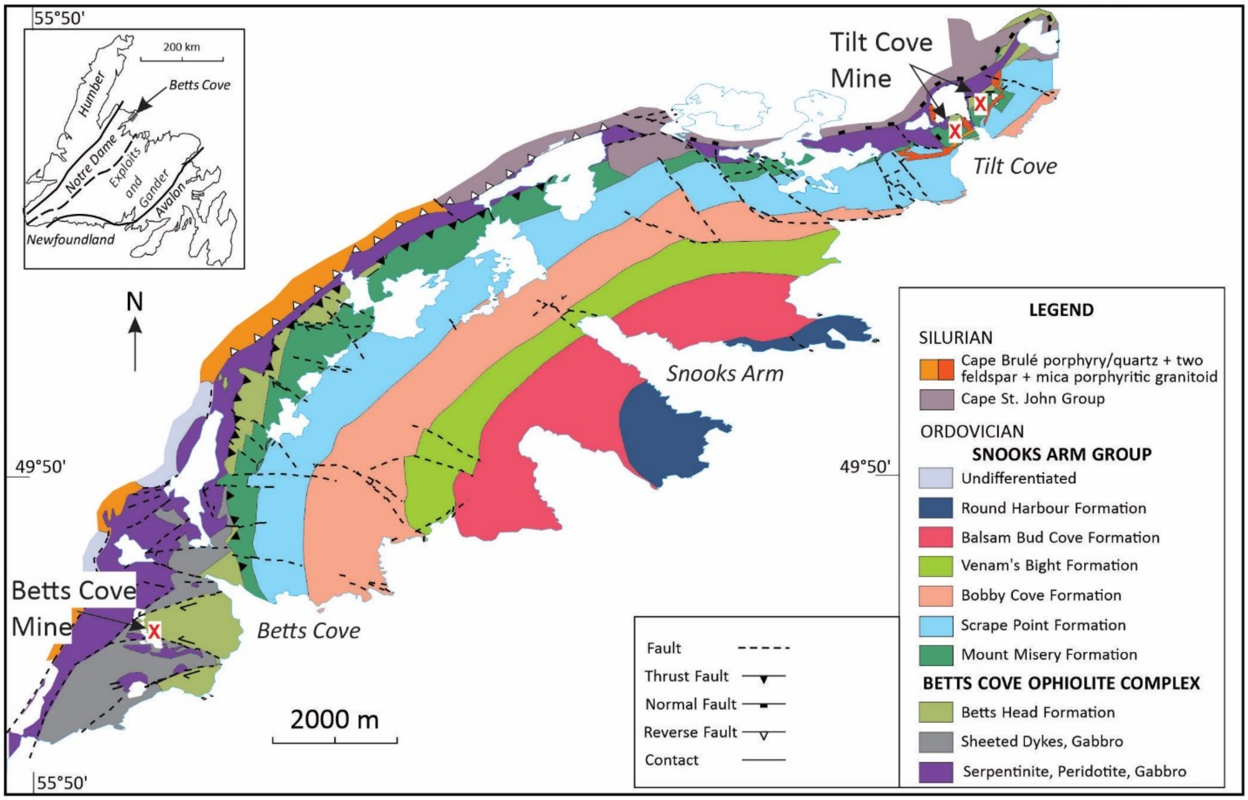

Figure 3.1. Geology of the Betts Cove ophiolite and locations of the Betts Cove and Tilt Cove deposits (from Bédard et al., 2000 and Sangster et al., 2007).

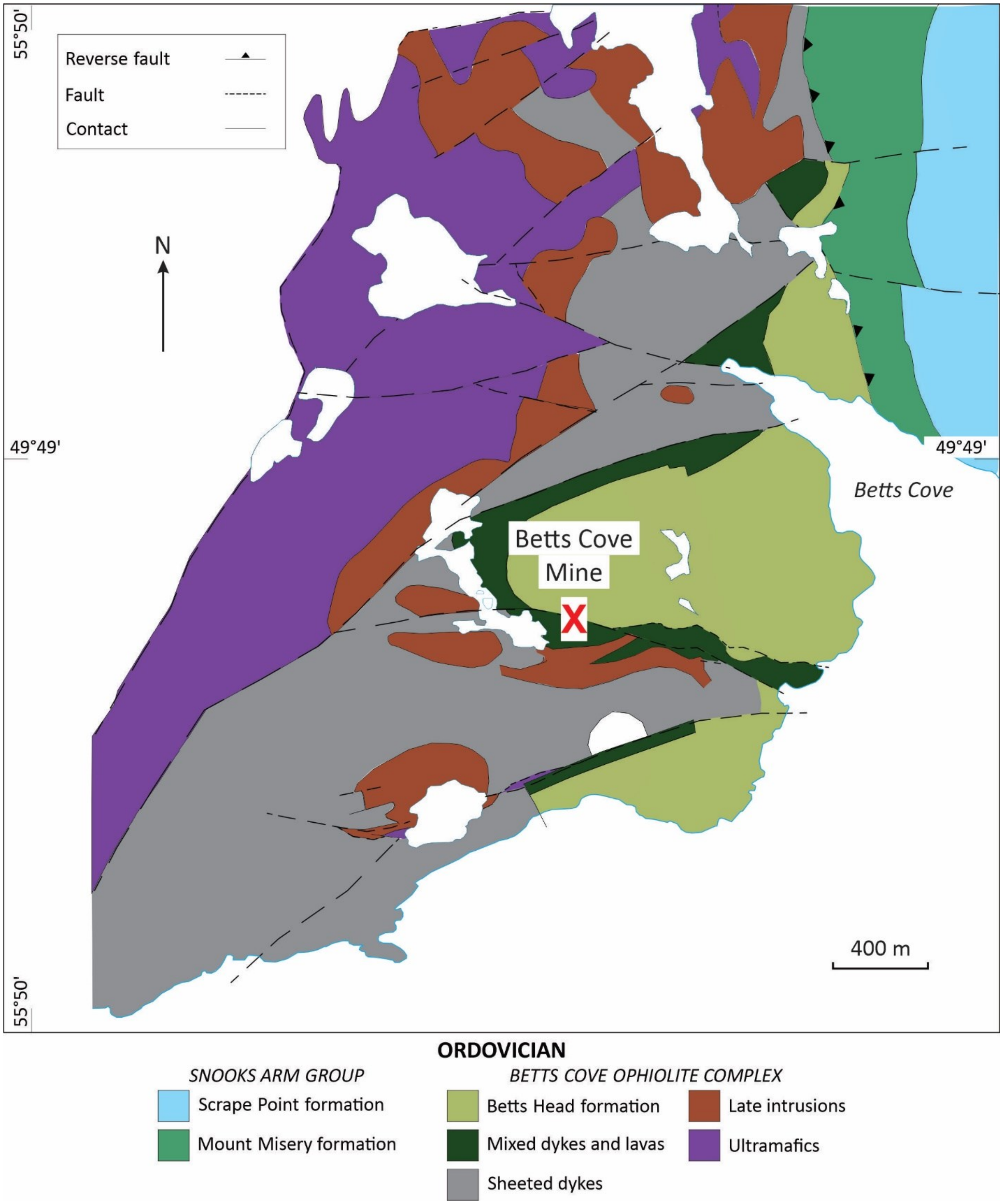

Figure 3.2. Geology of the Betts Cove deposit (from Bédard et al., 2000 and Sangster et al., 2007).

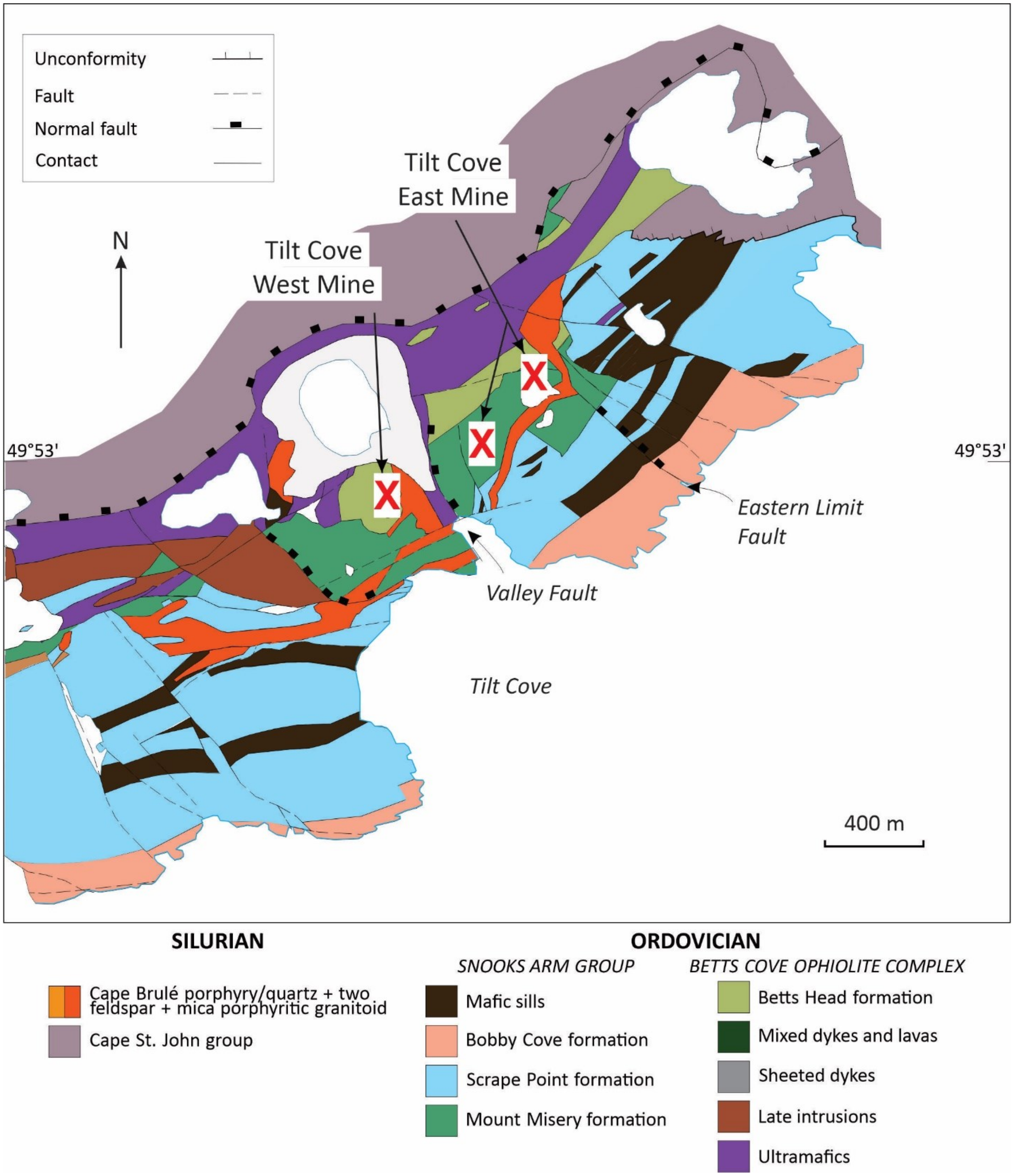

Figure 3.3. Geology of the Tilt Cove deposit (from Bédard et al., 2000 and Sangster et al., 2007).

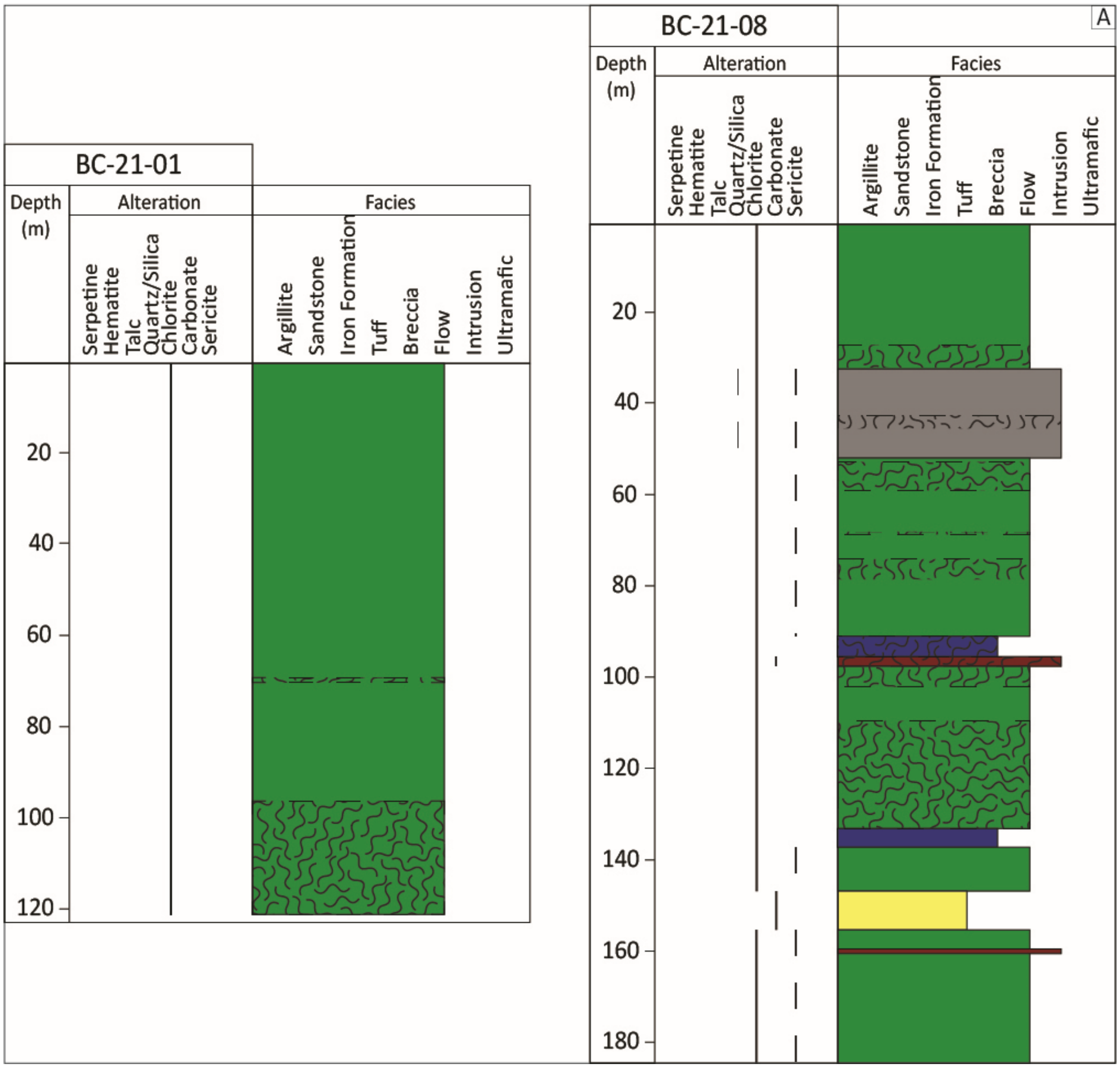

A
BC-21-01
Depth (m)
Alteration
Serpetine
Hematite
Talc
Quartz/Silica
Chlorite
Carbonate
Sericite
Facies
Argillite
Sandstone
Iron Formation
Tuff
Breccia
Flow
Intrusion
Ultramafic
20
40
60
80
100
120
BC-21-08
Depth (m)
Alteration
Serpetine
Hematite
Talc
Quartz/Silica
Chlorite
Carbonate
Sericite
Facies
Argillite
Sandstone
Iron Formation
Tuff
Breccia
Flow
Intrusion
Ultramafic
20
40
60
80
100
120
140
160
180

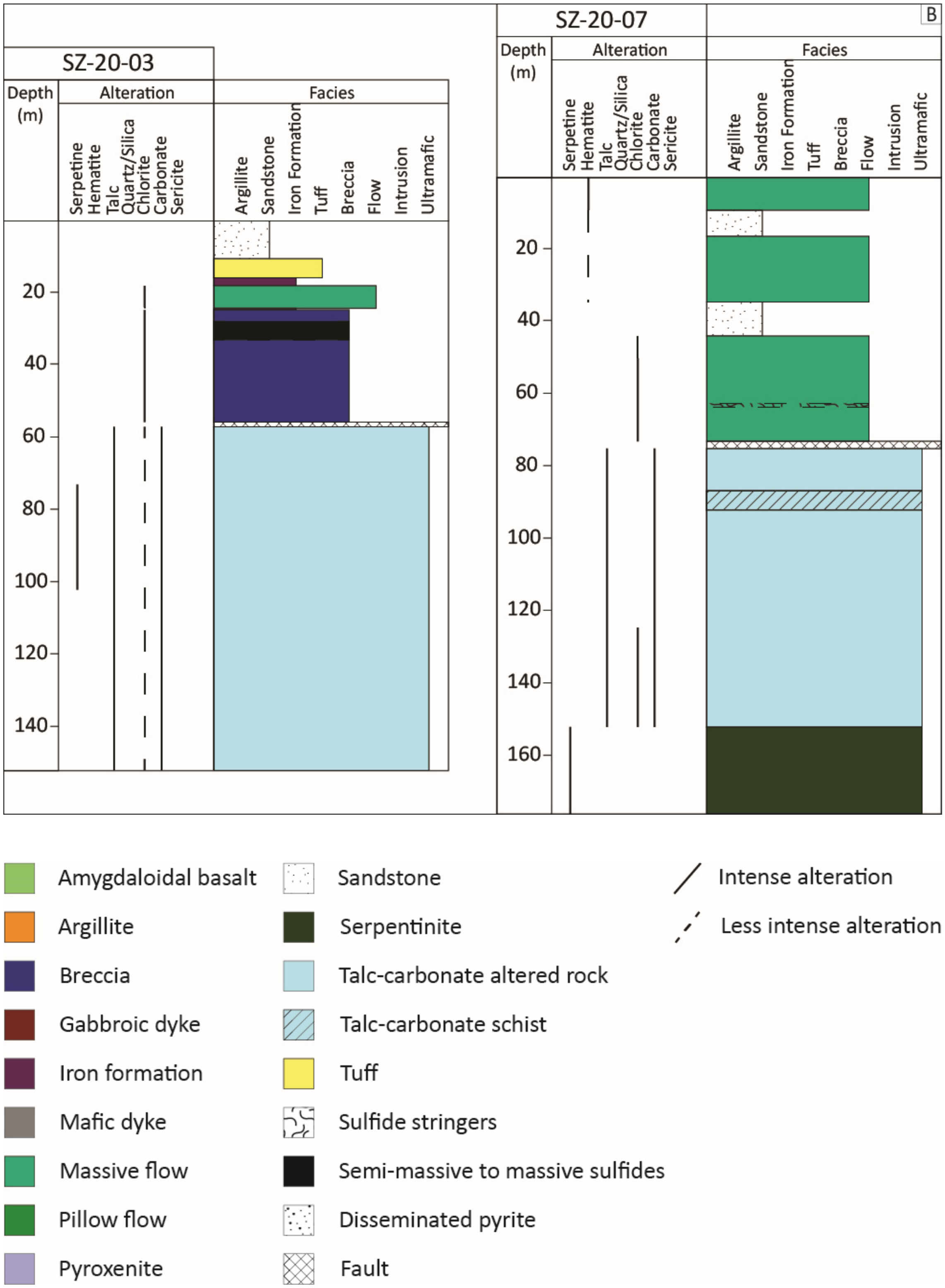

Figure 3.4. Representative graphic logs highlighting the main lithologies, alteration, and mineralization styles from: A) Betts Cove and B) Tilt Cove.

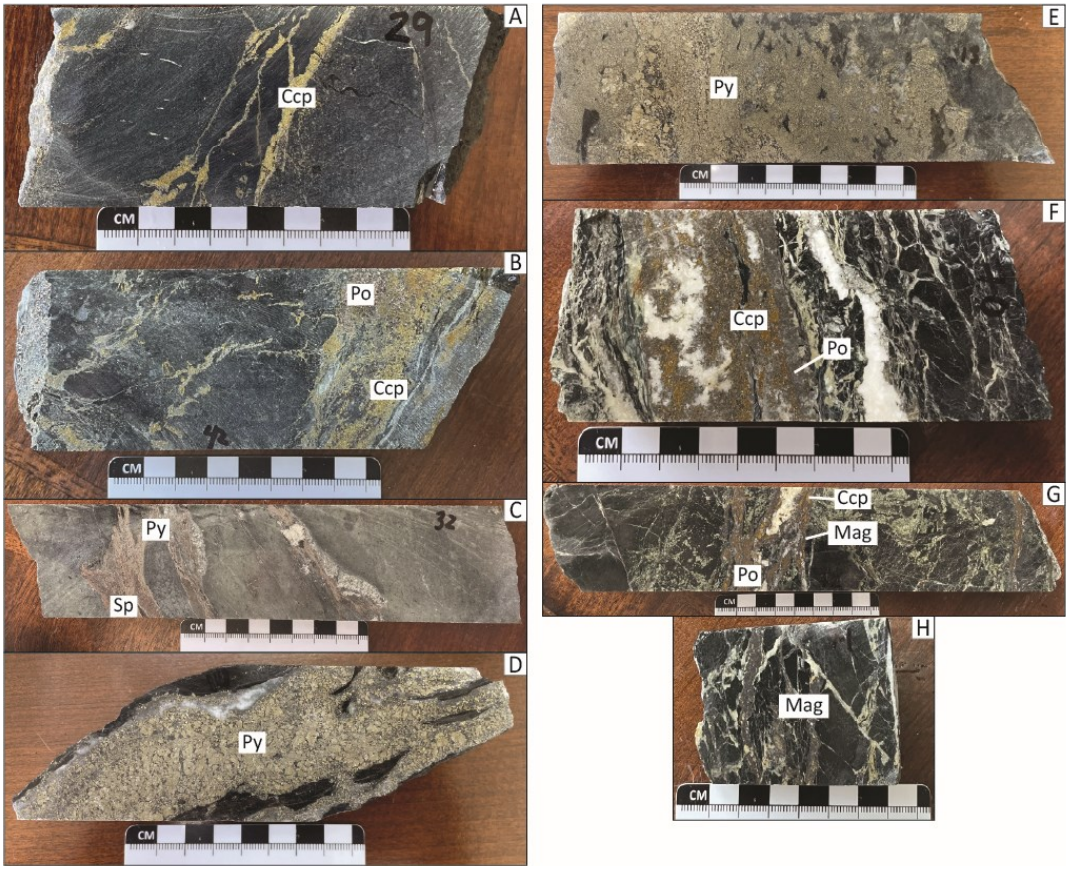

Figure 3.5. Main sulfide facies at Betts Cove, including: A) chalcopyrite-dominated facies; B) chalcopyrite-pyrrhotite-dominated facies; C) sphalerite-pyrite-dominated facies; D) pyrite-dominated facies, and at Tilt Cove, including: E) pyrite-dominated facies; F) chalcopyrite +/- pyrrhotite-dominated facies; G) pyrrhotite-dominated facies; and H) magnetite-dominated facies. Here, ccp = chalcopyrite, mag = magnetite, po = pyrrhotite, py = pyrite, and sp = sphalerite.

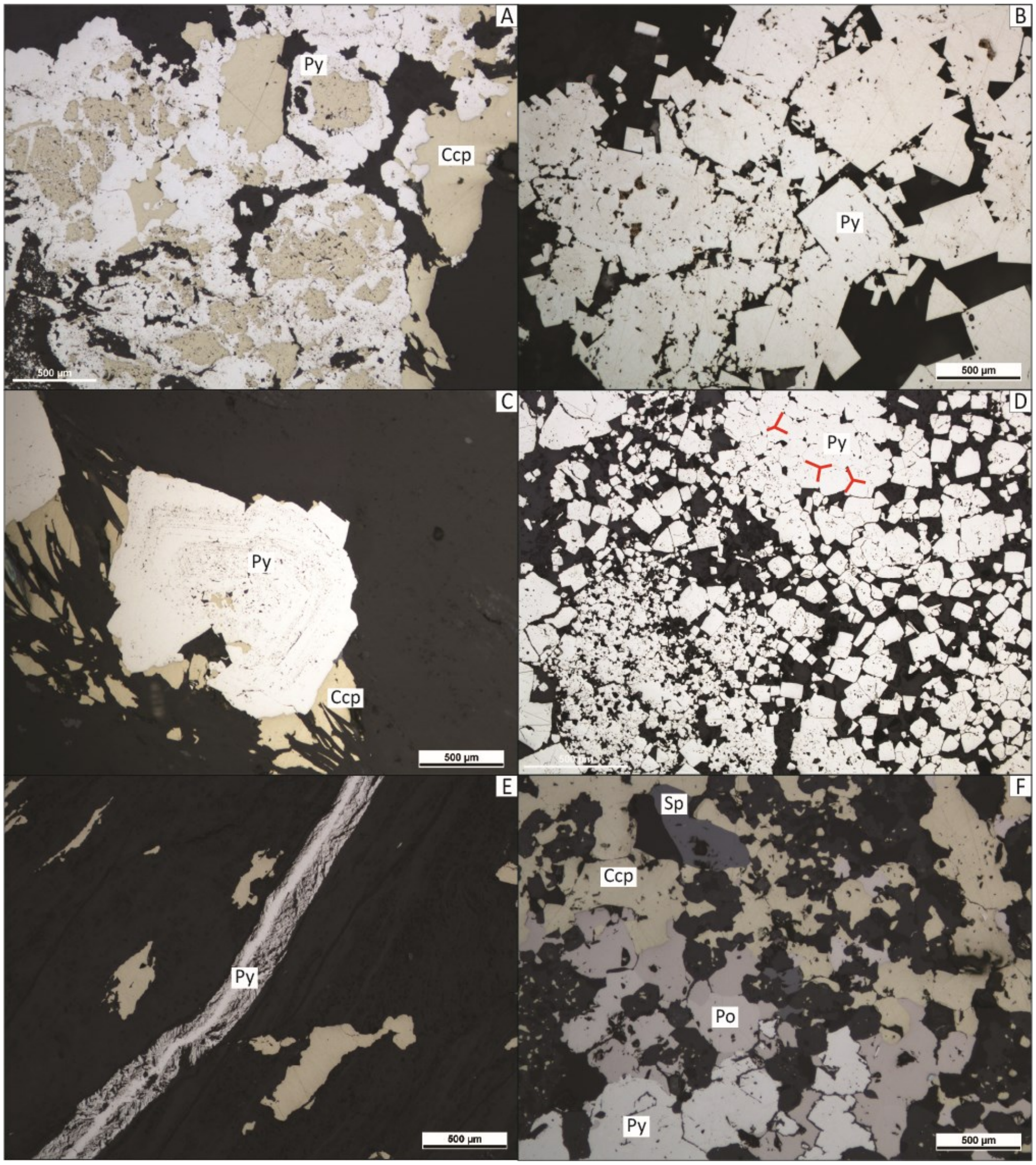
A
Py
Ccp
500 µm
B
Py
500 µm
C
Py
Ccp
500 µm
D
Py
E
Py
500 µm
F
Sp
Ccp
Po
Py
500 µm

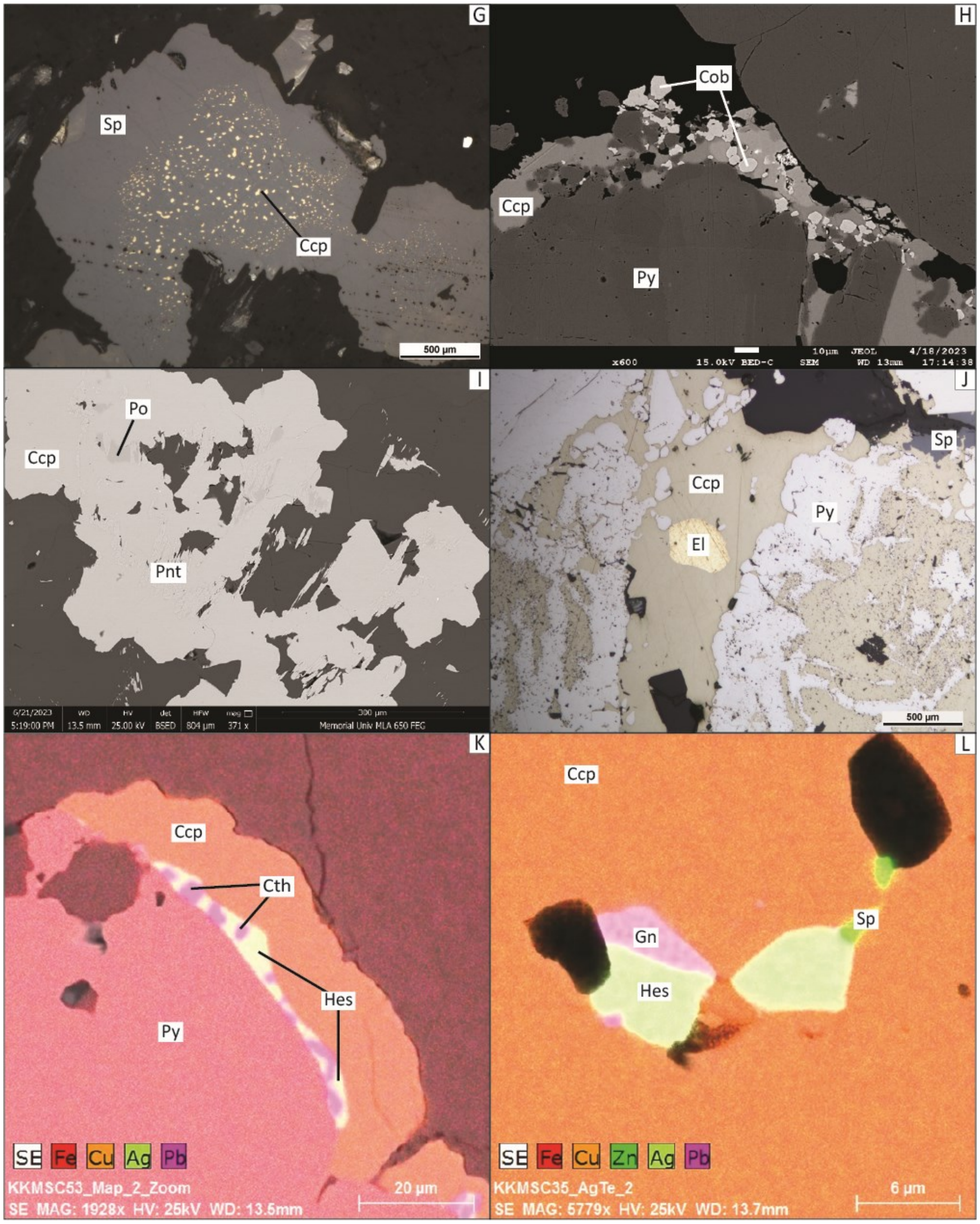
G
Sp
Ccp
500 µm
H
Cob
Ccp
Py
10µm JEOL 4/18/2023
x600 15.0kV BED-C SEM WD 13mm 17:14:38
I
Po
Ccp
Pnt
Memorial Univ MLA 650 FEG
J
Sp
Ccp
Py
El
500 µm
K
Ccp
Cth
Hes
Py
SE Fe Cu Ag Pb
KKMSC53_Map_2_Zoom
SE MAG: 1928x HV: 25kV WD: 13.5mm
20 µm
L
Ccp
Sp
Gn
Hes
SE Fe Cu Zn Ag Pb
KKMSC35_AgTe_2
SE MAG: 5779x HV: 25kV WD: 13.7mm
6 µm

Figure 3.6. Plane polarized reflected light and backscatter electron images of sulfide, selenide, and telluride mineral textures from Betts Cove, including: A) relic colloform pyrite being replaced by chalcopyrite; B) euhedral pyrite grains forming clusters; C) chalcopyrite forming a strain shadow around subhedral pyrite suggesting deformation; D) annealed pyrite grains suggesting deformation; E) pyrite vein following folliations in host rock; F) intergrown chalcopyrite-pyrrhotite assemblage (+ minor sphalerite and pyrite); G) chalcopyrite disease in sphalerite; H) subhedral cobalitite grains hosted in chalcopyrite; I) intergrown pentlandite and pyrrhotite within chalcopyrite; J) rounded electrum grain hosted in chalcopyrite; K) intergrown clausthalite and hessite along pyrite-chalcopyrite grain boundry; and L) intergrown galena and hessite in fracture in chalcopyrite. Here, ccp = chalcopyrite, cob = cobaltite, cth = clausthalite, el = electrum, gn = galena, hes = hessite, pnt = pentlandite, po = pyrrhotite, py = pyrite, and sp = sphalerite.

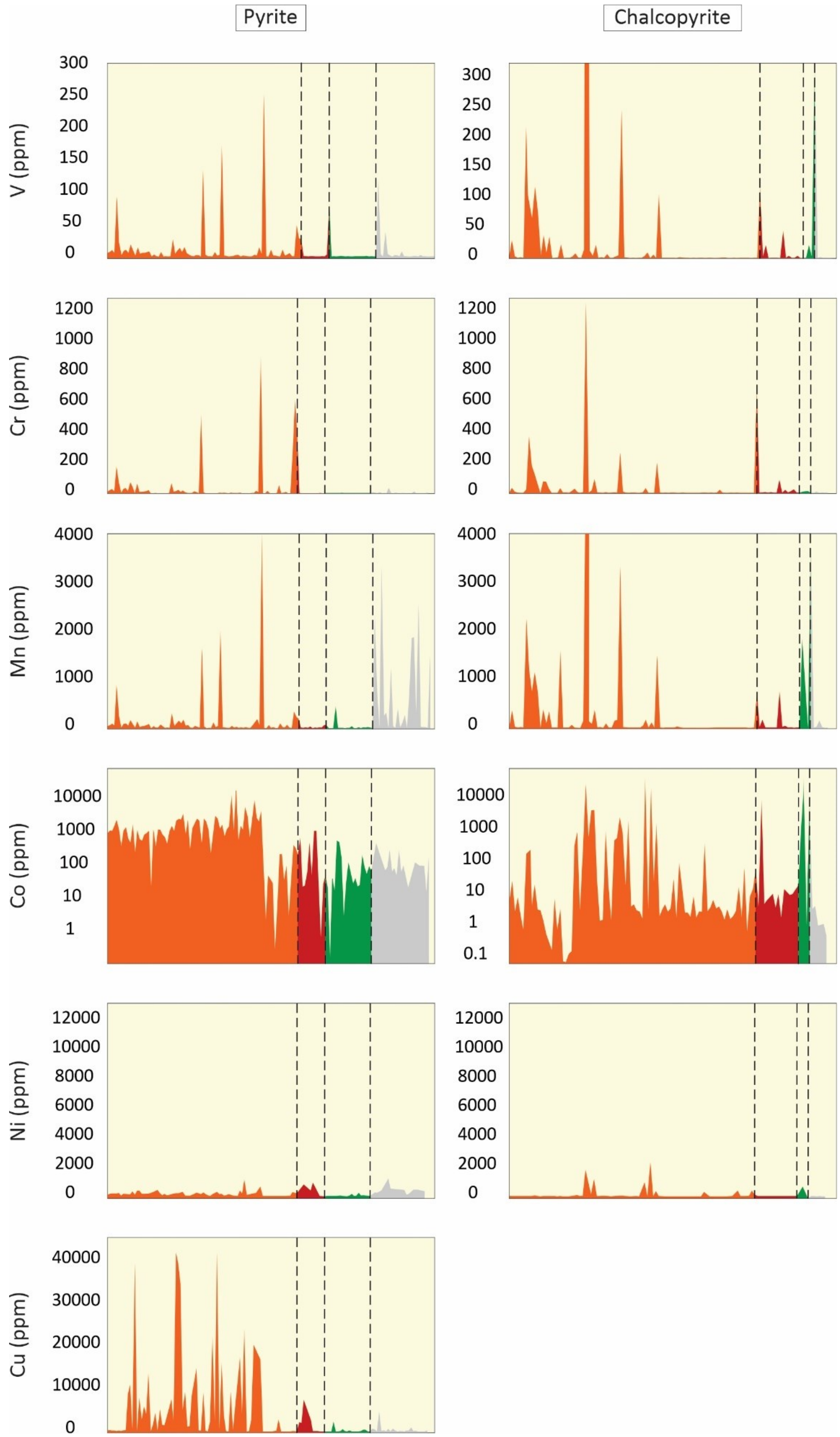
Pyrite
Chalcopyrite
V (ppm)
Cr (ppm)
Mn (ppm)
Co (ppm)
Ni (ppm)
Cu (ppm)
300
250
200
150
100
50
0
1200
1000
800
600
400
200
4000
3000
2000
1000
10000
100
10
1
0.1
12000
8000
6000
40000
30000
20000

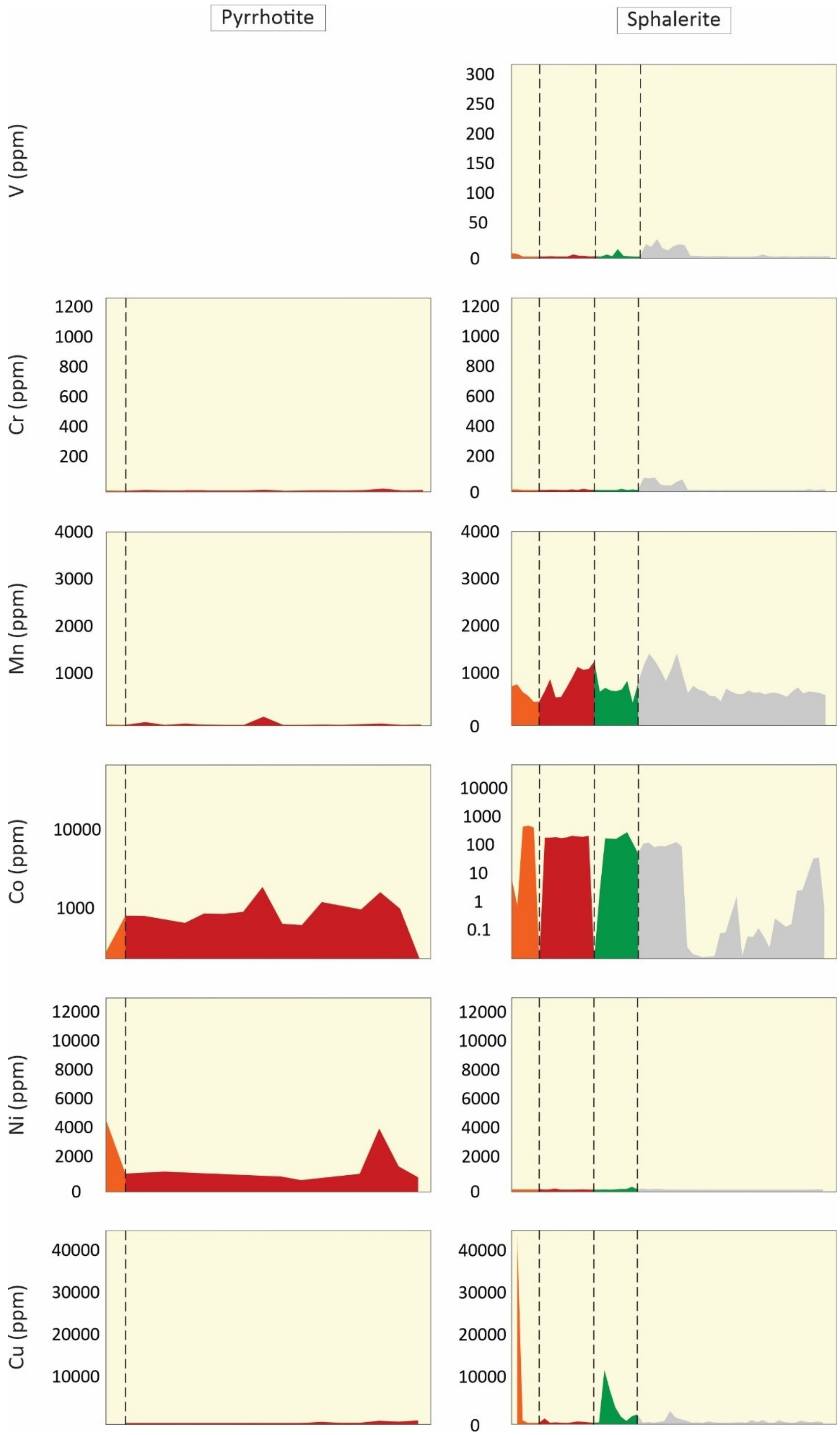

Pyrrhotite
Sphalerite
V (ppm)
300
250
200
150
100
50
0
Cr (ppm)
1200
1000
800
600
400
200
0
Mn (ppm)
4000
3000
2000
1000
0
Co (ppm)
10000
1000
100
10
1
0.1
Ni (ppm)
12000
10000
8000
6000
4000
2000
0
Cu (ppm)
40000
30000
20000
10000
0

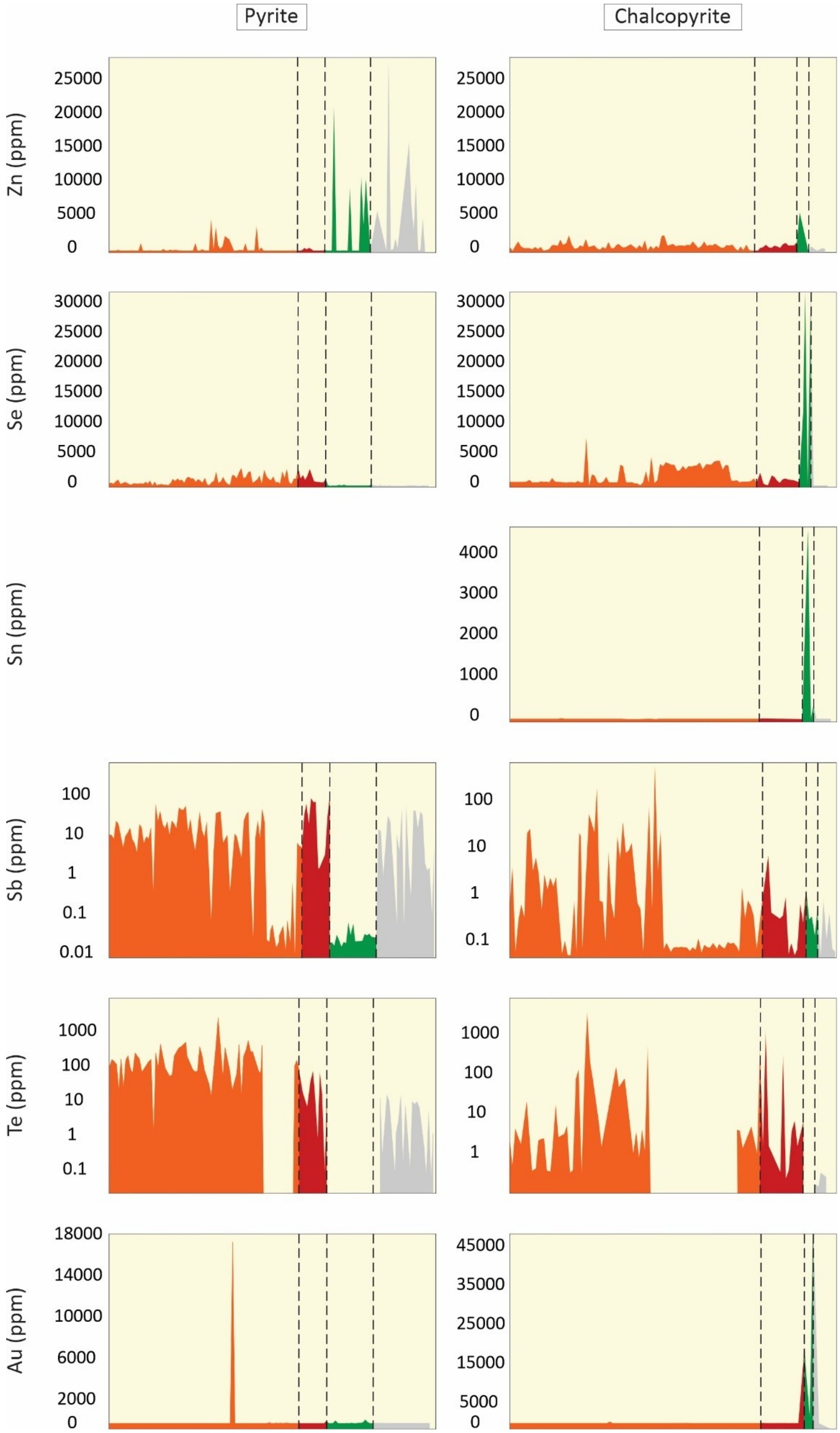
Pyrite
Chalcopyrite
Zn (ppm)
25000
20000
15000
10000
5000
0
Se (ppm)
30000
25000
20000
15000
10000
5000
0
Sn (ppm)
4000
3000
2000
1000
0
Sb (ppm)
100
10
1
0.1
0.01
Te (ppm)
1000
100
10
1
0.1
Au (ppm)
18000
14000
10000
6000
2000
0
45000
35000
25000
15000
5000
0

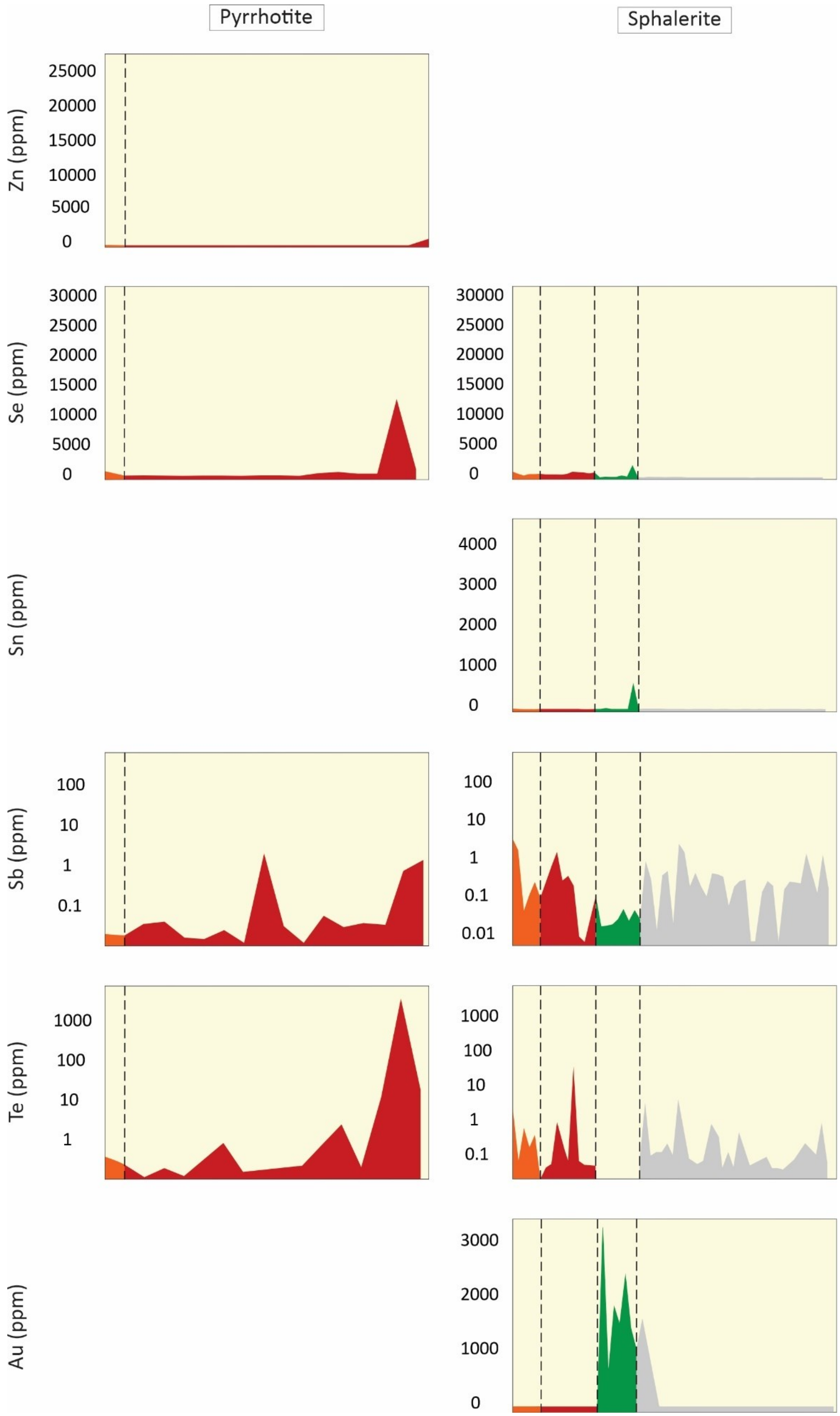
Pyrrhotite
Sphalerite
Zn (ppm)
25000
20000
15000
10000
5000
0
Se (ppm)
30000
25000
20000
15000
10000
5000
0
Sn (ppm)
4000
3000
2000
1000
0
Sb (ppm)
100
10
1
0.1
0.01
Te (ppm)
1000
100
10
1
0.1
Au (ppm)
3000
2000
1000
0

Figure 3.7. Trace element (V, Cr, Mn, Co, Ni, Cu, Zn, Se, Sn, Sb, Te, Au) variations between the main sulfide minerals (pyrite, chalcopyrite, pyrrhotite, sphalerite) composing the main sulfide facies at Betts Cove, where orange = chalcopyrite-dominated facies, red = chalcopyrite-pyrrhotite-dominated facies, green = pyrite-dominated facies, and light grey = sphalerite-pyrite-dominated facies.

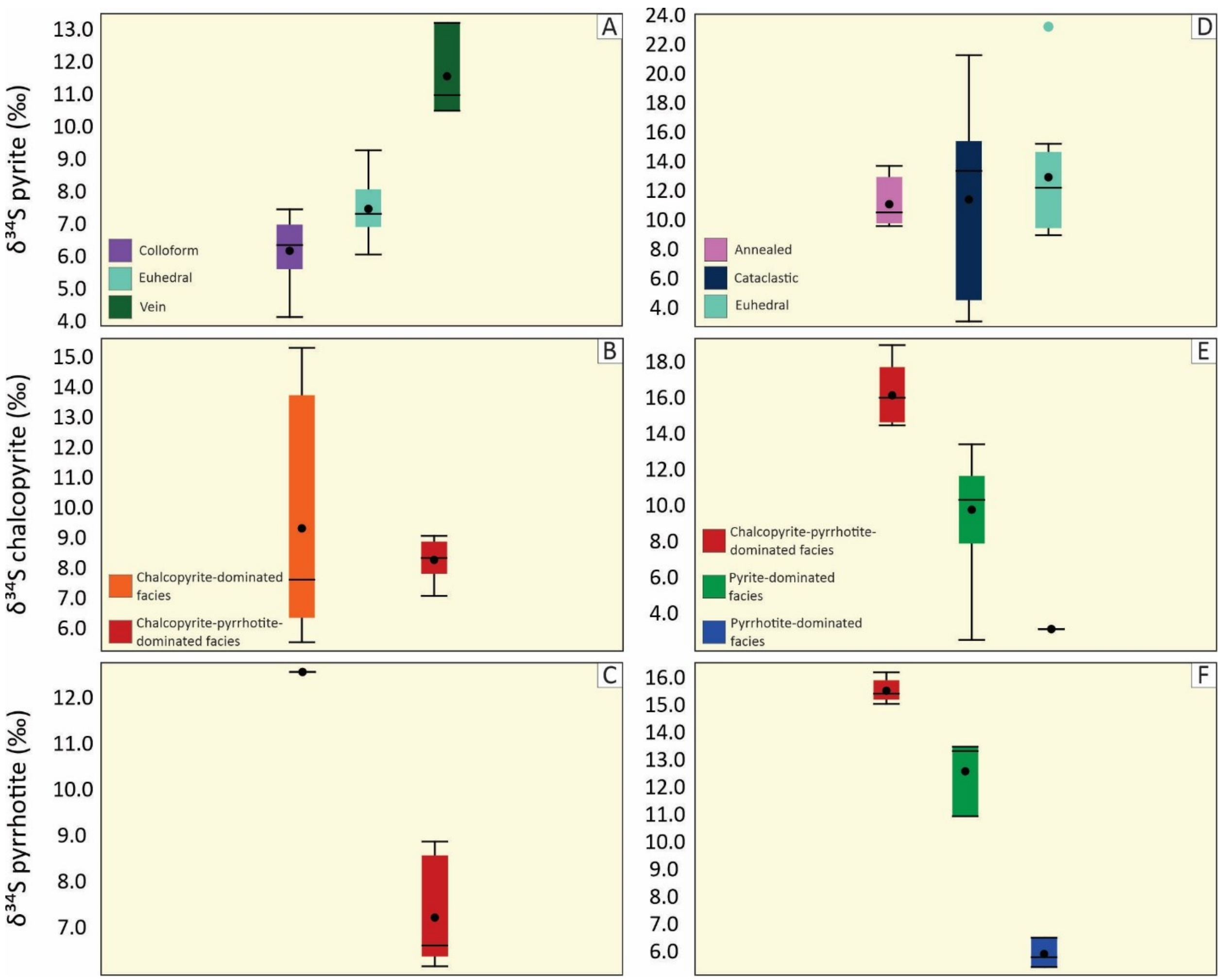

Figure 3.8. Sulfur isotope analyses ($\delta^{34}S$) of pyrite textures (A), chalcopyrite (B), and pyrrhotite (C) at Betts Cove (A-C) and Tilt Cove (D-F). Here, the boxes represents the interquartile range, the lines represents the median value, the black dots represents the mean value, the whiskers represent the minimum and maximum values, and the coloured dots represent any outliers.

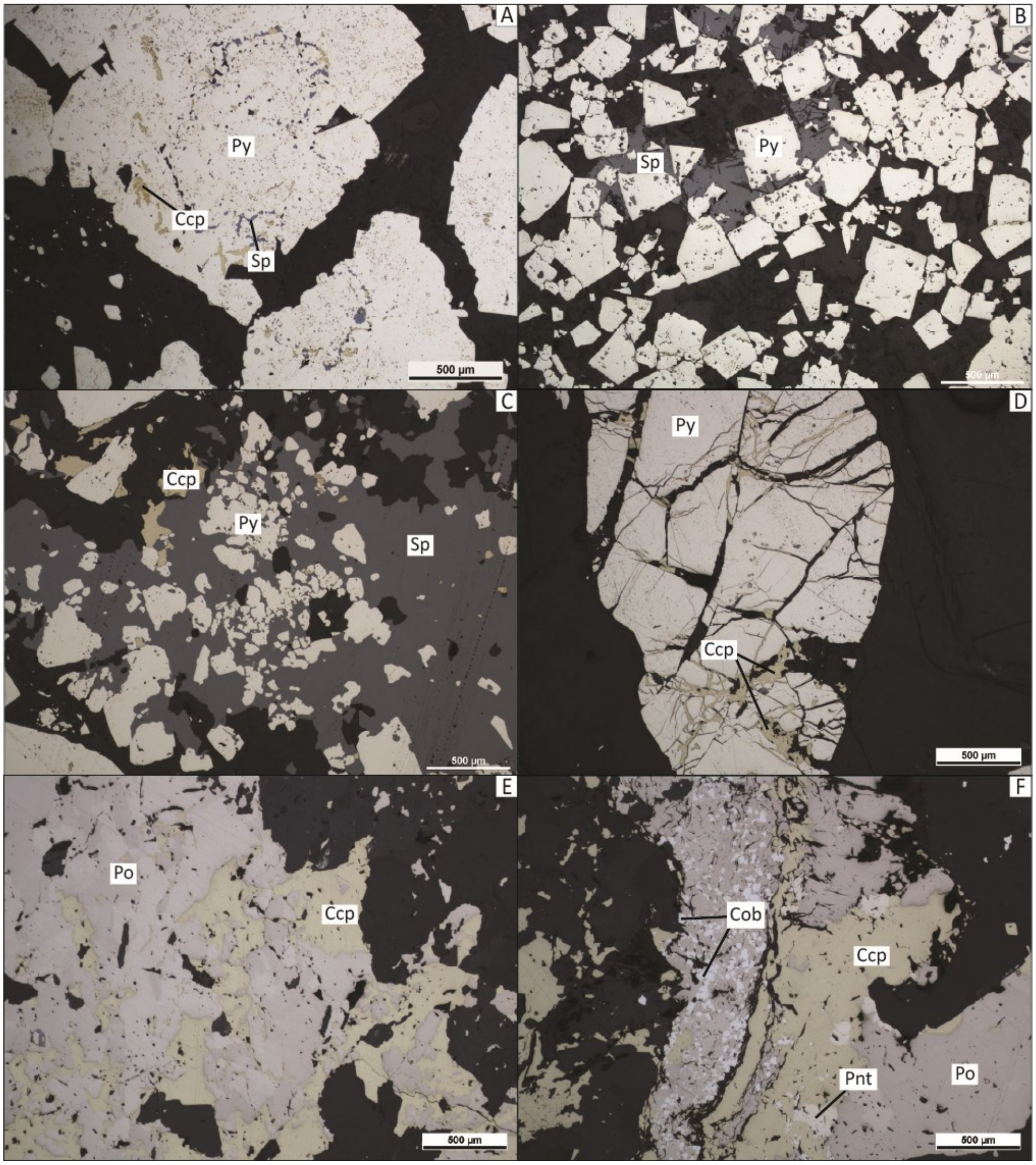
A
Py
Ccp
Sp
500 µm
B
Sp
Py
500 µm
C
Ccp
Py
Sp
500 µm
D
Py
Ccp
500 µm
E
Po
Ccp
500 µm
F
Cob
Ccp
Pnt
Po
500 µm

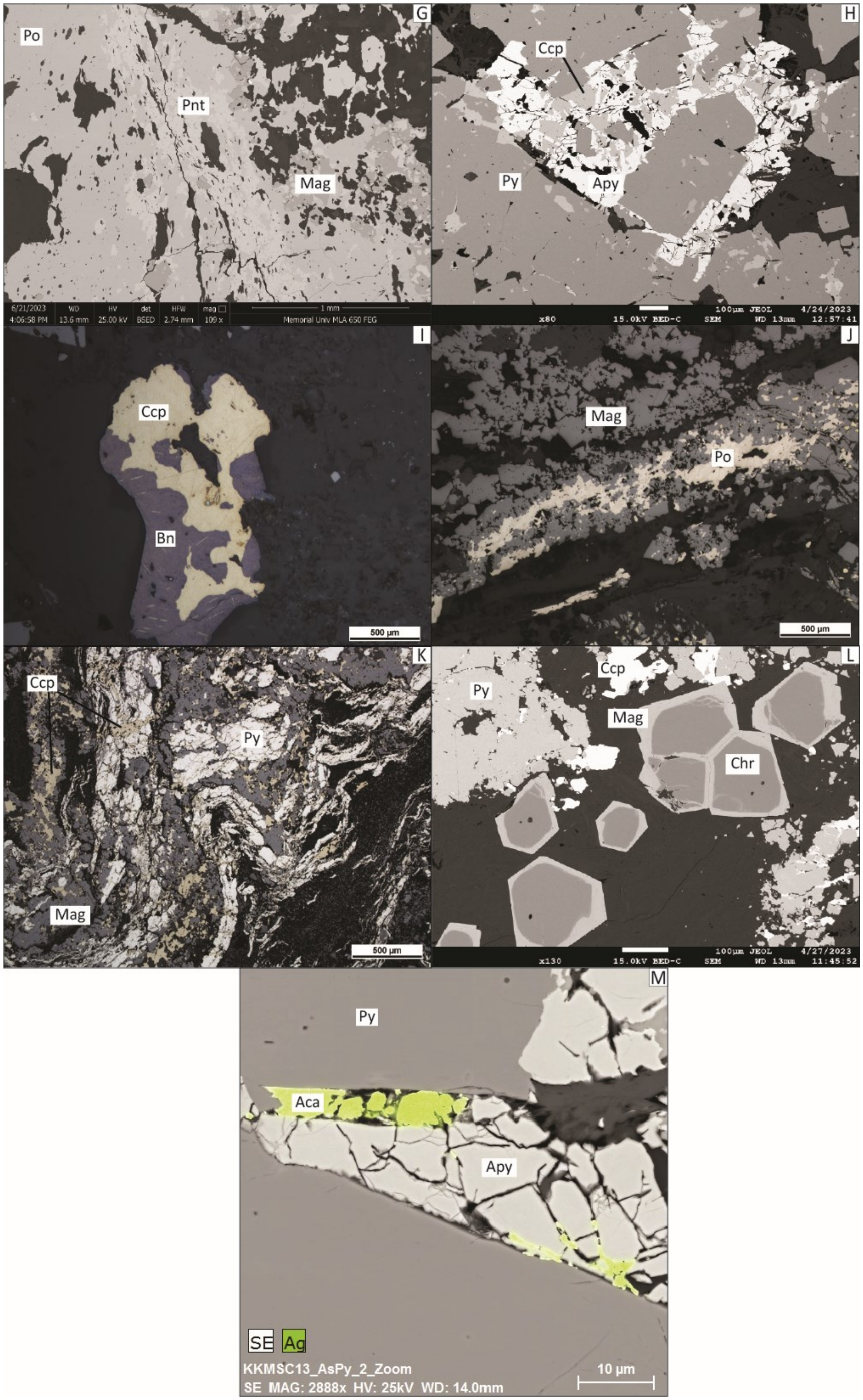
G
Po
Pnt
Mag
H
Ccp
Py
Apy
100µm JEOL 4/24/2023
x80 15.0kV BED-C SEM WD 13mm 12:57:41
I
Ccp
Bn
500 µm
J
Mag
Po
500 µm
K
Ccp
Py
Mag
500 µm
L
Py
Ccp
Mag
Chr
100µm JEOL 4/27/2023
x130 15.0kV BED-C SEM WD 13mm 11:45:52
M
Py
Aca
Apy
SE
Ag
KKMSC13_AsPy_2_Zoom
SE MAG: 2888x HV: 25kV WD: 14.0mm
10 µm

Figure 3.9. Plane polarized reflected light and backscatter electron images of sulfide and oxide mineral textures from Tilt Cove, including: A) relic colloform pyrite being replaced by chalcopyrite and sphalerite; B) euhedral pyrite grains; C) massive sphalerite surrounding pyrite grains; D) cataclastic pyrite with chalcopyrite infilling fracture spaces suggesting deformation; E) intergrown chalcopyrite-pyrrhotite assemblage; F) subhedral cobalitite grains hosted in pyrrhotite and chalcopyrite; G) pentlandite stringer hosted in pyrrhotite; H) arsenopyrite and chalcopyrite surrounding pyrite grains; I) bornite replacing chalcopyrite; J) magnetite surrounding pyrrhotite stringer; K) massive sulfide and magnetite showing folding as a result of deformation; L) euhedral chromite grains with magnetite rims; and M) acanthite and arsenopyrite in fracture in pyrite. Here, aca = acanthite, apy = arsenopyrite, bn = bornite, ccp = chalcopyrite, chr = chromite, cob = cobaltite, mag = magnetite, pnt = pentlandite, po = pyrrhotite, py = pyrite, and sp = sphalerite.

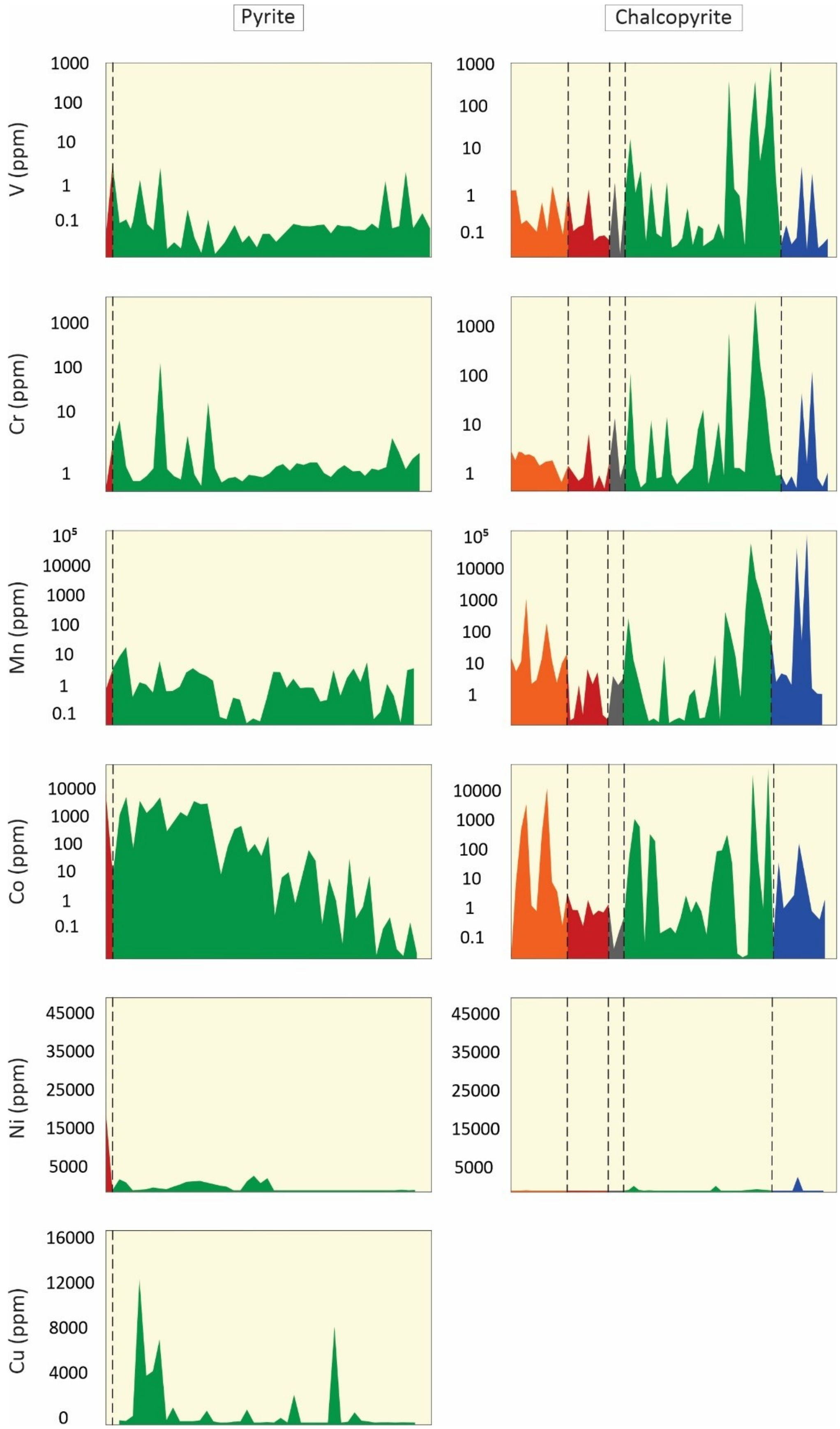

Pyrite
Chalcopyrite
V (ppm)
1000
100
10
1
0.1
Cr (ppm)
1000
100
10
1
Mn (ppm)
10^5
10000
1000
100
10
1
0.1
Co (ppm)
10000
1000
100
10
1
0.1
Ni (ppm)
45000
35000
25000
15000
5000
Cu (ppm)
16000
12000
8000
4000
0

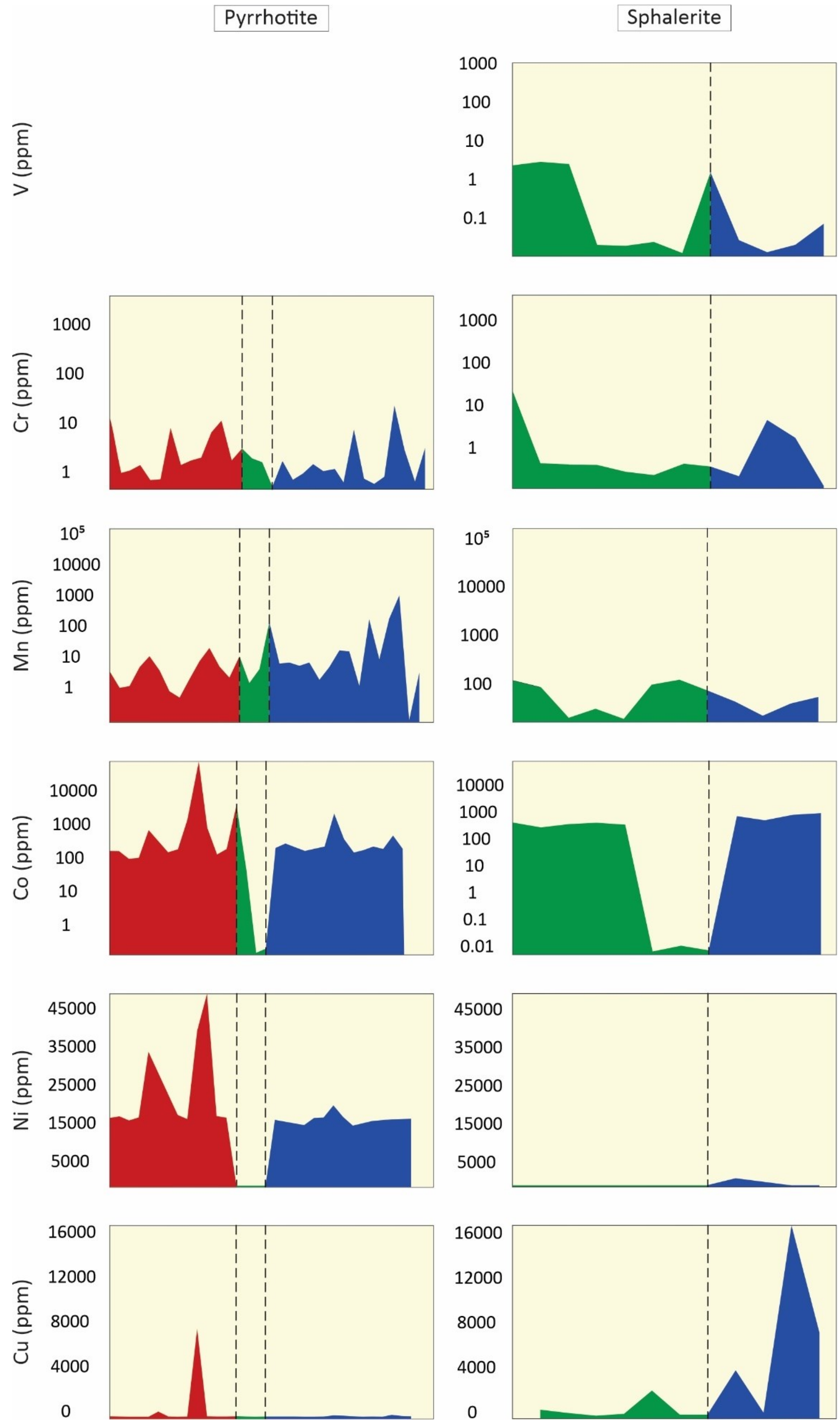
Pyrrhotite
Sphalerite
V (ppm)
1000
100
10
1
0.1
Cr (ppm)
1000
100
10
1
Mn (ppm)
10^5
10000
1000
100
10
1
Co (ppm)
10000
1000
100
10
1
0.1
0.01
Ni (ppm)
45000
35000
25000
15000
5000
Cu (ppm)
16000
12000
8000
4000
0

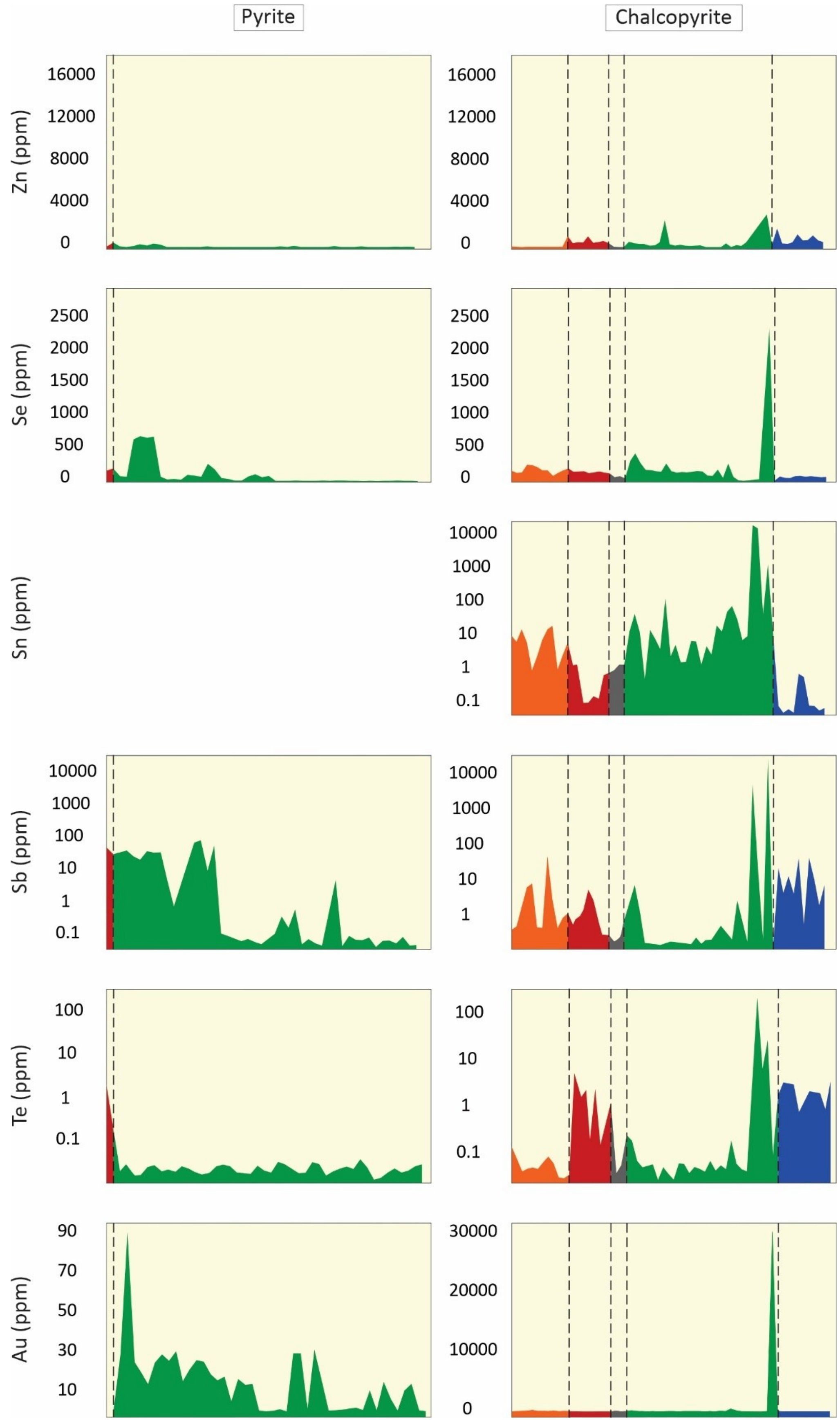
Pyrite
Chalcopyrite
Zn (ppm)
16000
12000
8000
4000
0
Se (ppm)
2500
2000
1500
1000
500
0
Sn (ppm)
10000
1000
100
10
1
0.1
Sb (ppm)
10000
1000
100
10
1
0.1
Te (ppm)
100
10
1
0.1
Au (ppm)
90
70
50
30
10
30000
20000
10000
0

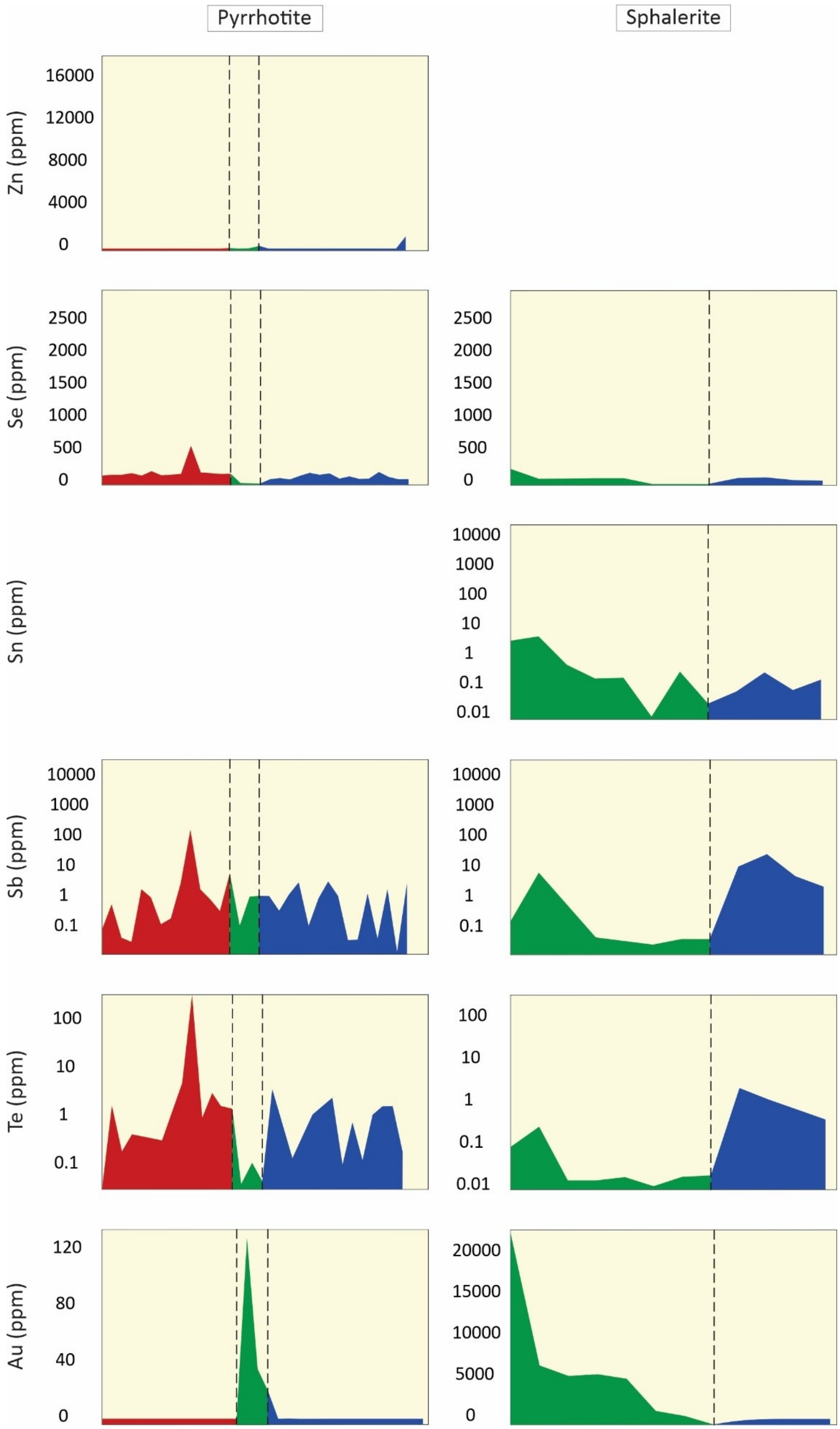

Pyrrhotite
Sphalerite
Zn (ppm)
16000
12000
8000
4000
0
Se (ppm)
2500
2000
1500
1000
500
0
Sn (ppm)
10000
1000
100
10
1
0.1
0.01
Sb (ppm)
10000
1000
100
10
1
0.1
Te (ppm)
100
10
1
0.1
0.01
Au (ppm)
120
80
40
0
20000
15000
10000
5000
0

Figure 3.10. Trace element (V, Cr, Mn, Co, Ni, Cu, Zn, Se, Sn, Sb, Te, Au) variations between the main sulfide minerals (pyrite, chalcopyrite, pyrrhotite, sphalerite) composing the main sulfide facies at Tilt Cove, where orange = chalcopyrite-dominated facies, red = chalcopyrite-pyrrhotite-dominated facies, dark grey = magnetite-dominated facies, green = pyrite-dominated facies, and blue = pyrrhotite-dominated facies.

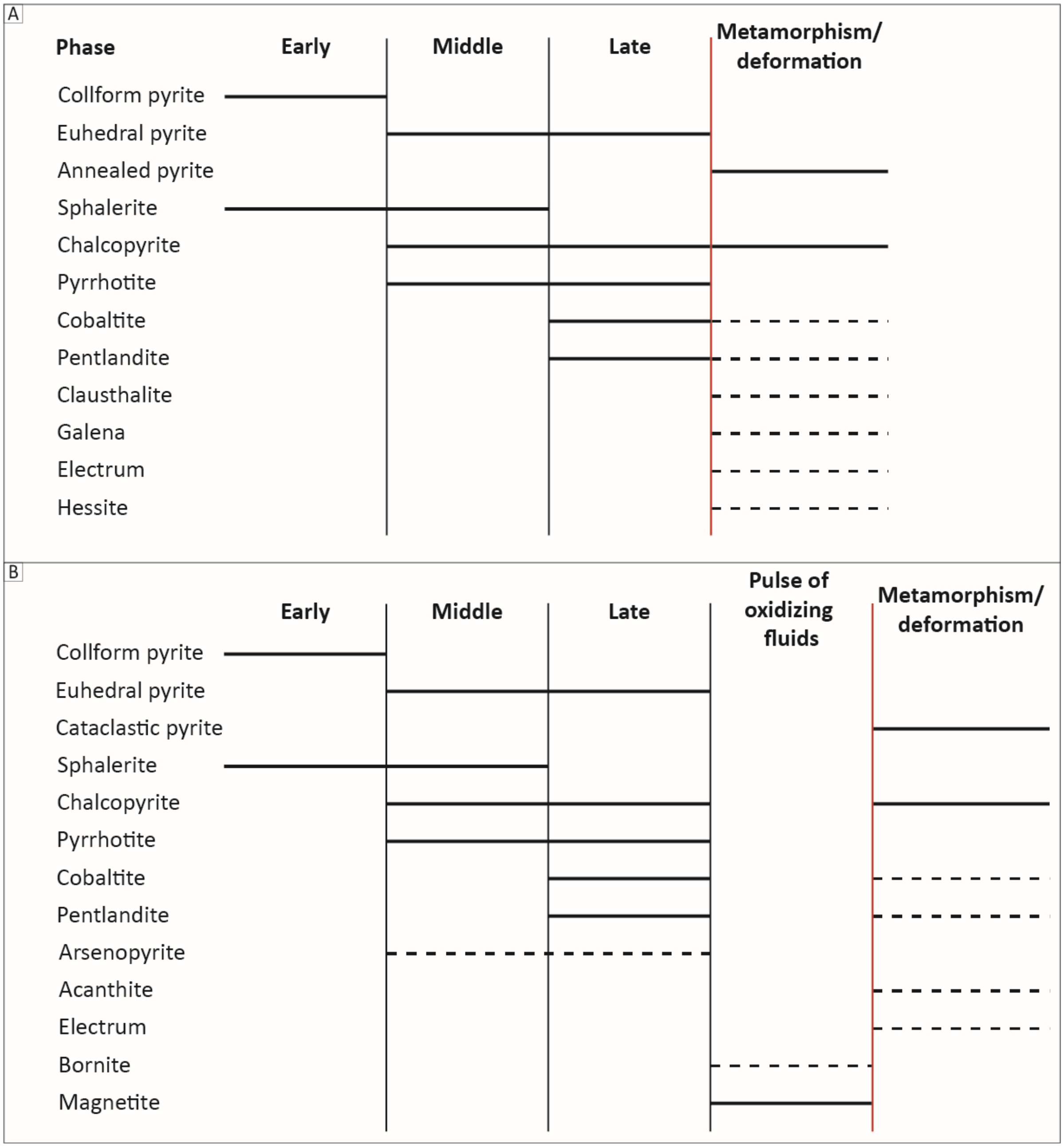

Figure 3.11. Mineral paragenesis at A) Betts Cove and B) Tilt Cove. Solid lines indicate that the mineral is abundant, and the timing is certain. Dashed lines indicate that the mineral is in minor to trace, and the timing has uncertainties.

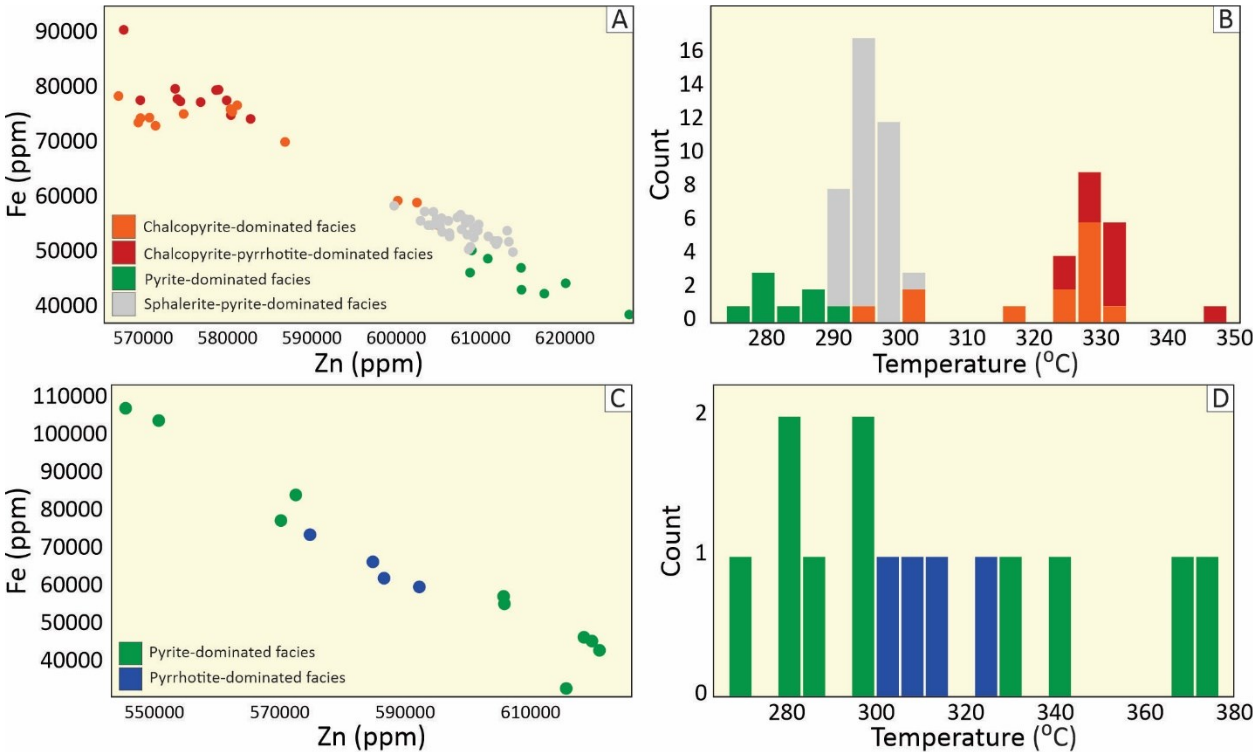

Figure 3.12. Electron microprobe results from Betts Cove and Tilt Cove, including: A/C) Fe/Zn plot for sphalerite; and B/D) calculated sphalerite crystallization temperatures using Fe/Zn ratios in sphalerite according to Keith et al., (2014).

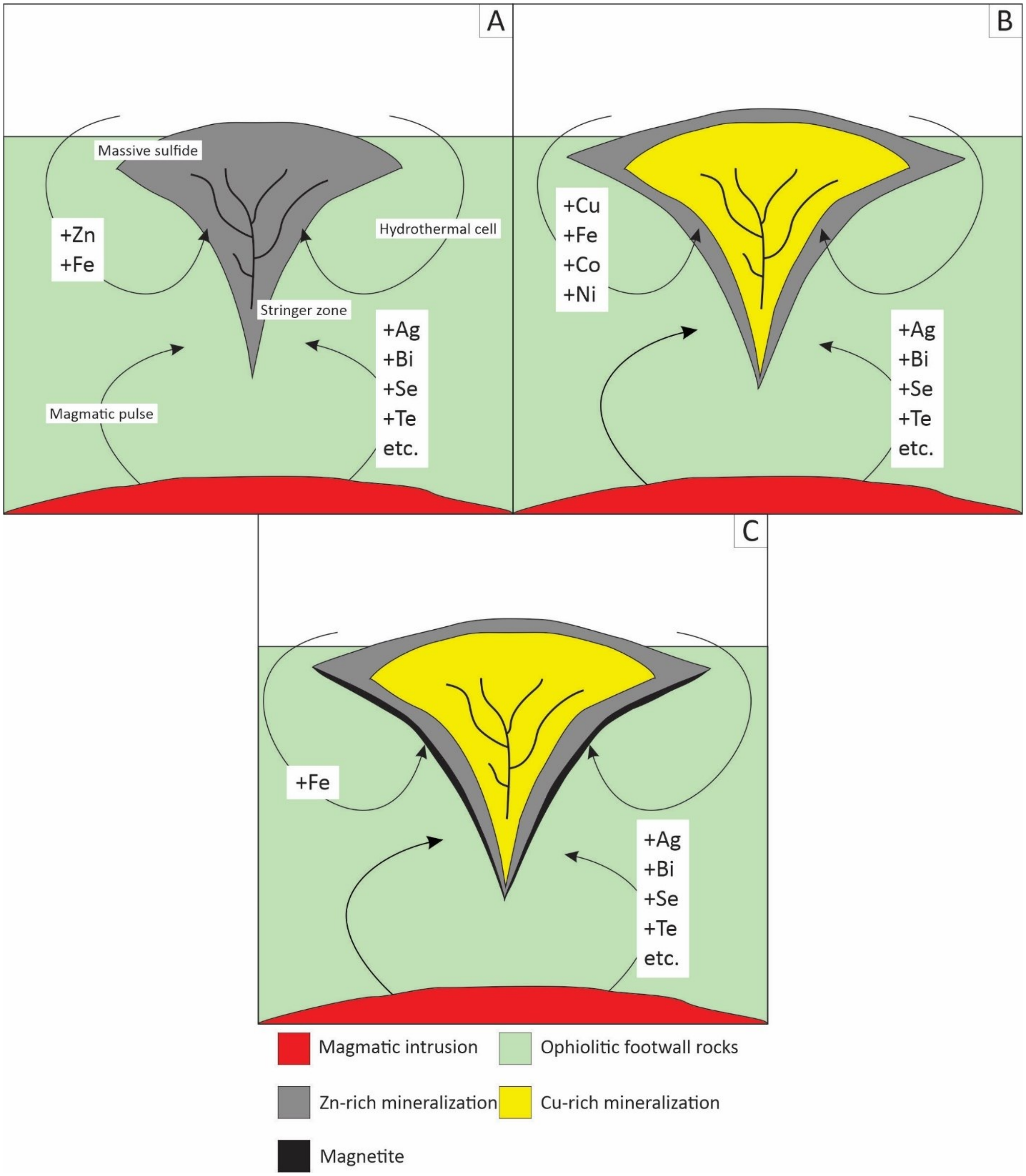

Figure 3.13. Schematic diagram showing the two-three stages of ore genesis at the Betts Cove and Tilt Cove deposits, including, A) low temperature (< 300ºC), near neutral pH, and reducing fluids that transported Zn and Fe and deposited sphalerite and pyrite by mixing with cold

seawater and possibly the addition of other trace metals through small magmatic pulses; B) high temperature (> 300ºC), acidic, and reducing fluids that transported Cu-Co-Ni and deposited chalcopyrite-pyrrhotite-(cobaltite-pentlandite)-rich assemblages, which also involved zone refining and replacement of earlier formed Zn-Fe-rich assemblages and possibly the addition of other trace metals through small magmatic pulses; and C) low temperature (< 300ºC), basic, oxidizing, and H_2S poor fluids that deposited magnetite at Tilt Cove.

Table 3.1. Median concentrations of select trace elements from Betts Cove for pyrite, chalcopyrite, pyrrhotite, and sphalerite.

Facies	**Chalcopyrite-dominated**				**Chalcopyrite-pyrrhotite-dominated**			
Mineral	Py	Ccp	Po	Sp	Py	Ccp	Po	Sp
Ti (ppm)	1	1	1	0	1	1	1	0
V (ppm)	3	0	0	0	0	0	0	0
Cr (ppm)	2	1	1	0	1	1	1	2
Mn (ppm)	40	5	3	644	10	7	0	969
Co (ppm)	1200	3	313	564	54	10	967	263
Ni (ppm)	149	6	4840	1	385	6	1010	1
Cu (ppm)	1500	-	-	313	1060	-	13	144
Zn (ppm)	28	681	69	-	70	738	10	-
As (ppm)	464	1	1	0	232	8	1	7
Se (ppm)	710	749	1200	600	1030	970	466	664
Ag (ppm)	14	51	37	6	8	31	1	4
Cd (ppm)	0	2	5	2770	0	4	0	2980
In (ppm)	1	1	-	5	1	19	0	147
Sn (ppm)	0	2	0	0	0	1	0	0
Sb (ppm)	11	0	0	0	36	0	0	0
Te (ppm)	140	4	0	0	15	2	0	0
Au (ppm)	3	46	-	0	1	0	0	0
Hg (ppm)	1	2	3	498	2	30	25	291
Tl (ppm)	1	1	11	0	4	0	0	0
Bi (ppm)	30	0	0	0	2	2	0	1
Pb (ppm)	178	26	157	66	190	23	7	44

Facies	**Pyrite-dominated**				**Sphalerite-pyrite-dominated**			

Mineral	Py	Ccp	Po	Sp	Py	Ccp	Po	Sp
Ti (ppm)	0	6	-	1	1	1	-	0
V (ppm)	0	11	-	0	0	0	-	0
Cr (ppm)	1	10	-	1	1	1	-	0
Mn (ppm)	1	1060	-	725	263	8	-	682
Co (ppm)	45	1110	-	222	103	1	-	0
Ni (ppm)	30	232	-	26	369	1	-	2
Cu (ppm)	26	-	-	1810	124	-	-	159
Zn (ppm)	5	4390	-	-	4730	296	-	-
As (ppm)	320	14980	-	78	524	1	-	0
Se (ppm)	37	20833	-	133	8	18	-	20
Ag (ppm)	0	0	-	19	13	292	-	10
Cd (ppm)	0	42	-	0	1	0	-	605
In (ppm)	0	152	-	2	0	0	-	0
Sn (ppm)	0	367	-	4	0	0	-	0
Sb (ppm)	0	0	-	0	10	0	-	0
Te (ppm)	-	-	-	-	2	0	-	0
Au (ppm)	4	26126	-	1570	2	0	-	0
Hg (ppm)	0	9	-	0	1	2	-	441
Tl (ppm)	7	11784	-	36	3	0	-	0
Bi (ppm)	0	-	-	-	0	0	-	0
Pb (ppm)	-	-	-	-	108	1	-	36

Table 3.2. Median concentrations of select trace elements from Tilt Cove for pyrite, chalcopyrite, pyrrhotite, and sphalerite.

Facies	**Chalcopyrite-dominated**				**Chalcopyrite-pyrrhotite-dominated**			
Mineral	Py	Ccp	Po	Sp	Py	Ccp	Po	Sp
Ti (ppm)	-	1	-	-	1	1	1	-
V (ppm)	-	0	-	-	2	0	0	-
Cr (ppm)	-	3	-	-	1	1	2	-
Mn (ppm)	-	16	-	-	3	0	3	-
Co (ppm)	-	10	-	-	5518	1	242	-
Ni (ppm)	-	5	-	-	10204	67	18121	-
Cu (ppm)	-	-	-	-	12746	-	14	-
Zn (ppm)	-	26	-	-	204	439	1	-
As (ppm)	-	76	-	-	11	30	19	-
Se (ppm)	-	164	-	-	177	143	152	-
Ag (ppm)	-	0	-	-	114	20	2	-
Cd (ppm)	-	11	-	-	20	12	0	-
In (ppm)	-	1	-	-	14	22	0	-
Sn (ppm)	-	7	-	-	0	1	0	-
Sb (ppm)	-	1	-	-	48	1	1	-
Te (ppm)	-	0	-	-	1	2	0	-
Au (ppm)	-	78	-	-	-	0	0	-
Hg (ppm)	-	113	-	-	66	2	21	-
Tl (ppm)	-	65	-	-	3	0	0	-
Bi (ppm)	-	0	-	-	5	0	1	-
Pb (ppm)	-	-	-	-	467	14	21	-

Facies	Magnetite-dominated				Pyrite-dominated				Pyrrhotite-dominated			
Mineral	Py	Ccp	Po	Sp	Py	Ccp	Po	Sp	Py	Ccp	Po	Sp
Ti (ppm)	-	8	-	-	1	-	13	0	0	1	1	0
V (ppm)	-	1	-	-	0	-	0	1	0	0	0	0
Cr (ppm)	-	1	-	-	1	-	1	0	1	1	1	1
Mn (ppm)	-	4	-	-	2	-	6	96	1	5	10	50
Co (ppm)	-	0	-	-	3	-	0	437	48	3	296	1080
Ni (ppm)	-	1	-	-	44	-	21	2	537	42	17421	944
Cu (ppm)	-	-	-	-	-	-	10	271	83	-	17	5810
Zn (ppm)	-	8	-	-	195	-	19	-	2	633	4	-
As (ppm)	-	38	-	-	77	-	175	2	715	1	1	0
Se (ppm)	-	56	-	-	146	-	3	85	8	66	88	77
Ag (ppm)	-	0	-	-	3	-	0	1580	0	59	2	23
Cd (ppm)	-	-	-	-	23	-	0	25	0	8	0	4070
In (ppm)	-	0	-	-	1	-	0	0	0	38	0	-
Sn (ppm)	-	2	-	-	11	-	0	0	1	0	0	0
Sb (ppm)	-	0	-	-	0	-	1	0	0	10	1	9
Te (ppm)	-	0	-	-	0	-	0	0	0	2	1	1
Au (ppm)	-	62	-	-	44	-	36	5080	15	0	0	2
Hg (ppm)	-	209	-	-	105	-	119	7210	26	6	19	293
Tl (ppm)	-	61	-	-	46	-	10	6	5	0	0	0
Bi (ppm)	-	-	-	-	-	-	-	-	-	0	1	1
Pb (ppm)	-	-	-	-	-	-	-	-	-	58	30	108

Table 3.3. TSR calculation results using Equations 3-7 showing $\delta^{34}S$ values for each of the main sulfide minerals if TSR was the source of reduced sulfur at the Betts Cove and Tilt Cove deposits at 250ºC and 350ºC. Here, py = pyrite, ccp = chalcopyrite, and po = pyrrhotite.

T(ºC)	T(K)	$\alpha_{H_2S-SO_4}$	f	$\delta^{34}S_{SO_4(parent,t=0)}$(‰)	$\delta^{34}S_{SO_4(parent,t)}$(‰)	$\delta^{34}S_{(TSR)}$ (‰)	$\delta^{34}S_{py(TSR)}$(‰)	$\delta^{34}S_{ccp(TSR)}$(‰)	$\delta^{34}S_{po(TSR)}$(‰)
250	523	0.975	1	30.0	30.0	5.10	6.56	5.28	5.46
350	623	0.981	1	30.0	30.0	10.6	11.7	10.8	10.9

Table 3.4. Mixing calculation results using Equation 8 showing $\delta^{34}S$ values for the main sulfide minerals if both TSR and leaching from igneous rocks were the sources of reduced sulfur at 250ºC and 350ºC.

	$\delta^{34}S_{(mix)}$(‰)	
b	**250 ºC**	**350 ºC**
1	5.10	10.6
0.9	4.59	9.58
0.8	4.08	8.52
0.7	3.57	7.45
0.6	3.06	6.39
0.5	2.55	5.32
0.4	2.04	4.26
0.3	1.53	3.19
0.2	1.02	2.13
0.1	0.51	1.06
0	0.00	0.00

Table 3.5. Leaching calculation results using Equation 9 for the Betts Cove deposit.

Contained Cu in the Betts Cove deposit (g)	**Density of boninites (t/m^3)**	**Concentration of Cu in boninites (g/t)**	**Leaching efficiency**	**Precipitation efficiency**	**Volume (km^3)**
1.19×10^{10}	2.87	60.0	1.00	0.10	0.69
1.19×10^{10}	2.87	60.0	1.00	0.38	0.18
1.19×10^{10}	2.87	60.0	1.00	0.99	0.07
Contained Cu in the Betts Cove deposit (g)	**Density of sheeted dykes (t/m^3)**	**Concentration of Cu in sheeted dykes (g/t)**	**Leaching efficiency**	**Precipitation efficiency**	**Volume (km^3)**
1.19×10^{10}	2.84	60.0	1.00	0.10	0.70
1.19×10^{10}	2.84	60.0	1.00	0.38	0.18
1.19×10^{10}	2.84	60.0	1.00	0.99	0.07
Contained Cu in the Betts Cove deposit (g)	**Density of ultramafics (t/m^3)**	**Concentration of Cu in ultramafics (g/t)**	**Leaching efficiency**	**Precipitation efficiency**	**Volume (km^3)**
1.19×10^{10}	2.92	2.50	1.00	0.10	16.2
1.19×10^{10}	2.92	2.50	1.00	0.38	4.27
1.19×10^{10}	2.92	2.50	1.00	0.99	1.64

Table 3.6. Leaching calculation results using Equation 9 for the Tilt Cove deposit.

Contained Cu in the Tilt Cove deposit (g)	**Density of boninites (t/m^3)**	**Concentration of Cu in boninites (g/t)**	**Leaching efficiency**	**Precipitation efficiency**	**Volume (km^3)**
5.30×10^{11}	2.87	60.0	1.00	0.10	30.8
5.30×10^{11}	2.87	60.0	1.00	0.38	8.11
5.30×10^{11}	2.87	60.0	1.00	0.99	3.11
Contained Cu in the Tilt Cove deposit (g)	**Density of sheeted dykes (t/m^3)**	**Concentration of Cu in sheeted dykes (g/t)**	**Leaching efficiency**	**Precipitation efficiency**	**Volume (km^3)**
5.30×10^{11}	2.84	60.0	1.00	0.10	31.1
5.30×10^{11}	2.84	60.0	1.00	0.38	8.19
5.30×10^{11}	2.84	60.0	1.00	0.99	3.14
Contained Cu in the Tilt Cove deposit (g)	**Density of ultramafics (t/m^3)**	**Concentration of Cu in ultramafics (g/t)**	**Leaching efficiency**	**Precipitation efficiency**	**Volume (km^3)**
5.30×10^{11}	2.92	2.50	1.00	0.10	727
5.30×10^{11}	2.92	2.50	1.00	0.38	191
5.30×10^{11}	2.92	2.50	1.00	0.99	73.4

Chapter 4

Summary and Conclusions

4.1. SUMMARY AND CONCLUSIONS

The goal of this thesis was to develop a descriptive framework and explore potential genetic models for the mafic-(Cyprus)-type Betts Cove and Tilt Cove VMS deposits hosted within the Betts Cove ophiolite, Baie Verte Peninsula, Newfoundland Appalachians using field, petrographic, geochemical, and microanalytical methods. The conclusions of this study are as follows:

1. The Betts Cove and Tilt Cove deposits consist of stringer-type stockwork mineralization dominated by pyrite, chalcopyrite, pyrrhotite, and sphalerite, and magnetite at Tilt Cove. Accessory minerals include cobaltite and pentlandite, which define two stages of deposit formation, including, (1) low temperature (< 300ºC), near neutral pH (pH ~7), and reducing fluids, that carried Zn and Fe (+/- Au) and deposited sphalerite and pyrite, and (2) high temperature (> 300ºC), acidic (pH < 7), and reducing fluids, that carried Cu, Fe, Co, and Ni (+/- Se) and deposited chalcopyrite and pyrrhotite (+/- pyrite, cobaltite, and pentlandite). The presence of late magnetite at the Tilt Cove deposit suggests a third stage of deposit formation for the Tilt Cove deposit and a shift in hydrothermal fluid conditions to low temperature (< 300ºC), basic (pH > 7), oxidizing, and H_2S poor, resulting in the deposition of magnetite over pyrite. Greenschist metamorphism and deformation in the area resulted in the redistribution of minor and trace elements (Ag, Au, Pb, Se, and Te) and the formation of secondary, trace phases in these deposits (acanthite, clausthalite, electrum, galena, and hessite).
2. Leaching of ophiolitic, Cu-, Co-, Ni-, As-, Au-, and Sb-bearing footwall rocks and episodic, short-lived magmatic pulses were most likely responsible for the metal budget of the Betts Cove and Tilt Cove deposits.

3. Variable and positive sulfur isotope compositions ($\delta^{34}S$) indicate that thermochemical sulfate reduction (TSR) of seawater sulfate and the mixing with igneous sulfur were the primary sources of reduced sulfur (H_2S) at Betts Cove and Tilt Cove. Some highly positive sulfur isotope compositions (> 10‰) may be explained by the replacement of sulfate minerals by sulfide minerals.

4.2. SUGGESTIONS FOR FURTHER RESEARCH

This thesis provides new insights into the mineralogy and genesis of the Betts Cove and Tilt Cove VMS deposits that can be applied to understand the formation of similar VMS deposits globally. Potential areas for future research that would add to the understanding of the Betts Cove and Tilt Cove deposits and similar VMS deposits globally, include:

1. A more detailed study of the hydrothermal fluids at Betts Cove and Tilt Cove using fluid inclusion analyses in quartz, carbonate, sulfates, or sulfides to determine other physiochemical conditions of the hydrothermal fluids that were outside of the scope of this project such as more accurate estimates of fluid temperature, salinity, and metal content. Whole rock oxygen isotopes can also be used to track hydrothermal fluid pathways. This would require further geological sampling, petrography, isotope ratio mass spectrometry, and/or SIMS.
2. A more detailed study of the sources of sulfur at Betts Cove and Tilt Cove using multiple sulfur isotopes and to test the idea of sulfate replacement by sulfide minerals. This would require further geological sampling, petrography, and multiple S isotopes by either SIMS or conventional methods and include the analysis of potential sulfate minerals present within the ophiolite or other deposits in the Baie Verte Peninsula. Multiple S isotopes

could also be used to further study the potential magmatic fluid contribution to these deposits.

3. A detailed study on regional stratigraphy, structure, and alteration would help understand the effects of deformation and metamorphism on the deposits. This would require further field work (i.e., mapping), geological sampling, and petrography.

Appendix A: Graphic Logs

Figure A1. Legend for graphic logs.

Figure A2. Compilation of graphic logs from Betts Cove.

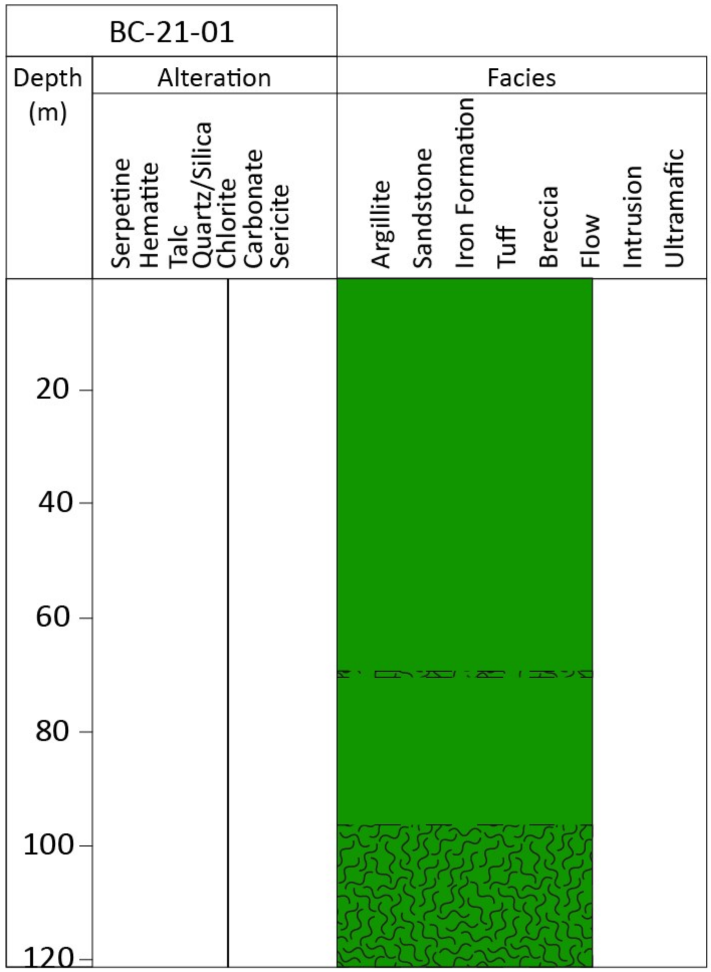
BC-21-01
Depth (m)
Alteration
Serpetine
Hematite
Talc
Quartz/Silica
Chlorite
Carbonate
Sericite
Facies
Argillite
Sandstone
Iron Formation
Tuff
Breccia
Flow
Intrusion
Ultramafic
20
40
60
80
100
120

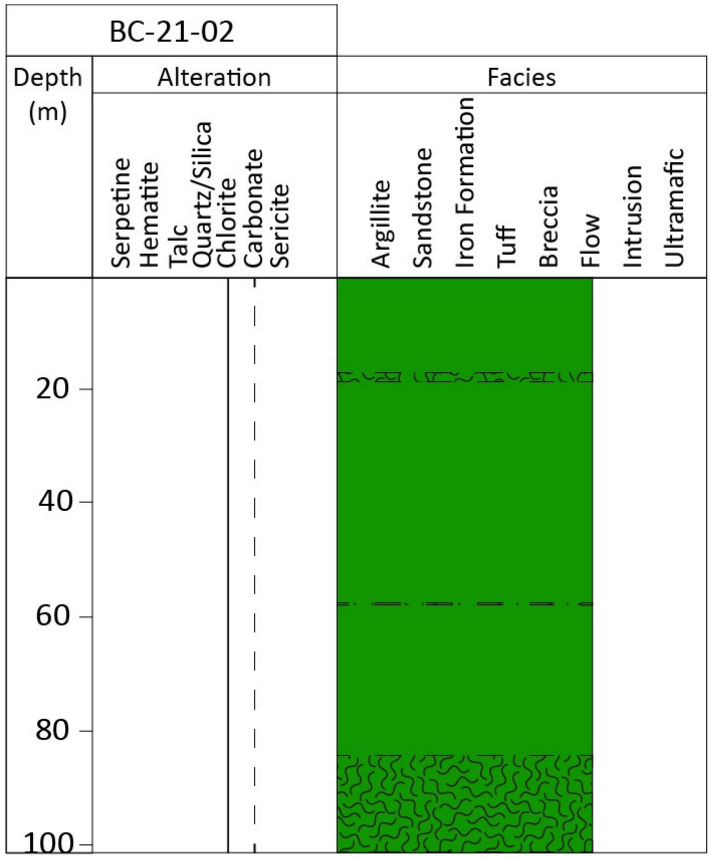
BC-21-02
Depth (m)
Alteration
Serpetine
Hematite
Talc
Quartz/Silica
Chlorite
Carbonate
Sericite
Facies
Argillite
Sandstone
Iron Formation
Tuff
Breccia
Flow
Intrusion
Ultramafic
20
40
60
80
100

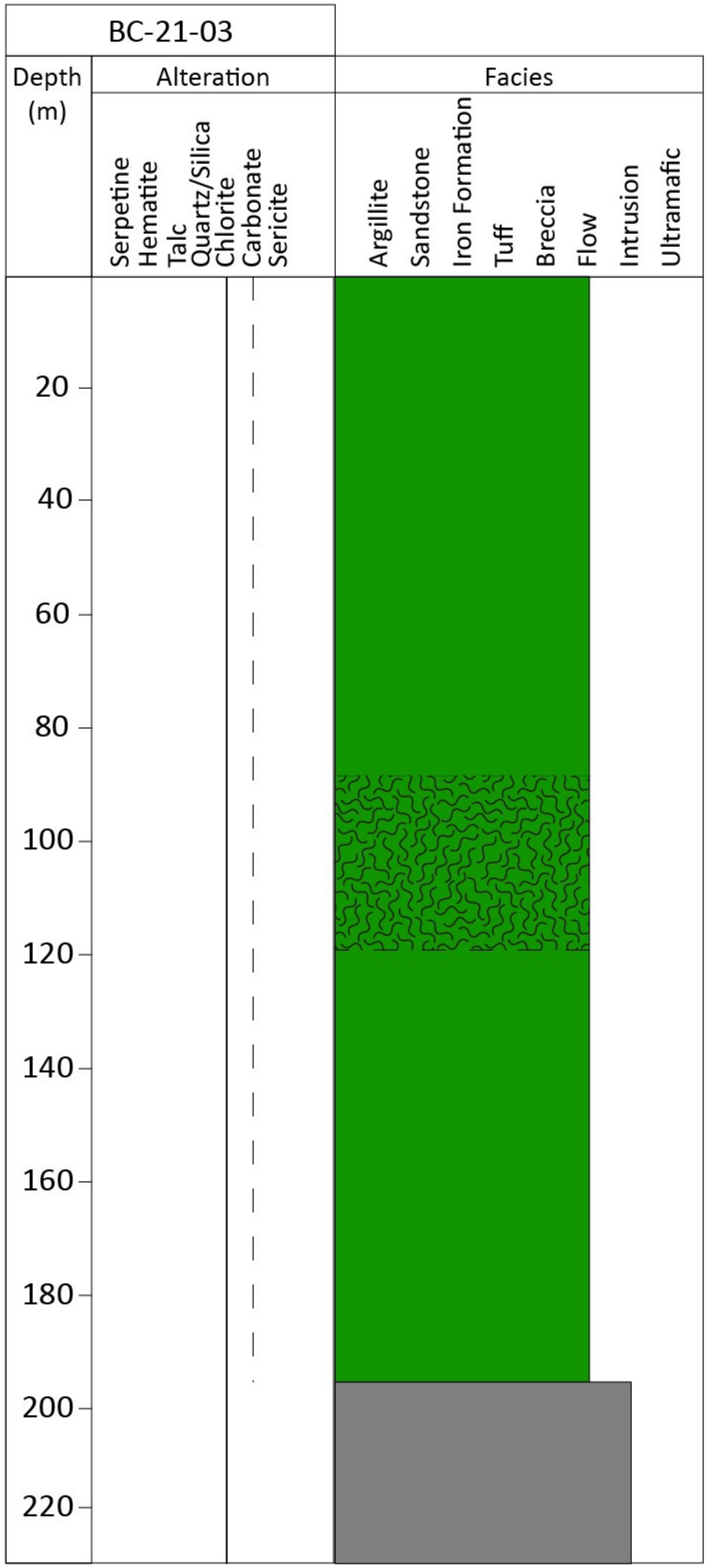
BC-21-03
Depth (m)
Alteration
Serpetine
Hematite
Talc
Quartz/Silica
Chlorite
Carbonate
Sericite
Facies
Argillite
Sandstone
Iron Formation
Tuff
Breccia
Flow
Intrusion
Ultramafic
20
40
60
80
100
120
140
160
180
200
220

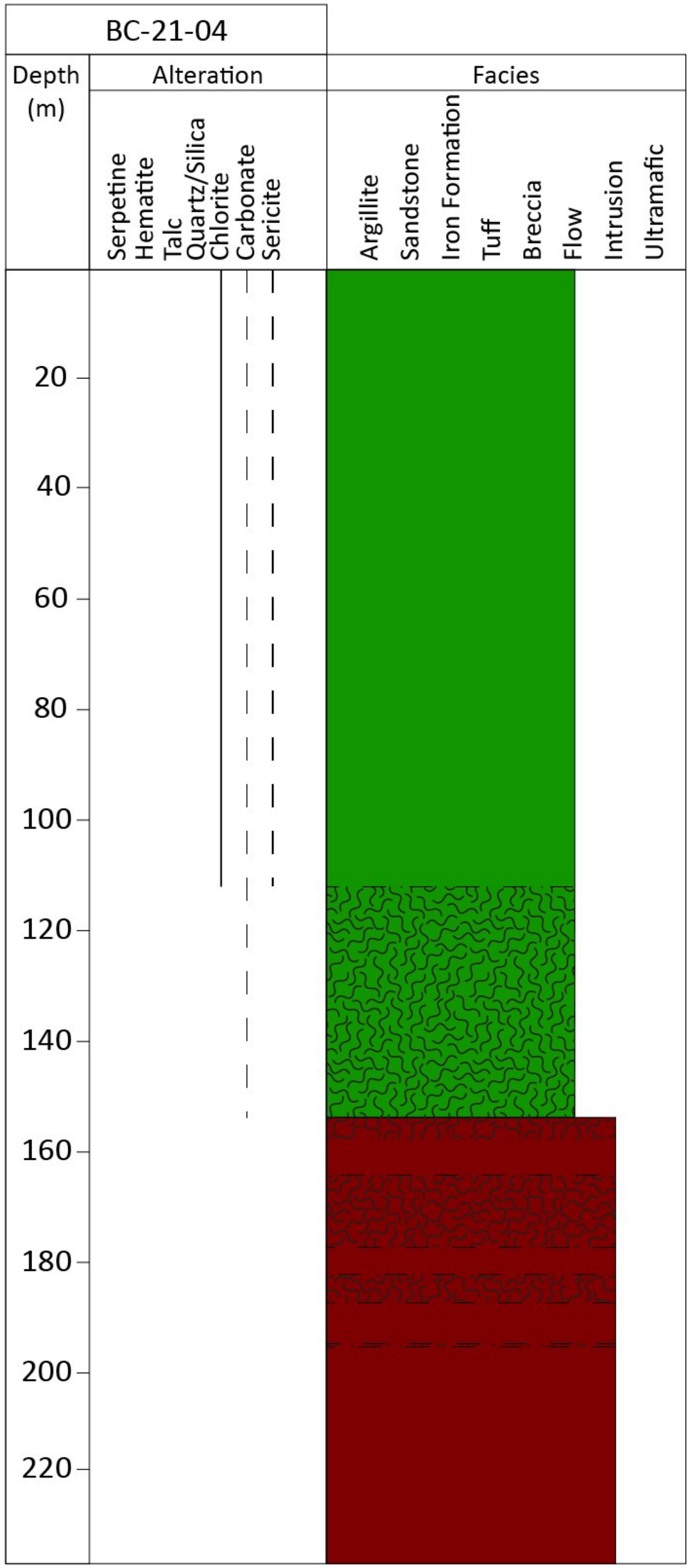
BC-21-04
Depth (m)
Alteration
Serpetine
Hematite
Talc
Quartz/Silica
Chlorite
Carbonate
Sericite
Facies
Argillite
Sandstone
Iron Formation
Tuff
Breccia
Flow
Intrusion
Ultramafic
20
40
60
80
100
120
140
160
180
200
220

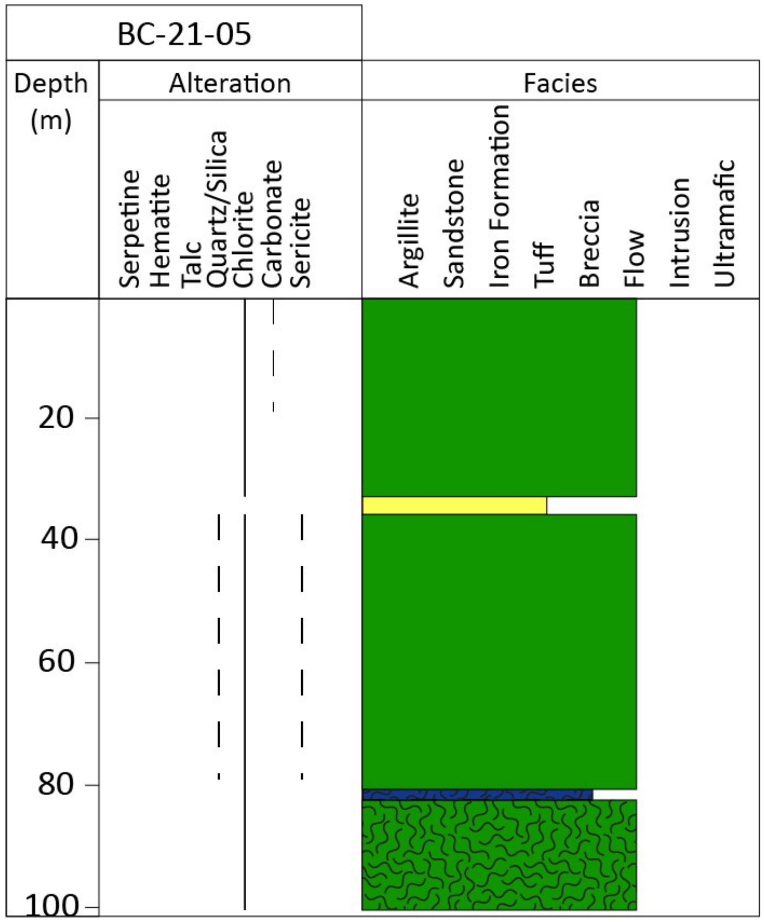
BC-21-05
Depth (m)
Alteration
Serpetine
Hematite
Talc
Quartz/Silica
Chlorite
Carbonate
Sericite
Facies
Argillite
Sandstone
Iron Formation
Tuff
Breccia
Flow
Intrusion
Ultramafic
20
40
60
80
100

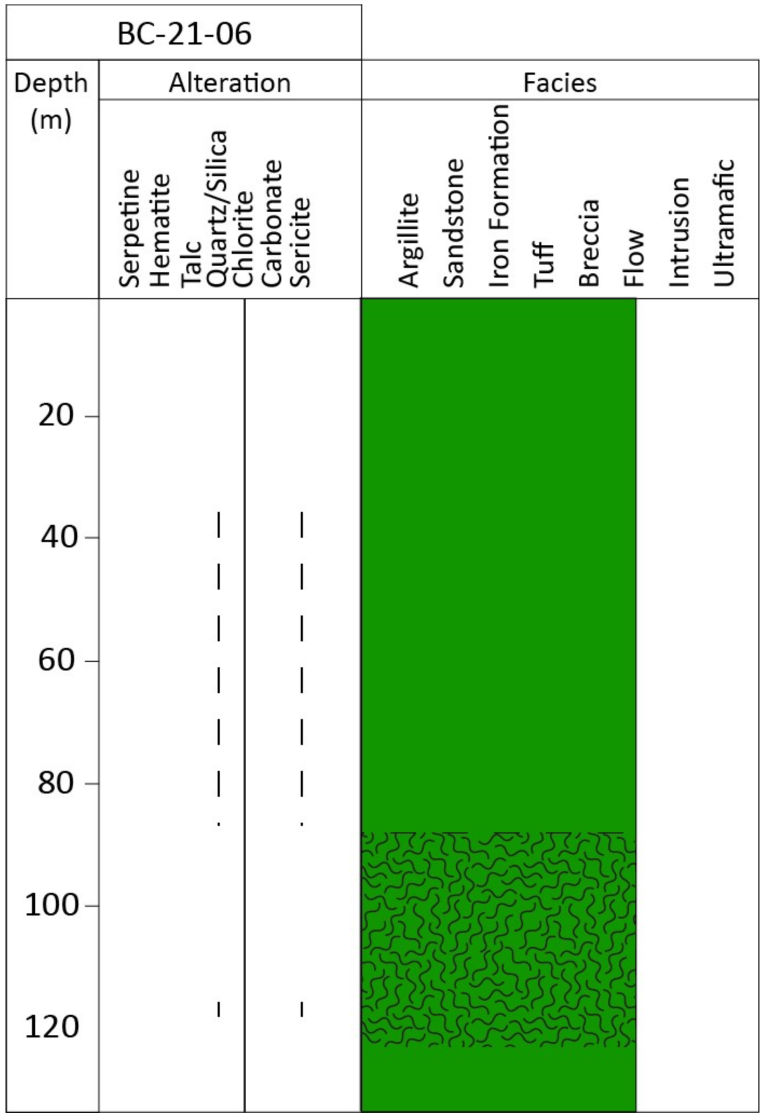
BC-21-06
Depth (m)
Alteration
Facies
Serpetine
Hematite
Talc
Quartz/Silica
Chlorite
Carbonate
Sericite
Argillite
Sandstone
Iron Formation
Tuff
Breccia
Flow
Intrusion
Ultramafic
20
40
60
80
100
120

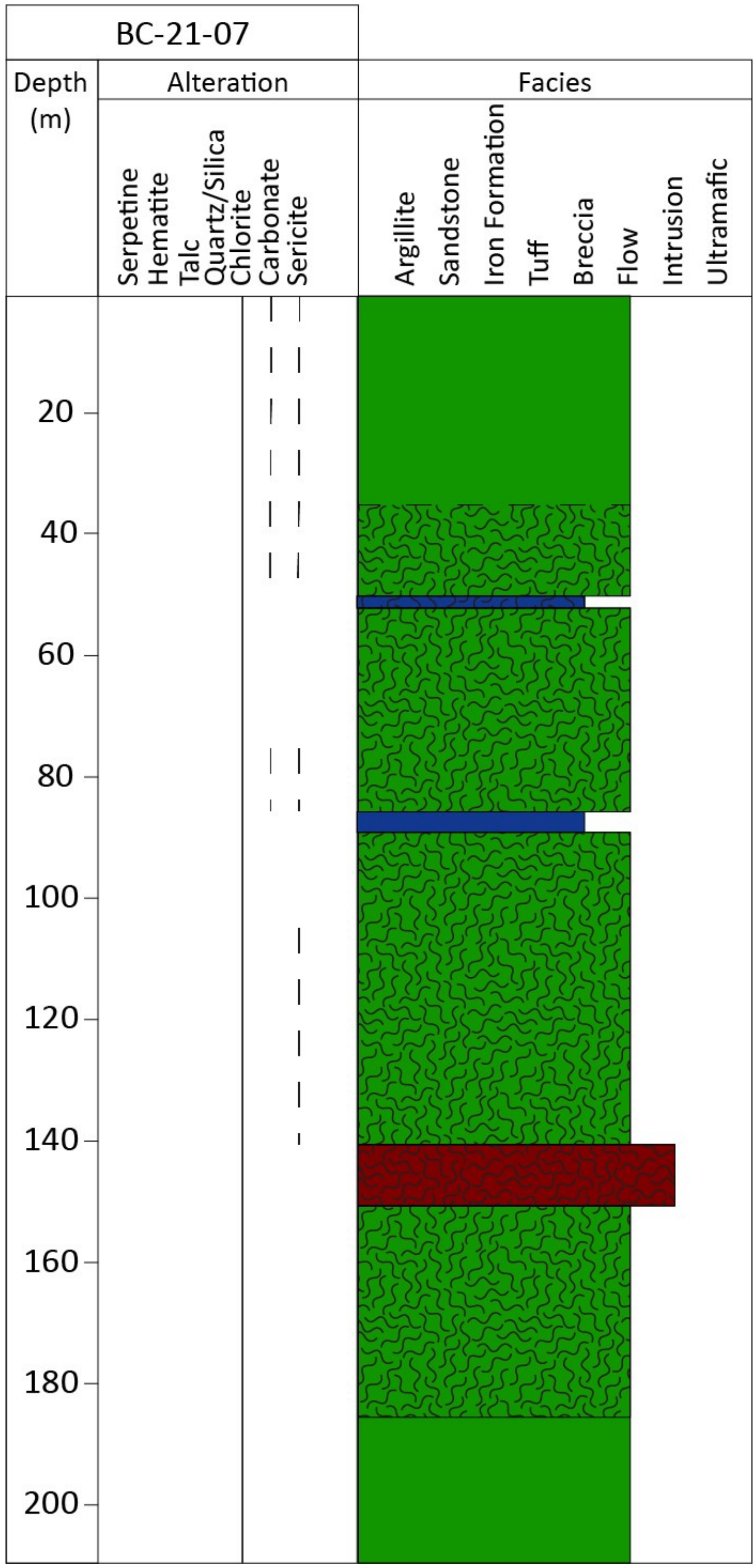
BC-21-07
Depth (m)
Alteration
Serpetine
Hematite
Talc
Quartz/Silica
Chlorite
Carbonate
Sericite
Facies
Argillite
Sandstone
Iron Formation
Tuff
Breccia
Flow
Intrusion
Ultramafic
20
40
60
80
100
120
140
160
180
200

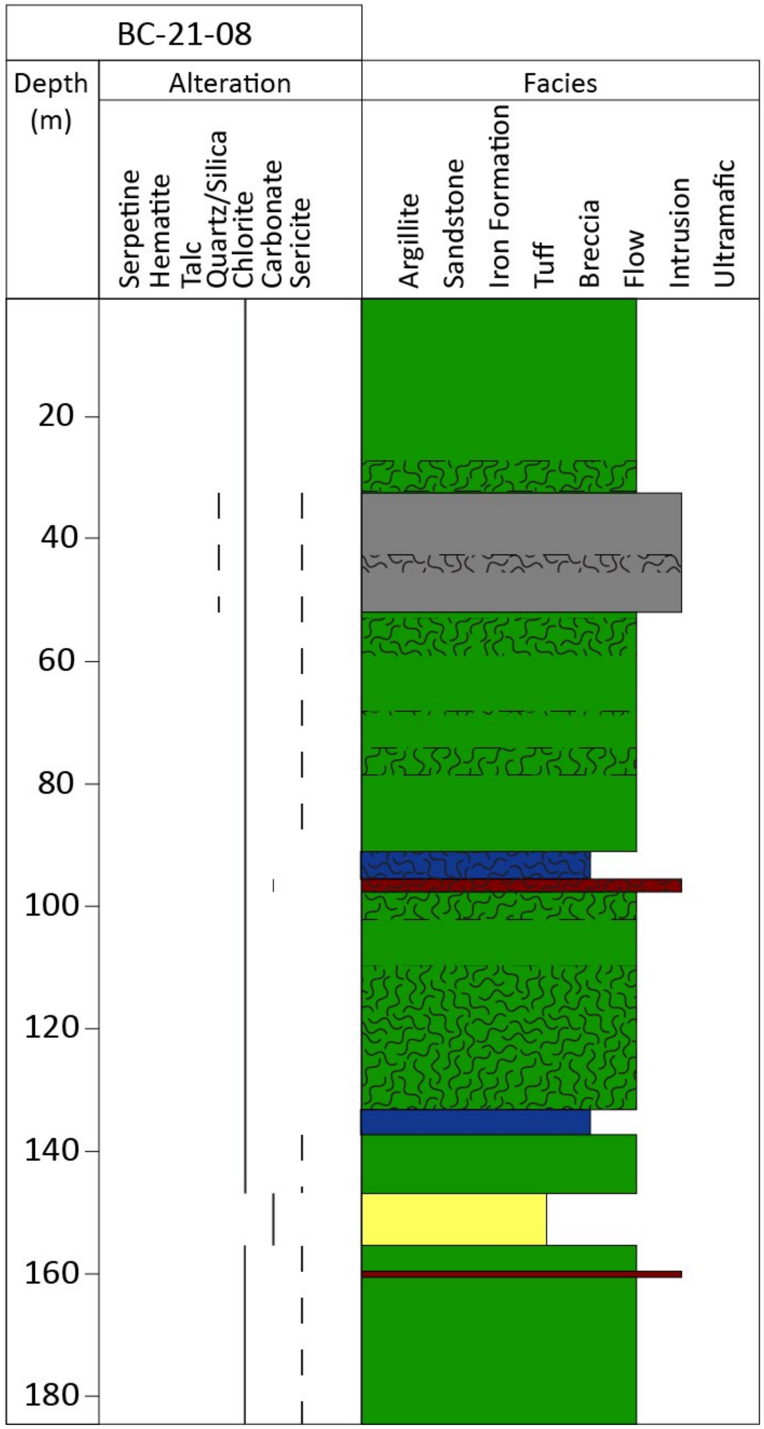
BC-21-08
Depth (m)
Alteration
Serpetine
Hematite
Talc
Quartz/Silica
Chlorite
Carbonate
Sericite
Facies
Argillite
Sandstone
Iron Formation
Tuff
Breccia
Flow
Intrusion
Ultramafic
20
40
60
80
100
120
140
160
180

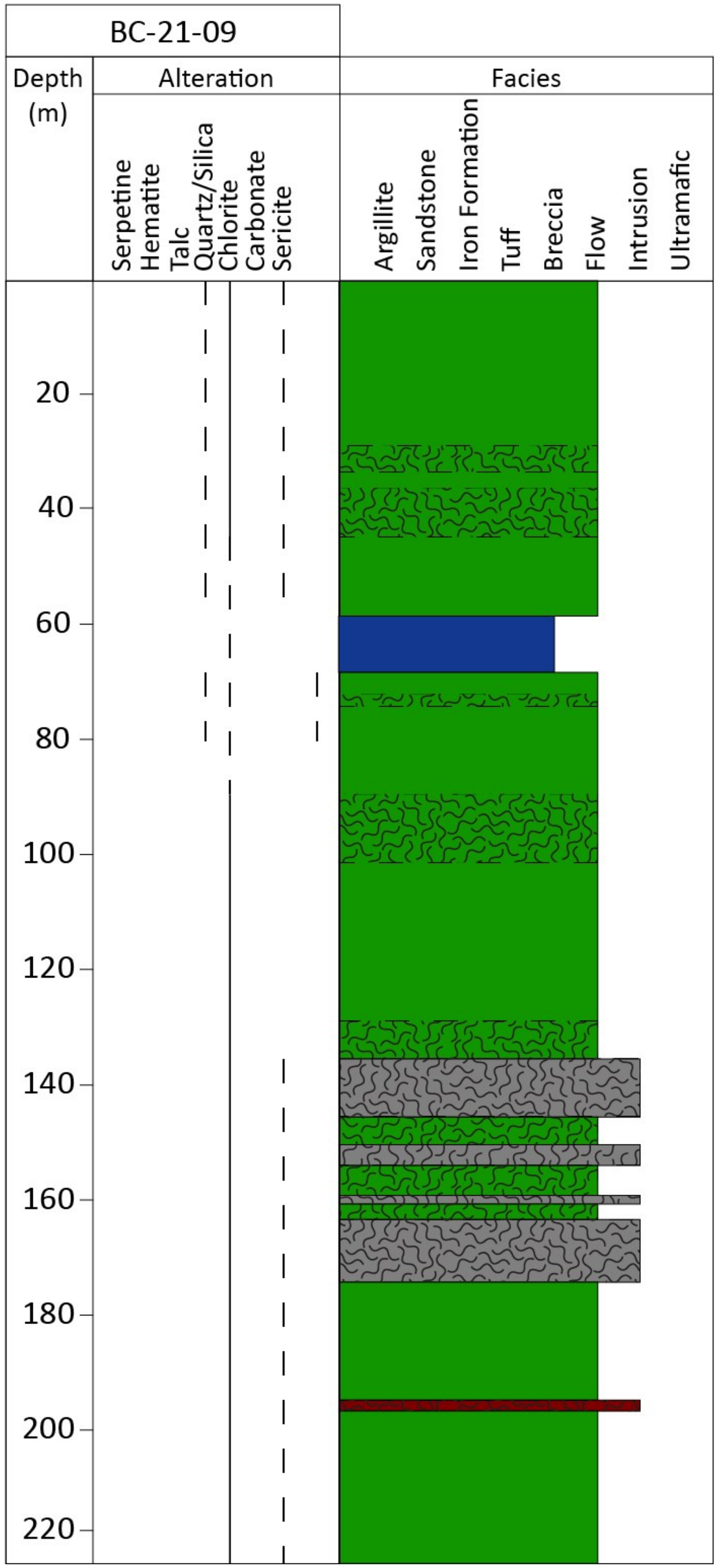
BC-21-09
Depth (m)
Alteration
Serpetine
Hematite
Talc
Quartz/Silica
Chlorite
Carbonate
Sericite
Facies
Argillite
Sandstone
Iron Formation
Tuff
Breccia
Flow
Intrusion
Ultramafic
20
40
60
80
100
120
140
160
180
200
220

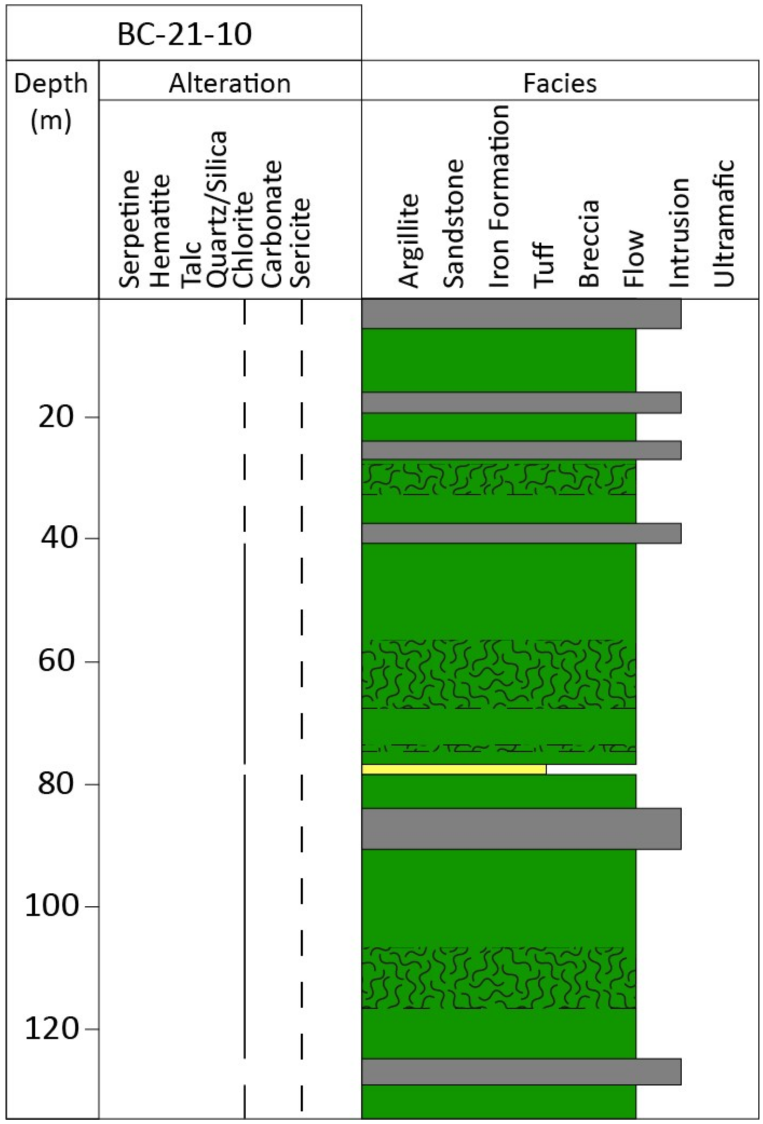
BC-21-10
Depth (m)
Alteration
Serpetine
Hematite
Talc
Quartz/Silica
Chlorite
Carbonate
Sericite
Facies
Argillite
Sandstone
Iron Formation
Tuff
Breccia
Flow
Intrusion
Ultramafic
20
40
60
80
100
120

Figure A3. Compilation of graphic logs from Tilt Cove.

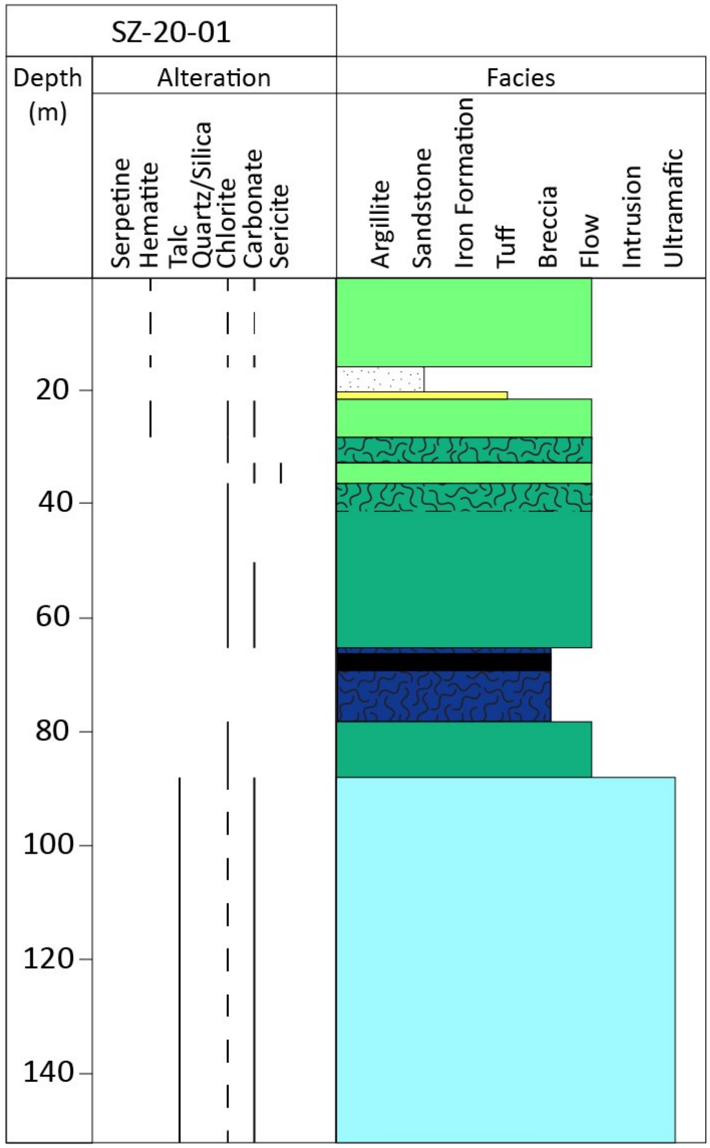
SZ-20-01
Depth (m)
Alteration
Serpetine
Hematite
Talc
Quartz/Silica
Chlorite
Carbonate
Sericite
Facies
Argillite
Sandstone
Iron Formation
Tuff
Breccia
Flow
Intrusion
Ultramafic
20
40
60
80
100
120
140

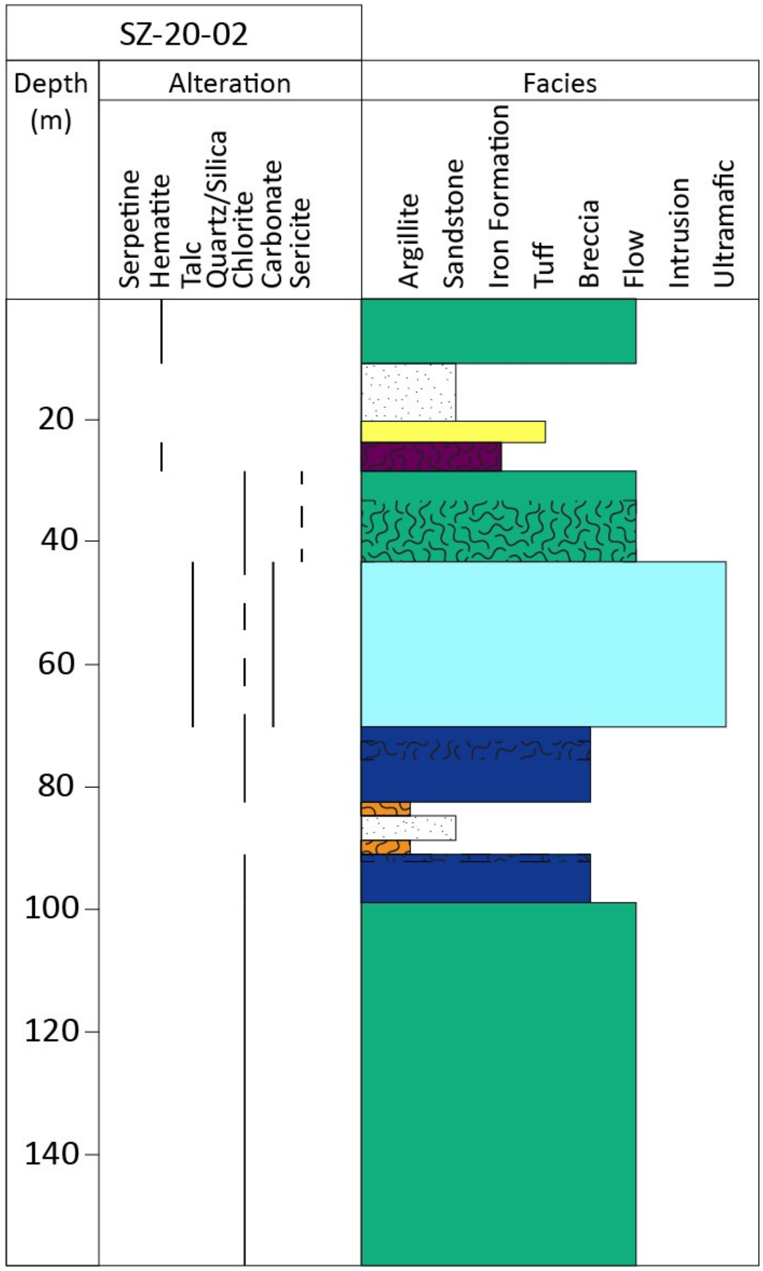

SZ-20-02
Depth (m)
Alteration
Serpetine
Hematite
Talc
Quartz/Silica
Chlorite
Carbonate
Sericite
Facies
Argillite
Sandstone
Iron Formation
Tuff
Breccia
Flow
Intrusion
Ultramafic
20
40
60
80
100
120
140

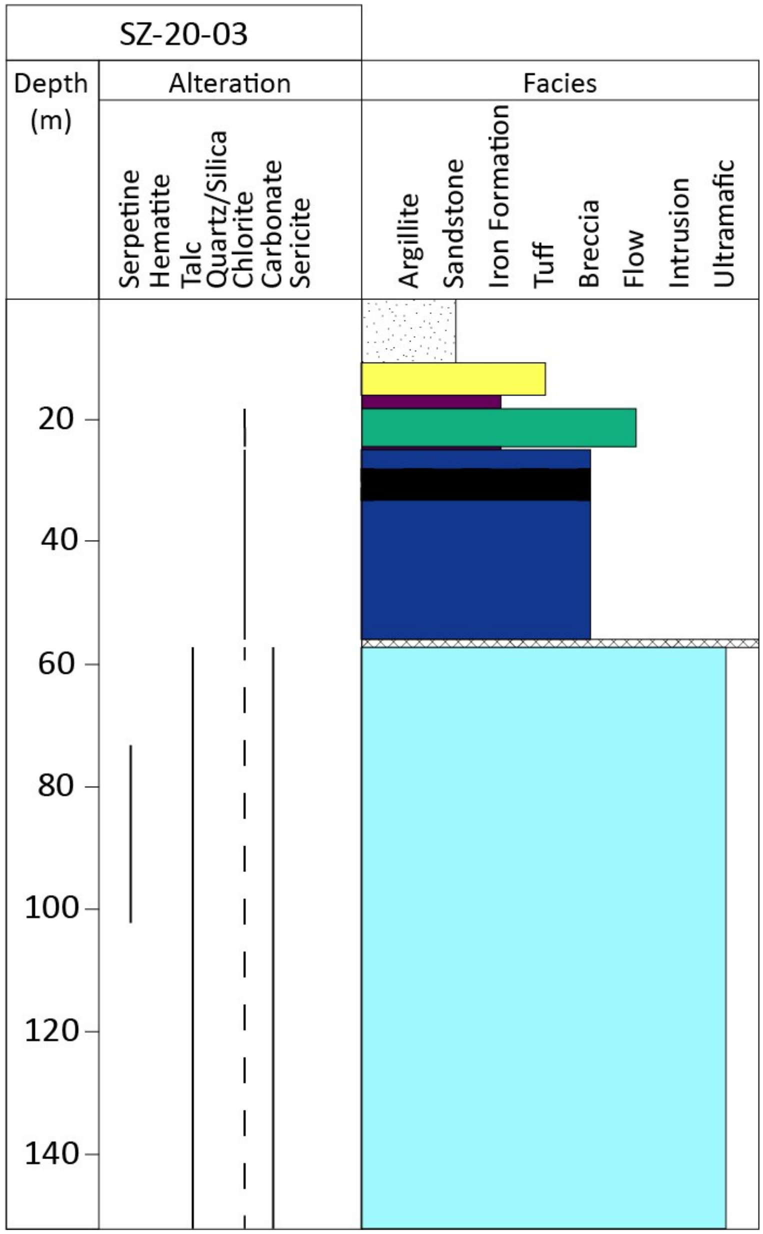
SZ-20-03
Depth (m)
Alteration
Serpetine
Hematite
Talc
Quartz/Silica
Chlorite
Carbonate
Sericite
Facies
Argillite
Sandstone
Iron Formation
Tuff
Breccia
Flow
Intrusion
Ultramafic
20
40
60
80
100
120
140

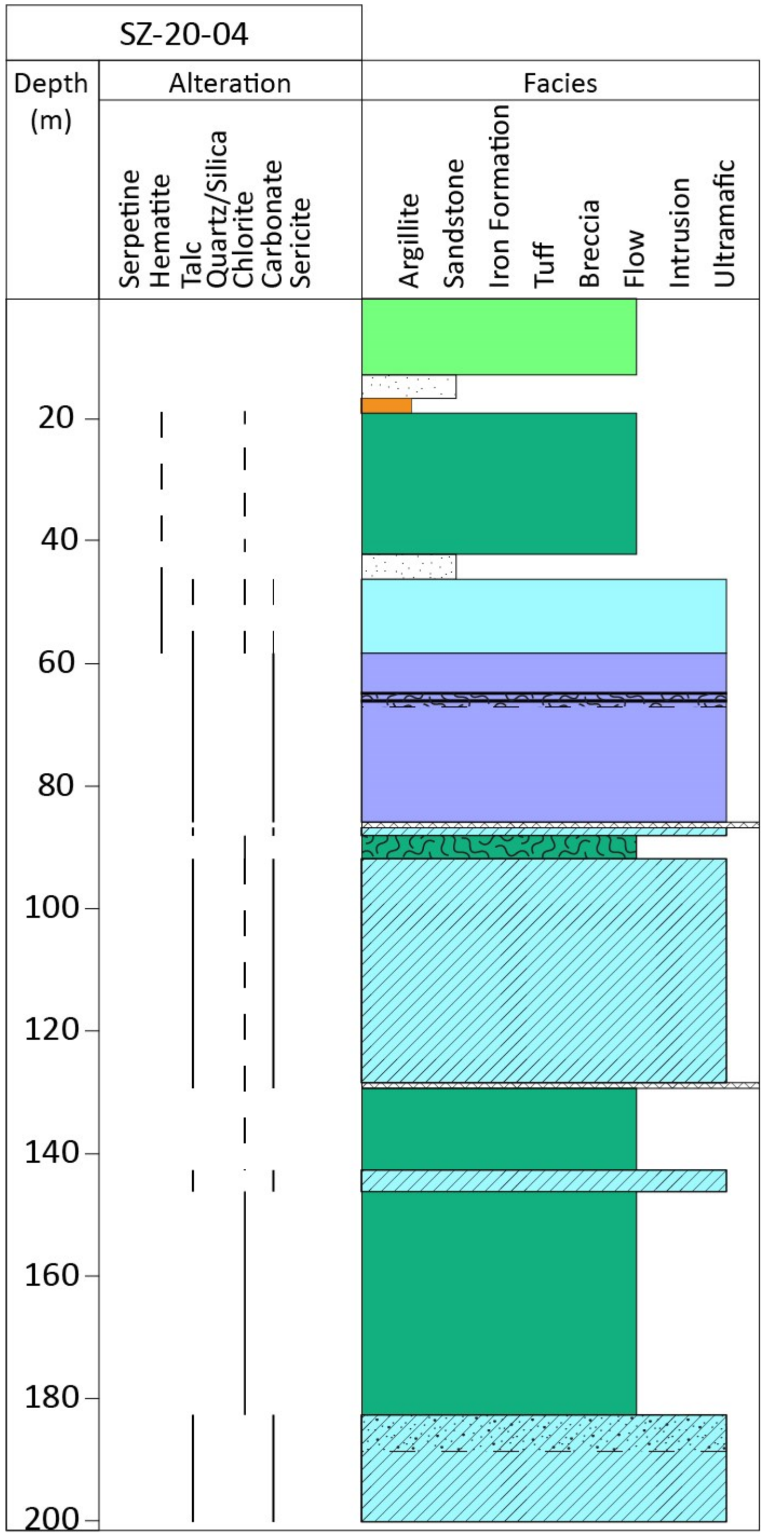
SZ-20-04
Depth (m)
Alteration
Facies
Serpetine
Hematite
Talc
Quartz/Silica
Chlorite
Carbonate
Sericite
Argillite
Sandstone
Iron Formation
Tuff
Breccia
Flow
Intrusion
Ultramafic
20
40
60
80
100
120
140
160
180
200

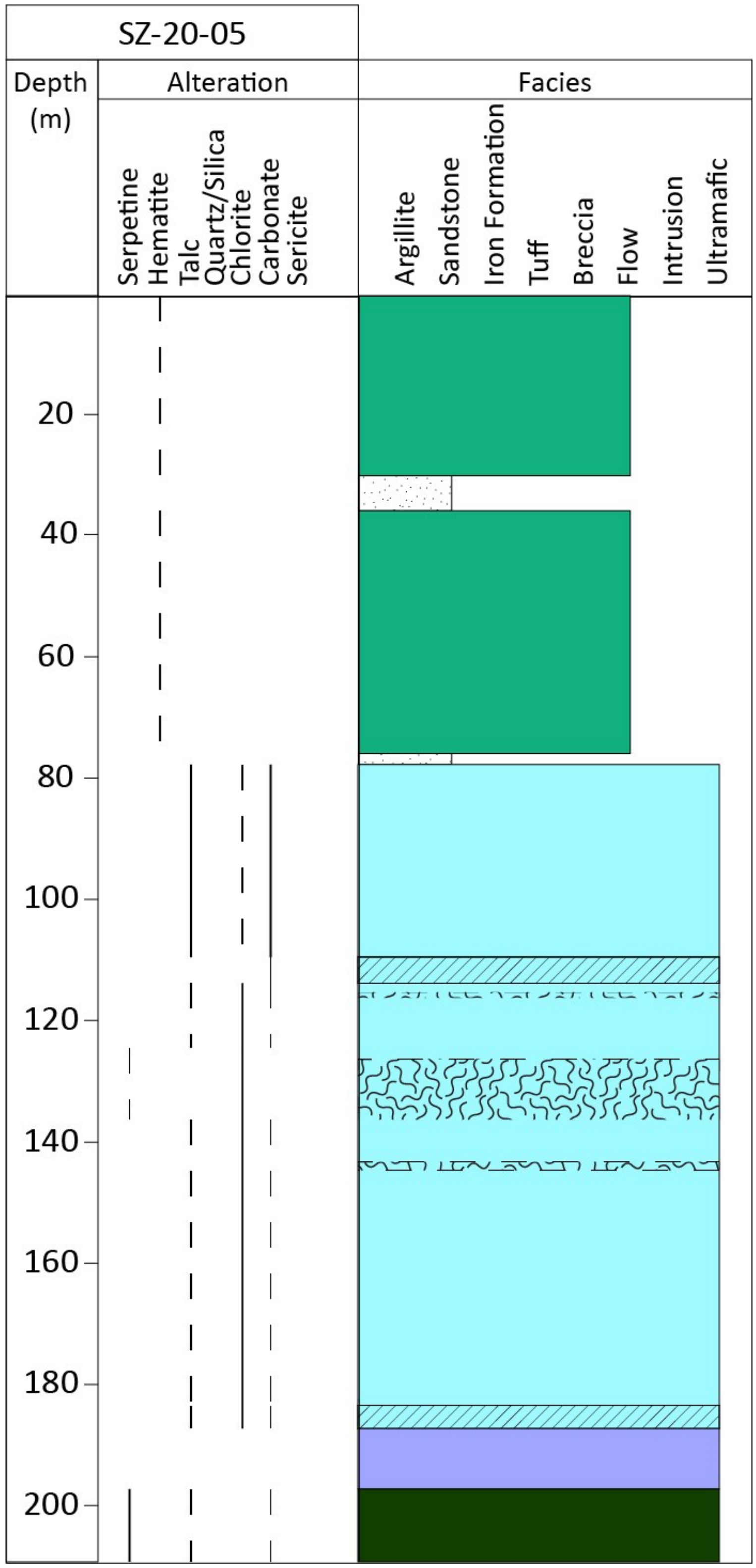
SZ-20-05
Depth (m)
Alteration
Serpetine
Hematite
Talc
Quartz/Silica
Chlorite
Carbonate
Sericite
Facies
Argillite
Sandstone
Iron Formation
Tuff
Breccia
Flow
Intrusion
Ultramafic
20
40
60
80
100
120
140
160
180
200

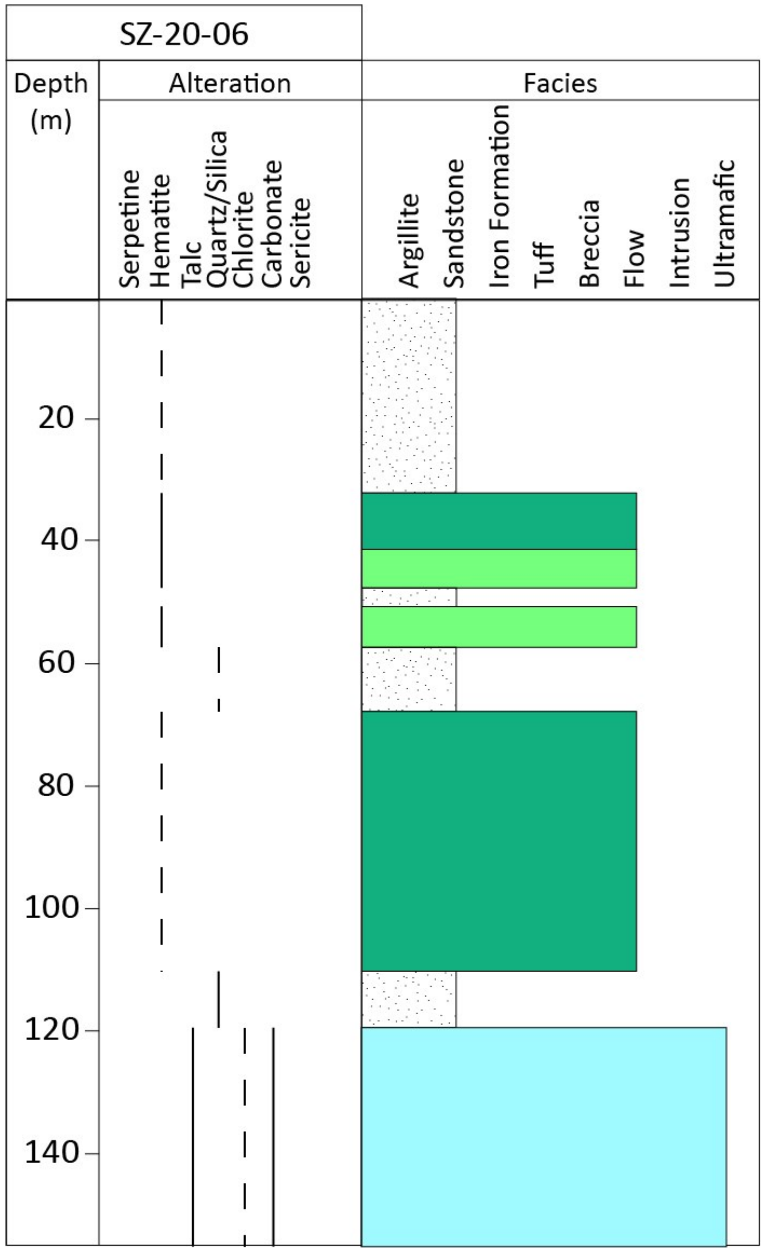
SZ-20-06
Depth (m)
Alteration
Serpetine
Hematite
Talc
Quartz/Silica
Chlorite
Carbonate
Sericite
Facies
Argillite
Sandstone
Iron Formation
Tuff
Breccia
Flow
Intrusion
Ultramafic
20
40
60
80
100
120
140

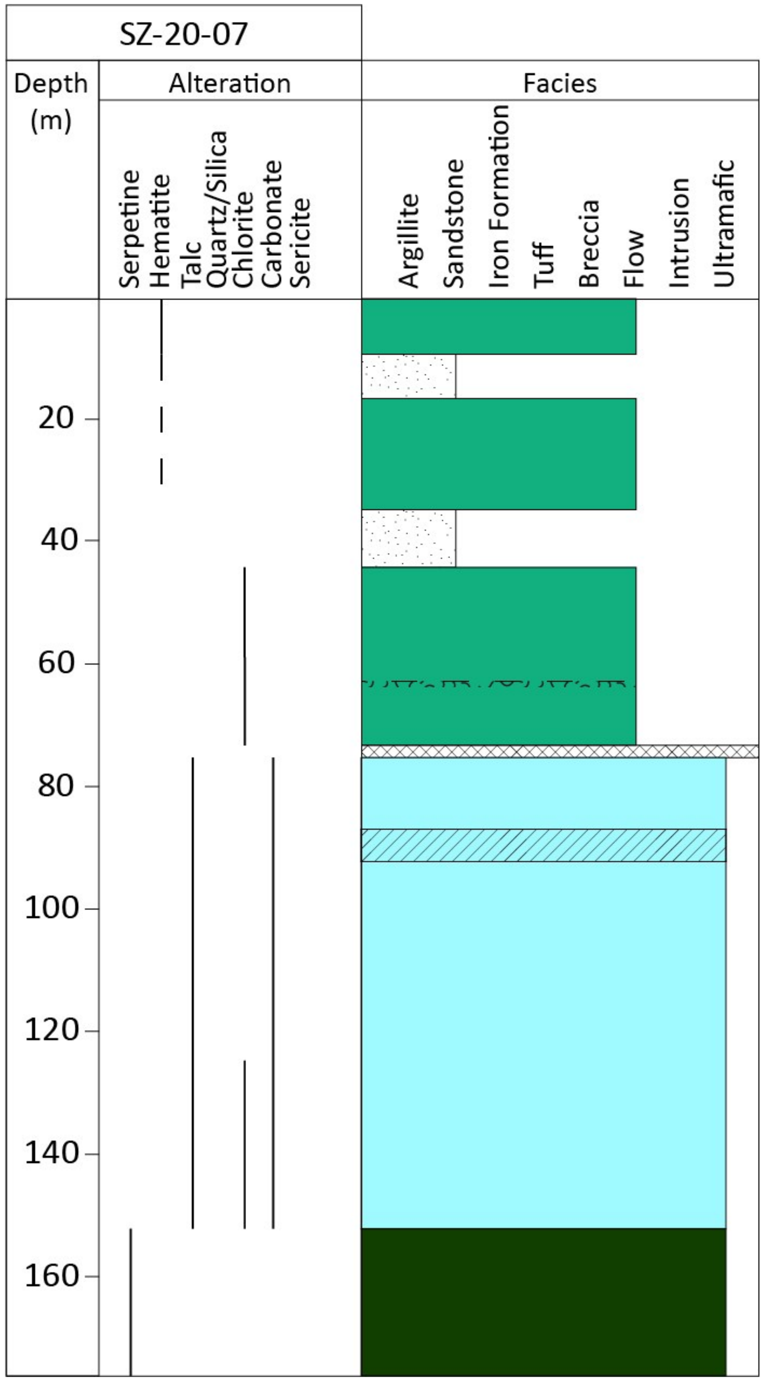
SZ-20-07
Depth (m)
Alteration
Facies
Serpetine
Hematite
Talc
Quartz/Silica
Chlorite
Carbonate
Sericite
Argillite
Sandstone
Iron Formation
Tuff
Breccia
Flow
Intrusion
Ultramafic
20
40
60
80
100
120
140
160

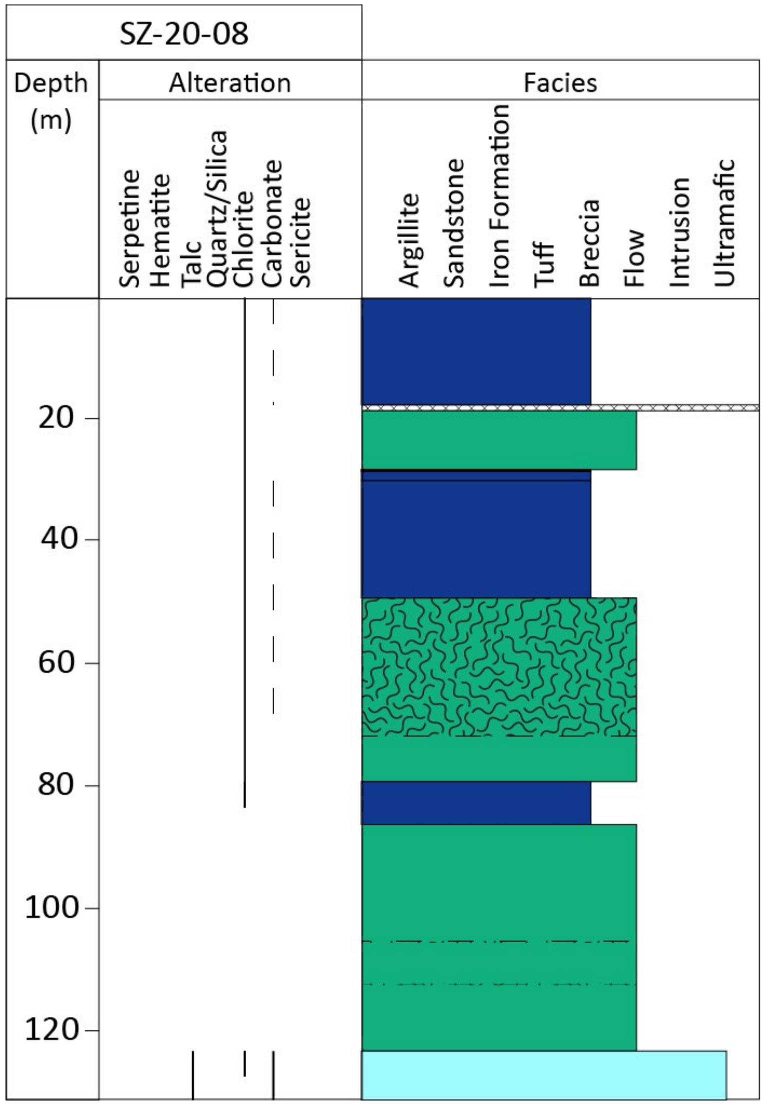

SZ-20-08
Depth (m)
Alteration
Serpetine
Hematite
Talc
Quartz/Silica
Chlorite
Carbonate
Sericite
Facies
Argillite
Sandstone
Iron Formation
Tuff
Breccia
Flow
Intrusion
Ultramafic
20
40
60
80
100
120

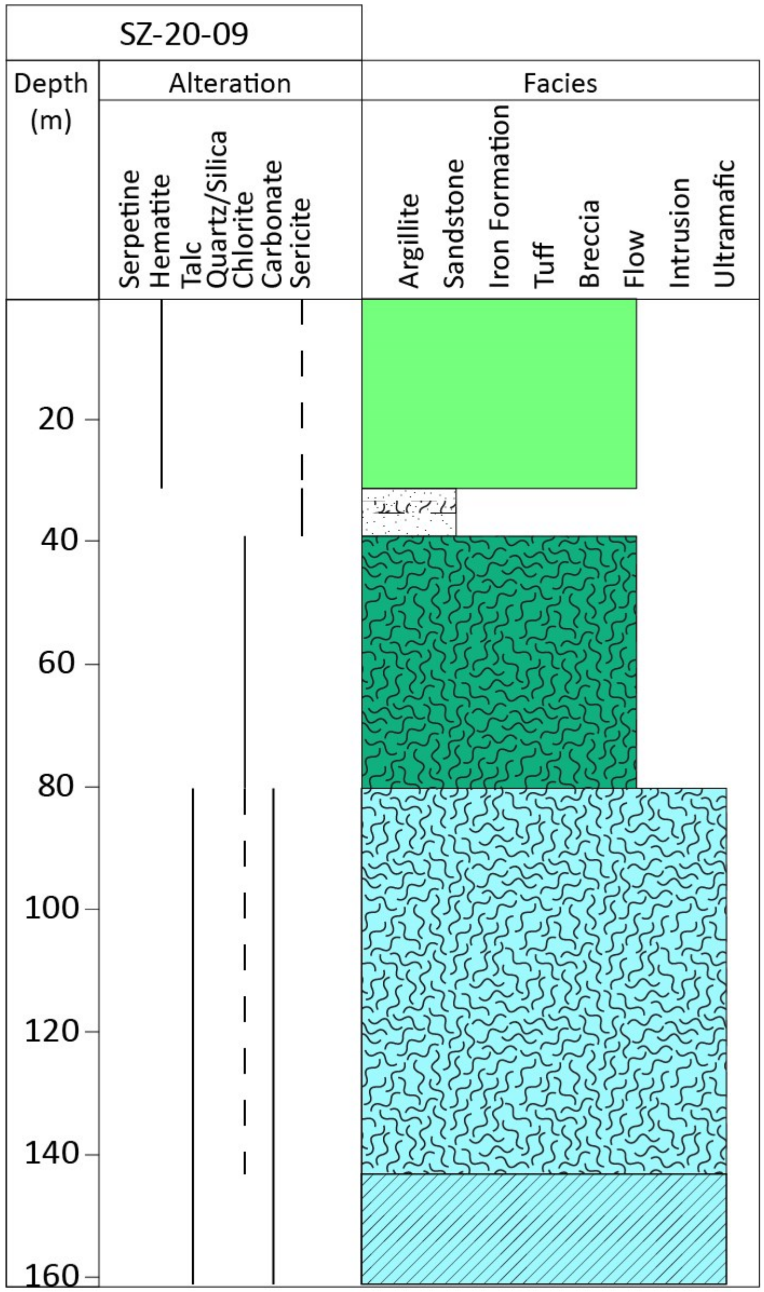
SZ-20-09
Depth (m)
Alteration
Serpetine
Hematite
Talc
Quartz/Silica
Chlorite
Carbonate
Sericite
Facies
Argillite
Sandstone
Iron Formation
Tuff
Breccia
Flow
Intrusion
Ultramafic
20
40
60
80
100
120
140
160

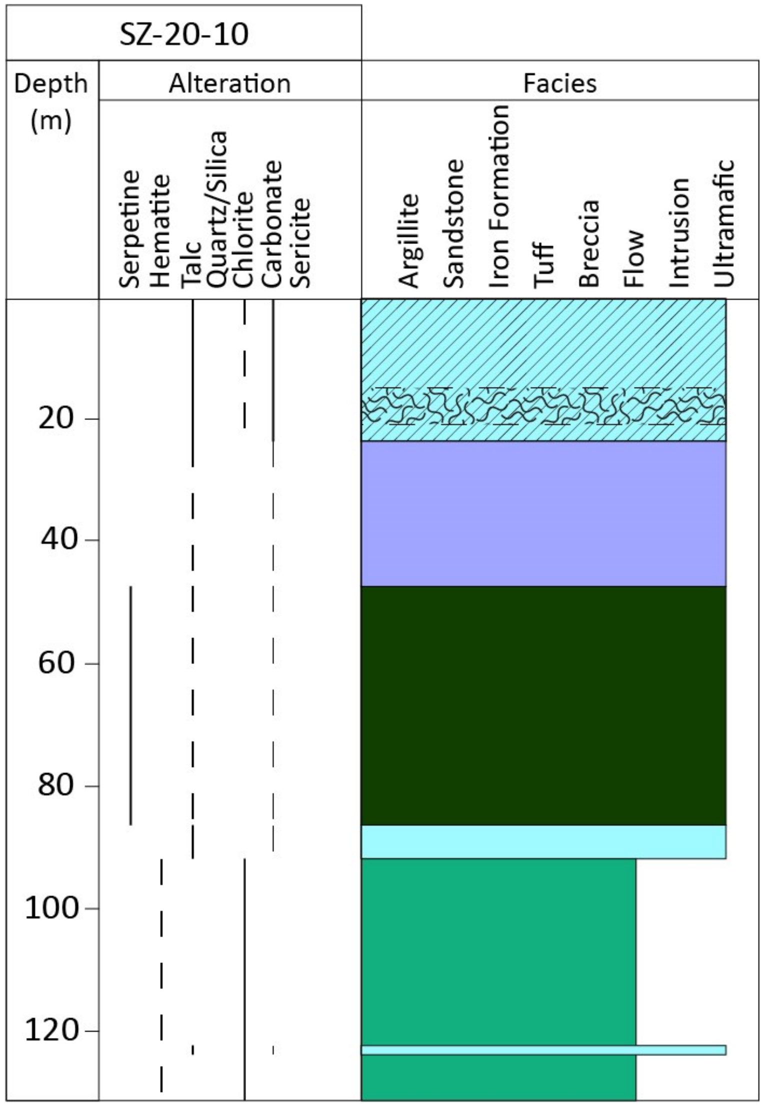
SZ-20-10
Depth (m)
Alteration
Serpetine
Hematite
Talc
Quartz/Silica
Chlorite
Carbonate
Sericite
Facies
Argillite
Sandstone
Iron Formation
Tuff
Breccia
Flow
Intrusion
Ultramafic
20
40
60
80
100
120

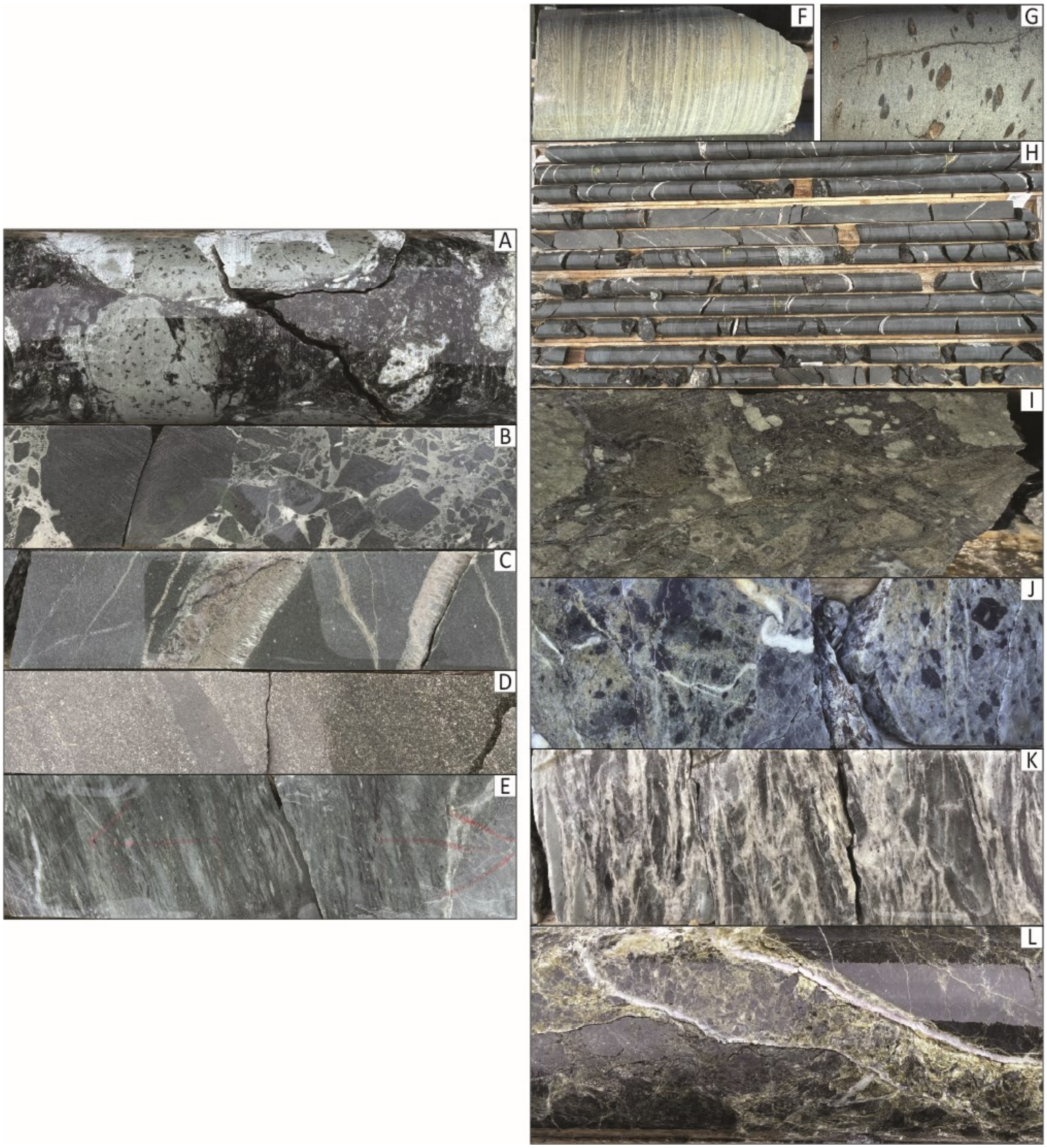

Figure A4. Photographs of lithological units from Betts Cove, including: A) pillow flows with chlorite surrounding individual pillows; B) breccia; C) mafic dyke from the sheeted dyke unit with quartz-sericite veining; D) gabbroic dyke; E) banded tuff, and from Tilt Cove, including, F) interbedded sandstone and siltstone from the Cape St. John group; G) amygdaloidal basalt from the Cape St. John group; H) massive and pillow flows; I) breccia; J) pyroxenite; K) talc-carbonate schist; and L) serpentinite.

Appendix B: Mineral Maps

Figure B1. Legend for mineral maps.

Figure B2. Mineral map of thin section KKMSC05B.

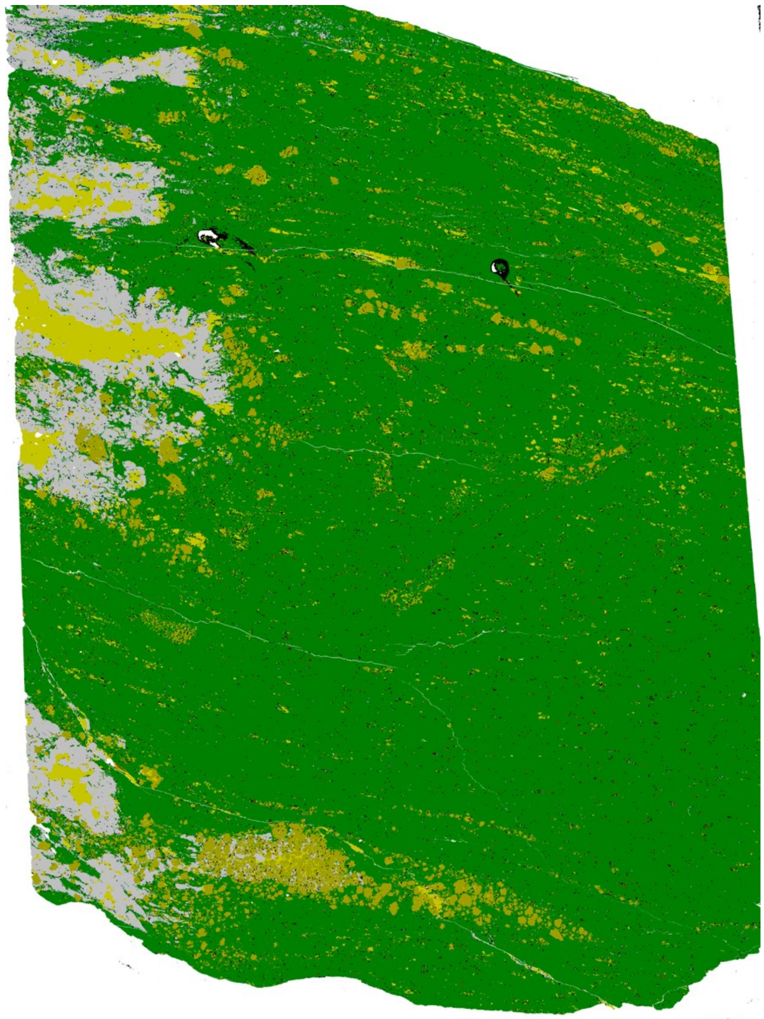

Figure B3. Mineral map of thin section KKMSC09.

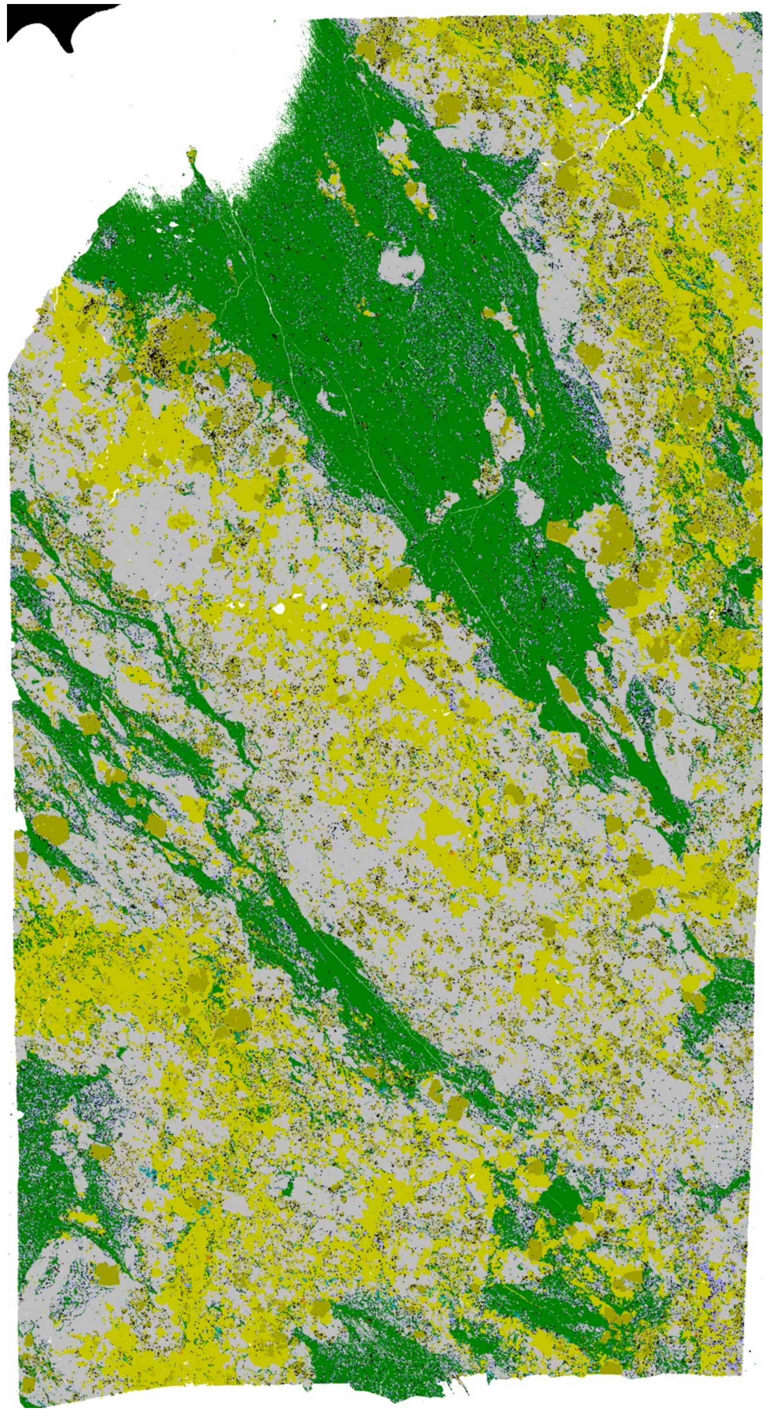

Figure B4. Mineral map of thin section KKMSC12.

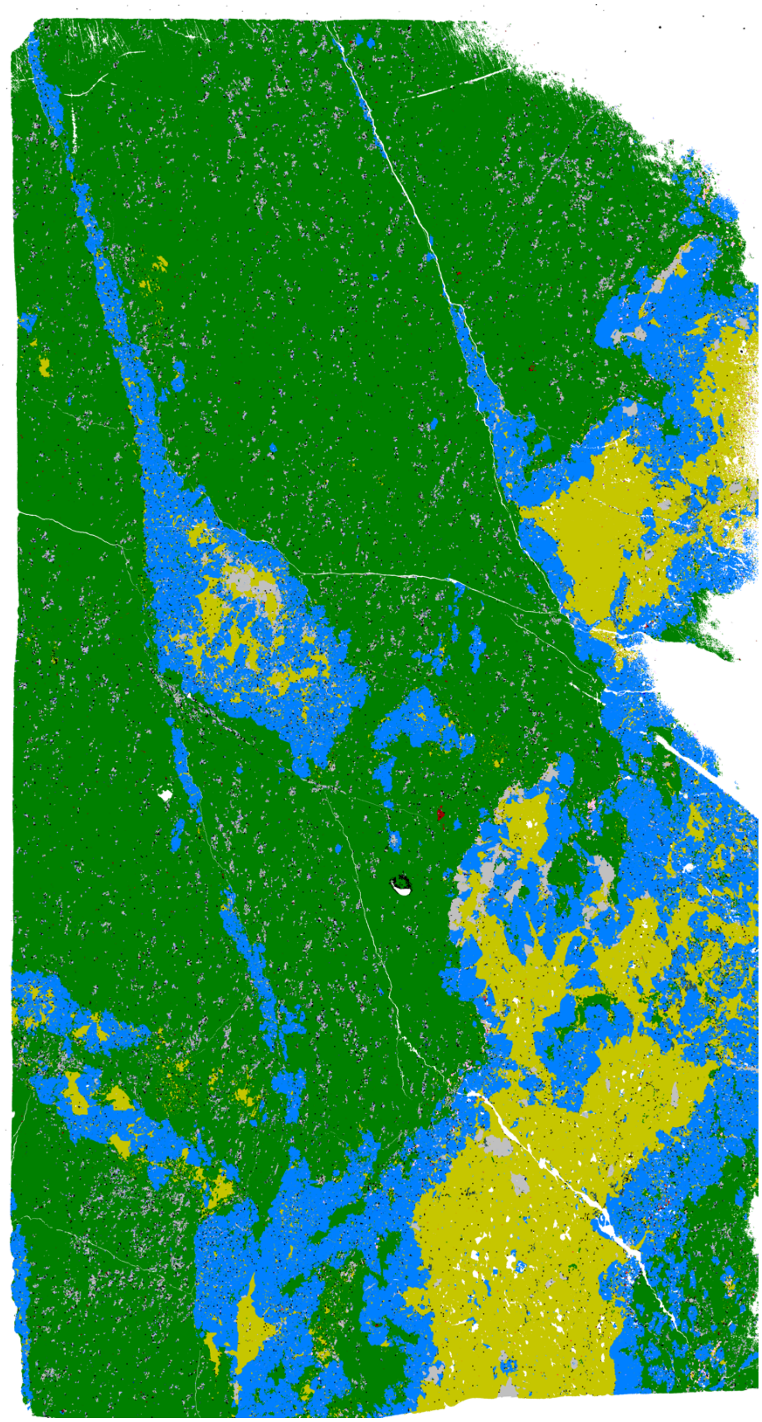

Figure B5. Mineral map of thin section KKMSC13.

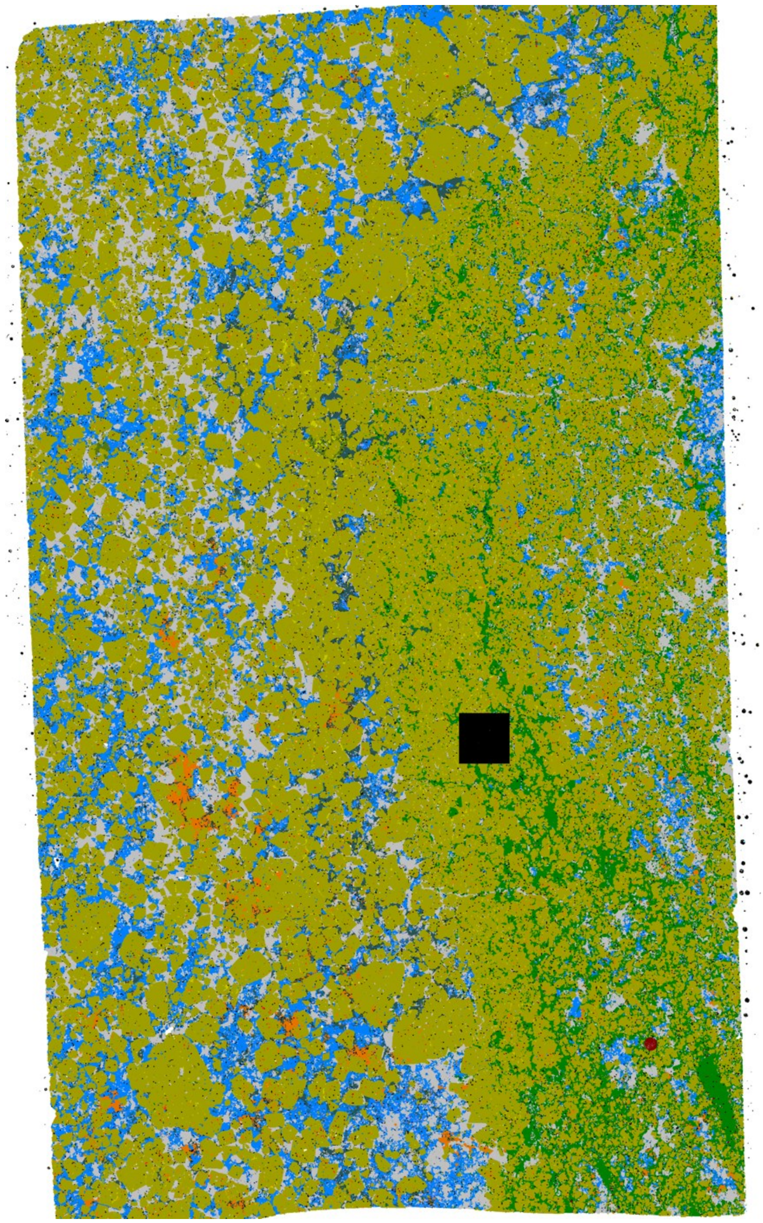

Figure B6. Mineral map of thin section KKMSC29.

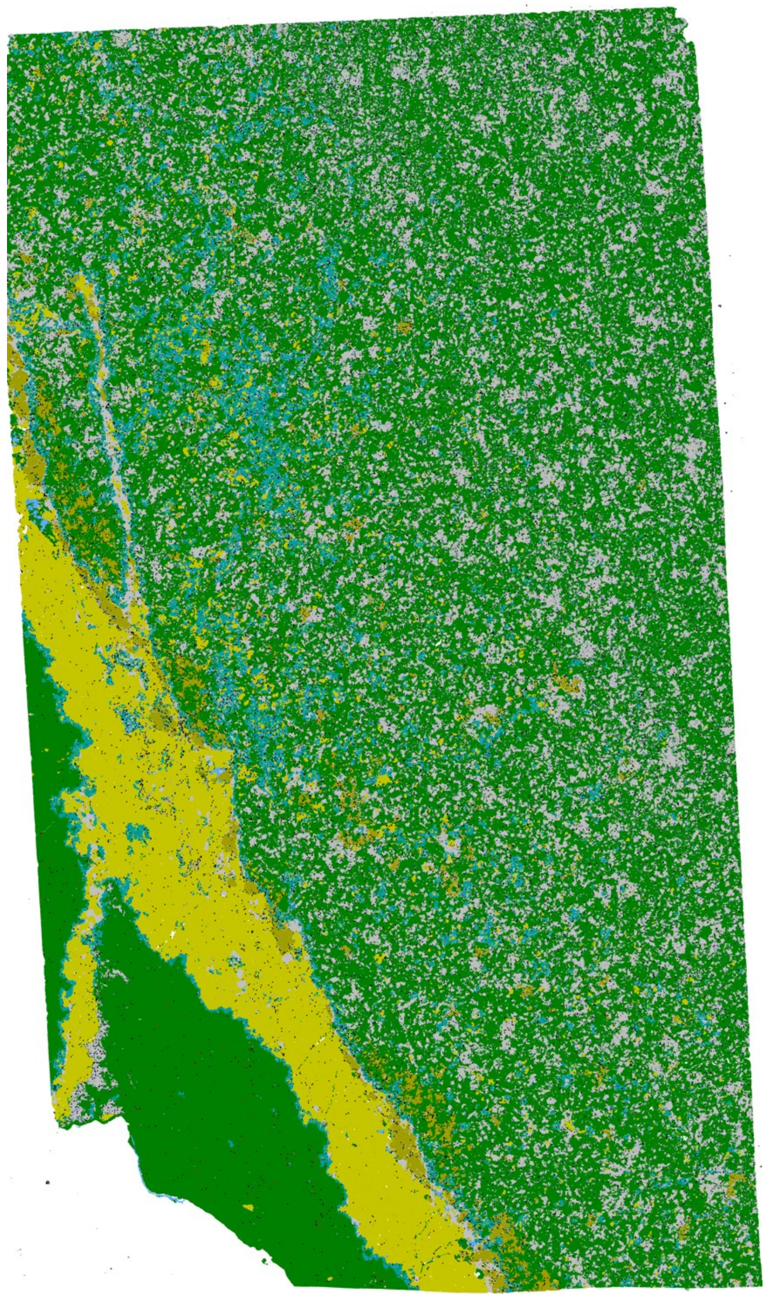

Figure B7. Mineral map of thin section KKMSC32.

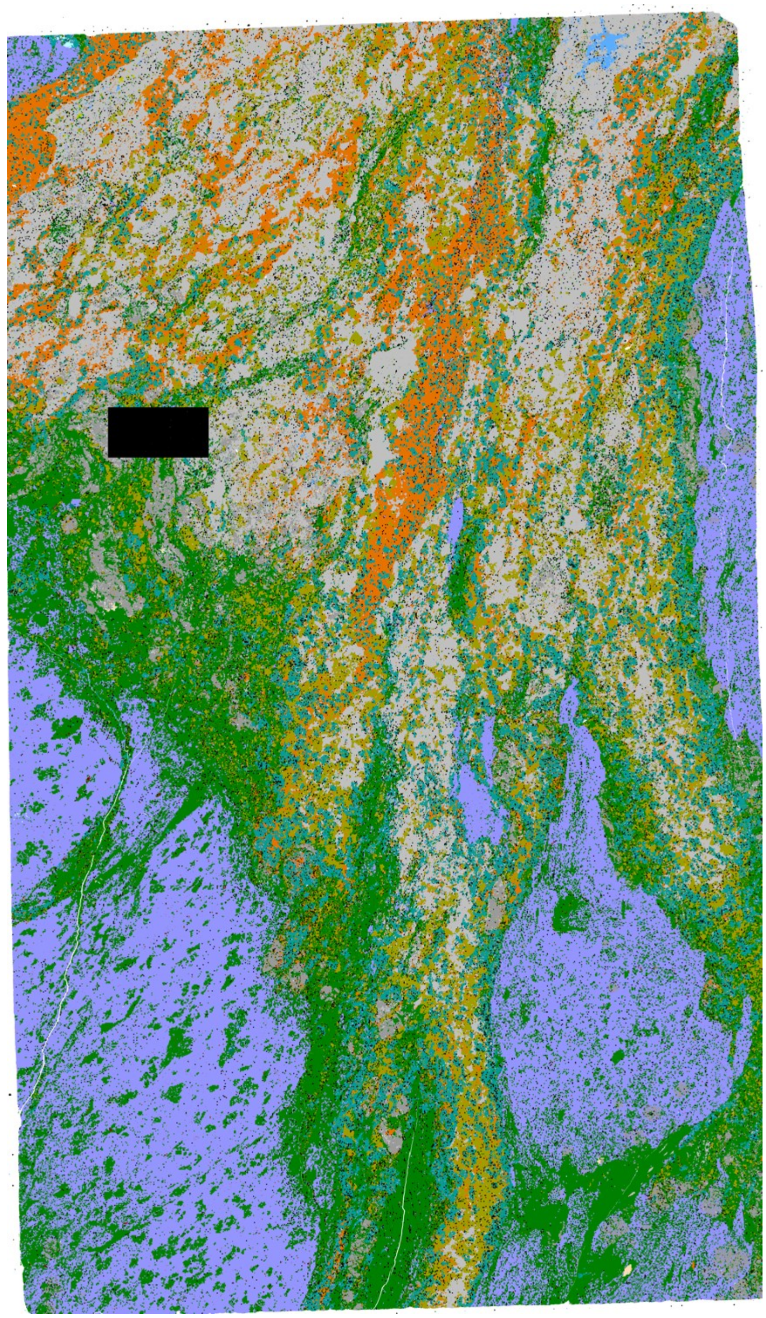

Figure B8. Mineral map of thin section KKMSC35.

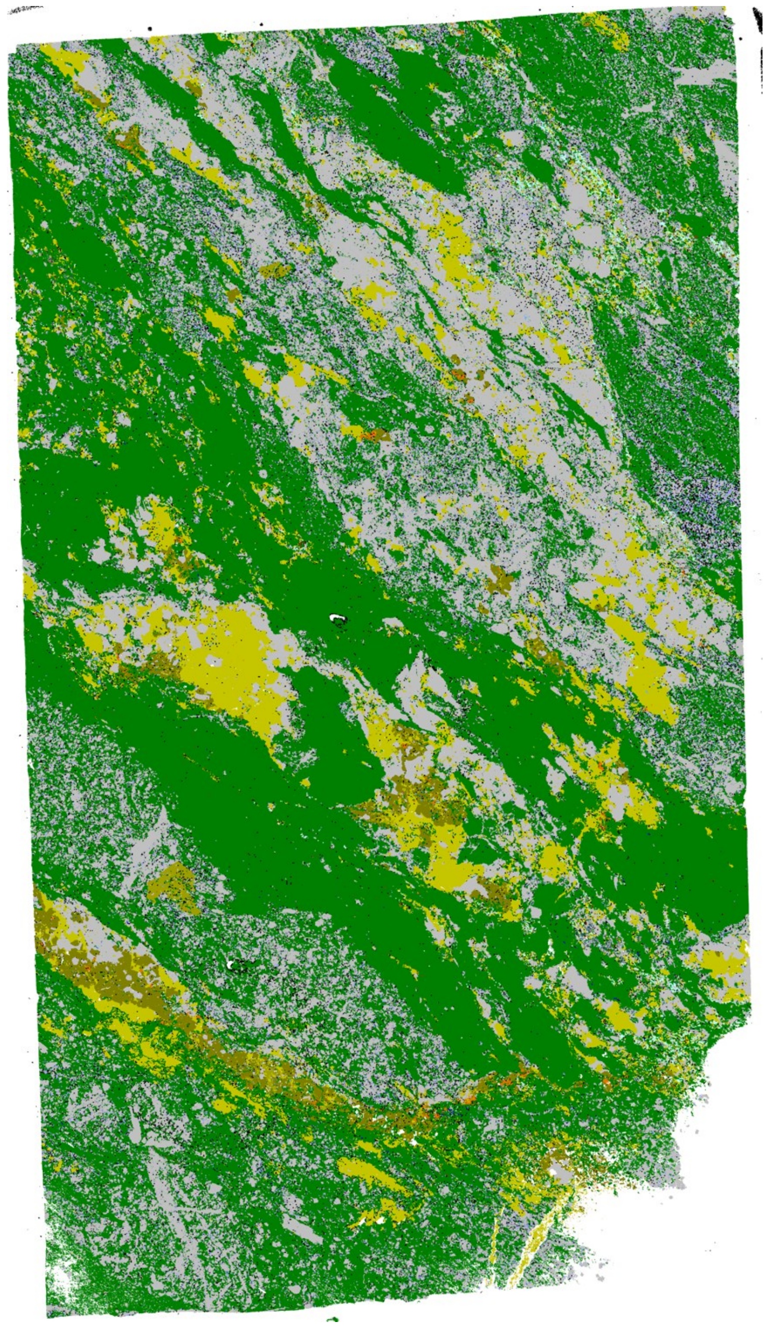

Figure B9. Mineral map of thin section KKMSC42.

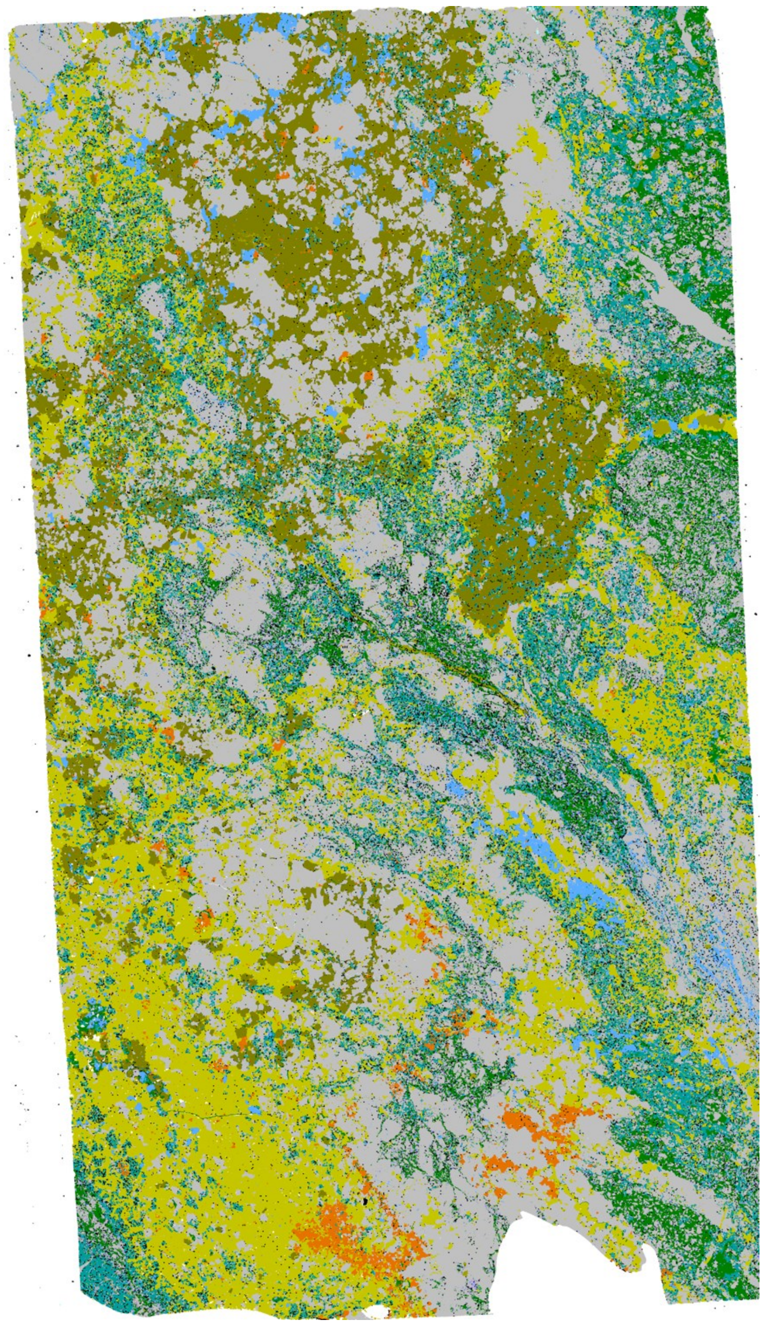

Figure B10. Mineral map of thin section KKMSC53.

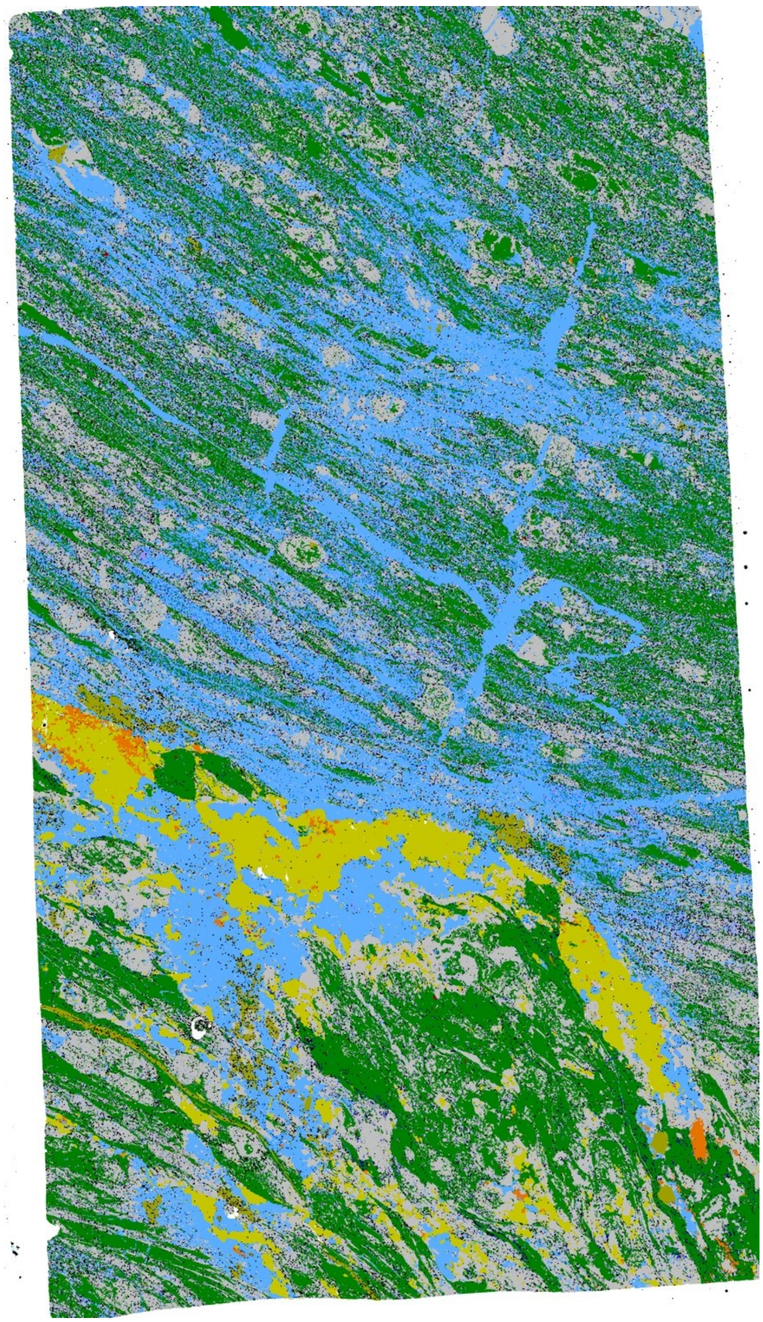

Figure B11. Mineral map of thin section KKMSC63.

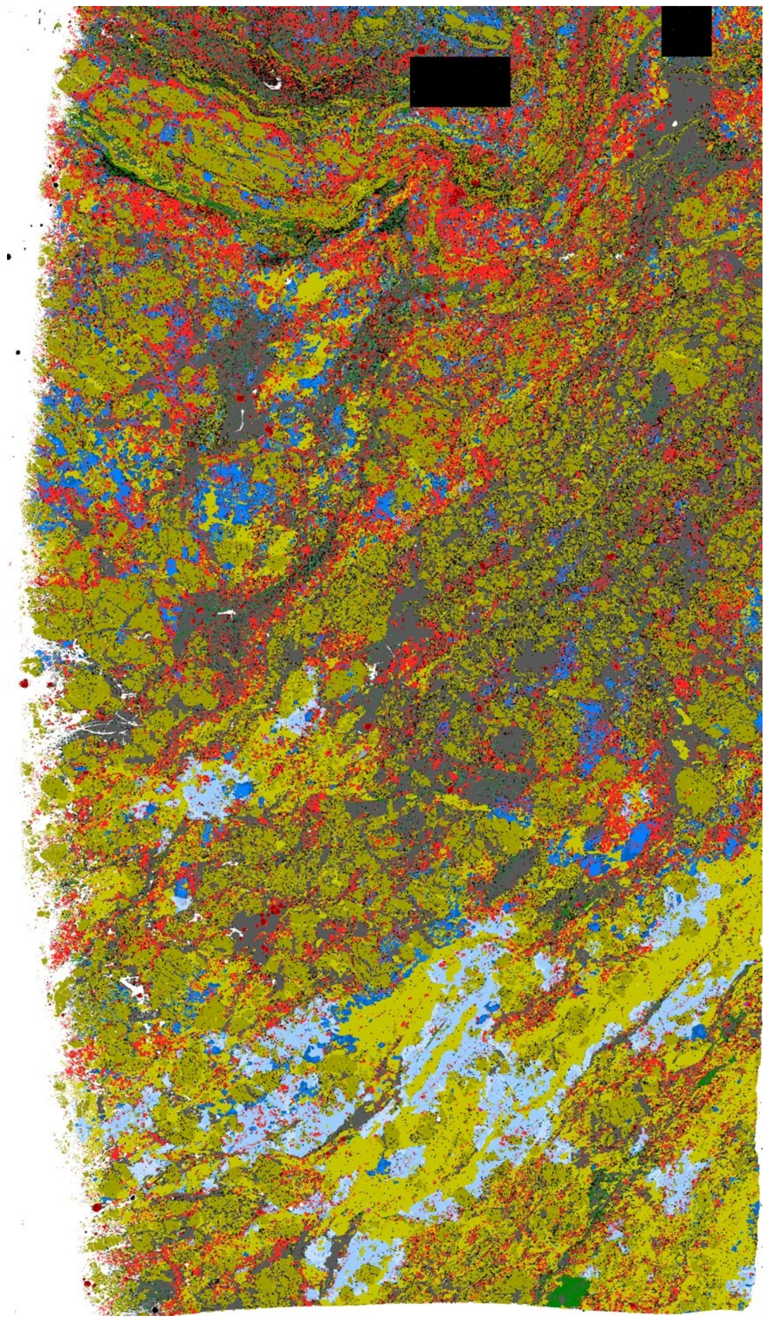

Figure B12. Mineral map of thin section KKMSC70.

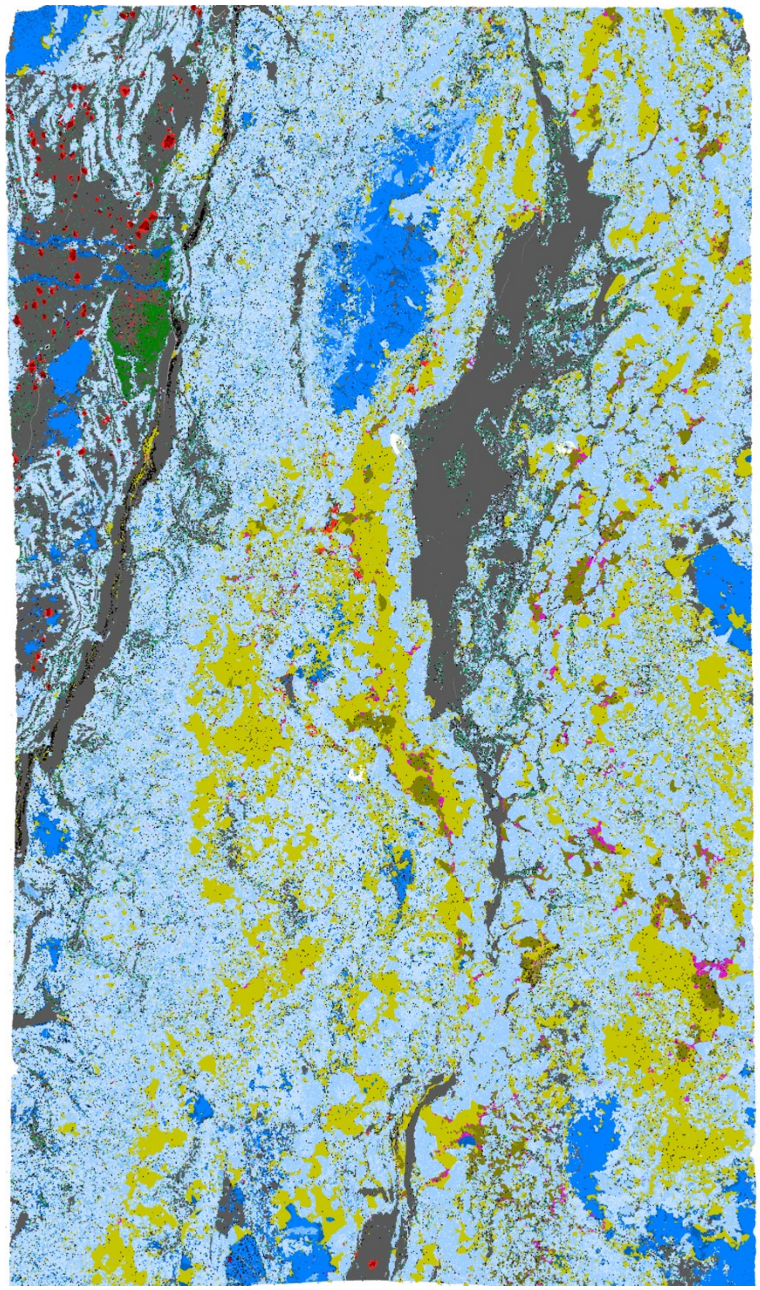

Figure B13. Mineral map of thin section KKMSC72.

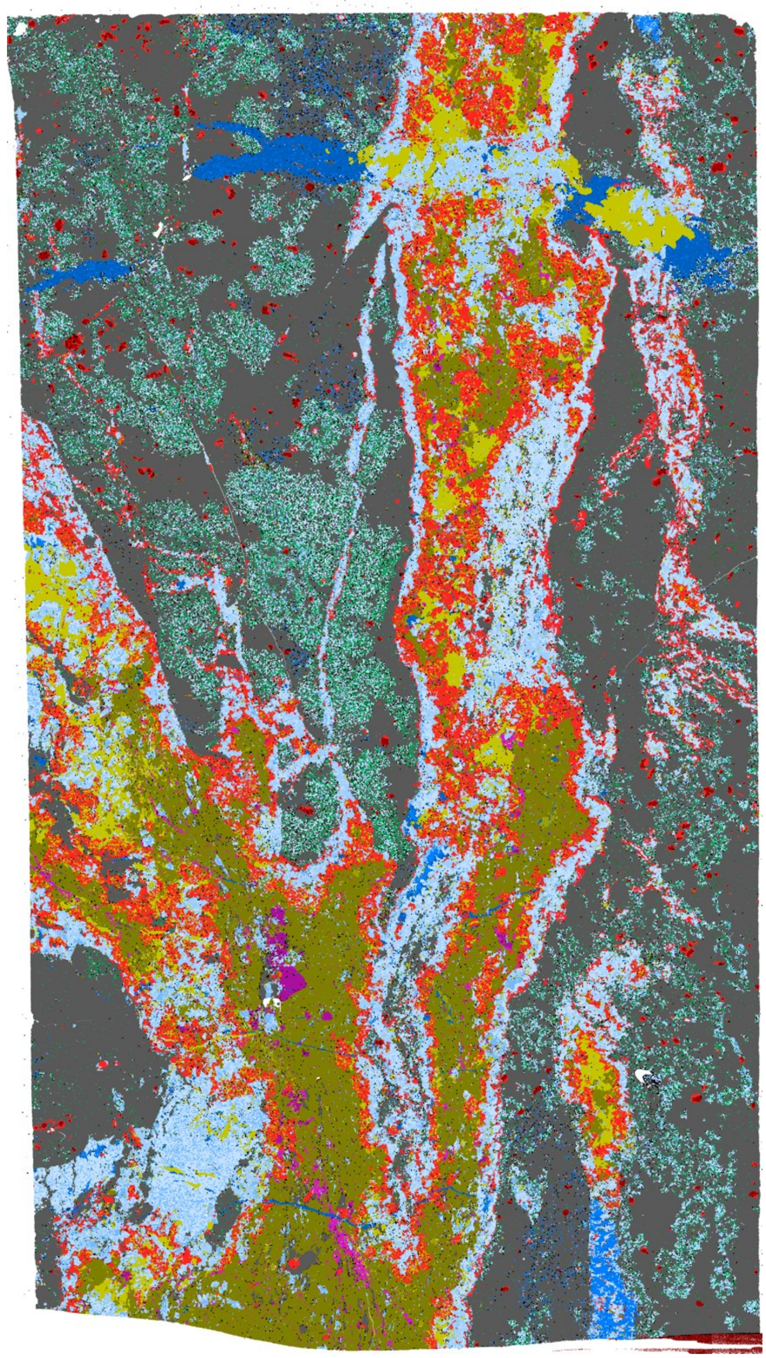

Appendix C: Electron Microprobe Analysis (EPMA) Results

Table C1. EPMA results for pyrite. Data in red was omitted in discussion due to results being outside of the total cut-off for EPMA or it is inconsistent with SEM and reflected light mineral ID.

Deposit	Betts Cove	Betts Cove	Betts Cove	Betts Cove	Betts Cove	Betts Cove	Betts Cove	Betts Cove	Betts Cove
Drill Hole	BC-21-01	BC-21-01	BC-21-01	BC-21-01	BC-21-01	BC-21-01	BC-21-01	BC-21-01	BC-21-01
Sample	KKMSC05B-Py1	KKMSC05B-Py2	KKMSC05B-Py3	KKMSC05B-Py4	KKMSC05B-Py5	KKMSC05B-Py6	KKMSC05B-Py7	KKMSC05B-Py8	KKMSC05B-Py9
Depth (m)	115.5	115.5	115.5	115.5	115.5	115.5	115.5	115.5	115.5
Date	2023_06_23	2023_06_23	2023_06_23	2023_06_23	2023_06_23	2023_06_23	2023_06_23	2023_06_23	2023_06_23
Facies	Chalcopyrite Dominated	Chalcopyrite Dominated	Chalcopyrite Dominated	Chalcopyrite Dominated	Chalcopyrite Dominated	Chalcopyrite Dominated	Chalcopyrite Dominated	Chalcopyrite Dominated	Chalcopyrite Dominated
Weight Percent (wt%)									
Zn	<0.01	<0.01	<0.01	<0.01	<0.01	<0.01	<0.01	<0.01	<0.01
Cu	0.02	<0.01	0.02	0.01	<0.01	0.02	0.02	<0.01	0.1
Ni	0.01	<0.01	<0.01	<0.01	0.01	0.03	0.01	<0.01	<0.01
Co	0.06	0.1	0.02	0.03	0.15	0.17	0.23	0.02	0.1
Fe	46.99	47.07	47.07	47.15	47.06	46.85	46.83	47.07	46.97
Sb	<0.01	<0.01	<0.01	<0.01	<0.01	<0.01	<0.01	<0.01	<0.01
Cd	<0.01	0.01	0.01	<0.01	<0.01	0.01	<0.01	<0.01	<0.01
Pb	0.06	0.03	0.04	0.03	0.05	<0.02	0.05	0.04	<0.02
S	53.72	53.78	53.66	53.46	53.42	53.58	54.14	53.95	53.46
As	<0.02	<0.02	<0.02	<0.02	<0.02	<0.02	0.05	<0.02	0.04
Se	0.08	0.07	<0.01	0.03	<0.01	0.2	0.04	0.04	0.16
Ag	<0.01	<0.01	<0.01	<0.01	<0.01	<0.01	<0.01	<0.01	<0.01
Au	<0.03	<0.03	<0.03	<0.03	<0.03	<0.03	<0.03	<0.03	<0.03
Total	100.87	100.92	100.71	100.48	100.62	100.75	101.27	101.03	100.78
Atoms Per Formula Unit (apfu)									
Zn	0.000	0.000	0.000	0.000	0.000	0.000	0.000	0.000	0.000
Cu	0.000	0.000	0.000	0.000	0.000	0.000	0.000	0.000	0.002
Ni	0.000	0.000	0.000	0.000	0.000	0.001	0.000	0.000	0.000
Co	0.001	0.002	0.000	0.001	0.003	0.003	0.005	0.000	0.002
Fe	1.005	1.005	1.007	1.013	1.012	1.004	0.993	1.002	1.009
Sb	0.000	0.000	0.000	0.000	0.000	0.000	0.000	0.000	0.000
Cd	0.000	0.000	0.000	0.000	0.000	0.000	0.000	0.000	0.000
Pb	0.000	0.000	0.000	0.000	0.000	0.000	0.000	0.000	0.000
S	2.000	2.000	2.000	2.000	2.000	2.000	2.000	2.000	2.000
As	0.000	0.000	0.000	0.000	0.000	0.000	0.001	0.000	0.001
Se	0.001	0.001	0.000	0.000	0.000	0.003	0.001	0.001	0.002
Ag	0.000	0.000	0.000	0.000	0.000	0.000	0.000	0.000	0.000
Au	0.000	0.000	0.000	0.000	0.000	0.000	0.000	0.000	0.000
Total	3.008	3.009	3.008	3.014	3.015	3.012	3.000	3.003	3.016

Table C1. EPMA results for pyrite continued.

Deposit	Betts Cove	Betts Cove	Betts Cove	Betts Cove	Betts Cove	Betts Cove	Betts Cove	Betts Cove	Betts Cove
Drill Hole	BC-21-01	BC-21-01	BC-21-01	BC-21-01	BC-21-01	BC-21-01	BC-21-01	BC-21-01	BC-21-01
Sample	KKMSC05B-Py10	KKMSC05B-Py11	KKMSC05B-Py12	KKMSC05B-Py13	KKMSC05B-Py14	KKMSC05B-Py15	KKMSC05B-Py16	KKMSC05B-Py17	KKMSC05B-Py18
Depth (m)	115.5	115.5	115.5	115.5	115.5	115.5	115.5	115.5	115.5
Date	2023_06_23	2023_06_23	2023_06_23	2023_06_23	2023_06_23	2023_06_23	2023_06_23	2023_06_23	2023_06_23
Facies	Chalcopyrite Dominated	Chalcopyrite Dominated	Chalcopyrite Dominated	Chalcopyrite Dominated	Chalcopyrite Dominated	Chalcopyrite Dominated	Chalcopyrite Dominated	Chalcopyrite Dominated	Chalcopyrite Dominated
Weight Percent (wt%)									
Zn	<0.01	<0.01	<0.01	<0.01	<0.01	<0.01	0.02	<0.01	<0.01
Cu	<0.01	0.01	0.04	0.03	0.03	0.02	0.03	0.01	0.05
Ni	<0.01	0.01	<0.01	<0.01	<0.01	<0.01	<0.01	<0.01	<0.01
Co	0.05	0.03	0.03	0.07	0.07	0.02	0.06	0.06	0.03
Fe	47	46.84	47.36	46.82	47.11	47.06	46.94	47.04	47.07
Sb	<0.01	<0.01	<0.01	<0.01	<0.01	<0.01	<0.01	<0.01	<0.01
Cd	0.02	<0.01	<0.01	<0.01	<0.01	0.02	<0.01	0.01	<0.01
Pb	<0.02	0.04	<0.02	0.03	0.05	0.06	0.04	<0.02	<0.02
S	53.41	53.57	53.65	53.76	54	54.02	53.85	53.39	53.94
As	<0.02	<0.02	0.05	<0.02	<0.02	<0.02	<0.02	<0.02	0.05
Se	0.07	0.04	<0.01	0.04	0.07	0.03	<0.01	<0.01	<0.01
Ag	<0.01	<0.01	<0.01	<0.01	<0.01	<0.01	<0.01	<0.01	<0.01
Au	<0.03	<0.03	<0.03	<0.03	<0.03	<0.03	<0.03	<0.03	<0.03
Total	100.40	100.44	101.07	100.64	101.26	101.12	100.88	100.34	101.10
Atoms Per Formula Unit (apfu)									
Zn	0.000	0.000	0.000	0.000	0.000	0.000	0.000	0.000	0.000
Cu	0.000	0.000	0.001	0.001	0.001	0.000	0.001	0.000	0.001
Ni	0.000	0.000	0.000	0.000	0.000	0.000	0.000	0.000	0.000
Co	0.001	0.001	0.001	0.001	0.001	0.000	0.001	0.001	0.001
Fe	1.011	1.004	1.014	1.000	1.002	1.000	1.001	1.012	1.002
Sb	0.000	0.000	0.000	0.000	0.000	0.000	0.000	0.000	0.000
Cd	0.000	0.000	0.000	0.000	0.000	0.000	0.000	0.000	0.000
Pb	0.000	0.000	0.000	0.000	0.000	0.000	0.000	0.000	0.000
S	2.000	2.000	2.000	2.000	2.000	2.000	2.000	2.000	2.000
As	0.000	0.000	0.001	0.000	0.000	0.000	0.000	0.000	0.001
Se	0.001	0.001	0.000	0.001	0.001	0.000	0.000	0.000	0.000
Ag	0.000	0.000	0.000	0.000	0.000	0.000	0.000	0.000	0.000
Au	0.000	0.000	0.000	0.000	0.000	0.000	0.000	0.000	0.000
Total	3.013	3.006	3.016	3.003	3.005	3.002	3.003	3.013	3.005

Table C1. EPMA results for pyrite continued.

Deposit	Betts Cove	Betts Cove	Betts Cove	Betts Cove	Betts Cove	Betts Cove	Betts Cove	Betts Cove	Betts Cove
Drill Hole	BC-21-01	BC-21-01	BC-21-01	BC-21-01	BC-21-01	BC-21-01	BC-21-01	BC-21-01	BC-21-01
Sample	KKMSC05B-Py19	KKMSC05B-Py20	KKMSC05B-Py21	KKMSC05B-Py22	KKMSC05B-Py23	KKMSC05B-Py24	KKMSC05B-Py25	KKMSC05B-Py26	KKMSC05B-Py27
Depth (m)	115.5	115.5	115.5	115.5	115.5	115.5	115.5	115.5	115.5
Date	2023_06_23	2023_06_23	2023_06_23	2023_06_23	2023_06_23	2023_06_23	2023_06_23	2023_06_23	2023_06_23
Facies	Chalcopyrite Dominated	Chalcopyrite Dominated	Chalcopyrite Dominated	Chalcopyrite Dominated	Chalcopyrite Dominated	Chalcopyrite Dominated	Chalcopyrite Dominated	Chalcopyrite Dominated	Chalcopyrite Dominated
Weight Percent (wt%)									
Zn	<0.01	0.19	<0.01	<0.01	<0.01	<0.01	<0.01	<0.01	<0.01
Cu	0.01	0.03	0.05	0.03	0.07	0.04	0.12	0.28	<0.01
Ni	<0.01	<0.01	<0.01	0.01	<0.01	<0.01	0.02	<0.01	0.02
Co	0.1	0.03	0.02	0.06	0.08	0.02	0.08	0.02	0.06
Fe	46.51	46.96	47.05	47.14	46.96	47.4	42.78	47.34	47.06
Sb	<0.01	<0.01	<0.01	<0.01	<0.01	<0.01	<0.01	<0.01	<0.01
Cd	<0.01	<0.01	<0.01	<0.01	<0.01	<0.01	0.01	<0.01	<0.01
Pb	0.03	0.03	0.03	0.05	<0.02	<0.02	<0.02	0.04	0.05
S	52.75	53.78	53.89	53.93	53.83	53.98	46.26	54.08	53.54
As	<0.02	<0.02	<0.02	<0.02	<0.02	<0.02	<0.04	<0.02	<0.02
Se	0.01	0.02	0.02	0.04	0.03	0.03	0.03	0.04	0.03
Ag	<0.01	<0.01	<0.01	<0.01	<0.01	<0.01	<0.01	<0.01	<0.01
Au	<0.03	<0.03	<0.03	<0.03	<0.03	<0.03	<0.03	<0.03	<0.03
Total	99.25	100.98	100.95	101.16	100.81	101.37	88.10	101.74	100.71
Atoms Per Formula Unit (apfu)									
Zn	0.000	0.004	0.000	0.000	0.000	0.000	0.000	0.000	0.000
Cu	0.000	0.001	0.001	0.001	0.001	0.001	0.003	0.005	0.000
Ni	0.000	0.000	0.000	0.000	0.000	0.000	0.001	0.000	0.000
Co	0.002	0.001	0.000	0.001	0.002	0.000	0.002	0.000	0.001
Fe	1.013	1.003	1.003	1.004	1.002	1.008	1.062	1.005	1.009
Sb	0.000	0.000	0.000	0.000	0.000	0.000	0.000	0.000	0.000
Cd	0.000	0.000	0.000	0.000	0.000	0.000	0.000	0.000	0.000
Pb	0.000	0.000	0.000	0.000	0.000	0.000	0.000	0.000	0.000
S	2.000	2.000	2.000	2.000	2.000	2.000	2.000	2.000	2.000
As	0.000	0.000	0.000	0.000	0.000	0.000	0.000	0.000	0.000
Se	0.000	0.000	0.000	0.001	0.000	0.000	0.000	0.001	0.000
Ag	0.000	0.000	0.000	0.000	0.000	0.000	0.000	0.000	0.000
Au	0.000	0.000	0.000	0.000	0.000	0.000	0.000	0.000	0.000
Total	3.015	3.008	3.005	3.007	3.005	3.010	3.068	3.012	3.012

Table C1. EPMA results for pyrite continued.

Deposit	Betts Cove	Betts Cove	Betts Cove	Betts Cove	Betts Cove	Betts Cove	Betts Cove	Betts Cove	Betts Cove
Drill Hole	BC-21-01	BC-21-01	BC-21-01	BC-21-01	BC-21-01	BC-21-01	BC-21-01	BC-21-01	BC-21-02
Sample	KKMSC05B-Py28	KKMSC05B-Py29	KKMSC05B-Py30	KKMSC05B-Py31	KKMSC05B-Py32	KKMSC05B-Py33	KKMSC05B-Py34	KKMSC05B-Py35	KKMSC09-Py1
Depth (m)	115.5	115.5	115.5	115.5	115.5	115.5	115.5	115.5	85.4
Date	2023 06 23	2023 06 23	2023 06 23	2023 06 23	2023 06 23	2023 06 23	2023 06 23	2023 06 23	2023 06 23
Facies	Chalcopyrite Dominated	Chalcopyrite Dominated	Chalcopyrite Dominated	Chalcopyrite Dominated	Chalcopyrite Dominated	Chalcopyrite Dominated	Chalcopyrite Dominated	Chalcopyrite Dominated	Chalcopyrite Dominated
Weight Percent (wt%)									
Zn	<0.01	<0.01	<0.01	<0.01	<0.01	<0.01	<0.01	<0.01	<0.01
Cu	0.01	0.06	<0.01	0.02	<0.01	<0.01	<0.01	0.02	0.05
Ni	0.01	<0.01	0.01	0.01	<0.01	<0.01	<0.01	<0.01	<0.01
Co	0.03	0.02	0.03	0.07	0.04	0.01	0.12	0.07	0.01
Fe	47.47	47.23	47.03	47.32	47.03	47.32	47.04	46.97	47.25
Sb	<0.01	<0.01	<0.01	<0.01	<0.01	<0.01	<0.01	<0.01	<0.01
Cd	<0.01	0.01	<0.01	0.01	<0.01	<0.01	<0.01	<0.01	<0.01
Pb	<0.02	<0.02	<0.02	<0.02	<0.02	0.02	0.04	0.04	<0.02
S	53.78	53.86	53.68	53.56	53.56	53.92	53.53	53.69	53.68
As	<0.02	<0.02	0.05	<0.02	<0.02	<0.02	<0.02	<0.02	0.13
Se	<0.01	<0.01	0.06	0.05	0.02	<0.01	0.01	0.03	0.12
Ag	<0.01	<0.01	<0.01	<0.01	<0.01	<0.01	<0.01	<0.01	<0.01
Au	<0.03	<0.03	<0.03	<0.03	<0.03	<0.03	<0.03	<0.03	<0.03
Total	101.17	101.13	100.78	101.01	100.57	101.18	100.70	100.71	101.18
Atoms Per Formula Unit (apfu)									
Zn	0.000	0.000	0.000	0.000	0.000	0.000	0.000	0.000	0.000
Cu	0.000	0.001	0.000	0.000	0.000	0.000	0.000	0.000	0.001
Ni	0.000	0.000	0.000	0.000	0.000	0.000	0.000	0.000	0.000
Co	0.001	0.000	0.001	0.001	0.001	0.000	0.002	0.001	0.000
Fe	1.014	1.007	1.006	1.015	1.008	1.008	1.009	1.005	1.011
Sb	0.000	0.000	0.000	0.000	0.000	0.000	0.000	0.000	0.000
Cd	0.000	0.000	0.000	0.000	0.000	0.000	0.000	0.000	0.000
Pb	0.000	0.000	0.000	0.000	0.000	0.000	0.000	0.000	0.000
S	2.000	2.000	2.000	2.000	2.000	2.000	2.000	2.000	2.000
As	0.000	0.000	0.001	0.000	0.000	0.000	0.000	0.000	0.002
Se	0.000	0.000	0.001	0.001	0.000	0.000	0.000	0.000	0.002
Ag	0.000	0.000	0.000	0.000	0.000	0.000	0.000	0.000	0.000
Au	0.000	0.000	0.000	0.000	0.000	0.000	0.000	0.000	0.000
Total	3.015	3.009	3.009	3.017	3.010	3.008	3.012	3.007	3.016

Table C1. EPMA results for pyrite continued.

Deposit	Betts Cove	Betts Cove	Betts Cove	Betts Cove	Betts Cove	Betts Cove	Betts Cove	Betts Cove	Betts Cove
Drill Hole	BC-21-02	BC-21-02	BC-21-02	BC-21-02	BC-21-02	BC-21-02	BC-21-02	BC-21-02	BC-21-02
Sample	KKMSC09-Py2	KKMSC09-Py3	KKMSC09-Py4	KKMSC09-Py5	KKMSC09-Py6	KKMSC09-Py7	KKMSC09-Py8	KKMSC09-Py9	KKMSC09-Py10
Depth (m)	85.4	85.4	85.4	85.4	85.4	85.4	85.4	85.4	85.4
Date	2023_06_23	2023_06_23	2023_06_23	2023_06_23	2023_06_23	2023_06_23	2023_06_23	2023_06_23	2023_06_23
Facies	Chalcopyrite Dominated	Chalcopyrite Dominated	Chalcopyrite Dominated	Chalcopyrite Dominated	Chalcopyrite Dominated	Chalcopyrite Dominated	Chalcopyrite Dominated	Chalcopyrite Dominated	Chalcopyrite Dominated
Weight Percent (wt%)									
Zn	<0.01	<0.01	<0.01	<0.01	<0.01	<0.01	<0.01	<0.01	<0.01
Cu	0.18	0.18	0.35	0.22	0.15	0.17	0.07	0.02	0.05
Ni	<0.01	0.01	0.02	<0.01	<0.01	0.02	<0.01	<0.01	<0.01
Co	0.01	0.1	0.2	0.09	0.11	0.3	0.02	0.01	0.01
Fe	47.23	46.99	46.65	46.73	47.01	46.61	46.9	47.09	46.67
Sb	<0.01	<0.01	<0.01	<0.01	<0.01	<0.01	<0.01	<0.01	<0.01
Cd	0.03	0.02	0.01	<0.01	0.01	<0.01	<0.01	<0.01	0.01
Pb	0.05	<0.02	0.11	0.03	0.04	0.05	0.04	0.03	0.03
S	53.6	53.38	53.23	53.29	53.54	53.85	53.25	53.5	53.33
As	<0.02	0.39	0.2	0.57	<0.02	<0.02	0.52	0.35	0.51
Se	0.09	0.23	0.08	0.12	0.04	0.08	0.14	0.11	0.1
Ag	<0.01	<0.01	<0.01	<0.01	<0.01	<0.01	<0.01	<0.01	<0.01
Au	<0.03	<0.03	<0.03	<0.03	<0.03	<0.03	<0.03	<0.03	<0.03
Total	101.07	101.23	100.74	100.95	100.80	101.03	100.87	101.07	100.67
Atoms Per Formula Unit (apfu)									
Zn	0.000	0.000	0.000	0.000	0.000	0.000	0.000	0.000	0.000
Cu	0.003	0.003	0.007	0.004	0.003	0.003	0.001	0.000	0.001
Ni	0.000	0.000	0.000	0.000	0.000	0.000	0.000	0.000	0.000
Co	0.000	0.002	0.004	0.002	0.002	0.006	0.000	0.000	0.000
Fe	1.012	1.011	1.006	1.007	1.008	0.994	1.011	1.011	1.005
Sb	0.000	0.000	0.000	0.000	0.000	0.000	0.000	0.000	0.000
Cd	0.000	0.000	0.000	0.000	0.000	0.000	0.000	0.000	0.000
Pb	0.000	0.000	0.001	0.000	0.000	0.000	0.000	0.000	0.000
S	2.000	2.000	2.000	2.000	2.000	2.000	2.000	2.000	2.000
As	0.000	0.006	0.003	0.009	0.000	0.000	0.008	0.006	0.008
Se	0.001	0.003	0.001	0.002	0.001	0.001	0.002	0.002	0.002
Ag	0.000	0.000	0.000	0.000	0.000	0.000	0.000	0.000	0.000
Au	0.000	0.000	0.000	0.000	0.000	0.000	0.000	0.000	0.000
Total	3.018	3.026	3.023	3.024	3.014	3.005	3.024	3.019	3.016

Table C1. EPMA results for pyrite continued.

Deposit	Betts Cove	Betts Cove	Betts Cove	Betts Cove	Betts Cove	Betts Cove	Betts Cove	Betts Cove	Betts Cove
Drill Hole	BC-21-02	BC-21-02	BC-21-02	BC-21-02	BC-21-02	BC-21-02	BC-21-02	BC-21-02	BC-21-02
Sample	KKMSC09-Py11	KKMSC09-Py12	KKMSC09-Py13	KKMSC09-Py14	KKMSC09-Py15	KKMSC09-Py16	KKMSC09-Py17	KKMSC09-Py18	KKMSC09-Py19
Depth (m)	85.4	85.4	85.4	85.4	85.4	85.4	85.4	85.4	85.4
Date	2023_06_23	2023_06_23	2023_06_23	2023_06_23	2023_06_23	2023_06_23	2023_06_23	2023_06_23	2023_06_23
Facies	Chalcopyrite Dominated	Chalcopyrite Dominated	Chalcopyrite Dominated	Chalcopyrite Dominated	Chalcopyrite Dominated	Chalcopyrite Dominated	Chalcopyrite Dominated	Chalcopyrite Dominated	Chalcopyrite Dominated
Weight Percent (wt%)									
Zn	<0.01	0.04	<0.01	<0.01	<0.01	<0.01	0.02	<0.01	1.7
Cu	0.04	0.16	0.12	0.05	<0.01	0.04	<0.01	0.15	0.12
Ni	<0.01	0.01	0.02	<0.01	<0.01	<0.01	<0.01	<0.01	0.01
Co	<0.01	0.05	0.23	0.01	<0.01	0.02	<0.01	0.24	0.07
Fe	47.22	47.12	46.47	47.2	47.08	47.11	46.99	46.42	45.89
Sb	<0.01	<0.01	0.02	<0.01	<0.01	<0.01	<0.01	<0.01	<0.01
Cd	0.02	<0.01	<0.01	<0.01	<0.01	<0.01	<0.01	<0.01	<0.01
Pb	0.04	0.03	0.04	<0.02	0.08	0.04	0.05	0.04	0.07
S	53.73	53.75	52.66	53.42	53.83	53.64	53.88	53.51	53.14
As	<0.02	<0.02	0.06	0.28	<0.02	0.1	<0.02	0.17	<0.02
Se	<0.01	0.06	0.03	0.26	0.08	0.16	0.04	0.11	0.06
Ag	<0.01	<0.01	<0.01	<0.01	<0.01	<0.01	<0.01	<0.01	<0.01
Au	<0.03	<0.03	<0.03	<0.03	<0.03	<0.03	<0.03	<0.03	<0.03
Total	100.96	101.20	99.59	101.13	100.98	101.06	100.97	100.58	101.01
Atoms Per Formula Unit (apfu)									
Zn	0.000	0.001	0.000	0.000	0.000	0.000	0.000	0.000	0.031
Cu	0.001	0.003	0.002	0.001	0.000	0.001	0.000	0.003	0.002
Ni	0.000	0.000	0.000	0.000	0.000	0.000	0.000	0.000	0.000
Co	0.000	0.001	0.005	0.000	0.000	0.000	0.000	0.005	0.001
Fe	1.009	1.007	1.013	1.015	1.004	1.009	1.002	0.996	0.992
Sb	0.000	0.000	0.000	0.000	0.000	0.000	0.000	0.000	0.000
Cd	0.000	0.000	0.000	0.000	0.000	0.000	0.000	0.000	0.000
Pb	0.000	0.000	0.000	0.000	0.000	0.000	0.000	0.000	0.000
S	2.000	2.000	2.000	2.000	2.000	2.000	2.000	2.000	2.000
As	0.000	0.000	0.001	0.005	0.000	0.002	0.000	0.003	0.000
Se	0.000	0.001	0.001	0.004	0.001	0.002	0.001	0.002	0.001
Ag	0.000	0.000	0.000	0.000	0.000	0.000	0.000	0.000	0.000
Au	0.000	0.000	0.000	0.000	0.000	0.000	0.000	0.000	0.000
Total	3.010	3.013	3.023	3.025	3.006	3.014	3.003	3.009	3.028

Table C1. EPMA results for pyrite continued.

Deposit	Betts Cove	Betts Cove	Betts Cove	Betts Cove	Betts Cove	Betts Cove	Betts Cove	Betts Cove	Betts Cove
Drill Hole	BC-21-02	BC-21-02	BC-21-02	BC-21-02	BC-21-02	BC-21-02	BC-21-02	BC-21-02	BC-21-02
Sample	KKMSC09-Py20	KKMSC09-Py21	KKMSC09-Py22	KKMSC09-Py23	KKMSC09-Py24	KKMSC09-Py25	KKMSC09-Py26	KKMSC09-Py27	KKMSC09-Py28
Depth (m)	85.4	85.4	85.4	85.4	85.4	85.4	85.4	85.4	85.4
Date	2023_06_23	2023_06_23	2023_06_23	2023_06_23	2023_06_23	2023_06_23	2023_06_23	2023_06_23	2023_06_23
Facies	Chalcopyrite Dominated	Chalcopyrite Dominated	Chalcopyrite Dominated	Chalcopyrite Dominated	Chalcopyrite Dominated	Chalcopyrite Dominated	Chalcopyrite Dominated	Chalcopyrite Dominated	Chalcopyrite Dominated
Weight Percent (wt%)									
Zn	<0.01	<0.01	<0.01	<0.01	<0.01	<0.01	<0.01	<0.01	1.08
Cu	0.3	0.05	0.09	0.17	0.02	0.37	0.04	0.09	0.34
Ni	<0.01	<0.01	<0.01	<0.01	<0.01	0.02	<0.01	0.01	0.01
Co	0.01	0.28	0.01	0.08	0.17	0.01	0.17	0.37	0.37
Fe	47.25	46.59	46.92	46.88	46.6	47.15	47.22	46.74	45.82
Sb	<0.01	0.01	<0.01	<0.01	0.01	<0.01	<0.01	<0.01	<0.01
Cd	0.01	<0.01	<0.01	<0.01	0.01	<0.01	<0.01	<0.01	<0.01
Pb	<0.02	0.04	0.03	0.05	<0.02	<0.02	0.06	<0.02	0.06
S	53.88	53.49	53.86	53.53	52.73	53.94	53.28	53.31	53.27
As	0.05	0.12	<0.02	0.04	<0.02	<0.02	<0.02	<0.02	<0.02
Se	0.08	0.05	0.08	0.05	<0.01	0.05	0.04	0.09	0.14
Ag	<0.01	<0.01	<0.01	<0.01	<0.01	<0.01	<0.01	<0.01	<0.01
Au	<0.03	<0.03	<0.03	<0.03	<0.03	<0.03	<0.03	<0.03	<0.03
Total	101.54	100.53	100.94	100.71	99.49	101.47	100.73	100.56	101.04
Atoms Per Formula Unit (apfu)									
Zn	0.000	0.000	0.000	0.000	0.000	0.000	0.000	0.000	0.020
Cu	0.006	0.001	0.002	0.003	0.000	0.007	0.001	0.002	0.007
Ni	0.000	0.000	0.000	0.000	0.000	0.000	0.000	0.000	0.000
Co	0.000	0.006	0.000	0.002	0.004	0.000	0.003	0.008	0.008
Fe	1.007	1.000	1.000	1.006	1.015	1.004	1.018	1.007	0.988
Sb	0.000	0.000	0.000	0.000	0.000	0.000	0.000	0.000	0.000
Cd	0.000	0.000	0.000	0.000	0.000	0.000	0.000	0.000	0.000
Pb	0.000	0.000	0.000	0.000	0.000	0.000	0.000	0.000	0.000
S	2.000	2.000	2.000	2.000	2.000	2.000	2.000	2.000	2.000
As	0.001	0.002	0.000	0.001	0.000	0.000	0.000	0.000	0.000
Se	0.001	0.001	0.001	0.001	0.000	0.001	0.001	0.001	0.002
Ag	0.000	0.000	0.000	0.000	0.000	0.000	0.000	0.000	0.000
Au	0.000	0.000	0.000	0.000	0.000	0.000	0.000	0.000	0.000
Total	3.015	3.010	3.004	3.012	3.019	3.012	3.023	3.018	3.024

Table C1. EPMA results for pyrite continued.

Deposit	Betts Cove	Betts Cove	Betts Cove	Betts Cove	Betts Cove	Betts Cove	Betts Cove	Betts Cove	Betts Cove
Drill Hole	BC-21-02	BC-21-02	BC-21-02	BC-21-02	BC-21-02	BC-21-02	BC-21-02	BC-21-02	BC-21-02
Sample	KKMSC09-Py29	KKMSC09-Py30	KKMSC09-Py31	KKMSC09-Py32	KKMSC09-Py33	KKMSC09-Py34	KKMSC10-Py1	KKMSC10-Py2	KKMSC10-Py3
Depth (m)	85.4	85.4	85.4	85.4	85.4	85.4	99.5	99.5	99.5
Date	2023_06_23	2023_06_23	2023_06_23	2023_06_23	2023_06_23	2023_06_23	2023_09_25	2023_09_25	2023_09_25
Facies	Chalcopyrite Dominated	Chalcopyrite Dominated	Chalcopyrite Dominated	Chalcopyrite Dominated	Chalcopyrite Dominated	Chalcopyrite Dominated	Pyrite Dominated	Pyrite Dominated	Pyrite Dominated
Weight Percent (wt%)									
Zn	<0.01	<0.01	<0.01	0.03	<0.01	<0.01	<0.01	<0.01	<0.01
Cu	0.08	0.32	0.43	0.18	0.03	0.05	<0.01	<0.01	<0.01
Ni	<0.01	<0.01	<0.01	0.02	<0.01	0.04	<0.01	<0.01	<0.01
Co	0.05	0.09	0.31	0.42	0.01	0.39	0.06	0.07	0.07
Fe	46.81	46.56	45.83	46.4	47.06	46.66	46.76	46.7	46.51
Sb	<0.01	<0.01	<0.01	<0.01	<0.01	<0.01	<0.01	<0.01	<0.01
Cd	<0.01	<0.01	0.01	<0.01	<0.01	0.01	<0.01	<0.01	<0.01
Pb	0.09	0.13	<0.02	0.02	<0.02	0.03	0.11	0.1	0.11
S	53.43	53.34	51.45	52.47	53.75	52.9	52.89	53.01	52.58
As	0.16	0.17	0.51	<0.02	<0.02	<0.02	<0.02	0.05	<0.02
Se	0.17	0.22	0.21	0.02	0.06	0.17	0.03	<0.01	<0.01
Ag	<0.01	<0.01	0.01	0.01	<0.01	<0.01	<0.01	<0.01	<0.01
Au	<0.03	<0.03	<0.03	<0.03	<0.03	<0.03	<0.02	<0.02	<0.02
Total	100.75	100.78	98.70	99.44	100.82	100.19	99.77	99.92	99.18
Atoms Per Formula Unit (apfu)									
Zn	0.000	0.000	0.000	0.000	0.000	0.000	0.000	0.000	0.000
Cu	0.001	0.006	0.009	0.003	0.000	0.001	0.000	0.000	0.000
Ni	0.000	0.000	0.000	0.000	0.000	0.001	0.000	0.000	0.000
Co	0.001	0.002	0.007	0.009	0.000	0.008	0.001	0.001	0.001
Fe	1.006	1.002	1.023	1.016	1.005	1.013	1.015	1.012	1.016
Sb	0.000	0.000	0.000	0.000	0.000	0.000	0.000	0.000	0.000
Cd	0.000	0.000	0.000	0.000	0.000	0.000	0.000	0.000	0.000
Pb	0.001	0.001	0.000	0.000	0.000	0.000	0.001	0.001	0.001
S	2.000	2.000	2.000	2.000	2.000	2.000	2.000	2.000	2.000
As	0.002	0.003	0.008	0.000	0.000	0.000	0.000	0.001	0.000
Se	0.003	0.003	0.003	0.000	0.001	0.003	0.000	0.000	0.000
Ag	0.000	0.000	0.000	0.000	0.000	0.000	0.000	0.000	0.000
Au	0.000	0.000	0.000	0.000	0.000	0.000	0.000	0.000	0.000
Total	3.014	3.017	3.050	3.029	3.007	3.026	3.017	3.015	3.018

Table C1. EPMA results for pyrite continued.

Deposit	Betts Cove	Betts Cove	Betts Cove	Betts Cove	Betts Cove	Betts Cove	Betts Cove	Betts Cove	Betts Cove
Drill Hole	BC-21-02	BC-21-02	BC-21-02	BC-21-02	BC-21-02	BC-21-02	BC-21-02	BC-21-02	BC-21-02
Sample	KKMSC10-Py4	KKMSC10-Py5	KKMSC10-Py6	KKMSC10-Py7	KKMSC10-Py8	KKMSC10-Py9	KKMSC10-Py10	KKMSC10-Py11	KKMSC10-Py12
Depth (m)	99.5	99.5	99.5	99.5	99.5	99.5	99.5	99.5	99.5
Date	2023 09 25	2023 09 25	2023 09 25	2023 09 25	2023 09 25	2023 09 25	2023 09 25	2023 09 25	2023 09 25
Facies	Pyrite Dominated	Pyrite Dominated	Pyrite Dominated	Pyrite Dominated	Pyrite Dominated	Pyrite Dominated	Pyrite Dominated	Pyrite Dominated	Pyrite Dominated
Weight Percent (wt%)									
Zn	<0.01	<0.01	<0.01	<0.01	0.02	<0.01	<0.01	<0.01	0.02
Cu	<0.01	<0.01	0.01	<0.01	<0.01	<0.01	<0.01	<0.01	0.01
Ni	<0.01	<0.01	<0.01	<0.01	<0.01	<0.01	<0.01	<0.01	0.05
Co	0.04	0.11	0.07	0.07	0.05	0.12	0.07	0.06	0.08
Fe	46.55	46.54	46.8	46.34	46.73	46.44	46.62	46.75	46.61
Sb	<0.01	<0.01	<0.01	<0.01	0.01	<0.01	<0.01	<0.01	<0.01
Cd	<0.01	<0.01	<0.01	<0.01	<0.01	0.01	<0.01	<0.01	<0.01
Pb	0.16	0.15	0.12	0.09	0.12	0.15	0.12	0.15	0.12
S	52.76	52.87	52.72	52.81	52.86	52.82	53.03	52.85	52.81
As	<0.02	<0.02	<0.02	<0.02	<0.02	<0.02	<0.02	<0.02	0.19
Se	<0.01	0.02	<0.01	0.01	0.02	<0.01	<0.01	0.01	<0.01
Ag	<0.01	<0.01	<0.01	<0.01	<0.01	<0.01	<0.01	<0.01	0.01
Au	<0.02	<0.02	<0.02	<0.02	<0.02	<0.02	<0.02	<0.02	<0.02
Total	99.41	99.66	99.69	99.21	99.73	99.43	99.79	99.74	99.84
Atoms Per Formula Unit (apfu)									
Zn	0.000	0.000	0.000	0.000	0.000	0.000	0.000	0.000	0.000
Cu	0.000	0.000	0.000	0.000	0.000	0.000	0.000	0.000	0.000
Ni	0.000	0.000	0.000	0.000	0.000	0.000	0.000	0.000	0.001
Co	0.001	0.002	0.001	0.002	0.001	0.002	0.001	0.001	0.002
Fe	1.013	1.011	1.019	1.008	1.015	1.009	1.009	1.016	1.013
Sb	0.000	0.000	0.000	0.000	0.000	0.000	0.000	0.000	0.000
Cd	0.000	0.000	0.000	0.000	0.000	0.000	0.000	0.000	0.000
Pb	0.001	0.001	0.001	0.001	0.001	0.001	0.001	0.001	0.001
S	2.000	2.000	2.000	2.000	2.000	2.000	2.000	2.000	2.000
As	0.000	0.000	0.000	0.000	0.000	0.000	0.000	0.000	0.003
Se	0.000	0.000	0.000	0.000	0.000	0.000	0.000	0.000	0.000
Ag	0.000	0.000	0.000	0.000	0.000	0.000	0.000	0.000	0.000
Au	0.000	0.000	0.000	0.000	0.000	0.000	0.000	0.000	0.000
Total	3.015	3.014	3.022	3.010	3.018	3.013	3.012	3.018	3.020

Table C1. EPMA results for pyrite continued.

Deposit	Betts Cove	Betts Cove	Betts Cove	Betts Cove	Betts Cove	Betts Cove	Betts Cove	Betts Cove	Betts Cove
Drill Hole	BC-21-02	BC-21-02	BC-21-02	BC-21-02	BC-21-02	BC-21-02	BC-21-02	BC-21-02	BC-21-07
Sample	KKMSC10-Py13	KKMSC10-Py14	KKMSC10-Py15	KKMSC10-Py16	KKMSC10-Py17	KKMSC10-Py18	KKMSC10-Py19	KKMSC10-Py20	KKMSC29-Py1
Depth (m)	99.5	99.5	99.5	99.5	99.5	99.5	99.5	99.5	107.6
Date	2023_09_25	2023_09_25	2023_09_25	2023_09_25	2023_09_25	2023_09_25	2023_09_25	2023_09_25	2023_06_27
Facies	Pyrite Dominated	Pyrite Dominated	Pyrite Dominated	Pyrite Dominated	Pyrite Dominated	Pyrite Dominated	Pyrite Dominated	Pyrite Dominated	Chalcopyrite Dominated
Weight Percent (wt%)									
Zn	<0.01	<0.01	<0.01	<0.01	0.03	0.06	<0.01	0.07	<0.01
Cu	<0.01	<0.01	0.01	<0.01	0.01	<0.01	<0.01	<0.01	<0.01
Ni	<0.01	<0.01	<0.01	0.03	0.01	<0.01	<0.01	<0.01	<0.01
Co	0.06	0.05	0.07	0.08	0.07	0.2	0.08	0.12	0.05
Fe	46.82	46.48	46.75	46.68	46.67	46.49	46.63	46.52	46.77
Sb	<0.01	<0.01	<0.01	<0.01	<0.01	<0.01	<0.01	<0.01	<0.01
Cd	<0.01	0.01	0.01	<0.01	<0.01	<0.01	<0.01	0.01	<0.01
Pb	0.15	0.11	0.14	0.13	0.12	0.14	0.1	0.12	0.11
S	52.85	52.76	52.73	52.8	52.78	52.72	52.73	52.7	53.44
As	<0.02	<0.02	<0.02	<0.02	0.03	<0.02	<0.02	<0.02	<0.02
Se	<0.01	<0.01	<0.01	0.02	0.03	0.01	<0.01	<0.01	0.32
Ag	<0.01	<0.01	<0.01	0.01	<0.01	<0.01	<0.01	<0.01	<0.01
Au	<0.02	<0.02	<0.02	<0.02	<0.02	<0.02	<0.02	<0.02	<0.03
Total	99.80	99.33	99.63	99.68	99.72	99.59	99.49	99.42	100.69
Atoms Per Formula Unit (apfu)									
Zn	0.000	0.000	0.000	0.000	0.001	0.001	0.000	0.001	0.000
Cu	0.000	0.000	0.000	0.000	0.000	0.000	0.000	0.000	0.000
Ni	0.000	0.000	0.000	0.001	0.000	0.000	0.000	0.000	0.000
Co	0.001	0.001	0.001	0.002	0.001	0.004	0.002	0.002	0.001
Fe	1.017	1.012	1.018	1.015	1.015	1.013	1.016	1.014	1.005
Sb	0.000	0.000	0.000	0.000	0.000	0.000	0.000	0.000	0.000
Cd	0.000	0.000	0.000	0.000	0.000	0.000	0.000	0.000	0.000
Pb	0.001	0.001	0.001	0.001	0.001	0.001	0.001	0.001	0.001
S	2.000	2.000	2.000	2.000	2.000	2.000	2.000	2.000	2.000
As	0.000	0.000	0.000	0.000	0.000	0.000	0.000	0.000	0.000
Se	0.000	0.000	0.000	0.000	0.000	0.000	0.000	0.000	0.005
Ag	0.000	0.000	0.000	0.000	0.000	0.000	0.000	0.000	0.000
Au	0.000	0.000	0.000	0.000	0.000	0.000	0.000	0.000	0.000
Total	3.019	3.014	3.020	3.019	3.019	3.019	3.018	3.018	3.012

Table C1. EPMA results for pyrite continued.

Deposit	Betts Cove	Betts Cove	Betts Cove	Betts Cove	Betts Cove	Betts Cove	Betts Cove	Betts Cove	Betts Cove
Drill Hole	BC-21-07	BC-21-07	BC-21-07	BC-21-07	BC-21-07	BC-21-07	BC-21-07	BC-21-07	BC-21-07
Sample	KKMSC29-Py2	KKMSC29-Py3	KKMSC29-Py4	KKMSC29-Py5	KKMSC29-Py6	KKMSC29-Py7	KKMSC29-Py8	KKMSC29-Py9	KKMSC29-Py10
Depth (m)	107.6	107.6	107.6	107.6	107.6	107.6	107.6	107.6	107.6
Date	2023_06_27	2023_06_27	2023_06_27	2023_06_27	2023_06_27	2023_06_27	2023_06_27	2023_06_27	2023_06_27
Facies	Chalcopyrite Dominated	Chalcopyrite Dominated	Chalcopyrite Dominated	Chalcopyrite Dominated	Chalcopyrite Dominated	Chalcopyrite Dominated	Chalcopyrite Dominated	Chalcopyrite Dominated	Chalcopyrite Dominated
Weight Percent (wt%)									
Zn	0.01	<0.01	<0.01	<0.01	<0.01	<0.01	<0.01	<0.01	<0.01
Cu	<0.01	0.01	<0.01	<0.01	0.04	<0.01	0.23	0.14	0.01
Ni	<0.01	<0.01	<0.01	<0.01	<0.01	<0.01	0.01	<0.01	0.01
Co	0.05	0.04	0.06	0.05	0.05	0.05	0.05	0.07	0.05
Fe	46.81	47.07	46.76	46.94	46.8	46.88	46.77	46.03	46.96
Sb	<0.01	<0.01	<0.01	<0.01	<0.01	<0.01	<0.01	<0.01	<0.01
Cd	<0.01	<0.01	<0.01	<0.01	0.01	0.01	<0.01	<0.01	0.01
Pb	0.09	0.16	0.14	0.14	0.17	0.12	0.1	0.14	0.15
S	53.75	53.76	53.96	53.88	53.85	54.06	53.67	52	53.81
As	<0.02	<0.02	<0.02	<0.02	<0.02	<0.02	<0.02	<0.03	<0.02
Se	0.13	<0.01	0.04	0.18	<0.01	<0.01	0.02	<0.01	0.26
Ag	<0.01	<0.01	<0.01	<0.01	<0.01	<0.01	<0.01	<0.01	<0.01
Au	<0.03	<0.03	<0.03	<0.03	<0.03	<0.03	<0.03	<0.03	<0.03
Total	100.78	100.94	100.89	101.14	100.86	101.10	100.70	98.03	101.21
Atoms Per Formula Unit (apfu)									
Zn	0.000	0.000	0.000	0.000	0.000	0.000	0.000	0.000	0.000
Cu	0.000	0.000	0.000	0.000	0.001	0.000	0.004	0.003	0.000
Ni	0.000	0.000	0.000	0.000	0.000	0.000	0.000	0.000	0.000
Co	0.001	0.001	0.001	0.001	0.001	0.001	0.001	0.001	0.001
Fe	1.000	1.006	0.995	1.000	0.998	0.996	1.001	1.017	1.002
Sb	0.000	0.000	0.000	0.000	0.000	0.000	0.000	0.000	0.000
Cd	0.000	0.000	0.000	0.000	0.000	0.000	0.000	0.000	0.000
Pb	0.001	0.001	0.001	0.001	0.001	0.001	0.001	0.001	0.001
S	2.000	2.000	2.000	2.000	2.000	2.000	2.000	2.000	2.000
As	0.000	0.000	0.000	0.000	0.000	0.000	0.000	0.000	0.000
Se	0.002	0.000	0.001	0.003	0.000	0.000	0.000	0.000	0.004
Ag	0.000	0.000	0.000	0.000	0.000	0.000	0.000	0.000	0.000
Au	0.000	0.000	0.000	0.000	0.000	0.000	0.000	0.000	0.000
Total	3.004	3.008	2.998	3.005	3.001	2.998	3.007	3.021	3.009

Table C1. EPMA results for pyrite continued.

Deposit	Betts Cove	Betts Cove	Betts Cove	Betts Cove	Betts Cove	Betts Cove	Betts Cove	Betts Cove	Betts Cove
Drill Hole	BC-21-07	BC-21-07	BC-21-07	BC-21-03	BC-21-03	BC-21-03	BC-21-03	BC-21-03	BC-21-03
Sample	KKMSC29-Py11	KKMSC29-Py12	KKMSC29-Py13	KKMSC32-Py1	KKMSC32-Py2	KKMSC32-Py3	KKMSC32-Py4	KKMSC32-Py5	KKMSC32-Py6
Depth (m)	107.6	107.6	107.6	88	88	88	88	88	88
Date	2023_06_27	2023_06_27	2023_06_27	2023_06_27	2023_06_27	2023_06_27	2023_06_27	2023_06_27	2023_06_27
Facies	Chalcopyrite Dominated	Chalcopyrite Dominated	Chalcopyrite Dominated	Sphalerite-pyrite Dominated	Sphalerite-pyrite Dominated	Sphalerite-pyrite Dominated	Sphalerite-pyrite Dominated	Sphalerite-pyrite Dominated	Sphalerite-pyrite Dominated
Weight Percent (wt%)									
Zn	<0.01	<0.01	<0.01	0.39	0.4	0.88	0.45	0.08	0.13
Cu	0.18	0.23	<0.01	<0.01	<0.01	0.01	<0.01	0.01	<0.01
Ni	<0.01	<0.01	<0.01	0.02	0.02	<0.01	0.04	0.02	<0.01
Co	0.05	0.06	0.05	0.08	0.13	0.05	0.06	0.05	0.05
Fe	46.82	46.79	47.03	46.71	46.83	46.69	46.89	46.79	47.03
Sb	<0.01	<0.01	<0.01	<0.01	<0.01	<0.01	<0.01	<0.01	<0.01
Cd	<0.01	<0.01	<0.01	<0.01	<0.01	<0.01	<0.01	<0.01	0.01
Pb	0.16	0.15	0.15	0.14	0.14	0.16	0.12	0.13	0.16
S	54.05	53.75	53.89	53.74	53.63	53.61	53.83	53.42	53.77
As	<0.02	<0.02	<0.02	<0.02	<0.02	0.29	<0.02	0.2	<0.02
Se	0.09	0.23	0.02	<0.01	<0.01	<0.01	<0.01	<0.01	<0.01
Ag	<0.01	<0.01	<0.01	<0.01	<0.01	<0.01	<0.01	<0.01	<0.01
Au	<0.03	<0.03	<0.03	<0.03	<0.03	<0.03	<0.03	<0.03	<0.03
Total	101.23	101.14	101.08	100.97	101.07	101.72	101.31	100.60	101.11
Atoms Per Formula Unit (apfu)									
Zn	0.000	0.000	0.000	0.007	0.007	0.016	0.008	0.001	0.002
Cu	0.003	0.004	0.000	0.000	0.000	0.000	0.000	0.000	0.000
Ni	0.000	0.000	0.000	0.000	0.000	0.000	0.001	0.000	0.000
Co	0.001	0.001	0.001	0.002	0.003	0.001	0.001	0.001	0.001
Fe	0.995	1.000	1.002	0.998	1.003	1.000	1.000	1.006	1.004
Sb	0.000	0.000	0.000	0.000	0.000	0.000	0.000	0.000	0.000
Cd	0.000	0.000	0.000	0.000	0.000	0.000	0.000	0.000	0.000
Pb	0.001	0.001	0.001	0.001	0.001	0.001	0.001	0.001	0.001
S	2.000	2.000	2.000	2.000	2.000	2.000	2.000	2.000	2.000
As	0.000	0.000	0.000	0.000	0.000	0.005	0.000	0.003	0.000
Se	0.001	0.003	0.000	0.000	0.000	0.000	0.000	0.000	0.000
Ag	0.000	0.000	0.000	0.000	0.000	0.000	0.000	0.000	0.000
Au	0.000	0.000	0.000	0.000	0.000	0.000	0.000	0.000	0.000
Total	3.001	3.010	3.004	3.008	3.014	3.023	3.011	3.013	3.009

Table C1. EPMA results for pyrite continued.

Deposit	Betts Cove	Betts Cove	Betts Cove	Betts Cove	Betts Cove	Betts Cove	Betts Cove	Betts Cove	Betts Cove
Drill Hole	BC-21-03	BC-21-03	BC-21-03	BC-21-03	BC-21-03	BC-21-03	BC-21-03	BC-21-03	BC-21-03
Sample	KKMSC32-Py7	KKMSC32-Py8	KKMSC32-Py9	KKMSC32-Py10	KKMSC32-Py11	KKMSC32-Py12	KKMSC32-Py13	KKMSC32-Py14	KKMSC32-Py15
Depth (m)	88	88	88	88	88	88	88	88	88
Date	2023_06_27	2023_06_27	2023_06_27	2023_06_27	2023_06_27	2023_06_27	2023_06_27	2023_06_27	2023_06_27
Facies	Sphalerite-pyrite Dominated	Sphalerite-pyrite Dominated	Sphalerite-pyrite Dominated	Sphalerite-pyrite Dominated	Sphalerite-pyrite Dominated	Sphalerite-pyrite Dominated	Sphalerite-pyrite Dominated	Sphalerite-pyrite Dominated	Sphalerite-pyrite Dominated
Weight Percent (wt%)									
Zn	0.06	0.05	0.06	0.02	0.09	0.12	0.04	0.03	0.05
Cu	<0.01	0.02	<0.01	<0.01	<0.01	<0.01	<0.01	<0.01	0.02
Ni	<0.01	<0.01	<0.01	<0.01	<0.01	<0.01	0.05	<0.01	<0.01
Co	0.05	0.04	0.06	0.05	0.05	0.07	0.09	0.05	0.04
Fe	46.86	46.88	46.86	46.89	46.88	46.88	46.91	46.49	46.38
Sb	<0.01	<0.01	<0.01	<0.01	<0.01	<0.01	<0.01	<0.01	<0.01
Cd	<0.01	<0.01	<0.01	0.01	0.01	0.01	<0.01	0.02	<0.01
Pb	0.14	0.15	0.14	0.15	0.12	0.11	0.13	0.12	0.12
S	53.73	53.5	53.88	53.83	53.45	53.93	53.82	53.69	53.91
As	<0.02	0.22	<0.02	<0.02	0.33	<0.02	0.05	0.11	<0.02
Se	0.01	<0.01	<0.01	<0.01	<0.01	<0.01	<0.01	<0.01	0.01
Ag	<0.01	<0.01	<0.01	<0.01	<0.01	<0.01	0.01	<0.01	<0.01
Au	<0.03	<0.03	<0.03	<0.03	<0.03	<0.03	<0.03	<0.03	<0.03
Total	100.81	100.82	100.96	100.92	100.94	101.10	101.06	100.44	100.49
Atoms Per Formula Unit (apfu)									
Zn	0.001	0.001	0.001	0.000	0.002	0.002	0.001	0.001	0.001
Cu	0.000	0.000	0.000	0.000	0.000	0.000	0.000	0.000	0.000
Ni	0.000	0.000	0.000	0.000	0.000	0.000	0.001	0.000	0.000
Co	0.001	0.001	0.001	0.001	0.001	0.001	0.002	0.001	0.001
Fe	1.002	1.006	0.999	1.000	1.007	0.998	1.001	0.994	0.988
Sb	0.000	0.000	0.000	0.000	0.000	0.000	0.000	0.000	0.000
Cd	0.000	0.000	0.000	0.000	0.000	0.000	0.000	0.000	0.000
Pb	0.001	0.001	0.001	0.001	0.001	0.001	0.001	0.001	0.001
S	2.000	2.000	2.000	2.000	2.000	2.000	2.000	2.000	2.000
As	0.000	0.004	0.000	0.000	0.005	0.000	0.001	0.002	0.000
Se	0.000	0.000	0.000	0.000	0.000	0.000	0.000	0.000	0.000
Ag	0.000	0.000	0.000	0.000	0.000	0.000	0.000	0.000	0.000
Au	0.000	0.000	0.000	0.000	0.000	0.000	0.000	0.000	0.000
Total	3.005	3.013	3.002	3.003	3.016	3.002	3.006	2.998	2.991

Table C1. EPMA results for pyrite continued.

Deposit	Betts Cove	Betts Cove	Betts Cove	Betts Cove	Betts Cove	Betts Cove	Betts Cove	Betts Cove	Betts Cove
Drill Hole	BC-21-03	BC-21-03	BC-21-03	BC-21-03	BC-21-03	BC-21-03	BC-21-03	BC-21-03	BC-21-03
Sample	KKMSC32-Py16	KKMSC32-Py17	KKMSC32-Py18	KKMSC32-Py19	KKMSC32-Py20	KKMSC32-Py21	KKMSC32-Py22	KKMSC32-Py23	KKMSC32-Py24
Depth (m)	88	88	88	88	88	88	88	88	88
Date	2023_06_27	2023_06_27	2023_06_27	2023_06_27	2023_06_27	2023_06_27	2023_06_27	2023_06_27	2023_06_27
Facies	Sphalerite-pyrite Dominated	Sphalerite-pyrite Dominated	Sphalerite-pyrite Dominated	Sphalerite-pyrite Dominated	Sphalerite-pyrite Dominated	Sphalerite-pyrite Dominated	Sphalerite-pyrite Dominated	Sphalerite-pyrite Dominated	Sphalerite-pyrite Dominated
Weight Percent (wt%)									
Zn	0.07	0.16	0.08	0.09	0.04	0.03	0.18	0.08	0.09
Cu	<0.01	<0.01	<0.01	<0.01	<0.01	<0.01	<0.01	<0.01	<0.01
Ni	0.05	0.01	0.02	<0.01	<0.01	0.01	<0.01	0.01	0.01
Co	0.07	0.06	0.07	0.05	0.05	0.05	0.05	0.05	0.06
Fe	46.96	47.04	47.03	46.78	46.46	47.01	46.87	46.78	46.91
Sb	<0.01	<0.01	<0.01	<0.01	0.05	<0.01	0.01	<0.01	<0.01
Cd	<0.01	<0.01	<0.01	0.01	0.02	<0.01	0.01	0.01	0.01
Pb	0.14	0.17	0.15	0.15	0.15	0.11	0.15	0.11	0.12
S	53.98	53.3	53.64	53.86	53.28	53.59	53.87	53.82	53.86
As	<0.02	<0.02	<0.02	<0.02	0.53	<0.02	<0.02	<0.02	<0.02
Se	<0.01	<0.01	<0.01	<0.01	0.03	<0.01	0.02	<0.01	<0.01
Ag	<0.01	0.01	<0.01	<0.01	<0.01	<0.01	<0.01	<0.01	<0.01
Au	<0.03	<0.03	<0.03	<0.03	<0.03	<0.03	<0.03	<0.03	<0.03
Total	101.18	100.65	100.96	100.86	100.60	100.75	101.09	100.78	101.00
Atoms Per Formula Unit (apfu)									
Zn	0.001	0.003	0.001	0.002	0.001	0.001	0.003	0.001	0.002
Cu	0.000	0.000	0.000	0.000	0.000	0.000	0.000	0.000	0.000
Ni	0.001	0.000	0.000	0.000	0.000	0.000	0.000	0.000	0.000
Co	0.001	0.001	0.001	0.001	0.001	0.001	0.001	0.001	0.001
Fe	0.999	1.014	1.007	0.997	1.001	1.007	0.999	0.998	1.000
Sb	0.000	0.000	0.000	0.000	0.001	0.000	0.000	0.000	0.000
Cd	0.000	0.000	0.000	0.000	0.000	0.000	0.000	0.000	0.000
Pb	0.001	0.001	0.001	0.001	0.001	0.001	0.001	0.001	0.001
S	2.000	2.000	2.000	2.000	2.000	2.000	2.000	2.000	2.000
As	0.000	0.000	0.000	0.000	0.008	0.000	0.000	0.000	0.000
Se	0.000	0.000	0.000	0.000	0.000	0.000	0.000	0.000	0.000
Ag	0.000	0.000	0.000	0.000	0.000	0.000	0.000	0.000	0.000
Au	0.000	0.000	0.000	0.000	0.000	0.000	0.000	0.000	0.000
Total	3.003	3.019	3.011	3.001	3.014	3.010	3.005	3.002	3.004

Table C1. EPMA results for pyrite continued.

Deposit	Betts Cove	Betts Cove	Betts Cove	Betts Cove	Betts Cove	Betts Cove	Betts Cove	Betts Cove	Betts Cove
Drill Hole	BC-21-03	BC-21-03	BC-21-03	BC-21-03	BC-21-03	BC-21-03	BC-21-03	BC-21-03	BC-21-03
Sample	KKMSC32-Py25	KKMSC35-Py1	KKMSC35-Py2	KKMSC35-Py3	KKMSC35-Py4	KKMSC35-Py5	KKMSC35-Py6	KKMSC35-Py7	KKMSC35-Py8
Depth (m)	88	116.9	116.9	116.9	116.9	116.9	116.9	116.9	116.9
Date	2023_06_27	2023_06_30	2023_06_30	2023_06_30	2023_06_30	2023_06_30	2023_06_30	2023_06_30	2023_06_30
Facies	Sphalerite-pyrite Dominated	Chalcopyrite-pyrrhotite Dominated	Chalcopyrite-pyrrhotite Dominated	Chalcopyrite-pyrrhotite Dominated	Chalcopyrite-pyrrhotite Dominated	Chalcopyrite-pyrrhotite Dominated	Chalcopyrite-pyrrhotite Dominated	Chalcopyrite-pyrrhotite Dominated	Chalcopyrite-pyrrhotite Dominated
Weight Percent (wt%)									
Zn	0.12	0.02	0.01	0.01	<0.01	0.02	0.01	<0.01	0.02
Cu	<0.01	0.12	0.04	0.37	0.12	0.17	0.07	0.14	0.35
Ni	0.03	<0.01	<0.01	0.01	0.02	0.04	0.1	<0.01	0.05
Co	0.07	0.04	0.05	0.04	0.05	0.05	0.05	0.05	0.05
Fe	46.89	46.37	46.64	46.63	46.23	46.52	46.56	46.75	46.42
Sb	<0.01	<0.01	<0.01	<0.01	<0.01	<0.01	<0.01	<0.01	0.01
Cd	<0.01	0.01	0.02	<0.01	0.01	<0.01	<0.01	<0.01	0.01
Pb	0.13	0.16	0.13	0.13	0.12	0.14	0.16	0.12	0.13
S	53.92	53.58	53.58	53.06	53.59	53.8	53.56	53.9	53.7
As	<0.02	0.09	<0.02	0.09	<0.02	<0.02	<0.02	<0.02	0.06
Se	<0.01	0.18	0.19	0.23	0.29	0.17	0.18	0.21	0.17
Ag	<0.01	<0.01	<0.01	<0.01	<0.01	<0.01	<0.01	<0.01	<0.01
Au	<0.03	<0.03	<0.03	<0.03	<0.03	<0.03	<0.03	<0.03	<0.03
Total	101.03	100.50	100.55	100.52	100.40	100.88	100.62	101.10	100.91
Atoms Per Formula Unit (apfu)									
Zn	0.002	0.000	0.000	0.000	0.000	0.000	0.000	0.000	0.000
Cu	0.000	0.002	0.001	0.007	0.002	0.003	0.001	0.003	0.007
Ni	0.001	0.000	0.000	0.000	0.000	0.001	0.002	0.000	0.001
Co	0.001	0.001	0.001	0.001	0.001	0.001	0.001	0.001	0.001
Fe	0.999	0.994	0.999	1.009	0.991	0.993	0.998	0.996	0.993
Sb	0.000	0.000	0.000	0.000	0.000	0.000	0.000	0.000	0.000
Cd	0.000	0.000	0.000	0.000	0.000	0.000	0.000	0.000	0.000
Pb	0.001	0.001	0.001	0.001	0.001	0.001	0.001	0.001	0.001
S	2.000	2.000	2.000	2.000	2.000	2.000	2.000	2.000	2.000
As	0.000	0.001	0.000	0.001	0.000	0.000	0.000	0.000	0.001
Se	0.000	0.003	0.003	0.003	0.004	0.003	0.003	0.003	0.003
Ag	0.000	0.000	0.000	0.000	0.000	0.000	0.000	0.000	0.000
Au	0.000	0.000	0.000	0.000	0.000	0.000	0.000	0.000	0.000
Total	3.003	3.002	3.005	3.023	3.000	3.002	3.006	3.004	3.006

Table C1. EPMA results for pyrite continued.

Deposit	Betts Cove	Betts Cove	Betts Cove	Betts Cove	Betts Cove	Betts Cove	Betts Cove	Betts Cove	Betts Cove
Drill Hole	BC-21-06	BC-21-06	BC-21-06	BC-21-06	BC-21-06	BC-21-06	BC-21-06	BC-21-08	BC-21-08
Sample	KKMSC42-Py1	KKMSC42-Py2	KKMSC42-Py3	KKMSC42-Py4	KKMSC42-Py5	KKMSC42-Py6	KKMSC53-Py1	KKMSC53-Py2	KKMSC53-Py3
Depth (m)	106.3	106.3	106.3	106.3	106.3	106.3	106.3	28.7	28.7
Date	2023_07_17	2023_07_17	2023_07_17	2023_07_17	2023_07_17	2023_07_17	2023_07_17	2023_07_19	2023_07_19
Facies	Chalcopyrite-pyrrhotite Dominated	Chalcopyrite-pyrrhotite Dominated	Chalcopyrite-pyrrhotite Dominated	Chalcopyrite-pyrrhotite Dominated	Chalcopyrite-pyrrhotite Dominated	Chalcopyrite-pyrrhotite Dominated	Chalcopyrite-pyrrhotite Dominated	Chalcopyrite Dominated	Chalcopyrite Dominated
Weight Percent (wt%)									
Zn	<0.01	<0.01	<0.01	<0.01	<0.01	<0.01	<0.01	<0.01	<0.01
Cu	0.01	<0.01	<0.01	<0.01	0.01	<0.01	<0.01	0.01	<0.01
Ni	<0.01	<0.01	<0.01	0.05	0.08	0.08	<0.01	<0.01	<0.01
Co	0.05	0.04	0.04	0.13	0.14	0.14	0.06	0.05	0.05
Fe	46.16	46.75	46.61	46.31	46.45	46.25	46.8	46.94	46.83
Sb	<0.01	<0.01	<0.01	<0.01	<0.01	<0.01	<0.01	<0.01	<0.01
Cd	<0.01	<0.01	<0.01	<0.01	<0.01	<0.01	<0.01	<0.01	<0.01
Pb	0.12	0.12	0.13	0.17	0.16	0.13	0.16	0.17	0.17
S	52.92	54.18	54.16	53.5	53.51	53.27	53.76	53.61	53.47
As	<0.03	<0.02	<0.02	<0.02	<0.02	<0.02	<0.02	<0.02	<0.02
Se	0.15	0.01	<0.01	0.17	0.08	0.12	0.4	0.46	0.38
Ag	<0.01	<0.01	<0.01	<0.01	<0.01	<0.01	<0.01	<0.01	<0.01
Au	<0.02	<0.03	<0.02	<0.02	<0.02	<0.02	<0.02	<0.02	<0.03
Total	99.18	100.99	100.89	100.25	100.40	99.92	101.07	101.17	100.77
Atoms Per Formula Unit (apfu)									
Zn	0.000	0.000	0.000	0.000	0.000	0.000	0.000	0.000	0.000
Cu	0.000	0.000	0.000	0.000	0.000	0.000	0.000	0.000	0.000
Ni	0.000	0.000	0.000	0.001	0.002	0.002	0.000	0.000	0.000
Co	0.001	0.001	0.001	0.003	0.003	0.003	0.001	0.001	0.001
Fe	1.002	0.991	0.988	0.994	0.997	0.997	1.000	1.006	1.006
Sb	0.000	0.000	0.000	0.000	0.000	0.000	0.000	0.000	0.000
Cd	0.000	0.000	0.000	0.000	0.000	0.000	0.000	0.000	0.000
Pb	0.001	0.001	0.001	0.001	0.001	0.001	0.001	0.001	0.001
S	2.000	2.000	2.000	2.000	2.000	2.000	2.000	2.000	2.000
As	0.000	0.000	0.000	0.000	0.000	0.000	0.000	0.000	0.000
Se	0.002	0.000	0.000	0.003	0.001	0.002	0.006	0.007	0.006
Ag	0.000	0.000	0.000	0.000	0.000	0.000	0.000	0.000	0.000
Au	0.000	0.000	0.000	0.000	0.000	0.000	0.000	0.000	0.000
Total	3.006	2.993	2.990	3.001	3.004	3.004	3.008	3.015	3.013

Table C1. EPMA results for pyrite continued.

Deposit	Betts Cove	Betts Cove	Tilt Cove	Tilt Cove	Tilt Cove	Tilt Cove	Tilt Cove	Tilt Cove	Tilt Cove
Drill Hole	BC-21-08	BC-21-08	SZ-20-01	SZ-20-01	SZ-20-01	SZ-20-01	SZ-20-01	SZ-20-01	SZ-20-01
Sample	KKMSC53-Py4	KKMSC53-Py5	KKMSC13-Py1	KKMSC13-Py2	KKMSC13-Py3	KKMSC13-Py4	KKMSC13-Py5	KKMSC13-Py6	KKMSC13-Py7
Depth (m)	28.7	28.7	66.6	66.6	66.6	66.6	66.6	66.6	66.6
Date	2023_07_19	2023_07_19	2023_07_17	2023_07_17	2023_07_17	2023_07_17	2023_07_17	2023_07_17	2023_07_17
Facies	Chalcopyrite Dominated	Chalcopyrite Dominated	Pyrite Dominated	Pyrite Dominated	Pyrite Dominated	Pyrite Dominated	Pyrite Dominated	Pyrite Dominated	Pyrite Dominated
Weight Percent (wt%)									
Zn	<0.01	<0.01	<0.01	<0.01	<0.01	0.02	<0.01	<0.01	<0.01
Cu	<0.01	<0.01	<0.01	<0.01	<0.01	<0.01	<0.01	<0.01	<0.01
Ni	<0.01	<0.01	<0.01	<0.01	0.02	<0.01	0.01	<0.01	0.01
Co	0.05	0.05	0.05	0.05	0.05	0.04	0.05	0.04	0.04
Fe	47.11	47.17	46.5	46.68	46.51	46.71	46.65	46.58	46.67
Sb	<0.01	<0.01	<0.01	<0.01	<0.01	<0.01	<0.01	<0.01	<0.01
Cd	<0.01	0.01	0.01	0.01	<0.01	<0.01	0.02	0.01	<0.01
Pb	0.17	0.13	0.17	0.13	0.18	0.14	0.15	0.14	0.12
S	53.97	53.93	54.05	53.95	54.05	53.88	53.87	54	53.86
As	<0.02	<0.02	<0.02	<0.02	0.38	0.11	0.29	0.35	0.23
Se	0.05	<0.01	<0.01	<0.01	0.02	<0.01	0.01	<0.01	<0.01
Ag	0.01	<0.01	<0.01	<0.01	<0.01	<0.01	<0.01	<0.01	<0.01
Au	<0.02	<0.02	<0.02	<0.02	<0.02	<0.02	<0.02	<0.02	<0.02
Total	101.31	101.21	100.72	100.72	101.14	100.83	100.99	101.09	100.82
Atoms Per Formula Unit (apfu)									
Zn	0.000	0.000	0.000	0.000	0.000	0.000	0.000	0.000	0.000
Cu	0.000	0.000	0.000	0.000	0.000	0.000	0.000	0.000	0.000
Ni	0.000	0.000	0.000	0.000	0.000	0.000	0.000	0.000	0.000
Co	0.001	0.001	0.001	0.001	0.001	0.001	0.001	0.001	0.001
Fe	1.002	1.005	0.988	0.993	0.988	0.995	0.994	0.991	0.995
Sb	0.000	0.000	0.000	0.000	0.000	0.000	0.000	0.000	0.000
Cd	0.000	0.000	0.000	0.000	0.000	0.000	0.000	0.000	0.000
Pb	0.001	0.001	0.001	0.001	0.001	0.001	0.001	0.001	0.001
S	2.000	2.000	2.000	2.000	2.000	2.000	2.000	2.000	2.000
As	0.000	0.000	0.000	0.000	0.006	0.002	0.005	0.006	0.004
Se	0.001	0.000	0.000	0.000	0.000	0.000	0.000	0.000	0.000
Ag	0.000	0.000	0.000	0.000	0.000	0.000	0.000	0.000	0.000
Au	0.000	0.000	0.000	0.000	0.000	0.000	0.000	0.000	0.000
Total	3.005	3.006	2.990	2.995	2.997	2.999	3.001	2.998	3.000

Table C1. EPMA results for pyrite continued.

Deposit	Tilt Cove	Tilt Cove	Tilt Cove	Tilt Cove	Tilt Cove	Tilt Cove	Tilt Cove	Tilt Cove	Tilt Cove
Drill Hole	SZ-20-01	SZ-20-01	SZ-20-01	SZ-20-01	SZ-20-01	SZ-20-01	SZ-20-01	SZ-20-01	SZ-20-01
Sample	KKMSC13-Py8	KKMSC13-Py9	KKMSC13-Py10	KKMSC13-Py11	KKMSC13-Py12	KKMSC13-Py13	KKMSC13-Py14	KKMSC13-Py15	KKMSC13-Py16
Depth (m)	66.6	66.6	66.6	66.6	66.6	66.6	66.6	66.6	66.6
Date	2023 07 17	2023 07 17	2023 07 17	2023 07 17	2023 07 17	2023 07 17	2023 07 17	2023 07 17	2023 07 17
Facies	Pyrite Dominated	Pyrite Dominated	Pyrite Dominated	Pyrite Dominated	Pyrite Dominated	Pyrite Dominated	Pyrite Dominated	Pyrite Dominated	Pyrite Dominated
Weight Percent (wt%)									
Zn	<0.01	<0.01	<0.01	0.01	<0.01	<0.01	<0.01	<0.01	0.02
Cu	<0.01	<0.01	<0.01	<0.01	<0.01	0.01	<0.01	<0.01	<0.01
Ni	<0.01	<0.01	<0.01	<0.01	<0.01	<0.01	<0.01	<0.01	<0.01
Co	0.05	0.05	0.05	0.05	0.08	0.05	0.05	0.04	0.05
Fe	46.58	46.72	46.59	46.6	46.5	46.62	46.58	46.69	46.7
Sb	<0.01	<0.01	<0.01	<0.01	<0.01	<0.01	<0.01	<0.01	0.01
Cd	0.02	0.01	<0.01	0.01	<0.01	<0.01	0.01	0.01	0.02
Pb	0.15	0.15	0.15	0.14	0.14	0.15	0.14	0.12	0.13
S	54.08	54.28	54.08	54.01	54.25	54.38	54.23	54.24	54.37
As	0.04	0.06	0.2	<0.02	<0.02	<0.02	0.18	<0.02	<0.02
Se	<0.01	<0.01	0.01	<0.01	<0.01	<0.01	<0.01	<0.01	<0.01
Ag	<0.01	<0.01	<0.01	<0.01	<0.01	<0.01	<0.01	0.01	<0.01
Au	<0.02	<0.03	<0.02	<0.02	<0.02	<0.02	<0.02	<0.02	<0.02
Total	100.80	101.18	101.04	100.75	100.93	101.14	101.16	101.02	101.21
Atoms Per Formula Unit (apfu)									
Zn	0.000	0.000	0.000	0.000	0.000	0.000	0.000	0.000	0.000
Cu	0.000	0.000	0.000	0.000	0.000	0.000	0.000	0.000	0.000
Ni	0.000	0.000	0.000	0.000	0.000	0.000	0.000	0.000	0.000
Co	0.001	0.001	0.001	0.001	0.002	0.001	0.001	0.001	0.001
Fe	0.989	0.989	0.989	0.991	0.984	0.985	0.986	0.989	0.986
Sb	0.000	0.000	0.000	0.000	0.000	0.000	0.000	0.000	0.000
Cd	0.000	0.000	0.000	0.000	0.000	0.000	0.000	0.000	0.000
Pb	0.001	0.001	0.001	0.001	0.001	0.001	0.001	0.001	0.001
S	2.000	2.000	2.000	2.000	2.000	2.000	2.000	2.000	2.000
As	0.001	0.001	0.003	0.000	0.000	0.000	0.003	0.000	0.000
Se	0.000	0.000	0.000	0.000	0.000	0.000	0.000	0.000	0.000
Ag	0.000	0.000	0.000	0.000	0.000	0.000	0.000	0.000	0.000
Au	0.000	0.000	0.000	0.000	0.000	0.000	0.000	0.000	0.000
Total	2.992	2.992	2.994	2.993	2.987	2.987	2.991	2.990	2.989

Table C1. EPMA results for pyrite continued.

Deposit	Tilt Cove	Tilt Cove	Tilt Cove	Tilt Cove	Tilt Cove	Tilt Cove	Tilt Cove	Tilt Cove	Tilt Cove
Drill Hole	SZ-20-01	SZ-20-01	SZ-20-01	SZ-20-04	SZ-20-04	SZ-20-04	SZ-20-04	SZ-20-04	SZ-20-04
Sample	KKMSC13-Py17	KKMSC13-Py18	KKMSC13-Py19	KKMSC63-Py1	KKMSC63-Py2	KKMSC63-Py3	KKMSC63-Py4	KKMSC63-Py5	KKMSC63-Py6
Depth (m)	66.6	66.6	66.6	64.45	64.45	64.45	64.45	64.45	64.45
Date	2023_07_17	2023_07_17	2023_07_17	2023_06_30	2023_06_30	2023_06_30	2023_06_30	2023_06_30	2023_06_30
Facies	Pyrite Dominated	Pyrite Dominated	Pyrite Dominated	Pyrite Dominated	Pyrite Dominated	Pyrite Dominated	Pyrite Dominated	Pyrite Dominated	Pyrite Dominated
Weight Percent (wt%)									
Zn	<0.01	<0.01	<0.01	0.01	<0.01	<0.01	<0.01	0.04	<0.01
Cu	0.01	<0.01	<0.01	0.81	0.19	0.2	0.37	0.03	0.04
Ni	<0.01	0.01	<0.01	0.08	0.04	0.05	0.37	0.22	0.03
Co	0.05	0.04	0.05	0.09	0.07	0.06	0.29	0.44	0.08
Fe	46.48	46.62	46.54	46.44	66.76	65.99	46.16	45.78	46.79
Sb	<0.01	<0.01	<0.01	<0.01	<0.01	<0.01	<0.01	<0.01	<0.01
Cd	<0.01	<0.01	<0.01	0.01	<0.01	<0.01	<0.01	<0.01	<0.01
Pb	0.15	0.17	0.13	0.12	0.08	0.05	0.14	0.12	0.1
S	54.2	54.13	54.38	53.22	0.02	0.09	53.1	53	53.78
As	<0.02	0.15	0.05	<0.02	<0.02	<0.02	0.06	0.12	<0.02
Se	<0.01	<0.01	<0.01	<0.01	<0.01	<0.01	0.01	<0.01	0.04
Ag	<0.01	<0.01	<0.01	<0.01	<0.01	<0.01	<0.01	<0.01	<0.01
Au	<0.02	<0.02	<0.02	<0.03	<0.02	<0.02	<0.03	<0.03	<0.03
Total	100.86	101.05	101.10	100.66	67.02	66.19	100.46	99.78	100.77
Atoms Per Formula Unit (apfu)									
Zn	0.000	0.000	0.000	0.000	0.000	0.000	0.000	0.001	0.000
Cu	0.000	0.000	0.000	0.015	10.484	2.203	0.007	0.001	0.001
Ni	0.000	0.000	0.000	0.002	2.125	0.599	0.008	0.005	0.001
Co	0.001	0.001	0.001	0.002	4.474	0.714	0.006	0.009	0.002
Fe	0.985	0.989	0.983	1.002	4259.320	814.840	0.998	0.992	0.999
Sb	0.000	0.000	0.000	0.000	0.000	0.000	0.000	0.000	0.000
Cd	0.000	0.000	0.000	0.000	0.000	0.000	0.000	0.000	0.000
Pb	0.001	0.001	0.001	0.001	1.358	0.166	0.001	0.001	0.001
S	2.000	2.000	2.000	2.000	2.000	2.000	2.000	2.000	2.000
As	0.000	0.002	0.001	0.000	0.000	0.000	0.001	0.002	0.000
Se	0.000	0.000	0.000	0.000	0.000	0.000	0.000	0.000	0.001
Ag	0.000	0.000	0.000	0.000	0.000	0.000	0.000	0.000	0.000
Au	0.000	0.000	0.000	0.000	0.000	0.000	0.000	0.000	0.000
Total	2.987	2.993	2.985	3.022	4279.761	820.522	3.021	3.010	3.003

Table C1. EPMA results for pyrite continued.

Deposit	Tilt Cove	Tilt Cove	Tilt Cove	Tilt Cove	Tilt Cove	Tilt Cove	Tilt Cove	Tilt Cove	Tilt Cove
Drill Hole	SZ-20-04	SZ-20-04	SZ-20-04	SZ-20-04	SZ-20-04	SZ-20-04	SZ-20-04	SZ-20-04	SZ-20-04
Sample	KKMSC63-Py7	KKMSC63-Py8	KKMSC63-Py9	KKMSC63-Py10	KKMSC63-Py11	KKMSC63-Py12	KKMSC63-Py13	KKMSC63-Py14	KKMSC63-Py15
Depth (m)	64.45	64.45	64.45	64.45	64.45	64.45	64.45	64.45	64.45
Date	2023 06 30	2023 06 30	2023 06 30	2023 06 30	2023 06 30	2023 06 30	2023 06 30	2023 06 30	2023 06 30
Facies	Pyrite Dominated	Pyrite Dominated	Pyrite Dominated	Pyrite Dominated	Pyrite Dominated	Pyrite Dominated	Pyrite Dominated	Pyrite Dominated	Pyrite Dominated
Weight Percent (wt%)									
Zn	<0.01	0.02	0.02	<0.01	1.26	<0.01	0.01	0.02	0.03
Cu	0.1	0.15	0.23	0.47	2.07	0.05	0.03	0.12	0.3
Ni	0.01	0.04	<0.01	0.21	0.15	0.16	0.31	0.25	0.08
Co	0.05	0.1	0.06	0.68	0.82	0.19	0.32	0.27	0.35
Fe	46.72	46.68	46.88	45.8	45.99	46.59	46.17	46.48	46.49
Sb	<0.01	<0.01	0.01	<0.01	<0.01	<0.01	<0.01	<0.01	<0.01
Cd	<0.01	<0.01	<0.01	<0.01	0.02	0.01	<0.01	<0.01	0.01
Pb	0.15	0.16	0.16	0.16	0.15	0.1	0.11	0.15	0.14
S	54.1	53.9	53.55	52.98	47.5	53.58	53.04	53.23	53.73
As	<0.02	<0.02	<0.02	0.17	0.23	<0.02	<0.02	<0.02	<0.02
Se	0.06	0.02	0.04	<0.01	0.02	0.01	0.02	<0.01	0.02
Ag	<0.01	<0.01	<0.01	<0.01	<0.01	<0.01	<0.01	<0.01	<0.01
Au	<0.03	<0.03	<0.03	<0.03	<0.03	<0.03	<0.03	<0.03	<0.03
Total	101.12	101.00	100.90	100.39	98.17	100.60	99.99	100.46	101.07
Atoms Per Formula Unit (apfu)									
Zn	0.000	0.000	0.000	0.000	0.026	0.000	0.000	0.000	0.001
Cu	0.002	0.003	0.004	0.009	0.044	0.001	0.000	0.002	0.006
Ni	0.000	0.001	0.000	0.004	0.003	0.003	0.006	0.005	0.002
Co	0.001	0.002	0.001	0.014	0.019	0.004	0.007	0.005	0.007
Fe	0.992	0.995	1.005	0.993	1.112	0.998	1.000	1.003	0.994
Sb	0.000	0.000	0.000	0.000	0.000	0.000	0.000	0.000	0.000
Cd	0.000	0.000	0.000	0.000	0.000	0.000	0.000	0.000	0.000
Pb	0.001	0.001	0.001	0.001	0.001	0.001	0.001	0.001	0.001
S	2.000	2.000	2.000	2.000	2.000	2.000	2.000	2.000	2.000
As	0.000	0.000	0.000	0.003	0.004	0.000	0.000	0.000	0.000
Se	0.001	0.000	0.001	0.000	0.000	0.000	0.000	0.000	0.000
Ag	0.000	0.000	0.000	0.000	0.000	0.000	0.000	0.000	0.000
Au	0.000	0.000	0.000	0.000	0.000	0.000	0.000	0.000	0.000
Total	2.997	3.002	3.013	3.023	3.210	3.007	3.014	3.017	3.010

Table C1. EPMA results for pyrite continued.

Deposit	Tilt Cove	Tilt Cove	Tilt Cove	Tilt Cove	Tilt Cove	Tilt Cove	Tilt Cove	Tilt Cove	Tilt Cove
Drill Hole	SZ-20-04	SZ-20-04	SZ-20-04	SZ-20-04	SZ-20-05	SZ-20-05	SZ-20-05	SZ-20-08	SZ-20-08
Sample	KKMSC63-Py16	KKMSC63-Py17	KKMSC63-Py18	KKMSC63-Py19	KKMSC70_Py1	KKMSC70_Py2	KKMSC70_Py3	KKMSC77-Py1	KKMSC77-Py2
Depth (m)	64.45	64.45	64.45	64.45	126.45	126.45	126.45	28.17	28.17
Date	2023_06_30	2023_06_30	2023_06_30	2023_06_30	2023_07_14	2023_07_14	2023_07_14	2023_09_25	2023_09_25
Facies	Pyrite Dominated	Pyrite Dominated	Pyrite Dominated	Pyrite Dominated	Chalcopyrite-pyrrhotite Dominated	Chalcopyrite-pyrrhotite Dominated	Chalcopyrite-pyrrhotite Dominated	Pyrite Dominated	Pyrite Dominated
Weight Percent (wt%)									
Zn	<0.01	<0.01	0.01	<0.01	<0.01	<0.01	<0.01	<0.01	<0.01
Cu	0.16	0.08	0.17	0.03	0.05	0.05	0.02	0.09	<0.01
Ni	0.08	0.04	0.13	0.08	0.91	2.02	4.41	0.15	0.2
Co	0.27	0.12	0.42	0.32	1.18	0.51	0.09	0.07	0.09
Fe	46.5	46.74	46.93	46.22	44.49	44.29	42.42	46.07	46.57
Sb	<0.01	<0.01	<0.01	<0.01	<0.01	<0.01	<0.01	<0.01	<0.01
Cd	<0.01	<0.01	0.01	<0.01	<0.01	<0.01	0.02	<0.01	0.01
Pb	0.13	0.11	0.17	0.13	0.14	0.17	0.14	0.13	0.14
S	53.44	53.53	52.12	53.03	53.8	53.86	54.13	51.9	52.85
As	0.05	<0.02	0.08	0.04	<0.02	<0.02	<0.02	<0.02	<0.02
Se	0.01	<0.01	<0.01	<0.01	<0.01	<0.01	<0.01	<0.01	<0.01
Ag	<0.01	<0.01	<0.01	<0.01	<0.01	<0.01	<0.01	<0.01	<0.01
Au	<0.03	<0.03	<0.03	<0.03	<0.02	<0.02	<0.02	<0.02	<0.02
Total	100.56	100.53	99.99	99.80	100.51	100.83	101.14	98.40	99.83
Atoms Per Formula Unit (apfu)									
Zn	0.000	0.000	0.000	0.000	0.000	0.000	0.000	0.000	0.000
Cu	0.003	0.002	0.003	0.001	0.001	0.001	0.000	0.002	0.000
Ni	0.002	0.001	0.003	0.002	0.019	0.041	0.089	0.003	0.004
Co	0.006	0.002	0.009	0.007	0.024	0.010	0.002	0.002	0.002
Fe	0.999	1.003	1.034	1.001	0.950	0.944	0.900	1.019	1.012
Sb	0.000	0.000	0.000	0.000	0.000	0.000	0.000	0.000	0.000
Cd	0.000	0.000	0.000	0.000	0.000	0.000	0.000	0.000	0.000
Pb	0.001	0.001	0.001	0.001	0.001	0.001	0.001	0.001	0.001
S	2.000	2.000	2.000	2.000	2.000	2.000	2.000	2.000	2.000
As	0.001	0.000	0.001	0.001	0.000	0.000	0.000	0.000	0.000
Se	0.000	0.000	0.000	0.000	0.000	0.000	0.000	0.000	0.000
Ag	0.000	0.000	0.000	0.000	0.000	0.000	0.000	0.000	0.000
Au	0.000	0.000	0.000	0.000	0.000	0.000	0.000	0.000	0.000
Total	3.011	3.008	3.051	3.011	2.994	2.997	2.992	3.027	3.019

Table C1. EPMA results for pyrite continued.

Deposit	Tilt Cove	Tilt Cove	Tilt Cove	Tilt Cove	Tilt Cove	Tilt Cove
Drill Hole	SZ-20-08	SZ-20-08	SZ-20-08	SZ-20-08	SZ-20-08	SZ-20-08
Sample	KKMSC77-Py3	KKMSC77-Py4	KKMSC77-Py5	KKMSC77-Py6	KKMSC77-Py7	KKMSC77-Py8
Depth (m)	28.17	28.17	28.17	28.17	28.17	28.17
Date	2023_09_25	2023_09_25	2023_09_25	2023_09_25	2023_09_25	2023_09_25
Facies	Pyrite Dominated	Pyrite Dominated	Pyrite Dominated	Pyrite Dominated	Pyrite Dominated	Pyrite Dominated
Weight Percent (wt%)						
Zn	<0.01	<0.01	<0.01	<0.01	<0.01	<0.01
Cu	0.02	0.03	<0.01	<0.01	<0.01	<0.01
Ni	0.26	0.22	0.08	0.1	<0.01	<0.01
Co	0.13	0.08	0.06	0.11	0.15	0.09
Fe	46.47	46.4	46.67	46.5	46.71	46.86
Sb	<0.01	<0.01	<0.01	<0.01	0.01	<0.01
Cd	<0.01	<0.01	<0.01	<0.01	<0.01	<0.01
Pb	0.11	0.12	0.11	0.15	0.1	0.14
S	52.67	52.73	52.59	52.52	52.73	52.9
As	<0.02	<0.02	0.02	<0.02	<0.02	<0.02
Se	0.01	<0.01	<0.01	<0.01	<0.01	<0.01
Ag	<0.01	<0.01	<0.01	<0.01	<0.01	<0.01
Au	<0.02	<0.02	<0.02	<0.02	<0.02	<0.02
Total	99.57	99.49	99.46	99.29	99.64	99.90
Atoms Per Formula Unit (apfu)						
Zn	0.000	0.000	0.000	0.000	0.000	0.000
Cu	0.000	0.001	0.000	0.000	0.000	0.000
Ni	0.005	0.004	0.002	0.002	0.000	0.000
Co	0.003	0.002	0.001	0.002	0.003	0.002
Fe	1.013	1.010	1.019	1.017	1.017	1.017
Sb	0.000	0.000	0.000	0.000	0.000	0.000
Cd	0.000	0.000	0.000	0.000	0.000	0.000
Pb	0.001	0.001	0.001	0.001	0.001	0.001
S	2.000	2.000	2.000	2.000	2.000	2.000
As	0.000	0.000	0.000	0.000	0.000	0.000
Se	0.000	0.000	0.000	0.000	0.000	0.000
Ag	0.000	0.000	0.000	0.000	0.000	0.000
Au	0.000	0.000	0.000	0.000	0.000	0.000
Total	3.022	3.018	3.023	3.022	3.021	3.020

Table C2. EPMA results for chalcopyrite. Data in red was omitted in discussion due to results being outside of the total cut-off for EPMA or it is inconsistent with SEM and reflected light mineral ID.

Deposit	Betts Cove	Betts Cove	Betts Cove	Betts Cove	Betts Cove	Betts Cove	Betts Cove	Betts Cove	Betts Cove
Drill Hole	BC-21-01	BC-21-01	BC-21-01	BC-21-01	BC-21-01	BC-21-01	BC-21-01	BC-21-01	BC-21-01
Sample	KKMSC05B-Cpy1	KKMSC05B-Cpy2	KKMSC05B-Cpy3	KKMSC05B-Cpy4	KKMSC05B-Cpy5	KKMSC05B-Cpy6	KKMSC05B-Cpy7	KKMSC05B-Cpy8	KKMSC05B-Cpy9
Depth (m)	115.5	115.5	115.5	115.5	115.5	115.5	115.5	115.5	115.5
Date	2023_06_23	2023_06_23	2023_06_23	2023_06_23	2023_06_23	2023_06_23	2023_06_23	2023_06_23	2023_06_23
Facies	Chalcopyrite Dominated	Chalcopyrite Dominated	Chalcopyrite Dominated	Chalcopyrite Dominated	Chalcopyrite Dominated	Chalcopyrite Dominated	Chalcopyrite Dominated	Chalcopyrite Dominated	Chalcopyrite Dominated
Weight Percent (wt%)									
Zn	0.04	0.03	0.06	0.2	0.05	0.04	0.04	0.04	<0.01
Cu	33.72	33.68	33.62	33.62	33.6	33.69	33.41	33.35	33.44
Ni	<0.01	<0.01	<0.01	<0.01	<0.01	<0.01	<0.01	<0.01	<0.01
Co	<0.01	0.01	<0.01	<0.01	0.01	<0.01	<0.01	<0.01	<0.01
Fe	31.35	31.31	31.13	31.08	31.28	31.25	31.46	31.47	31.38
Sb	<0.01	<0.01	<0.01	<0.01	<0.01	<0.01	<0.01	<0.01	<0.01
Cd	<0.01	<0.01	<0.01	<0.01	<0.01	<0.01	<0.01	<0.01	0.01
Pb	<0.02	0.02	0.03	<0.02	<0.02	0.05	<0.02	<0.02	0.04
S	35.85	35.51	35.37	35.33	35.31	35.23	35.46	35.28	35.39
As	<0.02	<0.02	<0.02	<0.02	<0.02	<0.02	<0.02	<0.02	<0.02
Se	0.05	0.03	0.01	0.06	0.02	0.06	0.05	0.03	0.04
Ag	<0.01	0.02	<0.01	<0.01	<0.01	<0.01	<0.01	<0.01	<0.01
Au	<0.03	<0.03	<0.03	<0.03	<0.03	<0.03	<0.03	<0.03	<0.03
Total	100.89	100.53	100.17	100.25	100.24	100.28	100.35	100.10	100.24
Atoms Per Formula Unit (apfu)									
Zn	0.001	0.001	0.002	0.006	0.001	0.001	0.001	0.001	0.000
Cu	0.949	0.957	0.959	0.960	0.960	0.965	0.951	0.954	0.954
Ni	0.000	0.000	0.000	0.000	0.000	0.000	0.000	0.000	0.000
Co	0.000	0.000	0.000	0.000	0.000	0.000	0.000	0.000	0.000
Fe	1.004	1.013	1.011	1.010	1.017	1.019	1.019	1.024	1.018
Sb	0.000	0.000	0.000	0.000	0.000	0.000	0.000	0.000	0.000
Cd	0.000	0.000	0.000	0.000	0.000	0.000	0.000	0.000	0.000
Pb	0.000	0.000	0.000	0.000	0.000	0.000	0.000	0.000	0.000
S	2.000	2.000	2.000	2.000	2.000	2.000	2.000	2.000	2.000
As	0.000	0.000	0.000	0.000	0.000	0.000	0.000	0.000	0.000
Se	0.001	0.001	0.000	0.001	0.000	0.001	0.001	0.001	0.001
Ag	0.000	0.000	0.000	0.000	0.000	0.000	0.000	0.000	0.000
Au	0.000	0.000	0.000	0.000	0.000	0.000	0.000	0.000	0.000
Total	3.956	3.972	3.972	3.977	3.980	3.987	3.972	3.980	3.973

Table C2. EPMA results for chalcopyrite continued.

Deposit	Betts Cove	Betts Cove	Betts Cove	Betts Cove	Betts Cove	Betts Cove	Betts Cove	Betts Cove	Betts Cove
Drill Hole	BC-21-01	BC-21-01	BC-21-01	BC-21-01	BC-21-01	BC-21-01	BC-21-01	BC-21-01	BC-21-01
Sample	KKMSC05B-Cpy10	KKMSC05B-Cpy11	KKMSC05B-Cpy12	KKMSC05B-Cpy13	KKMSC05B-Cpy14	KKMSC05B-Cpy15	KKMSC05B-Cpy16	KKMSC05B-Cpy17	KKMSC05B-Cpy18
Depth (m)	115.5	115.5	115.5	115.5	115.5	115.5	115.5	115.5	115.5
Date	2023_06_23	2023_06_23	2023_06_23	2023_06_23	2023_06_23	2023_06_23	2023_06_23	2023_06_23	2023_06_23
Facies	Chalcopyrite Dominated	Chalcopyrite Dominated	Chalcopyrite Dominated	Chalcopyrite Dominated	Chalcopyrite Dominated	Chalcopyrite Dominated	Chalcopyrite Dominated	Chalcopyrite Dominated	Chalcopyrite Dominated
Weight Percent (wt%)									
Zn	0.03	0.02	0.05	0.08	0.02	0.05	0.03	0.05	0.13
Cu	33.65	33.6	33.66	33.66	33.67	33.58	33.46	32.61	33.64
Ni	<0.01	<0.01	<0.01	<0.01	<0.01	<0.01	<0.01	<0.01	<0.01
Co	<0.01	0.01	<0.01	<0.01	0.02	<0.01	<0.01	0.01	0.01
Fe	31.45	31.43	31.52	31.27	31.38	31.2	31.2	31.98	31.14
Sb	<0.01	<0.01	<0.01	<0.01	<0.01	<0.01	<0.01	<0.01	<0.01
Cd	<0.01	<0.01	0.01	<0.01	<0.01	<0.01	<0.01	<0.01	<0.01
Pb	0.04	<0.02	<0.02	<0.02	<0.02	<0.02	0.05	<0.02	0.04
S	35.27	35.48	35.5	35.41	35.45	35.32	35.14	35.74	35.55
As	<0.02	<0.02	<0.02	<0.02	<0.02	<0.02	<0.02	<0.02	<0.02
Se	0.05	0.05	0.06	0.06	0.05	0.04	0.03	<0.01	<0.01
Ag	<0.01	<0.01	<0.01	<0.01	<0.01	<0.01	<0.01	<0.01	0.01
Au	<0.02	<0.03	<0.03	<0.03	<0.03	<0.03	<0.03	<0.03	<0.03
Total	100.47	100.54	100.74	100.43	100.52	100.12	99.84	100.36	100.44
Atoms Per Formula Unit (apfu)									
Zn	0.001	0.001	0.001	0.002	0.001	0.001	0.001	0.001	0.004
Cu	0.963	0.956	0.957	0.959	0.959	0.959	0.961	0.921	0.955
Ni	0.000	0.000	0.000	0.000	0.000	0.000	0.000	0.000	0.000
Co	0.000	0.000	0.000	0.000	0.001	0.000	0.000	0.000	0.000
Fe	1.024	1.017	1.020	1.014	1.017	1.014	1.020	1.028	1.006
Sb	0.000	0.000	0.000	0.000	0.000	0.000	0.000	0.000	0.000
Cd	0.000	0.000	0.000	0.000	0.000	0.000	0.000	0.000	0.000
Pb	0.000	0.000	0.000	0.000	0.000	0.000	0.000	0.000	0.000
S	2.000	2.000	2.000	2.000	2.000	2.000	2.000	2.000	2.000
As	0.000	0.000	0.000	0.000	0.000	0.000	0.000	0.000	0.000
Se	0.001	0.001	0.001	0.001	0.001	0.001	0.001	0.000	0.000
Ag	0.000	0.000	0.000	0.000	0.000	0.000	0.000	0.000	0.000
Au	0.000	0.000	0.000	0.000	0.000	0.000	0.000	0.000	0.000
Total	3.989	3.975	3.979	3.977	3.977	3.976	3.983	3.950	3.965

Table C2. EPMA results for chalcopyrite continued.

Deposit	Betts Cove	Betts Cove	Betts Cove	Betts Cove	Betts Cove	Betts Cove	Betts Cove	Betts Cove	Betts Cove
Drill Hole	BC-21-01	BC-21-01	BC-21-01	BC-21-01	BC-21-02	BC-21-02	BC-21-02	BC-21-02	BC-21-02
Sample	KKMSC05B-Cpy19	KKMSC05B-Cpy20	KKMSC05B-Cpy21	KKMSC05B-Cpy22	KKMSC09-Cpy1	KKMSC09-Cpy2	KKMSC09-Cpy3	KKMSC09-Cpy4	KKMSC09-Cpy5
Depth (m)	115.5	115.5	115.5	115.5	85.4	85.4	85.4	85.4	85.4
Date	2023_06_23	2023_06_23	2023_06_23	2023_06_23	2023_06_23	2023_06_23	2023_06_23	2023_06_23	2023_06_23
Facies	Chalcopyrite Dominated	Chalcopyrite Dominated	Chalcopyrite Dominated	Chalcopyrite Dominated	Chalcopyrite Dominated	Chalcopyrite Dominated	Chalcopyrite Dominated	Chalcopyrite Dominated	Chalcopyrite Dominated
Weight Percent (wt%)									
Zn	0.05	0.05	0.41	0.17	0.03	0.04	0.04	0.03	0.03
Cu	33.77	33.82	33.45	33.4	33.68	33.58	33.32	33.61	33.72
Ni	<0.01	<0.01	0.02	0.02	<0.01	<0.01	<0.01	<0.01	<0.01
Co	0.01	<0.01	<0.01	0.01	<0.01	0.01	<0.01	0.01	<0.01
Fe	31.29	31.35	30.99	30.96	31.21	31.17	31.31	31.17	31.22
Sb	<0.01	<0.01	<0.01	<0.01	<0.01	<0.01	<0.01	<0.01	<0.01
Cd	<0.01	<0.01	<0.01	0.01	<0.01	<0.01	<0.01	<0.01	<0.01
Pb	0.05	0.05	<0.02	0.04	0.05	<0.02	0.02	0.04	<0.02
S	35.44	35.41	35.47	35.36	35.72	35.37	35.37	35.35	35.77
As	<0.02	<0.02	<0.02	<0.02	<0.02	<0.02	<0.02	<0.02	<0.02
Se	0.02	0.04	<0.01	<0.01	0.02	0.05	0.03	0.04	0.03
Ag	<0.01	<0.01	<0.01	<0.01	<0.01	<0.01	0.01	<0.01	<0.01
Au	<0.03	<0.02	<0.03	<0.03	<0.03	<0.03	<0.03	<0.03	<0.03
Total	100.59	100.67	100.11	99.72	100.64	100.18	100.01	100.18	100.76
Atoms Per Formula Unit (apfu)									
Zn	0.001	0.001	0.011	0.005	0.001	0.001	0.001	0.001	0.001
Cu	0.962	0.964	0.952	0.953	0.952	0.958	0.951	0.960	0.951
Ni	0.000	0.000	0.001	0.001	0.000	0.000	0.000	0.000	0.000
Co	0.000	0.000	0.000	0.000	0.000	0.000	0.000	0.000	0.000
Fe	1.014	1.017	1.003	1.005	1.003	1.012	1.017	1.013	1.002
Sb	0.000	0.000	0.000	0.000	0.000	0.000	0.000	0.000	0.000
Cd	0.000	0.000	0.000	0.000	0.000	0.000	0.000	0.000	0.000
Pb	0.000	0.000	0.000	0.000	0.000	0.000	0.000	0.000	0.000
S	2.000	2.000	2.000	2.000	2.000	2.000	2.000	2.000	2.000
As	0.000	0.000	0.000	0.000	0.000	0.000	0.000	0.000	0.000
Se	0.000	0.001	0.000	0.000	0.000	0.001	0.001	0.001	0.001
Ag	0.000	0.000	0.000	0.000	0.000	0.000	0.000	0.000	0.000
Au	0.000	0.000	0.000	0.000	0.000	0.000	0.000	0.000	0.000
Total	3.978	3.983	3.967	3.965	3.957	3.973	3.969	3.974	3.955

Table C2. EPMA results for chalcopyrite continued.

Deposit	Betts Cove	Betts Cove	Betts Cove	Betts Cove	Betts Cove	Betts Cove	Betts Cove	Betts Cove	Betts Cove
Drill Hole	BC-21-02	BC-21-02	BC-21-02	BC-21-02	BC-21-02	BC-21-02	BC-21-02	BC-21-02	BC-21-02
Sample	KKMSC09-Cpy6	KKMSC09-Cpy7	KKMSC09-Cpy8	KKMSC09-Cpy9	KKMSC09-Cpy10	KKMSC09-Cpy11	KKMSC09-Cpy12	KKMSC09-Cpy13	KKMSC09-Cpy14
Depth (m)	85.4	85.4	85.4	85.4	85.4	85.4	85.4	85.4	85.4
Date	2023_06_23	2023_06_23	2023_06_23	2023_06_23	2023_06_23	2023_06_23	2023_06_23	2023_06_23	2023_06_23
Facies	Chalcopyrite Dominated	Chalcopyrite Dominated	Chalcopyrite Dominated	Chalcopyrite Dominated	Chalcopyrite Dominated	Chalcopyrite Dominated	Chalcopyrite Dominated	Chalcopyrite Dominated	Chalcopyrite Dominated
Weight Percent (wt%)									
Zn	0.04	0.03	0.04	0.05	0.01	0.04	0.02	0.03	0.06
Cu	33.16	33.52	33.15	33.33	33.2	33.44	33.65	33.77	32.13
Ni	<0.01	<0.01	<0.01	<0.01	<0.01	<0.01	<0.01	<0.01	<0.01
Co	0.01	<0.01	<0.01	<0.01	<0.01	0.09	0.03	0.01	0.04
Fe	31.34	31.54	31.37	31.44	31.02	31.21	31.28	31.22	32.11
Sb	<0.01	<0.01	<0.01	<0.01	<0.01	<0.01	<0.01	<0.01	<0.01
Cd	<0.01	<0.01	<0.01	<0.01	<0.01	<0.01	<0.01	<0.01	<0.01
Pb	<0.02	<0.02	<0.02	<0.02	0.03	0.04	<0.02	<0.02	0.06
S	35.46	35.35	35.33	35.31	35.41	35.36	35.41	35.34	35.98
As	<0.02	<0.02	<0.02	<0.02	<0.02	<0.02	<0.02	<0.02	<0.02
Se	<0.01	0.03	0.02	0.07	0.03	<0.01	<0.01	0.04	0.04
Ag	<0.01	<0.01	<0.01	<0.01	<0.01	<0.01	<0.01	<0.01	0.01
Au	<0.03	<0.03	<0.03	<0.03	<0.02	<0.03	<0.03	<0.03	<0.03
Total	99.95	100.39	99.80	100.14	99.64	100.12	100.30	100.37	100.39
Atoms Per Formula Unit (apfu)									
Zn	0.001	0.001	0.001	0.001	0.000	0.001	0.001	0.001	0.002
Cu	0.944	0.957	0.947	0.953	0.946	0.954	0.959	0.964	0.901
Ni	0.000	0.000	0.000	0.000	0.000	0.000	0.000	0.000	0.000
Co	0.000	0.000	0.000	0.000	0.000	0.003	0.001	0.000	0.001
Fe	1.015	1.025	1.020	1.022	1.006	1.014	1.014	1.014	1.025
Sb	0.000	0.000	0.000	0.000	0.000	0.000	0.000	0.000	0.000
Cd	0.000	0.000	0.000	0.000	0.000	0.000	0.000	0.000	0.000
Pb	0.000	0.000	0.000	0.000	0.000	0.000	0.000	0.000	0.001
S	2.000	2.000	2.000	2.000	2.000	2.000	2.000	2.000	2.000
As	0.000	0.000	0.000	0.000	0.000	0.000	0.000	0.000	0.000
Se	0.000	0.001	0.000	0.002	0.001	0.000	0.000	0.001	0.001
Ag	0.000	0.000	0.000	0.000	0.000	0.000	0.000	0.000	0.000
Au	0.000	0.000	0.000	0.000	0.000	0.000	0.000	0.000	0.000
Total	3.960	3.983	3.968	3.978	3.953	3.972	3.975	3.981	3.930

Table C2. EPMA results for chalcopyrite continued.

Deposit	Betts Cove	Betts Cove	Betts Cove	Betts Cove	Betts Cove	Betts Cove	Betts Cove	Betts Cove	Betts Cove
Drill Hole	BC-21-02	BC-21-02	BC-21-02	BC-21-02	BC-21-02	BC-21-02	BC-21-02	BC-21-02	BC-21-02
Sample	KKMSC09-Cpy15	KKMSC09-Cpy16	KKMSC09-Cpy17	KKMSC09-Cpy18	KKMSC09-Cpy19	KKMSC09-Cpy20	KKMSC09-Cpy21	KKMSC09-Cpy22	KKMSC09-Cpy23
Depth (m)	85.4	85.4	85.4	85.4	85.4	85.4	85.4	85.4	85.4
Date	2023 06 23	2023 06 23	2023 06 23	2023 06 23	2023 06 23	2023 06 23	2023 06 23	2023 06 23	2023 06 23
Facies	Chalcopyrite Dominated	Chalcopyrite Dominated	Chalcopyrite Dominated	Chalcopyrite Dominated	Chalcopyrite Dominated	Chalcopyrite Dominated	Chalcopyrite Dominated	Chalcopyrite Dominated	Chalcopyrite Dominated
Weight Percent (wt%)									
Zn	0.04	0.02	0.02	0.02	0.03	0.04	0.05	0.04	0.04
Cu	33.53	33.28	22.72	33.4	33.75	33.74	29.33	33.4	33.01
Ni	<0.01	<0.01	0.02	<0.01	<0.01	<0.01	0.01	<0.01	<0.01
Co	0.03	0.01	0.16	0.13	<0.01	0.01	0.04	0.01	0.04
Fe	31.31	31.36	35.91	31.09	31.2	31.44	33.06	30.92	31.42
Sb	<0.01	<0.01	0.01	<0.01	<0.01	<0.01	<0.01	<0.01	<0.01
Cd	<0.01	0.01	<0.01	<0.01	<0.01	<0.01	<0.01	<0.01	<0.01
Pb	<0.02	<0.02	0.07	0.03	<0.02	<0.02	0.06	0.02	0.06
S	35.17	35.21	39.98	35.31	35.45	35.37	36.96	35.63	35.38
As	<0.02	<0.02	<0.02	<0.02	<0.02	<0.02	<0.02	<0.02	<0.02
Se	0.01	0.05	0.03	0.04	0.05	0.04	0.04	0.03	0.01
Ag	0.01	<0.01	0.03	<0.01	<0.01	<0.01	0.01	<0.01	<0.01
Au	<0.03	<0.03	<0.02	<0.03	<0.03	<0.03	<0.03	<0.03	<0.03
Total	100.06	99.92	98.94	99.85	100.45	100.56	99.43	100.00	99.90
Atoms Per Formula Unit (apfu)									
Zn	0.001	0.001	0.000	0.001	0.001	0.001	0.001	0.001	0.001
Cu	0.962	0.954	0.574	0.955	0.961	0.963	0.801	0.946	0.942
Ni	0.000	0.000	0.001	0.000	0.000	0.000	0.000	0.000	0.000
Co	0.001	0.000	0.004	0.004	0.000	0.000	0.001	0.000	0.001
Fe	1.022	1.023	1.031	1.011	1.011	1.021	1.027	0.997	1.020
Sb	0.000	0.000	0.000	0.000	0.000	0.000	0.000	0.000	0.000
Cd	0.000	0.000	0.000	0.000	0.000	0.000	0.000	0.000	0.000
Pb	0.000	0.000	0.001	0.000	0.000	0.000	0.001	0.000	0.001
S	2.000	2.000	2.000	2.000	2.000	2.000	2.000	2.000	2.000
As	0.000	0.000	0.000	0.000	0.000	0.000	0.000	0.000	0.000
Se	0.000	0.001	0.001	0.001	0.001	0.001	0.001	0.001	0.000
Ag	0.000	0.000	0.000	0.000	0.000	0.000	0.000	0.000	0.000
Au	0.000	0.000	0.000	0.000	0.000	0.000	0.000	0.000	0.000
Total	3.987	3.979	3.612	3.971	3.973	3.986	3.832	3.945	3.965

Table C2. EPMA results for chalcopyrite continued.

Deposit	Betts Cove	Betts Cove	Betts Cove	Betts Cove	Betts Cove	Betts Cove	Betts Cove	Betts Cove	Betts Cove
Drill Hole	BC-21-02	BC-21-02	BC-21-02	BC-21-02	BC-21-02	BC-21-02	BC-21-07	BC-21-07	BC-21-07
Sample	KKMSC09-Cpy24	KKMSC10-Cpy1	KKMSC10-Cpy2	KKMSC10-Cpy3	KKMSC10-Cpy4	KKMSC10-Cpy5	KKMSC29-Cpy1	KKMSC29-Cpy2	KKMSC29-Cpy3
Depth (m)	85.4	99.5	99.5	99.5	99.5	99.5	107.6	107.6	107.6
Date	2023_06_23	2023_09_25	2023_09_25	2023_09_25	2023_09_25	2023_09_25	2023_06_27	2023_06_27	2023_06_27
Facies	Chalcopyrite Dominated	Pyrite Dominated	Pyrite Dominated	Pyrite Dominated	Pyrite Dominated	Pyrite Dominated	Chalcopyrite Dominated	Chalcopyrite Dominated	Chalcopyrite Dominated
Weight Percent (wt%)									
Zn	0.04	0.97	0.04	0.04	0.04	0.25	0.03	0.03	0.03
Cu	33.45	32.67	33.26	33.35	33.22	33.12	33.54	33.65	33.65
Ni	<0.01	<0.01	<0.01	<0.01	<0.01	<0.01	<0.01	<0.01	<0.01
Co	0.01	0.03	0.04	0.05	0.04	0.04	<0.01	<0.01	0.01
Fe	31.26	30.5	30.89	30.84	30.79	30.73	31.17	31.14	31.12
Sb	<0.01	<0.01	<0.01	<0.01	<0.01	<0.01	<0.01	<0.01	<0.01
Cd	<0.01	0.01	<0.01	<0.01	<0.01	<0.01	<0.01	<0.01	<0.01
Pb	0.05	0.1	0.04	0.08	0.12	0.05	0.05	0.06	0.03
S	35.35	34.83	34.89	35.19	35.03	35.05	35.1	35.14	35.09
As	<0.02	<0.02	<0.02	<0.02	<0.02	<0.02	<0.02	<0.02	<0.02
Se	<0.01	<0.01	<0.01	<0.01	0.03	<0.01	0.33	0.32	0.31
Ag	<0.01	<0.01	<0.01	<0.01	0.01	<0.01	<0.01	<0.01	<0.01
Au	<0.03	<0.02	<0.02	<0.02	<0.02	<0.02	<0.03	<0.03	<0.03
Total	100.11	99.01	99.06	99.54	99.23	99.20	100.18	100.25	100.14
Atoms Per Formula Unit (apfu)									
Zn	0.001	0.027	0.001	0.001	0.001	0.007	0.001	0.001	0.001
Cu	0.955	0.947	0.962	0.956	0.957	0.954	0.964	0.966	0.968
Ni	0.000	0.000	0.000	0.000	0.000	0.000	0.000	0.000	0.000
Co	0.000	0.001	0.001	0.002	0.001	0.001	0.000	0.000	0.000
Fe	1.015	1.006	1.017	1.006	1.009	1.007	1.020	1.018	1.018
Sb	0.000	0.000	0.000	0.000	0.000	0.000	0.000	0.000	0.000
Cd	0.000	0.000	0.000	0.000	0.000	0.000	0.000	0.000	0.000
Pb	0.000	0.001	0.000	0.001	0.001	0.000	0.000	0.001	0.000
S	2.000	2.000	2.000	2.000	2.000	2.000	2.000	2.000	2.000
As	0.000	0.000	0.000	0.000	0.000	0.000	0.000	0.000	0.000
Se	0.000	0.000	0.000	0.000	0.001	0.000	0.008	0.007	0.007
Ag	0.000	0.000	0.000	0.000	0.000	0.000	0.000	0.000	0.000
Au	0.000	0.000	0.000	0.000	0.000	0.000	0.000	0.000	0.000
Total	3.972	3.982	3.981	3.966	3.971	3.969	3.993	3.993	3.995

Table C2. EPMA results for chalcopyrite continued.

Deposit	Betts Cove	Betts Cove	Betts Cove	Betts Cove	Betts Cove	Betts Cove	Betts Cove	Betts Cove	Betts Cove
Drill Hole	BC-21-07	BC-21-07	BC-21-07	BC-21-07	BC-21-07	BC-21-07	BC-21-07	BC-21-07	BC-21-07
Sample	KKMSC29-Cpy4	KKMSC29-Cpy5	KKMSC29-Cpy6	KKMSC29-Cpy7	KKMSC29-Cpy8	KKMSC29-Cpy9	KKMSC29-Cpy10	KKMSC29-Cpy11	KKMSC29-Cpy12
Depth (m)	107.6	107.6	107.6	107.6	107.6	107.6	107.6	107.6	107.6
Date	2023 06 27	2023 06 27	2023 06 27	2023 06 27	2023 06 27	2023 06 27	2023 06 27	2023 06 27	2023 06 27
Facies	Chalcopyrite Dominated	Chalcopyrite Dominated	Chalcopyrite Dominated	Chalcopyrite Dominated	Chalcopyrite Dominated	Chalcopyrite Dominated	Chalcopyrite Dominated	Chalcopyrite Dominated	Chalcopyrite Dominated
Weight Percent (wt%)									
Zn	0.03	0.05	0.05	0.11	0.04	0.04	0.04	0.03	0.04
Cu	33.61	33.55	33.69	33.46	33.55	33.68	33.54	33.37	33.34
Ni	<0.01	<0.01	<0.01	<0.01	<0.01	<0.01	<0.01	<0.01	<0.01
Co	0.01	<0.01	0.01	<0.01	<0.01	<0.01	<0.01	<0.01	<0.01
Fe	30.98	31.21	30.93	31.23	31.05	31.16	31.02	31.12	31.25
Sb	<0.01	<0.01	<0.01	<0.01	<0.01	<0.01	<0.01	<0.01	<0.01
Cd	<0.01	<0.01	<0.01	<0.01	<0.01	<0.01	<0.01	0.01	<0.01
Pb	<0.02	0.05	0.05	0.06	0.04	<0.02	0.03	0.03	<0.02
S	35.17	35.12	35.24	35.34	34.85	35.17	35.09	35.24	35.1
As	<0.02	<0.02	<0.02	<0.02	<0.02	<0.02	<0.02	<0.02	<0.02
Se	0.3	0.3	0.33	0.29	0.32	0.3	0.36	0.25	0.26
Ag	<0.01	<0.01	<0.01	<0.01	<0.01	<0.01	<0.01	<0.01	<0.01
Au	<0.03	<0.03	<0.03	<0.02	<0.03	<0.03	<0.03	<0.03	<0.03
Total	100.02	100.24	100.21	100.43	99.76	100.27	100.01	99.99	99.96
Atoms Per Formula Unit (apfu)									
Zn	0.001	0.001	0.001	0.003	0.001	0.001	0.001	0.001	0.001
Cu	0.964	0.964	0.965	0.956	0.972	0.966	0.965	0.956	0.959
Ni	0.000	0.000	0.000	0.000	0.000	0.000	0.000	0.000	0.000
Co	0.000	0.000	0.000	0.000	0.000	0.000	0.000	0.000	0.000
Fe	1.012	1.021	1.008	1.015	1.023	1.017	1.015	1.014	1.022
Sb	0.000	0.000	0.000	0.000	0.000	0.000	0.000	0.000	0.000
Cd	0.000	0.000	0.000	0.000	0.000	0.000	0.000	0.000	0.000
Pb	0.000	0.000	0.000	0.001	0.000	0.000	0.000	0.000	0.000
S	2.000	2.000	2.000	2.000	2.000	2.000	2.000	2.000	2.000
As	0.000	0.000	0.000	0.000	0.000	0.000	0.000	0.000	0.000
Se	0.007	0.007	0.008	0.007	0.007	0.007	0.008	0.006	0.006
Ag	0.000	0.000	0.000	0.000	0.000	0.000	0.000	0.000	0.000
Au	0.000	0.000	0.000	0.000	0.000	0.000	0.000	0.000	0.000
Total	3.984	3.993	3.982	3.981	4.004	3.992	3.989	3.977	3.988

Table C2. EPMA results for chalcopyrite continued.

Deposit	Betts Cove	Betts Cove	Betts Cove	Betts Cove	Betts Cove	Betts Cove	Betts Cove	Betts Cove	Betts Cove
Drill Hole	BC-21-07	BC-21-07	BC-21-07	BC-21-07	BC-21-07	BC-21-07	BC-21-07	BC-21-07	BC-21-07
Sample	KKMSC29-Cpy13	KKMSC29-Cpy14	KKMSC29-Cpy15	KKMSC29-Cpy16	KKMSC29-Cpy17	KKMSC29-Cpy18	KKMSC29-Cpy19	KKMSC29-Cpy20	KKMSC29-Cpy21
Depth (m)	107.6	107.6	107.6	107.6	107.6	107.6	107.6	107.6	107.6
Date	2023 06 27	2023 06 27	2023 06 27	2023 06 27	2023 06 27	2023 06 27	2023 06 27	2023 06 27	2023 06 27
Facies	Chalcopyrite Dominated	Chalcopyrite Dominated	Chalcopyrite Dominated	Chalcopyrite Dominated	Chalcopyrite Dominated	Chalcopyrite Dominated	Chalcopyrite Dominated	Chalcopyrite Dominated	Chalcopyrite Dominated
Weight Percent (wt%)									
Zn	0.04	0.03	0.04	0.03	0.03	0.04	0.05	0.05	0.03
Cu	33.25	33.4	33.63	33.69	33.6	33.63	33.5	33.6	33.65
Ni	<0.01	<0.01	<0.01	<0.01	<0.01	<0.01	<0.01	<0.01	<0.01
Co	0.01	0.01	<0.01	0.01	0.01	0.01	<0.01	0.02	<0.01
Fe	31.24	31.04	31.15	31.11	31.15	31.17	31.04	30.88	31.11
Sb	<0.01	<0.01	<0.01	<0.01	<0.01	<0.01	<0.01	<0.01	<0.01
Cd	<0.01	<0.01	<0.01	<0.01	<0.01	<0.01	<0.01	<0.01	<0.01
Pb	<0.02	<0.02	<0.02	0.03	0.03	<0.02	0.04	0.03	0.03
S	35.11	35.4	35.15	35.05	35.11	35.33	35.25	35.2	35.08
As	<0.02	<0.02	<0.02	<0.02	<0.02	<0.02	<0.02	<0.02	<0.02
Se	0.25	0.23	0.4	0.42	0.3	0.29	0.34	0.32	0.38
Ag	<0.01	<0.01	<0.01	0.01	<0.01	<0.01	<0.01	<0.01	<0.01
Au	<0.03	<0.03	<0.03	<0.03	<0.03	<0.03	<0.03	<0.03	<0.03
Total	99.81	100.01	100.29	100.25	100.16	100.43	100.19	100.01	100.18
Atoms Per Formula Unit (apfu)									
Zn	0.001	0.001	0.001	0.001	0.001	0.001	0.001	0.001	0.001
Cu	0.956	0.952	0.966	0.970	0.966	0.961	0.959	0.963	0.968
Ni	0.000	0.000	0.000	0.000	0.000	0.000	0.000	0.000	0.000
Co	0.000	0.000	0.000	0.000	0.000	0.000	0.000	0.001	0.000
Fe	1.022	1.007	1.018	1.019	1.019	1.013	1.011	1.007	1.018
Sb	0.000	0.000	0.000	0.000	0.000	0.000	0.000	0.000	0.000
Cd	0.000	0.000	0.000	0.000	0.000	0.000	0.000	0.000	0.000
Pb	0.000	0.000	0.000	0.000	0.000	0.000	0.000	0.000	0.000
S	2.000	2.000	2.000	2.000	2.000	2.000	2.000	2.000	2.000
As	0.000	0.000	0.000	0.000	0.000	0.000	0.000	0.000	0.000
Se	0.006	0.005	0.009	0.010	0.007	0.007	0.008	0.007	0.009
Ag	0.000	0.000	0.000	0.000	0.000	0.000	0.000	0.000	0.000
Au	0.000	0.000	0.000	0.000	0.000	0.000	0.000	0.000	0.000
Total	3.985	3.966	3.994	4.001	3.993	3.982	3.980	3.980	3.996

Table C2. EPMA results for chalcopyrite continued.

Deposit	Betts Cove	Betts Cove	Betts Cove	Betts Cove	Betts Cove	Betts Cove	Betts Cove	Betts Cove	Betts Cove
Drill Hole	BC-21-07	BC-21-07	BC-21-03	BC-21-03	BC-21-03	BC-21-03	BC-21-03	BC-21-03	BC-21-03
Sample	KKMSC29-Cpy22	KKMSC29-Cpy23	KKMSC32-Cpy1	KKMSC32-Cpy2	KKMSC32-Cpy3	KKMSC32-Cpy4	KKMSC32-Cpy5	KKMSC32-Cpy6	KKMSC32-Cpy7
Depth (m)	107.6	107.6	88	88	88	88	88	88	88
Date	2023_06_27	2023_06_27	2023_06_27	2023_06_27	2023_06_27	2023_06_27	2023_06_27	2023_06_27	2023_06_27
Facies	Chalcopyrite Dominated	Chalcopyrite Dominated	Sphalerite-pyrite Dominated	Sphalerite-pyrite Dominated	Sphalerite-pyrite Dominated	Sphalerite-pyrite Dominated	Sphalerite-pyrite Dominated	Sphalerite-pyrite Dominated	Sphalerite-pyrite Dominated
Weight Percent (wt%)									
Zn	0.03	0.04	0.08	<0.01	0.04	0.06	0.05	0.1	0.04
Cu	33.6	33.5	21.11	1.67	33.58	33.69	33.7	33.51	33.4
Ni	<0.01	<0.01	0.87	22.86	<0.01	<0.01	<0.01	<0.01	<0.01
Co	<0.01	<0.01	0.58	0.04	<0.01	<0.01	<0.01	<0.01	0.01
Fe	31.17	30.93	16.83	31.66	31.03	30.9	31.12	30.92	30.69
Sb	<0.01	<0.01	<0.01	<0.01	<0.01	<0.01	<0.01	<0.01	<0.01
Cd	<0.01	<0.01	0.02	<0.01	<0.01	<0.01	<0.01	<0.01	0.01
Pb	<0.02	0.04	0.04	0.03	0.03	<0.02	<0.02	<0.02	0.04
S	35.09	34.81	21.5	32.08	35.56	35.56	35.43	35.41	35.58
As	<0.02	<0.02	<0.02	<0.02	<0.02	<0.02	<0.02	<0.02	<0.02
Se	0.28	0.39	<0.01	0.01	<0.01	<0.01	<0.01	<0.01	<0.01
Ag	<0.01	<0.01	0.32	12.1	<0.01	0.02	0.02	0.02	0.01
Au	<0.02	<0.03	<0.02	<0.03	<0.03	<0.03	<0.03	<0.03	<0.03
Total	100.11	99.62	61.20	100.40	100.21	100.18	100.27	99.91	99.75
Atoms Per Formula Unit (apfu)									
Zn	0.001	0.001	0.004	0.000	0.001	0.002	0.001	0.003	0.001
Cu	0.966	0.971	0.991	0.053	0.953	0.956	0.960	0.955	0.947
Ni	0.000	0.000	0.044	0.779	0.000	0.000	0.000	0.000	0.000
Co	0.000	0.000	0.029	0.001	0.000	0.000	0.000	0.000	0.000
Fe	1.020	1.020	0.899	1.133	1.002	0.998	1.009	1.003	0.991
Sb	0.000	0.000	0.000	0.000	0.000	0.000	0.000	0.000	0.000
Cd	0.000	0.000	0.001	0.000	0.000	0.000	0.000	0.000	0.000
Pb	0.000	0.000	0.001	0.000	0.000	0.000	0.000	0.000	0.000
S	2.000	2.000	2.000	2.000	2.000	2.000	2.000	2.000	2.000
As	0.000	0.000	0.000	0.000	0.000	0.000	0.000	0.000	0.000
Se	0.006	0.009	0.000	0.000	0.000	0.000	0.000	0.000	0.000
Ag	0.000	0.000	0.009	0.224	0.000	0.000	0.000	0.000	0.000
Au	0.000	0.000	0.000	0.000	0.000	0.000	0.000	0.000	0.000
Total	3.994	4.002	3.977	4.191	3.956	3.956	3.970	3.961	3.940

Table C2. EPMA results for chalcopyrite continued.

Deposit	Betts Cove	Betts Cove	Betts Cove	Betts Cove	Betts Cove	Betts Cove	Betts Cove	Betts Cove	Betts Cove
Drill Hole	BC-21-03	BC-21-03	BC-21-03	BC-21-03	BC-21-03	BC-21-03	BC-21-03	BC-21-03	BC-21-03
Sample	KKMSC32-Cpy8	KKMSC32-Cpy9	KKMSC35-Cpy1	KKMSC35-Cpy2	KKMSC35-Cpy3	KKMSC35-Cpy4	KKMSC35-Cpy5	KKMSC35-Cpy6	KKMSC35-Cpy7
Depth (m)	88	88	116.9	116.9	116.9	116.9	116.9	116.9	116.9
Date	2023 06 27	2023 06 27	2023 06 29	2023 06 29	2023 06 29	2023 06 29	2023 06 29	2023 06 29	2023 06 29
Facies	Sphalerite-pyrite Dominated	Sphalerite-pyrite Dominated	Chalcopyrite-pyrrhotite dominated	Chalcopyrite-pyrrhotite dominated	Chalcopyrite-pyrrhotite dominated	Chalcopyrite-pyrrhotite dominated	Chalcopyrite-pyrrhotite dominated	Chalcopyrite-pyrrhotite dominated	Chalcopyrite-pyrrhotite dominated
Weight Percent (wt%)									
Zn	0.03	0.06	0.08	0.05	0.04	0.06	0.21	0.16	0.04
Cu	33.58	33.05	33.4	33.58	33.62	33.2	32.99	33.12	33.09
Ni	<0.01	<0.01	0.01	<0.01	<0.01	<0.01	<0.01	<0.01	<0.01
Co	<0.01	<0.01	0.01	<0.01	<0.01	<0.01	<0.01	0.01	<0.01
Fe	31.21	30.75	30.99	30.83	30.94	31.02	31.09	30.81	31.51
Sb	<0.01	<0.01	<0.01	<0.01	<0.01	<0.01	<0.01	<0.01	<0.01
Cd	<0.01	<0.01	<0.01	0.01	<0.01	<0.01	0.02	<0.01	<0.01
Pb	0.06	0.03	<0.02	<0.02	<0.02	0.03	0.04	<0.02	0.07
S	35.65	35.72	35.35	35.44	35.32	35.38	35.51	35.07	35.58
As	<0.02	<0.02	<0.02	<0.02	<0.02	<0.02	<0.02	<0.02	<0.02
Se	<0.01	0.02	0.08	0.03	0.13	0.15	0.05	0.06	0.02
Ag	0.01	0.01	<0.01	0.01	<0.01	0.02	0.01	0.01	<0.01
Au	<0.03	<0.03	<0.03	<0.03	<0.03	<0.03	<0.03	<0.03	<0.03
Total	100.50	99.61	99.84	99.85	99.96	99.81	99.90	99.18	100.29
Atoms Per Formula Unit (apfu)									
Zn	0.001	0.002	0.002	0.001	0.001	0.002	0.006	0.004	0.001
Cu	0.951	0.934	0.954	0.956	0.961	0.947	0.938	0.953	0.939
Ni	0.000	0.000	0.000	0.000	0.000	0.000	0.000	0.000	0.000
Co	0.000	0.000	0.000	0.000	0.000	0.000	0.000	0.000	0.000
Fe	1.005	0.989	1.007	0.999	1.006	1.007	1.005	1.009	1.017
Sb	0.000	0.000	0.000	0.000	0.000	0.000	0.000	0.000	0.000
Cd	0.000	0.000	0.000	0.000	0.000	0.000	0.000	0.000	0.000
Pb	0.001	0.000	0.000	0.000	0.000	0.000	0.000	0.000	0.001
S	2.000	2.000	2.000	2.000	2.000	2.000	2.000	2.000	2.000
As	0.000	0.000	0.000	0.000	0.000	0.000	0.000	0.000	0.000
Se	0.000	0.000	0.002	0.001	0.003	0.003	0.001	0.001	0.000
Ag	0.000	0.000	0.000	0.000	0.000	0.000	0.000	0.000	0.000
Au	0.000	0.000	0.000	0.000	0.000	0.000	0.000	0.000	0.000
Total	3.957	3.925	3.965	3.958	3.971	3.960	3.951	3.968	3.958

Table C2. EPMA results for chalcopyrite continued.

Deposit	Betts Cove	Betts Cove	Betts Cove	Betts Cove	Betts Cove	Betts Cove	Betts Cove	Betts Cove	Betts Cove
Drill Hole	BC-21-03	BC-21-03	BC-21-03	BC-21-03	BC-21-06	BC-21-06	BC-21-06	BC-21-06	BC-21-06
Sample	KKMSC35-Cpy8	KKMSC35-Cpy9	KKMSC35-Cpy10	KKMSC35-Cpy11	KKMSC42-Cpy1	KKMSC42-Cpy2	KKMSC42-Cpy3	KKMSC42-Cpy4	KKMSC42-Cpy5
Depth (m)	116.9	116.9	116.9	116.9	106.3	106.3	106.3	106.3	106.3
Date	2023 06 29	2023 06 29	2023 06 29	2023 06 29	2023 07 18	2023 07 18	2023 07 18	2023 07 18	2023 07 18
Facies	Chalcopyrite-pyrrhotite dominated	Chalcopyrite-pyrrhotite dominated	Chalcopyrite-pyrrhotite dominated	Chalcopyrite-pyrrhotite dominated	Chalcopyrite-pyrrhotite dominated	Chalcopyrite-pyrrhotite dominated	Chalcopyrite-pyrrhotite dominated	Chalcopyrite-pyrrhotite dominated	Chalcopyrite-pyrrhotite dominated
Weight Percent (wt%)									
Zn	0.05	0.04	0.03	0.06	0.04	0.04	0.05	0.04	0.05
Cu	32.09	31.42	31.69	33.42	33.75	33.37	33.79	33.54	33.67
Ni	<0.01	<0.01	<0.01	<0.01	<0.01	<0.01	<0.01	<0.01	<0.01
Co	<0.01	0.01	0.02	<0.01	0.03	0.05	0.03	0.03	0.04
Fe	29.91	29.06	29.36	30.55	30.15	30.42	29.94	30.01	30.01
Sb	<0.01	<0.01	<0.01	<0.01	<0.01	<0.01	<0.01	<0.01	<0.01
Cd	<0.01	<0.01	<0.01	0.01	<0.01	<0.01	<0.01	<0.01	<0.01
Pb	<0.02	0.03	0.03	<0.02	0.11	0.08	0.11	0.08	0.07
S	35.43	35.72	35.8	35.46	35.76	35.36	35.63	35.76	35.54
As	<0.02	<0.02	<0.02	<0.02	<0.02	<0.02	<0.02	<0.02	<0.02
Se	0.07	0.04	0.07	0.07	0.04	0.06	0.08	0.08	0.08
Ag	<0.01	<0.01	0.01	0.01	0.01	<0.01	<0.01	<0.01	<0.01
Au	<0.02	<0.03	<0.03	<0.02	<0.02	<0.02	<0.02	<0.02	<0.02
Total	97.50	96.26	96.97	99.55	99.82	99.26	99.58	99.47	99.38
Atoms Per Formula Unit (apfu)									
Zn	0.001	0.001	0.001	0.002	0.001	0.001	0.001	0.001	0.001
Cu	0.914	0.888	0.893	0.951	0.952	0.952	0.957	0.947	0.956
Ni	0.000	0.000	0.000	0.000	0.000	0.000	0.000	0.000	0.000
Co	0.000	0.000	0.001	0.000	0.001	0.002	0.001	0.001	0.001
Fe	0.969	0.934	0.942	0.989	0.968	0.988	0.965	0.964	0.970
Sb	0.000	0.000	0.000	0.000	0.000	0.000	0.000	0.000	0.000
Cd	0.000	0.000	0.000	0.000	0.000	0.000	0.000	0.000	0.000
Pb	0.000	0.000	0.000	0.000	0.001	0.001	0.001	0.001	0.001
S	2.000	2.000	2.000	2.000	2.000	2.000	2.000	2.000	2.000
As	0.000	0.000	0.000	0.000	0.000	0.000	0.000	0.000	0.000
Se	0.002	0.001	0.002	0.002	0.001	0.001	0.002	0.002	0.002
Ag	0.000	0.000	0.000	0.000	0.000	0.000	0.000	0.000	0.000
Au	0.000	0.000	0.000	0.000	0.000	0.000	0.000	0.000	0.000
Total	3.886	3.825	3.839	3.944	3.925	3.945	3.927	3.915	3.931

Table C2. EPMA results for chalcopyrite continued.

Deposit	Betts Cove	Betts Cove	Betts Cove	Betts Cove	Betts Cove	Betts Cove	Betts Cove	Betts Cove	Betts Cove
Drill Hole	BC-21-06	BC-21-06	BC-21-06	BC-21-06	BC-21-08	BC-21-08	BC-21-08	BC-21-08	BC-21-08
Sample	KKMSC42-Cpy6	KKMSC42-Cpy7	KKMSC42-Cpy8	KKMSC42-Cpy9	KKMSC53-Cpy1	KKMSC53-Cpy2	KKMSC53-Cpy3	KKMSC53-Cpy4	KKMSC53-Cpy5
Depth (m)	106.3	106.3	106.3	106.3	28.7	28.7	28.7	28.7	28.7
Date	2023 07 18	2023 07 18	2023 07 18	2023 07 18	2023 07 19	2023 07 19	2023 07 19	2023 07 19	2023 07 19
Facies	Chalcopyrite-pyrrhotite dominated	Chalcopyrite-pyrrhotite dominated	Chalcopyrite-pyrrhotite dominated	Chalcopyrite-pyrrhotite dominated	Chalcopyrite Dominated	Chalcopyrite Dominated	Chalcopyrite Dominated	Chalcopyrite Dominated	Chalcopyrite Dominated
Weight Percent (wt%)									
Zn	0.15	0.24	0.04	0.04	0.04	0.25	0.03	0.03	0.04
Cu	33.3	33.41	33.39	33.54	33.77	33.67	33.88	33.75	33.62
Ni	<0.01	0.01	0.01	<0.01	<0.01	<0.01	<0.01	0.08	0.3
Co	0.03	0.04	0.04	0.03	0.03	0.03	0.03	0.04	0.07
Fe	29.56	29.74	29.66	29.68	30.27	30.16	30.2	30.09	30.24
Sb	<0.01	<0.01	<0.01	<0.01	<0.01	<0.01	<0.01	<0.01	<0.01
Cd	<0.01	<0.01	0.01	<0.01	<0.01	<0.01	<0.01	<0.01	<0.01
Pb	0.12	0.08	0.14	0.09	0.13	0.09	0.07	0.1	0.12
S	35.71	35.65	35.51	35.6	35.31	35.47	35.83	35.68	35.81
As	<0.02	<0.02	<0.02	<0.02	<0.02	<0.02	<0.02	<0.02	<0.02
Se	0.12	0.09	0.08	0.06	0.08	0.04	0.08	0.05	0.07
Ag	<0.01	<0.01	<0.01	<0.01	<0.01	<0.01	<0.01	<0.01	0.01
Au	<0.02	<0.02	<0.02	<0.02	<0.02	<0.02	<0.02	<0.02	<0.02
Total	98.98	99.20	98.85	98.99	99.58	99.64	100.05	99.72	100.19
Atoms Per Formula Unit (apfu)									
Zn	0.004	0.007	0.001	0.001	0.001	0.007	0.001	0.001	0.001
Cu	0.941	0.946	0.949	0.951	0.965	0.958	0.954	0.955	0.947
Ni	0.000	0.000	0.000	0.000	0.000	0.000	0.000	0.002	0.009
Co	0.001	0.001	0.001	0.001	0.001	0.001	0.001	0.001	0.002
Fe	0.951	0.958	0.959	0.957	0.984	0.976	0.968	0.968	0.970
Sb	0.000	0.000	0.000	0.000	0.000	0.000	0.000	0.000	0.000
Cd	0.000	0.000	0.000	0.000	0.000	0.000	0.000	0.000	0.000
Pb	0.001	0.001	0.001	0.001	0.001	0.001	0.001	0.001	0.001
S	2.000	2.000	2.000	2.000	2.000	2.000	2.000	2.000	2.000
As	0.000	0.000	0.000	0.000	0.000	0.000	0.000	0.000	0.000
Se	0.003	0.002	0.002	0.001	0.002	0.001	0.002	0.001	0.002
Ag	0.000	0.000	0.000	0.000	0.000	0.000	0.000	0.000	0.000
Au	0.000	0.000	0.000	0.000	0.000	0.000	0.000	0.000	0.000
Total	3.900	3.915	3.914	3.912	3.955	3.944	3.926	3.930	3.932

Table C2. EPMA results for chalcopyrite continued.

Deposit	Betts Cove	Betts Cove	Betts Cove	Betts Cove	Betts Cove	Betts Cove	Tilt Cove	Tilt Cove	Tilt Cove
Drill Hole	BC-21-08	BC-21-08	BC-21-08	BC-21-08	BC-21-08	BC-21-08	SZ-20-01	SZ-20-01	SZ-20-01
Sample	KKMSC53-Cpy6	KKMSC53-Cpy7	KKMSC53-Cpy8	KKMSC53-Cpy9	KKMSC53-Cpy10	KKMSC53-Cpy11	KKMSC12-Cpy1	KKMSC12-Cpy2	KKMSC12-Cpy3
Depth (m)	28.7	28.7	28.7	28.7	28.7	28.7	38.7	38.7	38.7
Date	2023 07 19	2023 07 19	2023 07 19	2023 07 19	2023 07 19	2023 07 19	2023 06 30	2023 06 30	2023 06 30
Facies	Chalcopyrite Dominated	Chalcopyrite Dominated	Chalcopyrite Dominated	Chalcopyrite Dominated	Chalcopyrite Dominated	Chalcopyrite Dominated	Chalcopyrite Dominated	Chalcopyrite Dominated	Chalcopyrite Dominated
Weight Percent (wt%)									
Zn	0.04	0.03	0.05	0.02	0.08	0.02	0.03	0.06	0.23
Cu	33.84	33.92	33.81	33.85	33.83	33.57	33.36	32.9	32.64
Ni	0.04	<0.01	0.03	0.04	<0.01	<0.01	0.01	0.03	<0.01
Co	0.04	0.03	0.04	0.03	0.03	0.03	0.25	1.56	1.66
Fe	30.24	30.2	30.17	30.19	30.33	29.94	30.83	30.29	30.3
Sb	<0.01	<0.01	<0.01	<0.01	<0.01	<0.01	<0.01	<0.01	<0.01
Cd	<0.01	<0.01	<0.01	<0.01	<0.01	<0.01	<0.01	<0.01	<0.01
Pb	0.07	0.11	0.1	0.11	0.08	0.12	0.09	0.08	0.08
S	35.68	35.77	35.28	35.56	35.65	35.49	35.54	35.55	35.31
As	<0.02	<0.02	<0.02	<0.02	<0.02	<0.02	<0.02	<0.02	<0.02
Se	0.05	0.04	0.05	0.07	0.02	0.15	<0.01	0.01	0.01
Ag	0.02	<0.01	<0.01	<0.01	<0.01	<0.01	<0.01	<0.01	<0.01
Au	<0.02	<0.02	<0.02	<0.02	<0.02	<0.02	<0.03	<0.03	<0.03
Total	99.96	100.07	99.45	99.82	99.99	99.21	100.06	100.42	100.16
Atoms Per Formula Unit (apfu)									
Zn	0.001	0.001	0.001	0.001	0.002	0.001	0.001	0.002	0.006
Cu	0.957	0.957	0.967	0.961	0.958	0.955	0.947	0.934	0.933
Ni	0.001	0.000	0.001	0.001	0.000	0.000	0.000	0.001	0.000
Co	0.001	0.001	0.001	0.001	0.001	0.001	0.008	0.048	0.051
Fe	0.973	0.970	0.982	0.975	0.977	0.969	0.996	0.978	0.985
Sb	0.000	0.000	0.000	0.000	0.000	0.000	0.000	0.000	0.000
Cd	0.000	0.000	0.000	0.000	0.000	0.000	0.000	0.000	0.000
Pb	0.001	0.001	0.001	0.001	0.001	0.001	0.001	0.001	0.001
S	2.000	2.000	2.000	2.000	2.000	2.000	2.000	2.000	2.000
As	0.000	0.000	0.000	0.000	0.000	0.000	0.000	0.000	0.000
Se	0.001	0.001	0.001	0.002	0.000	0.003	0.000	0.000	0.000
Ag	0.000	0.000	0.000	0.000	0.000	0.000	0.000	0.000	0.000
Au	0.000	0.000	0.000	0.000	0.000	0.000	0.000	0.000	0.000
Total	3.936	3.930	3.955	3.941	3.939	3.929	3.953	3.964	3.977

Table C2. EPMA results for chalcopyrite continued.

Deposit	Tilt Cove	Tilt Cove	Tilt Cove	Tilt Cove	Tilt Cove	Tilt Cove	Tilt Cove	Tilt Cove	Tilt Cove
Drill Hole	SZ-20-01	SZ-20-01	SZ-20-01	SZ-20-01	SZ-20-01	SZ-20-01	SZ-20-01	SZ-20-01	SZ-20-01
Sample	KKMSC12-Cpy4	KKMSC12-Cpy5	KKMSC12-Cpy6	KKMSC12-Cpy7	KKMSC12-Cpy8	KKMSC12-Cpy9	KKMSC12-Cpy10	KKMSC12-Cpy11	KKMSC12-Cpy12
Depth (m)	38.7	38.7	38.7	38.7	38.7	38.7	38.7	38.7	38.7
Date	2023 06 30	2023 06 30	2023 06 30	2023 06 30	2023 06 30	2023 06 30	2023 06 30	2023 06 30	2023 06 30
Facies	Chalcopyrite Dominated	Chalcopyrite Dominated	Chalcopyrite Dominated	Chalcopyrite Dominated	Chalcopyrite Dominated	Chalcopyrite Dominated	Chalcopyrite Dominated	Chalcopyrite Dominated	Chalcopyrite Dominated
Weight Percent (wt%)									
Zn	0.03	0.02	0.02	0.02	0.03	0.03	0.03	0.02	0.01
Cu	33.14	33.74	33.8	33.04	33.15	27.27	33.08	33.84	31.74
Ni	0.02	<0.01	<0.01	<0.01	0.02	0.29	<0.01	<0.01	0.01
Co	1.01	0.03	0.03	0.84	1.42	6.8	0.3	0.06	1.87
Fe	30.35	30.96	31.14	30.1	30.11	25.31	30.4	30.93	29.23
Sb	<0.01	<0.01	<0.01	<0.01	<0.01	<0.01	<0.02	<0.01	<0.01
Cd	<0.01	<0.01	0.01	<0.01	<0.01	<0.01	<0.01	<0.01	<0.01
Pb	0.09	0.1	0.07	0.1	0.1	0.07	0.09	0.08	0.09
S	35.56	35.82	35.88	35.63	35.52	32	35.32	35.75	33.97
As	<0.02	<0.02	<0.02	<0.02	<0.02	8.16	<0.02	<0.02	<0.03
Se	<0.01	<0.01	<0.01	<0.01	0.03	0.01	<0.01	0.02	<0.01
Ag	<0.01	<0.01	0.01	0.03	<0.01	<0.01	0.03	<0.01	0.03
Au	<0.03	<0.02	<0.03	<0.03	<0.03	<0.02	<0.03	<0.03	<0.03
Total	100.15	100.62	100.92	99.55	100.32	99.87	98.87	100.58	96.75
Atoms Per Formula Unit (apfu)									
Zn	0.001	0.001	0.001	0.001	0.001	0.001	0.001	0.001	0.000
Cu	0.941	0.951	0.951	0.936	0.942	0.860	0.945	0.955	0.943
Ni	0.001	0.000	0.000	0.000	0.001	0.010	0.000	0.000	0.000
Co	0.031	0.001	0.001	0.026	0.044	0.231	0.009	0.002	0.060
Fe	0.980	0.993	0.997	0.970	0.973	0.908	0.988	0.994	0.988
Sb	0.000	0.000	0.000	0.000	0.000	0.000	0.000	0.000	0.000
Cd	0.000	0.000	0.000	0.000	0.000	0.000	0.000	0.000	0.000
Pb	0.001	0.001	0.001	0.001	0.001	0.001	0.001	0.001	0.001
S	2.000	2.000	2.000	2.000	2.000	2.000	2.000	2.000	2.000
As	0.000	0.000	0.000	0.000	0.000	0.218	0.000	0.000	0.000
Se	0.000	0.000	0.000	0.000	0.001	0.000	0.000	0.000	0.000
Ag	0.000	0.000	0.000	0.001	0.000	0.000	0.001	0.000	0.001
Au	0.000	0.000	0.000	0.000	0.000	0.000	0.000	0.000	0.000
Total	3.954	3.945	3.950	3.934	3.962	4.230	3.945	3.952	3.993

Table C2. EPMA results for chalcopyrite continued.

Deposit	Tilt Cove	Tilt Cove	Tilt Cove	Tilt Cove	Tilt Cove	Tilt Cove	Tilt Cove	Tilt Cove	Tilt Cove
Drill Hole	SZ-20-01	SZ-20-01	SZ-20-01	SZ-20-01	SZ-20-01	SZ-20-01	SZ-20-01	SZ-20-01	SZ-20-01
Sample	KKMSC12-Cpy13	KKMSC12-Cpy14	KKMSC12-Cpy15	KKMSC12-Cpy16	KKMSC12-Cpy17	KKMSC12-Cpy18	KKMSC12-Cpy19	KKMSC12-Cpy20	KKMSC12-Cpy21
Depth (m)	38.7	38.7	38.7	38.7	38.7	38.7	38.7	38.7	38.7
Date	2023_06_30	2023_06_30	2023_06_30	2023_06_30	2023_06_30	2023_06_30	2023_06_30	2023_06_30	2023_06_30
Facies	Chalcopyrite Dominated	Chalcopyrite Dominated	Chalcopyrite Dominated	Chalcopyrite Dominated	Chalcopyrite Dominated	Chalcopyrite Dominated	Chalcopyrite Dominated	Chalcopyrite Dominated	Chalcopyrite Dominated
Weight Percent (wt%)									
Zn	0.02	0.03	0.02	0.03	0.03	0.02	0.03	0.02	<0.01
Cu	33.44	33.46	33.21	33.29	33.52	33.6	33.65	33.36	33.4
Ni	<0.01	0.01	<0.01	<0.01	<0.01	<0.01	<0.01	<0.01	<0.01
Co	0.12	0.05	0.05	0.29	0.03	0.03	0.04	0.1	0.04
Fe	30.35	30.47	30.72	30.25	30.63	30.6	30.68	30.54	30.66
Sb	<0.01	<0.01	<0.01	<0.01	<0.01	<0.01	<0.01	<0.01	<0.01
Cd	<0.01	<0.01	<0.01	<0.01	<0.01	<0.01	<0.01	<0.01	<0.01
Pb	0.1	0.07	0.07	0.12	0.1	0.07	0.1	0.09	0.13
S	35.79	35.58	35.84	35.58	35.45	35.58	35.28	35.65	35.19
As	0.06	<0.02	<0.02	<0.02	<0.02	<0.02	<0.02	<0.02	<0.02
Se	<0.01	<0.01	<0.01	<0.01	<0.01	<0.01	<0.01	<0.01	<0.01
Ag	<0.01	<0.01	<0.01	<0.01	<0.01	<0.01	<0.01	<0.01	<0.01
Au	<0.03	<0.03	<0.03	<0.03	<0.03	<0.03	<0.03	<0.03	<0.03
Total	99.81	99.56	99.74	99.46	99.59	99.80	99.67	99.67	99.22
Atoms Per Formula Unit (apfu)									
Zn	0.001	0.001	0.001	0.001	0.001	0.001	0.001	0.001	0.000
Cu	0.943	0.949	0.935	0.944	0.954	0.953	0.963	0.944	0.958
Ni	0.000	0.000	0.000	0.000	0.000	0.000	0.000	0.000	0.000
Co	0.004	0.002	0.002	0.009	0.001	0.001	0.001	0.003	0.001
Fe	0.974	0.983	0.984	0.976	0.992	0.988	0.999	0.984	1.001
Sb	0.000	0.000	0.000	0.000	0.000	0.000	0.000	0.000	0.000
Cd	0.000	0.000	0.000	0.000	0.000	0.000	0.000	0.000	0.000
Pb	0.001	0.001	0.001	0.001	0.001	0.001	0.001	0.001	0.001
S	2.000	2.000	2.000	2.000	2.000	2.000	2.000	2.000	2.000
As	0.001	0.000	0.000	0.000	0.000	0.000	0.000	0.000	0.000
Se	0.000	0.000	0.000	0.000	0.000	0.000	0.000	0.000	0.000
Ag	0.000	0.000	0.000	0.000	0.000	0.000	0.000	0.000	0.000
Au	0.000	0.000	0.000	0.000	0.000	0.000	0.000	0.000	0.000
Total	3.923	3.936	3.922	3.931	3.949	3.943	3.964	3.933	3.961

Table C2. EPMA results for chalcopyrite continued.

Deposit	Tilt Cove	Tilt Cove	Tilt Cove	Tilt Cove	Tilt Cove	Tilt Cove	Tilt Cove	Tilt Cove	Tilt Cove
Drill Hole	SZ-20-01	SZ-20-01	SZ-20-01	SZ-20-01	SZ-20-01	SZ-20-01	SZ-20-01	SZ-20-01	SZ-20-01
Sample	KKMSC12-Cpy22	KKMSC12-Cpy23	KKMSC12-Cpy24	KKMSC12-Cpy25	KKMSC12-Cpy26	KKMSC12-Cpy27	KKMSC12-Cpy28	KKMSC12-Cpy29	KKMSC12-Cpy30
Depth (m)	38.7	38.7	38.7	38.7	38.7	38.7	38.7	38.7	38.7
Date	2023 06 30	2023 06 30	2023 06 30	2023 06 30	2023 06 30	2023 06 30	2023 06 30	2023 06 30	2023 06 30
Facies	Chalcopyrite Dominated	Chalcopyrite Dominated	Chalcopyrite Dominated	Chalcopyrite Dominated	Chalcopyrite Dominated	Chalcopyrite Dominated	Chalcopyrite Dominated	Chalcopyrite Dominated	Chalcopyrite Dominated
Weight Percent (wt%)									
Zn	0.02	0.02	0.03	0.02	<0.01	0.03	0.02	0.04	0.05
Cu	33.38	33.46	33.19	33.32	33.39	33.44	33.32	28.76	28
Ni	<0.01	0.01	0.03	0.02	<0.01	<0.01	<0.01	0.03	<0.01
Co	0.29	0.38	0.69	0.41	0.06	0.04	0.09	1.32	1
Fe	30.38	30.18	30.09	30.44	30.37	30.31	30.27	25.14	24.51
Sb	<0.01	<0.01	<0.01	<0.01	<0.01	<0.01	<0.01	<0.01	<0.01
Cd	<0.01	<0.01	<0.01	<0.01	<0.01	<0.01	<0.01	<0.01	<0.01
Pb	0.08	0.08	0.1	0.09	0.06	0.09	0.11	0.09	0.09
S	35.45	35.45	35.25	35.55	35.69	35.67	35.56	30.35	30.14
As	<0.02	<0.02	<0.02	<0.02	<0.02	<0.02	<0.02	0.75	0.64
Se	0.02	0.03	<0.01	<0.01	<0.01	<0.01	<0.01	<0.01	<0.01
Ag	<0.01	0.01	0.02	<0.01	<0.01	<0.01	<0.01	<0.01	<0.01
Au	<0.03	<0.03	<0.03	<0.03	<0.03	<0.03	<0.03	<0.02	<0.02
Total	99.46	99.47	99.24	99.72	99.41	99.46	99.27	86.35	84.31
Atoms Per Formula Unit (apfu)									
Zn	0.001	0.001	0.001	0.001	0.000	0.001	0.001	0.001	0.002
Cu	0.950	0.953	0.950	0.946	0.944	0.946	0.946	0.956	0.938
Ni	0.000	0.000	0.001	0.001	0.000	0.000	0.000	0.001	0.000
Co	0.009	0.012	0.021	0.013	0.002	0.001	0.003	0.047	0.036
Fe	0.984	0.978	0.980	0.983	0.977	0.976	0.978	0.951	0.934
Sb	0.000	0.000	0.000	0.000	0.000	0.000	0.000	0.000	0.000
Cd	0.000	0.000	0.000	0.000	0.000	0.000	0.000	0.000	0.000
Pb	0.001	0.001	0.001	0.001	0.001	0.001	0.001	0.001	0.001
S	2.000	2.000	2.000	2.000	2.000	2.000	2.000	2.000	2.000
As	0.000	0.000	0.000	0.000	0.000	0.000	0.000	0.021	0.018
Se	0.000	0.001	0.000	0.000	0.000	0.000	0.000	0.000	0.000
Ag	0.000	0.000	0.000	0.000	0.000	0.000	0.000	0.000	0.000
Au	0.000	0.000	0.000	0.000	0.000	0.000	0.000	0.000	0.000
Total	3.945	3.944	3.955	3.944	3.924	3.925	3.927	3.979	3.928

Table C2. EPMA results for chalcopyrite continued.

Deposit	Tilt Cove	Tilt Cove	Tilt Cove	Tilt Cove	Tilt Cove	Tilt Cove	Tilt Cove	Tilt Cove	Tilt Cove
Drill Hole	SZ-20-01	SZ-20-01	SZ-20-01	SZ-20-01	SZ-20-01	SZ-20-01	SZ-20-01	SZ-20-01	SZ-20-01
Sample	KKMSC12-Cpy31	KKMSC13-Cpy1	KKMSC13-Cpy2	KKMSC13-Cpy3	KKMSC13-Cpy4	KKMSC13-Cpy5	KKMSC13-Cpy6	KKMSC13-Cpy7	KKMSC13-Cpy8
Depth (m)	38.7	66.6	66.6	66.6	66.6	66.6	66.6	66.6	66.6
Date	2023 06 30	2023 07 17	2023 07 17	2023 07 17	2023 07 17	2023 07 17	2023 07 17	2023 07 17	2023 07 17
Facies	Chalcopyrite Dominated	Pyrite Dominated	Pyrite Dominated	Pyrite Dominated	Pyrite Dominated	Pyrite Dominated	Pyrite Dominated	Pyrite Dominated	Pyrite Dominated
Weight Percent (wt%)									
Zn	0.06	0.05	0.02	0.04	0.04	0.03	0.02	0.09	0.02
Cu	31.08	33.63	33.64	33.7	33.75	32.7	33.32	32.97	32.93
Ni	<0.01	<0.01	<0.01	<0.01	<0.01	<0.01	<0.01	<0.01	<0.01
Co	0.49	0.04	0.04	0.01	0.03	0.03	0.03	0.04	0.03
Fe	27.77	30.18	30.13	30.29	30.3	29.76	30.37	30.6	30.5
Sb	<0.01	<0.01	<0.01	<0.01	<0.01	<0.01	<0.01	<0.01	<0.01
Cd	<0.01	<0.01	<0.01	<0.01	<0.01	<0.01	0.02	<0.01	<0.01
Pb	0.06	0.08	0.11	0.13	0.12	0.1	0.12	0.09	0.08
S	33.58	35.78	35.94	35.57	35.81	35.47	35.65	35.79	35.96
As	<0.02	<0.02	<0.02	<0.02	<0.02	0.36	<0.02	<0.02	<0.02
Se	0.03	<0.01	<0.01	<0.01	<0.01	<0.01	<0.01	<0.01	<0.01
Ag	<0.01	<0.01	0.01	<0.01	<0.01	<0.01	0.01	0.01	<0.01
Au	<0.02	<0.02	0.03	<0.02	<0.02	<0.02	<0.02	<0.02	<0.02
Total	92.87	99.69	99.90	99.64	99.97	98.38	99.50	99.52	99.44
Atoms Per Formula Unit (apfu)									
Zn	0.002	0.001	0.001	0.001	0.001	0.001	0.001	0.002	0.001
Cu	0.934	0.949	0.945	0.956	0.951	0.930	0.943	0.930	0.924
Ni	0.000	0.000	0.000	0.000	0.000	0.000	0.000	0.000	0.000
Co	0.016	0.001	0.001	0.000	0.001	0.001	0.001	0.001	0.001
Fe	0.950	0.969	0.963	0.978	0.972	0.963	0.978	0.982	0.974
Sb	0.000	0.000	0.000	0.000	0.000	0.000	0.000	0.000	0.000
Cd	0.000	0.000	0.000	0.000	0.000	0.000	0.000	0.000	0.000
Pb	0.001	0.001	0.001	0.001	0.001	0.001	0.001	0.001	0.001
S	2.000	2.000	2.000	2.000	2.000	2.000	2.000	2.000	2.000
As	0.000	0.000	0.000	0.000	0.000	0.009	0.000	0.000	0.000
Se	0.001	0.000	0.000	0.000	0.000	0.000	0.000	0.000	0.000
Ag	0.000	0.000	0.000	0.000	0.000	0.000	0.000	0.000	0.000
Au	0.000	0.000	0.000	0.000	0.000	0.000	0.000	0.000	0.000
Total	3.903	3.920	3.910	3.937	3.926	3.905	3.925	3.916	3.900

Table C2. EPMA results for chalcopyrite continued.

Deposit	Tilt Cove	Tilt Cove	Tilt Cove	Tilt Cove	Tilt Cove	Tilt Cove	Tilt Cove	Tilt Cove	Tilt Cove
Drill Hole	SZ-20-01	SZ-20-01	SZ-20-03	SZ-20-03	SZ-20-03	SZ-20-04	SZ-20-04	SZ-20-04	SZ-20-04
Sample	KKMSC13-Cpy9	KKMSC13-Cpy10	KKMSC23-Cpy1	KKMSC23-Cpy2	KKMSC23-Cpy3	KKMSC63-Cpy1	KKMSC63-Cpy2	KKMSC63-Cpy3	KKMSC63-Cpy4
Depth (m)	66.6	66.6	66.6	17	17	64.45	64.45	64.45	64.45
Date	2023_07_17	2023_07_17	2023_07_17	2023_06_29	2023_06_29	2023_06_30	2023_06_30	2023_06_30	2023_06_30
Facies	Pyrite Dominated	Pyrite Dominated	Pyrite Dominated	Magnetite Dominated	Magnetite Dominated	Pyrite Dominated	Pyrite Dominated	Pyrite Dominated	Pyrite Dominated
Weight Percent (wt%)									
Zn	0.02	0.03	<0.01	0.02	<0.01	0.03	0.02	0.03	0.03
Cu	33.42	32.91	34.43	33.77	33.85	33.6	33.48	33.56	33.42
Ni	<0.01	<0.01	<0.01	<0.01	<0.01	0.01	<0.01	<0.01	<0.01
Co	0.04	0.04	<0.01	<0.01	<0.01	0.03	0.03	0.04	0.03
Fe	29.91	30.43	30.61	30.97	31.06	31.18	31.57	31.45	31.65
Sb	<0.01	<0.01	<0.01	<0.01	<0.01	<0.01	<0.01	<0.01	<0.01
Cd	<0.01	<0.01	0.01	<0.01	<0.01	<0.01	<0.01	<0.01	<0.01
Pb	0.11	0.1	<0.02	<0.02	<0.02	0.11	0.11	0.11	0.09
S	35.63	35.65	35.33	35.35	35.51	35.43	35.82	35.6	35.5
As	<0.02	<0.02	<0.02	<0.02	<0.02	<0.02	<0.02	<0.02	<0.02
Se	<0.01	<0.01	<0.01	0.01	<0.01	0.03	0.03	0.03	<0.01
Ag	0.01	0.01	<0.01	<0.01	<0.01	<0.01	<0.01	<0.01	<0.01
Au	<0.02	<0.02	<0.03	<0.03	<0.03	<0.03	<0.03	<0.03	<0.03
Total	99.09	99.10	100.34	100.06	100.38	100.33	101.01	100.77	100.61
Atoms Per Formula Unit (apfu)									
Zn	0.001	0.001	0.000	0.001	0.000	0.001	0.001	0.001	0.001
Cu	0.947	0.932	0.983	0.964	0.962	0.957	0.943	0.951	0.950
Ni	0.000	0.000	0.000	0.000	0.000	0.000	0.000	0.000	0.000
Co	0.001	0.001	0.000	0.000	0.000	0.001	0.001	0.001	0.001
Fe	0.964	0.980	0.995	1.006	1.004	1.011	1.012	1.014	1.024
Sb	0.000	0.000	0.000	0.000	0.000	0.000	0.000	0.000	0.000
Cd	0.000	0.000	0.000	0.000	0.000	0.000	0.000	0.000	0.000
Pb	0.001	0.001	0.000	0.000	0.000	0.001	0.001	0.001	0.001
S	2.000	2.000	2.000	2.000	2.000	2.000	2.000	2.000	2.000
As	0.000	0.000	0.000	0.000	0.000	0.000	0.000	0.000	0.000
Se	0.000	0.000	0.000	0.000	0.000	0.001	0.001	0.001	0.000
Ag	0.000	0.000	0.000	0.000	0.000	0.000	0.000	0.000	0.000
Au	0.000	0.000	0.000	0.000	0.000	0.000	0.000	0.000	0.000
Total	3.913	3.915	3.979	3.971	3.966	3.971	3.958	3.970	3.976

Table C2. EPMA results for chalcopyrite continued.

Deposit	Tilt Cove	Tilt Cove	Tilt Cove	Tilt Cove	Tilt Cove	Tilt Cove	Tilt Cove	Tilt Cove	Tilt Cove
Drill Hole	SZ-20-04	SZ-20-04	SZ-20-04	SZ-20-04	SZ-20-04	SZ-20-04	SZ-20-04	SZ-20-04	SZ-20-04
Sample	KKMSC63-Cpy5	KKMSC63-Cpy6	KKMSC63-Cpy7	KKMSC63-Cpy8	KKMSC63-Cpy9	KKMSC63-Cpy10	KKMSC63-Cpy11	KKMSC63-Cpy12	KKMSC63-Cpy13
Depth (m)	64.45	64.45	64.45	64.45	64.45	64.45	64.45	64.45	64.45
Date	2023_06_30	2023_06_30	2023_06_30	2023_06_30	2023_06_30	2023_06_30	2023_06_30	2023_06_30	2023_06_30
Facies	Pyrite Dominated	Pyrite Dominated	Pyrite Dominated	Pyrite Dominated	Pyrite Dominated	Pyrite Dominated	Pyrite Dominated	Pyrite Dominated	Pyrite Dominated
Weight Percent (wt%)									
Zn	0.06	0.04	1.2	0.08	0.04	0.03	0.03	0.02	0.02
Cu	33.21	33.63	33.31	32.66	33.68	33.55	33.59	33.42	33.53
Ni	0.01	<0.01	0.01	<0.01	<0.01	<0.01	<0.01	<0.01	<0.01
Co	0.03	0.03	0.03	0.04	0.04	0.07	0.29	0.14	0.14
Fe	29.88	30.92	30.5	32.6	31.09	31.33	31.24	31.13	30.95
Sb	<0.01	0.01	<0.01	<0.01	<0.01	<0.01	<0.01	<0.01	<0.01
Cd	<0.01	<0.01	<0.01	<0.01	<0.01	<0.01	0.01	<0.01	<0.01
Pb	0.08	0.09	0.1	0.13	0.09	0.09	0.07	0.09	0.11
S	35.36	35.37	35.48	34.31	35.58	35.64	35.6	35.44	35.62
As	<0.02	<0.02	<0.02	<0.02	<0.02	<0.02	<0.02	<0.02	<0.02
Se	<0.01	<0.01	0.03	<0.01	<0.01	0.02	<0.01	<0.01	0.04
Ag	<0.01	<0.01	<0.01	<0.01	<0.01	<0.01	<0.01	<0.01	<0.01
Au	<0.03	<0.03	<0.02	<0.03	<0.03	<0.03	<0.03	<0.03	<0.03
Total	98.55	100.00	100.60	99.78	100.43	100.63	100.72	100.12	100.36
Atoms Per Formula Unit (apfu)									
Zn	0.002	0.001	0.033	0.002	0.001	0.001	0.001	0.001	0.001
Cu	0.948	0.960	0.947	0.961	0.955	0.950	0.952	0.952	0.950
Ni	0.000	0.000	0.000	0.000	0.000	0.000	0.000	0.000	0.000
Co	0.001	0.001	0.001	0.001	0.001	0.002	0.009	0.004	0.004
Fe	0.970	1.004	0.987	1.091	1.003	1.009	1.008	1.009	0.998
Sb	0.000	0.000	0.000	0.000	0.000	0.000	0.000	0.000	0.000
Cd	0.000	0.000	0.000	0.000	0.000	0.000	0.000	0.000	0.000
Pb	0.001	0.001	0.001	0.001	0.001	0.001	0.001	0.001	0.001
S	2.000	2.000	2.000	2.000	2.000	2.000	2.000	2.000	2.000
As	0.000	0.000	0.000	0.000	0.000	0.000	0.000	0.000	0.000
Se	0.000	0.000	0.001	0.000	0.000	0.000	0.000	0.000	0.001
Ag	0.000	0.000	0.000	0.000	0.000	0.000	0.000	0.000	0.000
Au	0.000	0.000	0.000	0.000	0.000	0.000	0.000	0.000	0.000
Total	3.922	3.966	3.971	4.057	3.962	3.964	3.970	3.966	3.954

Table C2. EPMA results for chalcopyrite continued.

Deposit	Tilt Cove	Tilt Cove	Tilt Cove	Tilt Cove	Tilt Cove	Tilt Cove	Tilt Cove	Tilt Cove	Tilt Cove
Drill Hole	SZ-20-04	SZ-20-04	SZ-20-04	SZ-20-04	SZ-20-04	SZ-20-04	SZ-20-04	SZ-20-04	SZ-20-04
Sample	KKMSC63-Cpy14	KKMSC63-Cpy15	KKMSC63-Cpy16	KKMSC63-Cpy17	KKMSC63-Cpy18	KKMSC63-Cpy19	KKMSC63-Cpy20	KKMSC63-Cpy21	KKMSC63-Cpy22
Depth (m)	64.45	64.45	64.45	64.45	64.45	64.45	64.45	64.45	64.45
Date	2023 06 30	2023 06 30	2023 06 30	2023 06 30	2023 06 30	2023 06 30	2023 06 30	2023 06 30	2023 06 30
Facies	Pyrite Dominated	Pyrite Dominated	Pyrite Dominated	Pyrite Dominated	Pyrite Dominated	Pyrite Dominated	Pyrite Dominated	Pyrite Dominated	Pyrite Dominated
Weight Percent (wt%)									
Zn	0.03	0.02	0.02	0.03	0.04	0.03	0.04	0.04	0.05
Cu	33.09	32.96	27.34	32.97	33.61	32.78	33.82	33.09	33.58
Ni	<0.01	0.01	0.41	0.01	<0.01	0.03	<0.01	0.03	0.01
Co	0.96	0.45	4.37	0.14	0.06	1.07	0.03	0.03	0.03
Fe	30.57	30.77	27.08	31.24	31.15	30.68	31.07	30.73	31.16
Sb	<0.01	0.01	<0.01	<0.01	<0.01	<0.01	<0.01	<0.01	<0.01
Cd	<0.01	<0.01	<0.01	<0.01	<0.01	<0.01	0.02	<0.01	0.01
Pb	0.08	0.08	0.11	0.11	0.09	0.07	0.06	0.08	0.05
S	35.48	35.45	33.9	35.43	35.36	35.36	35.82	35.75	35.51
As	<0.02	<0.02	11.1	<0.02	<0.02	<0.02	<0.02	<0.02	<0.02
Se	<0.01	0.03	0.02	<0.01	0.02	0.02	0.01	0.02	0.03
Ag	<0.01	<0.01	0.01	<0.01	<0.01	<0.01	<0.01	<0.01	<0.01
Au	<0.03	<0.03	<0.02	<0.03	<0.02	<0.03	<0.03	<0.03	<0.03
Total	100.17	99.74	104.31	99.76	100.29	99.95	100.77	99.70	100.35
Atoms Per Formula Unit (apfu)									
Zn	0.001	0.001	0.001	0.001	0.001	0.001	0.001	0.001	0.001
Cu	0.941	0.938	0.814	0.939	0.959	0.936	0.953	0.934	0.954
Ni	0.000	0.000	0.013	0.000	0.000	0.001	0.000	0.001	0.000
Co	0.029	0.014	0.140	0.004	0.002	0.033	0.001	0.001	0.001
Fe	0.989	0.997	0.917	1.013	1.012	0.996	0.996	0.987	1.008
Sb	0.000	0.000	0.000	0.000	0.000	0.000	0.000	0.000	0.000
Cd	0.000	0.000	0.000	0.000	0.000	0.000	0.000	0.000	0.000
Pb	0.001	0.001	0.001	0.001	0.001	0.001	0.001	0.001	0.000
S	2.000	2.000	2.000	2.000	2.000	2.000	2.000	2.000	2.000
As	0.000	0.000	0.280	0.000	0.000	0.000	0.000	0.000	0.000
Se	0.000	0.001	0.000	0.000	0.000	0.000	0.000	0.000	0.001
Ag	0.000	0.000	0.000	0.000	0.000	0.000	0.000	0.000	0.000
Au	0.000	0.000	0.000	0.000	0.000	0.000	0.000	0.000	0.000
Total	3.962	3.951	4.167	3.958	3.975	3.968	3.952	3.925	3.966

Table C2. EPMA results for chalcopyrite continued.

Deposit	Tilt Cove	Tilt Cove	Tilt Cove	Tilt Cove	Tilt Cove	Tilt Cove	Tilt Cove	Tilt Cove	Tilt Cove
Drill Hole	SZ-20-04	SZ-20-04	SZ-20-05	SZ-20-05	SZ-20-05	SZ-20-05	SZ-20-05	SZ-20-05	SZ-20-05
Sample	KKMSC63-Cpy23	KKMSC63-Cpy23	KKMSC70_Cpy 1	KKMSC70_Cpy 2	KKMSC70_Cpy 3	KKMSC70_Cpy 4	KKMSC70_Cpy 5	KKMSC70_Cpy 6	KKMSC70_Cpy 7
Depth (m)	64.45	64.45	126.45	126.45	126.45	126.45	126.45	126.45	126.45
Date	2023_06_30	2023_06_30	2023_07_14	2023_07_14	2023_07_14	2023_07_14	2023_07_14	2023_07_14	2023_07_14
Facies	Pyrite Dominated	Pyrite Dominated	Chalcopyrite-pyrrhotite Dominated	Chalcopyrite-pyrrhotite Dominated	Chalcopyrite-pyrrhotite Dominated	Chalcopyrite-pyrrhotite Dominated	Chalcopyrite-pyrrhotite Dominated	Chalcopyrite-pyrrhotite Dominated	Chalcopyrite-pyrrhotite Dominated
Weight Percent (wt%)									
Zn	0.04	0.04	0.07	0.05	0.04	0.04	0.05	0.04	0.04
Cu	33.56	33.7	33.59	33.63	33.45	33.64	33.48	33.58	33.53
Ni	0.02	<0.01	<0.01	0.02	0.02	<0.01	<0.01	0.01	<0.01
Co	0.02	0.03	0.04	0.04	0.04	0.03	0.03	0.03	0.03
Fe	31.24	30.94	30.18	30.16	30.07	30.23	29.96	30.02	30.25
Sb	<0.01	<0.01	<0.01	<0.01	<0.01	<0.01	<0.01	<0.01	<0.01
Cd	<0.01	<0.01	<0.01	<0.01	<0.01	0.01	<0.01	<0.01	<0.01
Pb	0.09	0.04	0.09	0.05	0.11	0.11	0.13	0.1	0.07
S	35.67	35.35	35.58	35.52	35.53	35.76	35.66	35.55	35.75
As	<0.02	<0.02	0.02	<0.02	<0.02	<0.02	<0.02	<0.02	<0.02
Se	<0.01	<0.01	0.03	<0.01	0.02	0.04	0.02	0.02	0.01
Ag	<0.01	<0.01	<0.01	0.01	<0.01	0.01	<0.01	<0.01	<0.01
Au	<0.03	<0.02	<0.02	<0.02	<0.02	<0.02	<0.02	<0.02	<0.02
Total	100.54	100.06	99.59	99.43	99.24	99.79	99.25	99.30	99.59
Atoms Per Formula Unit (apfu)									
Zn	0.001	0.001	0.002	0.001	0.001	0.001	0.001	0.001	0.001
Cu	0.949	0.962	0.953	0.955	0.950	0.949	0.947	0.953	0.947
Ni	0.001	0.000	0.000	0.001	0.001	0.000	0.000	0.000	0.000
Co	0.001	0.001	0.001	0.001	0.001	0.001	0.001	0.001	0.001
Fe	1.006	1.005	0.974	0.975	0.972	0.971	0.965	0.970	0.972
Sb	0.000	0.000	0.000	0.000	0.000	0.000	0.000	0.000	0.000
Cd	0.000	0.000	0.000	0.000	0.000	0.000	0.000	0.000	0.000
Pb	0.001	0.000	0.001	0.000	0.001	0.001	0.001	0.001	0.001
S	2.000	2.000	2.000	2.000	2.000	2.000	2.000	2.000	2.000
As	0.000	0.000	0.000	0.000	0.000	0.000	0.000	0.000	0.000
Se	0.000	0.000	0.001	0.000	0.000	0.001	0.000	0.000	0.000
Ag	0.000	0.000	0.000	0.000	0.000	0.000	0.000	0.000	0.000
Au	0.000	0.000	0.000	0.000	0.000	0.000	0.000	0.000	0.000
Total	3.958	3.970	3.932	3.934	3.926	3.924	3.916	3.927	3.921

Table C2. EPMA results for chalcopyrite continued.

Deposit	Tilt Cove	Tilt Cove	Tilt Cove	Tilt Cove	Tilt Cove	Tilt Cove	Tilt Cove	Tilt Cove	Tilt Cove
Drill Hole	SZ-20-05	SZ-20-05	SZ-20-05	SZ-20-05	SZ-20-05	SZ-20-05	SZ-20-05	SZ-20-05	SZ-20-05
Sample	KKMSC70_Cpy 8	KKMSC70_Cpy 9	KKMSC70_Cpy 10	KKMSC72_Cpy 1	KKMSC72_Cpy 2	KKMSC72_Cpy 3	KKMSC72_Cpy 4	KKMSC72_Cpy 5	KKMSC72_Cpy 6
Depth (m)	126.45	126.45	126.45	143.7	143.7	143.7	143.7	143.7	143.7
Date	2023 07 14	2023 07 14	2023 07 14	2023 07 14	2023 07 14	2023 07 14	2023 07 14	2023 07 14	2023 07 14
Facies	Chalcopyrite-pyrrhotite Dominated	Chalcopyrite-pyrrhotite Dominated	Chalcopyrite-pyrrhotite Dominated	Pyrrhotite Dominated	Pyrrhotite Dominated	Pyrrhotite Dominated	Pyrrhotite Dominated	Pyrrhotite Dominated	Pyrrhotite Dominated
Weight Percent (wt%)									
Zn	0.04	0.04	0.03	0.04	0.05	0.03	0.05	0.03	0.03
Cu	33.55	33.05	33.53	33.54	33.59	33.56	33.76	33.42	33.59
Ni	<0.01	0.01	<0.01	0.01	<0.01	0.02	<0.01	0.06	<0.01
Co	0.03	0.03	0.03	0.03	0.04	0.04	0.03	0.04	0.03
Fe	30.08	29.37	30.32	30.22	30.14	30.15	30.34	30.11	30.22
Sb	<0.01	<0.01	<0.01	<0.01	<0.01	<0.01	<0.01	<0.01	<0.01
Cd	<0.01	0.01	<0.01	<0.01	<0.01	<0.01	0.01	<0.01	<0.01
Pb	0.09	0.06	0.1	0.09	0.07	0.12	0.13	0.11	0.07
S	35.66	35.6	35.53	35.48	35.6	35.42	35.4	35.49	35.52
As	<0.02	<0.02	<0.02	<0.02	<0.02	<0.02	<0.02	<0.02	<0.02
Se	0.03	0.02	<0.01	0.01	<0.01	0.02	<0.01	<0.01	<0.01
Ag	<0.01	<0.01	0.01	<0.01	0.01	<0.01	0.01	<0.01	<0.01
Au	<0.02	<0.02	<0.02	<0.02	<0.02	<0.02	<0.02	<0.02	<0.02
Total	99.38	98.13	99.58	99.32	99.46	99.30	99.72	99.20	99.40
Atoms Per Formula Unit (apfu)									
Zn	0.001	0.001	0.001	0.001	0.001	0.001	0.001	0.001	0.001
Cu	0.949	0.937	0.952	0.954	0.952	0.956	0.962	0.950	0.954
Ni	0.000	0.000	0.000	0.000	0.000	0.001	0.000	0.002	0.000
Co	0.001	0.001	0.001	0.001	0.001	0.001	0.001	0.001	0.001
Fe	0.969	0.947	0.980	0.978	0.972	0.977	0.984	0.974	0.977
Sb	0.000	0.000	0.000	0.000	0.000	0.000	0.000	0.000	0.000
Cd	0.000	0.000	0.000	0.000	0.000	0.000	0.000	0.000	0.000
Pb	0.001	0.001	0.001	0.001	0.001	0.001	0.001	0.001	0.001
S	2.000	2.000	2.000	2.000	2.000	2.000	2.000	2.000	2.000
As	0.000	0.000	0.000	0.000	0.000	0.000	0.000	0.000	0.000
Se	0.001	0.000	0.000	0.000	0.000	0.000	0.000	0.000	0.000
Ag	0.000	0.000	0.000	0.000	0.000	0.000	0.000	0.000	0.000
Au	0.000	0.000	0.000	0.000	0.000	0.000	0.000	0.000	0.000
Total	3.922	3.888	3.935	3.935	3.928	3.938	3.950	3.929	3.934

Table C2. EPMA results for chalcopyrite continued.

Deposit	Tilt Cove	Tilt Cove	Tilt Cove	Tilt Cove	Tilt Cove	Tilt Cove	Tilt Cove	Tilt Cove	Tilt Cove
Drill Hole	SZ-20-05	SZ-20-05	SZ-20-05	SZ-20-05	SZ-20-05	SZ-20-05	SZ-20-08	SZ-20-08	SZ-20-08
Sample	KKMSC72_Cpy 7	KKMSC72_Cpy 8	KKMSC72_Cpy 9	KKMSC72_Cpy 10	KKMSC72_Cpy 11	KKMSC72_Cpy 12	KKMSC77-Cpy1	KKMSC77-Cpy2	KKMSC77-Cpy3
Depth (m)	143.7	143.7	143.7	143.7	143.7	143.7	28.17	28.17	28.17
Date	2023_07_14	2023_07_14	2023_07_14	2023_07_14	2023_07_14	2023_07_14	2023_09_25	2023_09_25	2023_09_25
Facies	Pyrrhotite Dominated	Pyrrhotite Dominated	Pyrrhotite Dominated	Pyrrhotite Dominated	Pyrrhotite Dominated	Pyrrhotite Dominated	Pyrite Dominated	Pyrite Dominated	Pyrite Dominated
Weight Percent (wt%)									
Zn	0.03	0.03	0.02	0.03	0.04	0.04	<0.01	0.02	0.02
Cu	33.41	33.69	33.15	33.54	33.56	33.58	33.32	33.53	33.39
Ni	0.02	<0.01	<0.01	<0.01	<0.01	<0.01	<0.01	<0.01	<0.01
Co	0.03	0.04	0.03	0.02	0.03	0.03	0.03	0.04	0.04
Fe	30.26	30.11	29.9	30.01	30.16	30.02	30.62	30.59	30.74
Sb	<0.01	<0.01	<0.01	<0.01	<0.01	<0.01	<0.01	<0.01	<0.01
Cd	<0.01	<0.01	<0.01	0.03	0.01	<0.01	<0.01	<0.01	<0.01
Pb	0.07	0.09	0.09	0.11	0.1	0.09	0.11	0.09	0.11
S	35.33	35.7	35.33	35.51	35.56	35.62	34.67	35.27	35.01
As	<0.02	<0.02	<0.02	<0.02	<0.02	<0.02	<0.02	<0.02	<0.02
Se	<0.01	0.03	0.01	0.02	<0.01	<0.01	<0.01	<0.01	<0.01
Ag	<0.01	0.01	<0.01	<0.01	<0.01	<0.01	0.01	<0.01	<0.01
Au	<0.02	<0.02	<0.02	<0.02	<0.02	<0.02	<0.02	<0.02	<0.02
Total	99.02	99.65	98.50	99.27	99.41	99.31	98.70	99.51	99.30
Atoms Per Formula Unit (apfu)									
Zn	0.001	0.001	0.001	0.001	0.001	0.001	0.000	0.001	0.001
Cu	0.954	0.952	0.947	0.953	0.952	0.951	0.970	0.959	0.962
Ni	0.001	0.000	0.000	0.000	0.000	0.000	0.000	0.000	0.000
Co	0.001	0.001	0.001	0.001	0.001	0.001	0.001	0.001	0.001
Fe	0.984	0.969	0.972	0.970	0.974	0.968	1.014	0.996	1.008
Sb	0.000	0.000	0.000	0.000	0.000	0.000	0.000	0.000	0.000
Cd	0.000	0.000	0.000	0.000	0.000	0.000	0.000	0.000	0.000
Pb	0.001	0.001	0.001	0.001	0.001	0.001	0.001	0.001	0.001
S	2.000	2.000	2.000	2.000	2.000	2.000	2.000	2.000	2.000
As	0.000	0.000	0.000	0.000	0.000	0.000	0.000	0.000	0.000
Se	0.000	0.001	0.000	0.000	0.000	0.000	0.000	0.000	0.000
Ag	0.000	0.000	0.000	0.000	0.000	0.000	0.000	0.000	0.000
Au	0.000	0.000	0.000	0.000	0.000	0.000	0.000	0.000	0.000
Total	3.941	3.925	3.921	3.927	3.929	3.922	3.986	3.958	3.974

Table C2. EPMA results for chalcopyrite continued.

Deposit	Tilt Cove	Tilt Cove	Tilt Cove	Tilt Cove	Tilt Cove
Drill Hole	SZ-20-08	SZ-20-08	SZ-20-08	SZ-20-08	SZ-20-08
Sample	KKMSC77-Cpy4	KKMSC77-Cpy5	KKMSC77-Cpy6	KKMSC77-Cpy7	KKMSC77-Cpy8
Depth (m)	28.17	28.17	28.17	28.17	28.17
Date	2023_09_25	2023_09_25	2023_09_25	2023_09_25	2023_09_25
Facies	Pyrite Dominated	Pyrite Dominated	Pyrite Dominated	Pyrite Dominated	Pyrite Dominated
Weight Percent (wt%)					
Zn	0.02	0.02	0.03	0.03	0.03
Cu	32.86	33.9	33.29	33.77	33.37
Ni	0.01	<0.01	<0.01	<0.01	<0.01
Co	0.04	0.04	0.04	0.04	0.05
Fe	31.03	30.73	30.94	30.61	30.76
Sb	<0.01	<0.01	<0.01	<0.01	<0.01
Cd	<0.01	<0.01	<0.01	<0.01	<0.01
Pb	0.12	0.12	0.11	0.08	0.06
S	35.13	35.03	35.08	35.15	34.96
As	<0.02	<0.02	<0.02	<0.02	<0.02
Se	<0.01	<0.01	<0.01	0.03	<0.01
Ag	<0.01	<0.01	<0.01	<0.01	<0.01
Au	<0.02	<0.02	<0.02	<0.02	<0.02
Total	99.12	99.77	99.47	99.62	99.15
Atoms Per Formula Unit (apfu)					
Zn	0.001	0.001	0.001	0.001	0.001
Cu	0.944	0.977	0.958	0.970	0.963
Ni	0.000	0.000	0.000	0.000	0.000
Co	0.001	0.001	0.001	0.001	0.002
Fe	1.014	1.007	1.013	1.000	1.010
Sb	0.000	0.000	0.000	0.000	0.000
Cd	0.000	0.000	0.000	0.000	0.000
Pb	0.001	0.001	0.001	0.001	0.001
S	2.000	2.000	2.000	2.000	2.000
As	0.000	0.000	0.000	0.000	0.000
Se	0.000	0.000	0.000	0.001	0.000
Ag	0.000	0.000	0.000	0.000	0.000
Au	0.000	0.000	0.000	0.000	0.000
Total	3.961	3.987	3.974	3.973	3.977

Table C3. EPMA results for pyrrhotite. Data in red was omitted in discussion due to results being outside of the total cut-off for EPMA or it is inconsistent with SEM and reflected light mineral ID.

Deposit	Betts Cove	Betts Cove	Betts Cove	Betts Cove	Betts Cove	Betts Cove	Betts Cove	Betts Cove	Betts Cove
Drill Hole	BC-21-03	BC-21-03	BC-21-03	BC-21-03	BC-21-03	BC-21-03	BC-21-03	BC-21-03	BC-21-03
Sample	KKMSC35-Po1	KKMSC35-Po2	KKMSC35-Po3	KKMSC35-Po4	KKMSC35-Po5	KKMSC35-Po6	KKMSC35-Po7	KKMSC35-Po8	KKMSC35-Po9
Depth (m)	116.9	116.9	116.9	116.9	116.9	116.9	116.9	116.9	116.9
Date	2023_06_29	2023_06_29	2023_06_29	2023_06_29	2023_06_29	2023_06_29	2023_06_29	2023_06_29	2023_06_29
Facies	Chalcopyrite-pyrrhotite Dominated	Chalcopyrite-pyrrhotite Dominated	Chalcopyrite-pyrrhotite Dominated	Chalcopyrite-pyrrhotite Dominated	Chalcopyrite-pyrrhotite Dominated	Chalcopyrite-pyrrhotite Dominated	Chalcopyrite-pyrrhotite Dominated	Chalcopyrite-pyrrhotite Dominated	Chalcopyrite-pyrrhotite Dominated
Weight Percent (wt%)									
Zn	0.02	0.02	<0.01	<0.01	<0.01	<0.01	0.01	<0.01	<0.01
Cu	<0.01	<0.01	<0.01	<0.01	<0.01	<0.01	0.01	<0.01	<0.01
Ni	0.12	0.14	0.10	0.13	0.08	0.10	0.10	0.13	0.11
Co	0.09	0.09	0.11	0.12	0.12	0.10	0.09	0.09	0.09
Fe	59.04	59.34	59.40	59.22	59.21	59.65	59.71	59.20	59.35
Sb	0.01	<0.01	<0.01	<0.01	<0.01	<0.01	<0.01	<0.01	<0.01
Cd	<0.01	<0.01	<0.01	0.01	<0.01	<0.01	0.01	<0.01	<0.01
Pb	0.04	0.05	<0.02	0.03	0.04	0.03	<0.02	<0.02	<0.02
S	39.85	39.88	39.76	39.79	39.91	39.31	39.57	39.72	39.23
As	<0.02	<0.02	<0.02	<0.02	<0.02	<0.02	<0.02	<0.02	<0.02
Se	0.05	0.03	0.04	0.04	0.06	0.04	0.02	0.07	0.04
Ag	<0.01	<0.01	<0.01	<0.01	<0.01	<0.01	<0.01	<0.01	<0.01
Au	<0.03	<0.03	<0.03	<0.03	<0.03	<0.03	<0.03	<0.03	<0.03
Total	99.14	99.48	99.33	99.22	99.31	99.11	99.45	99.15	98.72
Atoms Per Formula Unit (apfu)									
Zn	0.000	0.000	0.000	0.000	0.000	0.000	0.000	0.000	0.000
Cu	0.000	0.000	0.000	0.000	0.000	0.000	0.000	0.000	0.000
Ni	0.002	0.002	0.001	0.002	0.001	0.001	0.001	0.002	0.002
Co	0.001	0.001	0.002	0.002	0.002	0.001	0.001	0.001	0.001
Fe	0.851	0.854	0.858	0.855	0.852	0.871	0.866	0.856	0.869
Sb	0.000	0.000	0.000	0.000	0.000	0.000	0.000	0.000	0.000
Cd	0.000	0.000	0.000	0.000	0.000	0.000	0.000	0.000	0.000
Pb	0.000	0.000	0.000	0.000	0.000	0.000	0.000	0.000	0.000
S	1.000	1.000	1.000	1.000	1.000	1.000	1.000	1.000	1.000
As	0.000	0.000	0.000	0.000	0.000	0.000	0.000	0.000	0.000
Se	0.001	0.000	0.000	0.000	0.001	0.000	0.000	0.001	0.000
Ag	0.000	0.000	0.000	0.000	0.000	0.000	0.000	0.000	0.000
Au	0.000	0.000	0.000	0.000	0.000	0.000	0.000	0.000	0.000
Total	1.855	1.858	1.861	1.859	1.855	1.875	1.870	1.860	1.872

Table C3. EPMA results for pyrrhotite continued.

Deposit	Betts Cove	Betts Cove	Betts Cove	Betts Cove	Betts Cove	Betts Cove	Betts Cove	Betts Cove	Betts Cove
Drill Hole	BC-21-03	BC-21-03	BC-21-03	BC-21-03	BC-21-03	BC-21-06	BC-21-06	BC-21-06	BC-21-06
Sample	KKMSC35-Po10	KKMSC35-Po11	KKMSC35-Po12	KKMSC35-Po13	KKMSC35-Po14	KKMSC42-Po1	KKMSC42-Po2	KKMSC42-Po3	KKMSC42-Po4
Depth (m)	116.9	116.9	116.9	116.9	116.9	106.3	106.3	106.3	106.3
Date	2023_06_29	2023_06_29	2023_06_29	2023_06_29	2023_06_29	2023_07_18	2023_07_18	2023_07_18	2023_07_18
Facies	Chalcopyrite-pyrrhotite Dominated	Chalcopyrite-pyrrhotite Dominated	Chalcopyrite-pyrrhotite Dominated	Chalcopyrite-pyrrhotite Dominated	Chalcopyrite-pyrrhotite Dominated	Chalcopyrite-pyrrhotite Dominated	Chalcopyrite-pyrrhotite Dominated	Chalcopyrite-pyrrhotite Dominated	Chalcopyrite-pyrrhotite Dominated
Weight Percent (wt%)									
Zn	<0.01	<0.01	<0.01	<0.01	<0.01	<0.01	<0.01	<0.01	<0.01
Cu	<0.01	0.03	<0.01	0.08	<0.01	<0.01	<0.01	0.05	<0.01
Ni	0.09	0.02	0.03	0.06	0.11	0.09	0.08	0.08	0.08
Co	0.08	0.09	0.08	0.08	0.09	0.16	0.15	0.17	0.30
Fe	59.08	59.05	59.09	59.07	59.14	59.20	59.10	59.00	58.99
Sb	<0.01	<0.01	<0.01	<0.01	<0.01	<0.01	<0.01	<0.01	<0.01
Cd	<0.01	<0.01	<0.01	0.01	<0.01	<0.01	<0.01	0.01	<0.01
Pb	<0.02	<0.02	<0.02	0.05	<0.02	0.12	0.11	0.11	0.12
S	39.67	39.67	39.90	39.94	39.68	41.06	40.79	40.84	40.99
As	<0.02	<0.02	<0.02	<0.02	<0.02	<0.02	<0.02	<0.02	<0.02
Se	0.07	0.05	0.03	0.04	<0.01	0.07	0.06	0.05	<0.01
Ag	<0.01	<0.01	<0.01	<0.01	<0.01	<0.01	<0.01	<0.01	<0.01
Au	<0.03	<0.03	<0.03	<0.03	<0.03	<0.02	<0.02	<0.02	0.02
Total	98.94	98.84	99.04	99.27	98.91	100.59	100.17	100.21	100.50
Atoms Per Formula Unit (apfu)									
Zn	0.000	0.000	0.000	0.000	0.000	0.000	0.000	0.000	0.000
Cu	0.000	0.000	0.000	0.001	0.000	0.000	0.000	0.001	0.000
Ni	0.001	0.000	0.000	0.001	0.002	0.001	0.001	0.001	0.001
Co	0.001	0.001	0.001	0.001	0.001	0.002	0.002	0.002	0.004
Fe	0.855	0.855	0.850	0.849	0.856	0.828	0.832	0.829	0.826
Sb	0.000	0.000	0.000	0.000	0.000	0.000	0.000	0.000	0.000
Cd	0.000	0.000	0.000	0.000	0.000	0.000	0.000	0.000	0.000
Pb	0.000	0.000	0.000	0.000	0.000	0.000	0.000	0.000	0.000
S	1.000	1.000	1.000	1.000	1.000	1.000	1.000	1.000	1.000
As	0.000	0.000	0.000	0.000	0.000	0.000	0.000	0.000	0.000
Se	0.001	0.001	0.000	0.000	0.000	0.001	0.001	0.000	0.000
Ag	0.000	0.000	0.000	0.000	0.000	0.000	0.000	0.000	0.000
Au	0.000	0.000	0.000	0.000	0.000	0.000	0.000	0.000	0.000
Total	1.858	1.857	1.852	1.853	1.859	1.832	1.836	1.834	1.832

Table C3. EPMA results for pyrrhotite continued.

Deposit	Betts Cove	Betts Cove	Betts Cove	Betts Cove	Betts Cove	Tilt Cove	Tilt Cove	Tilt Cove	Tilt Cove
Drill Hole	BC-21-06	BC-21-06	BC-21-08	BC-21-08	BC-21-08	SZ-20-01	SZ-20-01	SZ-20-01	SZ-20-01
Sample	KKMSC42-Po5	KKMSC42-Po6	KKMSC53-Po1	KKMSC53-Po2	KKMSC53-Po3	KKMSC13-Po1	KKMSC13-Po2	KKMSC13-Po3	KKMSC13-Po4
Depth (m)	106.3	106.3	28.7	28.7	28.7	66.6	66.6	66.6	66.6
Date	2023_07_18	2023_07_18	2023_07_19	2023_07_19	2023_07_19	2023_07_18	2023_07_18	2023_07_18	2023_07_18
Facies	Chalcopyrite-pyrrhotite Dominated	Chalcopyrite-pyrrhotite Dominated	Chalcopyrite Dominated	Chalcopyrite Dominated	Chalcopyrite Dominated	Pyrite Dominated	Pyrite Dominated	Pyrite Dominated	Pyrite Dominated
Weight Percent (wt%)									
Zn	<0.01	<0.01	<0.01	<0.01	<0.01	<0.01	<0.01	<0.01	0.01
Cu	<0.01	<0.01	0.30	0.34	0.64	<0.01	<0.01	<0.01	0.20
Ni	0.09	0.08	0.56	0.23	0.31	<0.01	<0.01	<0.01	<0.01
Co	0.19	0.16	0.06	0.09	0.08	0.06	0.06	0.06	0.06
Fe	59.25	58.66	58.81	59.10	58.95	59.95	59.99	59.90	59.90
Sb	<0.01	<0.01	<0.01	<0.01	<0.01	<0.01	<0.01	<0.01	<0.01
Cd	0.01	<0.01	<0.01	<0.01	0.01	<0.01	<0.01	0.01	0.01
Pb	0.09	0.12	0.10	0.10	0.11	0.06	0.12	0.09	0.14
S	40.65	40.96	41.03	40.87	40.99	40.30	40.16	40.19	40.03
As	<0.02	<0.02	<0.02	<0.02	<0.02	<0.02	<0.02	<0.02	<0.02
Se	0.06	0.05	0.10	0.10	0.08	<0.01	<0.01	<0.01	<0.01
Ag	<0.01	<0.01	<0.01	<0.01	<0.01	<0.01	<0.01	<0.01	<0.01
Au	<0.02	<0.02	<0.02	<0.02	<0.02	<0.02	<0.02	<0.02	<0.02
Total	100.29	100.03	100.90	100.78	101.13	100.34	100.29	100.22	100.31
Atoms Per Formula Unit (apfu)									
Zn	0.000	0.000	0.000	0.000	0.000	0.000	0.000	0.000	0.000
Cu	0.000	0.000	0.004	0.004	0.008	0.000	0.000	0.000	0.003
Ni	0.001	0.001	0.007	0.003	0.004	0.000	0.000	0.000	0.000
Co	0.003	0.002	0.001	0.001	0.001	0.001	0.001	0.001	0.001
Fe	0.837	0.822	0.823	0.830	0.826	0.854	0.858	0.856	0.859
Sb	0.000	0.000	0.000	0.000	0.000	0.000	0.000	0.000	0.000
Cd	0.000	0.000	0.000	0.000	0.000	0.000	0.000	0.000	0.000
Pb	0.000	0.000	0.000	0.000	0.000	0.000	0.000	0.000	0.001
S	1.000	1.000	1.000	1.000	1.000	1.000	1.000	1.000	1.000
As	0.000	0.000	0.000	0.000	0.000	0.000	0.000	0.000	0.000
Se	0.001	0.000	0.001	0.001	0.001	0.000	0.000	0.000	0.000
Ag	0.000	0.000	0.000	0.000	0.000	0.000	0.000	0.000	0.000
Au	0.000	0.000	0.000	0.000	0.000	0.000	0.000	0.000	0.000
Total	1.842	1.826	1.836	1.840	1.840	1.855	1.859	1.857	1.863

Table C3. EPMA results for pyrrhotite continued.

Deposit	Tilt Cove	Tilt Cove	Tilt Cove	Tilt Cove	Tilt Cove	Tilt Cove	Tilt Cove	Tilt Cove	Tilt Cove
Drill Hole	SZ-20-05	SZ-20-05	SZ-20-05	SZ-20-05	SZ-20-05	SZ-20-05	SZ-20-05	SZ-20-05	SZ-20-05
Sample	KKMSC70_Po1	KKMSC70_Po2	KKMSC70_Po3	KKMSC70_Po4	KKMSC70_Po5	KKMSC70_Po6	KKMSC70_Po7	KKMSC70_Po8	KKMSC70_Po9
Depth (m)	126.45	126.45	126.45	126.45	126.45	126.45	126.45	126.45	126.45
Date	2023_07_14	2023_07_14	2023_07_14	2023_07_14	2023_07_14	2023_07_14	2023_07_14	2023_07_14	2023_07_14
Facies	Chalcopyrite-pyrrhotite Dominated	Chalcopyrite-pyrrhotite Dominated	Chalcopyrite-pyrrhotite Dominated	Chalcopyrite-pyrrhotite Dominated	Chalcopyrite-pyrrhotite Dominated	Chalcopyrite-pyrrhotite Dominated	Chalcopyrite-pyrrhotite Dominated	Chalcopyrite-pyrrhotite Dominated	Chalcopyrite-pyrrhotite Dominated
Weight Percent (wt%)									
Zn	<0.01	<0.01	<0.01	<0.01	<0.01	<0.01	<0.01	<0.01	<0.01
Cu	<0.01	<0.01	<0.01	<0.01	<0.01	0.01	<0.01	0.02	<0.01
Ni	1.66	1.63	1.51	1.63	1.74	1.72	1.58	1.63	1.63
Co	0.07	0.06	0.08	0.08	0.08	0.10	0.17	0.12	0.08
Fe	57.55	57.46	57.68	57.40	57.51	57.63	57.58	57.40	57.78
Sb	<0.01	<0.01	<0.01	<0.01	<0.01	<0.01	<0.01	<0.01	<0.01
Cd	0.01	0.01	<0.01	<0.01	<0.01	<0.01	<0.01	<0.01	0.02
Pb	<0.02	0.05	<0.02	0.04	<0.02	0.02	<0.02	0.03	0.05
S	40.74	40.71	40.67	40.41	40.86	40.66	40.82	40.57	40.58
As	<0.02	<0.02	<0.02	<0.02	<0.02	<0.02	<0.02	<0.02	<0.02
Se	<0.01	0.02	0.02	<0.01	<0.01	<0.01	0.03	0.03	<0.01
Ag	<0.01	<0.01	<0.01	<0.01	<0.01	<0.01	<0.01	<0.01	<0.01
Au	<0.02	<0.02	<0.02	<0.02	<0.02	<0.02	<0.02	<0.02	<0.02
Total	99.96	99.90	99.96	99.49	100.09	100.11	100.14	99.71	100.13
Atoms Per Formula Unit (apfu)									
Zn	0.000	0.000	0.000	0.000	0.000	0.000	0.000	0.000	0.000
Cu	0.000	0.000	0.000	0.000	0.000	0.000	0.000	0.000	0.000
Ni	0.022	0.022	0.020	0.022	0.023	0.023	0.021	0.022	0.022
Co	0.001	0.001	0.001	0.001	0.001	0.001	0.002	0.002	0.001
Fe	0.811	0.810	0.814	0.816	0.808	0.814	0.810	0.812	0.818
Sb	0.000	0.000	0.000	0.000	0.000	0.000	0.000	0.000	0.000
Cd	0.000	0.000	0.000	0.000	0.000	0.000	0.000	0.000	0.000
Pb	0.000	0.000	0.000	0.000	0.000	0.000	0.000	0.000	0.000
S	1.000	1.000	1.000	1.000	1.000	1.000	1.000	1.000	1.000
As	0.000	0.000	0.000	0.000	0.000	0.000	0.000	0.000	0.000
Se	0.000	0.000	0.000	0.000	0.000	0.000	0.000	0.000	0.000
Ag	0.000	0.000	0.000	0.000	0.000	0.000	0.000	0.000	0.000
Au	0.000	0.000	0.000	0.000	0.000	0.000	0.000	0.000	0.000
Total	1.834	1.834	1.836	1.839	1.832	1.838	1.834	1.837	1.841

Table C3. EPMA results for pyrrhotite continued.

Deposit	Tilt Cove	Tilt Cove	Tilt Cove	Tilt Cove	Tilt Cove	Tilt Cove	Tilt Cove	Tilt Cove	Tilt Cove
Drill Hole	SZ-20-05	SZ-20-05	SZ-20-05	SZ-20-05	SZ-20-05	SZ-20-05	SZ-20-05	SZ-20-05	SZ-20-05
Sample	KKMSC70_Po10	KKMSC70_Po11	KKMSC70_Po12	KKMSC70_Po13	KKMSC70_Po14	KKMSC70_Po15	KKMSC72_Po1	KKMSC72_Po2	KKMSC72_Po3
Depth (m)	126.45	126.45	126.45	126.45	126.45	126.45	143.7	143.7	143.7
Date	2023_07_14	2023_07_14	2023_07_14	2023_07_14	2023_07_14	2023_07_14	2023_07_14	2023_07_14	2023_07_14
Facies	Chalcopyrite-pyrrhotite Dominated	Chalcopyrite-pyrrhotite Dominated	Chalcopyrite-pyrrhotite Dominated	Chalcopyrite-pyrrhotite Dominated	Chalcopyrite-pyrrhotite Dominated	Chalcopyrite-pyrrhotite Dominated	Pyrrhotite Dominated	Pyrrhotite Dominated	Pyrrhotite Dominated
Weight Percent (wt%)									
Zn	<0.01	<0.01	<0.01	<0.01	<0.01	<0.01	<0.01	<0.01	<0.01
Cu	0.02	0.01	<0.01	0.01	0.02	<0.01	<0.01	<0.01	<0.01
Ni	1.62	1.66	1.51	1.52	1.54	1.64	1.70	6.52	1.59
Co	0.08	0.09	0.09	0.25	0.09	0.07	0.09	2.33	0.10
Fe	57.57	58.26	56.99	57.42	57.76	57.41	57.47	50.07	57.74
Sb	<0.01	<0.01	<0.01	<0.01	<0.01	<0.01	<0.01	<0.01	<0.01
Cd	0.03	0.01	<0.01	0.01	<0.01	<0.01	<0.01	<0.01	<0.01
Pb	<0.02	<0.02	0.04	0.03	0.03	<0.02	0.04	0.04	0.04
S	40.82	41.59	39.96	40.83	40.66	40.63	40.67	41.12	40.67
As	<0.02	<0.02	<0.02	<0.02	<0.02	<0.02	<0.02	<0.02	<0.02
Se	<0.01	<0.01	0.03	0.04	<0.01	0.03	<0.01	0.03	<0.01
Ag	<0.01	<0.01	<0.01	<0.01	<0.01	<0.01	<0.01	<0.01	<0.01
Au	<0.02	<0.02	<0.02	<0.02	<0.02	<0.02	<0.02	<0.02	<0.02
Total	100.06	101.57	98.45	100.03	100.05	99.75	99.86	100.08	100.07
Atoms Per Formula Unit (apfu)									
Zn	0.000	0.000	0.000	0.000	0.000	0.000	0.000	0.000	0.000
Cu	0.000	0.000	0.000	0.000	0.000	0.000	0.000	0.000	0.000
Ni	0.022	0.022	0.021	0.020	0.021	0.022	0.023	0.087	0.021
Co	0.001	0.001	0.001	0.003	0.001	0.001	0.001	0.031	0.001
Fe	0.810	0.804	0.819	0.807	0.816	0.811	0.811	0.699	0.815
Sb	0.000	0.000	0.000	0.000	0.000	0.000	0.000	0.000	0.000
Cd	0.000	0.000	0.000	0.000	0.000	0.000	0.000	0.000	0.000
Pb	0.000	0.000	0.000	0.000	0.000	0.000	0.000	0.000	0.000
S	1.000	1.000	1.000	1.000	1.000	1.000	1.000	1.000	1.000
As	0.000	0.000	0.000	0.000	0.000	0.000	0.000	0.000	0.000
Se	0.000	0.000	0.000	0.000	0.000	0.000	0.000	0.000	0.000
Ag	0.000	0.000	0.000	0.000	0.000	0.000	0.000	0.000	0.000
Au	0.000	0.000	0.000	0.000	0.000	0.000	0.000	0.000	0.000
Total	1.833	1.827	1.841	1.832	1.838	1.835	1.836	1.817	1.838

Table C3. EPMA results for pyrrhotite continued.

Deposit	Tilt Cove	Tilt Cove	Tilt Cove	Tilt Cove	Tilt Cove	Tilt Cove	Tilt Cove	Tilt Cove	Tilt Cove
Drill Hole	SZ-20-05	SZ-20-05	SZ-20-05	SZ-20-05	SZ-20-05	SZ-20-05	SZ-20-05	SZ-20-05	SZ-20-05
Sample	KKMSC72_Po4	KKMSC72_Po5	KKMSC72_Po6	KKMSC72-Po7	KKMSC72-Po8	KKMSC72-Po9	KKMSC72-Po10	KKMSC72-Po11	KKMSC72-Po12
Depth (m)	143.7	143.7	143.7	143.7	143.7	143.7	143.7	143.7	143.7
Date	2023_07_14	2023_07_14	2023_07_14	2023_07_14	2023_07_14	2023_07_14	2023_07_14	2023_07_14	2023_07_14
Facies	Pyrrhotite Dominated	Pyrrhotite Dominated	Pyrrhotite Dominated	Pyrrhotite Dominated	Pyrrhotite Dominated	Pyrrhotite Dominated	Pyrrhotite Dominated	Pyrrhotite Dominated	Pyrrhotite Dominated
Weight Percent (wt%)									
Zn	<0.01	<0.01	<0.01	<0.01	<0.01	<0.01	<0.01	<0.01	<0.01
Cu	<0.01	<0.01	<0.01	<0.01	<0.01	<0.01	<0.01	<0.01	<0.01
Ni	1.74	1.72	1.55	1.59	1.66	1.70	1.61	1.65	1.73
Co	0.09	0.10	0.11	0.10	0.10	0.08	0.09	0.09	0.09
Fe	57.77	57.42	57.58	57.89	57.87	57.89	57.50	57.93	57.54
Sb	<0.01	<0.01	<0.01	<0.01	<0.01	<0.01	<0.01	<0.01	<0.01
Cd	0.02	0.01	0.01	0.01	<0.01	<0.01	<0.01	0.01	<0.01
Pb	0.04	0.03	0.03	<0.02	0.04	0.03	0.04	0.07	0.04
S	40.74	40.65	40.50	40.73	40.94	40.74	40.47	40.84	40.80
As	<0.02	<0.02	<0.02	<0.02	<0.02	<0.02	<0.02	<0.02	<0.02
Se	<0.01	0.02	<0.01	0.01	<0.01	0.01	0.03	<0.01	<0.01
Ag	<0.01	<0.01	<0.01	<0.01	<0.01	<0.01	<0.01	<0.01	<0.01
Au	<0.02	<0.02	<0.02	<0.02	<0.02	<0.02	<0.02	<0.02	<0.02
Total	100.25	99.91	99.72	100.29	100.60	100.41	99.71	100.49	100.15
Atoms Per Formula Unit (apfu)									
Zn	0.000	0.000	0.000	0.000	0.000	0.000	0.000	0.000	0.000
Cu	0.000	0.000	0.000	0.000	0.000	0.000	0.000	0.000	0.000
Ni	0.023	0.023	0.021	0.021	0.022	0.023	0.022	0.022	0.023
Co	0.001	0.001	0.001	0.001	0.001	0.001	0.001	0.001	0.001
Fe	0.814	0.811	0.816	0.816	0.812	0.816	0.816	0.814	0.810
Sb	0.000	0.000	0.000	0.000	0.000	0.000	0.000	0.000	0.000
Cd	0.000	0.000	0.000	0.000	0.000	0.000	0.000	0.000	0.000
Pb	0.000	0.000	0.000	0.000	0.000	0.000	0.000	0.000	0.000
S	1.000	1.000	1.000	1.000	1.000	1.000	1.000	1.000	1.000
As	0.000	0.000	0.000	0.000	0.000	0.000	0.000	0.000	0.000
Se	0.000	0.000	0.000	0.000	0.000	0.000	0.000	0.000	0.000
Ag	0.000	0.000	0.000	0.000	0.000	0.000	0.000	0.000	0.000
Au	0.000	0.000	0.000	0.000	0.000	0.000	0.000	0.000	0.000
Total	1.839	1.836	1.839	1.839	1.835	1.840	1.839	1.838	1.834

Table C3. EPMA results for pyrrhotite continued.

Deposit	Tilt Cove	Tilt Cove	Tilt Cove
Drill Hole	SZ-20-05	SZ-20-05	SZ-20-05
Sample	KKMSC72-Po13	KKMSC72-Po14	KKMSC72-Po15
Depth (m)	143.7	143.7	143.7
Date	2023_07_14	2023_07_14	2023_07_14
Facies	Pyrrhotite Dominated	Pyrrhotite Dominated	Pyrrhotite Dominated
Weight Percent (wt%)			
Zn	<0.01	<0.01	<0.01
Cu	<0.01	<0.01	<0.01
Ni	1.68	1.68	1.86
Co	0.09	0.08	0.09
Fe	57.75	57.71	57.42
Sb	<0.01	<0.01	<0.01
Cd	<0.01	<0.01	<0.01
Pb	<0.02	<0.02	<0.02
S	40.66	40.71	40.73
As	<0.02	<0.02	<0.02
Se	<0.01	<0.01	<0.01
Ag	<0.01	<0.01	<0.01
Au	<0.02	<0.02	<0.02
Total	100.11	100.19	100.01
Atoms Per Formula Unit (apfu)			
Zn	0.000	0.000	0.000
Cu	0.000	0.000	0.000
Ni	0.023	0.023	0.025
Co	0.001	0.001	0.001
Fe	0.816	0.814	0.809
Sb	0.000	0.000	0.000
Cd	0.000	0.000	0.000
Pb	0.000	0.000	0.000
S	1.000	1.000	1.000
As	0.000	0.000	0.000
Se	0.000	0.000	0.000
Ag	0.000	0.000	0.000
Au	0.000	0.000	0.000
Total	1.839	1.838	1.836

Table C4. EPMA results for sphalerite. Data in red was omitted in discussion due to results being outside of the total cut-off for EPMA or it is inconsistent with SEM and reflected light mineral ID.

Deposit	Betts Cove	Betts Cove	Betts Cove	Betts Cove	Betts Cove	Betts Cove	Betts Cove	Betts Cove	Betts Cove
Drill Hole	BC-21-01	BC-21-01	BC-21-01	BC-21-02	BC-21-02	BC-21-02	BC-21-02	BC-21-02	BC-21-02
Sample	KKMSC05B-Sp1	KKMSC05B-Sp2	KKMSC05B-Sp3	KKMSC09-Sp1	KKMSC09-Sp2	KKMSC10-Sp1	KKMSC10-Sp2	KKMSC10-Sp3	KKMSC10-Sp4
Depth (m)	115.5	115.5	115.5	85.4	85.4	99.5	99.5	99.5	99.5
Date	2023 06 23	2023 06 23	2023 06 23	2023 06 23	2023 06 23	2023 09 25	2023 09 25	2023 09 25	2023 09 25
Facies	Chalcopyrite Dominated	Chalcopyrite Dominated	Chalcopyrite Dominated	Chalcopyrite Dominated	Chalcopyrite Dominated	Pyrite Dominated	Pyrite Dominated	Pyrite Dominated	Pyrite Dominated
Weight Percent (wt%)									
Zn	60.15	60.65	60.38	58.82	55.07	61.89	61.22	61.01	62.61
Cu	0.4	0.32	0.47	0.05	0.55	<0.01	0.09	0.46	0.05
Ni	<0.01	<0.01	<0.01	<0.01	<0.01	<0.01	<0.01	<0.01	<0.01
Co	<0.01	<0.01	<0.01	0.12	0.13	0.01	<0.01	<0.01	<0.01
Fe	5.99	5.53	5.96	7.06	7.15	4.3	4.93	4.68	3.91
Sb	<0.01	<0.01	<0.01	<0.01	<0.01	<0.01	<0.01	<0.01	<0.01
Cd	0.17	0.23	0.19	0.28	0.35	0.14	0.13	0.13	0.15
Pb	<0.02	0.04	<0.02	0.03	0.23	0.06	0.07	0.08	0.06
S	33.23	33.11	33.09	33.07	32.11	32.99	32.87	32.9	32.79
As	<0.02	<0.02	<0.02	<0.02	<0.02	<0.02	<0.02	<0.02	<0.02
Se	0.07	0.02	0.03	0.03	0.03	<0.01	<0.01	0.03	0.03
Ag	0.01	<0.01	<0.01	<0.01	0.44	<0.01	<0.01	<0.01	0.01
Au	<0.03	<0.03	<0.03	<0.03	0.81	<0.02	<0.02	<0.02	<0.02
Total	99.94	99.83	100.06	99.34	96.82	99.33	99.19	99.18	99.53
Atoms Per Formula Unit (apfu)									
Zn	0.888	0.898	0.895	0.872	0.841	0.920	0.913	0.909	0.936
Cu	0.006	0.005	0.007	0.001	0.009	0.000	0.001	0.007	0.001
Ni	0.000	0.000	0.000	0.000	0.000	0.000	0.000	0.000	0.000
Co	0.000	0.000	0.000	0.002	0.002	0.000	0.000	0.000	0.000
Fe	0.104	0.096	0.103	0.123	0.128	0.075	0.086	0.082	0.068
Sb	0.000	0.000	0.000	0.000	0.000	0.000	0.000	0.000	0.000
Cd	0.001	0.002	0.002	0.002	0.003	0.001	0.001	0.001	0.001
Pb	0.000	0.000	0.000	0.000	0.001	0.000	0.000	0.000	0.000
S	1.000	1.000	1.000	1.000	1.000	1.000	1.000	1.000	1.000
As	0.000	0.000	0.000	0.000	0.000	0.000	0.000	0.000	0.000
Se	0.001	0.000	0.000	0.000	0.000	0.000	0.000	0.000	0.000
Ag	0.000	0.000	0.000	0.000	0.004	0.000	0.000	0.000	0.000
Au	0.000	0.000	0.000	0.000	0.004	0.000	0.000	0.000	0.000
Total	2.000	2.002	2.008	2.001	1.993	1.997	2.002	2.000	2.008

Table C4. EPMA results for sphalerite continued.

Deposit	Betts Cove	Betts Cove	Betts Cove	Betts Cove	Betts Cove	Betts Cove	Betts Cove	Betts Cove	Betts Cove
Drill Hole	BC-21-02	BC-21-02	BC-21-02	BC-21-02	BC-21-07	BC-21-07	BC-21-07	BC-21-07	BC-21-07
Sample	KKMSC10-Sp5	KKMSC10-Sp6	KKMSC10-Sp7	KKMSC10-Sp8	KKMSC29-Sp1	KKMSC29-Sp2	KKMSC29-Sp3	KKMSC29-Sp4	KKMSC29-Sp5
Depth (m)	99.5	99.5	99.5	99.5	107.6	107.6	107.6	107.6	107.6
Date	2023_09_25	2023_09_25	2023_09_25	2023_09_25	2023_06_27	2023_06_27	2023_06_27	2023_06_27	2023_06_27
Facies	Pyrite Dominated	Pyrite Dominated	Pyrite Dominated	Pyrite Dominated	Chalcopyrite Dominated	Chalcopyrite Dominated	Chalcopyrite Dominated	Chalcopyrite Dominated	Chalcopyrite Dominated
Weight Percent (wt%)									
Zn	61.62	61.03	62.15	61.62	57.21	56.84	57.28	57.1	57.61
Cu	0.02	<0.01	0.04	0.35	0.75	1.01	1.46	1	0.96
Ni	<0.01	<0.01	<0.01	<0.01	<0.01	<0.01	<0.01	<0.01	<0.01
Co	0.01	<0.01	0.02	<0.01	0.13	0.12	0.14	0.13	0.13
Fe	4.77	5.09	4.49	4.37	7.51	7.9	7.36	7.5	7.57
Sb	<0.01	<0.01	<0.01	<0.01	<0.01	<0.01	<0.01	<0.01	<0.01
Cd	0.14	0.15	0.16	0.14	0.27	0.23	0.31	0.26	0.23
Pb	0.05	0.06	0.09	0.07	<0.02	<0.02	0.06	0.05	0.06
S	33.17	32.74	33.01	32.84	32.81	32.91	33.14	32.76	32.71
As	<0.02	<0.02	<0.02	<0.02	<0.02	<0.02	<0.02	<0.02	<0.02
Se	<0.01	<0.01	<0.01	<0.01	0.14	0.16	0.12	0.13	0.14
Ag	<0.01	<0.01	0.01	<0.01	<0.01	<0.01	0.01	<0.01	<0.01
Au	<0.02	<0.02	<0.02	<0.02	<0.03	<0.02	<0.03	<0.02	<0.03
Total	99.75	98.97	99.77	99.35	98.77	99.13	99.79	98.82	99.32
Atoms Per Formula Unit (apfu)									
Zn	0.911	0.914	0.923	0.920	0.855	0.847	0.848	0.855	0.864
Cu	0.000	0.000	0.001	0.005	0.012	0.015	0.022	0.015	0.015
Ni	0.000	0.000	0.000	0.000	0.000	0.000	0.000	0.000	0.000
Co	0.000	0.000	0.000	0.000	0.002	0.002	0.002	0.002	0.002
Fe	0.083	0.089	0.078	0.076	0.131	0.138	0.128	0.131	0.133
Sb	0.000	0.000	0.000	0.000	0.000	0.000	0.000	0.000	0.000
Cd	0.001	0.001	0.001	0.001	0.002	0.002	0.003	0.002	0.002
Pb	0.000	0.000	0.000	0.000	0.000	0.000	0.000	0.000	0.000
S	1.000	1.000	1.000	1.000	1.000	1.000	1.000	1.000	1.000
As	0.000	0.000	0.000	0.000	0.000	0.000	0.000	0.000	0.000
Se	0.000	0.000	0.000	0.000	0.002	0.002	0.001	0.002	0.002
Ag	0.000	0.000	0.000	0.000	0.000	0.000	0.000	0.000	0.000
Au	0.000	0.000	0.000	0.000	0.000	0.000	0.000	0.000	0.000
Total	1.996	2.005	2.004	2.004	2.004	2.006	2.004	2.008	2.018

Table C4. EPMA results for sphalerite continued.

Deposit	Betts Cove	Betts Cove	Betts Cove	Betts Cove	Betts Cove	Betts Cove	Betts Cove	Betts Cove	Betts Cove
Drill Hole	BC-21-07	BC-21-07	BC-21-03	BC-21-03	BC-21-03	BC-21-03	BC-21-03	BC-21-03	BC-21-03
Sample	KKMSC29-Sp6	KKMSC29-Sp7	KKMSC32-Sp1	KKMSC32-Sp2	KKMSC32-Sp3	KKMSC32-Sp4	KKMSC32-Sp5	KKMSC32-Sp6	KKMSC32-Sp7
Depth (m)	107.6	107.6	88	88	88	88	88	88	88
Date	2023_06_27	2023_06_27	2023_06_27	2023_06_27	2023_06_27	2023_06_27	2023_06_27	2023_06_27	2023_06_27
Facies	Chalcopyrite Dominated	Chalcopyrite Dominated	Sphalerite-pyrite Dominated	Sphalerite-pyrite Dominated	Sphalerite-pyrite Dominated	Sphalerite-pyrite Dominated	Sphalerite-pyrite Dominated	Sphalerite-pyrite Dominated	Sphalerite-pyrite Dominated
Weight Percent (wt%)									
Zn	57.08	0.19	60.56	60.68	60.77	60.65	60.77	61.1	61.23
Cu	1.41	32.81	<0.01	<0.01	<0.01	<0.01	<0.01	<0.01	<0.01
Ni	0.01	<0.01	<0.01	<0.01	<0.01	<0.01	<0.01	<0.01	<0.01
Co	0.14	<0.01	<0.01	<0.01	<0.01	<0.01	<0.01	<0.01	<0.01
Fe	7.42	29.24	5.54	5.42	5.34	5.53	5.4	5.45	5.34
Sb	<0.01	<0.01	<0.01	<0.01	<0.01	<0.01	<0.01	<0.01	<0.01
Cd	0.28	<0.01	0.08	0.09	0.08	0.06	0.08	0.08	0.08
Pb	<0.02	0.44	<0.02	<0.02	<0.02	<0.02	<0.02	<0.02	0.05
S	33.08	33.76	33.23	32.72	33.03	32.97	32.92	32.93	33.09
As	<0.02	<0.02	<0.02	<0.02	<0.02	<0.02	<0.02	<0.02	<0.02
Se	0.15	0.35	<0.01	0.03	0.04	<0.01	<0.01	<0.01	<0.01
Ag	<0.01	0.02	<0.01	<0.01	<0.01	<0.01	<0.01	<0.01	<0.01
Au	<0.03	<0.03	<0.03	<0.03	<0.02	<0.03	<0.03	<0.03	<0.03
Total	99.48	96.71	99.32	98.78	99.20	99.15	99.05	99.38	99.71
Atoms Per Formula Unit (apfu)									
Zn	0.846	0.003	0.894	0.910	0.902	0.902	0.905	0.910	0.908
Cu	0.022	0.490	0.000	0.000	0.000	0.000	0.000	0.000	0.000
Ni	0.000	0.000	0.000	0.000	0.000	0.000	0.000	0.000	0.000
Co	0.002	0.000	0.000	0.000	0.000	0.000	0.000	0.000	0.000
Fe	0.129	0.497	0.096	0.095	0.093	0.096	0.094	0.095	0.093
Sb	0.000	0.000	0.000	0.000	0.000	0.000	0.000	0.000	0.000
Cd	0.002	0.000	0.001	0.001	0.001	0.001	0.001	0.001	0.001
Pb	0.000	0.002	0.000	0.000	0.000	0.000	0.000	0.000	0.000
S	1.000	1.000	1.000	1.000	1.000	1.000	1.000	1.000	1.000
As	0.000	0.000	0.000	0.000	0.000	0.000	0.000	0.000	0.000
Se	0.002	0.004	0.000	0.000	0.000	0.000	0.000	0.000	0.000
Ag	0.000	0.000	0.000	0.000	0.000	0.000	0.000	0.000	0.000
Au	0.000	0.000	0.000	0.000	0.000	0.000	0.000	0.000	0.000
Total	2.003	1.997	1.990	2.006	1.996	1.999	2.000	2.006	2.001

Table C4. EPMA results for sphalerite continued.

Deposit	Betts Cove	Betts Cove	Betts Cove	Betts Cove	Betts Cove	Betts Cove	Betts Cove	Betts Cove	Betts Cove
Drill Hole	BC-21-03	BC-21-03	BC-21-03	BC-21-03	BC-21-03	BC-21-03	BC-21-03	BC-21-03	BC-21-03
Sample	KKMSC32-Sp8	KKMSC32-Sp9	KKMSC32-Sp10	KKMSC32-Sp11	KKMSC32-Sp12	KKMSC32-Sp13	KKMSC32-Sp14	KKMSC32-Sp15	KKMSC32-Sp16
Depth (m)	88	88	88	88	88	88	88	88	88
Date	2023_06_27	2023_06_27	2023_06_27	2023_06_27	2023_06_27	2023_06_27	2023_06_27	2023_06_27	2023_06_27
Facies	Sphalerite-pyrite Dominated	Sphalerite-pyrite Dominated	Sphalerite-pyrite Dominated	Sphalerite-pyrite Dominated	Sphalerite-pyrite Dominated	Sphalerite-pyrite Dominated	Sphalerite-pyrite Dominated	Sphalerite-pyrite Dominated	Sphalerite-pyrite Dominated
Weight Percent (wt%)									
Zn	61.32	61.34	60.98	61.05	60.67	60.42	60.95	61.52	61.06
Cu	<0.01	<0.01	<0.01	<0.01	<0.01	<0.01	<0.01	0.05	<0.01
Ni	<0.01	<0.01	<0.01	<0.01	<0.01	<0.01	<0.01	<0.01	<0.01
Co	<0.01	<0.01	<0.01	<0.01	<0.01	<0.01	<0.01	<0.01	<0.01
Fe	5.2	5.26	5.37	5.31	5.67	5.63	5.66	5.05	5.49
Sb	<0.01	<0.01	<0.01	<0.01	<0.01	<0.01	<0.01	<0.01	<0.01
Cd	0.08	0.09	0.09	0.08	0.08	0.1	0.09	0.09	0.08
Pb	<0.02	<0.02	<0.02	0.03	0.03	<0.02	<0.02	0.05	<0.02
S	33.09	33	32.84	33.13	32.97	32.96	32.94	32.88	32.87
As	<0.02	<0.02	<0.02	<0.02	<0.02	<0.02	<0.02	<0.02	<0.02
Se	<0.01	<0.01	0.03	<0.01	0.01	<0.01	<0.01	<0.01	<0.01
Ag	<0.01	<0.01	<0.01	<0.01	<0.01	<0.01	<0.01	<0.01	<0.01
Au	<0.03	<0.03	<0.03	<0.03	<0.02	<0.03	<0.03	<0.03	<0.03
Total	99.59	99.60	99.18	99.45	99.38	99.00	99.42	99.51	99.39
Atoms Per Formula Unit (apfu)									
Zn	0.909	0.912	0.911	0.904	0.902	0.899	0.907	0.918	0.911
Cu	0.000	0.000	0.000	0.000	0.000	0.000	0.000	0.001	0.000
Ni	0.000	0.000	0.000	0.000	0.000	0.000	0.000	0.000	0.000
Co	0.000	0.000	0.000	0.000	0.000	0.000	0.000	0.000	0.000
Fe	0.090	0.092	0.094	0.092	0.099	0.098	0.099	0.088	0.096
Sb	0.000	0.000	0.000	0.000	0.000	0.000	0.000	0.000	0.000
Cd	0.001	0.001	0.001	0.001	0.001	0.001	0.001	0.001	0.001
Pb	0.000	0.000	0.000	0.000	0.000	0.000	0.000	0.000	0.000
S	1.000	1.000	1.000	1.000	1.000	1.000	1.000	1.000	1.000
As	0.000	0.000	0.000	0.000	0.000	0.000	0.000	0.000	0.000
Se	0.000	0.000	0.000	0.000	0.000	0.000	0.000	0.000	0.000
Ag	0.000	0.000	0.000	0.000	0.000	0.000	0.000	0.000	0.000
Au	0.000	0.000	0.000	0.000	0.000	0.000	0.000	0.000	0.000
Total	2.000	2.004	2.006	1.997	2.002	1.998	2.007	2.008	2.008

Table C4. EPMA results for sphalerite continued.

Deposit	Betts Cove	Betts Cove	Betts Cove	Betts Cove	Betts Cove	Betts Cove	Betts Cove	Betts Cove	Betts Cove
Drill Hole	BC-21-03	BC-21-03	BC-21-03	BC-21-03	BC-21-03	BC-21-03	BC-21-03	BC-21-03	BC-21-03
Sample	KKMSC32-Sp17	KKMSC32-Sp18	KKMSC32-Sp19	KKMSC32-Sp20	KKMSC32-Sp21	KKMSC32-Sp22	KKMSC32-Sp23	KKMSC32-Sp24	KKMSC32-Sp25
Depth (m)	88	88	88	88	88	88	88	88	88
Date	2023_06_27	2023_06_27	2023_06_27	2023_06_27	2023_06_27	2023_06_27	2023_06_27	2023_06_27	2023_06_27
Facies	Sphalerite-pyrite Dominated	Sphalerite-pyrite Dominated	Sphalerite-pyrite Dominated	Sphalerite-pyrite Dominated	Sphalerite-pyrite Dominated	Sphalerite-pyrite Dominated	Sphalerite-pyrite Dominated	Sphalerite-pyrite Dominated	Sphalerite-pyrite Dominated
Weight Percent (wt%)									
Zn	60.61	60.47	59.3	60.91	61.01	61.47	60.77	61.3	60.96
Cu	<0.01	<0.01	0.11	<0.01	0.03	<0.01	<0.01	0.02	<0.01
Ni	<0.01	<0.01	<0.01	<0.01	<0.01	<0.01	<0.01	<0.01	<0.01
Co	<0.01	<0.01	<0.01	<0.01	<0.01	<0.01	<0.01	<0.01	<0.01
Fe	5.66	5.79	5.49	5.47	5.64	5.24	5.64	5.26	5.59
Sb	<0.01	<0.01	<0.02	<0.01	<0.01	<0.01	<0.01	<0.01	<0.01
Cd	0.08	0.08	0.09	0.09	0.09	0.09	0.09	0.09	0.08
Pb	<0.02	<0.02	<0.02	<0.02	<0.02	<0.02	<0.02	<0.02	<0.02
S	32.97	32.77	32.14	33.16	32.91	32.94	32.97	32.69	33.12
As	<0.02	<0.02	<0.03	<0.02	<0.02	<0.02	<0.02	<0.02	<0.02
Se	<0.01	<0.01	<0.01	<0.01	0.03	<0.01	<0.01	<0.01	<0.01
Ag	<0.01	<0.01	<0.01	<0.01	0.01	<0.01	<0.01	<0.01	<0.01
Au	<0.02	<0.03	<0.03	<0.03	<0.03	<0.02	<0.02	<0.03	<0.03
Total	99.25	99.00	96.30	99.51	99.66	99.67	99.39	99.25	99.68
Atoms Per Formula Unit (apfu)									
Zn	0.902	0.905	0.905	0.901	0.909	0.915	0.904	0.920	0.903
Cu	0.000	0.000	0.002	0.000	0.000	0.000	0.000	0.000	0.000
Ni	0.000	0.000	0.000	0.000	0.000	0.000	0.000	0.000	0.000
Co	0.000	0.000	0.000	0.000	0.000	0.000	0.000	0.000	0.000
Fe	0.099	0.101	0.098	0.095	0.098	0.091	0.098	0.092	0.097
Sb	0.000	0.000	0.000	0.000	0.000	0.000	0.000	0.000	0.000
Cd	0.001	0.001	0.001	0.001	0.001	0.001	0.001	0.001	0.001
Pb	0.000	0.000	0.000	0.000	0.000	0.000	0.000	0.000	0.000
S	1.000	1.000	1.000	1.000	1.000	1.000	1.000	1.000	1.000
As	0.000	0.000	0.000	0.000	0.000	0.000	0.000	0.000	0.000
Se	0.000	0.000	0.000	0.000	0.000	0.000	0.000	0.000	0.000
Ag	0.000	0.000	0.000	0.000	0.000	0.000	0.000	0.000	0.000
Au	0.000	0.000	0.000	0.000	0.000	0.000	0.000	0.000	0.000
Total	2.001	2.007	2.005	1.996	2.009	2.007	2.003	2.013	2.000

Table C4. EPMA results for sphalerite continued.

Deposit	Betts Cove	Betts Cove	Betts Cove	Betts Cove	Betts Cove	Betts Cove	Betts Cove	Betts Cove	Betts Cove
Drill Hole	BC-21-03	BC-21-03	BC-21-03	BC-21-03	BC-21-03	BC-21-03	BC-21-03	BC-21-03	BC-21-03
Sample	KKMSC32-Sp26	KKMSC32-Sp27	KKMSC32-Sp28	KKMSC32-Sp29	KKMSC32-Sp30	KKMSC32-Sp31	KKMSC32-Sp32	KKMSC32-Sp33	KKMSC32-Sp34
Depth (m)	88	88	88	88	88	88	88	88	88
Date	2023 06 27	2023 06 27	2023 06 27	2023 06 27	2023 06 27	2023 06 27	2023 06 27	2023 06 27	2023 06 27
Facies	Sphalerite-pyrite Dominated	Sphalerite-pyrite Dominated	Sphalerite-pyrite Dominated	Sphalerite-pyrite Dominated	Sphalerite-pyrite Dominated	Sphalerite-pyrite Dominated	Sphalerite-pyrite Dominated	Sphalerite-pyrite Dominated	Sphalerite-pyrite Dominated
Weight Percent (wt%)									
Zn	60.11	60.75	60.86	61.02	60.52	60.58	60.99	60.6	61.11
Cu	<0.01	<0.01	0.22	<0.01	0.03	<0.01	0.19	<0.01	<0.01
Ni	<0.01	<0.01	<0.01	<0.01	<0.01	<0.01	<0.01	<0.01	<0.01
Co	0.02	0.02	<0.01	0.03	0.02	0.01	0.02	0.01	0.01
Fe	5.9	5.62	5.68	5.15	5.54	5.79	5.1	5.78	5.56
Sb	<0.01	<0.01	<0.01	<0.01	<0.01	<0.01	<0.01	<0.01	<0.01
Cd	0.08	0.09	0.09	0.1	0.08	0.09	0.07	0.08	0.11
Pb	<0.02	<0.02	<0.02	0.03	<0.02	<0.02	0.03	<0.02	<0.02
S	32.7	32.93	32.97	32.94	32.96	32.93	32.98	32.89	33.03
As	<0.02	<0.02	<0.02	<0.02	<0.02	<0.02	<0.02	<0.02	<0.02
Se	<0.01	<0.01	<0.01	<0.01	0.01	<0.01	<0.01	<0.01	<0.01
Ag	<0.01	<0.01	<0.01	<0.01	<0.01	<0.01	<0.01	<0.01	<0.01
Au	<0.02	<0.02	<0.03	<0.02	<0.03	<0.03	<0.02	<0.03	<0.02
Total	98.79	99.36	99.69	99.17	99.12	99.30	99.35	99.27	99.77
Atoms Per Formula Unit (apfu)									
Zn	0.902	0.905	0.905	0.909	0.901	0.902	0.907	0.904	0.907
Cu	0.000	0.000	0.003	0.000	0.000	0.000	0.003	0.000	0.000
Ni	0.000	0.000	0.000	0.000	0.000	0.000	0.000	0.000	0.000
Co	0.000	0.000	0.000	0.000	0.000	0.000	0.000	0.000	0.000
Fe	0.104	0.098	0.099	0.090	0.097	0.101	0.089	0.101	0.097
Sb	0.000	0.000	0.000	0.000	0.000	0.000	0.000	0.000	0.000
Cd	0.001	0.001	0.001	0.001	0.001	0.001	0.001	0.001	0.001
Pb	0.000	0.000	0.000	0.000	0.000	0.000	0.000	0.000	0.000
S	1.000	1.000	1.000	1.000	1.000	1.000	1.000	1.000	1.000
As	0.000	0.000	0.000	0.000	0.000	0.000	0.000	0.000	0.000
Se	0.000	0.000	0.000	0.000	0.000	0.000	0.000	0.000	0.000
Ag	0.000	0.000	0.000	0.000	0.000	0.000	0.000	0.000	0.000
Au	0.000	0.000	0.000	0.000	0.000	0.000	0.000	0.000	0.000
Total	2.006	2.004	2.008	2.000	1.999	2.004	2.000	2.005	2.005

Table C4. EPMA results for sphalerite continued.

Deposit	Betts Cove	Betts Cove	Betts Cove	Betts Cove	Betts Cove	Betts Cove	Betts Cove	Betts Cove	Betts Cove
Drill Hole	BC-21-03	BC-21-03	BC-21-03	BC-21-05	BC-21-05	BC-21-05	BC-21-05	BC-21-06	BC-21-06
Sample	KKMSC32-Sp35	KKMSC32-Sp36	KKMSC32-Sp37	KKMSC35-Sp1	KKMSC35-Sp2	KKMSC35-Sp3	KKMSC35-Sp4	KKMSC42-Sp1	KKMSC42-Sp2
Depth (m)	88	88	88	116.9	116.9	116.9	116.9	106.3	106.3
Date	2023 06 27	2023 06 27	2023 06 27	2023 06 29	2023 06 29	2023 06 29	2023 06 29	2023 07 18	2023 07 18
Facies	Sphalerite-pyrite Dominated	Sphalerite-pyrite Dominated	Sphalerite-pyrite Dominated	Chalcopyrite-pyrrhotite Dominated	Chalcopyrite-pyrrhotite Dominated	Chalcopyrite-pyrrhotite Dominated	Chalcopyrite-pyrrhotite Dominated	Chalcopyrite-pyrrhotite Dominated	Chalcopyrite-pyrrhotite Dominated
Weight Percent (wt%)									
Zn	61.45	60.9	61.06	58.45	58.03	58.41	58	57.51	58.13
Cu	0.01	<0.01	0.05	0.07	0.03	0.06	0.05	0.26	<0.01
Ni	<0.01	<0.01	<0.01	<0.01	<0.01	<0.01	<0.01	<0.01	<0.01
Co	<0.01	<0.01	<0.01	0.06	0.04	0.04	0.05	0.06	0.05
Fe	5.44	5.73	5.32	7.82	8.01	7.48	8.01	8.03	7.82
Sb	<0.01	<0.01	<0.01	<0.01	<0.01	<0.01	<0.01	<0.01	<0.01
Cd	0.1	0.1	0.12	0.55	0.51	0.56	0.54	0.24	0.22
Pb	<0.02	<0.02	<0.02	0.08	0.06	0.09	0.05	0.06	0.1
S	32.89	32.99	33.03	33.78	33.9	34.02	33.79	33.09	33.43
As	<0.02	<0.02	<0.02	<0.02	<0.02	<0.02	<0.02	<0.02	<0.02
Se	0.01	<0.01	<0.01	0.02	0.05	0.04	0.05	0.05	0.08
Ag	<0.01	<0.01	<0.01	<0.01	<0.01	<0.01	<0.01	<0.01	0.01
Au	<0.03	<0.03	<0.02	<0.03	<0.02	<0.03	<0.02	<0.02	<0.02
Total	99.84	99.56	99.51	100.72	100.57	100.51	100.50	99.26	99.77
Atoms Per Formula Unit (apfu)									
Zn	0.916	0.905	0.907	0.849	0.840	0.842	0.842	0.852	0.853
Cu	0.000	0.000	0.001	0.001	0.000	0.001	0.001	0.004	0.000
Ni	0.000	0.000	0.000	0.000	0.000	0.000	0.000	0.000	0.000
Co	0.000	0.000	0.000	0.001	0.001	0.001	0.001	0.001	0.001
Fe	0.095	0.100	0.092	0.133	0.136	0.126	0.136	0.139	0.134
Sb	0.000	0.000	0.000	0.000	0.000	0.000	0.000	0.000	0.000
Cd	0.001	0.001	0.001	0.005	0.004	0.005	0.005	0.002	0.002
Pb	0.000	0.000	0.000	0.000	0.000	0.000	0.000	0.000	0.000
S	1.000	1.000	1.000	1.000	1.000	1.000	1.000	1.000	1.000
As	0.000	0.000	0.000	0.000	0.000	0.000	0.000	0.000	0.000
Se	0.000	0.000	0.000	0.000	0.001	0.000	0.001	0.001	0.001
Ag	0.000	0.000	0.000	0.000	0.000	0.000	0.000	0.000	0.000
Au	0.000	0.000	0.000	0.000	0.000	0.000	0.000	0.000	0.000
Total	2.012	2.006	2.001	1.989	1.981	1.975	1.985	2.000	1.991

Table C4. EPMA results for sphalerite continued.

Deposit	Betts Cove	Betts Cove	Betts Cove	Betts Cove	Betts Cove	Betts Cove	Betts Cove	Betts Cove	Betts Cove
Drill Hole	BC-21-06	BC-21-06	BC-21-06	BC-21-06	BC-21-06	BC-21-06	BC-21-08	BC-21-08	BC-21-08
Sample	KKMSC42-Sp3	KKMSC42-Sp4	KKMSC42-Sp5	KKMSC42-Sp6	KKMSC42-Sp7	KKMSC42-Sp8	KKMSC53-Sp1	KKMSC53-Sp2	KKMSC53-Sp3
Depth (m)	106.3	106.3	106.3	106.3	106.3	106.3	28.7	28.7	28.7
Date	2023_07_18	2023_07_18	2023_07_18	2023_07_18	2023_07_18	2023_07_18	2023_07_19	2023_07_19	2023_07_19
Facies	Chalcopyrite-pyrrhotite Dominated	Chalcopyrite-pyrrhotite Dominated	Chalcopyrite-pyrrhotite Dominated	Chalcopyrite-pyrrhotite Dominated	Chalcopyrite-pyrrhotite Dominated	Chalcopyrite-pyrrhotite Dominated	Chalcopyrite Dominated	Chalcopyrite Dominated	Chalcopyrite Dominated
Weight Percent (wt%)									
Zn	58.17	57.82	57.58	57.54	57.1	56.9	58.19	58.17	58.25
Cu	0.09	<0.01	0.14	0.09	0.07	<0.01	0.03	<0.01	0.06
Ni	<0.01	<0.01	<0.01	<0.01	<0.01	<0.01	<0.01	<0.01	<0.01
Co	0.07	0.06	0.05	0.06	0.05	0.05	0.13	0.11	0.11
Fe	7.55	7.79	7.8	7.85	7.82	9.11	7.61	7.66	7.73
Sb	<0.01	<0.01	<0.01	<0.01	<0.01	<0.01	<0.01	<0.01	<0.01
Cd	0.23	0.23	0.23	0.24	0.24	0.22	0.33	0.35	0.34
Pb	0.09	0.09	0.08	0.08	0.08	0.09	0.09	0.13	0.07
S	33.27	33.1	33.21	33.22	33.37	33.29	33.06	33.08	33.39
As	<0.02	<0.02	<0.02	<0.02	<0.02	<0.02	<0.02	<0.02	<0.02
Se	0.04	0.08	0.08	0.06	0.1	0.1	0.07	0.07	0.07
Ag	<0.01	0.01	<0.01	<0.01	<0.01	<0.01	<0.01	<0.01	<0.01
Au	<0.02	<0.02	<0.02	<0.02	<0.02	<0.02	<0.02	<0.02	<0.02
Total	99.45	99.10	99.12	99.04	98.78	99.69	99.44	99.49	99.98
Atoms Per Formula Unit (apfu)									
Zn	0.857	0.857	0.850	0.849	0.839	0.838	0.863	0.862	0.856
Cu	0.001	0.000	0.002	0.001	0.001	0.000	0.000	0.000	0.001
Ni	0.000	0.000	0.000	0.000	0.000	0.000	0.000	0.000	0.000
Co	0.001	0.001	0.001	0.001	0.001	0.001	0.002	0.002	0.002
Fe	0.130	0.135	0.135	0.136	0.135	0.157	0.132	0.133	0.133
Sb	0.000	0.000	0.000	0.000	0.000	0.000	0.000	0.000	0.000
Cd	0.002	0.002	0.002	0.002	0.002	0.002	0.003	0.003	0.003
Pb	0.000	0.000	0.000	0.000	0.000	0.000	0.000	0.001	0.000
S	1.000	1.000	1.000	1.000	1.000	1.000	1.000	1.000	1.000
As	0.000	0.000	0.000	0.000	0.000	0.000	0.000	0.000	0.000
Se	0.000	0.001	0.001	0.001	0.001	0.001	0.001	0.001	0.001
Ag	0.000	0.000	0.000	0.000	0.000	0.000	0.000	0.000	0.000
Au	0.000	0.000	0.000	0.000	0.000	0.000	0.000	0.000	0.000
Total	1.993	1.996	1.991	1.991	1.979	2.000	2.002	2.002	1.995

Table C4. EPMA results for sphalerite continued.

Deposit	Tilt Cove	Tilt Cove	Tilt Cove	Tilt Cove	Tilt Cove	Tilt Cove	Tilt Cove	Tilt Cove	Tilt Cove
Drill Hole	SZ-20-01	SZ-20-01	SZ-20-01	SZ-20-01	SZ-20-01	SZ-20-01	SZ-20-04	SZ-20-04	SZ-20-04
Sample	KKMSC13-Sp1	KKMSC13-Sp2	KKMSC13-Sp3	KKMSC13-Sp4	KKMSC13-Sp5	KKMSC13-Sp6	KKMSC63-Sp1	KKMSC63-Sp2	KKMSC63-Sp3
Depth (m)	66.6	66.6	66.6	66.6	66.6	66.6	64.45	64.45	64.45
Date	2023_07_18	2023_07_18	2023_07_18	2023_07_18	2023_07_18	2023_07_18	2023_06_30	2023_06_30	2023_06_30
Facies	Pyrite Dominated	Pyrite Dominated	Pyrite Dominated	Pyrite Dominated	Pyrite Dominated	Pyrite Dominated	Pyrite Dominated	Pyrite Dominated	Pyrite Dominated
Weight Percent (wt%)									
Zn	57.21	55.26	54.73	57.44	60.76	60.77	61.76	62.29	62.17
Cu	1.1	<0.01	0.09	<0.01	0.03	0.14	0.2	0.14	0.1
Ni	<0.01	<0.01	<0.01	<0.01	<0.01	<0.01	<0.01	<0.01	<0.01
Co	<0.01	0.01	0.01	<0.01	<0.01	0.01	0.03	0.06	0.06
Fe	7.81	10.45	10.78	8.48	5.8	5.6	3.36	4.37	4.61
Sb	<0.01	<0.01	<0.01	<0.01	<0.01	<0.01	<0.01	<0.01	<0.01
Cd	0.1	0.09	0.12	0.09	0.12	0.12	0.38	0.29	0.26
Pb	0.11	0.08	0.14	0.06	0.07	0.1	0.09	0.1	0.1
S	33.55	33.37	33.6	32.91	32.98	32.92	33.67	33.72	33.61
As	<0.02	<0.02	<0.02	<0.02	<0.02	<0.02	<0.02	<0.02	<0.02
Se	<0.01	<0.01	<0.01	<0.01	<0.01	<0.01	<0.01	0.01	0.01
Ag	<0.01	<0.01	<0.01	<0.01	<0.01	<0.01	<0.01	<0.01	<0.01
Au	<0.02	<0.02	<0.02	<0.02	<0.02	<0.02	<0.03	<0.03	<0.03
Total	99.81	99.19	99.35	98.91	99.69	99.57	99.34	100.90	100.86
Atoms Per Formula Unit (apfu)									
Zn	0.836	0.812	0.799	0.856	0.904	0.905	0.900	0.906	0.907
Cu	0.017	0.000	0.001	0.000	0.000	0.002	0.003	0.002	0.002
Ni	0.000	0.000	0.000	0.000	0.000	0.000	0.000	0.000	0.000
Co	0.000	0.000	0.000	0.000	0.000	0.000	0.000	0.001	0.001
Fe	0.134	0.180	0.184	0.148	0.101	0.098	0.057	0.074	0.079
Sb	0.000	0.000	0.000	0.000	0.000	0.000	0.000	0.000	0.000
Cd	0.001	0.001	0.001	0.001	0.001	0.001	0.003	0.002	0.002
Pb	0.001	0.000	0.001	0.000	0.000	0.000	0.000	0.000	0.000
S	1.000	1.000	1.000	1.000	1.000	1.000	1.000	1.000	1.000
As	0.000	0.000	0.000	0.000	0.000	0.000	0.000	0.000	0.000
Se	0.000	0.000	0.000	0.000	0.000	0.000	0.000	0.000	0.000
Ag	0.000	0.000	0.000	0.000	0.000	0.000	0.000	0.000	0.000
Au	0.000	0.000	0.000	0.000	0.000	0.000	0.000	0.000	0.000
Total	1.988	1.993	1.986	2.005	2.006	2.007	1.964	1.986	1.991

Table C4. EPMA results for sphalerite continued.

Deposit	Tilt Cove	Tilt Cove	Tilt Cove	Tilt Cove	Tilt Cove
Drill Hole	SZ-20-04	SZ-20-05	SZ-20-05	SZ-20-05	SZ-20-05
Sample	KKMSC63-Sp4	KKMSC72_Sp1	KKMSC72_Sp2	KKMSC72_Sp3	KKMSC72_Sp4
Depth (m)	64.45	143.7	143.7	143.7	143.7
Date	2023_06_30	2023_07_14	2023_07_14	2023_07_14	2023_07_14
Facies	Pyrite Dominated	Pyrrhotite Dominated	Pyrrhotite Dominated	Pyrrhotite Dominated	Pyrrhotite Dominated
Weight Percent (wt%)					
Zn	62.04	58.67	59.42	57.67	58.85
Cu	0.26	0.07	0.08	0.06	0.29
Ni	<0.01	0.23	<0.01	0.05	<0.01
Co	0.06	0.42	0.17	0.26	0.21
Fe	4.71	6.71	6.05	7.43	6.28
Sb	<0.01	<0.01	<0.01	<0.01	<0.01
Cd	0.28	0.46	0.47	0.47	0.39
Pb	0.09	0.05	0.06	0.08	0.08
S	33.75	33.23	33.13	33.08	33.15
As	<0.02	<0.02	<0.02	<0.02	<0.02
Se	0.02	<0.01	<0.01	0.01	<0.01
Ag	<0.01	<0.01	0.01	<0.01	<0.01
Au	<0.03	<0.02	<0.02	<0.02	<0.02
Total	101.07	99.75	99.34	99.03	99.11
Atoms Per Formula Unit (apfu)					
Zn	0.902	0.866	0.880	0.855	0.871
Cu	0.004	0.001	0.001	0.001	0.004
Ni	0.000	0.004	0.000	0.001	0.000
Co	0.001	0.007	0.003	0.004	0.003
Fe	0.080	0.116	0.105	0.129	0.109
Sb	0.000	0.000	0.000	0.000	0.000
Cd	0.002	0.004	0.004	0.004	0.003
Pb	0.000	0.000	0.000	0.000	0.000
S	1.000	1.000	1.000	1.000	1.000
As	0.000	0.000	0.000	0.000	0.000
Se	0.000	0.000	0.000	0.000	0.000
Ag	0.000	0.000	0.000	0.000	0.000
Au	0.000	0.000	0.000	0.000	0.000
Total	1.990	1.998	1.993	1.995	1.991

Table C5. EPMA results for cobaltite. Data in red was omitted in discussion due to results being outside of the total cut-off for EPMA or it is inconsistent with SEM and reflected light mineral ID.

Deposit	Betts Cove	Betts Cove	Betts Cove	Betts Cove	Betts Cove	Betts Cove	Betts Cove	Betts Cove	Betts Cove
Drill Hole	BC-21-02	BC-21-02	BC-21-02	BC-21-02	BC-21-02	BC-21-02	BC-21-02	BC-21-02	BC-21-02
Sample	KKMSC09-Cob1	KKMSC09-Cob2	KKMSC09-Cob3	KKMSC09-Cob4	KKMSC09-Cob5	KKMSC09-Cob6	KKMSC09-Cob7	KKMSC09-Cob8	KKMSC09-Cob9
Depth (m)	85.4	85.4	85.4	85.4	85.4	85.4	85.4	85.4	85.4
Date	2023 06 23	2023 06 23	2023 06 23	2023 06 23	2023 06 23	2023 06 23	2023 06 23	2023 06 23	2023 06 23
Facies	Chalcopyrite Dominated	Chalcopyrite Dominated	Chalcopyrite Dominated	Chalcopyrite Dominated	Chalcopyrite Dominated	Chalcopyrite Dominated	Chalcopyrite Dominated	Chalcopyrite Dominated	Chalcopyrite Dominated
Weight Percent (wt%)									
Zn	0.05	<0.01	<0.01	<0.01	<0.01	<0.01	<0.01	<0.01	<0.01
Cu	2.21	1.29	0.93	0.92	0.84	2.6	0.74	1.16	11.35
Ni	0.3	0.15	0.14	0.33	0.19	0.43	0.18	0.25	0.28
Co	29.62	24.26	30.96	30.83	30.97	27.04	31.06	29.74	13.49
Fe	6.72	14.06	6.12	5.84	5.73	8.79	5.89	6.89	12.08
Sb	<0.01	<0.01	<0.01	<0.01	<0.01	<0.01	<0.01	<0.01	<0.01
Cd	<0.01	<0.01	<0.01	<0.01	<0.01	<0.01	<0.01	<0.01	0.01
Pb	0.03	0.05	0.04	<0.02	0.06	<0.02	<0.02	0.09	0.04
S	23.59	31.99	23.3	22.75	22.74	27.51	23.4	22.86	22.82
As	38.68	32.72	39.61	40.1	39.37	36.14	39.66	38.79	19.69
Se	<0.02	0.1	0.06	0.03	0.02	0.13	0.04	<0.02	0.05
Ag	0.01	<0.01	<0.01	<0.01	<0.01	<0.01	<0.01	0.01	0.04
Au	<0.03	<0.02	<0.03	<0.02	<0.02	<0.03	<0.02	<0.03	<0.02
Total	101.11	104.59	101.14	100.76	99.86	102.58	100.88	99.69	79.85
Atoms Per Formula Unit (apfu)									
Zn	0.001	0.000	0.000	0.000	0.000	0.000	0.000	0.000	0.000
Cu	0.047	0.020	0.020	0.020	0.019	0.048	0.016	0.026	0.251
Ni	0.007	0.003	0.003	0.008	0.005	0.009	0.004	0.006	0.007
Co	0.683	0.413	0.723	0.737	0.741	0.535	0.722	0.708	0.322
Fe	0.164	0.252	0.151	0.147	0.145	0.183	0.145	0.173	0.304
Sb	0.000	0.000	0.000	0.000	0.000	0.000	0.000	0.000	0.000
Cd	0.000	0.000	0.000	0.000	0.000	0.000	0.000	0.000	0.000
Pb	0.000	0.000	0.000	0.000	0.000	0.000	0.000	0.001	0.000
S	1.000	1.000	1.000	1.000	1.000	1.000	1.000	1.000	1.000
As	0.702	0.438	0.728	0.754	0.741	0.562	0.725	0.726	0.369
Se	0.000	0.001	0.001	0.001	0.000	0.002	0.001	0.000	0.001
Ag	0.000	0.000	0.000	0.000	0.000	0.000	0.000	0.000	0.001
Au	0.000	0.000	0.000	0.000	0.000	0.000	0.000	0.000	0.000
Total	2.604	2.127	2.626	2.668	2.651	2.339	2.613	2.639	2.254

Table C5. EPMA results for cobaltite continued.

Deposit	Betts Cove	Betts Cove	Betts Cove	Betts Cove	Betts Cove	Betts Cove	Betts Cove	Betts Cove	Betts Cove
Drill Hole	BC-21-02	BC-21-02	BC-21-02	BC-21-02	BC-21-02	BC-21-02	BC-21-02	BC-21-02	BC-21-02
Sample	KKMSC09-Cob10	KKMSC09-Cob11	KKMSC09-Cob12	KKMSC09-Cob13	KKMSC09-Cob14	KKMSC09-Cob15	KKMSC09-Cob16	KKMSC09-Cob17	KKMSC09-Cob18
Depth (m)	85.4	85.4	85.4	85.4	85.4	85.4	85.4	85.4	85.4
Date	2023 06 23	2023 06 23	2023 06 23	2023 06 23	2023 06 23	2023 06 23	2023 06 23	2023 06 23	2023 06 23
Facies	Chalcopyrite Dominated	Chalcopyrite Dominated	Chalcopyrite Dominated	Chalcopyrite Dominated	Chalcopyrite Dominated	Chalcopyrite Dominated	Chalcopyrite Dominated	Chalcopyrite Dominated	Chalcopyrite Dominated
Weight Percent (wt%)									
Zn	0.02	<0.01	<0.01	0.02	<0.01	0.01	0.06	<0.01	<0.01
Cu	0.18	0.4	1.01	1.87	0.94	0.77	0.99	0.28	0.63
Ni	0.25	0.3	0.12	0.32	0.22	0.24	0.24	0.39	0.4
Co	12.6	30.89	30.6	30.49	31.64	31.19	30.77	31.33	28.61
Fe	14.93	5.66	7.05	5.98	5.44	5.9	6.32	5.62	8.97
Sb	<0.01	<0.01	<0.01	<0.01	<0.01	<0.01	<0.01	<0.01	<0.01
Cd	<0.01	<0.01	<0.01	0.01	<0.01	<0.01	<0.01	<0.01	<0.01
Pb	0.04	<0.02	<0.02	0.03	0.04	0.04	0.04	<0.02	0.03
S	14.58	23.03	24.34	23.3	22.99	23.43	23.36	22.51	27.21
As	15.49	40.27	38.06	40.46	40.67	39.41	39.39	40.22	36.6
Se	0.11	0.02	0.1	<0.02	<0.02	0.07	<0.02	0.04	0.11
Ag	<0.01	0.01	<0.01	<0.01	<0.01	0.01	<0.01	<0.01	<0.01
Au	<0.02	<0.02	<0.02	<0.03	<0.02	<0.03	<0.03	<0.03	<0.03
Total	58.17	100.55	101.22	102.42	101.92	101.03	101.09	100.33	102.44
Atoms Per Formula Unit (apfu)									
Zn	0.001	0.000	0.000	0.000	0.000	0.000	0.001	0.000	0.000
Cu	0.006	0.009	0.021	0.040	0.021	0.017	0.021	0.006	0.012
Ni	0.009	0.007	0.003	0.008	0.005	0.006	0.006	0.009	0.008
Co	0.470	0.730	0.684	0.712	0.749	0.724	0.717	0.757	0.572
Fe	0.588	0.141	0.166	0.147	0.136	0.145	0.155	0.143	0.189
Sb	0.000	0.000	0.000	0.000	0.000	0.000	0.000	0.000	0.000
Cd	0.000	0.000	0.000	0.000	0.000	0.000	0.000	0.000	0.000
Pb	0.000	0.000	0.000	0.000	0.000	0.000	0.000	0.000	0.000
S	1.000	1.000	1.000	1.000	1.000	1.000	1.000	1.000	1.000
As	0.455	0.748	0.669	0.743	0.757	0.720	0.722	0.765	0.576
Se	0.003	0.000	0.002	0.000	0.000	0.001	0.000	0.001	0.002
Ag	0.000	0.000	0.000	0.000	0.000	0.000	0.000	0.000	0.000
Au	0.000	0.000	0.000	0.000	0.000	0.000	0.000	0.000	0.000
Total	2.533	2.636	2.545	2.651	2.668	2.613	2.622	2.682	2.359

Table C5. EPMA results for cobaltite continued.

Deposit	Betts Cove	Betts Cove	Betts Cove	Betts Cove	Betts Cove	Betts Cove	Betts Cove	Betts Cove	Betts Cove
Drill Hole	BC-21-02	BC-21-02	BC-21-02	BC-21-02	BC-21-02	BC-21-02	BC-21-02	BC-21-02	BC-21-02
Sample	KKMSC09-Cob19	KKMSC09-Cob20	KKMSC09-Cob21	KKMSC09-Cob22	KKMSC09-Cob23	KKMSC09-Cob24	KKMSC09-Cob25	KKMSC09-Cob26	KKMSC09-Cob27
Depth (m)	85.4	85.4	85.4	85.4	85.4	85.4	85.4	85.4	85.4
Date	2023_06_23	2023_06_23	2023_06_23	2023_06_23	2023_06_23	2023_06_23	2023_06_23	2023_06_23	2023_06_23
Facies	Chalcopyrite Dominated	Chalcopyrite Dominated	Chalcopyrite Dominated	Chalcopyrite Dominated	Chalcopyrite Dominated	Chalcopyrite Dominated	Chalcopyrite Dominated	Chalcopyrite Dominated	Chalcopyrite Dominated
Weight Percent (wt%)									
Zn	0.03	<0.01	<0.01	<0.01	<0.01	<0.01	<0.01	<0.01	<0.01
Cu	21.33	0.14	0.65	0.64	1.24	1.15	0.99	1.21	0.75
Ni	0.31	0.62	0.19	0.26	0.19	0.4	0.29	0.22	0.27
Co	12.01	28.11	31.31	30.93	31.34	30.84	30.12	30.72	31.32
Fe	19.67	8.07	5.79	5.84	5.68	5.56	6.83	6.04	5.32
Sb	<0.01	<0.01	<0.01	<0.01	<0.01	<0.01	<0.01	<0.01	<0.01
Cd	0.01	<0.01	<0.01	<0.01	<0.01	<0.01	<0.01	<0.01	<0.01
Pb	0.05	0.1	<0.02	0.05	0.04	<0.02	<0.02	<0.02	<0.02
S	30.38	27.78	23.2	22.93	22.92	22.62	25.15	23.34	22.59
As	20.01	35.4	39.59	40.71	40.29	40.6	39.09	40.14	39.2
Se	0.1	0.18	0.05	0.06	0.08	<0.02	0.05	0.03	0.02
Ag	0.06	0.02	<0.01	<0.01	<0.01	<0.01	0.01	<0.01	<0.01
Au	<0.02	<0.03	<0.03	<0.02	<0.03	<0.03	<0.02	<0.02	<0.02
Total	103.94	100.35	100.69	101.34	101.66	101.08	102.47	101.66	99.45
Atoms Per Formula Unit (apfu)									
Zn	0.000	0.000	0.000	0.000	0.000	0.000	0.000	0.000	0.000
Cu	0.354	0.003	0.014	0.014	0.027	0.026	0.020	0.026	0.017
Ni	0.006	0.012	0.004	0.006	0.005	0.010	0.006	0.005	0.007
Co	0.215	0.551	0.734	0.734	0.744	0.742	0.652	0.716	0.754
Fe	0.372	0.167	0.143	0.146	0.142	0.141	0.156	0.149	0.135
Sb	0.000	0.000	0.000	0.000	0.000	0.000	0.000	0.000	0.000
Cd	0.000	0.000	0.000	0.000	0.000	0.000	0.000	0.000	0.000
Pb	0.000	0.001	0.000	0.000	0.000	0.000	0.000	0.000	0.000
S	1.000	1.000	1.000	1.000	1.000	1.000	1.000	1.000	1.000
As	0.282	0.545	0.730	0.760	0.752	0.768	0.665	0.736	0.743
Se	0.001	0.003	0.001	0.001	0.001	0.000	0.001	0.001	0.000
Ag	0.001	0.000	0.000	0.000	0.000	0.000	0.000	0.000	0.000
Au	0.000	0.000	0.000	0.000	0.000	0.000	0.000	0.000	0.000
Total	2.231	2.281	2.627	2.662	2.672	2.686	2.500	2.633	2.656

Table C5. EPMA results for cobaltite continued.

Deposit	Betts Cove	Betts Cove	Betts Cove	Betts Cove	Betts Cove	Betts Cove	Betts Cove	Tilt Cove	Tilt Cove
Drill Hole	BC-21-02	BC-21-02	BC-21-02	BC-21-02	BC-21-02	BC-21-02	BC-21-02	SZ-20-01	SZ-20-01
Sample	KKMSC09-Cob28	KKMSC09-Cob29	KKMSC09-Cob30	KKMSC09-Cob31	KKMSC09-Cob32	KKMSC09-Cob33	KKMSC09-Cob34	KKMSC12-Cob1	KKMSC12-Cob2
Depth (m)	85.4	85.4	85.4	85.4	85.4	85.4	85.4	38.7	38.7
Date	2023_06_23	2023_06_23	2023_06_23	2023_06_23	2023_06_23	2023_06_23	2023_06_23	2023_06_29	2023_06_29
Facies	Chalcopyrite Dominated	Chalcopyrite Dominated	Chalcopyrite Dominated	Chalcopyrite Dominated	Chalcopyrite Dominated	Chalcopyrite Dominated	Chalcopyrite Dominated	Chalcopyrite Dominated	Chalcopyrite Dominated
Weight Percent (wt%)									
Zn	0.02	0.06	<0.01	<0.01	0.16	<0.01	<0.01	<0.01	<0.01
Cu	1.03	0.27	0.23	1.25	0.82	1.38	0.22	0.21	0.04
Ni	0.39	0.2	0.19	0.38	0.15	0.18	0.15	0.26	0.04
Co	31.02	31.06	30.92	30.7	30.38	30.54	30.97	31.68	33.06
Fe	5.6	6.04	6.24	5.88	6.87	6.54	5.99	5.88	4.96
Sb	<0.01	<0.01	<0.01	<0.01	<0.01	<0.01	<0.01	<0.01	<0.01
Cd	<0.01	<0.01	<0.01	<0.01	<0.01	<0.01	<0.01	<0.01	<0.01
Pb	<0.02	0.05	<0.02	<0.02	0.04	<0.02	<0.02	0.03	0.07
S	22.6	22.87	23.14	22.91	23.72	23.45	22.85	24.46	24.52
As	40.23	39.54	39.18	39.53	39.41	38.66	39.04	38.85	38.41
Se	<0.02	0.04	0.05	0.05	0.1	0.1	<0.02	<0.02	<0.02
Ag	<0.01	<0.01	<0.01	<0.01	<0.01	<0.01	<0.01	<0.01	<0.01
Au	<0.03	<0.03	<0.02	<0.03	<0.03	<0.03	<0.03	<0.03	<0.02
Total	100.78	99.96	99.87	100.57	101.57	100.75	99.18	101.27	100.98
Atoms Per Formula Unit (apfu)									
Zn	0.000	0.001	0.000	0.000	0.003	0.000	0.000	0.000	0.000
Cu	0.023	0.006	0.005	0.028	0.017	0.030	0.005	0.004	0.001
Ni	0.009	0.005	0.004	0.009	0.003	0.004	0.004	0.006	0.001
Co	0.747	0.739	0.727	0.729	0.697	0.709	0.737	0.705	0.734
Fe	0.142	0.152	0.155	0.147	0.166	0.160	0.151	0.138	0.116
Sb	0.000	0.000	0.000	0.000	0.000	0.000	0.000	0.000	0.000
Cd	0.000	0.000	0.000	0.000	0.000	0.000	0.000	0.000	0.000
Pb	0.000	0.000	0.000	0.000	0.000	0.000	0.000	0.000	0.000
S	1.000	1.000	1.000	1.000	1.000	1.000	1.000	1.000	1.000
As	0.762	0.740	0.725	0.738	0.711	0.706	0.731	0.680	0.670
Se	0.000	0.001	0.001	0.001	0.002	0.002	0.000	0.000	0.000
Ag	0.000	0.000	0.000	0.000	0.000	0.000	0.000	0.000	0.000
Au	0.000	0.000	0.000	0.000	0.000	0.000	0.000	0.000	0.000
Total	2.684	2.644	2.617	2.652	2.600	2.610	2.628	2.533	2.522

Table C5. EPMA results for cobaltite continued.

Deposit	Tilt Cove	Tilt Cove	Tilt Cove	Tilt Cove	Tilt Cove	Tilt Cove	Tilt Cove	Tilt Cove	Tilt Cove
Drill Hole	SZ-20-01	SZ-20-01	SZ-20-01	SZ-20-01	SZ-20-01	SZ-20-01	SZ-20-01	SZ-20-01	SZ-20-01
Sample	KKMSC12-Cob3	KKMSC12-Cob4	KKMSC12-Cob5	KKMSC12-Cob6	KKMSC12-Cob7	KKMSC12-Cob8	KKMSC12-Cob9	KKMSC12-Cob10	KKMSC12-Cob11
Depth (m)	38.7	38.7	38.7	38.7	38.7	38.7	38.7	38.7	38.7
Date	2023 06 29	2023 06 29	2023 06 29	2023 06 29	2023 06 29	2023 06 29	2023 06 29	2023 06 29	2023 06 29
Facies	Chalcopyrite Dominated	Chalcopyrite Dominated	Chalcopyrite Dominated	Chalcopyrite Dominated	Chalcopyrite Dominated	Chalcopyrite Dominated	Chalcopyrite Dominated	Chalcopyrite Dominated	Chalcopyrite Dominated
Weight Percent (wt%)									
Zn	<0.01	<0.01	<0.01	<0.01	<0.01	<0.01	<0.01	<0.01	<0.01
Cu	0.06	0.04	<0.01	0.08	0.04	0.09	0.04	0.07	3.4
Ni	0.04	<0.02	0.08	<0.01	0.04	<0.02	<0.02	<0.02	23.44
Co	33.18	33.96	31.87	33.52	33.37	32.86	33.89	33.47	4.14
Fe	4.66	3.58	5.34	4.82	4.59	5.35	4.29	4.64	8.44
Sb	<0.01	<0.01	<0.01	<0.01	<0.01	<0.01	<0.01	<0.01	<0.01
Cd	<0.01	<0.01	<0.01	<0.01	<0.01	<0.01	<0.01	<0.01	<0.01
Pb	0.07	0.07	0.06	0.04	0.05	0.05	0.05	0.05	0.05
S	23.67	22.69	23.44	25.79	24.13	25.47	25.13	24.44	20.67
As	39.44	40.69	39.56	36.46	38.39	37.18	37.23	38.46	44.4
Se	<0.02	<0.02	<0.02	<0.02	<0.02	<0.02	0.03	<0.02	<0.02
Ag	<0.01	<0.01	<0.01	<0.01	<0.01	<0.01	<0.01	<0.01	<0.01
Au	<0.03	<0.02	<0.03	<0.02	<0.02	<0.03	<0.02	<0.03	<0.03
Total	101.03	100.93	100.15	100.62	100.56	100.85	100.58	101.01	104.39
Atoms Per Formula Unit (apfu)									
Zn	0.000	0.000	0.000	0.000	0.000	0.000	0.000	0.000	0.000
Cu	0.001	0.001	0.000	0.002	0.001	0.002	0.001	0.001	0.083
Ni	0.001	0.000	0.002	0.000	0.001	0.000	0.000	0.000	0.620
Co	0.763	0.814	0.740	0.707	0.752	0.702	0.734	0.745	0.109
Fe	0.113	0.091	0.131	0.107	0.109	0.121	0.098	0.109	0.234
Sb	0.000	0.000	0.000	0.000	0.000	0.000	0.000	0.000	0.000
Cd	0.000	0.000	0.000	0.000	0.000	0.000	0.000	0.000	0.000
Pb	0.000	0.000	0.000	0.000	0.000	0.000	0.000	0.000	0.000
S	1.000	1.000	1.000	1.000	1.000	1.000	1.000	1.000	1.000
As	0.713	0.767	0.722	0.605	0.681	0.625	0.634	0.673	0.919
Se	0.000	0.000	0.000	0.000	0.000	0.000	0.000	0.000	0.000
Ag	0.000	0.000	0.000	0.000	0.000	0.000	0.000	0.000	0.000
Au	0.000	0.000	0.000	0.000	0.000	0.000	0.000	0.000	0.000
Total	2.592	2.674	2.595	2.421	2.545	2.449	2.467	2.529	2.966

Table C5. EPMA results for cobaltite continued.

Deposit	Tilt Cove	Tilt Cove	Tilt Cove	Tilt Cove	Tilt Cove	Tilt Cove	Tilt Cove	Tilt Cove	Tilt Cove
Drill Hole	SZ-20-01	SZ-20-01	SZ-20-01	SZ-20-01	SZ-20-01	SZ-20-01	SZ-20-01	SZ-20-01	SZ-20-01
Sample	KKMSC12-Cob12	KKMSC12-Cob13	KKMSC12-Cob14	KKMSC12-Cob15	KKMSC12-Cob16	KKMSC12-Cob17	KKMSC12-Cob18	KKMSC12-Cob19	KKMSC12-Cob20
Depth (m)	38.7	38.7	38.7	38.7	38.7	38.7	38.7	38.7	38.7
Date	2023 06 29	2023 06 29	2023 06 29	2023 06 29	2023 06 29	2023 06 29	2023 06 29	2023 06 29	2023 06 29
Facies	Chalcopyrite Dominated	Chalcopyrite Dominated	Chalcopyrite Dominated	Chalcopyrite Dominated	Chalcopyrite Dominated	Chalcopyrite Dominated	Chalcopyrite Dominated	Chalcopyrite Dominated	Chalcopyrite Dominated
Weight Percent (wt%)									
Zn	<0.01	<0.01	<0.01	<0.01	<0.01	0.01	<0.01	<0.01	<0.01
Cu	<0.01	0.15	<0.01	<0.01	<0.01	<0.01	0.01	<0.01	1.2
Ni	0.02	<0.01	0.03	0.18	3.45	<0.01	<0.01	<0.01	<0.01
Co	33.44	32.75	32.84	32.21	27.41	32.48	32.59	32.34	32.44
Fe	4.74	5.5	4.95	5.01	5.03	5.46	4.37	5.4	4.34
Sb	<0.01	<0.01	<0.01	<0.01	<0.01	<0.01	<0.02	<0.01	<0.01
Cd	<0.01	<0.01	<0.01	<0.01	<0.01	<0.01	<0.01	<0.01	<0.01
Pb	0.06	0.08	0.05	0.04	0.09	0.03	0.03	0.05	0.07
S	24.64	25.78	24.45	23.8	20.96	25.78	24.3	25.67	23.47
As	38.31	36.98	38.65	39.38	43.1	36.32	38.47	35.97	40.01
Se	<0.02	<0.02	<0.02	<0.02	<0.02	<0.02	<0.02	0.04	<0.02
Ag	<0.01	<0.01	<0.01	<0.01	<0.01	<0.01	<0.01	<0.01	<0.01
Au	<0.02	<0.02	<0.03	<0.02	<0.03	<0.02	<0.03	<0.02	<0.03
Total	101.17	101.07	100.80	100.51	99.79	99.86	99.45	99.37	101.34
Atoms Per Formula Unit (apfu)									
Zn	0.000	0.000	0.000	0.000	0.000	0.000	0.000	0.000	0.000
Cu	0.000	0.003	0.000	0.000	0.000	0.000	0.000	0.000	0.026
Ni	0.000	0.000	0.001	0.004	0.090	0.000	0.000	0.000	0.000
Co	0.738	0.691	0.731	0.736	0.712	0.685	0.730	0.685	0.752
Fe	0.110	0.122	0.116	0.121	0.138	0.122	0.103	0.121	0.106
Sb	0.000	0.000	0.000	0.000	0.000	0.000	0.000	0.000	0.000
Cd	0.000	0.000	0.000	0.000	0.000	0.000	0.000	0.000	0.000
Pb	0.000	0.000	0.000	0.000	0.001	0.000	0.000	0.000	0.000
S	1.000	1.000	1.000	1.000	1.000	1.000	1.000	1.000	1.000
As	0.665	0.614	0.677	0.708	0.880	0.603	0.678	0.600	0.730
Se	0.000	0.000	0.000	0.000	0.000	0.000	0.000	0.001	0.000
Ag	0.000	0.000	0.000	0.000	0.000	0.000	0.000	0.000	0.000
Au	0.000	0.000	0.000	0.000	0.000	0.000	0.000	0.000	0.000
Total	2.515	2.431	2.525	2.570	2.820	2.410	2.511	2.407	2.614

Table C5. EPMA results for cobaltite continued.

Deposit	Tilt Cove	Tilt Cove	Tilt Cove	Tilt Cove	Tilt Cove	Tilt Cove	Tilt Cove	Tilt Cove	Tilt Cove
Drill Hole	SZ-20-01	SZ-20-01	SZ-20-01	SZ-20-01	SZ-20-01	SZ-20-01	SZ-20-01	SZ-20-01	SZ-20-01
Sample	KKMSC12-Cob21	KKMSC12-Cob22	KKMSC12-Cob23	KKMSC12-Cob24	KKMSC12-Cob25	KKMSC12-Cob26	KKMSC12-Cob27	KKMSC12-Cob28	KKMSC12-Cob29
Depth (m)	38.7	38.7	38.7	38.7	38.7	38.7	38.7	38.7	38.7
Date	2023_06_29	2023_06_29	2023_06_29	2023_06_29	2023_06_29	2023_06_29	2023_06_29	2023_06_29	2023_06_29
Facies	Chalcopyrite Dominated	Chalcopyrite Dominated	Chalcopyrite Dominated	Chalcopyrite Dominated	Chalcopyrite Dominated	Chalcopyrite Dominated	Chalcopyrite Dominated	Chalcopyrite Dominated	Chalcopyrite Dominated
Weight Percent (wt%)									
Zn	0.02	0.01	<0.01	<0.01	<0.01	<0.01	0.02	<0.01	<0.01
Cu	0.19	0.48	0.36	0.52	0.97	0.69	27.08	0.14	0.08
Ni	<0.01	<0.01	<0.01	1.09	0.5	0.34	0.5	0.08	1.2
Co	32.58	32.98	32.77	31.63	30.94	31.61	5.47	31.6	18.81
Fe	4.95	3.78	4.51	3.64	5.22	4.99	25.77	5.67	10.65
Sb	<0.01	<0.01	<0.01	<0.01	<0.01	<0.01	<0.01	<0.01	<0.01
Cd	<0.01	0.01	<0.01	<0.01	<0.01	<0.01	<0.01	<0.01	<0.01
Pb	0.07	0.09	0.04	0.05	0.09	0.06	0.12	0.06	0.06
S	24.65	22.7	23.39	21.29	22.98	23.73	29.47	24.7	13.26
As	37.41	40.44	39.32	42.1	38.62	38.58	14.93	38.17	19.8
Se	<0.02	<0.02	<0.02	<0.02	<0.02	<0.02	<0.01	<0.02	<0.01
Ag	<0.01	<0.01	<0.01	<0.01	<0.01	0.01	0.06	<0.01	<0.01
Au	<0.02	<0.03	<0.03	<0.03	<0.02	<0.02	<0.02	<0.02	<0.02
Total	99.74	100.35	100.25	100.11	99.15	99.91	103.38	100.34	63.75
Atoms Per Formula Unit (apfu)									
Zn	0.000	0.000	0.000	0.000	0.000	0.000	0.000	0.000	0.000
Cu	0.004	0.011	0.008	0.012	0.021	0.015	0.464	0.003	0.003
Ni	0.000	0.000	0.000	0.028	0.012	0.008	0.009	0.002	0.049
Co	0.719	0.790	0.762	0.808	0.733	0.725	0.101	0.696	0.772
Fe	0.115	0.096	0.111	0.098	0.130	0.121	0.502	0.132	0.461
Sb	0.000	0.000	0.000	0.000	0.000	0.000	0.000	0.000	0.000
Cd	0.000	0.000	0.000	0.000	0.000	0.000	0.000	0.000	0.000
Pb	0.000	0.001	0.000	0.000	0.001	0.000	0.001	0.000	0.001
S	1.000	1.000	1.000	1.000	1.000	1.000	1.000	1.000	1.000
As	0.650	0.762	0.719	0.846	0.719	0.696	0.217	0.661	0.639
Se	0.000	0.000	0.000	0.000	0.000	0.000	0.000	0.000	0.000
Ag	0.000	0.000	0.000	0.000	0.000	0.000	0.001	0.000	0.000
Au	0.000	0.000	0.000	0.000	0.000	0.000	0.000	0.000	0.000
Total	2.489	2.660	2.600	2.793	2.616	2.564	2.294	2.494	2.925

Table C5. EPMA results for cobaltite continued.

Deposit	Tilt Cove	Tilt Cove	Tilt Cove	Tilt Cove	Tilt Cove	Tilt Cove	Tilt Cove	Tilt Cove	Tilt Cove
Drill Hole	SZ-20-01	SZ-20-01	SZ-20-01	SZ-20-01	SZ-20-01	SZ-20-01	SZ-20-01	SZ-20-01	SZ-20-01
Sample	KKMSC12-Cob30	KKMSC12-Cob31	KKMSC12-Cob32	KKMSC12-Cob33	KKMSC12-Cob34	KKMSC12-Cob35	KKMSC12-Cob36	KKMSC12-Cob37	KKMSC12-Cob38
Depth (m)	38.7	38.7	38.7	38.7	38.7	38.7	38.7	38.7	38.7
Date	2023_06_29	2023_06_29	2023_06_29	2023_06_29	2023_06_29	2023_06_29	2023_06_29	2023_06_29	2023_06_29
Facies	Chalcopyrite Dominated	Chalcopyrite Dominated	Chalcopyrite Dominated	Chalcopyrite Dominated	Chalcopyrite Dominated	Chalcopyrite Dominated	Chalcopyrite Dominated	Chalcopyrite Dominated	Chalcopyrite Dominated
Weight Percent (wt%)									
Zn	<0.01	<0.01	0.02	<0.01	<0.01	<0.01	<0.01	0.01	<0.01
Cu	0.08	0.12	5.89	0.23	0.01	0.28	0.71	11.47	1.39
Ni	0.08	1.58	2.25	1.94	<0.01	0.03	1.59	3.2	3.57
Co	32.7	31.02	23.71	29.96	32.8	33.65	30.15	16.83	26.24
Fe	4.25	3.67	9.02	4.5	5.01	3.3	4.55	14.63	6.34
Sb	<0.01	<0.01	<0.01	<0.01	<0.01	<0.01	<0.01	<0.01	<0.01
Cd	<0.01	<0.01	<0.01	<0.01	<0.01	<0.01	<0.01	0.01	<0.01
Pb	0.05	0.06	0.04	0.07	0.06	0.06	0.07	0.09	0.06
S	23.74	21.6	23.65	21.74	25	22.83	21.02	24.69	21.56
As	38.81	41.73	37.97	42.27	37.3	40.68	41.83	24.03	42.26
Se	<0.02	<0.02	<0.02	<0.02	<0.02	<0.02	<0.02	<0.01	<0.02
Ag	<0.01	<0.01	<0.01	<0.01	<0.01	<0.01	<0.01	<0.01	<0.01
Au	<0.02	<0.02	<0.03	<0.03	<0.03	<0.03	<0.03	<0.03	<0.02
Total	99.58	99.65	102.46	100.39	99.92	100.57	99.66	94.78	101.16
Atoms Per Formula Unit (apfu)									
Zn	0.000	0.000	0.000	0.000	0.000	0.000	0.000	0.000	0.000
Cu	0.002	0.003	0.126	0.005	0.000	0.006	0.017	0.234	0.033
Ni	0.002	0.040	0.052	0.049	0.000	0.001	0.041	0.071	0.090
Co	0.749	0.781	0.545	0.750	0.714	0.802	0.780	0.371	0.662
Fe	0.103	0.098	0.219	0.119	0.115	0.083	0.124	0.340	0.169
Sb	0.000	0.000	0.000	0.000	0.000	0.000	0.000	0.000	0.000
Cd	0.000	0.000	0.000	0.000	0.000	0.000	0.000	0.000	0.000
Pb	0.000	0.000	0.000	0.000	0.000	0.000	0.001	0.001	0.000
S	1.000	1.000	1.000	1.000	1.000	1.000	1.000	1.000	1.000
As	0.700	0.827	0.687	0.832	0.639	0.763	0.852	0.417	0.839
Se	0.000	0.000	0.000	0.000	0.000	0.000	0.000	0.000	0.000
Ag	0.000	0.000	0.000	0.000	0.000	0.000	0.000	0.000	0.000
Au	0.000	0.000	0.000	0.000	0.000	0.000	0.000	0.000	0.000
Total	2.556	2.749	2.630	2.755	2.468	2.655	2.815	2.434	2.793

Table C5. EPMA results for cobaltite continued.

Deposit	Tilt Cove	Tilt Cove	Tilt Cove	Tilt Cove	Tilt Cove	Tilt Cove	Tilt Cove	Tilt Cove	Tilt Cove
Drill Hole	SZ-20-01	SZ-20-01	SZ-20-01	SZ-20-01	SZ-20-01	SZ-20-01	SZ-20-01	SZ-20-01	SZ-20-01
Sample	KKMSC12-Cob39	KKMSC12-Cob40	KKMSC12-Cob41	KKMSC12-Cob42	KKMSC12-Cob43	KKMSC12-Cob44	KKMSC12-Cob45	KKMSC12-Cob46	KKMSC12-Cob47
Depth (m)	38.7	38.7	38.7	38.7	38.7	38.7	38.7	38.7	38.7
Date	2023 06 29	2023 06 29	2023 06 29	2023 06 29	2023 06 29	2023 06 29	2023 06 29	2023 06 29	2023 06 29
Facies	Chalcopyrite Dominated	Chalcopyrite Dominated	Chalcopyrite Dominated	Chalcopyrite Dominated	Chalcopyrite Dominated	Chalcopyrite Dominated	Chalcopyrite Dominated	Chalcopyrite Dominated	Chalcopyrite Dominated
Weight Percent (wt%)									
Zn	0.05	<0.01	0.01	<0.01	<0.01	<0.01	<0.01	<0.01	<0.01
Cu	23.71	5.61	20.6	1.75	6.19	0.08	0.17	0.25	0.21
Ni	0.16	2.42	1.38	0.13	4.42	0.16	0.02	<0.01	<0.01
Co	0.83	23.95	10.91	31.6	19.99	32.52	33.1	32.86	32.32
Fe	27.06	8.35	20.36	4.96	10.79	3.78	3.64	4.83	5.35
Sb	<0.01	<0.01	<0.01	<0.01	<0.01	<0.01	<0.01	<0.01	<0.01
Cd	<0.01	<0.01	<0.01	<0.01	<0.01	<0.01	<0.01	<0.01	<0.01
Pb	0.05	0.06	0.09	0.05	0.1	0.05	0.08	0.05	0.08
S	21.56	22.87	26.74	23.27	23.31	22.64	22.9	25.04	25.15
As	<0.14	37.68	20.89	39.61	35.87	41.04	40.34	37.12	37.28
Se	<0.01	<0.02	<0.01	0.02	<0.02	<0.02	<0.02	<0.02	<0.02
Ag	0.06	<0.01	<0.01	<0.01	<0.01	0.01	<0.01	0.02	<0.01
Au	<0.02	<0.03	<0.03	<0.02	<0.03	<0.02	<0.03	<0.03	<0.03
Total	64.43	100.85	100.82	101.34	100.54	100.12	100.08	100.11	100.24
Atoms Per Formula Unit (apfu)									
Zn	0.001	0.000	0.000	0.000	0.000	0.000	0.000	0.000	0.000
Cu	0.555	0.124	0.389	0.038	0.134	0.002	0.004	0.005	0.004
Ni	0.004	0.058	0.028	0.003	0.104	0.004	0.000	0.000	0.000
Co	0.021	0.570	0.222	0.739	0.467	0.782	0.786	0.714	0.699
Fe	0.721	0.210	0.437	0.122	0.266	0.096	0.091	0.111	0.122
Sb	0.000	0.000	0.000	0.000	0.000	0.000	0.000	0.000	0.000
Cd	0.000	0.000	0.000	0.000	0.000	0.000	0.000	0.000	0.000
Pb	0.000	0.000	0.001	0.000	0.001	0.000	0.001	0.000	0.000
S	1.000	1.000	1.000	1.000	1.000	1.000	1.000	1.000	1.000
As	0.000	0.705	0.334	0.729	0.659	0.776	0.754	0.634	0.634
Se	0.000	0.000	0.000	0.000	0.000	0.000	0.000	0.000	0.000
Ag	0.001	0.000	0.000	0.000	0.000	0.000	0.000	0.000	0.000
Au	0.000	0.000	0.000	0.000	0.000	0.000	0.000	0.000	0.000
Total	2.303	2.667	2.411	2.631	2.629	2.659	2.636	2.465	2.460

Table C5. EPMA results for cobaltite continued.

Deposit	Tilt Cove	Tilt Cove	Tilt Cove	Tilt Cove	Tilt Cove	Tilt Cove	Tilt Cove	Tilt Cove	Tilt Cove
Drill Hole	SZ-20-01	SZ-20-01	SZ-20-01	SZ-20-04	SZ-20-04	SZ-20-04	SZ-20-04	SZ-20-04	SZ-20-04
Sample	KKMSC12-Cob48	KKMSC12-Cob49	KKMSC12-Cob50	KKMSC63-Cob1	KKMSC63-Cob2	KKMSC63-Cob3	KKMSC63-Cob4	KKMSC63-Cob5	KKMSC63-Cob6
Depth (m)	38.7	38.7	38.7	64.45	64.45	64.45	64.45	64.45	64.45
Date	2023 06 29	2023 06 29	2023 06 29	2023 06 29	2023 06 29	2023 06 29	2023 06 29	2023 06 29	2023 06 29
Facies	Chalcopyrite Dominated	Chalcopyrite Dominated	Chalcopyrite Dominated	Pyrite Dominated	Pyrite Dominated	Pyrite Dominated	Pyrite Dominated	Pyrite Dominated	Pyrite Dominated
Weight Percent (wt%)									
Zn	<0.01	<0.01	<0.01	<0.01	<0.01	<0.01	<0.01	<0.01	<0.01
Cu	0.02	0.02	<0.01	0.96	0.62	0.74	0.63	1.23	19.03
Ni	0.12	0.13	<0.01	0.14	0.16	0.08	0.28	0.15	0.1
Co	31.17	32.25	29.06	31.84	32.21	31.08	31.99	31.58	1.89
Fe	5.63	3.8	4.26	6.13	6.28	7.94	5.48	5.95	34.05
Sb	<0.01	<0.01	<0.01	<0.01	<0.01	<0.01	<0.01	<0.01	<0.01
Cd	<0.01	<0.01	<0.01	<0.01	<0.01	<0.01	<0.01	<0.01	0.01
Pb	0.09	0.05	0.03	0.07	0.03	0.05	0.06	0.03	0.07
S	24.8	22.74	23.24	24.45	24.18	25.59	23.57	24.23	21.37
As	37.36	40.7	34.53	38.32	38.14	36.6	39.53	38.76	<0.08
Se	<0.02	<0.02	<0.02	<0.02	<0.02	<0.02	<0.02	<0.02	<0.01
Ag	<0.01	<0.01	<0.01	<0.01	<0.01	<0.01	<0.01	<0.01	<0.01
Au	<0.02	<0.02	<0.02	<0.03	<0.02	<0.02	<0.02	<0.02	<0.02
Total	99.08	99.49	90.96	101.81	101.52	102.00	101.36	101.74	75.63
Atoms Per Formula Unit (apfu)									
Zn	0.000	0.000	0.000	0.000	0.000	0.000	0.000	0.000	0.000
Cu	0.000	0.000	0.000	0.020	0.013	0.015	0.013	0.026	0.449
Ni	0.003	0.003	0.000	0.003	0.004	0.002	0.006	0.003	0.003
Co	0.684	0.772	0.680	0.709	0.725	0.661	0.738	0.709	0.048
Fe	0.130	0.096	0.105	0.144	0.149	0.178	0.133	0.141	0.915
Sb	0.000	0.000	0.000	0.000	0.000	0.000	0.000	0.000	0.000
Cd	0.000	0.000	0.000	0.000	0.000	0.000	0.000	0.000	0.000
Pb	0.001	0.000	0.000	0.000	0.000	0.000	0.000	0.000	0.001
S	1.000	1.000	1.000	1.000	1.000	1.000	1.000	1.000	1.000
As	0.645	0.766	0.636	0.671	0.675	0.612	0.718	0.685	0.000
Se	0.000	0.000	0.000	0.000	0.000	0.000	0.000	0.000	0.000
Ag	0.000	0.000	0.000	0.000	0.000	0.000	0.000	0.000	0.000
Au	0.000	0.000	0.000	0.000	0.000	0.000	0.000	0.000	0.000
Total	2.463	2.637	2.422	2.547	2.566	2.468	2.610	2.564	2.416

Table C5. EPMA results for cobaltite continued.

Deposit	Tilt Cove	Tilt Cove	Tilt Cove	Tilt Cove	Tilt Cove	Tilt Cove	Tilt Cove	Tilt Cove	Tilt Cove
Drill Hole	SZ-20-04	SZ-20-04	SZ-20-04	SZ-20-04	SZ-20-04	SZ-20-04	SZ-20-04	SZ-20-04	SZ-20-05
Sample	KKMSC63-Cob7	KKMSC63-Cob8	KKMSC63-Cob9	KKMSC63-Cob10	KKMSC63-Cob11	KKMSC63-Cob12	KKMSC63-Cob13	KKMSC63-Cob14	KKMSC70-Cob1
Depth (m)	64.45	64.45	64.45	64.45	64.45	64.45	64.45	64.45	126.45
Date	2023 06 29	2023 06 29	2023 06 29	2023 06 29	2023 06 29	2023 06 29	2023 06 29	2023 06 29	2023 07 14
Facies	Pyrite Dominated	Pyrite Dominated	Pyrite Dominated	Pyrite Dominated	Pyrite Dominated	Pyrite Dominated	Pyrite Dominated	Pyrite Dominated	Chalcopyrite-pyrrhotite Dominated
Weight Percent (wt%)									
Zn	<0.01	<0.01	0.03	<0.01	<0.01	0.02	0.09	0.01	<0.01
Cu	0.23	9.56	0.42	0.25	0.23	0.96	0.29	0.24	0.04
Ni	0.48	1.25	0.16	0.58	0.05	0.48	1.52	0.15	6.11
Co	32.42	19.89	31.56	31.56	32.34	30.12	30.1	28.77	26.76
Fe	4.99	14.08	7.06	5.65	5.8	7.7	6.12	12.41	4.09
Sb	<0.01	<0.01	<0.01	<0.01	<0.01	<0.01	<0.01	<0.01	<0.01
Cd	<0.01	<0.01	0.01	<0.01	<0.01	<0.01	<0.01	<0.01	<0.01
Pb	0.06	0.11	0.08	0.05	0.09	0.13	0.17	0.05	<0.02
S	23.62	26.64	24.25	23.1	24.61	25.01	23.15	21.42	19.36
As	39.94	33.67	38.67	39.78	37.9	37.52	37.37	33.85	44.64
Se	<0.02	<0.02	<0.02	<0.02	<0.02	<0.02	<0.02	<0.02	<0.02
Ag	<0.01	0.01	<0.01	<0.01	<0.01	<0.01	0.09	<0.01	<0.01
Au	<0.03	<0.03	<0.02	<0.02	<0.03	<0.03	0.53	<0.02	<0.02
Total	101.61	105.12	102.14	100.83	100.84	101.83	99.32	96.85	100.79
Atoms Per Formula Unit (apfu)									
Zn	0.000	0.000	0.001	0.000	0.000	0.000	0.002	0.000	0.000
Cu	0.005	0.181	0.009	0.005	0.005	0.019	0.006	0.006	0.001
Ni	0.011	0.026	0.004	0.014	0.001	0.010	0.036	0.004	0.172
Co	0.747	0.406	0.708	0.743	0.715	0.655	0.707	0.731	0.752
Fe	0.121	0.303	0.167	0.140	0.135	0.177	0.152	0.333	0.121
Sb	0.000	0.000	0.000	0.000	0.000	0.000	0.000	0.000	0.000
Cd	0.000	0.000	0.000	0.000	0.000	0.000	0.000	0.000	0.000
Pb	0.000	0.001	0.001	0.000	0.001	0.001	0.001	0.000	0.000
S	1.000	1.000	1.000	1.000	1.000	1.000	1.000	1.000	1.000
As	0.724	0.541	0.682	0.737	0.659	0.642	0.691	0.676	0.987
Se	0.000	0.000	0.000	0.000	0.000	0.000	0.000	0.000	0.000
Ag	0.000	0.000	0.000	0.000	0.000	0.000	0.001	0.000	0.000
Au	0.000	0.000	0.000	0.000	0.000	0.000	0.004	0.000	0.000
Total	2.608	2.458	2.571	2.640	2.516	2.505	2.600	2.750	3.034

Table C5. EPMA results for cobaltite continued.

Deposit	Tilt Cove	Tilt Cove	Tilt Cove	Tilt Cove	Tilt Cove	Tilt Cove	Tilt Cove	Tilt Cove	Tilt Cove
Drill Hole	SZ-20-05	SZ-20-05	SZ-20-05	SZ-20-05	SZ-20-05	SZ-20-05	SZ-20-05	SZ-20-05	SZ-20-05
Sample	KKMSC70-Cob2	KKMSC70-Cob3	KKMSC70-Cob4	KKMSC70-Cob5	KKMSC70-Cob6	KKMSC70-Cob7	KKMSC70-Cob8	KKMSC70-Cob9	KKMSC70-Cob10
Depth (m)	126.45	126.45	126.45	126.45	126.45	126.45	126.45	126.45	126.45
Date	2023_07_14	2023_07_14	2023_07_14	2023_07_14	2023_07_14	2023_07_14	2023_07_14	2023_07_14	2023_07_14
Facies	Chalcopyrite-pyrrhotite Dominated	Chalcopyrite-pyrrhotite Dominated	Chalcopyrite-pyrrhotite Dominated	Chalcopyrite-pyrrhotite Dominated	Chalcopyrite-pyrrhotite Dominated	Chalcopyrite-pyrrhotite Dominated	Chalcopyrite-pyrrhotite Dominated	Chalcopyrite-pyrrhotite Dominated	Chalcopyrite-pyrrhotite Dominated
Weight Percent (wt%)									
Zn	<0.01	<0.01	<0.01	<0.01	<0.01	<0.01	<0.01	<0.01	<0.01
Cu	0.03	0.01	0.32	0.93	0.47	0.04	0.03	0.13	0.02
Ni	3.09	0.19	1	0.32	0.5	0.61	2.84	0.26	0.27
Co	30.22	33.57	33.1	33.7	33.35	34.34	31.9	33.81	33.51
Fe	3.31	3.49	3.21	2.51	2.38	1.67	1.77	2.87	3.39
Sb	<0.01	<0.01	<0.01	<0.01	<0.01	<0.01	<0.01	<0.01	<0.01
Cd	<0.01	<0.01	<0.01	<0.01	<0.01	<0.01	<0.01	<0.01	<0.01
Pb	<0.02	<0.02	<0.02	<0.02	0.03	<0.02	<0.02	<0.02	<0.02
S	19.53	21.12	20.9	20.76	20.21	19.99	19.57	21.51	21.56
As	44.28	41.93	42.15	43.63	43.61	43.63	44.38	41.98	41.35
Se	<0.02	<0.02	<0.02	<0.02	<0.02	<0.02	<0.02	<0.02	<0.02
Ag	<0.01	<0.01	<0.01	<0.01	<0.01	0.01	<0.01	<0.01	<0.01
Au	<0.02	<0.02	<0.02	<0.02	<0.02	<0.02	<0.02	<0.02	<0.02
Total	100.22	100.18	100.46	101.71	100.36	100.15	100.34	100.34	99.95
Atoms Per Formula Unit (apfu)									
Zn	0.000	0.000	0.000	0.000	0.000	0.000	0.000	0.000	0.000
Cu	0.001	0.000	0.008	0.023	0.012	0.001	0.001	0.003	0.000
Ni	0.086	0.005	0.026	0.008	0.014	0.017	0.079	0.007	0.007
Co	0.842	0.865	0.862	0.883	0.898	0.935	0.887	0.855	0.846
Fe	0.097	0.095	0.088	0.069	0.068	0.048	0.052	0.077	0.090
Sb	0.000	0.000	0.000	0.000	0.000	0.000	0.000	0.000	0.000
Cd	0.000	0.000	0.000	0.000	0.000	0.000	0.000	0.000	0.000
Pb	0.000	0.000	0.000	0.000	0.000	0.000	0.000	0.000	0.000
S	1.000	1.000	1.000	1.000	1.000	1.000	1.000	1.000	1.000
As	0.970	0.850	0.863	0.899	0.924	0.934	0.971	0.835	0.821
Se	0.000	0.000	0.000	0.000	0.000	0.000	0.000	0.000	0.000
Ag	0.000	0.000	0.000	0.000	0.000	0.000	0.000	0.000	0.000
Au	0.000	0.000	0.000	0.000	0.000	0.000	0.000	0.000	0.000
Total	2.997	2.815	2.847	2.883	2.914	2.935	2.989	2.777	2.764

Table C5. EPMA results for cobaltite continued.

Deposit	Tilt Cove	Tilt Cove	Tilt Cove	Tilt Cove	Tilt Cove	Tilt Cove	Tilt Cove
Drill Hole	SZ-20-05	SZ-20-05	SZ-20-05	SZ-20-05	SZ-20-05	SZ-20-05	SZ-20-05
Sample	KKMSC70-Cob11	KKMSC70-Cob12	KKMSC70-Cob13	KKMSC70-Cob14	KKMSC70-Cob15	KKMSC70-Cob16	KKMSC70-Cob17
Depth (m)	126.45	126.45	126.45	126.45	126.45	126.45	126.45
Date	2023_07_14	2023_07_14	2023_07_14	2023_07_14	2023_07_14	2023_07_14	2023_07_14
Facies	Chalcopyrite-pyrrhotite Dominated	Chalcopyrite-pyrrhotite Dominated	Chalcopyrite-pyrrhotite Dominated	Chalcopyrite-pyrrhotite Dominated	Chalcopyrite-pyrrhotite Dominated	Chalcopyrite-pyrrhotite Dominated	Chalcopyrite-pyrrhotite Dominated
Weight Percent (wt%)							
Zn	<0.01	<0.01	<0.01	<0.01	<0.01	<0.01	<0.01
Cu	0.06	0.1	0.06	0.03	0.05	0.02	0.22
Ni	1.14	6.5	1	0.61	0.23	0.59	0.66
Co	32.92	26.08	32.88	34.24	33.96	33.53	32.77
Fe	2.53	4.77	3.11	2.14	2.58	3.19	3.03
Sb	<0.01	<0.01	<0.01	<0.01	<0.01	<0.01	<0.01
Cd	<0.01	<0.01	<0.01	<0.01	<0.01	<0.01	<0.01
Pb	0.06	0.05	<0.02	<0.02	<0.02	0.03	0.03
S	20.1	19.45	20.48	20.7	21.19	22.01	21.23
As	43.67	45.13	42.6	42.81	41.49	40.64	41.71
Se	<0.02	<0.02	<0.02	<0.02	<0.02	<0.02	<0.02
Ag	<0.01	<0.01	<0.01	<0.01	<0.01	0.01	<0.01
Au	<0.02	<0.02	<0.02	<0.02	<0.02	<0.02	<0.02
Total	100.27	101.80	99.97	100.33	99.34	99.94	99.43
Atoms Per Formula Unit (apfu)							
Zn	0.000	0.000	0.000	0.000	0.000	0.000	0.000
Cu	0.002	0.003	0.001	0.001	0.001	0.000	0.005
Ni	0.031	0.183	0.027	0.016	0.006	0.015	0.017
Co	0.891	0.730	0.874	0.900	0.872	0.829	0.840
Fe	0.072	0.141	0.087	0.059	0.070	0.083	0.082
Sb	0.000	0.000	0.000	0.000	0.000	0.000	0.000
Cd	0.000	0.000	0.000	0.000	0.000	0.000	0.000
Pb	0.000	0.000	0.000	0.000	0.000	0.000	0.000
S	1.000	1.000	1.000	1.000	1.000	1.000	1.000
As	0.930	0.993	0.890	0.885	0.838	0.790	0.841
Se	0.000	0.000	0.000	0.000	0.000	0.000	0.000
Ag	0.000	0.000	0.000	0.000	0.000	0.000	0.000
Au	0.000	0.000	0.000	0.000	0.000	0.000	0.000
Total	2.926	3.049	2.879	2.861	2.787	2.718	2.785

Table C6. EPMA results for pentlandite. Data in red was omitted in discussion due to results being outside of the total cut-off for EPMA or it is inconsistent with SEM and reflected light mineral ID.

Deposit	Betts Cove	Betts Cove	Betts Cove	Betts Cove	Betts Cove	Betts Cove	Betts Cove	Betts Cove	Betts Cove
Drill Hole	BC-21-03	BC-21-03	BC-21-08	BC-21-08	BC-21-08	BC-21-08	BC-21-08	BC-21-08	BC-21-08
Sample	KKMSC32-Pnt2	KKMSC32-Pnt3	KKMSC53-Pnt1	KKMSC53-Pnt2	KKMSC53-Pnt3	KKMSC53-Pnt4	KKMSC53-Pnt5	KKMSC53-Pnt6	KKMSC53-Pnt7
Depth (m)	88	88	28.7	28.7	28.7	28.7	28.7	28.7	28.7
Date	2023_06_27	2023_06_27	2023_07_19	2023_07_19	2023_07_19	2023_07_19	2023_07_19	2023_07_19	2023_07_19
Facies	Sphalerite-pyrite Dominated	Sphalerite-pyrite Dominated	Chalcopyrite Dominated	Chalcopyrite Dominated	Chalcopyrite Dominated	Chalcopyrite Dominated	Chalcopyrite Dominated	Chalcopyrite Dominated	Chalcopyrite Dominated
Weight Percent (wt%)									
Zn	<0.01	0.02	<0.01	<0.01	<0.01	<0.01	<0.01	<0.01	0.05
Cu	0.16	0.38	0.24	0.86	2.31	0.33	5.79	0.49	0.41
Ni	23.21	22.75	35.44	37.33	30.1	40.28	33.49	38.16	35.17
Co	<0.01	<0.01	0.46	1.92	2.35	1.61	1.45	1.7	3.39
Fe	32.06	32.04	30.98	27.54	32.02	25.36	26.27	26.42	28.49
Sb	<0.01	<0.01	<0.01	<0.01	<0.01	<0.01	<0.01	<0.02	<0.01
Cd	0.1	0.1	<0.01	0.01	<0.01	0.03	<0.01	<0.01	<0.01
Pb	<0.02	0.08	0.07	0.12	0.09	0.1	0.1	0.12	0.11
S	31.24	31.26	33.63	33.06	33.54	33.12	33.24	33.18	32.96
As	<0.02	<0.02	<0.02	<0.02	<0.02	<0.02	<0.02	<0.02	<0.02
Se	<0.01	<0.01	0.05	0.08	0.04	0.05	0.03	0.05	0.05
Ag	12.8	12.95	<0.01	<0.01	<0.01	<0.01	<0.01	<0.01	<0.01
Au	<0.03	<0.03	<0.02	<0.02	<0.02	<0.02	<0.02	<0.02	<0.02
Total	99.44	99.46	100.85	100.88	100.41	100.68	100.19	99.59	100.53
Atoms Per Formula Unit (apfu)									
Zn	0.000	0.003	0.000	0.000	0.000	0.000	0.000	0.000	0.006
Cu	0.021	0.049	0.029	0.105	0.278	0.040	0.703	0.060	0.050
Ni	3.247	3.181	4.606	4.935	3.922	5.315	4.403	5.026	4.664
Co	0.000	0.000	0.060	0.253	0.305	0.212	0.190	0.223	0.448
Fe	4.714	4.708	4.231	3.826	4.385	3.517	3.630	3.658	3.970
Sb	0.000	0.000	0.000	0.000	0.000	0.000	0.000	0.000	0.000
Cd	0.007	0.007	0.000	0.001	0.000	0.002	0.000	0.000	0.000
Pb	0.000	0.003	0.003	0.004	0.003	0.004	0.004	0.004	0.004
S	8.000	8.000	8.000	8.000	8.000	8.000	8.000	8.000	8.000
As	0.000	0.000	0.000	0.000	0.000	0.000	0.000	0.000	0.000
Se	0.000	0.000	0.005	0.008	0.004	0.005	0.003	0.005	0.005
Ag	0.974	0.985	0.000	0.000	0.000	0.000	0.000	0.000	0.000
Au	0.000	0.000	0.000	0.000	0.000	0.000	0.000	0.000	0.000
Total	16.963	16.936	16.933	17.132	16.898	17.095	16.933	16.976	17.147

Table C6. EPMA results for pentlandite continued.

Deposit	Tilt Cove	Tilt Cove	Tilt Cove	Tilt Cove	Tilt Cove	Tilt Cove	Tilt Cove	Tilt Cove	Tilt Cove
Drill Hole	SZ-20-04	SZ-20-04	SZ-20-04	SZ-20-04	SZ-20-04	SZ-20-04	SZ-20-04	SZ-20-04	SZ-20-04
Sample	KKMSC63-Pnt1	KKMSC63-Pnt2	KKMSC63-Pnt3	KKMSC63-Pnt4	KKMSC63-Pnt5	KKMSC63-Pnt6	KKMSC63-Pnt7	KKMSC63-Pnt8	KKMSC63-Pnt9
Depth (m)	64.45	64.45	64.45	64.45	64.45	64.45	64.45	64.45	64.45
Date	2023_06_30	2023_06_30	2023_06_30	2023_06_30	2023_06_30	2023_06_30	2023_06_30	2023_06_30	2023_06_30
Facies	Pyrite Dominated	Pyrite Dominated	Pyrite Dominated	Pyrite Dominated	Pyrite Dominated	Pyrite Dominated	Pyrite Dominated	Pyrite Dominated	Pyrite Dominated
Weight Percent (wt%)									
Zn	<0.01	<0.01	<0.01	<0.01	<0.01	<0.01	<0.01	0.04	0.06
Cu	0.11	0.17	0.18	0.19	0.47	0.58	0.07	0.29	0.37
Ni	39.66	28.77	39.32	39.6	27.26	28.89	39.6	26.69	30.98
Co	0.24	0.3	0.48	0.46	0.49	0.46	0.46	0.46	0.39
Fe	27.58	26.89	27.37	27.65	26.93	26.87	27.13	26.85	25.07
Sb	<0.01	<0.01	<0.01	<0.01	<0.01	<0.01	<0.01	<0.01	<0.01
Cd	<0.01	0.01	<0.01	<0.01	<0.01	0.01	<0.01	<0.01	<0.01
Pb	<0.02	0.04	<0.02	<0.02	0.1	0.14	0.04	0.08	0.09
S	32.94	39.4	33.08	33.15	37.49	34.13	33	37.16	36.42
As	<0.02	<0.02	<0.02	<0.02	<0.02	<0.02	0.02	<0.02	<0.02
Se	<0.01	0.02	<0.01	<0.01	<0.01	0.04	<0.01	<0.01	0.02
Ag	<0.01	<0.01	<0.01	<0.01	0.03	0.06	<0.01	<0.01	0.01
Au	<0.03	<0.03	<0.02	<0.03	<0.03	<0.03	<0.03	<0.03	<0.03
Total	100.41	95.56	100.31	100.93	92.68	90.96	100.24	91.48	93.32
Atoms Per Formula Unit (apfu)									
Zn	0.000	0.000	0.000	0.000	0.000	0.000	0.000	0.004	0.006
Cu	0.013	0.017	0.022	0.023	0.051	0.069	0.009	0.032	0.041
Ni	5.262	3.191	5.195	5.221	3.178	3.700	5.245	3.139	3.718
Co	0.032	0.033	0.063	0.060	0.057	0.059	0.061	0.054	0.047
Fe	3.846	3.135	3.801	3.831	3.300	3.616	3.776	3.319	3.162
Sb	0.000	0.000	0.000	0.000	0.000	0.000	0.000	0.000	0.000
Cd	0.000	0.001	0.000	0.000	0.000	0.001	0.000	0.000	0.000
Pb	0.000	0.001	0.000	0.000	0.003	0.005	0.002	0.003	0.003
S	8.000	8.000	8.000	8.000	8.000	8.000	8.000	8.000	8.000
As	0.000	0.000	0.000	0.000	0.000	0.000	0.002	0.000	0.000
Se	0.000	0.002	0.000	0.000	0.000	0.004	0.000	0.000	0.002
Ag	0.000	0.000	0.000	0.000	0.002	0.004	0.000	0.000	0.001
Au	0.000	0.000	0.000	0.000	0.000	0.000	0.000	0.000	0.000
Total	17.153	14.380	17.081	17.136	14.590	15.457	17.094	14.550	14.979

Table C6. EPMA results for pentlandite continued.

Deposit	Tilt Cove	Tilt Cove	Tilt Cove	Tilt Cove	Tilt Cove	Tilt Cove	Tilt Cove	Tilt Cove	Tilt Cove
Drill Hole	SZ-20-04	SZ-20-04	SZ-20-04	SZ-20-04	SZ-20-04	SZ-20-05	SZ-20-05	SZ-20-05	SZ-20-05
Sample	KKMSC63-Pnt10	KKMSC63-Pnt11	KKMSC63-Pnt12	KKMSC63-Pnt13	KKMSC63-Pnt14	KKMSC70_Pnt 1	KKMSC70_Pnt 2	KKMSC70_Pnt 3	KKMSC70_Pnt 4
Depth (m)	64.45	64.45	64.45	64.45	64.45	126.45	126.45	126.45	126.45
Date	2023 06 30	2023 06 30	2023 06 30	2023 06 30	2023 06 30	2023 07 14	2023 07 14	2023 07 14	2023 07 14
Facies	Pyrite Dominated	Pyrite Dominated	Pyrite Dominated	Pyrite Dominated	Pyrite Dominated	Chalcopyrite-pyrrhotite Dominated	Chalcopyrite-pyrrhotite Dominated	Chalcopyrite-pyrrhotite Dominated	Chalcopyrite-pyrrhotite Dominated
Weight Percent (wt%)									
Zn	0.03	<0.01	0.02	<0.01	0.03	<0.01	<0.01	<0.01	<0.01
Cu	0.64	0.1	0.19	0.09	0.48	0.05	0.08	0.07	0.04
Ni	28.31	39.6	26.87	39.77	27.58	37.5	37.64	37.53	37.65
Co	0.38	0.2	0.21	0.17	0.18	1.03	0.87	0.82	1.08
Fe	26.72	27.38	26.53	27.45	25.42	28.35	28.12	28.59	28.1
Sb	0.02	<0.01	0.04	<0.01	0.03	<0.01	<0.01	<0.01	<0.01
Cd	<0.01	<0.01	<0.01	<0.01	<0.01	<0.01	<0.01	<0.01	<0.01
Pb	0.13	0.02	0.09	<0.02	0.14	0.03	<0.02	0.03	<0.02
S	39.64	33.08	39.72	33.11	38.04	32.94	32.92	32.89	32.89
As	<0.02	<0.02	<0.02	<0.02	<0.02	<0.02	<0.02	<0.02	<0.02
Se	0.03	<0.01	0.02	0.03	<0.01	<0.01	0.01	0.02	<0.01
Ag	<0.01	<0.01	<0.01	<0.01	<0.01	<0.01	<0.01	<0.01	<0.01
Au	<0.03	<0.02	<0.03	<0.03	<0.03	<0.02	<0.02	<0.02	<0.02
Total	95.73	100.33	93.60	100.53	91.79	99.82	99.50	99.85	99.70
Atoms Per Formula Unit (apfu)									
Zn	0.003	0.000	0.002	0.000	0.003	0.000	0.000	0.000	0.000
Cu	0.065	0.012	0.019	0.011	0.051	0.006	0.010	0.009	0.005
Ni	3.121	5.232	2.957	5.250	3.169	4.976	4.997	4.987	5.003
Co	0.042	0.026	0.023	0.022	0.021	0.136	0.115	0.109	0.143
Fe	3.096	3.802	3.068	3.808	3.070	3.953	3.924	3.993	3.924
Sb	0.001	0.000	0.002	0.000	0.002	0.000	0.000	0.000	0.000
Cd	0.000	0.000	0.000	0.000	0.000	0.000	0.000	0.000	0.000
Pb	0.004	0.001	0.003	0.000	0.005	0.001	0.000	0.001	0.000
S	8.000	8.000	8.000	8.000	8.000	8.000	8.000	8.000	8.000
As	0.000	0.000	0.000	0.000	0.000	0.000	0.000	0.000	0.000
Se	0.002	0.000	0.002	0.003	0.000	0.000	0.001	0.002	0.000
Ag	0.000	0.000	0.000	0.000	0.000	0.000	0.000	0.000	0.000
Au	0.000	0.000	0.000	0.000	0.000	0.000	0.000	0.000	0.000
Total	14.335	17.073	14.076	17.094	14.319	17.072	17.047	17.100	17.075

Table C6. EPMA results for pentlandite continued.

Deposit	Tilt Cove	Tilt Cove	Tilt Cove	Tilt Cove	Tilt Cove	Tilt Cove	Tilt Cove	Tilt Cove	Tilt Cove
Drill Hole	SZ-20-05	SZ-20-05	SZ-20-05	SZ-20-05	SZ-20-05	SZ-20-05	SZ-20-05	SZ-20-05	SZ-20-05
Sample	KKMSC70_Pnt 5	KKMSC70_Pnt 6	KKMSC70_Pnt 7	KKMSC70_Pnt 8	KKMSC70_Pnt 9	KKMSC70_Pnt 10	KKMSC70_Pnt 11	KKMSC70_Pnt 12	KKMSC70_Pnt 13
Depth (m)	126.45	126.45	126.45	126.45	126.45	126.45	126.45	126.45	126.45
Date	2023_07_14	2023_07_14	2023_07_14	2023_07_14	2023_07_14	2023_07_14	2023_07_14	2023_07_14	2023_07_14
Facies	Chalcopyrite-pyrrhotite Dominated	Chalcopyrite-pyrrhotite Dominated	Chalcopyrite-pyrrhotite Dominated	Chalcopyrite-pyrrhotite Dominated	Chalcopyrite-pyrrhotite Dominated	Chalcopyrite-pyrrhotite Dominated	Chalcopyrite-pyrrhotite Dominated	Chalcopyrite-pyrrhotite Dominated	Chalcopyrite-pyrrhotite Dominated
Weight Percent (wt%)									
Zn	<0.01	0.05	<0.01	<0.01	<0.01	<0.01	<0.01	<0.01	<0.01
Cu	0.01	33.5	0.03	0.03	0.12	0.07	0.02	0.24	0.01
Ni	37.56	0.04	37.65	37.23	37.57	37.62	37.63	37.58	37.5
Co	1.24	0.01	1.27	1.37	1.37	1.39	0.85	0.93	1.32
Fe	28.11	30.59	27.59	28.02	27.83	27.55	28.13	28.1	27.97
Sb	<0.01	<0.01	<0.01	<0.01	<0.01	<0.01	<0.01	<0.01	<0.01
Cd	<0.01	<0.01	<0.01	<0.01	<0.01	0.01	<0.01	0.01	<0.01
Pb	0.03	<0.02	0.02	<0.02	<0.02	<0.02	0.03	0.03	0.05
S	32.79	34.26	32.82	32.74	33.03	32.73	32.96	33.13	32.76
As	<0.02	<0.02	<0.02	<0.02	<0.02	<0.02	<0.02	<0.02	<0.02
Se	<0.01	0.04	0.02	<0.01	<0.01	0.03	<0.01	<0.01	0.03
Ag	<0.01	0.01	<0.01	<0.01	<0.01	<0.01	<0.01	<0.01	<0.01
Au	<0.02	<0.02	<0.02	<0.02	<0.02	<0.02	<0.02	<0.02	<0.02
Total	99.63	98.43	99.30	99.30	99.88	99.34	99.52	99.94	99.54
Atoms Per Formula Unit (apfu)									
Zn	0.000	0.006	0.000	0.000	0.000	0.000	0.000	0.000	0.000
Cu	0.001	3.947	0.004	0.004	0.015	0.009	0.002	0.029	0.001
Ni	5.006	0.005	5.014	4.970	4.971	5.023	4.990	4.958	5.003
Co	0.165	0.001	0.168	0.182	0.181	0.185	0.112	0.122	0.175
Fe	3.938	4.101	3.861	3.931	3.870	3.866	3.920	3.896	3.922
Sb	0.000	0.000	0.000	0.000	0.000	0.000	0.000	0.000	0.000
Cd	0.000	0.000	0.000	0.000	0.000	0.001	0.000	0.001	0.000
Pb	0.001	0.000	0.001	0.000	0.000	0.000	0.001	0.001	0.002
S	8.000	8.000	8.000	8.000	8.000	8.000	8.000	8.000	8.000
As	0.000	0.000	0.000	0.000	0.000	0.000	0.000	0.000	0.000
Se	0.000	0.004	0.002	0.000	0.000	0.003	0.000	0.000	0.003
Ag	0.000	0.001	0.000	0.000	0.000	0.000	0.000	0.000	0.000
Au	0.000	0.000	0.000	0.000	0.000	0.000	0.000	0.000	0.000
Total	17.111	16.065	17.050	17.087	17.037	17.087	17.026	17.007	17.106

Table C6. EPMA results for pentlandite continued.

Deposit	Tilt Cove	Tilt Cove	Tilt Cove	Tilt Cove	Tilt Cove	Tilt Cove	Tilt Cove	Tilt Cove	Tilt Cove
Drill Hole	SZ-20-05	SZ-20-05	SZ-20-05	SZ-20-05	SZ-20-05	SZ-20-05	SZ-20-05	SZ-20-05	SZ-20-05
Sample	KKMSC70_Pnt 14	KKMSC70_Pnt 15	KKMSC70_Pnt 16	KKMSC70_Pnt 17	KKMSC70_Pnt 18	KKMSC72_Pnt 1	KKMSC72_Pnt 2	KKMSC72_Pnt 3	KKMSC72_Pnt 4
Depth (m)	126.45	126.45	126.45	126.45	126.45	143.7	143.7	143.7	143.7
Date	2023_07_14	2023_07_14	2023_07_14	2023_07_14	2023_07_14	2023_07_14	2023_07_14	2023_07_14	2023_07_14
Facies	Chalcopyrite-pyrrhotite Dominated	Chalcopyrite-pyrrhotite Dominated	Chalcopyrite-pyrrhotite Dominated	Chalcopyrite-pyrrhotite Dominated	Chalcopyrite-pyrrhotite Dominated	Pyrrhotite Dominated	Pyrrhotite Dominated	Pyrrhotite Dominated	Pyrrhotite Dominated
Weight Percent (wt%)									
Zn	<0.01	<0.01	<0.01	<0.01	<0.01	<0.01	<0.01	<0.01	<0.01
Cu	0.02	0.03	0.02	0.06	0.03	<0.01	<0.01	0.02	0.02
Ni	37.25	37.42	35.31	37.6	37.76	26.08	25.41	36.91	37.51
Co	1.39	1.42	3.16	1.34	1.4	20.07	22.79	2.47	2.05
Fe	27.9	27.81	25.94	27.89	27.86	11.37	9.33	27.05	27.33
Sb	<0.01	<0.01	<0.01	<0.01	<0.01	<0.01	<0.01	<0.01	<0.01
Cd	<0.01	0.02	<0.01	<0.01	<0.01	<0.01	<0.01	<0.01	<0.01
Pb	<0.02	<0.02	0.04	0.03	<0.02	0.03	<0.02	<0.02	<0.02
S	32.75	32.76	30.36	33.26	32.95	42.1	41.96	32.95	32.77
As	<0.02	<0.02	2.27	<0.02	<0.02	<0.02	<0.02	<0.02	<0.02
Se	0.02	<0.01	<0.01	<0.01	0.01	0.02	<0.01	0.02	<0.01
Ag	<0.01	<0.01	<0.01	<0.01	<0.01	<0.01	<0.01	<0.01	<0.01
Au	<0.02	<0.02	<0.02	<0.02	<0.02	<0.02	<0.02	<0.02	<0.02
Total	99.25	99.35	97.06	100.05	99.94	99.60	99.36	99.38	99.59
Atoms Per Formula Unit (apfu)									
Zn	0.000	0.000	0.000	0.000	0.000	0.000	0.000	0.000	0.000
Cu	0.002	0.004	0.003	0.007	0.004	0.000	0.000	0.002	0.002
Ni	4.971	4.992	5.083	4.941	5.009	2.707	2.647	4.896	5.003
Co	0.185	0.189	0.453	0.175	0.185	2.075	2.364	0.326	0.272
Fe	3.913	3.899	3.925	3.852	3.884	1.241	1.021	3.771	3.831
Sb	0.000	0.000	0.000	0.000	0.000	0.000	0.000	0.000	0.000
Cd	0.000	0.001	0.000	0.000	0.000	0.000	0.000	0.000	0.000
Pb	0.000	0.000	0.002	0.001	0.000	0.001	0.000	0.000	0.000
S	8.000	8.000	8.000	8.000	8.000	8.000	8.000	8.000	8.000
As	0.000	0.000	0.256	0.000	0.000	0.000	0.000	0.000	0.000
Se	0.002	0.000	0.000	0.000	0.001	0.002	0.000	0.002	0.000
Ag	0.000	0.000	0.000	0.000	0.000	0.000	0.000	0.000	0.000
Au	0.000	0.000	0.000	0.000	0.000	0.000	0.000	0.000	0.000
Total	17.073	17.085	17.721	16.976	17.082	14.025	14.032	16.997	17.108

Table C6. EPMA results for pentlandite continued.

Deposit	Tilt Cove	Tilt Cove	Tilt Cove	Tilt Cove	Tilt Cove	Tilt Cove	Tilt Cove	Tilt Cove	Tilt Cove
Drill Hole	SZ-20-05	SZ-20-05	SZ-20-05	SZ-20-05	SZ-20-05	SZ-20-05	SZ-20-05	SZ-20-05	SZ-20-05
Sample	KKMSC72_Pnt 5	KKMSC72_Pnt 6	KKMSC72_Pnt 7	KKMSC72_Pnt 8	KKMSC72_Pnt 9	KKMSC72_Pnt 10	KKMSC72_Pnt 11	KKMSC72_Pnt 12	KKMSC72_Pnt 13
Depth (m)	143.7	143.7	143.7	143.7	143.7	143.7	143.7	143.7	143.7
Date	2023_07_14	2023_07_14	2023_07_14	2023_07_14	2023_07_14	2023_07_14	2023_07_14	2023_07_14	2023_07_14
Facies	Pyrrhotite Dominated	Pyrrhotite Dominated	Pyrrhotite Dominated	Pyrrhotite Dominated	Pyrrhotite Dominated	Pyrrhotite Dominated	Pyrrhotite Dominated	Pyrrhotite Dominated	Pyrrhotite Dominated
Weight Percent (wt%)									
Zn	<0.01	<0.01	<0.01	<0.01	<0.01	<0.01	<0.01	<0.01	<0.01
Cu	0.03	0.02	<0.01	0.02	0.01	0.01	<0.01	0.02	<0.01
Ni	37.39	37.45	26.09	37.08	25.62	36.97	25.9	37.63	26.2
Co	1.77	1.91	20.57	2.19	21.67	2.46	21.9	1.93	20.16
Fe	27.55	27.71	10.68	27.34	10.05	27.49	9.95	27.47	11.1
Sb	<0.01	<0.01	<0.01	<0.01	<0.01	<0.01	<0.01	<0.01	<0.01
Cd	<0.01	<0.01	<0.01	<0.01	<0.01	<0.01	<0.01	<0.01	<0.01
Pb	<0.02	<0.02	0.06	0.03	0.02	<0.02	<0.02	0.05	<0.02
S	32.96	32.88	41.81	32.73	42.02	32.82	41.92	32.53	41.89
As	<0.02	<0.02	<0.02	<0.02	<0.02	<0.02	<0.02	<0.02	<0.02
Se	<0.01	<0.01	0.02	0.02	<0.01	<0.01	0.01	<0.01	0.01
Ag	<0.01	<0.01	<0.01	<0.01	<0.01	<0.01	<0.01	<0.01	<0.01
Au	<0.02	<0.02	<0.02	<0.02	<0.02	<0.02	<0.02	<0.02	<0.02
Total	99.60	99.87	99.08	99.32	99.26	99.69	99.63	99.53	99.26
Atoms Per Formula Unit (apfu)									
Zn	0.000	0.000	0.000	0.000	0.000	0.000	0.000	0.000	0.000
Cu	0.004	0.002	0.000	0.002	0.001	0.001	0.000	0.002	0.000
Ni	4.958	4.978	2.727	4.951	2.665	4.923	2.700	5.056	2.734
Co	0.234	0.253	2.141	0.291	2.245	0.326	2.274	0.258	2.095
Fe	3.839	3.871	1.173	3.837	1.099	3.847	1.090	3.879	1.217
Sb	0.000	0.000	0.000	0.000	0.000	0.000	0.000	0.000	0.000
Cd	0.000	0.000	0.000	0.000	0.000	0.000	0.000	0.000	0.000
Pb	0.000	0.000	0.002	0.001	0.001	0.000	0.000	0.002	0.000
S	8.000	8.000	8.000	8.000	8.000	8.000	8.000	8.000	8.000
As	0.000	0.000	0.000	0.000	0.000	0.000	0.000	0.000	0.000
Se	0.000	0.000	0.002	0.002	0.000	0.000	0.001	0.000	0.001
Ag	0.000	0.000	0.000	0.000	0.000	0.000	0.000	0.000	0.000
Au	0.000	0.000	0.000	0.000	0.000	0.000	0.000	0.000	0.000
Total	17.035	17.104	14.045	17.085	14.010	17.098	14.065	17.197	14.046

Table C6. EPMA results for pentlandite continued.

Deposit	Tilt Cove	Tilt Cove	Tilt Cove	Tilt Cove	Tilt Cove	Tilt Cove	Tilt Cove	Tilt Cove	Tilt Cove
Drill Hole	SZ-20-05	SZ-20-05	SZ-20-05	SZ-20-05	SZ-20-05	SZ-20-05	SZ-20-05	SZ-20-05	SZ-20-05
Sample	KKMSC72_Pnt 14	KKMSC72_Pnt 15	KKMSC72_Pnt 16	KKMSC72_Pnt 17	KKMSC72_Pnt 18	KKMSC72_Pnt 19	KKMSC72_Pnt 20	KKMSC72_Pnt 21	KKMSC72_Pnt 22
Depth (m)	143.7	143.7	143.7	143.7	143.7	143.7	143.7	143.7	143.7
Date	2023 07 14	2023 07 14	2023 07 14	2023 07 14	2023 07 14	2023 07 14	2023 07 14	2023 07 14	2023 07 14
Facies	Pyrrhotite Dominated	Pyrrhotite Dominated	Pyrrhotite Dominated	Pyrrhotite Dominated	Pyrrhotite Dominated	Pyrrhotite Dominated	Pyrrhotite Dominated	Pyrrhotite Dominated	Pyrrhotite Dominated
Weight Percent (wt%)									
Zn	<0.01	<0.01	<0.01	<0.01	<0.01	<0.01	<0.01	<0.01	<0.01
Cu	0.02	0.09	0.02	0.11	0.07	0.04	0.04	0.03	0.02
Ni	36.89	37.28	37.26	36.83	36.46	37.06	37.6	37.43	37.34
Co	2.08	2.54	2.39	2.56	2.51	2.45	2.25	2.13	2.09
Fe	27.39	27.05	27.45	27.4	27.57	27.67	27.47	27.41	27.54
Sb	<0.01	<0.01	<0.01	<0.01	<0.01	<0.01	<0.01	<0.01	<0.01
Cd	<0.01	<0.01	<0.01	<0.01	<0.01	<0.01	<0.01	<0.01	<0.01
Pb	0.03	0.03	<0.02	0.03	0.05	0.03	0.03	<0.02	0.03
S	32.9	32.97	32.93	32.76	32.8	32.99	32.97	32.92	32.87
As	<0.02	<0.02	<0.02	<0.02	<0.02	<0.02	<0.02	<0.02	<0.02
Se	0.03	0.02	0.01	<0.01	<0.01	<0.01	<0.01	<0.01	<0.01
Ag	<0.01	<0.01	<0.01	<0.01	<0.01	<0.01	<0.01	<0.01	<0.01
Au	<0.02	<0.02	<0.02	<0.02	<0.02	<0.02	<0.02	<0.02	<0.02
Total	99.26	99.90	99.98	99.61	99.36	100.18	100.28	99.80	99.86
Atoms Per Formula Unit (apfu)									
Zn	0.000	0.000	0.000	0.000	0.000	0.000	0.000	0.000	0.000
Cu	0.002	0.011	0.002	0.014	0.009	0.005	0.005	0.004	0.002
Ni	4.901	4.942	4.945	4.913	4.858	4.910	4.984	4.969	4.965
Co	0.275	0.335	0.316	0.340	0.333	0.323	0.297	0.282	0.277
Fe	3.824	3.769	3.829	3.842	3.861	3.853	3.827	3.825	3.849
Sb	0.000	0.000	0.000	0.000	0.000	0.000	0.000	0.000	0.000
Cd	0.000	0.000	0.000	0.000	0.000	0.000	0.000	0.000	0.000
Pb	0.001	0.001	0.000	0.001	0.002	0.001	0.001	0.000	0.001
S	8.000	8.000	8.000	8.000	8.000	8.000	8.000	8.000	8.000
As	0.000	0.000	0.000	0.000	0.000	0.000	0.000	0.000	0.000
Se	0.003	0.002	0.001	0.000	0.000	0.000	0.000	0.000	0.000
Ag	0.000	0.000	0.000	0.000	0.000	0.000	0.000	0.000	0.000
Au	0.000	0.000	0.000	0.000	0.000	0.000	0.000	0.000	0.000
Total	17.006	17.060	17.094	17.110	17.063	17.092	17.114	17.079	17.094

Table C6. EPMA results for pentlandite continued.

Deposit	Tilt Cove
Drill Hole	SZ-20-05
Sample	KKMSC72_Pnt23
Depth (m)	143.7
Date	2023_07_14
Facies	Pyrrhotite Dominated
Weight Percent (wt%)	
Zn	<0.01
Cu	0.01
Ni	27.35
Co	16.95
Fe	13.3
Sb	<0.01
Cd	<0.01
Pb	0.04
S	42.02
As	<0.02
Se	<0.01
Ag	<0.01
Au	<0.02
Total	99.59
Atoms Per Formula Unit (apfu)	
Zn	0.000
Cu	0.001
Ni	2.845
Co	1.756
Fe	1.454
Sb	0.000
Cd	0.000
Pb	0.001
S	8.000
As	0.000
Se	0.000
Ag	0.000
Au	0.000
Total	14.057

Table C7. EPMA results for acanthite. Data in red was omitted in discussion due to results being outside of the total cut-off for EPMA or it is inconsistent with SEM and reflected light mineral ID.

Deposit	Tilt Cove	Tilt Cove	Tilt Cove	Tilt Cove	Tilt Cove
Drill Hole	SZ-20-01	SZ-20-01	SZ-20-01	SZ-20-01	SZ-20-01
Sample	KKMSC13-Aca1	KKMSC13-Aca2	KKMSC13-Aca3	KKMSC13-Acanthite4	KKMSC13-Aca5
Depth (m)	66.6	66.6	66.6	66.6	66.6
Date	2023 07 17	2023 07 17	2023 07 17	2023 07 17	2023 07 17
Facies	Pyrite Dominated	Pyrite Dominated	Pyrite Dominated	Pyrite Dominated	Pyrite Dominated
Weight Percent (wt%)					
Zn	<0.02	<0.02	<0.02	0.03	<0.02
Cu	0.37	0.43	2.18	0.85	0.11
Ni	<0.01	<0.01	<0.01	<0.01	<0.01
Co	<0.01	<0.01	<0.01	<0.01	0.01
Fe	1.36	1.4	5.37	1.37	1.57
Sb	12.67	13.35	8.95	5.73	11.34
Cd	0.57	0.56	0.51	0.58	0.57
Pb	0.06	0.04	0.04	0.05	0.06
S	16.04	15.86	15.7	13.69	15.66
As	1.46	0.73	4.87	0.4	1.58
Se	<0.02	<0.02	<0.02	<0.02	<0.01
Ag	67.31	69.45	62	72.4	68.16
Au	0.04	<0.03	1.55	0.33	0.09
Total	99.88	101.84	101.11	95.39	99.11
Atoms Per Formula Unit (apfu)					
Zn	0.000	0.000	0.000	0.001	0.000
Cu	0.012	0.014	0.070	0.031	0.004
Ni	0.000	0.000	0.000	0.000	0.000
Co	0.000	0.000	0.000	0.000	0.000
Fe	0.049	0.051	0.196	0.057	0.058
Sb	0.208	0.222	0.150	0.110	0.191
Cd	0.010	0.010	0.009	0.012	0.010
Pb	0.001	0.000	0.000	0.001	0.001
S	1.000	1.000	1.000	1.000	1.000
As	0.039	0.020	0.133	0.013	0.043
Se	0.000	0.000	0.000	0.000	0.000
Ag	1.247	1.302	1.174	1.572	1.294
Au	0.000	0.000	0.016	0.004	0.001
Total	2.566	2.618	2.749	2.801	2.601

Table C8. EPMA results for arsenopyrite. Data in red was omitted in discussion due to results being outside of the total cut-off for EPMA or it is inconsistent with SEM and reflected light mineral ID.

Deposit	Tilt Cove	Tilt Cove	Tilt Cove	Tilt Cove	Tilt Cove	Tilt Cove	Tilt Cove	Tilt Cove	Tilt Cove
Drill Hole	SZ-20-01	SZ-20-01	SZ-20-01	SZ-20-01	SZ-20-01	SZ-20-01	SZ-20-01	SZ-20-01	SZ-20-01
Sample	KKMSC13-Apy1	KKMSC13-Apy2	KKMSC13-Apy3	KKMSC13-Apy4	KKMSC13-Apy5	KKMSC13-Apy6	KKMSC13-Apy7	KKMSC13-Apy8	KKMSC13-Apy9
Depth (m)	66.6	66.6	66.6	66.6	66.6	66.6	66.6	66.6	66.6
Date	2023_07_17	2023_07_17	2023_07_17	2023_07_17	2023_07_17	2023_07_17	2023_07_17	2023_07_17	2023_07_17
Facies	Pyrite Dominated	Pyrite Dominated	Pyrite Dominated	Pyrite Dominated	Pyrite Dominated	Pyrite Dominated	Pyrite Dominated	Pyrite Dominated	Pyrite Dominated
Weight Percent (wt%)									
Zn	0.01	<0.01	<0.01	<0.01	<0.01	<0.01	<0.01	<0.01	<0.01
Cu	<0.01	0.16	<0.01	0.05	0.17	0.01	<0.01	0.02	<0.01
Ni	<0.01	0.02	<0.01	<0.01	0.05	<0.01	<0.01	<0.01	<0.01
Co	0.04	0.04	0.02	0.04	0.04	0.03	0.04	0.03	0.04
Fe	34.15	34.24	34.11	34.46	34.2	34.37	34.31	34.13	34.33
Sb	<0.01	<0.01	0.02	<0.01	0.02	<0.01	<0.01	<0.01	<0.01
Cd	<0.01	<0.01	<0.01	0.01	0.01	<0.01	<0.01	<0.01	<0.01
Pb	0.06	0.09	0.06	0.06	0.08	0.05	0.05	0.03	0.06
S	21.02	21.47	20.92	22.07	21.69	21.68	21.15	20.75	21.11
As	44.03	43.49	44.64	42.74	43.18	43.32	44.21	44.58	44.62
Se	<0.02	<0.02	<0.02	<0.02	<0.02	<0.02	<0.02	<0.02	<0.02
Ag	<0.01	<0.01	<0.01	<0.01	<0.01	<0.01	<0.01	<0.01	<0.01
Au	<0.02	<0.02	<0.02	<0.02	<0.02	<0.02	<0.02	<0.02	<0.02
Total	99.17	99.34	99.60	99.34	99.29	99.32	99.61	99.43	99.96
Atoms Per Formula Unit (apfu)									
Zn	0.000	0.000	0.000	0.000	0.000	0.000	0.000	0.000	0.000
Cu	0.000	0.004	0.000	0.001	0.004	0.000	0.000	0.000	0.000
Ni	0.000	0.001	0.000	0.000	0.001	0.000	0.000	0.000	0.000
Co	0.001	0.001	0.001	0.001	0.001	0.001	0.001	0.001	0.001
Fe	0.933	0.916	0.936	0.897	0.905	0.910	0.931	0.944	0.934
Sb	0.000	0.000	0.000	0.000	0.000	0.000	0.000	0.000	0.000
Cd	0.000	0.000	0.000	0.000	0.000	0.000	0.000	0.000	0.000
Pb	0.000	0.001	0.000	0.000	0.001	0.000	0.000	0.000	0.000
S	1.000	1.000	1.000	1.000	1.000	1.000	1.000	1.000	1.000
As	0.896	0.867	0.913	0.829	0.852	0.855	0.895	0.919	0.905
Se	0.000	0.000	0.000	0.000	0.000	0.000	0.000	0.000	0.000
Ag	0.000	0.000	0.000	0.000	0.000	0.000	0.000	0.000	0.000
Au	0.000	0.000	0.000	0.000	0.000	0.000	0.000	0.000	0.000
Total	2.831	2.789	2.851	2.728	2.765	2.767	2.827	2.865	2.840

Table C8. EPMA results for arsenopyrite continued.

Deposit	Tilt Cove	Tilt Cove	Tilt Cove	Tilt Cove
Drill Hole	SZ-20-01	SZ-20-01	SZ-20-01	SZ-20-01
Sample	KKMSC13-Apy10	KKMSC13-Apy11	KKMSC13-Apy12	KKMSC13-Apy13
Depth (m)	66.6	66.6	66.6	66.6
Date	2023_07_17	2023_07_17	2023_07_17	2023_07_17
Facies	Pyrite Dominated	Pyrite Dominated	Pyrite Dominated	Pyrite Dominated
Weight Percent (wt%)				
Zn	<0.01	0.03	<0.01	<0.01
Cu	<0.01	<0.01	<0.01	<0.01
Ni	<0.01	<0.01	<0.01	<0.01
Co	0.04	0.04	0.04	0.04
Fe	34.65	34.53	34.57	34.52
Sb	<0.01	<0.01	0.01	<0.01
Cd	0.01	<0.01	<0.01	<0.01
Pb	0.06	0.07	0.09	0.06
S	21.72	22.06	21.01	21.99
As	43.32	42.86	44.33	43.09
Se	<0.02	<0.02	<0.02	<0.02
Ag	<0.01	<0.01	<0.01	<0.01
Au	<0.02	<0.02	<0.02	<0.02
Total	99.70	99.48	99.86	99.54
Atoms Per Formula Unit (apfu)				
Zn	0.000	0.001	0.000	0.000
Cu	0.000	0.000	0.000	0.000
Ni	0.000	0.000	0.000	0.000
Co	0.001	0.001	0.001	0.001
Fe	0.916	0.899	0.945	0.901
Sb	0.000	0.000	0.000	0.000
Cd	0.000	0.000	0.000	0.000
Pb	0.000	0.000	0.001	0.000
S	1.000	1.000	1.000	1.000
As	0.854	0.832	0.903	0.839
Se	0.000	0.000	0.000	0.000
Ag	0.000	0.000	0.000	0.000
Au	0.000	0.000	0.000	0.000
Total	2.771	2.732	2.850	2.741

Table C9. EPMA results for bornite. Data in red was omitted in discussion due to results being outside of the total cut-off for EPMA or it is inconsistent with SEM and reflected light mineral ID.

Deposit	Tilt Cove	Tilt Cove	Tilt Cove	Tilt Cove	Tilt Cove	Tilt Cove	Tilt Cove	Tilt Cove	Tilt Cove
Drill Hole	SZ-20-03	SZ-20-03	SZ-20-03	SZ-20-03	SZ-20-03	SZ-20-03	SZ-20-03	SZ-20-03	SZ-20-03
Sample	KKMSC23-Bn1	KKMSC23-Bn2	KKMSC23-Bn3	KKMSC23-Bn4	KKMSC23-Bn5	KKMSC23-Bn6	KKMSC23-Bn7	KKMSC23-Bn8	KKMSC23-Bn9
Depth (m)	17	17	17	17	17	17	17	17	17
Date	2023/06/30	2023/06/30	2023/06/30	2023/06/30	2023/06/30	2023/06/30	2023/06/30	2023/06/30	2023/06/30
Facies	Magnetite Dominated	Magnetite Dominated	Magnetite Dominated	Magnetite Dominated	Magnetite Dominated	Magnetite Dominated	Magnetite Dominated	Magnetite Dominated	Magnetite Dominated
Weight Percent (wt%)									
Zn	0.03	0.03	0.04	0.04	0.05	0.04	0.04	0.04	0.04
Cu	61.12	60.89	60.47	62.29	61.91	61.91	60.85	61.92	61.55
Ni	<0.01	<0.01	<0.01	<0.01	<0.01	<0.01	<0.01	<0.01	<0.01
Co	<0.01	<0.01	0.01	<0.01	<0.01	<0.01	<0.01	<0.01	<0.01
Fe	11.79	12.4	12.23	11.53	11.43	11.35	12.29	11.61	12.48
Sb	<0.01	<0.01	<0.01	<0.01	<0.01	<0.01	<0.01	<0.01	<0.01
Cd	0.01	<0.01	<0.01	<0.01	<0.01	<0.01	0.01	<0.01	<0.01
Pb	<0.02	<0.02	<0.02	<0.02	0.03	<0.02	0.03	<0.02	<0.02
S	26.45	26.43	26.59	26.05	26.23	26.18	26.55	26.59	26.52
As	<0.02	<0.02	<0.02	<0.02	<0.02	<0.02	<0.02	<0.02	<0.02
Se	<0.01	<0.01	<0.01	<0.01	0.02	<0.01	<0.01	<0.01	<0.01
Ag	0.03	0.05	0.05	0.07	0.05	0.05	0.05	0.03	0.04
Au	<0.03	<0.03	<0.03	<0.03	<0.03	<0.02	<0.03	<0.03	<0.03
Total	99.38	99.74	99.32	99.83	99.61	99.45	99.71	100.04	100.56
Atoms Per Formula Unit (apfu)									
Zn	0.002	0.002	0.003	0.003	0.004	0.003	0.003	0.003	0.003
Cu	4.664	4.650	4.590	4.826	4.764	4.773	4.626	4.700	4.684
Ni	0.000	0.000	0.000	0.000	0.000	0.000	0.000	0.000	0.000
Co	0.000	0.000	0.001	0.000	0.000	0.000	0.000	0.000	0.000
Fe	1.024	1.078	1.056	1.017	1.001	0.996	1.063	1.003	1.081
Sb	0.000	0.000	0.000	0.000	0.000	0.000	0.000	0.000	0.000
Cd	0.000	0.000	0.000	0.000	0.000	0.000	0.000	0.000	0.000
Pb	0.000	0.000	0.000	0.000	0.001	0.000	0.001	0.000	0.000
S	4.000	4.000	4.000	4.000	4.000	4.000	4.000	4.000	4.000
As	0.000	0.000	0.000	0.000	0.000	0.000	0.000	0.000	0.000
Se	0.000	0.000	0.000	0.000	0.001	0.000	0.000	0.000	0.000
Ag	0.001	0.002	0.002	0.003	0.002	0.002	0.002	0.001	0.002
Au	0.000	0.000	0.000	0.000	0.000	0.000	0.000	0.000	0.000
Total	9.692	9.732	9.652	9.849	9.773	9.774	9.695	9.707	9.770

Table C9. EPMA results for bornite continued.

Deposit	Tilt Cove	Tilt Cove
Drill Hole	SZ-20-03	SZ-20-03
Sample	KKMSC23-Bn10	KKMSC23-Bn11
Depth (m)	17	17
Date	2023/06/30	2023/06/30
Facies	Magnetite Dominated	Magnetite Dominated
Weight Percent (wt%)		
Zn	0.06	0.04
Cu	62.08	62.37
Ni	<0.01	<0.01
Co	<0.01	0.01
Fe	11.63	11.69
Sb	<0.01	<0.01
Cd	<0.01	<0.01
Pb	<0.02	0.03
S	26.39	26.33
As	<0.02	<0.02
Se	<0.01	<0.01
Ag	0.04	0.05
Au	<0.03	<0.03
Total	100.08	100.33
Atoms Per Formula Unit (apfu)		
Zn	0.004	0.003
Cu	4.748	4.781
Ni	0.000	0.000
Co	0.000	0.001
Fe	1.012	1.020
Sb	0.000	0.000
Cd	0.000	0.000
Pb	0.000	0.001
S	4.000	4.000
As	0.000	0.000
Se	0.000	0.000
Ag	0.002	0.002
Au	0.000	0.000
Total	9.766	9.808

Table C10. EPMA results for clausthalite. Data in red was omitted in discussion due to results being outside of the total cut-off for EPMA or it is inconsistent with SEM and reflected light mineral ID.

Deposit	Betts Cove	Betts Cove	Betts Cove	Betts Cove	Betts Cove	Betts Cove	Betts Cove	Betts Cove	Betts Cove
Drill Hole	BC-21-07	BC-21-07	BC-21-07	BC-21-07	BC-21-07	BC-21-07	BC-21-07	BC-21-07	BC-21-07
Sample	KKMSC29-Cth1	KKMSC29-Cth2	KKMSC29-Cth8	KKMSC29-Cth9	KKMSC29-Cth10	KKMSC29-Cth11	KKMSC29-Cth17	KKMSC29-Cth18	KKMSC29-Cth21
Depth (m)	107.6	107.6	107.6	107.6	107.6	107.6	107.6	107.6	107.6
Date	2023_06_27	2023_06_27	2023_06_27	2023_06_27	2023_06_27	2023_06_27	2023_06_27	2023_06_27	2023_06_27
Facies	Chalcopyrite Dominated	Chalcopyrite Dominated	Chalcopyrite Dominated	Chalcopyrite Dominated	Chalcopyrite Dominated	Chalcopyrite Dominated	Chalcopyrite Dominated	Chalcopyrite Dominated	Chalcopyrite Dominated
Weight Percent (wt%)									
Zn	<0.02	<0.02	<0.02	<0.02	<0.02	0.14	<0.02	<0.02	<0.02
Cu	1.02	0.54	1.02	0.88	0.64	0.85	0.83	0.71	0.57
Ni	<0.02	<0.02	<0.02	<0.02	<0.02	<0.02	<0.02	<0.02	<0.02
Co	<0.01	<0.01	<0.01	<0.01	<0.01	<0.01	<0.01	<0.01	<0.01
Fe	0.63	0.3	0.63	0.58	0.4	0.49	0.48	0.43	0.33
Sb	<0.01	0.01	<0.01	<0.01	0.02	<0.01	<0.01	0.03	0.04
Cd	<0.01	<0.01	<0.01	0.03	<0.01	0.02	0.02	0.02	<0.01
Pb	68.3	68.41	68.81	68.74	68.12	68.01	68.81	70.01	65.74
S	1.15	1.37	1.12	1.19	1.27	1.15	1.08	1.16	1.01
As	<0.04	<0.04	<0.03	<0.04	<0.03	<0.04	<0.04	<0.04	<0.04
Se	19.82	19.35	19.37	18.86	18	19.22	19.19	19.24	18.89
Te	3.32	3.79	3.9	4.24	5.38	4.07	4.53	4.51	4.85
Ag	<0.01	<0.01	<0.01	<0.01	<0.01	<0.01	<0.01	<0.01	<0.01
Au	<0.01	<0.01	<0.01	<0.01	<0.01	<0.01	<0.01	<0.01	<0.01
Total	94.05	93.55	94.64	94.30	93.71	93.70	94.76	95.95	91.28
Atoms Per Formula Unit (apfu)									
Zn	0.000	0.000	0.000	0.000	0.000	0.002	0.000	0.000	0.000
Cu	0.016	0.008	0.016	0.014	0.010	0.013	0.013	0.011	0.009
Ni	0.000	0.000	0.000	0.000	0.000	0.000	0.000	0.000	0.000
Co	0.000	0.000	0.000	0.000	0.000	0.000	0.000	0.000	0.000
Fe	0.011	0.005	0.011	0.010	0.007	0.009	0.009	0.008	0.006
Sb	0.000	0.000	0.000	0.000	0.000	0.000	0.000	0.000	0.000
Cd	0.000	0.000	0.000	0.000	0.000	0.000	0.000	0.000	0.000
Pb	0.330	0.330	0.332	0.332	0.329	0.328	0.332	0.338	0.317
S	0.036	0.043	0.035	0.037	0.040	0.036	0.034	0.036	0.031
As	0.000	0.000	0.000	0.000	0.000	0.000	0.000	0.000	0.000
Se	0.251	0.245	0.245	0.239	0.228	0.243	0.243	0.244	0.239
Te	0.026	0.030	0.031	0.033	0.042	0.032	0.036	0.035	0.038
Ag	0.000	0.000	0.000	0.000	0.000	0.000	0.000	0.000	0.000
Au	0.000	0.000	0.000	0.000	0.000	0.000	0.000	0.000	0.000
Total	0.670	0.662	0.670	0.665	0.656	0.664	0.666	0.672	0.641

Table C10. EPMA results for clausthalite continued.

Deposit	Betts Cove	Betts Cove	Betts Cove	Betts Cove	Betts Cove	Betts Cove	Betts Cove	Betts Cove	Betts Cove
Drill Hole	BC-21-07	BC-21-07	BC-21-07	BC-21-07	BC-21-07	BC-21-07	BC-21-07	BC-21-07	BC-21-07
Sample	KKMSC29-Cth23	KKMSC29-Cth24	KKMSC29-Cth25	KKMSC29-Cth26	KKMSC29-Cth27	KKMSC29-Cth32	KKMSC29-Cth34	KKMSC29-Cth35	KKMSC29-Cth38
Depth (m)	107.6	107.6	107.6	107.6	107.6	107.6	107.6	107.6	107.6
Date	2023_06_27	2023_06_27	2023_06_27	2023_06_27	2023_06_27	2023_06_27	2023_06_27	2023_06_27	2023_06_27
Facies	Chalcopyrite Dominated	Chalcopyrite Dominated	Chalcopyrite Dominated	Chalcopyrite Dominated	Chalcopyrite Dominated	Chalcopyrite Dominated	Chalcopyrite Dominated	Chalcopyrite Dominated	Chalcopyrite Dominated
Weight Percent (wt%)									
Zn	<0.02	0.18	<0.02	0.04	<0.02	<0.02	<0.02	<0.02	<0.02
Cu	0.67	1.01	0.38	0.85	0.83	1.25	0.82	0.92	0.62
Ni	<0.02	<0.02	<0.02	<0.02	<0.02	<0.02	<0.02	<0.02	<0.02
Co	<0.01	<0.01	<0.01	<0.01	<0.01	<0.01	<0.01	0.01	0.02
Fe	0.42	0.64	0.25	0.57	0.53	0.8	0.57	0.58	0.39
Sb	<0.01	<0.01	<0.01	<0.01	<0.01	<0.01	<0.01	<0.01	<0.01
Cd	<0.01	<0.01	<0.01	<0.01	<0.01	<0.01	<0.01	<0.01	<0.01
Pb	68.03	67.01	68.63	67.78	69.06	68.62	68.1	67.87	68.4
S	0.87	1.01	1.28	1.23	1.27	1.32	1.29	1.37	1.43
As	<0.03	<0.04	<0.04	<0.04	<0.04	<0.04	<0.04	<0.04	<0.04
Se	19.5	18.97	19.13	19.42	20.23	19.4	18.74	19.52	18.89
Te	3.92	3.89	3.64	2.94	2.83	2.92	2.61	2.96	2.79
Ag	0.02	<0.01	<0.01	<0.01	<0.01	<0.01	<0.01	<0.01	<0.01
Au	0.02	<0.01	<0.01	<0.01	<0.01	<0.01	<0.01	<0.01	<0.01
Total	93.27	92.52	93.14	92.62	94.57	94.05	91.79	93.02	92.32
Atoms Per Formula Unit (apfu)									
Zn	0.000	0.003	0.000	0.001	0.000	0.000	0.000	0.000	0.000
Cu	0.011	0.016	0.006	0.013	0.013	0.020	0.013	0.014	0.010
Ni	0.000	0.000	0.000	0.000	0.000	0.000	0.000	0.000	0.000
Co	0.000	0.000	0.000	0.000	0.000	0.000	0.000	0.000	0.000
Fe	0.008	0.011	0.004	0.010	0.009	0.014	0.010	0.010	0.007
Sb	0.000	0.000	0.000	0.000	0.000	0.000	0.000	0.000	0.000
Cd	0.000	0.000	0.000	0.000	0.000	0.000	0.000	0.000	0.000
Pb	0.328	0.323	0.331	0.327	0.333	0.331	0.329	0.328	0.330
S	0.027	0.031	0.040	0.038	0.040	0.041	0.040	0.043	0.045
As	0.000	0.000	0.000	0.000	0.000	0.000	0.000	0.000	0.000
Se	0.247	0.240	0.242	0.246	0.256	0.246	0.237	0.247	0.239
Te	0.031	0.030	0.029	0.023	0.022	0.023	0.020	0.023	0.022
Ag	0.000	0.000	0.000	0.000	0.000	0.000	0.000	0.000	0.000
Au	0.000	0.000	0.000	0.000	0.000	0.000	0.000	0.000	0.000
Total	0.651	0.656	0.652	0.659	0.674	0.675	0.650	0.666	0.653

Table C10. EPMA results for clausthalite continued.

Deposit	Betts Cove	Betts Cove	Betts Cove	Betts Cove	Betts Cove	Betts Cove	Betts Cove	Betts Cove
Drill Hole	BC-21-07	BC-21-06	BC-21-06	BC-21-06	BC-21-08	BC-21-08	BC-21-08	BC-21-08
Sample	KKMSC29-Cth42	KKMSC42-Cth1	KKMSC42-Cth2	KKMSC42-Cth3	KKMSC53-Cth1	KKMSC53-Cth2	KKMSC53-Cth3	KKMSC53-Cth4
Depth (m)	107.6	106.3	106.3	106.3	43.9	43.9	43.9	43.9
Date	2023_06_27	2023_07_17	2023_07_17	2023_07_17	2023_07_19	2023_07_19	2023_07_19	2023_07_19
Facies	Chalcopyrite Dominated	Chalcopyrite-pyrrhotite Dominated	Chalcopyrite-pyrrhotite Dominated	Chalcopyrite-pyrrhotite Dominated	Chalcopyrite Dominated	Chalcopyrite Dominated	Chalcopyrite Dominated	Chalcopyrite Dominated
Weight Percent (wt%)								
Zn	<0.02	<0.02	<0.02	<0.02	<0.02	<0.02	<0.02	<0.02
Cu	0.59	0.33	0.32	<0.02	0.95	0.83	0.05	<0.02
Ni	<0.02	<0.02	<0.02	<0.02	<0.02	<0.02	<0.02	0.04
Co	<0.01	<0.01	<0.01	<0.01	<0.01	<0.01	<0.01	0.01
Fe	0.34	0.17	0.17	1.78	1.56	1.63	1.12	0.76
Sb	0.02	<0.01	<0.01	<0.01	<0.01	0.02	<0.02	<0.02
Cd	<0.01	<0.01	<0.01	<0.01	0.02	0.09	<0.01	<0.01
Pb	68.01	75.79	75.08	73.62	67.9	63.56	69.25	69.2
S	1.41	6.13	4.84	5.55	0.96	1.37	0.49	0.97
As	<0.03	<0.03	<0.03	<0.03	<0.04	<0.04	<0.04	<0.04
Se	18.71	11.9	13.92	12.58	22.35	19.67	23.18	21.39
Te	3.18	<0.01	0.02	0.02	1.1	9.66	0.37	<0.01
Ag	<0.01	<0.03	<0.03	<0.03	<0.03	<0.03	<0.03	<0.03
Au	<0.01	<0.03	<0.03	<0.03	<0.03	<0.03	<0.03	<0.03
Total	91.97	95.58	95.69	94.95	95.48	102.31	94.63	92.86
Atoms Per Formula Unit (apfu)								
Zn	0.000	0.000	0.000	0.000	0.000	0.000	0.000	0.000
Cu	0.009	0.005	0.005	0.000	0.015	0.013	0.001	0.000
Ni	0.000	0.000	0.000	0.000	0.000	0.000	0.000	0.001
Co	0.000	0.000	0.000	0.000	0.000	0.000	0.000	0.000
Fe	0.006	0.003	0.003	0.032	0.028	0.029	0.020	0.014
Sb	0.000	0.000	0.000	0.000	0.000	0.000	0.000	0.000
Cd	0.000	0.000	0.000	0.000	0.000	0.001	0.000	0.000
Pb	0.328	0.366	0.362	0.355	0.328	0.307	0.334	0.334
S	0.044	0.191	0.151	0.173	0.030	0.043	0.015	0.030
As	0.000	0.000	0.000	0.000	0.000	0.000	0.000	0.000
Se	0.237	0.151	0.176	0.159	0.283	0.249	0.294	0.271
Te	0.025	0.000	0.000	0.000	0.009	0.076	0.003	0.000
Ag	0.000	0.000	0.000	0.000	0.000	0.000	0.000	0.000
Au	0.000	0.000	0.000	0.000	0.000	0.000	0.000	0.000
Total	0.650	0.716	0.698	0.720	0.692	0.718	0.667	0.650

Table C11. EPMA results for electrum. Data in red was omitted in discussion due to results being outside of the total cut-off for EPMA or it is inconsistent with SEM and reflected light mineral ID.

Deposit	Betts Cove	Betts Cove	Betts Cove	Betts Cove	Betts Cove	Betts Cove	Betts Cove	Betts Cove	Tilt Cove
Drill Hole	BC-21-02	BC-21-02	BC-21-02	BC-21-02	BC-21-02	BC-21-02	BC-21-02	BC-21-03	SZ-20-01
Sample	KKMSC09-El1	KKMSC09-El2	KKMSC09-El3	KKMSC09-El4	KKMSC09-El5	KKMSC09-El6	KKMSC09-El7	KKMSC32-El1	KKMSC13-El1
Depth (m)	85.4	85.4	85.4	85.4	85.4	85.4	85.4	88	66.6
Date	2023_06_23	2023_06_23	2023_06_23	2023_06_23	2023_06_23	2023_06_23	2023_06_23	2023_06_27	2023_07_17
Facies	Chalcopyrite Dominated	Chalcopyrite Dominated	Chalcopyrite Dominated	Chalcopyrite Dominated	Chalcopyrite Dominated	Chalcopyrite Dominated	Chalcopyrite Dominated	Sphalerite-pyrite Dominated	Pyrite Dominated
Weight Percent (wt%)									
Zn	<0.02	<0.02	<0.02	<0.02	<0.02	<0.02	<0.02	1.73	1.01
Cu	0.4	0.86	<0.02	0.15	<0.02	0.09	0.04	<0.01	0.1
Ni	<0.02	<0.02	<0.02	<0.02	<0.02	<0.02	<0.02	0.02	<0.01
Co	<0.01	<0.01	<0.01	<0.01	<0.01	<0.01	<0.01	0.03	0.02
Fe	0.63	1.76	1.12	0.1	<0.01	0.06	0.62	15.09	0.94
Sb	<0.01	<0.01	<0.01	<0.01	<0.01	<0.01	<0.01	<0.01	<0.01
Cd	0.14	0.18	0.14	0.13	0.11	0.13	0.19	0.3	0.46
Pb	<0.03	<0.03	<0.03	<0.03	<0.03	<0.03	<0.03	<0.03	<0.03
S	0.04	0.06	0.09	0.07	0.04	0.06	0.07	22.87	0.11
As	<0.03	<0.03	<0.03	<0.03	<0.03	<0.03	<0.03	<0.03	<0.03
Se	0.07	0.08	0.13	0.1	0.08	0.06	0.11	0.02	<0.02
Ag	16.53	17.73	14.9	13.35	11.83	13.45	21.43	26.31	52.11
Au	82.74	79.24	84.86	87.06	88.57	85	77.93	33.88	47.51
Total	100.34	99.77	101.03	100.74	100.44	98.59	100.21	100.04	102.05
Au Proportion	0.73	0.71	0.76	0.78	0.80	0.78	0.67	0.41	0.33

Table C12. EPMA results for galena. Data in red was omitted in discussion due to results being outside of the total cut-off for EPMA or it is inconsistent with SEM and reflected light mineral ID.

Deposit	Betts Cove	Betts Cove	Betts Cove	Betts Cove	Betts Cove	Betts Cove	Betts Cove	Betts Cove	Betts Cove
Drill Hole	BC-21-03	BC-21-03	BC-21-03	BC-21-03	BC-21-03	BC-21-03	BC-21-03	BC-21-03	BC-21-03
Sample	KKMSC32-Gn1	KKMSC32-Gn3	KKMSC32-Gn4	KKMSC32-Gn7	KKMSC32-Gn8	KKMSC32-Gn9	KKMSC32-Gn10	KKMSC32-Gn11	KKMSC32-Gn12
Depth (m)	88	88	88	88	88	88	88	88	88
Date	2023_06_27	2023_06_27	2023_06_27	2023_06_27	2023_06_27	2023_06_27	2023_06_27	2023_06_27	2023_06_27
Facies	Sphalerite-pyrite Dominated	Sphalerite-pyrite Dominated	Sphalerite-pyrite Dominated	Sphalerite-pyrite Dominated	Sphalerite-pyrite Dominated	Sphalerite-pyrite Dominated	Sphalerite-pyrite Dominated	Sphalerite-pyrite Dominated	Sphalerite-pyrite Dominated
Weight Percent (wt%)									
Zn	1.51	0.69	0.32	0.28	0.24	0.19	0.75	0.18	0.41
Cu	0.07	13.57	0.05	<0.01	0.02	0.02	<0.02	0.04	<0.02
Ni	<0.02	0.01	<0.01	0.04	0.02	<0.01	<0.02	<0.01	<0.01
Co	<0.01	0.05	<0.01	0.08	0.05	0.02	<0.01	<0.01	<0.01
Fe	2.87	30.11	8.38	45.91	36.09	14.19	1.27	7.69	9.61
Sb	<0.01	<0.01	<0.01	<0.01	<0.01	<0.01	<0.01	<0.01	<0.01
Cd	0.02	0.02	<0.01	0.01	<0.01	0.03	<0.01	<0.01	<0.01
Pb	85.13	22.39	73.99	2.08	27.27	66.45	85.28	73.45	68.46
S	13.54	36.66	18.67	54.07	43.29	25.09	13.56	17.75	19.57
As	<0.04	<0.03	<0.04	<0.02	<0.02	<0.03	<0.03	<0.03	<0.03
Se	0.29	0.07	0.34	<0.01	0.07	0.23	0.3	0.43	0.21
Ag	<0.01	<0.01	<0.01	<0.01	<0.01	<0.01	<0.01	<0.01	<0.01
Au	<0.04	<0.03	<0.03	<0.03	<0.03	<0.03	<0.04	<0.03	<0.03
Total	102.95	103.27	101.36	102.41	106.85	105.82	100.94	99.27	97.96
Atoms Per Formula Unit (apfu)									
Zn	0.055	0.009	0.008	0.003	0.003	0.004	0.027	0.005	0.010
Cu	0.003	0.187	0.001	0.000	0.000	0.000	0.000	0.001	0.000
Ni	0.000	0.000	0.000	0.000	0.000	0.000	0.000	0.000	0.000
Co	0.000	0.001	0.000	0.001	0.001	0.000	0.000	0.000	0.000
Fe	0.122	0.472	0.258	0.488	0.479	0.325	0.054	0.249	0.282
Sb	0.000	0.000	0.000	0.000	0.000	0.000	0.000	0.000	0.000
Cd	0.000	0.000	0.000	0.000	0.000	0.000	0.000	0.000	0.000
Pb	0.973	0.095	0.613	0.006	0.097	0.410	0.973	0.640	0.541
S	1.000	1.000	1.000	1.000	1.000	1.000	1.000	1.000	1.000
As	0.000	0.000	0.000	0.000	0.000	0.000	0.000	0.000	0.000
Se	0.009	0.001	0.007	0.000	0.001	0.004	0.009	0.010	0.004
Ag	0.000	0.000	0.000	0.000	0.000	0.000	0.000	0.000	0.000
Au	0.000	0.000	0.000	0.000	0.000	0.000	0.000	0.000	0.000
Total	2.161	1.764	1.888	1.497	1.581	1.743	2.063	1.905	1.838

Table C12. EPMA results for galena continued.

Deposit	Betts Cove	Betts Cove
Drill Hole	BC-21-03	BC-21-07
Sample	KKMSC32-Gn14	KKMSC35-Gn1
Depth (m)	88	116.9
Date	2023_06_27	2023_06_29
Facies	Sphalerite-pyrite Dominated	Chalcopyrite-pyrrhotite Dominated
Weight Percent (wt%)		
Zn	0.39	<0.02
Cu	0.04	2.11
Ni	<0.02	<0.02
Co	<0.01	<0.01
Fe	4.33	1.51
Sb	<0.02	<0.02
Cd	0.02	0.01
Pb	78.65	73.5
S	15.1	4.55
As	<0.04	<0.03
Se	0.31	14.86
Ag	0.56	<0.01
Au	1.21	<0.03
Total	100.08	96.32
Atoms Per Formula Unit (apfu)		
Zn	0.013	0.000
Cu	0.001	0.234
Ni	0.000	0.000
Co	0.000	0.000
Fe	0.165	0.191
Sb	0.000	0.000
Cd	0.000	0.001
Pb	0.806	2.500
S	1.000	1.000
As	0.000	0.000
Se	0.008	1.326
Ag	0.011	0.000
Au	0.013	0.000
Total	2.017	5.251

Table C13. EPMA results for hessite. Data in red was omitted in discussion due to results being outside of the total cut-off for EPMA or it is inconsistent with SEM and reflected light mineral ID.

Deposit	Betts Cove	Betts Cove	Betts Cove	Betts Cove
Drill Hole	BC-21-03	BC-21-03	BC-21-08	BC-21-08
Sample	KKMSC35-AgTe1	KKMSC35-AgTe2	KKMSC53-AgTe1	KKMSC53-AgTe2
Depth (m)	116.9	116.9	28.7	28.7
Date	2023_06_29	2023_06_29	2023_07_19	2023_07_19
Facies	Chalcopyrite-pyrrhotite Dominated	Chalcopyrite-pyrrhotite Dominated	Chalcopyrite Dominated	Chalcopyrite Dominated
Weight Percent (wt%)				
Zn	0.04	0.02	<0.02	<0.02
Cu	1.07	1.44	0.51	0.24
Ni	<0.01	<0.01	<0.01	<0.01
Co	<0.01	<0.01	<0.01	<0.01
Fe	0.71	1.05	0.88	0.68
Sb	0.15	0.19	0.19	0.13
Cd	0.53	0.54	0.44	0.48
Pb	0.03	<0.03	0.05	0.05
S	0.08	0.13	0.14	0.17
As	<0.03	<0.03	<0.03	<0.04
Se	<0.02	<0.02	<0.04	<0.04
Te	37.77	37.27	40.03	39.67
Ag	61.23	60.57	58.81	58.76
Au	<0.03	0.17	<0.03	<0.03
Total	101.17	100.90	100.50	99.56
Atoms Per Formula Unit (apfu)				
Zn	0.002	0.001	0.000	0.000
Cu	0.057	0.078	0.026	0.012
Ni	0.000	0.000	0.000	0.000
Co	0.000	0.000	0.000	0.000
Fe	0.043	0.064	0.050	0.039
Sb	0.004	0.005	0.005	0.003
Cd	0.016	0.016	0.012	0.014
Pb	0.000	0.000	0.001	0.001
S	0.008	0.014	0.014	0.017
As	0.000	0.000	0.000	0.000
Se	0.000	0.000	0.000	0.000
Te	1.000	1.000	1.000	1.000
Ag	1.918	1.922	1.738	1.752
Au	0.000	0.003	0.000	0.000
Total	3.049	3.104	2.846	2.838

Table C14. EPMA results for magnetite. Data in red was omitted in discussion due to results being outside of the total cut-off for EPMA or it is inconsistent with SEM and reflected light mineral ID.

Deposit	Tilt Cove	Tilt Cove	Tilt Cove	Tilt Cove	Tilt Cove	Tilt Cove	Tilt Cove	Tilt Cove	Tilt Cove
Drill Hole	SZ-20-01	SZ-20-01	SZ-20-01	SZ-20-01	SZ-20-03	SZ-20-03	SZ-20-03	SZ-20-03	SZ-20-03
Sample	KKMSC13-Mag1	KKMSC13-Mag2	KKMSC13-Mag3	KKMSC13-Mag4	KKMSC23-Mag1	KKMSC23-Mag2	KKMSC23-Mag3	KKMSC23-Mag4	KKMSC23-Mag5
Depth (m)	66.6	66.6	66.6	66.6	17	17	17	17	17
Date	2023_07_17	2023_07_17	2023_07_17	2023_07_17	2023_06_29	2023_06_29	2023_06_29	2023_06_29	2023_06_29
Facies	Pyrite Dominated	Pyrite Dominated	Pyrite Dominated	Pyrite Dominated	Magnetite Dominated	Magnetite Dominated	Magnetite Dominated	Magnetite Dominated	Magnetite Dominated
Weight Percent (wt%)									
ZnO	<0.01	0.02	0.03	0.01	0.03	0.02	0.04	0.02	0.02
CoO	0.03	0.05	0.05	0.05	0.11	0.1	0.09	0.1	0.11
FeO	46.5	47.67	46.76	47.9	91.12	91.54	91.53	91.44	91.87
MnO	0.43	1.93	2.07	2.3	<0.01	<0.01	<0.01	<0.01	<0.01
Cr2O3	<0.01	<0.01	<0.01	<0.01	0.02	0.02	<0.01	0.03	<0.02
Al2O3	<0.01	<0.01	<0.01	<0.01	<0.01	<0.01	<0.01	<0.01	<0.01
V2O3	<0.01	<0.01	<0.01	<0.01	0.04	0.03	0.03	0.04	0.03
TiO2	<0.01	<0.01	<0.01	<0.01	<0.02	<0.02	<0.02	<0.02	<0.02
Total	46.95	49.65	48.89	50.23	91.33	91.72	91.67	91.65	92.03
Atoms Per Formula Unit (apfu)									
Fe3+	16.000	16.000	16.000	16.000	15.985	15.988	15.992	15.983	15.992
Fe2+	7.763	7.024	6.935	6.861	7.965	7.970	7.968	7.970	7.968
Zn	0.000	0.009	0.013	0.004	0.007	0.005	0.009	0.005	0.005
Co	0.015	0.023	0.024	0.023	0.028	0.025	0.023	0.025	0.028
Mn	0.223	0.944	1.028	1.112	0.000	0.000	0.000	0.000	0.000
Cr	0.000	0.000	0.000	0.000	0.005	0.005	0.000	0.007	0.000
Al	0.000	0.000	0.000	0.000	0.000	0.000	0.000	0.000	0.000
V	0.000	0.000	0.000	0.000	0.010	0.008	0.008	0.010	0.008
Ti	0.000	0.000	0.000	0.000	0.000	0.000	0.000	0.000	0.000
Total	24.000	24.000	24.000	24.000	24.000	24.000	24.000	24.000	24.000

Table C14. EPMA results for magnetite continued.

Deposit	Tilt Cove	Tilt Cove	Tilt Cove	Tilt Cove	Tilt Cove	Tilt Cove	Tilt Cove	Tilt Cove	Tilt Cove
Drill Hole	SZ-20-04	SZ-20-04	SZ-20-04	SZ-20-04	SZ-20-04	SZ-20-04	SZ-20-04	SZ-20-04	SZ-20-04
Sample	KKMSC63-Mag1	KKMSC63-Mag2	KKMSC63-Mag3	KKMSC63-Mag4	KKMSC63-Mag5	KKMSC63-Mag6	KKMSC63-Mag7	KKMSC63-Mag8	KKMSC63-Mag9
Depth (m)	64.45	64.45	64.45	64.45	64.45	64.45	64.45	64.45	64.45
Date	2023 06 30	2023 06 30	2023 06 30	2023 06 30	2023 06 30	2023 06 30	2023 06 30	2023 06 30	2023 06 30
Facies	Pyrite Dominated	Pyrite Dominated	Pyrite Dominated	Pyrite Dominated	Pyrite Dominated	Pyrite Dominated	Pyrite Dominated	Pyrite Dominated	Pyrite Dominated
Weight Percent (wt%)									
ZnO	<0.01	<0.01	0.05	<0.01	<0.01	<0.01	<0.01	<0.01	<0.01
CoO	0.09	0.11	0.07	0.11	0.09	0.1	0.58	0.1	0.22
FeO	88.8	58.45	88.29	90.52	88.97	90.05	57.71	89.63	58.31
MnO	<0.01	<0.01	<0.02	<0.02	<0.01	<0.01	<0.01	<0.01	<0.01
Cr2O3	0.03	<0.01	2.17	2.73	0.18	0.03	<0.01	<0.01	0.03
Al2O3	<0.01	<0.01	<0.01	<0.01	<0.01	<0.01	<0.01	<0.01	<0.01
V2O3	0.03	<0.01	0.03	0.04	0.03	0.02	<0.01	0.01	<0.01
TiO2	0.05	<0.02	0.09	0.02	0.05	0.05	<0.02	0.03	<0.02
Total	88.97	58.51	90.53	93.23	89.31	90.21	58.27	89.74	58.51
Atoms Per Formula Unit (apfu)									
Fe3+	15.960	16.000	15.406	15.317	15.922	15.963	16.000	15.983	15.988
Fe2+	7.989	7.957	7.992	7.977	7.989	7.986	7.771	7.982	7.914
Zn	0.000	0.000	0.012	0.000	0.000	0.000	0.000	0.000	0.000
Co	0.023	0.043	0.018	0.027	0.023	0.026	0.229	0.026	0.086
Mn	0.000	0.000	0.000	0.000	0.000	0.000	0.000	0.000	0.000
Cr	0.008	0.000	0.544	0.664	0.046	0.008	0.000	0.000	0.012
Al	0.000	0.000	0.000	0.000	0.000	0.000	0.000	0.000	0.000
V	0.008	0.000	0.008	0.010	0.008	0.005	0.000	0.003	0.000
Ti	0.012	0.000	0.021	0.005	0.012	0.012	0.000	0.007	0.000
Total	24.000	24.000	24.000	24.000	24.000	24.000	24.000	24.000	24.000

Table C14. EPMA results for magnetite continued.

Deposit	Tilt Cove	Tilt Cove	Tilt Cove	Tilt Cove	Tilt Cove	Tilt Cove	Tilt Cove	Tilt Cove	Tilt Cove
Drill Hole	SZ-20-04	SZ-20-04	SZ-20-04	SZ-20-04	SZ-20-04	SZ-20-04	SZ-20-04	SZ-20-04	SZ-20-04
Sample	KKMSC63-Mag10	KKMSC63-Mag11	KKMSC63-Mag12	KKMSC63-Mag13	KKMSC63-Mag14	KKMSC63-Mag15	KKMSC63-Mag16	KKMSC63-Mag17	KKMSC63-Mag18
Depth (m)	64.45	64.45	64.45	64.45	64.45	64.45	64.45	64.45	64.45
Date	2023 06 30	2023 06 30	2023 06 30	2023 06 30	2023 06 30	2023 06 30	2023 06 30	2023 06 30	2023 06 30
Facies	Pyrite Dominated	Pyrite Dominated	Pyrite Dominated	Pyrite Dominated	Pyrite Dominated	Pyrite Dominated	Pyrite Dominated	Pyrite Dominated	Pyrite Dominated
Weight Percent (wt%)									
ZnO	<0.01	0.02	0.01	<0.01	<0.01	<0.01	<0.01	<0.01	<0.01
CoO	0.12	0.1	0.1	0.09	0.09	0.11	0.08	0.09	0.09
FeO	90.62	90.64	89.75	90.92	88.45	90.74	88.05	90.43	90.03
MnO	<0.01	0.02	<0.01	<0.02	<0.02	<0.01	<0.01	<0.01	<0.01
Cr2O3	<0.02	<0.01	0.02	0.85	2.34	0.7	0.53	0.63	0.59
Al2O3	<0.01	<0.01	<0.01	<0.01	<0.01	<0.01	<0.01	<0.01	<0.01
V2O3	0.02	0.02	<0.01	0.04	0.02	0.03	0.03	0.04	0.02
TiO2	0.03	0.03	0.02	0.03	0.05	<0.02	0.05	0.02	0.02
Total	90.74	90.80	89.90	91.82	90.79	91.51	88.69	91.14	90.66
Atoms Per Formula Unit (apfu)									
Fe3+	15.981	15.981	15.985	15.766	15.387	15.819	15.832	15.824	15.838
Fe2+	7.977	7.972	7.977	7.985	7.989	7.972	7.991	7.982	7.982
Zn	0.000	0.005	0.002	0.000	0.000	0.000	0.000	0.000	0.000
Co	0.030	0.025	0.026	0.023	0.023	0.028	0.021	0.023	0.023
Mn	0.000	0.005	0.000	0.000	0.000	0.000	0.000	0.000	0.000
Cr	0.000	0.000	0.005	0.210	0.585	0.174	0.136	0.157	0.148
Al	0.000	0.000	0.000	0.000	0.000	0.000	0.000	0.000	0.000
V	0.005	0.005	0.000	0.010	0.005	0.008	0.008	0.010	0.005
Ti	0.007	0.007	0.005	0.007	0.012	0.000	0.012	0.005	0.005
Total	24.000	24.000	24.000	24.000	24.000	24.000	24.000	24.000	24.000

Table C14. EPMA results for magnetite continued.

Deposit	Tilt Cove	Tilt Cove	Tilt Cove	Tilt Cove	Tilt Cove	Tilt Cove	Tilt Cove	Tilt Cove	Tilt Cove
Drill Hole	SZ-20-04	SZ-20-05	SZ-20-05	SZ-20-05	SZ-20-05	SZ-20-05	SZ-20-05	SZ-20-05	SZ-20-05
Sample	KKMSC63-Mag19	KKMSC72-Mag1	KKMSC72-Mag2	KKMSC72-Mag3	KKMSC72-Mag4	KKMSC72-Mag5	KKMSC72-Mag6	KKMSC72-Mag7	KKMSC72-Mag8
Depth (m)	64.45	143.7	143.7	143.7	143.7	143.7	143.7	143.7	143.7
Date	2023 06 30	2023 07 14	2023 07 14	2023 07 14	2023 07 14	2023 07 14	2023 07 14	2023 07 14	2023 07 14
Facies	Pyrite Dominated	Pyrrhotite Dominated	Pyrrhotite Dominated	Pyrrhotite Dominated	Pyrrhotite Dominated	Pyrrhotite Dominated	Pyrrhotite Dominated	Pyrrhotite Dominated	Pyrrhotite Dominated
Weight Percent (wt%)									
ZnO	<0.01	<0.01	<0.01	<0.01	<0.01	<0.01	<0.01	<0.01	<0.01
CoO	0.1	0.1	0.1	0.09	0.1	0.11	0.1	0.1	0.09
FeO	88.38	91.4	91.37	92.1	91.98	91.86	91.47	91.76	91.2
MnO	<0.01	0.02	<0.01	<0.01	0.03	<0.01	<0.01	<0.01	0.01
Cr2O3	0.4	<0.01	0.49	<0.01	<0.01	<0.01	<0.01	<0.01	<0.01
Al2O3	<0.01	<0.01	<0.01	<0.01	<0.01	<0.01	<0.01	<0.01	<0.01
V2O3	0.03	<0.01	0.01	<0.01	0.01	<0.01	<0.01	<0.01	<0.01
TiO2	0.08	<0.02	<0.02	<0.02	<0.02	<0.02	<0.02	<0.02	<0.02
Total	88.97	91.51	91.92	92.17	92.11	91.94	91.56	91.85	91.31
Atoms Per Formula Unit (apfu)									
Fe3+	15.851	16.000	15.877	16.000	15.998	16.000	16.000	16.000	16.000
Fe2+	7.994	7.970	7.975	7.978	7.967	7.972	7.975	7.975	7.975
Zn	0.000	0.000	0.000	0.000	0.000	0.000	0.000	0.000	0.000
Co	0.026	0.025	0.025	0.022	0.025	0.028	0.025	0.025	0.023
Mn	0.000	0.005	0.000	0.000	0.008	0.000	0.000	0.000	0.003
Cr	0.102	0.000	0.121	0.000	0.000	0.000	0.000	0.000	0.000
Al	0.000	0.000	0.000	0.000	0.000	0.000	0.000	0.000	0.000
V	0.008	0.000	0.003	0.000	0.002	0.000	0.000	0.000	0.000
Ti	0.019	0.000	0.000	0.000	0.000	0.000	0.000	0.000	0.000
Total	24.000	24.000	24.000	24.000	24.000	24.000	24.000	24.000	24.000

Table C14. EPMA results for magnetite continued.

Deposit	Tilt Cove	Tilt Cove	Tilt Cove	Tilt Cove	Tilt Cove	Tilt Cove	Tilt Cove	Tilt Cove	Tilt Cove
Drill Hole	SZ-20-05	SZ-20-05	SZ-20-05	SZ-20-05	SZ-20-05	SZ-20-05	SZ-20-05	SZ-20-05	SZ-20-05
Sample	KKMSC72-Mag9	KKMSC72-Mag10	KKMSC72-Mag11	KKMSC72-Mag12	KKMSC72-Mag13	KKMSC72-Mag14	KKMSC72-Mag15	KKMSC72-Mag16	KKMSC72-Mag17
Depth (m)	143.7	143.7	143.7	143.7	143.7	143.7	143.7	143.7	143.7
Date	2023_07_14	2023_07_14	2023_07_14	2023_07_14	2023_07_14	2023_07_14	2023_07_14	2023_07_14	2023_07_14
Facies	Pyrrhotite Dominated	Pyrrhotite Dominated	Pyrrhotite Dominated	Pyrrhotite Dominated	Pyrrhotite Dominated	Pyrrhotite Dominated	Pyrrhotite Dominated	Pyrrhotite Dominated	Pyrrhotite Dominated
Weight Percent (wt%)									
ZnO	<0.01	<0.01	<0.01	<0.01	<0.01	<0.01	<0.01	0.02	<0.01
CoO	0.09	0.1	0.1	0.1	0.09	0.11	0.09	0.09	0.1
FeO	91.74	91.88	91.81	91.88	92.29	91.92	91.87	91.92	91.02
MnO	0.02	<0.01	<0.01	0.02	<0.01	0.02	0.03	<0.01	<0.01
Cr2O3	<0.01	<0.01	<0.01	<0.01	<0.01	<0.01	<0.01	0.48	0.46
Al2O3	<0.01	<0.01	<0.01	<0.01	<0.01	<0.01	<0.01	<0.01	<0.01
V2O3	<0.01	<0.01	<0.01	<0.01	<0.01	<0.01	<0.01	0.02	0.02
TiO2	0.02	<0.02	0.02	<0.02	<0.02	0.02	<0.02	0.03	<0.02
Total	91.83	91.93	91.92	91.97	92.39	92.03	91.93	92.49	91.56
Atoms Per Formula Unit (apfu)									
Fe3+	15.991	16.000	15.991	16.000	16.000	15.991	16.000	15.863	15.881
Fe2+	7.977	7.975	7.980	7.970	7.978	7.972	7.970	7.980	7.975
Zn	0.000	0.000	0.000	0.000	0.000	0.000	0.000	0.005	0.000
Co	0.023	0.025	0.025	0.025	0.022	0.027	0.023	0.022	0.025
Mn	0.005	0.000	0.000	0.005	0.000	0.005	0.008	0.000	0.000
Cr	0.000	0.000	0.000	0.000	0.000	0.000	0.000	0.118	0.114
Al	0.000	0.000	0.000	0.000	0.000	0.000	0.000	0.000	0.000
V	0.000	0.000	0.000	0.000	0.000	0.000	0.000	0.005	0.005
Ti	0.005	0.000	0.005	0.000	0.000	0.005	0.000	0.007	0.000
Total	24.000	24.000	24.000	24.000	24.000	24.000	24.000	24.000	24.000

Table C14. EPMA results for magnetite continued.

Deposit	Tilt Cove	Tilt Cove
Drill Hole	SZ-20-05	SZ-20-05
Sample	KKMSC72-Mag18	KKMSC72-Mag19
Depth (m)	143.7	143.7
Date	2023_07_14	2023_07_14
Facies	Pyrrhotite Dominated	Pyrrhotite Dominated
Weight Percent (wt%)		
ZnO	<0.01	<0.01
CoO	0.09	0.1
FeO	91.48	90.43
MnO	<0.01	<0.02
Cr2O3	0.21	1.49
Al2O3	<0.01	<0.01
V2O3	0.01	0.02
TiO2	0.02	<0.02
Total	91.80	91.91
Atoms Per Formula Unit (apfu)		
Fe3+	15.936	15.627
Fe2+	7.982	7.975
Zn	0.000	0.000
Co	0.023	0.025
Mn	0.000	0.000
Cr	0.052	0.368
Al	0.000	0.000
V	0.003	0.005
Ti	0.005	0.000
Total	24.000	24.000

Table C15. EPMA results for chromite. Data in red was omitted in discussion due to results being outside of the total cut-off for EPMA or it is inconsistent with SEM and reflected light mineral ID.

Deposit	Tilt Cove	Tilt Cove	Tilt Cove	Tilt Cove	Tilt Cove	Tilt Cove	Tilt Cove	Tilt Cove	Tilt Cove
Drill Hole	SZ-20-04	SZ-20-04	SZ-20-04	SZ-20-04	SZ-20-04	SZ-20-04	SZ-20-04	SZ-20-04	SZ-20-04
Sample	KKMSC63-Chr1	KKMSC63-Chr2	KKMSC63-Chr3	KKMSC63-Chr4	KKMSC63-Chr5	KKMSC63-Chr6	KKMSC63-Chr7	KKMSC63-Chr8	KKMSC63-Chr9
Depth (m)	64.45	64.45	64.45	64.45	64.45	64.45	64.45	64.45	64.45
Date	2023 07 19	2023 07 19	2023 07 19	2023 07 19	2023 07 19	2023 07 19	2023 07 19	2023 07 19	2023 07 19
Facies	Pyrite Dominated	Pyrite Dominated	Pyrite Dominated	Pyrite Dominated	Pyrite Dominated	Pyrite Dominated	Pyrite Dominated	Pyrite Dominated	Pyrite Dominated
Weight Percent (wt%)									
ZnO	0.12	0.13	0.11	0.13	0.12	0.12	0.12	0.12	0.13
CoO	0.07	0.07	0.07	0.08	0.08	0.06	0.07	0.06	0.06
FeO	24.7	24.97	25.6	26.4	25.96	25.54	25.86	25.56	24.36
MnO	0.32	0.31	0.34	0.34	0.34	0.34	0.33	0.34	0.32
Cr2O3	50.79	50.37	49.89	49.28	49.29	49.45	49.05	49.81	49.23
Al2O3	13.03	13.27	13.02	13.11	13.51	13.38	14.08	12.91	14.22
MgO	9.72	9.58	9.22	8.92	9.17	9.37	9.28	9.12	9.61
V2O3	0.19	0.2	0.2	0.22	0.21	0.21	0.21	0.2	0.21
TiO2	0.32	0.32	0.32	0.3	0.3	0.33	0.29	0.32	0.32
Total	99.25	99.22	98.77	98.79	98.97	98.80	99.29	98.44	98.46
Atoms Per Formula Unit (apfu)									
Fe3+	1.268	1.275	1.344	1.426	1.377	1.360	1.340	1.334	1.177
Fe2+	4.152	4.206	4.317	4.420	4.342	4.271	4.323	4.341	4.184
Zn	0.023	0.025	0.021	0.025	0.023	0.023	0.023	0.024	0.025
Co	0.015	0.015	0.015	0.017	0.017	0.013	0.015	0.013	0.013
Mn	0.071	0.069	0.076	0.076	0.076	0.076	0.073	0.076	0.071
Cr	10.536	10.452	10.429	10.317	10.266	10.307	10.156	10.456	10.242
Al	4.029	4.105	4.057	4.091	4.194	4.157	4.346	4.040	4.410
Mg	3.802	3.748	3.634	3.521	3.601	3.683	3.623	3.610	3.770
V	0.040	0.042	0.042	0.047	0.044	0.044	0.044	0.043	0.044
Ti	0.063	0.063	0.064	0.060	0.059	0.065	0.057	0.064	0.063
Total	24.000	24.000	24.000	24.000	24.000	24.000	24.000	24.000	24.000

Table C15. EPMA results for chromite continued.

Deposit	Tilt Cove	Tilt Cove	Tilt Cove	Tilt Cove	Tilt Cove	Tilt Cove
Drill Hole	SZ-20-04	SZ-20-04	SZ-20-05	SZ-20-05	SZ-20-05	SZ-20-05
Sample	KKMSC63-Chr10	KKMSC63-Chr11	KKMSC72-Chr1	KKMSC72-Chr2	KKMSC72-Chr3	KKMSC72-Chr4
Depth (m)	64.45	64.45	143.7	143.7	143.7	143.7
Date	2023_07_19	2023_07_19	2023_07_14	2023_07_14	2023_07_14	2023_07_14
Facies	Pyrite Dominated	Pyrite Dominated	Pyrrhotite Dominated	Pyrrhotite Dominated	Pyrrhotite Dominated	Pyrrhotite Dominated
Weight Percent (wt%)						
ZnO	0.13	0.13	0.11	0.13	0.12	0.13
CoO	0.07	0.07	0.05	0.05	0.06	0.06
FeO	26.28	25.7	18.29	18.49	18.47	18.82
MnO	0.33	0.32	0.1	0.11	0.09	0.11
Cr2O3	48.37	49.04	33.22	33.5	32.24	33.74
Al2O3	13.51	13.41	30.9	30.75	31.42	30.23
MgO	8.93	9.16	14.44	14.31	14.52	14.15
V2O3	0.19	0.21	0.24	0.25	0.25	0.25
TiO2	0.31	0.35	0.46	0.43	0.47	0.41
Total	98.13	98.39	97.81	98.02	97.64	97.89
Atoms Per Formula Unit (apfu)						
Fe3+	1.435	1.355	0.782	0.784	0.835	0.833
Fe2+	4.408	4.340	2.880	2.917	2.858	2.949
Zn	0.026	0.025	0.019	0.023	0.021	0.023
Co	0.015	0.015	0.010	0.010	0.012	0.012
Mn	0.074	0.072	0.020	0.022	0.018	0.022
Cr	10.167	10.273	6.288	6.339	6.094	6.410
Al	4.233	4.188	8.719	8.674	8.854	8.561
Mg	3.539	3.618	5.154	5.106	5.175	5.069
V	0.040	0.045	0.046	0.048	0.048	0.048
Ti	0.062	0.070	0.083	0.077	0.085	0.074
Total	24.000	24.000	24.000	24.000	24.000	24.000

Table C16. Detection limits EMPA.

Mineral	Pyrite		Chalcopyrite		Pyrrhotite		Sphalerite		Cobaltite		Pentlandite	
Element	LOD Min	LOD Max	LOD Min	LOD Max	LOD Min	LOD Max	LOD Min	LOD Max	LOD Min	LOD Max	LOD Min	LOD Max
Zn (ppm)	34.27	36.21	34.67	38.79	35.08	36.82	53.24	60.06	33.67	41.50	35.45	39.61
Cu (ppm)	28.37	30.23	40.57	47.68	29.34	30.74	32.02	34.75	27.95	34.85	29.77	33.14
Ni (ppm)	26.38	28.16	26.87	32.22	27.37	28.80	29.50	32.09	32.49	46.77	41.95	50.61
Co (ppm)	23.70	31.74	23.42	33.98	24.84	26.38	26.17	34.41	34.49	43.01	25.31	28.01
Fe (ppm)	37.39	40.79	35.87	173.33	37.99	41.85	27.45	29.93	29.68	36.91	35.39	39.95
Sb (ppm)	29.81	33.13	31.99	45.98	31.03	32.96	32.64	47.92	31.20	45.91	32.20	51.19
Cd (ppm)	25.42	29.19	26.01	30.84	26.63	28.59	27.90	29.61	25.29	30.82	26.90	31.02
Pb (ppm)	56.23	75.62	60.64	72.55	67.32	73.38	64.72	70.55	55.04	70.85	64.85	72.21
S (ppm)	10.25	28.20	19.96	102.07	24.23	27.00	21.10	29.42	18.01	24.66	24.54	27.97
As (ppm)	59.98	132.51	57.37	88.86	60.61	67.58	57.43	81.65	97.31	459.59	58.99	65.98
Se (ppm)	32.71	37.45	32.92	43.77	33.88	37.15	32.48	36.46	34.82	50.89	33.02	37.45
Te (ppm)	-	-	-	-	-	-	-	-	-	-	-	-
Ag (ppm)	26.21	30.35	26.52	30.83	27.66	29.52	28.14	30.27	26.85	31.78	27.55	31.01
Au (ppm)	68.41	83.79	66.64	81.78	66.82	81.89	65.01	80.69	66.37	82.00	66.62	81.39

Table C16. Detection limits EMPA continued.

Mineral	Acanthite		Arsenopyrite		Bornite		Clausthalite		Electrum		Galena	
Element	LOD Min	LOD Max	LOD Min	LOD Max	LOD Min	LOD Max	LOD Min	LOD Max	LOD Min	LOD Max	LOD Min	LOD Max
Zn (ppm)	48.12	53.07	39.67	41.04	39.61	40.47	45.86	61.53	52.99	66.73	35.91	62.02
Cu (ppm)	39.92	44.12	33.15	34.06	48.32	50.44	38.19	51.09	44.53	55.05	29.72	51.01
Ni (ppm)	37.99	41.15	31.33	31.91	31.20	31.97	35.57	47.83	41.79	50.73	27.51	47.86
Co (ppm)	32.19	35.13	27.76	28.68	26.83	28.26	31.49	40.90	36.44	43.95	25.44	40.98
Fe (ppm)	33.08	36.57	37.39	40.27	41.17	43.78	34.80	44.12	38.63	45.23	27.98	43.26
Sb (ppm)	35.53	38.97	34.37	35.20	33.88	34.89	36.82	46.30	41.05	45.00	30.98	47.18
Cd (ppm)	39.27	47.22	29.56	30.47	29.10	30.20	29.86	40.48	36.44	41.22	26.36	39.84
Pb (ppm)	76.16	80.67	65.08	68.72	64.25	69.15	74.63	179.43	85.00	90.69	105.97	182.01
S (ppm)	22.14	26.24	25.78	27.52	22.09	24.13	10.63	26.32	16.69	19.78	23.38	38.03
As (ppm)	80.27	103.17	125.59	132.71	60.32	64.57	92.57	147.87	86.65	99.36	63.03	118.76
Se (ppm)	41.38	48.22	48.83	50.86	33.64	35.27	65.67	97.14	44.72	57.45	35.53	55.50
Te (ppm)	-	-	-	-	-	-	32.86	49.95	-	-	-	-
Ag (ppm)	57.17	67.15	30.73	31.67	29.25	30.53	32.69	101.67	49.95	60.49	26.98	42.16
Au (ppm)	79.31	85.55	66.71	69.99	74.65	80.25	39.81	110.89	126.12	168.14	81.13	114.59

Table C16. Detection limits EMPA continued.

Mineral	Hessite	
Element	LOD Min	LOD Max
Zn (ppm)	39.47	61.16
Cu (ppm)	33.65	49.84
Ni (ppm)	31.08	46.81
Co (ppm)	27.65	40.06
Fe (ppm)	29.96	41.52
Sb (ppm)	35.47	50.55
Cd (ppm)	30.38	47.32
Pb (ppm)	69.30	125.20
S (ppm)	15.90	25.69
As (ppm)	64.88	124.65
Se (ppm)	36.27	142.54
Te (ppm)	46.24	75.70
Ag (ppm)	44.23	67.82
Au (ppm)	76.19	100.89

Table C16. Detection limits EMPA continued.

Mineral	Magnetite		Chromite	
Element	LOD Min	LOD Max	LOD Min	LOD Max
ZnO (ppm)	35.55	44.04	36.23	41.01
CoO (ppm)	25.68	32.80	25.26	28.38
FeO (ppm)	39.89	52.51	27.24	32.38
MnO (ppm)	31.69	58.18	32.04	38.12
Cr2O3 (ppm)	35.47	46.87	22.16	28.68
Al2O3 (ppm)	33.34	42.63	37.64	39.34
MgO (ppm)	-	-	39.51	44.36
V2O3 (ppm)	32.44	41.37	32.70	38.53
TiO2 (ppm)	41.35	53.36	43.57	50.14

Appendix D: Laser Ablation Inductively Coupled Plasma Mass Spectrometry (LA-ICP-MS) Results

Table D1. Trace element data for pyrite.

Deposit	Betts Cove	Betts Cove	Betts Cove	Betts Cove	Betts Cove	Betts Cove	Betts Cove	Betts Cove	Betts Cove
Sample	KKMSC05B_Py1	KKMSC05B_Py2	KKMSC05B_Py4	KKMSC05B_Py6	KKMSC05B_Py7	KKMSC05B_Py5	KKMSC05B_Py9	KKMSC05B_Py11	KKMSC05B_Py12
Date	2023-11-20	2023-11-20	2023-11-20	2023-11-20	2023-11-20	2023-11-20	2023-11-20	2023-11-20	2023-11-20
Facies	Chalcopyrite-dominated	Chalcopyrite-dominated	Chalcopyrite-dominated	Chalcopyrite-dominated	Chalcopyrite-dominated	Chalcopyrite-dominated	Chalcopyrite-dominated	Chalcopyrite-dominated	Chalcopyrite-dominated
Li7 (ppm)	BDL	BDL	BDL	BDL	9	BDL	BDL	BDL	BDL
Be9 (ppm)	BDL	BDL	-	BDL	BDL	BDL	BDL	-	BDL
B11 (ppm)	BDL	BDL	BDL	BDL	BDL	BDL	BDL	BDL	BDL
Na23 (ppm)	BDL	BDL	BDL	BDL	BDL	BDL	BDL	BDL	48
Mg24 (ppm)	2045	3550	4465	2738	38480	11358	1129	4456	4637
Al27 (ppm)	2186	3612	4129	2308	39545	10583	886	4092	4335
Si29 (ppm)	3351	5219	6087	3463	49699	14597	BDL	6092	6527
P31 (ppm)	BDL	BDL	BDL	BDL	BDL	BDL	BDL	BDL	BDL
S32 (ppm)	453302	477665	481674	448281	513213	504005	482569	494880	445288
K39 (ppm)	BDL	BDL	BDL	BDL	50	BDL	BDL	BDL	16
Ca44 (ppm)	BDL	BDL	BDL	BDL	4124	BDL	BDL	BDL	BDL
Sc45 (ppm)	1	2	2	BDL	14	4	BDL	2	2
Ti47 (ppm)	34	16	13	7	86	24	4	10	14
V51 (ppm)	5	7	10	6	94	21	2	9	10
Cr52 (ppm)	12	21	28	16	179	75	4	30	36
Mn55 (ppm)	44	59	90	55	904	250	11	87	96
Fe57 (ppm)	-	-	-	-	-	-	-	-	-
Co59 (ppm)	1015	1203	1186	1655	2536	1272	406	1200	1508
Ni60 (ppm)	100	167	176	-	182	222	56	165	-
Cu63 (ppm)	270	336	244	209	72	226	91	290	329
Zn66 (ppm)	8	11	13	18	128	31	4	13	20
Ga71 (ppm)	-	0	0	-	-	1	-	0	-
Ge73 (ppm)	BDL	BDL	BDL	-	BDL	BDL	BDL	-	BDL
As75 (ppm)	378	314	400	518	675	609	132	356	434
Se77 (ppm)	381	496	321	702	981	248	432	575	434
Rb85 (ppm)	BDL	BDL	BDL	BDL	0	BDL	BDL	BDL	BDL
Sr88 (ppm)	0	-	0	-	-	0	BDL	0	-
Y89 (ppm)	-	4	-	-	0	-	-	-	-
Zr90 (ppm)	-	-	BDL	BDL	-	-	-	BDL	BDL
Nb93 (ppm)	-	BDL	BDL	-	BDL	-	-	BDL	-
Mo95 (ppm)	-	2	1	2	-	1	3	1	0
Ru101 (ppm)	BDL	-	-	-	BDL	-	BDL	-	-
Rh103 (ppm)	BDL	BDL	-	-	-	-	-	BDL	BDL
Pd104 (ppm)	BDL	BDL	BDL	BDL	-	-	BDL	-	-

Pd105 (ppm)	-	-	BDL	BDL	-	BDL	BDL	BDL	-
Pd106 (ppm)	BDL	BDL	BDL	BDL	BDL	BDL	BDL	BDL	BDL
Ag107 (ppm)	1	3	5	3	1	14	0	2	2
Cd111 (ppm)	-	BDL	BDL	1	-	BDL	BDL	BDL	BDL
In115 (ppm)	-	0	-	-	0	BDL	-	BDL	BDL
Sn118 (ppm)	BDL	BDL	BDL	BDL	BDL	BDL	BDL	BDL	BDL
Sb121 (ppm)	12	12	9	26	22	12	6	11	13
Te125 (ppm)	103	166	147	120	22	171	25	157	215
Cs133 (ppm)	BDL	BDL	BDL	BDL	BDL	BDL	BDL	BDL	BDL
Ba137 (ppm)	-	BDL	-	-	-	-	-	-	-
La139 (ppm)	-	-	-	BDL	BDL	-	-	-	-
Ce140 (ppm)	BDL	-	BDL	BDL	BDL	-	BDL	-	-
Pr141 (ppm)	-	-	BDL	-	BDL	BDL	BDL	BDL	-
Nd146 (ppm)	-	-	-	-	-	-	-	-	-
Sm147 (ppm)	-	-	-	-	-	-	-	BDL	-
Eu153 (ppm)	-	BDL	-	-	-	-	-	-	-
Gd157 (ppm)	-	-	-	-	-	-	-	BDL	-
Tb159 (ppm)	-	-	-	BDL	BDL	-	-	-	-
Dy163 (ppm)	-	-	-	BDL	-	-	-	-	-
Ho165 (ppm)	BDL	-	-	-	-	-	-	-	-
Er166 (ppm)	-	-	-	-	-	-	-	-	-
Tm169 (ppm)	-	-	-	-	-	-	BDL	-	-
Yb172 (ppm)	-	-	-	-	-	-	-	-	-
Lu175 (ppm)	-	-	BDL	-	BDL	BDL	BDL	BDL	-
Hf178 (ppm)	-	-	-	-	BDL	-	-	-	-
Ta181 (ppm)	BDL	BDL	-	-	-	-	BDL	-	BDL
W182 (ppm)	-	-	BDL	-	-	BDL	-	-	BDL
Re185 (ppm)	-	BDL	BDL	BDL	BDL	BDL	BDL	BDL	BDL
Os189 (ppm)	BDL	BDL	BDL	BDL	BDL	BDL	BDL	BDL	BDL
Ir193 (ppm)	-	-	BDL	BDL	BDL	BDL	-	-	-
Pt195 (ppm)	-	BDL	BDL	BDL	-	BDL	BDL	BDL	-
Au197 (ppm)	-	-	-	-	-	2	-	2	-
Hg202 (ppm)	BDL	BDL	BDL	BDL	BDL	BDL	BDL	BDL	BDL
Pb204 (ppm)	138	130	114	153	BDL	138	BDL	154	182
Tl205 (ppm)	0	0	0	2	0	0	0	0	0
Pb206 (ppm)	102	-	126	160	-	151	-	154	192
Pb207 (ppm)	102	145	126	160	-	147	42	154	192
Pb208 (ppm)	99	146	125	161	17	-	44	155	191
Bi209 (ppm)	35	47	45	35	4	54	11	50	71
Th232 (ppm)	-	0	BDL	-	BDL	BDL	BDL	BDL	-
U238 (ppm)	-	-	-	BDL	-	BDL	-	BDL	BDL
PbTotal (ppm)	101	145	125	160	17	149	43	154	191

Table D1. Trace element data for pyrite continued.

Deposit	Betts Cove	Betts Cove	Betts Cove	Betts Cove	Betts Cove	Betts Cove	Betts Cove	Betts Cove	Betts Cove
Sample	KKMSC05B_Py13	KKMSC05B_Py15	KKMSC05B_Py17	KKMSC05B_Py18	KKMSC05B_Py19	KKMSC05B_Py20	KKMSC05B_Py21	KKMSC05B_Py22	KKMSC05B_Py24
Date	2023-11-20	2023-11-20	2023-11-20	2023-11-20	2023-11-20	2023-11-20	2023-11-20	2023-11-20	2023-11-20
Facies	Chalcopyrite-dominated	Chalcopyrite-dominated	Chalcopyrite-dominated	Chalcopyrite-dominated	Chalcopyrite-dominated	Chalcopyrite-dominated	Chalcopyrite-dominated	Chalcopyrite-dominated	Chalcopyrite-dominated
Li7 (ppm)	BDL	BDL	BDL	BDL	BDL	BDL	BDL	BDL	BDL
Be9 (ppm)	BDL	BDL	-	BDL	BDL	BDL	-	BDL	BDL
B11 (ppm)	BDL	BDL	BDL	BDL	BDL	BDL	BDL	BDL	BDL
Na23 (ppm)	BDL	42	57	BDL	43	BDL	BDL	38	BDL
Mg24 (ppm)	2165	7079	4315	374	5890	1048	2186	2201	2859
Al27 (ppm)	2157	7673	4500	247	5944	1561	2235	2348	3044
Si29 (ppm)	3550	9958	5968	BDL	8548	2187	3777	3523	4096
P31 (ppm)	BDL	BDL	BDL	BDL	BDL	BDL	BDL	BDL	BDL
S32 (ppm)	498400	484175	433402	508944	405626	464244	488326	465560	458947
K39 (ppm)	BDL	BDL	23	BDL	BDL	BDL	BDL	BDL	BDL
Ca44 (ppm)	BDL	BDL	BDL	353	BDL	BDL	BDL	BDL	BDL
Sc45 (ppm)	BDL	3	2	BDL	3	BDL	BDL	1	1
Ti47 (ppm)	7	15	12	BDL	12	6	5	8	8
V51 (ppm)	5	19	10	1	14	4	5	6	7
Cr52 (ppm)	15	74	43	BDL	63	10	10	11	16
Mn55 (ppm)	48	167	82	8	136	23	41	46	59
Fe57 (ppm)	-	-	-	-	-	-	-	-	-
Co59 (ppm)	699	518	1878	260	1254	661	595	900	1000
Ni60 (ppm)	137	126	330	106	381	383	153	165	-
Cu63 (ppm)	8837	11114	404	39612	191	7991	2734	5915	4146
Zn66 (ppm)	18	44	9	28	18	1121	12	33	21
Ga71 (ppm)	0	-	-	BDL	0	-	-	-	0
Ge73 (ppm)	BDL	BDL	-	-	BDL	-	BDL	BDL	-
As75 (ppm)	292	224	371	223	829	268	115	162	388
Se77 (ppm)	221	213	407	258	228	374	327	633	329
Rb85 (ppm)	BDL	BDL	BDL	BDL	BDL	BDL	BDL	BDL	BDL
Sr88 (ppm)	-	-	-	0	-	-	-	0	-
Y89 (ppm)	-	-	-	BDL	0	-	-	BDL	-
Zr90 (ppm)	-	-	-	-	-	-	-	-	-
Nb93 (ppm)	-	-	-	-	-	-	BDL	-	-
Mo95 (ppm)	1	3	1	1	1	-	11	3	-
Ru101 (ppm)	-	-	-	-	-	-	-	-	-
Rh103 (ppm)	-	-	-	-	-	0	-	0	BDL
Pd104 (ppm)	-	BDL	-	BDL	-	BDL	BDL	BDL	-

Pd105 (ppm)	BDL	BDL	BDL	1	-	0	BDL	-	BDL
Pd106 (ppm)	BDL	BDL	BDL	BDL	BDL	0	BDL	BDL	BDL
Ag107 (ppm)	10	18	2	6	8	5	13	23	14
Cd111 (ppm)	BDL	-	0	BDL	BDL	5	-	BDL	-
In115 (ppm)	-	0	-	2	BDL	2	-	-	-
Sn118 (ppm)	BDL	BDL	BDL	BDL	BDL	1	BDL	BDL	BDL
Sb121 (ppm)	18	9	7	4	22	18	7	11	9
Te125 (ppm)	90	65	259	-	166	-	84	-	140
Cs133 (ppm)	BDL	BDL	BDL	BDL	0	BDL	BDL	BDL	BDL
Ba137 (ppm)	-	-	-	-	-	-	-	-	-
La139 (ppm)	-	-	-	-	BDL	-	-	BDL	BDL
Ce140 (ppm)	-	-	-	-	-	-	-	BDL	-
Pr141 (ppm)	-	-	-	-	-	-	-	-	BDL
Nd146 (ppm)	-	-	BDL	-	BDL	-	-	-	-
Sm147 (ppm)	-	-	BDL	-	-	-	-	-	-
Eu153 (ppm)	BDL	-	-	-	-	-	-	-	-
Gd157 (ppm)	-	-	-	-	-	-	-	-	-
Tb159 (ppm)	-	-	-	-	-	-	-	-	-
Dy163 (ppm)	-	-	-	-	-	-	-	-	-
Ho165 (ppm)	-	-	-	-	-	-	-	-	-
Er166 (ppm)	-	-	-	-	-	-	-	-	-
Tm169 (ppm)	-	-	-	-	-	-	-	-	-
Yb172 (ppm)	-	-	-	-	-	-	-	-	-
Lu175 (ppm)	-	BDL	-	-	-	-	-	-	-
Hf178 (ppm)	-	-	-	-	-	-	1	-	-
Ta181 (ppm)	-	-	-	BDL	-	-	-	-	-
W182 (ppm)	BDL	BDL	BDL	-	-	-	-	-	-
Re185 (ppm)	-	BDL	-	BDL	-	BDL	0	BDL	BDL
Os189 (ppm)	BDL	BDL	BDL	BDL	BDL	BDL	BDL	BDL	BDL
Ir193 (ppm)	-	BDL	BDL	-	BDL	-	-	-	BDL
Pt195 (ppm)	BDL	BDL	-	-	-	-	BDL	BDL	BDL
Au197 (ppm)	-	-	-	-	-	-	-	1	-
Hg202 (ppm)	BDL	BDL	BDL	BDL	BDL	BDL	6	BDL	8
Pb204 (ppm)	106	80	144	58	162	83	141	127	120
Tl205 (ppm)	0	0	1	BDL	0	0	0	0	0
Pb206 (ppm)	-	-	159	43	-	83	-	108	109
Pb207 (ppm)	-	82	161	45	172	84	-	-	-
Pb208 (ppm)	101	79	159	44	178	81	63	90	107
Bi209 (ppm)	30	31	65	3	53	23	30	33	43
Th232 (ppm)	-	-	-	-	-	-	-	-	BDL
U238 (ppm)	BDL	-	-	-	-	BDL	-	-	-
PbTotal (ppm)	102	80	159	44	178	82	65	107	108

Table D1. Trace element data for pyrite continued.

Deposit	Betts Cove	Betts Cove	Betts Cove	Betts Cove	Betts Cove	Betts Cove	Betts Cove	Betts Cove	Betts Cove
Sample	KKMSC05B_Py25	KKMSC05B_Py26	KKMSC05B_Py27	KKMSC05B_Py28	KKMSC05B_Py29	KKMSC05B_Py30	KKMSC05B_Py31	KKMSC05B_Py32	KKMSC05B_Py33
Date	2023-11-20	2023-11-20	2023-11-20	2023-11-20	2023-11-20	2023-11-20	2023-11-20	2023-11-20	2023-11-20
Facies	Chalcopyrite-dominated	Chalcopyrite-dominated	Chalcopyrite-dominated	Chalcopyrite-dominated	Chalcopyrite-dominated	Chalcopyrite-dominated	Chalcopyrite-dominated	Chalcopyrite-dominated	Chalcopyrite-dominated
Li7 (ppm)	BDL	BDL	BDL	BDL	BDL	BDL	BDL	BDL	BDL
Be9 (ppm)	-	BDL	BDL	BDL	BDL	-	BDL	BDL	BDL
B11 (ppm)	BDL	BDL	BDL	BDL	BDL	BDL	BDL	BDL	BDL
Na23 (ppm)	BDL	BDL	BDL	BDL	BDL	BDL	BDL	BDL	BDL
Mg24 (ppm)	3448	BDL	1526	110	60	2977	381	103	217
Al27 (ppm)	3439	BDL	1297	110	29	2939	24	59	40
Si29 (ppm)	5317	BDL	2887	BDL	BDL	17331	BDL	BDL	1264
P31 (ppm)	BDL	BDL	BDL	BDL	BDL	BDL	BDL	BDL	BDL
S32 (ppm)	522809	476802	403384	376987	403661	428015	429540	430493	476548
K39 (ppm)	BDL	BDL	23	BDL	BDL	BDL	BDL	BDL	BDL
Ca44 (ppm)	BDL	BDL	BDL	BDL	BDL	BDL	BDL	BDL	BDL
Sc45 (ppm)	2	BDL	BDL	BDL	BDL	BDL	BDL	BDL	BDL
Ti47 (ppm)	7	BDL	BDL	BDL	BDL	BDL	BDL	BDL	BDL
V51 (ppm)	8	BDL	3	BDL	BDL	7	BDL	BDL	BDL
Cr52 (ppm)	21	BDL	BDL	BDL	BDL	BDL	BDL	BDL	BDL
Mn55 (ppm)	86	1	39	7	7	72	39	6	7
Fe57 (ppm)	-	-	-	-	-	-	-	-	-
Co59 (ppm)	1176	25	1315	403	1287	1282	918	759	478
Ni60 (ppm)	189	-	331	-	423	207	59	165	64
Cu63 (ppm)	13646	63	1685	4405	270	5144	1563	1434	1149
Zn66 (ppm)	40	BDL	16	21	4	27	266	4	5
Ga71 (ppm)	-	-	-	-	-	-	-	BDL	BDL
Ge73 (ppm)	-	BDL	BDL	BDL	-	BDL	BDL	-	BDL
As75 (ppm)	402	90	778	360	604	446	604	438	439
Se77 (ppm)	837	21	693	80	224	243	184	174	73
Rb85 (ppm)	BDL	BDL	BDL	BDL	BDL	BDL	BDL	BDL	BDL
Sr88 (ppm)	-	-	-	-	-	-	-	-	-
Y89 (ppm)	-	-	-	-	-	BDL	-	BDL	-
Zr90 (ppm)	-	-	BDL	-	-	-	-	-	BDL
Nb93 (ppm)	BDL	BDL	BDL	-	-	BDL	-	-	-
Mo95 (ppm)	-	0	-	5	-	-	1	-	4
Ru101 (ppm)	-	-	-	-	-	-	-	-	-
Rh103 (ppm)	-	-	-	BDL	-	-	-	-	-
Pd104 (ppm)	0	BDL	2	0	1	-	-	BDL	BDL

Pd105 (ppm)	0	BDL	BDL	BDL	-	0	BDL	BDL	BDL
Pd106 (ppm)	BDL	BDL	-	0	1	-	-	-	-
Ag107 (ppm)	77	0	58	6	4	29	7	9	12
Cd111 (ppm)	-	BDL	BDL	-	0	BDL	2	-	BDL
In115 (ppm)	1	-	0	-	-	0	0	-	0
Sn118 (ppm)	BDL	BDL	BDL	BDL	BDL	BDL	BDL	BDL	BDL
Sb121 (ppm)	19	0	71	26	47	22	17	25	12
Te125 (ppm)	168	1	252	95	453	-	93	75	55
Cs133 (ppm)	BDL	BDL	BDL	BDL	BDL	BDL	BDL	BDL	BDL
Ba137 (ppm)	-	-	-	BDL	-	-	-	-	-
La139 (ppm)	-	-	-	-	-	-	-	-	-
Ce140 (ppm)	-	-	BDL	-	-	-	-	-	-
Pr141 (ppm)	-	-	-	-	-	-	-	-	-
Nd146 (ppm)	-	-	-	-	-	-	-	-	-
Sm147 (ppm)	-	-	-	-	-	-	-	-	-
Eu153 (ppm)	-	-	-	-	-	-	-	-	-
Gd157 (ppm)	-	BDL	-	-	-	-	-	-	-
Tb159 (ppm)	-	-	-	-	-	-	-	-	-
Dy163 (ppm)	-	-	-	-	-	-	-	-	-
Ho165 (ppm)	-	-	-	-	-	-	-	-	-
Er166 (ppm)	BDL	-	-	-	-	-	-	-	-
Tm169 (ppm)	-	-	-	-	-	BDL	-	-	-
Yb172 (ppm)	-	-	-	-	-	-	-	-	-
Lu175 (ppm)	BDL	-	-	-	-	-	-	-	-
Hf178 (ppm)	BDL	-	-	-	-	-	-	-	-
Ta181 (ppm)	-	-	-	-	-	-	-	-	-
W182 (ppm)	-	-	0	-	-	-	-	-	-
Re185 (ppm)	BDL	BDL	BDL	BDL	BDL	BDL	BDL	-	-
Os189 (ppm)	BDL	BDL	BDL	BDL	BDL	BDL	BDL	BDL	BDL
Ir193 (ppm)	BDL	-	-	-	-	-	BDL	-	-
Pt195 (ppm)	BDL	BDL	-	BDL	BDL	-	BDL	BDL	BDL
Au197 (ppm)	-	-	-	2	11	1	1	-	-
Hg202 (ppm)	BDL	BDL	BDL	3	BDL	BDL	BDL	BDL	BDL
Pb204 (ppm)	225	BDL	3709	122	382	140	382	131	198
Tl205 (ppm)	0	1	1	2	14	0	0	0	1
Pb206 (ppm)	211	4	-	103	412	-	458	119	-
Pb207 (ppm)	-	-	4464	97	422	-	426	125	185
Pb208 (ppm)	212	4	4485	113	430	154	426	-	201
Bi209 (ppm)	45	0	80	35	174	45	28	31	26
Th232 (ppm)	-	BDL	-	-	-	-	-	-	-
U238 (ppm)	-	-	-	-	-	-	-	-	-
PbTotal (ppm)	211	4	4416	107	423	144	433	123	194

Table D1. Trace element data for pyrite continued.

Deposit	Betts Cove	Betts Cove	Betts Cove	Betts Cove	Betts Cove	Betts Cove	Betts Cove	Betts Cove	Betts Cove
Sample	KKMSC05B_Py34	KKMSC09_Py1	KKMSC09_Py2	KKMSC09_Py3	KKMSC09_Py4	KKMSC09_Py5	KKMSC09_Py6	KKMSC09_Py8	KKMSC09_Py9
Date	2023-11-20	2023-11-20	2023-11-20	2023-11-20	2023-11-20	2023-11-20	2023-11-20	2023-11-20	2023-11-20
Facies	Chalcopyrite-dominated	Chalcopyrite-dominated	Chalcopyrite-dominated	Chalcopyrite-dominated	Chalcopyrite-dominated	Chalcopyrite-dominated	Chalcopyrite-dominated	Chalcopyrite-dominated	Chalcopyrite-dominated
Li7 (ppm)	BDL	5	3	BDL	BDL	BDL	BDL	BDL	BDL
Be9 (ppm)	BDL	BDL	BDL	-	BDL	BDL	BDL	BDL	BDL
B11 (ppm)	BDL	BDL	BDL	BDL	BDL	BDL	BDL	BDL	BDL
Na23 (ppm)	BDL	BDL	BDL	BDL	BDL	BDL	35	BDL	BDL
Mg24 (ppm)	158	7729	891	2471	3456	1959	3880	1209	645
Al27 (ppm)	91	9932	1152	2856	4458	1942	4903	1621	723
Si29 (ppm)	1225	12419	2757	4845	5998	3401	6114	2739	1327
P31 (ppm)	BDL	BDL	BDL	BDL	BDL	BDL	BDL	BDL	BDL
S32 (ppm)	525966	534215	447059	427104	425186	401005	366614	444767	411177
K39 (ppm)	BDL	BDL	BDL	41	55	55	51	BDL	BDL
Ca44 (ppm)	BDL	BDL	BDL	BDL	BDL	BDL	BDL	BDL	BDL
Sc45 (ppm)	BDL	4	BDL	BDL	3	1	3	BDL	BDL
Ti47 (ppm)	BDL	39	BDL	10	12	5	12	BDL	BDL
V51 (ppm)	BDL	27	4	9	13	7	15	5	3
Cr52 (ppm)	BDL	67	12	16	23	10	19	7	BDL
Mn55 (ppm)	5	309	48	99	155	98	179	48	64
Fe57 (ppm)	-	-	-	-	-	-	-	-	-
Co59 (ppm)	1137	1663	1180	2375	2675	2590	3809	945	2523
Ni60 (ppm)	79	148	-	197	205	-	299	47	-
Cu63 (ppm)	60368	7791	2536	42167	39511	34788	5101	9311	1128
Zn66 (ppm)	181	56	145	108	53	31	28	29	13
Ga71 (ppm)	BDL	1	-	-	-	-	-	0	0
Ge73 (ppm)	-	15	4	5	2	3	4	-	3
As75 (ppm)	467	3645	1316	3339	3799	3472	1444	5687	2097
Se77 (ppm)	458	1127	770	1172	853	980	444	1311	1453
Rb85 (ppm)	BDL	BDL	BDL	BDL	BDL	BDL	BDL	BDL	BDL
Sr88 (ppm)	-	-	-	-	-	-	-	-	-
Y89 (ppm)	-	-	-	-	-	-	-	-	-
Zr90 (ppm)	-	-	-	-	121	-	-	12	-
Nb93 (ppm)	-	-	BDL	BDL	-	-	BDL	BDL	BDL
Mo95 (ppm)	1	-	66	16	15	26	14	3	21
Ru101 (ppm)	BDL	-	-	-	-	-	BDL	-	-
Rh103 (ppm)	-	BDL	-	-	-	0	-	-	BDL
Pd104 (ppm)	-	-	-	-	-	-	-	-	2

Pd105 (ppm)	-	-	BDL	1	1	-	-	BDL	-
Pd106 (ppm)	-	BDL	BDL	BDL	0	0	0	BDL	-
Ag107 (ppm)	17	52	38	147	128	157	129	28	47
Cd111 (ppm)	-	BDL	1	-	1	-	-	-	-
In115 (ppm)	-	-	1	-	-	-	1	-	-
Sn118 (ppm)	1	BDL	BDL	BDL	BDL	BDL	BDL	BDL	BDL
Sb121 (ppm)	27	22	17	58	51	50	64	14	30
Te125 (ppm)	58	212	-	363	394	-	527	-	229
Cs133 (ppm)	BDL	BDL	BDL	BDL	BDL	BDL	BDL	BDL	BDL
Ba137 (ppm)	-	-	-	-	-	-	-	-	-
La139 (ppm)	-	-	-	-	BDL	-	-	-	-
Ce140 (ppm)	0	-	-	-	-	-	-	-	-
Pr141 (ppm)	BDL	-	BDL	BDL	-	-	-	-	-
Nd146 (ppm)	-	-	-	-	-	-	-	-	-
Sm147 (ppm)	-	-	-	-	-	-	-	-	-
Eu153 (ppm)	-	-	-	-	-	-	-	-	-
Gd157 (ppm)	-	-	BDL	-	-	-	-	-	-
Tb159 (ppm)	-	-	-	-	-	-	-	-	-
Dy163 (ppm)	-	-	-	-	-	-	-	-	-
Ho165 (ppm)	-	-	-	-	-	-	-	-	-
Er166 (ppm)	-	-	-	-	-	-	-	-	-
Tm169 (ppm)	-	-	-	-	-	-	-	-	-
Yb172 (ppm)	-	-	-	-	-	-	-	-	-
Lu175 (ppm)	-	-	-	-	-	-	-	-	-
Hf178 (ppm)	-	-	-	-	3	-	-	-	-
Ta181 (ppm)	-	-	-	-	-	-	-	-	-
W182 (ppm)	-	BDL	-	-	-	-	-	-	-
Re185 (ppm)	BDL	BDL	BDL	BDL	BDL	0	BDL	BDL	BDL
Os189 (ppm)	BDL	BDL	BDL	BDL	BDL	BDL	BDL	-	BDL
Ir193 (ppm)	-	-	-	-	-	BDL	-	-	BDL
Pt195 (ppm)	BDL	-	-	-	BDL	BDL	-	BDL	-
Au197 (ppm)	-	-	1	2	-	-	-	-	-
Hg202 (ppm)	BDL	BDL	BDL	BDL	BDL	BDL	BDL	BDL	BDL
Pb204 (ppm)	125	968	287	4904	2516	3455	2831	1139	2471
Tl205 (ppm)	0	1	1	3	2	2	2	1	1
Pb206 (ppm)	124	963	-	5454	2751	3623	3171	1188	2647
Pb207 (ppm)	-	-	-	5502	2714	3743	3074	1189	2610
Pb208 (ppm)	-	933	313	5354	2690	3712	3146	1299	2604
Bi209 (ppm)	17	36	29	88	75	77	98	22	52
Th232 (ppm)	-	-	-	-	-	-	-	-	-
U238 (ppm)	-	-	-	-	-	-	-	-	-
PbTotal (ppm)	112	938	312	5404	2708	3693	3133	1246	2615

Table D1. Trace element data for pyrite continued.

Deposit	Betts Cove	Betts Cove	Betts Cove	Betts Cove	Betts Cove	Betts Cove	Betts Cove	Betts Cove	Betts Cove
Sample	KKMSC09_Py10	KKMSC09_Py11	KKMSC09_Py12	KKMSC09_Py13	KKMSC09_Py14	KKMSC09_Py15	KKMSC09_Py16	KKMSC09_Py17	KKMSC09_Py18
Date	2023-11-20	2023-11-20	2023-11-20	2023-11-20	2023-11-20	2023-11-20	2023-11-20	2023-11-20	2023-11-20
Facies	Chalcopyrite-dominated	Chalcopyrite-dominated	Chalcopyrite-dominated	Chalcopyrite-dominated	Chalcopyrite-dominated	Chalcopyrite-dominated	Chalcopyrite-dominated	Chalcopyrite-dominated	Chalcopyrite-dominated
Li7 (ppm)	BDL	BDL	BDL	BDL	BDL	8	BDL	BDL	BDL
Be9 (ppm)	BDL	BDL	BDL	BDL	-	BDL	BDL	BDL	BDL
B11 (ppm)	BDL	BDL	BDL	BDL	BDL	BDL	BDL	BDL	BDL
Na23 (ppm)	BDL	BDL	BDL	BDL	BDL	BDL	BDL	BDL	BDL
Mg24 (ppm)	259	-	500	613	45	38732	634	BDL	26
Al27 (ppm)	276	174	682	510	13	50623	782	BDL	23
Si29 (ppm)	BDL	BDL	6184	27480	BDL	124067	2012	BDL	BDL
P31 (ppm)	BDL	BDL	BDL	BDL	BDL	BDL	BDL	BDL	54
S32 (ppm)	395502	429060	435551	437580	412463	444311	392829	424653	407842
K39 (ppm)	BDL	BDL	BDL	BDL	BDL	BDL	BDL	BDL	BDL
Ca44 (ppm)	BDL	BDL	BDL	BDL	BDL	274	BDL	BDL	BDL
Sc45 (ppm)	BDL	BDL	BDL	BDL	BDL	23	BDL	BDL	BDL
Ti47 (ppm)	BDL	BDL	BDL	BDL	2	50	15	BDL	BDL
V51 (ppm)	1	0	1	2	BDL	136	2	BDL	BDL
Cr52 (ppm)	BDL	BDL	13	8	BDL	525	6	BDL	BDL
Mn55 (ppm)	11	5	43	26	10	1676	32	BDL	3
Fe57 (ppm)	-	-	-	-	-	-	-	-	-
Co59 (ppm)	327	1398	1996	2755	2374	508	2752	2256	1295
Ni60 (ppm)	37	-	153	248	-	136	263	134	72
Cu63 (ppm)	1231	8532	93379	15284	273	221	9153	134	29
Zn66 (ppm)	16	26	1142	29	12	206	47	BDL	20
Ga71 (ppm)	0	-	0	-	BDL	-	-	-	-
Ge73 (ppm)	-	-	4	4	2	-	3	BDL	BDL
As75 (ppm)	4822	4123	2223	4870	2060	958	3355	30	4
Se77 (ppm)	1182	1209	623	1086	845	480	1329	254	87
Rb85 (ppm)	BDL	BDL	BDL	BDL	BDL	BDL	BDL	BDL	BDL
Sr88 (ppm)	-	-	0	-	-	-	-	-	1
Y89 (ppm)	-	-	-	-	-	-	BDL	-	-
Zr90 (ppm)	-	-	-	-	-	-	-	-	-
Nb93 (ppm)	-	BDL	-	-	-	-	-	BDL	-
Mo95 (ppm)	9	-	-	-	17	2553	-	-	-
Ru101 (ppm)	-	-	-	-	-	-	-	-	-
Rh103 (ppm)	BDL	0	-	0	BDL	-	-	-	-
Pd104 (ppm)	-	-	-	-	-	-	-	-	BDL

Pd105 (ppm)	-	-	-	1	BDL	-	0	-	-
Pd106 (ppm)	BDL	-	BDL	BDL	BDL	1	BDL	BDL	BDL
Ag107 (ppm)	13	34	38	130	20	18	277	1	5
Cd111 (ppm)	BDL	-	-	-	BDL	BDL	-	BDL	BDL
In115 (ppm)	-	-	11	-	-	0	-	-	-
Sn118 (ppm)	BDL	BDL	BDL	BDL	BDL	BDL	BDL	BDL	BDL
Sb121 (ppm)	11	6	13	46	15	10	25	2	0
Te125 (ppm)	85	75	75	385	209	84	-	32	17
Cs133 (ppm)	BDL	BDL	BDL	BDL	BDL	0	BDL	BDL	BDL
Ba137 (ppm)	-	-	-	-	-	-	-	-	2
La139 (ppm)	-	-	-	-	-	-	-	BDL	-
Ce140 (ppm)	-	-	-	BDL	-	-	-	-	-
Pr141 (ppm)	-	-	-	-	-	-	-	-	-
Nd146 (ppm)	-	-	-	-	-	-	-	-	-
Sm147 (ppm)	-	-	-	-	-	-	-	-	-
Eu153 (ppm)	-	-	-	-	-	-	-	-	-
Gd157 (ppm)	-	-	-	-	-	BDL	-	-	-
Tb159 (ppm)	-	-	-	-	-	-	-	-	-
Dy163 (ppm)	-	-	-	-	-	-	-	-	-
Ho165 (ppm)	-	-	-	-	-	-	-	-	-
Er166 (ppm)	-	-	-	-	-	-	-	-	BDL
Tm169 (ppm)	-	-	-	BDL	-	-	-	-	-
Yb172 (ppm)	-	-	-	-	-	-	-	-	-
Lu175 (ppm)	-	-	-	-	-	-	-	-	-
Hf178 (ppm)	-	-	-	-	-	-	-	-	-
Ta181 (ppm)	-	-	-	-	-	-	-	-	-
W182 (ppm)	-	BDL	-	-	0	-	0	-	-
Re185 (ppm)	BDL	BDL	BDL	-	BDL	7	-	BDL	BDL
Os189 (ppm)	BDL	BDL	BDL	BDL	BDL	BDL	BDL	BDL	BDL
Ir193 (ppm)	-	-	-	-	-	BDL	BDL	-	BDL
Pt195 (ppm)	BDL	BDL	-	BDL	BDL	BDL	-	-	BDL
Au197 (ppm)	-	3	-	-	16	-	-	-	-
Hg202 (ppm)	BDL	BDL	BDL	BDL	BDL	BDL	BDL	BDL	8
Pb204 (ppm)	778	2004	156	2112	380	353	1877	BDL	51
Tl205 (ppm)	1	1	1	1	1	1	1	1	BDL
Pb206 (ppm)	1004	2536	-	-	-	-	2096	32	6
Pb207 (ppm)	869	2196	178	2425	371	-	-	31	6
Pb208 (ppm)	901	2294	-	2468	369	397	1994	32	6
Bi209 (ppm)	17	13	19	76	28	22	48	5	BDL
Th232 (ppm)	-	-	-	-	-	-	-	-	-
U238 (ppm)	-	-	-	-	-	-	-	-	-
PbTotal (ppm)	918	2329	171	2467	372	398	2022	32	6

Table D1. Trace element data for pyrite continued.

Deposit	Betts Cove	Betts Cove	Betts Cove	Betts Cove	Betts Cove	Betts Cove	Betts Cove	Betts Cove	Betts Cove
Sample	KKMSC09_Py19	KKMSC09_Py20	KKMSC09_Py21	KKMSC09_Py22	KKMSC09_Py23	KKMSC09_Py24	KKMSC09_Py25	KKMSC09_Py26	KKMSC09_Py28
Date	2023-11-20	2023-11-20	2023-11-20	2023-11-20	2023-11-20	2023-11-20	2023-11-20	2023-11-20	2023-11-20
Facies	Chalcopyrite-dominated	Chalcopyrite-dominated	Chalcopyrite-dominated	Chalcopyrite-dominated	Chalcopyrite-dominated	Chalcopyrite-dominated	Chalcopyrite-dominated	Chalcopyrite-dominated	Chalcopyrite-dominated
Li7 (ppm)	BDL	BDL	BDL	BDL	7	BDL	4	BDL	BDL
Be9 (ppm)	BDL	BDL	-	BDL	BDL	BDL	BDL	BDL	BDL
B11 (ppm)	BDL	BDL	BDL	BDL	BDL	BDL	BDL	BDL	BDL
Na23 (ppm)	BDL	BDL	BDL	BDL	BDL	BDL	BDL	BDL	BDL
Mg24 (ppm)	2	2983	143	968	64353	380	192	25	37
Al27 (ppm)	BDL	3357	58	970	73715	390	212	32	46
Si29 (ppm)	BDL	4735	939	2056	81660	1275	BDL	630	BDL
P31 (ppm)	BDL	BDL	BDL	BDL	BDL	BDL	59	BDL	BDL
S32 (ppm)	407107	469536	444090	405505	396392	531857	553643	457751	407512
K39 (ppm)	BDL	25	BDL	BDL	BDL	BDL	BDL	BDL	BDL
Ca44 (ppm)	BDL	BDL	BDL	BDL	BDL	BDL	BDL	BDL	BDL
Sc45 (ppm)	BDL	BDL	BDL	BDL	11	BDL	BDL	BDL	BDL
Ti47 (ppm)	BDL	BDL	3	BDL	68	BDL	BDL	BDL	BDL
V51 (ppm)	BDL	7	1	3	175	1	1	BDL	BDL
Cr52 (ppm)	BDL	BDL	BDL	BDL	BDL	BDL	3	BDL	BDL
Mn55 (ppm)	1	118	19	43	2051	21	11	5	3
Fe57 (ppm)	-	-	-	-	-	-	-	-	-
Co59 (ppm)	256	916	3337	2724	1368	1788	819	1334	1612
Ni60 (ppm)	16	149	-	305	147	155	40	71	145
Cu63 (ppm)	2381	22338	2462	42002	530	16203	3870	63	49
Zn66 (ppm)	4642	202	3561	833	320	674	2187	1704	12
Ga71 (ppm)	BDL	-	BDL	-	8	-	-	-	-
Ge73 (ppm)	-	-	-	BDL	BDL	BDL	-	-	-
As75 (ppm)	460	1799	1599	1023	1555	2063	1228	548	36
Se77 (ppm)	549	791	2336	448	718	1455	738	309	110
Rb85 (ppm)	BDL	BDL	BDL	0	BDL	BDL	BDL	BDL	BDL
Sr88 (ppm)	-	-	-	-	-	-	-	1	-
Y89 (ppm)	-	-	BDL	-	-	-	-	-	-
Zr90 (ppm)	-	-	-	-	-	-	-	-	-
Nb93 (ppm)	-	-	-	BDL	BDL	-	-	-	-
Mo95 (ppm)	BDL	0	-	-	BDL	1	BDL	-	-
Ru101 (ppm)	-	-	-	-	-	-	-	-	-
Rh103 (ppm)	-	0	-	-	BDL	-	-	-	-
Pd104 (ppm)	BDL	-	-	1	-	-	-	-	-

Pd105 (ppm)	-	-	-	-	-	-	BDL	-	-
Pd106 (ppm)	1	-	-	0	BDL	0	0	-	BDL
Ag107 (ppm)	12	112	4602	256	31	109	23	3	0
Cd111 (ppm)	-	4	14	-	-	5	-	3	-
In115 (ppm)	-	-	-	-	-	6	-	10	-
Sn118 (ppm)	BDL	BDL	1	BDL	BDL	BDL	BDL	BDL	BDL
Sb121 (ppm)	4	41	-	46	7	-	12	0	-
Te125 (ppm)	-	408	2651	510	51	362	140	80	21
Cs133 (ppm)	BDL	BDL	BDL	BDL	BDL	BDL	BDL	BDL	BDL
Ba137 (ppm)	-	-	-	-	-	-	-	-	-
La139 (ppm)	-	-	-	-	-	-	-	-	-
Ce140 (ppm)	-	-	-	-	-	-	-	-	-
Pr141 (ppm)	BDL	BDL	-	-	-	BDL	-	BDL	-
Nd146 (ppm)	-	-	-	-	-	-	-	-	-
Sm147 (ppm)	-	-	-	-	-	-	-	-	-
Eu153 (ppm)	-	-	-	-	-	-	-	-	-
Gd157 (ppm)	-	-	-	-	-	-	-	-	-
Tb159 (ppm)	-	BDL	-	-	-	-	-	-	-
Dy163 (ppm)	-	-	-	-	-	-	-	-	-
Ho165 (ppm)	-	-	-	-	-	-	-	-	-
Er166 (ppm)	-	-	-	-	-	-	-	-	-
Tm169 (ppm)	-	-	-	-	-	-	-	-	-
Yb172 (ppm)	-	-	-	-	-	-	-	-	-
Lu175 (ppm)	-	-	-	-	-	-	-	-	-
Hf178 (ppm)	-	-	-	-	-	-	-	-	-
Ta181 (ppm)	-	-	-	-	-	-	-	-	-
W182 (ppm)	-	-	-	-	BDL	-	-	-	-
Re185 (ppm)	BDL	BDL	BDL	BDL	BDL	-	BDL	BDL	BDL
Os189 (ppm)	BDL	BDL	BDL	BDL	BDL	BDL	BDL	BDL	BDL
Ir193 (ppm)	-	-	-	BDL	BDL	BDL	-	-	-
Pt195 (ppm)	-	-	BDL	-	BDL	BDL	BDL	BDL	BDL
Au197 (ppm)	30	7	-	-	BDL	10	-	25	-
Hg202 (ppm)	BDL	16	16	8	14	14	13	8	7
Pb204 (ppm)	80	946	17657	1495	750	2515	497	38	32
Tl205 (ppm)	0	2	1	3	0	1	0	BDL	0
Pb206 (ppm)	49	-	19588	1525	864	2345	-	10	4
Pb207 (ppm)	-	-	19579	1539	782	-	-	10	4
Pb208 (ppm)	52	877	19406	1979	763	2349	429	10	4
Bi209 (ppm)	8	62	-	78	11	58	20	3	-
Th232 (ppm)	-	-	-	-	-	-	-	-	-
U238 (ppm)	-	BDL	BDL	-	BDL	-	-	-	-
PbTotal (ppm)	52	915	19465	1766	792	2375	437	11	4

Table D1. Trace element data for pyrite continued.

Deposit	Betts Cove	Betts Cove	Betts Cove	Betts Cove	Betts Cove	Betts Cove	Betts Cove	Betts Cove	Betts Cove
Sample	KKMSC09_Py29	KKMSC09_Py30	KKMSC09_Py42	KKMSC09_Py32	KKMSC09_Py34	KKMSC09_Py35	KKMSC09_Py36	KKMSC09_Py37	KKMSC09_Py38
Date	2023-11-20	2023-11-20	2023-11-20	2023-11-20	2023-11-20	2023-11-20	2023-11-20	2023-11-20	2023-11-20
Facies	Chalcopyrite-dominated	Chalcopyrite-dominated	Chalcopyrite-dominated	Chalcopyrite-dominated	Chalcopyrite-dominated	Chalcopyrite-dominated	Chalcopyrite-dominated	Chalcopyrite-dominated	Chalcopyrite-dominated
Li7 (ppm)	BDL	BDL	BDL	4	BDL	3	BDL	BDL	BDL
Be9 (ppm)	BDL	-	-	BDL	-	BDL	BDL	-	-
B11 (ppm)	BDL	BDL	BDL	BDL	BDL	BDL	BDL	BDL	BDL
Na23 (ppm)	BDL	BDL	BDL	BDL	BDL	BDL	BDL	BDL	BDL
Mg24 (ppm)	244	323	522	113	381	85	42	BDL	12
Al27 (ppm)	333	279	679	70	535	135	26	6	12
Si29 (ppm)	14429	6907	87695	1326	10335	4771	3381	BDL	BDL
P31 (ppm)	63	BDL	BDL	101	BDL	42	41	BDL	BDL
S32 (ppm)	487508	522833	443904	517756	484853	502487	399382	527475	527455
K39 (ppm)	BDL	BDL	BDL	BDL	BDL	18	BDL	BDL	BDL
Ca44 (ppm)	BDL	BDL	BDL	BDL	BDL	BDL	BDL	BDL	BDL
Sc45 (ppm)	BDL	BDL	BDL	BDL	BDL	BDL	BDL	BDL	BDL
Ti47 (ppm)	BDL	2	BDL	BDL	BDL	3	BDL	BDL	BDL
V51 (ppm)	1	2	3	BDL	1	1	BDL	BDL	BDL
Cr52 (ppm)	5	BDL	BDL	BDL	4	BDL	BDL	BDL	BDL
Mn55 (ppm)	46	11	28	6	16	5	19	2	5
Fe57 (ppm)	-	-	-	-	-	-	-	-	-
Co59 (ppm)	14101	1223	19169	595	1673	1283	6148	3259	748
Ni60 (ppm)	-	54	-	12	387	177	1157	79	-
Cu63 (ppm)	9320	262	5887	213846	17675	4040	24215	40	69
Zn66 (ppm)	67572	6	12	108	130	61	1106	15	51
Ga71 (ppm)	-	-	-	-	-	-	0	-	BDL
Ge73 (ppm)	-	BDL	BDL	3	-	BDL	-	2	-
As75 (ppm)	31074	1884	39584	1367	921	600	1414	3269	4938
Se77 (ppm)	1759	1676	1217	2225	2965	1207	1395	2244	2408
Rb85 (ppm)	BDL	BDL	BDL	BDL	BDL	BDL	BDL	BDL	BDL
Sr88 (ppm)	-	-	-	-	-	0	-	-	-
Y89 (ppm)	-	-	-	BDL	-	-	-	-	BDL
Zr90 (ppm)	BDL	-	-	-	BDL	0	-	-	-
Nb93 (ppm)	BDL	-	-	BDL	-	-	-	-	-
Mo95 (ppm)	204	BDL	6	3	-	2	-	-	1
Ru101 (ppm)	-	-	-	-	-	-	-	-	-
Rh103 (ppm)	-	-	-	-	-	BDL	-	-	BDL
Pd104 (ppm)	7	BDL	-	BDL	-	1	-	BDL	BDL

Pd105 (ppm)	-	BDL	BDL	-	-	-	-	-	-
Pd106 (ppm)	-	BDL	-	-	BDL	-	0	BDL	-
Ag107 (ppm)	7449	-	163	-	653	68	461	0	BDL
Cd111 (ppm)	626	BDL	-	3	-	-	5	1	-
In115 (ppm)	-	0	0	-	2	-	20	-	-
Sn118 (ppm)	BDL	BDL	BDL	BDL	BDL	1	0	BDL	BDL
Sb121 (ppm)	13	10	-	3	26	39	44	1	BDL
Te125 (ppm)	-	64	442	17	202	312	583	274	290
Cs133 (ppm)	BDL	BDL	BDL	BDL	BDL	BDL	BDL	BDL	BDL
Ba137 (ppm)	-	-	-	-	-	-	-	-	-
La139 (ppm)	-	-	-	-	-	-	-	-	-
Ce140 (ppm)	-	-	-	-	-	-	-	-	-
Pr141 (ppm)	BDL	-	BDL	-	-	0	-	-	-
Nd146 (ppm)	-	-	-	-	-	-	-	-	-
Sm147 (ppm)	-	-	-	-	-	-	-	-	-
Eu153 (ppm)	-	-	-	-	-	-	-	-	-
Gd157 (ppm)	-	-	-	-	-	-	-	-	-
Tb159 (ppm)	-	-	-	-	-	-	-	-	-
Dy163 (ppm)	-	-	-	-	-	-	-	-	-
Ho165 (ppm)	BDL	-	-	-	-	-	-	-	-
Er166 (ppm)	-	-	-	-	-	-	-	-	-
Tm169 (ppm)	-	-	-	-	-	-	-	-	-
Yb172 (ppm)	-	BDL	-	-	-	-	-	-	-
Lu175 (ppm)	-	-	-	-	-	-	-	-	-
Hf178 (ppm)	-	-	-	-	-	-	BDL	-	-
Ta181 (ppm)	-	-	-	-	-	-	-	-	-
W182 (ppm)	-	-	-	-	-	-	-	-	-
Re185 (ppm)	1	BDL	BDL	BDL	BDL	BDL	BDL	BDL	BDL
Os189 (ppm)	BDL	BDL	BDL	BDL	BDL	-	BDL	BDL	BDL
Ir193 (ppm)	BDL	-	-	-	BDL	BDL	-	-	-
Pt195 (ppm)	BDL	-	-	-	BDL	-	BDL	BDL	-
Au197 (ppm)	17557	-	-	0	-	-	13	-	-
Hg202 (ppm)	59	BDL	BDL	9	BDL	BDL	BDL	11	10
Pb204 (ppm)	8573	368	2758	100	4601	2391	697	33	37
Tl205 (ppm)	3	0	1	1	2	1	2	BDL	1
Pb206 (ppm)	8907	384	-	-	4675	2665	851	-	2
Pb207 (ppm)	9049	379	-	-	4899	2390	844	1	1
Pb208 (ppm)	8914	367	-	90	4554	3775	-	1	2
Bi209 (ppm)	22	18	99	5	-	83	81	1	BDL
Th232 (ppm)	-	-	-	-	-	-	BDL	-	-
U238 (ppm)	-	-	-	-	-	-	-	-	-
PbTotal (ppm)	8937	374	2828	90	4659	3185	788	2	2

Table D1. Trace element data for pyrite continued.

Deposit	Betts Cove	Betts Cove	Betts Cove	Betts Cove	Betts Cove	Betts Cove	Betts Cove	Betts Cove	Betts Cove
Sample	KKMSC09_Py39	KKMSC09_Py40	KKMSC09_Py41	KKMSC09_Py44	KKMSC09_Py45	KKMSC10_Py1	KKMSC10_Py2	KKMSC10_Py3	KKMSC10_Py4
Date	2023-11-20	2023-11-20	2023-11-20	2023-11-20	2023-11-20	2023-11-20	2023-11-20	2023-11-20	2023-11-20
Facies	Chalcopyrite-dominated	Chalcopyrite-dominated	Chalcopyrite-dominated	Chalcopyrite-dominated	Chalcopyrite-dominated	Pyrite-dominated	Pyrite-dominated	Pyrite-dominated	Pyrite-dominated
Li7 (ppm)	7	BDL	BDL	BDL	18	BDL	BDL	3	BDL
Be9 (ppm)	-	-	BDL	BDL	BDL	-	BDL	-	BDL
B11 (ppm)	BDL	BDL	BDL	BDL	BDL	BDL	BDL	BDL	BDL
Na23 (ppm)	BDL	BDL	BDL	BDL	BDL	BDL	BDL	BDL	BDL
Mg24 (ppm)	598	317	4513	1325	70928	BDL	BDL	13	BDL
Al27 (ppm)	670	354	5114	1404	88609	BDL	BDL	16	4
Si29 (ppm)	1531	5708	22892	38886	187788	BDL	BDL	BDL	BDL
P31 (ppm)	55	BDL	BDL	60	173	BDL	BDL	BDL	BDL
S32 (ppm)	420839	420656	430589	445221	345619	485545	453546	489537	475356
K39 (ppm)	BDL	BDL	BDL	24	99	BDL	BDL	BDL	BDL
Ca44 (ppm)	BDL	245	BDL	BDL	588	BDL	BDL	BDL	BDL
Sc45 (ppm)	BDL	1	1	BDL	34	BDL	BDL	BDL	BDL
Ti47 (ppm)	BDL	3	BDL	BDL	71	-	BDL	-	BDL
V51 (ppm)	3	2	14	4	255	BDL	BDL	BDL	BDL
Cr52 (ppm)	BDL	BDL	18	8	908	BDL	BDL	BDL	BDL
Mn55 (ppm)	55	124	188	60	4007	BDL	BDL	1	462
Fe57 (ppm)	-	-	-	-	-	-	-	-	-
Co59 (ppm)	2462	10088	2915	2274	4639	23	0	43	19
Ni60 (ppm)	158	-	229	-	660	2	-	-	-
Cu63 (ppm)	2717	20401	83264	57096	17295	BDL	BDL	6	2296
Zn66 (ppm)	48	35	3670	60	508	1	BDL	5	21315
Ga71 (ppm)	0	-	-	-	-	-	-	-	-
Ge73 (ppm)	BDL	BDL	4	BDL	BDL	-	-	-	2
As75 (ppm)	359	12155	259	5078	2629	16	1036	5	454
Se77 (ppm)	438	783	1030	1673	365	65	5	46	7
Rb85 (ppm)	BDL	BDL	BDL	BDL	BDL	-	BDL	BDL	BDL
Sr88 (ppm)	-	-	-	-	-	-	-	-	-
Y89 (ppm)	-	-	-	-	-	-	-	-	-
Zr90 (ppm)	-	-	BDL	-	-	-	-	-	2
Nb93 (ppm)	-	-	-	-	-	BDL	-	-	-
Mo95 (ppm)	17	-	16	3	1506	-	BDL	-	-
Ru101 (ppm)	-	BDL	-	-	BDL	-	-	-	3
Rh103 (ppm)	-	-	-	0	-	BDL	BDL	BDL	0
Pd104 (ppm)	BDL	0	BDL	-	-	BDL	BDL	BDL	-

Pd105 (ppm)	BDL	1	1	2	1	-	BDL	BDL	26
Pd106 (ppm)	-	BDL	1	BDL	BDL	-	-	BDL	75
Ag107 (ppm)	15	88	47	328	125	BDL	-	BDL	-
Cd111 (ppm)	-	-	17	1	2	BDL	BDL	BDL	BDL
In115 (ppm)	-	-	44	5	4	BDL	BDL	BDL	22
Sn118 (ppm)	BDL	BDL	BDL	BDL	BDL	BDL	BDL	BDL	BDL
Sb121 (ppm)	9	27	10	53	24	BDL	BDL	BDL	BDL
Te125 (ppm)	114	-	80	-	322	-	-	-	-
Cs133 (ppm)	BDL	BDL	BDL	BDL	BDL	-	-	-	-
Ba137 (ppm)	-	-	-	-	-	-	-	-	-
La139 (ppm)	-	-	-	-	-	-	-	-	-
Ce140 (ppm)	-	-	-	-	-	-	-	-	-
Pr141 (ppm)	-	-	-	-	-	-	-	-	-
Nd146 (ppm)	-	-	-	BDL	-	-	-	-	-
Sm147 (ppm)	-	-	-	-	-	-	BDL	-	-
Eu153 (ppm)	-	-	-	-	-	-	-	-	-
Gd157 (ppm)	-	-	-	-	-	-	-	-	-
Tb159 (ppm)	-	-	-	-	-	-	-	-	-
Dy163 (ppm)	-	-	-	-	-	-	-	-	-
Ho165 (ppm)	-	-	-	-	-	-	-	-	-
Er166 (ppm)	-	-	-	-	-	-	-	-	-
Tm169 (ppm)	-	-	-	-	-	-	-	-	-
Yb172 (ppm)	-	-	-	-	-	-	-	-	-
Lu175 (ppm)	-	-	-	-	-	-	-	-	-
Hf178 (ppm)	-	-	-	-	-	-	BDL	BDL	BDL
Ta181 (ppm)	BDL	-	-	-	-	0	BDL	BDL	BDL
W182 (ppm)	-	-	-	-	1	BDL	BDL	BDL	BDL
Re185 (ppm)	-	BDL	BDL	BDL	-	-	-	BDL	-
Os189 (ppm)	BDL	BDL	0	BDL	BDL	BDL	-	-	-
Ir193 (ppm)	-	BDL	-	-	-	-	-	-	-
Pt195 (ppm)	BDL	-	-	BDL	BDL	BDL	BDL	BDL	BDL
Au197 (ppm)	-	4	-	-	3	BDL	BDL	BDL	291
Hg202 (ppm)	BDL	11	BDL	BDL	BDL	BDL	BDL	BDL	1
Pb204 (ppm)	497	1972	137	1913	1415	0	-	2	-
Tl205 (ppm)	1	3	1	2	4	0	-	2	294
Pb206 (ppm)	421	2132	142	-	1477	0	0	2	293
Pb207 (ppm)	-	2146	149	-	1275	BDL	BDL	BDL	1
Pb208 (ppm)	427	2151	136	2062	1468	-	-	-	-
Bi209 (ppm)	16	39	22	-	48	-	-	-	-
Th232 (ppm)	-	-	-	-	-	BDL	1	2	308
U238 (ppm)	-	-	-	-	-	-	-	-	-
PbTotal (ppm)	438	2143	140	2076	1486	-	-	-	-

Table D1. Trace element data for pyrite continued.

Deposit	Betts Cove	Betts Cove	Betts Cove	Betts Cove	Betts Cove	Betts Cove	Betts Cove	Betts Cove	Betts Cove
Sample	KKMSC10_Py5	KKMSC10_Py6	KKMSC10_Py7	KKMSC10_Py8	KKMSC10_Py9	KKMSC10_Py1 0	KKMSC10_Py1 1	KKMSC10_Py1 2	KKMSC10_Py1 3
Date	2023-11-20	2023-11-20	2023-11-20	2023-11-20	2023-11-20	2023-11-20	2023-11-20	2023-11-20	2023-11-20
Facies	Pyrite-dominated	Pyrite-dominated	Pyrite-dominated	Pyrite-dominated	Pyrite-dominated	Pyrite-dominated	Pyrite-dominated	Pyrite-dominated	Pyrite-dominated
Li7 (ppm)	BDL	BDL	BDL	BDL	BDL	4	2	BDL	BDL
Be9 (ppm)	BDL	-	-	BDL	-	-	-	-	BDL
B11 (ppm)	BDL	BDL	BDL	BDL	BDL	15	BDL	BDL	BDL
Na23 (ppm)	BDL	BDL	BDL	BDL	BDL	BDL	BDL	BDL	BDL
Mg24 (ppm)	78	-	1	22	BDL	62	10	BDL	1
Al27 (ppm)	80	BDL	2	30	BDL	20	5	BDL	BDL
Si29 (ppm)	BDL	BDL	BDL	BDL	BDL	BDL	BDL	BDL	BDL
P31 (ppm)	BDL	BDL	BDL	BDL	BDL	BDL	BDL	BDL	BDL
S32 (ppm)	466687	495507	460528	532571	477037	567076	440646	508264	474616
K39 (ppm)	BDL	BDL	BDL	BDL	BDL	BDL	BDL	BDL	BDL
Ca44 (ppm)	BDL	BDL	BDL	BDL	BDL	BDL	BDL	BDL	BDL
Sc45 (ppm)	BDL	BDL	BDL	BDL	BDL	BDL	BDL	BDL	BDL
Ti47 (ppm)	BDL	BDL	BDL	BDL	-	BDL	BDL	-	BDL
V51 (ppm)	1	BDL	BDL	BDL	BDL	BDL	BDL	BDL	BDL
Cr52 (ppm)	BDL	BDL	BDL	BDL	BDL	BDL	BDL	BDL	BDL
Mn55 (ppm)	4	1	1	1	1	2	41	BDL	BDL
Fe57 (ppm)	-	-	-	-	-	-	-	-	-
Co59 (ppm)	603	540	184	3	35	133	-	30	45
Ni60 (ppm)	15	-	58	1	-	1	51	163	5
Cu63 (ppm)	8	11	80	541	61	7	198	16	3
Zn66 (ppm)	4	7	35	54	1	3	9337	BDL	3
Ga71 (ppm)	-	-	BDL	-	-	-	-	-	-
Ge73 (ppm)	2	-	-	-	BDL	-	-	BDL	-
As75 (ppm)	186	278	361	5	1077	BDL	373	739	3
Se77 (ppm)	41	138	42	161	23	32	33	23	41
Rb85 (ppm)	BDL	BDL	BDL	-	BDL	BDL	BDL	BDL	BDL
Sr88 (ppm)	-	-	-	-	-	-	-	BDL	BDL
Y89 (ppm)	-	BDL	-	-	-	-	-	-	-
Zr90 (ppm)	BDL	-	-	BDL	2	7	8	BDL	-
Nb93 (ppm)	-	-	BDL	-	-	-	-	-	-
Mo95 (ppm)	-	BDL	BDL	-	BDL	BDL	-	-	-
Ru101 (ppm)	BDL	BDL	BDL	BDL	-	BDL	-	BDL	BDL
Rh103 (ppm)	-	-	-	BDL	-	-	-	-	-
Pd104 (ppm)	BDL	BDL	BDL	-	-	BDL	-	BDL	BDL

Pd105 (ppm)	BDL	BDL	0	BDL	BDL	BDL	2	BDL	BDL
Pd106 (ppm)	BDL	-	-	BDL	-	-	-	-	-
Ag107 (ppm)	-	-	-	-	-	-	1	-	-
Cd111 (ppm)	BDL	BDL	BDL	BDL	BDL	BDL	BDL	BDL	BDL
In115 (ppm)	BDL	4	0	BDL	2	0	-	-	BDL
Sn118 (ppm)	BDL	79	1	-	1	5	BDL	BDL	BDL
Sb121 (ppm)	BDL	BDL	BDL	BDL	BDL	BDL	BDL	BDL	BDL
Te125 (ppm)	-	-	-	-	-	-	-	-	-
Cs133 (ppm)	-	-	-	-	-	-	-	-	-
Ba137 (ppm)	-	-	-	-	-	-	-	-	-
La139 (ppm)	-	-	-	-	-	-	-	-	-
Ce140 (ppm)	-	-	-	-	-	-	-	-	-
Pr141 (ppm)	-	-	-	-	-	-	-	-	-
Nd146 (ppm)	-	-	-	-	-	-	-	-	-
Sm147 (ppm)	-	-	-	-	-	-	-	-	-
Eu153 (ppm)	-	-	-	-	-	-	-	-	-
Gd157 (ppm)	-	-	-	-	-	-	-	-	-
Tb159 (ppm)	-	-	-	-	-	-	-	-	-
Dy163 (ppm)	-	-	-	-	-	-	-	-	-
Ho165 (ppm)	-	-	-	-	-	-	-	-	-
Er166 (ppm)	-	-	-	-	-	-	-	-	-
Tm169 (ppm)	-	-	-	-	-	-	-	-	-
Yb172 (ppm)	-	-	-	-	-	-	-	-	-
Lu175 (ppm)	-	-	-	-	-	-	-	-	-
Hf178 (ppm)	-	-	BDL	-	BDL	-	-	BDL	BDL
Ta181 (ppm)	BDL	0	BDL	0	BDL	BDL	BDL	BDL	BDL
W182 (ppm)	BDL	BDL	0	BDL	BDL	BDL	BDL	BDL	BDL
Re185 (ppm)	-	BDL	BDL	BDL	BDL	-	-	BDL	-
Os189 (ppm)	BDL	BDL	-	BDL	BDL	-	BDL	BDL	BDL
Ir193 (ppm)	-	-	-	-	-	-	-	-	BDL
Pt195 (ppm)	BDL	BDL	BDL	BDL	BDL	BDL	11	BDL	BDL
Au197 (ppm)	BDL	BDL	BDL	BDL	BDL	BDL	47	19	BDL
Hg202 (ppm)	BDL	0	BDL	BDL	0	0	0	BDL	BDL
Pb204 (ppm)	4	8	9	-	21	4	50	5	0
Tl205 (ppm)	4	8	7	-	-	5	48	4	1
Pb206 (ppm)	4	9	7	2	19	5	52	4	-
Pb207 (ppm)	0	0	0	10	BDL	1	BDL	BDL	BDL
Pb208 (ppm)	-	-	-	-	-	-	-	-	-
Bi209 (ppm)	-	-	-	-	-	-	-	-	-
Th232 (ppm)	4	9	7	2	20	5	52	5	1
U238 (ppm)	-	-	-	-	-	-	-	-	-
PbTotal (ppm)	-	-	-	-	-	-	-	-	-

Table D1. Trace element data for pyrite continued.

Deposit	Betts Cove	Betts Cove	Betts Cove	Betts Cove	Betts Cove	Betts Cove	Betts Cove	Betts Cove	Betts Cove
Sample	KKMSC10_Py14	KKMSC10_Py15	KKMSC10_Py16	KKMSC10_Py17	KKMSC10_Py18	KKMSC10_Py19	KKMSC10_Py20	KKMSC29_Py1	KKMSC29_Py2
Date	2023-11-20	2023-11-20	2023-11-20	2023-11-20	2023-11-20	2023-11-20	2023-11-20	2023-11-20	2023-11-20
Facies	Pyrite-dominated	Pyrite-dominated	Pyrite-dominated	Pyrite-dominated	Pyrite-dominated	Pyrite-dominated	Pyrite-dominated	Chalcopyrite-dominated	Chalcopyrite-dominated
Li7 (ppm)	BDL	4	BDL	4	BDL	BDL	BDL	BDL	BDL
Be9 (ppm)	BDL	BDL	-	BDL	BDL	-	BDL	BDL	BDL
B11 (ppm)	BDL	BDL	BDL	BDL	BDL	BDL	BDL	BDL	BDL
Na23 (ppm)	BDL	BDL	BDL	BDL	BDL	BDL	BDL	BDL	BDL
Mg24 (ppm)	22	32	13	106	38	1	BDL	58	1
Al27 (ppm)	20	28	9	62	30	BDL	BDL	148	BDL
Si29 (ppm)	BDL	BDL	4982	583	BDL	BDL	BDL	BDL	BDL
P31 (ppm)	BDL	BDL	BDL	BDL	BDL	BDL	BDL	BDL	BDL
S32 (ppm)	481129	479240	461282	529663	477803	505794	483841	528578	550092
K39 (ppm)	BDL	BDL	BDL	BDL	BDL	BDL	BDL	BDL	BDL
Ca44 (ppm)	BDL	BDL	BDL	BDL	BDL	BDL	BDL	BDL	BDL
Sc45 (ppm)	BDL	BDL	BDL	BDL	BDL	BDL	BDL	BDL	BDL
Ti47 (ppm)	BDL	BDL	BDL	BDL	-	BDL	BDL	BDL	-
V51 (ppm)	BDL	0	1	BDL	BDL	BDL	BDL	1	BDL
Cr52 (ppm)	BDL	BDL	BDL	BDL	BDL	BDL	BDL	BDL	BDL
Mn55 (ppm)	16	1	18	7	21	10	BDL	6	BDL
Fe57 (ppm)	-	-	-	-	-	-	-	-	-
Co59 (ppm)	25	28	224	97	60	102	71	96	2
Ni60 (ppm)	37	233	42	63	-	24	8	19	2
Cu63 (ppm)	16	35	79	435	385	7	36	28	11
Zn66 (ppm)	3	BDL	11004	3830	10601	5229	3	27	1
Ga71 (ppm)	-	BDL	-	-	-	-	-	-	-
Ge73 (ppm)	BDL	-	-	-	BDL	BDL	BDL	-	BDL
As75 (ppm)	1519	1458	232	413	1337	168	37	BDL	BDL
Se77 (ppm)	17	12	50	18	13	42	149	2667	1600
Rb85 (ppm)	BDL	-	BDL	BDL	BDL	-	BDL	BDL	BDL
Sr88 (ppm)	-	-	-	-	-	BDL	-	-	-
Y89 (ppm)	-	-	-	-	BDL	-	BDL	-	BDL
Zr90 (ppm)	1	1	-	BDL	-	-	BDL	-	BDL
Nb93 (ppm)	-	-	-	-	-	-	-	-	-
Mo95 (ppm)	-	BDL	-	BDL	-	BDL	-	-	-
Ru101 (ppm)	-	BDL	-	-	-	-	-	BDL	-
Rh103 (ppm)	-	-	-	-	BDL	-	BDL	BDL	-
Pd104 (ppm)	BDL	BDL	-	1	2	2	-	-	BDL

Pd105 (ppm)	0	BDL	9	5	2	0	BDL	BDL	BDL
Pd106 (ppm)	-	-	-	-	-	-	-	-	0
Ag107 (ppm)	-	-	-	-	-	0	BDL	-	BDL
Cd111 (ppm)	BDL	BDL	BDL	BDL	BDL	BDL	BDL	BDL	BDL
In115 (ppm)	65	0	5	10	5	0	BDL	BDL	0
Sn118 (ppm)	BDL	-	17	12	1	1	14	1	1
Sb121 (ppm)	BDL	BDL	BDL	BDL	BDL	BDL	BDL	BDL	BDL
Te125 (ppm)	-	-	-	-	-	-	-	-	-
Cs133 (ppm)	-	-	-	-	-	-	-	-	-
Ba137 (ppm)	-	-	-	-	-	BDL	-	-	-
La139 (ppm)	-	-	-	-	-	-	-	-	-
Ce140 (ppm)	-	-	-	-	-	-	-	-	-
Pr141 (ppm)	-	-	-	-	-	-	-	-	-
Nd146 (ppm)	-	-	-	-	-	-	-	-	-
Sm147 (ppm)	BDL	-	-	-	-	-	-	-	-
Eu153 (ppm)	-	-	-	-	-	-	-	-	-
Gd157 (ppm)	-	-	-	-	-	-	-	-	-
Tb159 (ppm)	-	-	-	-	-	-	-	-	-
Dy163 (ppm)	-	-	-	-	-	-	-	-	-
Ho165 (ppm)	-	-	-	-	-	-	-	-	-
Er166 (ppm)	-	-	-	-	-	-	-	-	-
Tm169 (ppm)	-	-	-	-	-	-	-	-	BDL
Yb172 (ppm)	-	-	-	-	-	-	-	-	-
Lu175 (ppm)	-	-	-	BDL	-	-	-	-	-
Hf178 (ppm)	-	-	BDL	BDL	-	-	-	-	-
Ta181 (ppm)	BDL	BDL	1	BDL	BDL	BDL	0	BDL	BDL
W182 (ppm)	BDL	BDL	BDL	BDL	BDL	BDL	BDL	BDL	BDL
Re185 (ppm)	-	BDL	-	-	BDL	BDL	-	BDL	BDL
Os189 (ppm)	BDL	-	BDL	BDL	BDL	-	BDL	BDL	-
Ir193 (ppm)	-	-	-	-	-	-	-	-	BDL
Pt195 (ppm)	BDL	BDL	BDL	43	21	BDL	BDL	BDL	BDL
Au197 (ppm)	37	31	103	355	130	BDL	BDL	BDL	BDL
Hg202 (ppm)	3	BDL	0	0	0	BDL	BDL	0	0
Pb204 (ppm)	-	15	96	438	-	6	5	1	1
Tl205 (ppm)	30	-	99	321	111	6	-	1	1
Pb206 (ppm)	33	15	95	-	104	7	8	1	1
Pb207 (ppm)	0	BDL	9	7	1	1	1	BDL	BDL
Pb208 (ppm)	-	-	-	-	-	-	-	-	-
Bi209 (ppm)	-	BDL	BDL	-	-	-	BDL	-	BDL
Th232 (ppm)	32	15	96	403	106	6	8	2	1
U238 (ppm)	-	-	-	-	-	-	-	-	-
PbTotal (ppm)	-	-	-	-	-	-	-	-	-

Table D1. Trace element data for pyrite continued.

Deposit	Betts Cove	Betts Cove	Betts Cove	Betts Cove	Betts Cove	Betts Cove	Betts Cove	Betts Cove	Betts Cove
Sample	KKMSC29_Py3	KKMSC29_Py4	KKMSC29_Py5	KKMSC29_Py6	KKMSC29_Py7	KKMSC29_Py8	KKMSC29_Py1 0	KKMSC29_Py1 1	KKMSC29_Py1 3
Date	2023-11-20	2023-11-20	2023-11-20	2023-11-20	2023-11-20	2023-11-20	2023-11-20	2023-11-20	2023-11-20
Facies	Chalcopyrite-dominated	Chalcopyrite-dominated	Chalcopyrite-dominated	Chalcopyrite-dominated	Chalcopyrite-dominated	Chalcopyrite-dominated	Chalcopyrite-dominated	Chalcopyrite-dominated	Chalcopyrite-dominated
Li7 (ppm)	2	BDL	BDL	BDL	BDL	BDL	BDL	BDL	BDL
Be9 (ppm)	-	BDL	-	-	-	-	-	-	-
B11 (ppm)	BDL	BDL	BDL	BDL	BDL	BDL	BDL	BDL	BDL
Na23 (ppm)	BDL	BDL	BDL	BDL	BDL	BDL	BDL	129	BDL
Mg24 (ppm)	2163	198	468	1	19	3379	408	391	1073
Al27 (ppm)	3177	175	606	BDL	14	3672	532	504	1405
Si29 (ppm)	5543	BDL	1445	BDL	BDL	9291	1270	2593	2801
P31 (ppm)	86	BDL	28	BDL	BDL	162	BDL	BDL	BDL
S32 (ppm)	455679	489993	495201	490650	423249	388082	541071	373311	518859
K39 (ppm)	BDL	BDL	BDL	BDL	BDL	BDL	BDL	BDL	BDL
Ca44 (ppm)	890	BDL	243	BDL	BDL	1822	BDL	362	157
Sc45 (ppm)	1	BDL	1	BDL	BDL	BDL	BDL	BDL	BDL
Ti47 (ppm)	628	279	222	-	BDL	-	-	-	260
V51 (ppm)	11	1	1	0	BDL	11	1	3	5
Cr52 (ppm)	18	BDL	BDL	BDL	BDL	54	BDL	4	9
Mn55 (ppm)	64	7	22	BDL	2	96	19	13	65
Fe57 (ppm)	-	-	-	-	-	-	-	-	-
Co59 (ppm)	53	-	31	0	7	238	236	40	105
Ni60 (ppm)	5	2	2	1	13	-	-	-	17
Cu63 (ppm)	40	23	18	95	129	2909	28	32	36
Zn66 (ppm)	12	3	2	BDL	12	30	1	8	5
Ga71 (ppm)	-	-	0	-	-	-	-	0	-
Ge73 (ppm)	BDL	-	BDL	BDL	-	-	-	BDL	-
As75 (ppm)	27	BDL	18	286	65	120	26	30	13
Se77 (ppm)	1136	909	1521	575	643	336	2347	1275	2833
Rb85 (ppm)	-	BDL	BDL	BDL	-	BDL	BDL	BDL	BDL
Sr88 (ppm)	-	-	-	-	-	-	-	-	-
Y89 (ppm)	-	-	-	-	-	-	-	-	-
Zr90 (ppm)	-	-	BDL	BDL	BDL	BDL	BDL	-	BDL
Nb93 (ppm)	-	-	-	-	-	-	-	-	-
Mo95 (ppm)	-	BDL	-	-	BDL	BDL	BDL	BDL	-
Ru101 (ppm)	-	-	-	-	-	-	-	-	BDL
Rh103 (ppm)	-	-	-	-	-	-	-	-	-
Pd104 (ppm)	BDL	-	-	-	BDL	BDL	-	-	BDL

Pd105 (ppm)	0	BDL	1	2	14	7	1	1	1
Pd106 (ppm)	-	BDL	0	-	1	0	-	-	-
Ag107 (ppm)	BDL	-	-	BDL	-	-	BDL	-	BDL
Cd111 (ppm)	BDL	BDL	BDL	BDL	BDL	BDL	BDL	BDL	BDL
In115 (ppm)	-	1	-	4	11	2	1	1	-
Sn118 (ppm)	11	BDL	10	-	3	62	-	14	7
Sb121 (ppm)	BDL	BDL	BDL	BDL	BDL	BDL	BDL	BDL	BDL
Te125 (ppm)	-	-	-	-	-	-	-	-	-
Cs133 (ppm)	-	-	-	-	-	-	-	-	-
Ba137 (ppm)	-	-	-	-	-	-	-	-	-
La139 (ppm)	-	-	-	-	BDL	-	-	-	-
Ce140 (ppm)	-	-	-	-	-	-	-	-	-
Pr141 (ppm)	-	-	-	-	-	-	-	-	-
Nd146 (ppm)	-	-	-	-	-	-	-	-	-
Sm147 (ppm)	-	-	-	BDL	-	BDL	-	-	-
Eu153 (ppm)	-	-	-	-	-	-	-	-	-
Gd157 (ppm)	-	-	-	-	-	-	-	-	-
Tb159 (ppm)	-	-	-	-	-	-	-	-	-
Dy163 (ppm)	-	-	-	-	-	-	-	-	-
Ho165 (ppm)	-	-	-	-	-	-	-	-	-
Er166 (ppm)	-	-	-	-	-	-	-	-	-
Tm169 (ppm)	-	-	-	-	-	-	-	-	-
Yb172 (ppm)	-	-	-	-	-	-	-	-	-
Lu175 (ppm)	-	BDL	-	-	BDL	-	-	-	-
Hf178 (ppm)	-	-	-	BDL	BDL	-	-	BDL	-
Ta181 (ppm)	BDL	BDL	BDL	BDL	BDL	BDL	BDL	BDL	BDL
W182 (ppm)	BDL	BDL	BDL	BDL	0	BDL	BDL	BDL	BDL
Re185 (ppm)	-	-	-	-	-	BDL	BDL	-	-
Os189 (ppm)	BDL	-	BDL	-	BDL	BDL	-	BDL	-
Ir193 (ppm)	-	-	0	-	-	-	-	-	-
Pt195 (ppm)	42	BDL	BDL	BDL	20	BDL	BDL	36	BDL
Au197 (ppm)	98	21	BDL	27	22	31	BDL	46	24
Hg202 (ppm)	1	0	0	1	4	1	0	0	0
Pb204 (ppm)	-	9	10	6	11	-	-	-	-
Tl205 (ppm)	15	9	9	6	11	-	17	-	-
Pb206 (ppm)	-	9	9	6	12	20	17	11	13
Pb207 (ppm)	0	BDL	0	BDL	BDL	1	5	1	0
Pb208 (ppm)	-	-	-	-	-	-	-	-	-
Bi209 (ppm)	-	-	-	-	-	-	-	-	-
Th232 (ppm)	16	9	9	6	12	20	17	11	13
U238 (ppm)	-	-	-	-	-	-	-	-	-
PbTotal (ppm)	-	-	-	-	-	-	-	-	-

Table D1. Trace element data for pyrite continued.

Deposit	Tilt Cove	Tilt Cove	Tilt Cove	Tilt Cove	Tilt Cove	Tilt Cove	Tilt Cove	Tilt Cove	Tilt Cove
Sample	KKMSC63_Py1	KKMSC63_Py2	KKMSC63_Py3	KKMSC63_Py4	KKMSC63_Py5	KKMSC63_Py6	KKMSC63_Py19	KKMSC63_Py17	KKMSC63_Py11
Date	2023-11-21	2023-11-21	2023-11-21	2023-11-21	2023-11-21	2023-11-21	2023-11-21	2023-11-21	2023-11-21
Facies	Pyrite-dominated	Pyrite-dominated	Pyrite-dominated	Pyrite-dominated	Pyrite-dominated	Pyrite-dominated	Pyrite-dominated	Pyrite-dominated	Pyrite-dominated
Li7 (ppm)	3	5	BDL	BDL	BDL	BDL	BDL	BDL	1
Be9 (ppm)	-	-	BDL	-	-	-	-	-	-
B11 (ppm)	BDL	BDL	BDL	BDL	BDL	BDL	BDL	BDL	BDL
Na23 (ppm)	BDL	51	BDL	BDL	BDL	BDL	81	BDL	BDL
Mg24 (ppm)	812	404	8	2147	105	14	7746	27	10
Al27 (ppm)	92	88	BDL	90	6	4	248	BDL	2
Si29 (ppm)	BDL	3553	BDL	2496	BDL	BDL	9603	BDL	704
P31 (ppm)	BDL	BDL	BDL	BDL	BDL	BDL	BDL	BDL	BDL
S32 (ppm)	461397	507991	475837	480195	474824	516361	448404	447316	429351
K39 (ppm)	BDL	20	BDL	BDL	BDL	BDL	BDL	BDL	BDL
Ca44 (ppm)	169	386	BDL	BDL	BDL	BDL	BDL	BDL	BDL
Sc45 (ppm)	BDL	BDL	BDL	BDL	BDL	BDL	1	BDL	BDL
Ti47 (ppm)	BDL	BDL	BDL	BDL	BDL	BDL	3	-	-
V51 (ppm)	BDL	BDL	BDL	1	BDL	BDL	3	BDL	BDL
Cr52 (ppm)	8	BDL	BDL	BDL	BDL	BDL	161	BDL	BDL
Mn55 (ppm)	12	25	BDL	2	1	1	8	1	1
Fe57 (ppm)	-	-	-	-	-	-	-	-	-
Co59 (ppm)	1701	7398	102	5317	1925	3332	7245	429	-
Ni60 (ppm)	2886	2137	40	-	320	755	-	283	-
Cu63 (ppm)	180	137	583	12746	4143	4554	7378	198	1341
Zn66 (ppm)	49	9	70	250	131	322	240	2	2
Ga71 (ppm)	-	-	-	-	-	-	-	BDL	-
Ge73 (ppm)	-	BDL	BDL	-	-	-	BDL	BDL	BDL
As75 (ppm)	717	913	5	3929	1541	2948	11304	114	26
Se77 (ppm)	73	67	645	696	670	689	65	25	33
Rb85 (ppm)	BDL	BDL	BDL	BDL	BDL	BDL	BDL	BDL	BDL
Sr88 (ppm)	-	-	-	-	-	-	-	-	-
Y89 (ppm)	-	-	-	-	-	-	-	-	-
Zr90 (ppm)	-	-	-	-	-	-	-	BDL	-
Nb93 (ppm)	10	3	2	-	1	-	-	0	-
Mo95 (ppm)	BDL	-	-	BDL	-	-	-	-	-
Ru101 (ppm)	-	BDL	-	-	-	-	-	-	-
Rh103 (ppm)	-	BDL	BDL	BDL	-	BDL	-	BDL	-
Pd104 (ppm)	-	-	BDL	-	0	-	0	-	-

Pd105 (ppm)	BDL	-	BDL	-	BDL	BDL	0	-	BDL
Pd106 (ppm)	0	1	2	5	4	4	43	BDL	0
Ag107 (ppm)	1	BDL	3	-	-	2	3	BDL	-
Cd111 (ppm)	BDL	-	-	-	8	-	-	-	-
In115 (ppm)	BDL	BDL	BDL	BDL	BDL	BDL	BDL	BDL	BDL
Sn118 (ppm)	4	52	1	19	10	6	86	3	1
Sb121 (ppm)	-	47	31	24	45	41	40	6	1
Te125 (ppm)	BDL	BDL	BDL	BDL	BDL	BDL	BDL	BDL	BDL
Cs133 (ppm)	-	-	-	-	-	-	-	-	-
Ba137 (ppm)	-	-	-	-	-	-	-	-	-
La139 (ppm)	-	-	-	-	-	-	-	-	-
Ce140 (ppm)	-	-	-	-	-	-	-	-	-
Pr141 (ppm)	-	-	-	-	-	-	-	-	-
Nd146 (ppm)	-	-	-	-	-	-	-	-	-
Sm147 (ppm)	-	-	-	-	-	-	-	-	-
Eu153 (ppm)	-	-	-	-	BDL	-	-	-	-
Gd157 (ppm)	-	-	-	-	-	-	-	-	-
Tb159 (ppm)	-	-	-	-	-	-	-	-	-
Dy163 (ppm)	-	-	-	-	-	-	-	-	-
Ho165 (ppm)	-	-	-	-	-	-	-	-	-
Er166 (ppm)	-	-	-	-	-	-	-	-	-
Tm169 (ppm)	-	-	-	-	BDL	-	-	-	-
Yb172 (ppm)	-	-	-	-	-	-	-	-	-
Lu175 (ppm)	-	BDL	-	-	-	-	-	-	-
Hf178 (ppm)	-	-	-	-	-	-	-	-	BDL
Ta181 (ppm)	-	-	-	-	-	-	BDL	BDL	-
W182 (ppm)	BDL	BDL	BDL	BDL	BDL	BDL	BDL	BDL	BDL
Re185 (ppm)	BDL	BDL	BDL	BDL	BDL	BDL	BDL	BDL	BDL
Os189 (ppm)	BDL	-	BDL	BDL	BDL	BDL	-	-	BDL
Ir193 (ppm)	-	BDL	0	BDL	BDL	BDL	BDL	-	BDL
Pt195 (ppm)	1	9	0	-	-	1	-	-	0
Au197 (ppm)	30	89	26	20	BDL	26	30	27	31
Hg202 (ppm)	68	268	27	71	82	49	511	45	45
Pb204 (ppm)	0	0	BDL	0	0	0	15	BDL	0
Tl205 (ppm)	19	185	1	35	50	23	-	-	3
Pb206 (ppm)	21	184	1	37	52	-	478	12	3
Pb207 (ppm)	14	133	1	29	42	19	453	12	3
Pb208 (ppm)	1	6	1	2	2	1	5	1	0
Bi209 (ppm)	-	-	-	-	-	-	-	-	-
Th232 (ppm)	-	-	-	-	BDL	-	-	-	-
U238 (ppm)	17	155	1	32	46	21	461	12	4
PbTotal (ppm)	-	-	-	-	-	-	-	-	-

Table D1. Trace element data for pyrite continued.

Deposit	Tilt Cove	Tilt Cove	Tilt Cove	Tilt Cove	Tilt Cove	Tilt Cove	Tilt Cove	Tilt Cove	Tilt Cove
Sample	KKMSC63_Py10	KKMSC63_Py9	KKMSC63_Py10	KKMSC63_Py16	KKMSC63_Py15	KKMSC63_Py14	KKMSC77_Py5	KKMSC77_Py6	KKMSC77_Py8
Date	2023-11-21	2023-11-21	2023-11-21	2023-11-21	2023-11-21	2023-11-21	2023-11-21	2023-11-21	2023-11-21
Facies	Pyrite-dominated	Pyrite-dominated	Pyrite-dominated	Pyrite-dominated	Pyrite-dominated	Pyrite-dominated	Pyrite-dominated	Pyrite-dominated	Pyrite-dominated
Li7 (ppm)	BDL	BDL	1	BDL	BDL	BDL	BDL	BDL	BDL
Be9 (ppm)	-	-	-	BDL	-	-	-	BDL	BDL
B11 (ppm)	BDL	BDL	BDL	BDL	BDL	BDL	BDL	BDL	BDL
Na23 (ppm)	BDL	BDL	BDL	BDL	BDL	BDL	BDL	BDL	BDL
Mg24 (ppm)	6	1221	56	74	6563	30	1	BDL	BDL
Al27 (ppm)	BDL	31	BDL	9	116	7	BDL	BDL	BDL
Si29 (ppm)	BDL	1725	BDL	BDL	7434	BDL	BDL	BDL	BDL
P31 (ppm)	BDL	BDL	BDL	BDL	BDL	BDL	BDL	BDL	BDL
S32 (ppm)	436812	444665	423955	429750	426806	437336	560347	588095	608998
K39 (ppm)	BDL	BDL	BDL	BDL	BDL	BDL	BDL	BDL	BDL
Ca44 (ppm)	BDL	BDL	BDL	BDL	BDL	BDL	BDL	BDL	BDL
Sc45 (ppm)	BDL	BDL	BDL	BDL	BDL	BDL	BDL	BDL	BDL
Ti47 (ppm)	BDL	-	BDL	BDL	3	BDL	-	BDL	-
V51 (ppm)	BDL	0	BDL	BDL	0	BDL	BDL	BDL	BDL
Cr52 (ppm)	BDL	4	BDL	BDL	20	BDL	BDL	BDL	BDL
Mn55 (ppm)	1	3	5	3	3	2	BDL	BDL	0
Fe57 (ppm)	-	-	-	-	-	-	-	-	-
Co59 (ppm)	2052	1485	5156	3997	4237	-	11	121	498
Ni60 (ppm)	1568	2228	-	2497	-	-	1257	978	42
Cu63 (ppm)	121	114	115	184	1040	97	2	BDL	62
Zn66 (ppm)	3	3	1	2	63	BDL	BDL	BDL	BDL
Ga71 (ppm)	-	-	-	-	-	-	BDL	-	BDL
Ge73 (ppm)	-	-	BDL	-	-	-	BDL	-	BDL
As75 (ppm)	119	76	1173	1555	1589	1085	1414	122	16
Se77 (ppm)	21	97	84	65	265	183	47	31	7
Rb85 (ppm)	-	BDL	BDL	-	BDL	BDL	BDL	BDL	BDL
Sr88 (ppm)	-	-	-	-	-	-	-	-	-
Y89 (ppm)	-	-	-	-	-	-	-	-	-
Zr90 (ppm)	-	-	-	-	-	-	-	-	-
Nb93 (ppm)	3	3	-	1	-	BDL	-	BDL	BDL
Mo95 (ppm)	-	-	-	BDL	-	-	-	-	-
Ru101 (ppm)	-	-	BDL	-	-	-	-	-	BDL
Rh103 (ppm)	-	BDL	-	-	BDL	-	-	-	BDL
Pd104 (ppm)	-	BDL	BDL	BDL	-	BDL	-	-	BDL

Pd105 (ppm)	BDL	-	BDL	BDL	-	BDL	-	-	BDL
Pd106 (ppm)	1	1	1	1	2	1	BDL	-	0
Ag107 (ppm)	BDL	-	BDL	-	1	BDL	BDL	BDL	-
Cd111 (ppm)	-	-	-	BDL	-	-	-	-	-
In115 (ppm)	BDL	BDL	BDL	BDL	BDL	BDL	BDL	BDL	BDL
Sn118 (ppm)	8	3	47	57	13	35	0	0	6
Sb121 (ppm)	-	-	82	99	11	67	-	BDL	BDL
Te125 (ppm)	BDL	BDL	BDL	BDL	BDL	BDL	BDL	BDL	BDL
Cs133 (ppm)	-	-	0	-	-	-	-	-	-
Ba137 (ppm)	-	-	-	-	-	-	-	-	-
La139 (ppm)	-	-	-	-	-	-	-	-	-
Ce140 (ppm)	-	-	-	-	-	BDL	-	-	-
Pr141 (ppm)	-	-	-	-	-	-	-	-	-
Nd146 (ppm)	-	-	-	-	-	-	-	-	-
Sm147 (ppm)	-	-	-	-	-	-	-	-	-
Eu153 (ppm)	-	-	BDL	-	-	-	-	-	-
Gd157 (ppm)	-	-	-	-	-	-	-	-	-
Tb159 (ppm)	-	-	-	-	-	-	-	-	-
Dy163 (ppm)	-	-	-	-	-	-	-	-	-
Ho165 (ppm)	-	-	-	-	-	-	-	-	-
Er166 (ppm)	-	-	-	-	-	-	-	-	-
Tm169 (ppm)	-	-	-	-	-	-	-	-	-
Yb172 (ppm)	-	-	-	-	-	-	-	-	-
Lu175 (ppm)	-	-	-	-	-	-	-	-	-
Hf178 (ppm)	BDL	BDL	-	-	-	-	-	-	-
Ta181 (ppm)	-	-	-	-	-	-	-	-	BDL
W182 (ppm)	BDL	BDL	BDL	BDL	0	BDL	BDL	BDL	BDL
Re185 (ppm)	BDL	BDL	BDL	BDL	BDL	BDL	BDL	BDL	BDL
Os189 (ppm)	BDL	BDL	BDL	-	-	BDL	BDL	-	-
Ir193 (ppm)	BDL	BDL	-	BDL	-	BDL	BDL	BDL	BDL
Pt195 (ppm)	-	1	-	6	-	4	BDL	-	0
Au197 (ppm)	16	22	27	26	20	17	19	BDL	17
Hg202 (ppm)	46	35	229	293	74	203	BDL	BDL	19
Pb204 (ppm)	0	0	0	0	0	1	BDL	BDL	0
Tl205 (ppm)	23	10	220	-	54	-	1	0	5
Pb206 (ppm)	22	-	-	-	55	203	1	-	5
Pb207 (ppm)	23	9	217	303	55	200	-	-	5
Pb208 (ppm)	1	1	8	10	-	7	BDL	BDL	0
Bi209 (ppm)	-	-	-	-	-	-	-	-	-
Th232 (ppm)	-	BDL	-	-	-	-	-	-	-
U238 (ppm)	23	10	216	299	55	202	2	BDL	5
PbTotal (ppm)	-	-	-	-	-	-	-	-	-

Table D1. Trace element data for pyrite continued.

Deposit	Tilt Cove	Tilt Cove	Tilt Cove	Tilt Cove	Tilt Cove	Betts Cove	Betts Cove	Betts Cove	Betts Cove
Sample	KKMSC77_Py7	KKMSC77_Py1	KKMSC77_Py2	KKMSC77_Py4	KKMSC77_Py3	KKMSC32_Py1	KKMSC32_Py2	KKMSC32_Py3	KKMSC32_Py4
Date	2023-11-21	2023-11-21	2023-11-21	2023-11-21	2023-11-21	2023-11-21	2023-11-21	2023-11-21	2023-11-21
Facies	Pyrite-dominated	Pyrite-dominated	Pyrite-dominated	Pyrite-dominated	Pyrite-dominated	Sphalerite-pyrite-dominated	Sphalerite-pyrite-dominated	Sphalerite-pyrite-dominated	Sphalerite-pyrite-dominated
Li7 (ppm)	BDL	BDL	BDL	BDL	BDL	1	1	BDL	BDL
Be9 (ppm)	-	BDL	-	-	-	BDL	-	BDL	-
B11 (ppm)	BDL	BDL	BDL	BDL	BDL	BDL	BDL	BDL	BDL
Na23 (ppm)	BDL	BDL	BDL	BDL	BDL	32	BDL	BDL	BDL
Mg24 (ppm)	BDL	7	BDL	BDL	35	245	2525	153	-
Al27 (ppm)	BDL	5	BDL	BDL	3	42562	2397	143	8005
Si29 (ppm)	BDL	745	BDL	BDL	BDL	64157	4585	BDL	19355
P31 (ppm)	BDL	BDL	BDL	BDL	BDL	107	BDL	BDL	255
S32 (ppm)	542593	577900	617494	553895	553892	1294915	851095	483822	1821891
K39 (ppm)	BDL	BDL	BDL	BDL	BDL	BDL	BDL	BDL	BDL
Ca44 (ppm)	BDL	BDL	BDL	BDL	BDL	46610	BDL	BDL	6062
Sc45 (ppm)	BDL	BDL	BDL	BDL	BDL	BDL	BDL	BDL	BDL
Ti47 (ppm)	BDL	BDL	BDL	BDL	BDL	57	-	-	11
V51 (ppm)	BDL	BDL	BDL	BDL	BDL	121	3	BDL	38
Cr52 (ppm)	BDL	BDL	BDL	BDL	BDL	7	BDL	BDL	8
Mn55 (ppm)	0	BDL	BDL	BDL	BDL	2384	755	7	3400
Fe57 (ppm)	-	-	-	-	-	-	-	-	-
Co59 (ppm)	662	72	143	53	284	179	505	-	-
Ni60 (ppm)	51	2372	3807	1909	3109	152	265	-	-
Cu63 (ppm)	83	1134	5	1	45	649	455	5	4647
Zn66 (ppm)	BDL	BDL	BDL	BDL	BDL	2640181	925612	5888	4407484
Ga71 (ppm)	BDL	BDL	-	-	-	-	-	-	-
Ge73 (ppm)	BDL	-	-	BDL	-	BDL	-	-	BDL
As75 (ppm)	21	93	98	59	67	380	300	243	152
Se77 (ppm)	8	73	105	56	81	68	25	5	100
Rb85 (ppm)	BDL	BDL	BDL	BDL	BDL	BDL	BDL	BDL	-
Sr88 (ppm)	-	-	-	-	-	-	-	-	-
Y89 (ppm)	-	-	-	-	-	-	-	-	-
Zr90 (ppm)	-	-	-	-	-	-	-	-	-
Nb93 (ppm)	BDL	-	-	BDL	-	-	-	-	-
Mo95 (ppm)	-	-	-	-	-	55	81	-	110
Ru101 (ppm)	-	-	BDL	BDL	-	-	-	-	-
Rh103 (ppm)	BDL	-	BDL	-	BDL	-	-	-	BDL
Pd104 (ppm)	BDL	BDL	-	-	BDL	-	154	-	740
Pd105 (ppm)	BDL	-	-	-	BDL	-	BDL	-	-

Pd106 (ppm)	0	2	BDL	BDL	1	-	-	-	-
Ag107 (ppm)	BDL	0	BDL	BDL	-	72	62	-	101
Cd111 (ppm)	-	-	-	-	BDL	-	-	-	-
In115 (ppm)	BDL	BDL	BDL	BDL	BDL	-	-	-	-
Sn118 (ppm)	6	4	BDL	BDL	2	7	BDL	BDL	1
Sb121 (ppm)	BDL	BDL	BDL	BDL	-	16	14	1	7
Te125 (ppm)	BDL	BDL	BDL	BDL	BDL	-	13	BDL	2
Cs133 (ppm)	-	-	-	-	-	BDL	BDL	BDL	BDL
Ba137 (ppm)	-	-	-	-	-	-	-	-	-
La139 (ppm)	-	-	-	-	-	-	-	-	-
Ce140 (ppm)	-	-	-	-	-	-	-	-	-
Pr141 (ppm)	-	-	-	-	-	-	-	-	-
Nd146 (ppm)	-	-	-	-	-	-	-	-	-
Sm147 (ppm)	-	-	-	-	-	-	-	-	-
Eu153 (ppm)	-	-	-	-	-	-	-	-	-
Gd157 (ppm)	-	-	-	-	-	-	-	-	-
Tb159 (ppm)	-	-	-	-	-	-	-	-	-
Dy163 (ppm)	-	-	-	-	-	-	-	-	-
Ho165 (ppm)	-	-	-	-	-	-	-	-	-
Er166 (ppm)	-	-	-	-	-	-	-	-	-
Tm169 (ppm)	-	-	0	-	-	-	-	-	-
Yb172 (ppm)	-	-	-	-	-	-	-	-	-
Lu175 (ppm)	-	-	-	-	-	-	-	-	-
Hf178 (ppm)	-	-	-	-	-	-	-	-	-
Ta181 (ppm)	-	-	-	BDL	-	-	-	-	-
W182 (ppm)	BDL	BDL	BDL	BDL	BDL	-	-	BDL	-
Re185 (ppm)	BDL	BDL	BDL	BDL	BDL	BDL	BDL	BDL	BDL
Os189 (ppm)	-	-	-	BDL	-	BDL	BDL	BDL	BDL
Ir193 (ppm)	BDL	-	BDL	BDL	BDL	-	-	-	BDL
Pt195 (ppm)	-	-	BDL	-	-	BDL	BDL	BDL	BDL
Au197 (ppm)	15	15	BDL	BDL	BDL	-	-	-	BDL
Hg202 (ppm)	31	43	BDL	BDL	34	1472	33	BDL	2045
Pb204 (ppm)	1	0	BDL	BDL	0	7430	337	BDL	9630
Tl205 (ppm)	5	-	0	BDL	21	1	3	BDL	0
Pb206 (ppm)	4	37	-	BDL	20	-	201	-	-
Pb207 (ppm)	-	-	0	0	21	-	-	15	158
Pb208 (ppm)	0	0	BDL	-	0	211	207	16	149
Bi209 (ppm)	-	-	-	-	-	BDL	BDL	BDL	BDL
Th232 (ppm)	-	-	-	-	-	-	-	-	-
U238 (ppm)	5	37	0	BDL	21	-	-	-	BDL
PbTotal (ppm)	-	-	-	-	-	313	203	16	295

Table D1. Trace element data for pyrite continued.

Deposit	Betts Cove	Betts Cove	Betts Cove	Betts Cove	Betts Cove	Betts Cove	Betts Cove	Betts Cove	Betts Cove
Sample	KKMSC32_Py5	KKMSC32_Py6	KKMSC32_Py7	KKMSC32_Py8	KKMSC32_Py9	KKMSC32_Py1 0	KKMSC32_Py1 1	KKMSC32_Py1 2	KKMSC32_Py1 8
Date	2023-11-21	2023-11-21	2023-11-21	2023-11-21	2023-11-21	2023-11-21	2023-11-21	2023-11-21	2023-11-21
Facies	Sphalerite-pyrite-dominated	Sphalerite-pyrite-dominated	Sphalerite-pyrite-dominated	Sphalerite-pyrite-dominated	Sphalerite-pyrite-dominated	Sphalerite-pyrite-dominated	Sphalerite-pyrite-dominated	Sphalerite-pyrite-dominated	Sphalerite-pyrite-dominated
Li7 (ppm)	BDL	BDL	BDL	BDL	BDL	BDL	BDL	BDL	BDL
Be9 (ppm)	-	-	-	BDL	-	BDL	-	BDL	-
B11 (ppm)	BDL	BDL	BDL	BDL	BDL	BDL	BDL	BDL	BDL
Na23 (ppm)	BDL	27	BDL	BDL	BDL	BDL	34	BDL	BDL
Mg24 (ppm)	1760	472	7	166	407	200	456	313	47
Al27 (ppm)	1717	405	3	174	377	147	591	282	5
Si29 (ppm)	3437	1561	BDL	17900	BDL	BDL	1681	BDL	BDL
P31 (ppm)	BDL	BDL	BDL	BDL	BDL	BDL	BDL	BDL	BDL
S32 (ppm)	504992	409998	503187	439849	466881	530771	380348	502094	439856
K39 (ppm)	15	32	BDL	20	BDL	BDL	93	BDL	BDL
Ca44 (ppm)	BDL	BDL	BDL	BDL	BDL	BDL	BDL	BDL	BDL
Sc45 (ppm)	BDL	BDL	BDL	BDL	BDL	BDL	1	BDL	BDL
Ti47 (ppm)	-	3	-	-	BDL	BDL	-	-	BDL
V51 (ppm)	4	1	BDL	2	1	BDL	8	1	BDL
Cr52 (ppm)	BDL	BDL	BDL	37	BDL	BDL	4	BDL	BDL
Mn55 (ppm)	261	325	BDL	1246	41	6	409	8	109
Fe57 (ppm)	-	-	-	-	-	-	-	-	-
Co59 (ppm)	-	76	96	310	70	89	53	307	68
Ni60 (ppm)	397	-	-	1208	530	265	-	-	-
Cu63 (ppm)	152	267	12	577	19	678	233	3	61
Zn66 (ppm)	144590	1077	5	28139	138	207	1837	417	569
Ga71 (ppm)	-	-	-	-	0	-	-	-	-
Ge73 (ppm)	BDL	-	BDL	BDL	-	BDL	-	BDL	-
As75 (ppm)	1497	1876	295	5036	710	190	2967	226	547
Se77 (ppm)	8	16	7	11	5	6	BDL	5	BDL
Rb85 (ppm)	BDL	0	BDL	BDL	BDL	-	0	-	BDL
Sr88 (ppm)	-	-	-	-	-	-	1	-	-
Y89 (ppm)	-	-	-	-	-	-	-	-	-
Zr90 (ppm)	-	-	-	-	-	-	-	-	-
Nb93 (ppm)	-	BDL	-	-	-	-	-	-	-
Mo95 (ppm)	59	15	1	-	12	BDL	15	8	-
Ru101 (ppm)	-	-	-	-	-	-	-	-	-
Rh103 (ppm)	-	-	BDL	-	-	0	-	-	-
Pd104 (ppm)	-	-	-	-	BDL	-	-	-	-

Pd105 (ppm)	-	-	-	-	-	BDL	-	BDL	-
Pd106 (ppm)	-	0	-	4	BDL	BDL	1	BDL	-
Ag107 (ppm)	30	14	BDL	22	1	5	16	0	11
Cd111 (ppm)	122	-	-	25	BDL	BDL	-	1	1
In115 (ppm)	-	-	BDL	0	-	-	-	-	BDL
Sn118 (ppm)	BDL	BDL	BDL	BDL	BDL	BDL	BDL	BDL	BDL
Sb121 (ppm)	36	25	0	-	13	4	52	0	60
Te125 (ppm)	16	10	BDL	-	1	3	15	BDL	8
Cs133 (ppm)	BDL	BDL	BDL	BDL	BDL	BDL	BDL	BDL	BDL
Ba137 (ppm)	-	-	-	-	-	-	-	-	-
La139 (ppm)	-	-	-	-	-	-	-	-	-
Ce140 (ppm)	-	-	-	-	-	-	-	-	-
Pr141 (ppm)	-	-	-	-	-	-	-	-	-
Nd146 (ppm)	-	-	-	-	-	-	-	-	-
Sm147 (ppm)	-	-	-	-	-	BDL	-	-	-
Eu153 (ppm)	-	-	-	-	-	-	-	-	-
Gd157 (ppm)	-	-	-	-	-	-	-	-	-
Tb159 (ppm)	-	-	-	-	-	-	-	-	-
Dy163 (ppm)	-	-	-	-	-	-	-	-	-
Ho165 (ppm)	-	-	-	-	-	-	-	-	-
Er166 (ppm)	-	-	-	-	-	-	-	-	-
Tm169 (ppm)	-	-	-	-	-	-	-	-	-
Yb172 (ppm)	-	-	-	-	-	-	-	-	-
Lu175 (ppm)	-	-	-	-	-	-	-	-	-
Hf178 (ppm)	-	-	-	-	-	-	-	-	-
Ta181 (ppm)	-	-	-	BDL	-	-	-	BDL	-
W182 (ppm)	-	-	-	-	-	-	-	BDL	BDL
Re185 (ppm)	BDL	BDL	BDL	BDL	BDL	BDL	BDL	BDL	BDL
Os189 (ppm)	BDL	BDL	BDL	BDL	BDL	BDL	BDL	BDL	BDL
Ir193 (ppm)	BDL	BDL	BDL	BDL	BDL	-	-	-	BDL
Pt195 (ppm)	BDL	BDL	BDL	-	-	BDL	-	-	BDL
Au197 (ppm)	-	-	-	-	2	-	-	BDL	-
Hg202 (ppm)	BDL	BDL	BDL	4	4	BDL	BDL	BDL	BDL
Pb204 (ppm)	270	311	BDL	225	33	94	190	BDL	591
Tl205 (ppm)	26	22	BDL	94	3	BDL	54	BDL	7
Pb206 (ppm)	287	-	-	-	29	39	192	5	666
Pb207 (ppm)	297	332	0	-	-	36	194	5	-
Pb208 (ppm)	298	341	1	221	29	39	192	5	671
Bi209 (ppm)	0	0	BDL	0	BDL	0	0	BDL	0
Th232 (ppm)	-	-	-	-	-	-	-	-	-
U238 (ppm)	-	-	-	1	-	-	0	-	-
PbTotal (ppm)	294	336	1	217	29	39	193	5	657

Table D1. Trace element data for pyrite continued.

Deposit	Betts Cove	Betts Cove	Betts Cove	Betts Cove	Betts Cove	Betts Cove	Betts Cove	Betts Cove	Betts Cove
Sample	KKMSC32_Py17	KKMSC32_Py16	KKMSC32_Py19	KKMSC32_Py22	KKMSC32_Py21	KKMSC32_Py20	KKMSC32_Py14	KKMSC32_Py13	KKMSC32_Py25
Date	2023-11-21	2023-11-21	2023-11-21	2023-11-21	2023-11-21	2023-11-21	2023-11-21	2023-11-21	2023-11-21
Facies	Sphalerite-pyrite-dominated	Sphalerite-pyrite-dominated	Sphalerite-pyrite-dominated	Sphalerite-pyrite-dominated	Sphalerite-pyrite-dominated	Sphalerite-pyrite-dominated	Sphalerite-pyrite-dominated	Sphalerite-pyrite-dominated	Sphalerite-pyrite-dominated
Li7 (ppm)	1	BDL	BDL	BDL	BDL	BDL	BDL	BDL	BDL
Be9 (ppm)	-	-	-	-	-	-	-	-	-
B11 (ppm)	BDL	BDL	BDL	BDL	BDL	BDL	BDL	BDL	BDL
Na23 (ppm)	BDL	BDL	BDL	BDL	BDL	BDL	BDL	BDL	BDL
Mg24 (ppm)	40	-	290	121	69	53	2	34	43
Al27 (ppm)	47	105	174	96	34	472	BDL	45	56
Si29 (ppm)	1205	BDL	1397	BDL	BDL	1821	BDL	BDL	BDL
P31 (ppm)	BDL	BDL	BDL	BDL	BDL	BDL	BDL	BDL	BDL
S32 (ppm)	655481	499308	483638	424502	410313	533156	428460	522725	462903
K39 (ppm)	BDL	BDL	BDL	BDL	BDL	BDL	BDL	BDL	BDL
Ca44 (ppm)	BDL	BDL	BDL	BDL	BDL	638	BDL	BDL	BDL
Sc45 (ppm)	BDL	BDL	BDL	BDL	BDL	BDL	BDL	BDL	BDL
Ti47 (ppm)	-	-	BDL	-	-	-	BDL	BDL	BDL
V51 (ppm)	BDL	BDL	1	1	BDL	2	BDL	BDL	BDL
Cr52 (ppm)	BDL	BDL	BDL	BDL	BDL	12	BDL	BDL	BDL
Mn55 (ppm)	263	3	691	1895	1910	336	2601	25	21
Fe57 (ppm)	-	-	-	-	-	-	-	-	-
Co59 (ppm)	106	-	23	-	-	133	-	104	-
Ni60 (ppm)	-	423	107	167	-	444	-	-	405
Cu63 (ppm)	112	2	193	241	911	76	124	28	16
Zn66 (ppm)	235127	70	5923	16080	7109	2987	10068	121	8
Ga71 (ppm)	-	-	-	-	-	-	-	-	-
Ge73 (ppm)	-	-	-	-	BDL	-	-	BDL	BDL
As75 (ppm)	260	400	1836	2538	551	1699	1097	553	307
Se77 (ppm)	10	6	36	25	16	15	5	6	8
Rb85 (ppm)	-	-	-	-	BDL	BDL	BDL	BDL	BDL
Sr88 (ppm)	-	-	-	-	-	-	-	-	-
Y89 (ppm)	-	-	-	-	-	-	-	-	-
Zr90 (ppm)	-	-	-	-	-	-	-	-	-
Nb93 (ppm)	-	-	-	-	-	-	-	-	-
Mo95 (ppm)	4	3	33	31	18	36	30	-	10
Ru101 (ppm)	-	-	-	-	-	-	-	-	-
Rh103 (ppm)	-	-	-	-	-	BDL	-	-	-
Pd104 (ppm)	-	BDL	1	-	-	BDL	2	-	BDL

Pd105 (ppm)	-	-	-	-	-	-	-	BDL	BDL
Pd106 (ppm)	-	-	-	3	-	1	-	-	-
Ag107 (ppm)	-	-	20	29	20	12	8	2	2
Cd111 (ppm)	-	BDL	5	-	6	3	-	BDL	BDL
In115 (ppm)	-	-	-	BDL	-	-	-	-	-
Sn118 (ppm)	BDL	BDL	BDL	BDL	BDL	BDL	BDL	BDL	BDL
Sb121 (ppm)	2	0	49	46	17	45	37	2	1
Te125 (ppm)	1	BDL	10	9	10	7	2	1	BDL
Cs133 (ppm)	BDL	BDL	BDL	BDL	BDL	BDL	BDL	BDL	BDL
Ba137 (ppm)	-	-	-	-	-	-	-	-	-
La139 (ppm)	-	-	-	-	-	-	-	-	-
Ce140 (ppm)	BDL	-	-	-	-	-	-	-	-
Pr141 (ppm)	-	-	-	-	-	-	-	-	-
Nd146 (ppm)	-	-	-	-	-	-	-	-	-
Sm147 (ppm)	-	-	-	-	-	-	-	-	-
Eu153 (ppm)	-	-	-	-	-	-	-	-	-
Gd157 (ppm)	-	-	-	-	-	-	-	-	-
Tb159 (ppm)	-	-	-	-	-	-	-	-	-
Dy163 (ppm)	-	-	-	-	-	-	BDL	BDL	-
Ho165 (ppm)	-	-	-	-	-	-	-	-	-
Er166 (ppm)	-	-	-	-	-	-	-	-	-
Tm169 (ppm)	-	-	-	-	-	-	-	-	-
Yb172 (ppm)	-	-	-	-	-	-	-	-	-
Lu175 (ppm)	-	-	-	-	BDL	-	-	-	-
Hf178 (ppm)	-	-	-	-	-	-	-	-	-
Ta181 (ppm)	-	-	-	-	-	-	-	-	-
W182 (ppm)	-	-	-	-	-	-	BDL	-	-
Re185 (ppm)	BDL	BDL	BDL	BDL	BDL	BDL	BDL	BDL	BDL
Os189 (ppm)	BDL	BDL	BDL	BDL	BDL	BDL	BDL	BDL	BDL
Ir193 (ppm)	BDL	BDL	-	-	BDL	BDL	-	BDL	BDL
Pt195 (ppm)	-	BDL	-	BDL	-	-	BDL	BDL	-
Au197 (ppm)	-	-	-	-	-	11	-	2	-
Hg202 (ppm)	7	BDL	BDL	BDL	BDL	BDL	BDL	BDL	BDL
Pb204 (ppm)	60	BDL	268	207	424	108	30	47	23
Tl205 (ppm)	BDL	0	28	33	16	18	202	5	2
Pb206 (ppm)	39	5	-	-	-	102	23	42	-
Pb207 (ppm)	37	4	-	222	369	-	-	-	-
Pb208 (ppm)	39	5	296	245	409	-	17	36	10
Bi209 (ppm)	BDL	BDL	0	0	0	0	BDL	BDL	BDL
Th232 (ppm)	-	-	-	-	-	-	-	-	-
U238 (ppm)	-	-	BDL	-	-	-	-	-	-
PbTotal (ppm)	47	5	292	236	393	108	17	37	10

Table D1. Trace element data for pyrite continued.

Deposit	Betts Cove	Betts Cove	Betts Cove	Betts Cove	Betts Cove	Betts Cove	Betts Cove	Betts Cove	Betts Cove
Sample	KKMSC32_Py24	KKMSC32_Py23	KKMSC32_Py38	KKMSC35_Py1	KKMSC35_Py5	KKMSC35_Py4	KKMSC35_Py3	KKMSC35_Py7	KKMSC35_Py6
Date	2023-11-21	2023-11-21	2023-11-21	2023-11-21	2023-11-21	2023-11-21	2023-11-21	2023-11-21	2023-11-21
Facies	Sphalerite-pyrite-dominated	Sphalerite-pyrite-dominated	Sphalerite-pyrite-dominated	Chalcopyrite-pyrrhotite-dominated	Chalcopyrite-pyrrhotite-dominated	Chalcopyrite-pyrrhotite-dominated	Chalcopyrite-pyrrhotite-dominated	Chalcopyrite-pyrrhotite-dominated	Chalcopyrite-pyrrhotite-dominated
Li7 (ppm)	BDL	BDL	BDL	BDL	BDL	BDL	BDL	BDL	BDL
Be9 (ppm)	BDL	-	-	BDL	-	-	BDL	-	-
B11 (ppm)	BDL	BDL	BDL	BDL	BDL	BDL	BDL	BDL	BDL
Na23 (ppm)	BDL	BDL	BDL	32	BDL	BDL	BDL	69	BDL
Mg24 (ppm)	57	55	35	26	17	-	22	147	1
Al27 (ppm)	50	42	89	79	BDL	7	23	130	BDL
Si29 (ppm)	BDL	BDL	BDL	BDL	BDL	BDL	BDL	BDL	BDL
P31 (ppm)	BDL	BDL	83	BDL	BDL	BDL	BDL	BDL	BDL
S32 (ppm)	491547	479982	896881	356081	505720	433399	462288	464608	446916
K39 (ppm)	BDL	BDL	43	BDL	BDL	BDL	BDL	BDL	BDL
Ca44 (ppm)	BDL	BDL	BDL	BDL	BDL	182	BDL	729	BDL
Sc45 (ppm)	BDL	BDL	BDL	BDL	BDL	BDL	BDL	BDL	BDL
Ti47 (ppm)	-	BDL	10	BDL	BDL	-	BDL	BDL	BDL
V51 (ppm)	BDL	BDL	BDL	BDL	BDL	BDL	BDL	BDL	BDL
Cr52 (ppm)	BDL	BDL	BDL	BDL	BDL	BDL	BDL	BDL	BDL
Mn55 (ppm)	20	3	1528	7	1	14	2	31	BDL
Fe57 (ppm)	-	-	-	-	-	-	-	-	-
Co59 (ppm)	103	17	192	729	25	27	68	516	54
Ni60 (ppm)	-	341	-	244	-	808	-	-	385
Cu63 (ppm)	42	2	242	2195	2013	7529	3227	99660	3070
Zn66 (ppm)	4725	13	1618573	37	103	429	238	431	275
Ga71 (ppm)	-	BDL	-	-	-	-	-	-	-
Ge73 (ppm)	-	-	-	-	-	-	BDL	BDL	-
As75 (ppm)	524	294	270	614	1668	2	637	2165	1157
Se77 (ppm)	30	6	41	1195	1796	990	1588	2776	1667
Rb85 (ppm)	BDL	BDL	BDL	-	BDL	BDL	BDL	BDL	BDL
Sr88 (ppm)	-	-	-	-	-	-	-	-	-
Y89 (ppm)	-	-	-	-	-	-	-	-	-
Zr90 (ppm)	-	-	-	-	-	-	-	-	-
Nb93 (ppm)	-	-	-	-	-	-	-	-	-
Mo95 (ppm)	14	23	6	BDL	BDL	BDL	BDL	BDL	BDL
Ru101 (ppm)	-	-	-	-	-	-	-	-	-
Rh103 (ppm)	-	BDL	-	-	-	-	BDL	-	-
Pd104 (ppm)	-	-	-	-	-	-	-	-	-

Pd105 (ppm)	-	-	-	BDL	-	0	BDL	-	-
Pd106 (ppm)	-	-	-	BDL	-	0	BDL	0	-
Ag107 (ppm)	2	0	27	49	3	51	-	83	7
Cd111 (ppm)	-	BDL	-	-	BDL	4	1	-	-
In115 (ppm)	-	-	-	-	1	-	1	3	-
Sn118 (ppm)	BDL	BDL	BDL	BDL	BDL	8	0	3	0
Sb121 (ppm)	2	0	5	36	72	23	98	77	80
Te125 (ppm)	5	BDL	1	40	13	7	41	78	12
Cs133 (ppm)	BDL	BDL	BDL	BDL	BDL	BDL	BDL	BDL	BDL
Ba137 (ppm)	-	-	-	-	-	-	-	-	-
La139 (ppm)	-	-	-	-	BDL	-	-	-	-
Ce140 (ppm)	-	-	-	-	-	-	-	-	-
Pr141 (ppm)	-	-	-	-	-	-	-	-	-
Nd146 (ppm)	-	-	-	-	-	-	-	-	-
Sm147 (ppm)	-	-	-	-	-	-	-	-	-
Eu153 (ppm)	-	-	-	-	-	-	-	-	-
Gd157 (ppm)	-	-	-	-	-	-	-	-	-
Tb159 (ppm)	-	-	-	-	-	-	-	-	-
Dy163 (ppm)	-	-	-	-	-	-	-	-	-
Ho165 (ppm)	-	-	-	-	-	-	-	-	-
Er166 (ppm)	-	-	-	-	-	-	-	-	-
Tm169 (ppm)	-	-	-	-	-	-	-	-	-
Yb172 (ppm)	-	-	-	-	-	-	-	-	-
Lu175 (ppm)	-	-	-	-	-	-	-	-	-
Hf178 (ppm)	-	-	-	-	-	-	-	-	-
Ta181 (ppm)	-	-	BDL	-	BDL	-	-	BDL	-
W182 (ppm)	-	BDL	-	-	-	-	-	-	BDL
Re185 (ppm)	BDL	BDL	BDL	BDL	BDL	BDL	BDL	BDL	BDL
Os189 (ppm)	BDL	BDL	BDL	BDL	BDL	BDL	BDL	BDL	BDL
Ir193 (ppm)	-	-	-	BDL	BDL	BDL	BDL	BDL	-
Pt195 (ppm)	BDL	-	-	-	BDL	BDL	-	-	BDL
Au197 (ppm)	-	-	-	-	-	1	-	-	-
Hg202 (ppm)	BDL	BDL	214	14	BDL	4	4	BDL	BDL
Pb204 (ppm)	50	23	955	384	194	64	355	8421	186
Tl205 (ppm)	1	BDL	BDL	1	0	6	1	1	1
Pb206 (ppm)	53	5	150	-	-	65	-	8507	-
Pb207 (ppm)	-	-	137	326	-	-	-	-	-
Pb208 (ppm)	61	5	146	309	186	68	396	9591	192
Bi209 (ppm)	BDL	BDL	BDL	7	0	1	2	20	2
Th232 (ppm)	-	-	-	-	-	-	-	-	-
U238 (ppm)	BDL	-	-	-	-	BDL	-	-	-
PbTotal (ppm)	57	5	157	314	188	66	382	9254	191

Table D1. Trace element data for pyrite continued.

Deposit	Betts Cove	Betts Cove	Betts Cove	Betts Cove	Betts Cove	Betts Cove	Betts Cove	Betts Cove	Betts Cove
Sample	KKMSC53_Py4	KKMSC53_Py5	KKMSC53_Py1	KKMSC53_Py2	KKMSC53_Py3	KKMSC42_Py6	KKMSC42_Py5	KKMSC42_Py4	KKMSC42_Py1
Date	2023-11-22	2023-11-22	2023-11-22	2023-11-22	2023-11-22	2023-11-22	2023-11-22	2023-11-22	2023-11-22
Facies	Chalcopyrite-dominated	Chalcopyrite-dominated	Chalcopyrite-dominated	Chalcopyrite-dominated	Chalcopyrite-dominated	Chalcopyrite-pyrrhotite-dominated	Chalcopyrite-pyrrhotite-dominated	Chalcopyrite-pyrrhotite-dominated	Chalcopyrite-pyrrhotite-dominated
Li7 (ppm)	6	2	2	1	3	BDL	BDL	BDL	3
Be9 (ppm)	BDL	-	-	-	BDL	-	-	-	-
B11 (ppm)	BDL	BDL	BDL	BDL	BDL	BDL	BDL	BDL	BDL
Na23 (ppm)	BDL	BDL	120	66	86	BDL	BDL	BDL	26
Mg24 (ppm)	62	91	25665	17971	-	14	17	185	106
Al27 (ppm)	73	41	26116	16611	14070	13	4	58	1141
Si29 (ppm)	BDL	BDL	18237	12648	10332	BDL	2931	BDL	9603
P31 (ppm)	BDL	BDL	31	BDL	703	BDL	BDL	BDL	BDL
S32 (ppm)	527995	529134	452916	410939	462362	411346	392203	306645	463142
K39 (ppm)	BDL	BDL	37	BDL	24	18	55	BDL	509
Ca44 (ppm)	BDL	BDL	551	294	2382	BDL	BDL	BDL	BDL
Sc45 (ppm)	BDL	BDL	9	6	5	BDL	8	BDL	BDL
Ti47 (ppm)	BDL	BDL	-	10	11	3	-	-	-
V51 (ppm)	BDL	BDL	49	29	27	BDL	BDL	BDL	BDL
Cr52 (ppm)	BDL	BDL	293	620	398	BDL	BDL	BDL	BDL
Mn55 (ppm)	7	4	348	232	192	12	6	18	8
Fe57 (ppm)	-	-	-	-	-	-	-	-	-
Co59 (ppm)	3	34	439	359	229	1174	1171	-	1
Ni60 (ppm)	-	34	273	204	-	942	-	-	-
Cu63 (ppm)	18	10	103	85	56	110	78	75	15
Zn66 (ppm)	6	5	53	33	30	2	19	5	2
Ga71 (ppm)	-	-	-	-	-	-	-	-	-
Ge73 (ppm)	BDL	BDL	BDL	-	BDL	-	-	BDL	BDL
As75 (ppm)	BDL	33	37	34	25	12	BDL	24	9
Se77 (ppm)	595	255	1119	1195	2935	734	648	606	535
Rb85 (ppm)	BDL	-	BDL	-	0	BDL	0	BDL	1
Sr88 (ppm)	-	-	-	-	-	1	-	-	-
Y89 (ppm)	-	-	-	0	-	-	-	-	-
Zr90 (ppm)	-	-	-	-	-	BDL	-	-	-
Nb93 (ppm)	-	-	-	-	BDL	-	-	-	-
Mo95 (ppm)	BDL	BDL	-	BDL	-	8	BDL	60	BDL
Ru101 (ppm)	BDL	-	-	-	-	BDL	-	-	-
Rh103 (ppm)	BDL	-	-	-	-	-	BDL	-	BDL
Pd104 (ppm)	-	-	BDL	-	BDL	-	BDL	-	BDL
Pd105 (ppm)	-	-	-	-	-	-	-	-	-

Pd106 (ppm)	-	-	BDL	BDL	BDL	BDL	BDL	-	-
Ag107 (ppm)	-	BDL	-	10	4	0	-	2	-
Cd111 (ppm)	-	1	1	0	-	-	BDL	-	-
In115 (ppm)	BDL	-	-	-	-	-	BDL	-	-
Sn118 (ppm)	BDL	BDL	BDL	BDL	BDL	BDL	1	BDL	BDL
Sb121 (ppm)	1	BDL	7	6	6	2	2	-	4
Te125 (ppm)	-	106	156	85	20	1	71	16	BDL
Cs133 (ppm)	BDL	BDL	0	0	0	BDL	BDL	BDL	BDL
Ba137 (ppm)	-	-	-	-	-	-	-	-	-
La139 (ppm)	-	-	-	-	-	-	-	-	-
Ce140 (ppm)	-	-	-	-	-	-	-	-	-
Pr141 (ppm)	-	-	-	-	-	-	-	-	-
Nd146 (ppm)	-	-	-	-	-	-	-	-	-
Sm147 (ppm)	-	-	-	-	-	-	-	-	-
Eu153 (ppm)	-	-	-	-	-	-	-	-	BDL
Gd157 (ppm)	-	-	-	-	-	-	-	-	-
Tb159 (ppm)	-	-	-	-	-	-	-	-	-
Dy163 (ppm)	BDL	-	-	-	-	-	-	-	-
Ho165 (ppm)	-	-	-	-	-	-	-	-	-
Er166 (ppm)	-	-	-	-	-	-	-	-	-
Tm169 (ppm)	-	-	-	-	-	-	-	-	-
Yb172 (ppm)	-	-	-	-	-	-	-	-	-
Lu175 (ppm)	-	-	-	-	-	-	-	-	-
Hf178 (ppm)	-	-	-	-	-	-	-	-	-
Ta181 (ppm)	-	-	-	-	-	-	BDL	-	-
W182 (ppm)	BDL	-	BDL	-	-	1	BDL	BDL	BDL
Re185 (ppm)	BDL	0	BDL	BDL	BDL	BDL	BDL	1	BDL
Os189 (ppm)	BDL	BDL	BDL	BDL	BDL	BDL	BDL	BDL	0
Ir193 (ppm)	-	-	-	BDL	BDL	-	BDL	BDL	-
Pt195 (ppm)	BDL	BDL	-	BDL	BDL	BDL	BDL	BDL	-
Au197 (ppm)	BDL	-	-	-	BDL	-	-	BDL	-
Hg202 (ppm)	BDL	6	5	6	BDL	26	BDL	BDL	BDL
Pb204 (ppm)	BDL	31	116	111	92	121	1024	362	23
Tl205 (ppm)	0	0	3	2	2	39	27	28	1
Pb206 (ppm)	-	4	101	82	84	22	2092	391	13
Pb207 (ppm)	1	4	104	-	82	29	1840	492	16
Pb208 (ppm)	1	5	107	93	86	32	1759	391	16
Bi209 (ppm)	BDL	0	BDL	BDL	BDL	1	40	14	0
Th232 (ppm)	-	-	-	-	-	-	-	-	-
U238 (ppm)	-	-	-	-	-	BDL	-	-	BDL
PbTotal (ppm)	1	5	105	89	85	30	1848	412	15

Table D1. Trace element data for pyrite continued.

Deposit	Betts Cove	Betts Cove	Tilt Cove	Tilt Cove	Tilt Cove	Tilt Cove	Tilt Cove	Tilt Cove	Tilt Cove
Sample	KKMSC42_Py2	KKMSC42_Py3	KKMSC70_Py1	KKMSC70_Py10	KKMSC13_Py10	KKMSC13_Py11	KKMSC13_Py9	KKMSC13_Py13	KKMSC13_Py12
Date	2023-11-22	2023-11-22	2023-11-22	2023-11-22	2023-11-23	2023-11-23	2023-11-23	2023-11-23	2023-11-23
Facies	Chalcopyrite-pyrrhotite-dominated	Chalcopyrite-pyrrhotite-dominated	Chalcopyrite-pyrrhotite-dominated	Chalcopyrite-pyrrhotite-dominated	Pyrite-dominated	Pyrite-dominated	Pyrite-dominated	Pyrite-dominated	Pyrite-dominated
Li7 (ppm)	BDL	BDL	BDL	BDL	2	BDL	1	1	1
Be9 (ppm)	-	-	-	-	-	-	BDL	-	-
B11 (ppm)	BDL	246	BDL	BDL	BDL	BDL	BDL	BDL	BDL
Na23 (ppm)	BDL	BDL	350	150	BDL	BDL	BDL	BDL	BDL
Mg24 (ppm)	1847	BDL	138	84	25	-	89	387	77
Al27 (ppm)	1893	2052	6	BDL	19	9	51	25	11
Si29 (ppm)	BDL	BDL	BDL	BDL	1976	BDL	BDL	BDL	BDL
P31 (ppm)	BDL	1867	BDL	BDL	BDL	BDL	BDL	BDL	BDL
S32 (ppm)	322345	316438	494293	818504	560842	456367	520734	493015	517210
K39 (ppm)	BDL	BDL	14	BDL	BDL	BDL	BDL	BDL	BDL
Ca44 (ppm)	591	BDL	105	BDL	BDL	BDL	BDL	BDL	BDL
Sc45 (ppm)	BDL	36	BDL	7	BDL	BDL	BDL	BDL	BDL
Ti47 (ppm)	BDL	BDL	BDL	BDL	BDL	-	BDL	-	-
V51 (ppm)	3	83	BDL	3	BDL	BDL	BDL	BDL	BDL
Cr52 (ppm)	BDL	BDL	BDL	BDL	BDL	BDL	BDL	BDL	BDL
Mn55 (ppm)	61	61	1	4	4	4	1	2	1
Fe57 (ppm)	-	-	-	-	-	-	-	-	-
Co59 (ppm)	31	53	11025	11	0	9	14	1	-
Ni60 (ppm)	-	BDL	20326	81	-	-	-	-	13
Cu63 (ppm)	51	30	1447	679589	2	416	6	2459	2
Zn66 (ppm)	8	129	14	394	5	46	2	113	2
Ga71 (ppm)	-	-	-	-	BDL	BDL	-	-	BDL
Ge73 (ppm)	-	-	BDL	BDL	BDL	BDL	BDL	-	-
As75 (ppm)	35	428	5	17	657	335	179	90673	715
Se77 (ppm)	539	1079	159	195	BDL	BDL	BDL	7	4
Rb85 (ppm)	BDL	-	-	BDL	BDL	BDL	BDL	BDL	BDL
Sr88 (ppm)	-	-	-	-	-	-	-	-	-
Y89 (ppm)	-	-	-	-	-	-	-	-	-
Zr90 (ppm)	-	-	-	-	-	-	-	BDL	-
Nb93 (ppm)	-	-	-	-	BDL	-	-	-	6
Mo95 (ppm)	BDL	BDL	BDL	BDL	-	-	-	-	-
Ru101 (ppm)	BDL	-	BDL	BDL	-	-	-	-	-
Rh103 (ppm)	-	-	0	8	BDL	-	-	-	-
Pd104 (ppm)	-	-	-	-	BDL	BDL	BDL	-	BDL

Pd105 (ppm)	BDL	-	-	-	-	-	-	BDL	-
Pd106 (ppm)	-	BDL	-	-	BDL	3	1	6	-
Ag107 (ppm)	9	-	-	114	BDL	BDL	BDL	-	BDL
Cd111 (ppm)	-	BDL	2	37	-	-	BDL	-	-
In115 (ppm)	-	-	-	13	BDL	BDL	BDL	BDL	BDL
Sn118 (ppm)	BDL	15	BDL	BDL	0	7	2	17	-
Sb121 (ppm)	31	120	59	36	BDL	0	BDL	1	BDL
Te125 (ppm)	21	BDL	2	BDL	BDL	BDL	BDL	BDL	BDL
Cs133 (ppm)	BDL	BDL	BDL	1	-	-	-	-	-
Ba137 (ppm)	-	-	-	-	-	-	-	-	-
La139 (ppm)	-	-	-	-	-	-	-	-	-
Ce140 (ppm)	-	-	-	-	-	-	-	-	-
Pr141 (ppm)	-	-	-	-	-	-	-	-	-
Nd146 (ppm)	-	-	-	-	-	-	-	-	-
Sm147 (ppm)	BDL	-	-	-	-	-	-	-	-
Eu153 (ppm)	-	-	-	-	-	-	-	-	-
Gd157 (ppm)	-	-	-	-	-	-	-	-	-
Tb159 (ppm)	-	-	-	-	-	-	-	-	-
Dy163 (ppm)	-	-	-	-	-	-	-	-	-
Ho165 (ppm)	-	BDL	-	-	-	-	-	-	-
Er166 (ppm)	-	-	-	-	-	-	-	-	-
Tm169 (ppm)	-	-	-	-	BDL	-	-	-	-
Yb172 (ppm)	-	-	-	-	-	BDL	-	-	-
Lu175 (ppm)	-	-	-	-	-	-	-	-	-
Hf178 (ppm)	-	-	-	-	-	-	-	-	-
Ta181 (ppm)	-	-	BDL	BDL	-	BDL	-	-	-
W182 (ppm)	-	-	-	-	BDL	BDL	BDL	BDL	BDL
Re185 (ppm)	BDL	4	BDL	BDL	BDL	BDL	-	BDL	BDL
Os189 (ppm)	BDL	29	BDL	BDL	BDL	BDL	BDL	BDL	BDL
Ir193 (ppm)	-	BDL	BDL	BDL	-	BDL	BDL	BDL	BDL
Pt195 (ppm)	-	BDL	-	BDL	BDL	BDL	-	0	-
Au197 (ppm)	-	215	-	-	BDL	BDL	30	30	BDL
Hg202 (ppm)	BDL	191	3	129	BDL	26	64	82	BDL
Pb204 (ppm)	BDL	BDL	413	1281	BDL	BDL	BDL	0	BDL
Tl205 (ppm)	7	29	2	4	4	-	12	30	-
Pb206 (ppm)	185	123	447	492	2	37	12	22	-
Pb207 (ppm)	-	54	457	457	2	30	15	29	1
Pb208 (ppm)	183	137	491	427	BDL	1	0	1	BDL
Bi209 (ppm)	0	6	3	7	-	-	-	-	-
Th232 (ppm)	-	-	-	-	-	BDL	0	-	-
U238 (ppm)	-	-	-	-	3	31	14	29	1
PbTotal (ppm)	187	70	472	462	-	-	-	-	-

Table D1. Trace element data for pyrite continued.

Deposit	Tilt Cove	Tilt Cove	Tilt Cove	Tilt Cove	Tilt Cove	Tilt Cove	Tilt Cove	Tilt Cove	Tilt Cove
Sample	KKMSC13_Py1 4	KKMSC13_Py1 6	KKMSC13_Py1 5	KKMSC13_Py2 3	KKMSC13_Py1 9	KKMSC13_Py2 1	KKMSC13_Py2 2	KKMSC13_Py1 6	KKMSC13_Py1 5
Date	2023-11-23	2023-11-23	2023-11-23	2023-11-23	2023-11-23	2023-11-23	2023-11-23	2023-11-23	2023-11-23
Facies	Pyrite-dominated	Pyrite-dominated	Pyrite-dominated	Pyrite-dominated	Pyrite-dominated	Pyrite-dominated	Pyrite-dominated	Pyrite-dominated	Pyrite-dominated
Li7 (ppm)	2	1	BDL	BDL	BDL	BDL	2	1	BDL
Be9 (ppm)	-	-	-	BDL	-	-	-	-	-
B11 (ppm)	BDL	BDL	BDL	BDL	BDL	BDL	BDL	BDL	BDL
Na23 (ppm)	BDL	BDL	BDL	BDL	BDL	BDL	BDL	BDL	BDL
Mg24 (ppm)	27	16	9	BDL	85	BDL	35	-	6
Al27 (ppm)	17	17	3	BDL	41	BDL	41	22	4
Si29 (ppm)	BDL	BDL	BDL	BDL	BDL	BDL	BDL	BDL	BDL
P31 (ppm)	BDL	BDL	BDL	BDL	BDL	BDL	BDL	BDL	BDL
S32 (ppm)	518516	486391	494161	504699	471270	517637	497626	444346	572080
K39 (ppm)	BDL	BDL	BDL	BDL	BDL	BDL	BDL	BDL	BDL
Ca44 (ppm)	BDL	BDL	BDL	BDL	BDL	BDL	BDL	BDL	BDL
Sc45 (ppm)	BDL	BDL	BDL	BDL	BDL	BDL	BDL	BDL	BDL
Ti47 (ppm)	BDL	-	-	-	BDL	BDL	BDL	6	BDL
V51 (ppm)	BDL	BDL	BDL	BDL	BDL	BDL	BDL	BDL	BDL
Cr52 (ppm)	BDL	BDL	BDL	BDL	BDL	BDL	BDL	BDL	BDL
Mn55 (ppm)	1	1	BDL	BDL	4	BDL	2	5	2
Fe57 (ppm)	-	-	-	-	-	-	-	-	-
Co59 (ppm)	87	35	BDL	8	1	BDL	42	0	1
Ni60 (ppm)	32	-	57	-	-	-	-	-	-
Cu63 (ppm)	2	2	4	5	8493	6	77	890	160
Zn66 (ppm)	1	2	BDL	BDL	86	BDL	2	7	46
Ga71 (ppm)	-	BDL	-	-	-	-	-	-	BDL
Ge73 (ppm)	-	BDL	2	-	-	BDL	-	BDL	-
As75 (ppm)	576	105	2846	926	130323	4386	143	696	193
Se77 (ppm)	BDL	BDL	8	BDL	7	6	4	BDL	BDL
Rb85 (ppm)	BDL	BDL	BDL	BDL	BDL	BDL	BDL	BDL	BDL
Sr88 (ppm)	-	-	-	-	-	-	-	-	-
Y89 (ppm)	-	-	-	-	-	-	-	-	-
Zr90 (ppm)	-	-	-	BDL	-	-	-	-	-
Nb93 (ppm)	BDL	1	0	BDL	-	BDL	-	BDL	BDL
Mo95 (ppm)	-	-	BDL	-	-	-	-	-	-
Ru101 (ppm)	-	-	-	-	0	-	-	-	-
Rh103 (ppm)	BDL	-	BDL	-	BDL	-	-	BDL	-
Pd104 (ppm)	-	-	-	BDL	-	-	BDL	-	BDL

Pd105 (ppm)	BDL	-	BDL	BDL	-	-	BDL	BDL	BDL
Pd106 (ppm)	BDL	BDL	0	1	81	-	2	2	5
Ag107 (ppm)	-	BDL	BDL	BDL	BDL	-	BDL	-	-
Cd111 (ppm)	-	-	BDL	BDL	0	BDL	-	-	-
In115 (ppm)	BDL	BDL	0	BDL	BDL	BDL	BDL	BDL	BDL
Sn118 (ppm)	BDL	0	1	1	55	1	2	1	1
Sb121 (ppm)	BDL	BDL	BDL	-	6	BDL	BDL	BDL	BDL
Te125 (ppm)	BDL	BDL	BDL	BDL	BDL	BDL	BDL	BDL	BDL
Cs133 (ppm)	-	-	-	-	-	-	-	-	-
Ba137 (ppm)	-	-	-	-	-	-	-	-	-
La139 (ppm)	-	-	-	-	-	-	-	-	-
Ce140 (ppm)	-	-	-	-	-	-	-	-	-
Pr141 (ppm)	-	-	-	-	-	-	-	-	-
Nd146 (ppm)	-	-	-	-	-	-	-	-	-
Sm147 (ppm)	-	-	-	-	-	-	-	-	-
Eu153 (ppm)	-	-	-	-	-	-	-	-	-
Gd157 (ppm)	-	-	-	-	-	-	-	-	-
Tb159 (ppm)	-	-	-	-	-	-	-	-	-
Dy163 (ppm)	-	-	-	-	-	-	-	-	-
Ho165 (ppm)	-	-	-	-	-	-	-	-	-
Er166 (ppm)	-	-	-	-	-	-	-	-	-
Tm169 (ppm)	-	-	-	-	-	-	-	-	-
Yb172 (ppm)	-	-	-	-	-	-	-	-	-
Lu175 (ppm)	-	-	-	-	-	-	-	-	-
Hf178 (ppm)	-	-	BDL	-	-	-	BDL	-	-
Ta181 (ppm)	BDL	-	-	-	-	-	BDL	-	BDL
W182 (ppm)	BDL	BDL	BDL	BDL	BDL	BDL	BDL	BDL	BDL
Re185 (ppm)	BDL	BDL	BDL	BDL	BDL	BDL	BDL	BDL	BDL
Os189 (ppm)	BDL	BDL	-	-	BDL	-	-	-	-
Ir193 (ppm)	BDL	BDL	BDL	BDL	BDL	BDL	BDL	-	BDL
Pt195 (ppm)	BDL	-	0	0	13	BDL	-	-	-
Au197 (ppm)	32	17	BDL	BDL	BDL	BDL	BDL	BDL	11
Hg202 (ppm)	45	20	BDL	19	65	BDL	23	BDL	BDL
Pb204 (ppm)	BDL	BDL	BDL	BDL	0	BDL	0	BDL	BDL
Tl205 (ppm)	BDL	-	9	-	75	5	-	14	-
Pb206 (ppm)	-	0	8	8	72	-	13	15	5
Pb207 (ppm)	0	0	11	12	73	5	11	14	6
Pb208 (ppm)	BDL	BDL	BDL	0	2	BDL	1	0	0
Bi209 (ppm)	-	-	-	-	-	-	-	-	-
Th232 (ppm)	-	-	BDL	-	-	-	-	-	BDL
U238 (ppm)	1	1	10	12	73	5	13	15	6
PbTotal (ppm)	-	-	-	-	-	-	-	-	-

Table D1. Trace element data for pyrite continued.

Deposit	Tilt Cove	Tilt Cove	Tilt Cove	Tilt Cove	Tilt Cove	Tilt Cove	Tilt Cove	Tilt Cove
Sample	KKMSC13_Py1	KKMSC13_Py2	KKMSC13_Py4	KKMSC13_Py3	KKMSC13_Py6	KKMSC13_Py5	KKMSC13_Py8	KKMSC13_Py7
Date	2023-11-23	2023-11-23	2023-11-23	2023-11-23	2023-11-23	2023-11-23	2023-11-23	2023-11-23
Facies	Pyrite-dominated	Pyrite-dominated	Pyrite-dominated	Pyrite-dominated	Pyrite-dominated	Pyrite-dominated	Pyrite-dominated	Pyrite-dominated
Li7 (ppm)	2	BDL	BDL	2	BDL	BDL	4	0
Be9 (ppm)	-	-	-	-	-	BDL	BDL	-
B11 (ppm)	BDL	BDL	BDL	BDL	BDL	BDL	BDL	BDL
Na23 (ppm)	BDL	BDL	BDL	BDL	BDL	BDL	BDL	BDL
Mg24 (ppm)	41	-	-	BDL	BDL	1	BDL	21
Al27 (ppm)	53	BDL	BDL	2	BDL	BDL	22	BDL
Si29 (ppm)	BDL	BDL	BDL	BDL	BDL	BDL	BDL	BDL
P31 (ppm)	57	BDL	BDL	BDL	BDL	BDL	BDL	BDL
S32 (ppm)	520289	476418	527917	486332	464001	435840	480083	517689
K39 (ppm)	BDL	BDL	BDL	30	BDL	BDL	BDL	BDL
Ca44 (ppm)	BDL	BDL	BDL	BDL	BDL	BDL	BDL	BDL
Sc45 (ppm)	BDL	BDL	BDL	BDL	BDL	BDL	BDL	BDL
Ti47 (ppm)	142	-	BDL	BDL	BDL	-	BDL	BDL
V51 (ppm)	1	BDL	BDL	1	BDL	BDL	BDL	BDL
Cr52 (ppm)	BDL	BDL	BDL	3	BDL	BDL	BDL	BDL
Mn55 (ppm)	8	BDL	BDL	1	1	BDL	4	5
Fe57 (ppm)	-	-	-	-	-	-	-	-
Co59 (ppm)	10	BDL	0	0	BDL	BDL	0	BDL
Ni60 (ppm)	-	-	10	-	1	167	26	-
Cu63 (ppm)	96	4	9	15	3	7	8	2
Zn66 (ppm)	BDL	BDL	6	10	15	15	16	4
Ga71 (ppm)	-	BDL	BDL	-	-	-	-	-
Ge73 (ppm)	BDL	-	BDL	BDL	-	-	-	-
As75 (ppm)	39	59	1520	3083	7426	3806	2691	3689
Se77 (ppm)	1	BDL	BDL	BDL	8	3	4	BDL
Rb85 (ppm)	BDL	BDL	-	0	BDL	BDL	BDL	BDL
Sr88 (ppm)	-	-	-	-	-	-	-	-
Y89 (ppm)	-	-	-	-	-	-	-	-
Zr90 (ppm)	-	BDL	-	-	-	-	-	-
Nb93 (ppm)	0	-	BDL	-	0	BDL	-	78
Mo95 (ppm)	-	BDL	-	-	-	BDL	-	-
Ru101 (ppm)	-	-	BDL	-	-	-	BDL	-
Rh103 (ppm)	BDL	-	BDL	-	BDL	-	-	BDL
Pd104 (ppm)	0	BDL	-	-	-	BDL	BDL	-
Pd105 (ppm)	-	-	BDL	-	BDL	-	BDL	BDL

Pd106 (ppm)	7	BDL	BDL	BDL	BDL	-	1	0
Ag107 (ppm)	-	BDL	BDL	-	-	BDL	-	BDL
Cd111 (ppm)	BDL	-	BDL	-	-	BDL	-	-
In115 (ppm)	BDL	BDL	BDL	BDL	BDL	BDL	BDL	BDL
Sn118 (ppm)	0	BDL	BDL	BDL	BDL	BDL	0	0
Sb121 (ppm)	BDL	BDL	BDL	BDL	BDL	BDL	BDL	BDL
Te125 (ppm)	BDL	BDL	BDL	BDL	BDL	BDL	BDL	BDL
Cs133 (ppm)	-	-	-	-	-	-	-	-
Ba137 (ppm)	-	-	-	-	-	-	-	-
La139 (ppm)	-	-	-	-	-	-	-	-
Ce140 (ppm)	-	-	-	-	-	-	-	-
Pr141 (ppm)	-	-	-	-	-	-	-	-
Nd146 (ppm)	-	-	-	-	-	-	-	-
Sm147 (ppm)	-	-	-	-	-	-	-	-
Eu153 (ppm)	-	-	-	-	-	-	-	-
Gd157 (ppm)	-	-	-	-	-	-	-	-
Tb159 (ppm)	-	-	-	-	-	-	-	-
Dy163 (ppm)	-	-	-	-	-	-	-	-
Ho165 (ppm)	-	-	-	-	-	-	-	-
Er166 (ppm)	-	-	-	-	-	-	-	-
Tm169 (ppm)	-	-	-	-	-	-	-	-
Yb172 (ppm)	-	-	-	-	-	-	-	-
Lu175 (ppm)	-	-	-	-	-	-	-	-
Hf178 (ppm)	-	-	-	-	-	-	-	-
Ta181 (ppm)	-	BDL	-	-	-	-	-	BDL
W182 (ppm)	BDL	BDL	BDL	BDL	BDL	BDL	BDL	BDL
Re185 (ppm)	BDL	BDL	BDL	BDL	BDL	BDL	BDL	BDL
Os189 (ppm)	-	-	BDL	-	BDL	BDL	BDL	-
Ir193 (ppm)	-	BDL	-	BDL	BDL	-	BDL	BDL
Pt195 (ppm)	BDL	-	BDL	-	-	BDL	-	-
Au197 (ppm)	BDL	16	BDL	BDL	12	15	BDL	BDL
Hg202 (ppm)	BDL	BDL	BDL	BDL	BDL	BDL	22	BDL
Pb204 (ppm)	0	BDL	BDL	BDL	BDL	BDL	1	BDL
Tl205 (ppm)	2	-	0	0	BDL	-	-	3
Pb206 (ppm)	-	0	0	0	0	1	15	-
Pb207 (ppm)	2	0	0	-	0	1	11	3
Pb208 (ppm)	0	BDL	BDL	BDL	-	BDL	BDL	0
Bi209 (ppm)	-	-	-	-	-	-	-	-
Th232 (ppm)	-	-	BDL	-	-	-	-	-
U238 (ppm)	2	BDL	BDL	BDL	BDL	1	12	3
PbTotal (ppm)	-	-	-	-	-	-	-	-

Table D2. Trace element data for chalcopyrite.

Deposit	Betts Cove	Betts Cove	Betts Cove	Betts Cove	Betts Cove	Betts Cove	Betts Cove	Betts Cove	Betts Cove
Sample	KKMSC05B_C py1	KKMSC05B_C py2	KKMSC05B_C py3	KKMSC05B_C py4	KKMSC05B_C py5	KKMSC05B_C py6	KKMSC05B_C py7	KKMSC05B_C py9	KKMSC05B_C py10
Date	2023-11-20	2023-11-20	2023-11-20	2023-11-20	2023-11-20	2023-11-20	2023-11-20	2023-11-20	2023-11-20
Facies	Chalcopyrite-dominated	Chalcopyrite-dominated	Chalcopyrite-dominated	Chalcopyrite-dominated	Chalcopyrite-dominated	Chalcopyrite-dominated	Chalcopyrite-dominated	Chalcopyrite-dominated	Chalcopyrite-dominated
Li7 (ppm)	BDL	5	BDL	BDL	BDL	BDL	22	15	14
Be9 (ppm)	BDL	BDL	BDL	BDL	BDL	BDL	BDL	BDL	BDL
B11 (ppm)	BDL	BDL	BDL	BDL	BDL	BDL	BDL	BDL	BDL
Na23 (ppm)	BDL	BDL	BDL	249	BDL	BDL	BDL	109	BDL
Mg24 (ppm)	724	11172	1028	195	396	240	82836	46424	27254
Al27 (ppm)	661	11589	1094	99	436	171	89276	45817	29204
Si29 (ppm)	BDL	15927	4381	BDL	BDL	BDL	102246	60089	34692
P31 (ppm)	BDL	BDL	BDL	BDL	BDL	BDL	BDL	BDL	BDL
S32 (ppm)	393952	377359	406466	359834	357805	355946	455278	699949	280061
K39 (ppm)	BDL	64	BDL	BDL	BDL	BDL	BDL	BDL	BDL
Ca44 (ppm)	BDL	BDL	BDL	BDL	BDL	BDL	775	1104	BDL
Sc45 (ppm)	BDL	4	BDL	BDL	BDL	BDL	25	18	8
Ti47 (ppm)	BDL	14	BDL	BDL	BDL	BDL	87	51	BDL
V51 (ppm)	1	30	2	1	1	BDL	219	103	67
Cr52 (ppm)	BDL	34	BDL	BDL	BDL	BDL	202	375	180
Mn55 (ppm)	15	305	23	4	13	4	2076	1212	763
Fe57 (ppm)	263659	289820	278334	257144	275153	285602	425237	571419	290268
Co59 (ppm)	6	25	2	8	2	1	185	250	4
Ni60 (ppm)	-	-	-	-	BDL	2	101	-	-
Cu63 (ppm)	-	-	-	-	-	-	-	-	-
Zn66 (ppm)	569	330	761	1359	653	375	398	380	234
Ga71 (ppm)	0	1	BDL	-	-	BDL	-	-	-
Ge73 (ppm)	BDL	BDL	-	BDL	BDL	BDL	-	BDL	BDL
As75 (ppm)	BDL	BDL	BDL	BDL	BDL	BDL	127	2332	BDL
Se77 (ppm)	649	635	707	645	659	635	659	1065	548
Rb85 (ppm)	BDL	BDL	BDL	BDL	BDL	BDL	BDL	BDL	BDL
Sr88 (ppm)	-	-	-	BDL	-	-	3	5	-
Y89 (ppm)	-	BDL	-	-	BDL	BDL	-	-	-
Zr90 (ppm)	-	-	-	-	-	BDL	-	-	-
Nb93 (ppm)	BDL	-	BDL	-	-	BDL	BDL	-	BDL
Mo95 (ppm)	-	BDL	-	-	-	BDL	BDL	BDL	BDL
Ru101 (ppm)	-	-	-	BDL	-	-	-	-	-
Rh103 (ppm)	3	3	3	-	-	3	-	-	-
Pd104 (ppm)	-	-	-	BDL	BDL	-	BDL	BDL	BDL

Pd105 (ppm)	6	9	7	7	8	-	6	8	-
Pd106 (ppm)	1	BDL	BDL	1	BDL	BDL	-	BDL	BDL
Ag107 (ppm)	41	41	43	45	51	36	113	348	69
Cd111 (ppm)	5	2	3	9	-	2	2	-	BDL
In115 (ppm)	14	15	14	-	13	-	-	16	14
Sn118 (ppm)	3	2	3	1	3	2	BDL	4	2
Sb121 (ppm)	1	4	BDL	0	1	0	23	29	4
Te125 (ppm)	3	BDL	4	3	2	-	24	-	BDL
Cs133 (ppm)	BDL	BDL	BDL	BDL	BDL	BDL	BDL	BDL	BDL
Ba137 (ppm)	-	-	-	-	-	-	-	-	-
La139 (ppm)	-	-	-	-	-	BDL	-	-	-
Ce140 (ppm)	BDL	-	-	-	-	-	-	-	BDL
Pr141 (ppm)	-	-	-	-	-	BDL	-	BDL	-
Nd146 (ppm)	-	-	-	-	-	-	-	-	BDL
Sm147 (ppm)	-	-	-	-	-	-	-	BDL	-
Eu153 (ppm)	-	-	-	-	-	-	-	-	-
Gd157 (ppm)	-	BDL	-	-	-	BDL	-	-	-
Tb159 (ppm)	BDL	-	-	BDL	-	BDL	-	BDL	-
Dy163 (ppm)	-	-	-	BDL	-	-	-	-	-
Ho165 (ppm)	-	-	BDL	-	-	-	-	BDL	-
Er166 (ppm)	-	-	-	-	-	-	-	-	-
Tm169 (ppm)	-	-	BDL	-	-	-	BDL	-	-
Yb172 (ppm)	-	-	-	-	-	-	-	-	-
Lu175 (ppm)	BDL	-	BDL	-	-	-	-	BDL	BDL
Hf178 (ppm)	-	-	-	-	-	BDL	-	-	-
Ta181 (ppm)	-	-	-	-	BDL	-	-	-	-
W182 (ppm)	BDL	-	-	BDL	-	BDL	-	BDL	-
Re185 (ppm)	BDL	BDL	BDL	BDL	BDL	BDL	BDL	BDL	BDL
Os189 (ppm)	BDL	BDL	BDL	BDL	BDL	BDL	BDL	BDL	BDL
Ir193 (ppm)	-	BDL	BDL	BDL	-	-	-	BDL	-
Pt195 (ppm)	BDL	BDL	BDL	BDL	BDL	-	BDL	-	-
Au197 (ppm)	-	-	-	-	-	-	-	-	-
Hg202 (ppm)	17	BDL	BDL	BDL	BDL	BDL	BDL	BDL	BDL
Pb204 (ppm)	BDL	BDL	BDL	BDL	BDL	88	BDL	292	BDL
Tl205 (ppm)	BDL	BDL	BDL	BDL	BDL	BDL	1	36	BDL
Pb206 (ppm)	4	-	1	4	2	-	57	309	23
Pb207 (ppm)	4	8	1	4	-	1	62	327	19
Pb208 (ppm)	4	8	1	3	2	1	57	330	-
Bi209 (ppm)	BDL	BDL	BDL	BDL	BDL	0	16	12	0
Th232 (ppm)	-	-	BDL	-	-	BDL	-	BDL	-
U238 (ppm)	-	BDL	-	BDL	BDL	-	-	-	-
PbTotal (ppm)	5	8	1	4	2	3	58	323	21

Table D2. Trace element data for chalcopyrite continued.

Deposit	Betts Cove	Betts Cove	Betts Cove	Betts Cove	Betts Cove	Betts Cove	Betts Cove	Betts Cove	Betts Cove
Sample	KKMSC05B_C py11	KKMSC05B_C py12	KKMSC05B_C py13	KKMSC05B_C py14	KKMSC05B_C py15	KKMSC05B_C py16	KKMSC05B_C py19	KKMSC05B_C py20	KKMSC05B_C py18
Date	2023-11-20	2023-11-20	2023-11-20	2023-11-20	2023-11-20	2023-11-20	2023-11-20	2023-11-20	2023-11-20
Facies	Chalcopyrite-dominated	Chalcopyrite-dominated	Chalcopyrite-dominated	Chalcopyrite-dominated	Chalcopyrite-dominated	Chalcopyrite-dominated	Chalcopyrite-dominated	Chalcopyrite-dominated	Chalcopyrite-dominated
Li7 (ppm)	12	9	BDL	BDL	BDL	BDL	BDL	BDL	BDL
Be9 (ppm)	BDL	BDL	BDL	BDL	BDL	BDL	BDL	BDL	BDL
B11 (ppm)	BDL	BDL	BDL	BDL	BDL	BDL	BDL	BDL	BDL
Na23 (ppm)	BDL	BDL	BDL	BDL	BDL	BDL	BDL	BDL	BDL
Mg24 (ppm)	44907	28015	239	16081	3479	13634	111	121	66
Al27 (ppm)	48761	28323	241	15551	2617	14473	66	116	52
Si29 (ppm)	57138	36985	BDL	18019	5079	18639	BDL	BDL	BDL
P31 (ppm)	BDL	BDL	BDL	BDL	BDL	BDL	BDL	BDL	BDL
S32 (ppm)	325481	340290	368593	332283	420862	337540	365564	437089	377917
K39 (ppm)	126	BDL	BDL	BDL	BDL	BDL	BDL	BDL	BDL
Ca44 (ppm)	BDL	BDL	BDL	BDL	BDL	BDL	BDL	BDL	BDL
Sc45 (ppm)	13	9	10	5	BDL	6	BDL	BDL	BDL
Ti47 (ppm)	62	22	5299	31	BDL	11	BDL	BDL	BDL
V51 (ppm)	116	78	1	38	8	36	BDL	BDL	BDL
Cr52 (ppm)	128	60	BDL	76	73	27	BDL	BDL	BDL
Mn55 (ppm)	1172	764	10	383	90	342	3	3	2
Fe57 (ppm)	341908	307720	247677	303000	267277	266235	242918	332725	255679
Co59 (ppm)	20	3	3	1	1	-	BDL	7	BDL
Ni60 (ppm)	34	16	-	13	3	9	-	6	-
Cu63 (ppm)	-	-	-	-	-	-	-	-	-
Zn66 (ppm)	562	262	550	270	301	224	822	880	719
Ga71 (ppm)	-	-	0	1	-	-	-	0	-
Ge73 (ppm)	-	BDL	-	BDL	BDL	BDL	BDL	BDL	BDL
As75 (ppm)	BDL	BDL	BDL	BDL	BDL	BDL	BDL	BDL	BDL
Se77 (ppm)	532	517	720	640	661	574	606	692	611
Rb85 (ppm)	0	BDL	BDL	BDL	BDL	BDL	BDL	BDL	BDL
Sr88 (ppm)	-	-	BDL	-	-	-	-	BDL	BDL
Y89 (ppm)	BDL	-	-	-	-	BDL	-	-	-
Zr90 (ppm)	-	-	-	-	-	-	-	-	-
Nb93 (ppm)	-	BDL	-	-	BDL	-	BDL	BDL	-
Mo95 (ppm)	-	BDL	-	-	BDL	BDL	BDL	-	BDL
Ru101 (ppm)	-	-	-	-	-	-	-	-	-
Rh103 (ppm)	-	-	4	-	-	-	-	-	-
Pd104 (ppm)	BDL	BDL	BDL	-	BDL	-	BDL	-	BDL

Pd105 (ppm)	5	-	-	-	-	6	6	-	7
Pd106 (ppm)	BDL	BDL	-	-	-	BDL	0	0	0
Ag107 (ppm)	82	59	13	48	44	47	16	16	25
Cd111 (ppm)	-	-	-	3	-	-	7	-	-
In115 (ppm)	-	13	-	16	14	-	-	23	-
Sn118 (ppm)	2	2	3	2	2	2	3	3	2
Sb121 (ppm)	7	3	1	3	1	3	2	3	BDL
Te125 (ppm)	BDL	2	3	3	BDL	BDL	2	19	3
Cs133 (ppm)	BDL	BDL	BDL	BDL	BDL	BDL	BDL	BDL	BDL
Ba137 (ppm)	-	BDL	-	-	-	-	-	-	-
La139 (ppm)	-	-	-	-	-	-	-	BDL	BDL
Ce140 (ppm)	BDL	-	-	-	-	-	-	-	-
Pr141 (ppm)	BDL	-	-	BDL	-	-	BDL	-	-
Nd146 (ppm)	-	-	-	-	-	-	-	-	-
Sm147 (ppm)	-	-	-	-	-	-	-	-	-
Eu153 (ppm)	-	-	-	-	-	-	BDL	-	BDL
Gd157 (ppm)	-	-	-	-	-	-	-	-	-
Tb159 (ppm)	-	-	-	-	-	BDL	-	-	-
Dy163 (ppm)	-	-	-	-	-	BDL	-	-	-
Ho165 (ppm)	-	-	BDL	-	-	-	-	BDL	-
Er166 (ppm)	-	-	-	-	-	-	-	BDL	-
Tm169 (ppm)	-	-	-	-	-	-	-	-	-
Yb172 (ppm)	-	-	-	-	-	-	-	-	-
Lu175 (ppm)	-	-	BDL	-	BDL	-	-	-	-
Hf178 (ppm)	-	-	-	-	-	-	-	-	-
Ta181 (ppm)	BDL	-	-	-	BDL	-	-	-	-
W182 (ppm)	-	BDL	-	-	-	-	-	-	-
Re185 (ppm)	BDL	BDL	BDL	BDL	BDL	BDL	BDL	BDL	BDL
Os189 (ppm)	BDL	BDL	BDL	BDL	BDL	BDL	BDL	BDL	BDL
Ir193 (ppm)	-	-	-	BDL	-	-	-	-	-
Pt195 (ppm)	BDL	BDL	-	-	BDL	BDL	BDL	BDL	-
Au197 (ppm)	-	-	-	BDL	-	-	-	-	-
Hg202 (ppm)	BDL	BDL	13	16	11	12	BDL	BDL	BDL
Pb204 (ppm)	BDL	BDL	BDL	73	86	100	BDL	130	58
Tl205 (ppm)	1	BDL	0	BDL	BDL	0	BDL	BDL	BDL
Pb206 (ppm)	47	-	-	7	-	18	-	9	0
Pb207 (ppm)	48	-	-	6	7	17	17	-	0
Pb208 (ppm)	48	19	2	15	6	18	-	10	1
Bi209 (ppm)	1	0	BDL	0	0	BDL	0	2	BDL
Th232 (ppm)	-	-	-	-	-	-	-	-	-
U238 (ppm)	-	BDL	BDL	-	-	-	-	-	-
PbTotal (ppm)	48	18	3	12	7	19	17	12	1

Table D2. Trace element data for chalcopyrite continued.

Deposit	Betts Cove	Betts Cove	Betts Cove	Betts Cove	Betts Cove	Betts Cove	Betts Cove	Betts Cove	Betts Cove
Sample	KKMSC05B_Cpy21	KKMSC05B_Cpy22	KKMSC05B_Cpy23	KKMSC05B_Cpy24	KKMSC05B_Cpy25	KKMSC09_Cpy3	KKMSC09_Cpy1	KKMSC09_Cpy4	KKMSC09_Cpy6
Date	2023-11-20	2023-11-20	2023-11-20	2023-11-20	2023-11-20	2023-11-20	2023-11-20	2023-11-20	2023-11-20
Facies	Chalcopyrite-dominated	Chalcopyrite-dominated	Chalcopyrite-dominated	Chalcopyrite-dominated	Chalcopyrite-dominated	Chalcopyrite-dominated	Chalcopyrite-dominated	Chalcopyrite-dominated	Chalcopyrite-dominated
Li7 (ppm)	143	BDL	6	15	18	BDL	BDL	BDL	BDL
Be9 (ppm)	BDL	BDL	BDL	BDL	BDL	BDL	BDL	BDL	BDL
B11 (ppm)	1011	BDL	BDL	BDL	BDL	BDL	BDL	BDL	BDL
Na23 (ppm)	1492065	BDL	BDL	BDL	BDL	81	BDL	166	BDL
Mg24 (ppm)	347305	99	141	496	1053	3184	300	78	3256
Al27 (ppm)	132497	74	120	474	742	3348	325	89	3676
Si29 (ppm)	5213803	1853	BDL	BDL	BDL	6638	36260	BDL	5750
P31 (ppm)	601	BDL	BDL	BDL	BDL	BDL	BDL	BDL	BDL
S32 (ppm)	1795492	383105	431645	590559	721455	375602	525944	331625	398829
K39 (ppm)	50083	BDL	80	BDL	154	69	BDL	BDL	86
Ca44 (ppm)	922673	BDL	274	BDL	BDL	BDL	BDL	BDL	BDL
Sc45 (ppm)	92	BDL	BDL	BDL	BDL	BDL	BDL	BDL	BDL
Ti47 (ppm)	2703	BDL	BDL	BDL	BDL	BDL	BDL	BDL	BDL
V51 (ppm)	23	BDL	BDL	BDL	2	8	BDL	BDL	14
Cr52 (ppm)	33	BDL	BDL	BDL	12	28	BDL	BDL	7
Mn55 (ppm)	1402	2	4	7	26	100	13	2	149
Fe57 (ppm)	287463	265702	265066	277565	312973	294400	460380	279065	325558
Co59 (ppm)	3	BDL	BDL	BDL	BDL	326	882	3	276
Ni60 (ppm)	5	BDL	1	BDL	5	50	92	2	27
Cu63 (ppm)	-	-	-	-	-	-	-	-	-
Zn66 (ppm)	1655	1018	1117	2272	924	320	375	780	599
Ga71 (ppm)	-	-	0	-	-	-	BDL	BDL	0
Ge73 (ppm)	BDL	BDL	BDL	BDL	-	BDL	-	-	4
As75 (ppm)	BDL	BDL	BDL	12	25	230	563	8	222
Se77 (ppm)	1652	524	475	582	596	476	777	549	522
Rb85 (ppm)	447	BDL	BDL	BDL	BDL	BDL	BDL	BDL	BDL
Sr88 (ppm)	-	-	-	-	-	-	-	-	-
Y89 (ppm)	-	-	-	-	-	-	-	-	-
Zr90 (ppm)	-	BDL	-	-	-	-	-	-	-
Nb93 (ppm)	-	-	-	-	BDL	-	-	-	-
Mo95 (ppm)	-	BDL	BDL	2	BDL	-	-	-	-
Ru101 (ppm)	-	-	-	-	-	-	-	-	-
Rh103 (ppm)	-	-	3	-	-	-	-	-	-
Pd104 (ppm)	-	-	BDL	-	BDL	-	-	-	BDL

Pd105 (ppm)	-	-	7	5	5	5	7	-	6
Pd106 (ppm)	-	0	-	-	BDL	BDL	-	0	-
Ag107 (ppm)	BDL	5	6	4	6	153	111	57	-
Cd111 (ppm)	-	-	-	12	4	-	2	5	6
In115 (ppm)	-	-	-	17	-	24	-	25	27
Sn118 (ppm)	17	3	3	2	2	BDL	1	1	1
Sb121 (ppm)	BDL	BDL	BDL	1	BDL	24	21	BDL	11
Te125 (ppm)	-	4	6	BDL	BDL	109	150	BDL	99
Cs133 (ppm)	BDL	BDL	BDL	BDL	3	BDL	BDL	BDL	BDL
Ba137 (ppm)	-	-	-	-	-	-	-	-	-
La139 (ppm)	-	-	-	-	-	-	-	-	-
Ce140 (ppm)	-	-	-	-	-	-	-	-	-
Pr141 (ppm)	-	-	-	-	-	-	-	-	-
Nd146 (ppm)	-	-	-	-	-	-	-	-	-
Sm147 (ppm)	-	-	-	-	-	-	-	-	-
Eu153 (ppm)	-	-	-	-	-	-	BDL	-	-
Gd157 (ppm)	-	-	-	-	-	-	-	-	-
Tb159 (ppm)	-	-	-	-	-	-	-	BDL	-
Dy163 (ppm)	-	-	-	BDL	-	-	-	-	-
Ho165 (ppm)	-	-	-	-	-	-	-	-	-
Er166 (ppm)	-	-	-	-	-	-	-	-	-
Tm169 (ppm)	-	-	-	-	-	-	-	-	-
Yb172 (ppm)	-	-	-	BDL	-	-	-	-	-
Lu175 (ppm)	-	-	-	-	-	-	-	-	-
Hf178 (ppm)	-	-	-	-	-	-	-	-	-
Ta181 (ppm)	-	-	-	-	-	-	-	-	-
W182 (ppm)	-	-	-	-	-	BDL	-	-	-
Re185 (ppm)	BDL	BDL	BDL	BDL	BDL	BDL	BDL	BDL	-
Os189 (ppm)	-	BDL	BDL	BDL	BDL	BDL	BDL	BDL	-
Ir193 (ppm)	-	-	BDL	BDL	-	BDL	-	-	BDL
Pt195 (ppm)	1	BDL	BDL	BDL	BDL	-	BDL	BDL	BDL
Au197 (ppm)	-	-	-	-	-	-	1	-	-
Hg202 (ppm)	325	14	31	109	145	BDL	BDL	BDL	BDL
Pb204 (ppm)	2024	71	252	609	803	327	765	BDL	334
Tl205 (ppm)	BDL	BDL	BDL	BDL	BDL	3	1	0	5
Pb206 (ppm)	154	1	0	-	5	332	763	3	395
Pb207 (ppm)	131	-	1	1	2	309	774	-	378
Pb208 (ppm)	137	1	0	1	-	325	754	3	394
Bi209 (ppm)	1	BDL	BDL	BDL	0	26	37	0	24
Th232 (ppm)	-	-	-	-	-	-	-	-	-
U238 (ppm)	-	-	BDL	-	-	-	-	-	-
PbTotal (ppm)	169	2	4	11	15	323	761	3	390

Table D2. Trace element data for chalcopyrite continued.

Deposit	Betts Cove	Betts Cove	Betts Cove	Betts Cove	Betts Cove	Betts Cove	Betts Cove	Betts Cove	Betts Cove
Sample	KKMSC09_Cpy 7	KKMSC09_Cpy 8	KKMSC09_Cpy 9	KKMSC09_Cpy 10	KKMSC09_Cpy 2	KKMSC09_Cpy 5	KKMSC09_Cpy 11	KKMSC09_Cpy 12	KKMSC09_Cpy 13
Date	2023-11-20	2023-11-20	2023-11-20	2023-11-20	2023-11-20	2023-11-20	2023-11-20	2023-11-20	2023-11-20
Facies	Chalcopyrite-dominated	Chalcopyrite-dominated	Chalcopyrite-dominated	Chalcopyrite-dominated	Chalcopyrite-dominated	Chalcopyrite-dominated	Chalcopyrite-dominated	Chalcopyrite-dominated	Chalcopyrite-dominated
Li7 (ppm)	101	BDL	BDL	BDL	5	BDL	BDL	BDL	BDL
Be9 (ppm)	BDL	BDL	BDL	BDL	BDL	BDL	BDL	BDL	BDL
B11 (ppm)	BDL	BDL	BDL	BDL	BDL	BDL	BDL	BDL	BDL
Na23 (ppm)	1353	160	BDL	236	BDL	BDL	BDL	BDL	BDL
Mg24 (ppm)	208935	3947	617	7967	218	290	8	2103	BDL
Al27 (ppm)	290308	4106	1014	7977	189	392	13	2667	15
Si29 (ppm)	309114	6599	3934	17399	BDL	BDL	BDL	5395	BDL
P31 (ppm)	894	BDL	BDL	144	BDL	BDL	BDL	BDL	BDL
S32 (ppm)	5621558	361902	1171208	927676	388228	345647	385917	1244391	353979
K39 (ppm)	1287	148	BDL	372	BDL	BDL	BDL	BDL	BDL
Ca44 (ppm)	3065	BDL	BDL	BDL	BDL	BDL	BDL	BDL	BDL
Sc45 (ppm)	111	BDL	BDL	3	BDL	BDL	BDL	BDL	BDL
Ti47 (ppm)	185	BDL	BDL	BDL	BDL	BDL	BDL	BDL	BDL
V51 (ppm)	608	12	4	20	BDL	1	BDL	7	BDL
Cr52 (ppm)	1262	30	17	93	BDL	BDL	BDL	10	BDL
Mn55 (ppm)	8809	138	80	376	12	13	BDL	90	BDL
Fe57 (ppm)	6051450	351151	1054846	919845	276409	265625	291414	1022518	244931
Co59 (ppm)	28255	624	4252	4362	25	1	2	963	18
Ni60 (ppm)	1835	-	147	1184	6	1	28	-	9
Cu63 (ppm)	-	-	-	-	-	-	-	-	-
Zn66 (ppm)	1751	556	659	811	344	122	549	377	1310
Ga71 (ppm)	-	-	0	-	-	-	-	-	-
Ge73 (ppm)	BDL	BDL	-	6	-	-	BDL	-	BDL
As75 (ppm)	24098	303	5243	3620	13	BDL	BDL	496	BDL
Se77 (ppm)	7836	409	1875	1688	542	429	663	1447	519
Rb85 (ppm)	BDL	1	BDL	2	BDL	BDL	BDL	BDL	BDL
Sr88 (ppm)	-	-	-	-	-	-	-	-	-
Y89 (ppm)	-	-	BDL	-	-	-	-	-	-
Zr90 (ppm)	-	-	-	-	-	-	-	-	-
Nb93 (ppm)	-	-	-	-	-	BDL	-	BDL	-
Mo95 (ppm)	-	-	-	269	1	-	-	15	BDL
Ru101 (ppm)	-	-	BDL	-	-	BDL	-	BDL	-
Rh103 (ppm)	-	-	-	-	-	2	2	2	-
Pd104 (ppm)	-	-	-	-	BDL	BDL	-	BDL	-

Pd105 (ppm)	-	-	5	-	-	5	-	-	5
Pd106 (ppm)	4	1	-	-	0	-	BDL	-	BDL
Ag107 (ppm)	1688	344	93	623	29	36	46	173	210
Cd111 (ppm)	21	-	10	-	-	3	10	-	16
In115 (ppm)	-	26	-	-	24	-	-	19	-
Sn118 (ppm)	5	BDL	BDL	2	BDL	BDL	BDL	BDL	BDL
Sb121 (ppm)	-	52	15	160	1	1	BDL	9	1
Te125 (ppm)	4247	222	83	-	7	BDL	3	-	-
Cs133 (ppm)	5	1	BDL	BDL	BDL	BDL	BDL	BDL	BDL
Ba137 (ppm)	-	-	-	-	-	-	-	-	-
La139 (ppm)	-	-	-	-	-	-	-	-	-
Ce140 (ppm)	-	-	-	-	-	-	-	-	-
Pr141 (ppm)	-	-	-	-	-	-	-	-	-
Nd146 (ppm)	-	-	-	-	-	-	-	-	-
Sm147 (ppm)	-	-	-	-	-	-	-	-	-
Eu153 (ppm)	-	-	-	-	-	-	-	-	-
Gd157 (ppm)	-	-	-	-	-	-	-	-	-
Tb159 (ppm)	-	-	-	-	-	-	-	-	-
Dy163 (ppm)	-	-	-	-	-	-	-	-	-
Ho165 (ppm)	-	-	-	-	-	-	-	-	-
Er166 (ppm)	-	-	-	-	-	-	-	-	-
Tm169 (ppm)	-	-	-	-	BDL	-	-	-	-
Yb172 (ppm)	-	-	-	-	-	-	-	-	-
Lu175 (ppm)	-	-	-	BDL	-	-	-	-	-
Hf178 (ppm)	-	-	-	-	-	-	-	-	-
Ta181 (ppm)	-	-	-	-	-	BDL	-	-	-
W182 (ppm)	BDL	-	-	-	-	BDL	BDL	-	-
Re185 (ppm)	BDL	BDL	1	1	BDL	-	BDL	BDL	BDL
Os189 (ppm)	BDL	BDL	1	BDL	BDL	BDL	BDL	BDL	BDL
Ir193 (ppm)	BDL	-	BDL	BDL	BDL	-	-	-	-
Pt195 (ppm)	2	BDL	BDL	-	-	-	-	BDL	-
Au197 (ppm)	-	-	-	-	-	-	-	-	394
Hg202 (ppm)	BDL	BDL	BDL	BDL	BDL	BDL	16	19	29
Pb204 (ppm)	11393	832	475	4965	BDL	63	BDL	308	208
Tl205 (ppm)	-	10	3	14	0	0	BDL	2	1
Pb206 (ppm)	12526	-	586	5314	27	58	-	-	-
Pb207 (ppm)	-	-	-	5279	28	-	3	-	87
Pb208 (ppm)	11897	838	572	5177	30	61	2	272	81
Bi209 (ppm)	594	67	-	251	1	0	BDL	15	0
Th232 (ppm)	-	-	-	-	BDL	-	-	-	-
U238 (ppm)	-	-	-	-	-	-	-	-	-
PbTotal (ppm)	12088	853	576	5231	29	59	3	281	86

Table D2. Trace element data for chalcopyrite continued.

Deposit	Betts Cove	Betts Cove	Betts Cove	Betts Cove	Betts Cove	Betts Cove	Betts Cove	Betts Cove	Betts Cove
Sample	KKMSC09_Cpy 14	KKMSC09_Cpy 15	KKMSC09_Cpy 16	KKMSC09_Cpy 17	KKMSC09_Cpy 18	KKMSC09_Cpy 19	KKMSC09_Cpy 27	KKMSC09_Cpy 21	KKMSC09_Cpy 22
Date	2023-11-20	2023-11-20	2023-11-20	2023-11-20	2023-11-20	2023-11-20	2023-11-20	2023-11-20	2023-11-20
Facies	Chalcopyrite-dominated	Chalcopyrite-dominated	Chalcopyrite-dominated	Chalcopyrite-dominated	Chalcopyrite-dominated	Chalcopyrite-dominated	Chalcopyrite-dominated	Chalcopyrite-dominated	Chalcopyrite-dominated
Li7 (ppm)	BDL	BDL	BDL	23	BDL	BDL	BDL	BDL	BDL
Be9 (ppm)	BDL	-	BDL	BDL	-	-	-	BDL	BDL
B11 (ppm)	BDL	BDL	BDL	BDL	BDL	BDL	BDL	BDL	BDL
Na23 (ppm)	BDL	61	BDL	BDL	BDL	BDL	BDL	BDL	BDL
Mg24 (ppm)	32	4071	5000	98814	515	160	91	50	53
Al27 (ppm)	29	4301	5632	121547	526	253	150	70	53
Si29 (ppm)	BDL	7653	7796	286919	4032	BDL	5039	BDL	BDL
P31 (ppm)	104	BDL	BDL	422	BDL	BDL	BDL	BDL	BDL
S32 (ppm)	371523	461003	424487	2106982	1531164	404592	423368	363796	346145
K39 (ppm)	BDL	94	BDL	BDL	BDL	BDL	BDL	BDL	BDL
Ca44 (ppm)	BDL	BDL	BDL	BDL	BDL	BDL	BDL	BDL	BDL
Sc45 (ppm)	BDL	BDL	BDL	23	BDL	BDL	BDL	BDL	BDL
Ti47 (ppm)	BDL	BDL	BDL	98	BDL	BDL	BDL	BDL	-
V51 (ppm)	BDL	6	10	248	1	1	BDL	BDL	BDL
Cr52 (ppm)	BDL	BDL	BDL	265	8	BDL	BDL	BDL	BDL
Mn55 (ppm)	3	150	161	3398	16	9	6	3	5
Fe57 (ppm)	279416	337502	349645	1831630	1275268	286234	328064	297631	290729
Co59 (ppm)	1	477	571	4241	976	109	1998	3	4
Ni60 (ppm)	-	76	29	-	49	-	-	BDL	-
Cu63 (ppm)	-	-	-	-	-	-	-	-	-
Zn66 (ppm)	364	377	938	999	517	511	602	973	622
Ga71 (ppm)	-	-	-	-	-	-	-	0	-
Ge73 (ppm)	-	BDL	-	BDL	-	BDL	BDL	BDL	-
As75 (ppm)	BDL	310	384	2469	547	68	5314	BDL	8
Se77 (ppm)	519	421	535	3498	3249	532	548	584	414
Rb85 (ppm)	BDL	BDL	BDL	BDL	BDL	BDL	BDL	BDL	BDL
Sr88 (ppm)	-	-	-	-	-	-	-	-	BDL
Y89 (ppm)	-	-	BDL	BDL	-	-	-	-	BDL
Zr90 (ppm)	-	-	BDL	BDL	-	-	-	-	BDL
Nb93 (ppm)	-	-	-	-	-	-	-	-	-
Mo95 (ppm)	-	BDL	BDL	3130	-	-	-	-	1
Ru101 (ppm)	-	-	-	-	-	-	-	-	-
Rh103 (ppm)	-	2	-	-	-	-	2	2	-
Pd104 (ppm)	-	BDL	-	BDL	-	-	-	-	-

Pd105 (ppm)	-	6	6	-	-	6	-	7	-
Pd106 (ppm)	0	-	-	-	-	-	BDL	-	-
Ag107 (ppm)	82	192	108	345	98	-	132	130	97
Cd111 (ppm)	-	-	10	7	6	-	-	-	-
In115 (ppm)	-	-	-	-	-	-	-	26	-
Sn118 (ppm)	BDL	BDL	BDL	BDL	1	BDL	BDL	BDL	BDL
Sb121 (ppm)	0	19	6	39	9	10	14	-	1
Te125 (ppm)	-	180	54	-	89	41	-	BDL	4
Cs133 (ppm)	BDL	BDL	BDL	BDL	BDL	BDL	BDL	BDL	BDL
Ba137 (ppm)	-	-	-	-	-	-	-	-	-
La139 (ppm)	-	-	-	-	-	-	-	-	-
Ce140 (ppm)	-	-	-	-	-	-	-	BDL	-
Pr141 (ppm)	-	-	BDL	-	-	-	-	-	-
Nd146 (ppm)	-	-	-	-	-	-	-	-	-
Sm147 (ppm)	-	-	-	-	-	-	-	-	-
Eu153 (ppm)	BDL	-	-	-	-	BDL	-	-	-
Gd157 (ppm)	-	-	-	-	-	-	-	-	-
Tb159 (ppm)	-	-	-	-	-	-	-	-	-
Dy163 (ppm)	-	-	-	-	-	-	-	-	-
Ho165 (ppm)	-	-	-	-	-	-	-	-	-
Er166 (ppm)	BDL	-	-	-	-	-	-	-	-
Tm169 (ppm)	-	-	-	-	-	-	-	-	-
Yb172 (ppm)	-	-	-	-	-	-	-	-	-
Lu175 (ppm)	-	-	-	-	-	-	-	-	-
Hf178 (ppm)	-	-	-	-	-	-	-	-	-
Ta181 (ppm)	-	-	-	-	-	-	-	BDL	-
W182 (ppm)	BDL	-	-	BDL	-	-	-	-	-
Re185 (ppm)	BDL	BDL	BDL	15	1	BDL	BDL	-	BDL
Os189 (ppm)	BDL	BDL	BDL	BDL	BDL	-	-	BDL	BDL
Ir193 (ppm)	-	BDL	-	BDL	-	-	-	-	BDL
Pt195 (ppm)	BDL	-	BDL	BDL	-	BDL	BDL	-	BDL
Au197 (ppm)	25	-	-	-	30	-	-	-	-
Hg202 (ppm)	25	21	BDL	BDL	BDL	BDL	BDL	24	BDL
Pb204 (ppm)	92	406	172	1798	3798	141	1078	125	53
Tl205 (ppm)	0	4	2	7	3	1	2	BDL	BDL
Pb206 (ppm)	-	-	131	1924	4076	-	1136	3	14
Pb207 (ppm)	-	347	138	-	-	-	1061	4	-
Pb208 (ppm)	-	330	137	1823	4097	96	1067	4	14
Bi209 (ppm)	0	31	-	76	20	12	-	0	0
Th232 (ppm)	-	-	-	-	-	-	-	-	-
U238 (ppm)	-	-	-	-	-	-	-	-	-
PbTotal (ppm)	26	336	136	1853	4112	98	1083	5	15

Table D2. Trace element data for chalcopyrite continued.

Deposit	Betts Cove	Betts Cove	Betts Cove	Betts Cove	Betts Cove	Betts Cove	Betts Cove	Betts Cove	Betts Cove
Sample	KKMSC09_Cpy 23	KKMSC09_Cpy 24	KKMSC09_Cpy 25	KKMSC09_Cpy 26	KKMSC09_Cpy 28	KKMSC09_Cpy 29	KKMSC09_Cpy 30	KKMSC09_Cpy 33	KKMSC10_Cpy 1
Date	2023-11-20	2023-11-20	2023-11-20	2023-11-20	2023-11-20	2023-11-20	2023-11-20	2023-11-20	2023-11-20
Facies	Chalcopyrite-dominated	Chalcopyrite-dominated	Chalcopyrite-dominated	Chalcopyrite-dominated	Chalcopyrite-dominated	Chalcopyrite-dominated	Chalcopyrite-dominated	Chalcopyrite-dominated	Pyrite-dominated
Li7 (ppm)	BDL	BDL	BDL	11	BDL	24	BDL	28	63
Be9 (ppm)	BDL	-	-	-	BDL	-	-	BDL	-
B11 (ppm)	BDL	BDL	BDL	BDL	BDL	BDL	BDL	34	BDL
Na23 (ppm)	BDL	BDL	BDL	BDL	BDL	200	BDL	BDL	5646
Mg24 (ppm)	49	5	763	3576	47	876	38	34383	291
Al27 (ppm)	41	10	1460	4276	57	1353	37	47898	BDL
Si29 (ppm)	2073	BDL	BDL	255603	BDL	885253	BDL	51715	1276221
P31 (ppm)	BDL	BDL	BDL	BDL	BDL	521	BDL	252	38269
S32 (ppm)	313321	358539	340610	1155190	318776	3032820	340725	575396	990874906
K39 (ppm)	BDL	BDL	BDL	BDL	BDL	BDL	BDL	BDL	BDL
Ca44 (ppm)	BDL	BDL	BDL	621	BDL	1267	BDL	815	22623
Sc45 (ppm)	BDL	BDL	BDL	7	BDL	14	BDL	10	160
Ti47 (ppm)	BDL	BDL	BDL	BDL	BDL	BDL	-	BDL	-
V51 (ppm)	BDL	BDL	3	11	BDL	6	BDL	101	BDL
Cr52 (ppm)	BDL	BDL	BDL	31	BDL	BDL	BDL	199	BDL
Mn55 (ppm)	3	BDL	44	167	BDL	112	2	1520	1879
Fe57 (ppm)	292850	264176	278924	840862	291452	2873455	264308	442147	813768438
Co59 (ppm)	3	3	2	44553	3	22193	23	16089	1111
Ni60 (ppm)	4	BDL	-	961	BDL	2352	4	356	463
Cu63 (ppm)	-	-	-	-	-	-	-	-	-
Zn66 (ppm)	314	1047	247	1957	204	755	244	806	5735
Ga71 (ppm)	-	-	BDL	-	-	-	-	-	-
Ge73 (ppm)	-	-	BDL	BDL	BDL	BDL	BDL	BDL	571
As75 (ppm)	BDL	BDL	5	117451	32	24440	26	52538	2765592
Se77 (ppm)	339	710	500	2369	481	4070	454	887	10130
Rb85 (ppm)	BDL	BDL	BDL	BDL	-	1	BDL	BDL	BDL
Sr88 (ppm)	-	-	-	13	-	-	-	-	-
Y89 (ppm)	-	-	-	-	-	-	BDL	BDL	-
Zr90 (ppm)	-	-	-	2	-	-	-	-	BDL
Nb93 (ppm)	-	-	-	-	-	-	-	-	-
Mo95 (ppm)	BDL	BDL	BDL	BDL	-	-	BDL	-	BDL
Ru101 (ppm)	BDL	-	-	-	-	-	-	-	BDL
Rh103 (ppm)	2	-	-	-	2	-	2	-	BDL
Pd104 (ppm)	-	-	-	-	-	-	-	-	-

Pd105 (ppm)	-	-	7	-	-	-	-	7	14
Pd106 (ppm)	BDL	BDL	BDL	-	-	3	BDL	-	-
Ag107 (ppm)	102	-	132	1016	46	5751	74	213	BDL
Cd111 (ppm)	-	-	-	13	-	-	-	-	79
In115 (ppm)	-	23	-	-	-	-	-	-	-
Sn118 (ppm)	BDL	BDL	BDL	BDL	BDL	BDL	BDL	BDL	-
Sb121 (ppm)	1	BDL	-	86	1	618	3	27	BDL
Te125 (ppm)	BDL	5	-	-	BDL	-	10	221	-
Cs133 (ppm)	BDL	BDL	BDL	BDL	BDL	BDL	BDL	BDL	-
Ba137 (ppm)	-	-	-	-	-	-	-	-	-
La139 (ppm)	BDL	-	-	-	-	-	-	-	-
Ce140 (ppm)	-	-	-	-	-	-	-	-	-
Pr141 (ppm)	-	-	-	-	-	BDL	-	-	-
Nd146 (ppm)	-	-	-	-	-	-	-	-	-
Sm147 (ppm)	-	-	-	-	-	-	-	-	-
Eu153 (ppm)	-	-	-	-	-	-	-	-	-
Gd157 (ppm)	-	-	-	-	-	-	-	-	-
Tb159 (ppm)	-	-	-	-	BDL	-	-	-	-
Dy163 (ppm)	-	-	-	-	-	-	-	-	-
Ho165 (ppm)	-	-	-	-	-	-	-	-	-
Er166 (ppm)	-	-	-	-	-	-	-	-	-
Tm169 (ppm)	-	-	-	-	-	-	-	-	-
Yb172 (ppm)	-	-	-	-	-	-	-	-	-
Lu175 (ppm)	-	-	-	-	-	-	-	-	-
Hf178 (ppm)	-	-	-	-	-	-	-	-	-
Ta181 (ppm)	-	BDL	-	-	-	-	-	-	BDL
W182 (ppm)	-	-	-	-	-	-	-	-	BDL
Re185 (ppm)	BDL	BDL	BDL	BDL	BDL	BDL	-	BDL	BDL
Os189 (ppm)	BDL	BDL	BDL	BDL	BDL	BDL	BDL	BDL	BDL
Ir193 (ppm)	-	-	-	-	-	-	BDL	-	-
Pt195 (ppm)	BDL	BDL	BDL	-	-	-	BDL	BDL	16054
Au197 (ppm)	-	-	-	-	-	-	-	-	18541
Hg202 (ppm)	BDL	BDL	BDL	52	22	BDL	24	BDL	BDL
Pb204 (ppm)	BDL	BDL	69	2349	105	21556	169	732	2786
Tl205 (ppm)	0	BDL	1	4	BDL	20	1	4	1849
Pb206 (ppm)	21	1	-	-	-	-	114	-	2034
Pb207 (ppm)	18	1	30	-	11	24113	121	-	94
Pb208 (ppm)	20	1	31	2425	10	-	118	587	-
Bi209 (ppm)	0	BDL	BDL	-	0	-	4	44	-
Th232 (ppm)	-	-	-	-	-	-	-	-	3446
U238 (ppm)	-	-	-	-	-	-	-	-	-
PbTotal (ppm)	20	1	31	2482	12	23632	119	603	-

Table D2. Trace element data for chalcopyrite continued.

Deposit	Betts Cove	Betts Cove	Betts Cove	Betts Cove	Betts Cove	Betts Cove	Betts Cove	Betts Cove	Betts Cove
Sample	KKMSC10_Cpy 2	KKMSC10_Cpy 3	KKMSC10_Cpy 4	KKMSC29_Cpy 1	KKMSC29_Cpy 3	KKMSC29_Cpy 4	KKMSC29_Cpy 6	KKMSC29_Cpy 7	KKMSC29_Cpy 8
Date	2023-11-20	2023-11-20	2023-11-20	2023-11-20	2023-11-20	2023-11-20	2023-11-20	2023-11-20	2023-11-20
Facies	Pyrite-dominated	Pyrite-dominated	Pyrite-dominated	Chalcopyrite-dominated	Chalcopyrite-dominated	Chalcopyrite-dominated	Chalcopyrite-dominated	Chalcopyrite-dominated	Chalcopyrite-dominated
Li7 (ppm)	237	BDL	6403	BDL	BDL	BDL	BDL	BDL	BDL
Be9 (ppm)	-	-	BDL	-	BDL	-	BDL	BDL	BDL
B11 (ppm)	BDL	BDL	3444	BDL	BDL	BDL	BDL	BDL	BDL
Na23 (ppm)	BDL	BDL	BDL	BDL	BDL	BDL	BDL	BDL	BDL
Mg24 (ppm)	82	62	45820	108	BDL	8	34	57	98
Al27 (ppm)	BDL	91	78748	132	BDL	6	46	55	21
Si29 (ppm)	523113	BDL	1270143	BDL	BDL	BDL	BDL	BDL	BDL
P31 (ppm)	30653	BDL	68455	BDL	BDL	BDL	BDL	BDL	BDL
S32 (ppm)	502786824	415554	850868658	350621	314053	318729	346815	317246	316010
K39 (ppm)	2170	BDL	12048	BDL	BDL	BDL	BDL	BDL	BDL
Ca44 (ppm)	13639	BDL	95894	BDL	BDL	BDL	BDL	BDL	BDL
Sc45 (ppm)	BDL	BDL	144	BDL	BDL	BDL	BDL	BDL	BDL
Ti47 (ppm)	BDL	6	2154	BDL	BDL	-	BDL	BDL	BDL
V51 (ppm)	22	BDL	317	0	BDL	BDL	BDL	BDL	BDL
Cr52 (ppm)	BDL	11	BDL	BDL	BDL	BDL	BDL	BDL	BDL
Mn55 (ppm)	248	5	3796	4	BDL	1	2	2	1
Fe57 (ppm)	477420682	312038	639512513	257780	249610	242287	284331	262586	257100
Co59 (ppm)	175087	1	67463	2	3	4	3	3	29
Ni60 (ppm)	-	1	-	3	BDL	-	-	2	-
Cu63 (ppm)	-	-	-	-	-	-	-	-	-
Zn66 (ppm)	3047	588	2746579	526	2008	2096	766	893	998
Ga71 (ppm)	-	-	BDL	-	-	-	-	-	-
Ge73 (ppm)	-	-	-	BDL	-	BDL	BDL	BDL	-
As75 (ppm)	2016841	BDL	29958	BDL	BDL	BDL	BDL	BDL	BDL
Se77 (ppm)	31705	64	31536	3620	3243	3875	3683	3474	3458
Rb85 (ppm)	BDL	BDL	BDL	BDL	BDL	BDL	-	BDL	-
Sr88 (ppm)	-	-	-	-	-	-	-	-	-
Y89 (ppm)	-	-	-	-	-	-	BDL	-	BDL
Zr90 (ppm)	BDL	BDL	105	-	BDL	-	-	-	BDL
Nb93 (ppm)	-	-	-	-	-	-	-	-	-
Mo95 (ppm)	BDL	-	-	-	-	5	-	-	-
Ru101 (ppm)	BDL	-	-	-	BDL	-	-	BDL	BDL
Rh103 (ppm)	-	-	274	-	-	13	-	-	13
Pd104 (ppm)	BDL	BDL	310	1	-	-	-	0	-

Pd105 (ppm)	669	4	510	0	-	2	2	3	2
Pd106 (ppm)	75	2	-	-	-	-	12	-	14
Ag107 (ppm)	-	-	-	9	-	-	-	-	-
Cd111 (ppm)	BDL	6	274	BDL	BDL	BDL	BDL	BDL	BDL
In115 (ppm)	2325	BDL	152	BDL	BDL	BDL	0	BDL	0
Sn118 (ppm)	4630	4	367	5	6	-	5	5	6
Sb121 (ppm)	BDL	BDL	BDL	BDL	BDL	BDL	BDL	BDL	BDL
Te125 (ppm)	-	-	-	-	-	-	-	-	-
Cs133 (ppm)	-	-	-	-	-	-	-	-	-
Ba137 (ppm)	-	-	-	-	-	-	-	-	-
La139 (ppm)	-	-	-	-	-	-	-	-	-
Ce140 (ppm)	-	-	-	-	-	-	-	-	-
Pr141 (ppm)	-	-	-	-	-	-	-	-	-
Nd146 (ppm)	-	-	-	-	-	-	-	-	-
Sm147 (ppm)	-	-	-	-	BDL	-	-	-	-
Eu153 (ppm)	-	-	-	-	-	-	-	-	-
Gd157 (ppm)	-	-	-	-	-	-	-	-	-
Tb159 (ppm)	-	-	-	-	-	-	-	-	-
Dy163 (ppm)	-	-	-	-	-	-	-	-	-
Ho165 (ppm)	-	-	-	-	-	-	-	-	-
Er166 (ppm)	-	-	-	-	-	-	BDL	-	-
Tm169 (ppm)	-	-	-	-	-	-	-	-	-
Yb172 (ppm)	-	-	-	-	-	-	-	-	-
Lu175 (ppm)	-	BDL	-	-	-	-	-	-	-
Hf178 (ppm)	BDL	-	-	-	BDL	-	-	-	-
Ta181 (ppm)	40	BDL	21	BDL	BDL	BDL	BDL	BDL	BDL
W182 (ppm)	173	BDL	BDL	BDL	BDL	BDL	BDL	BDL	BDL
Re185 (ppm)	BDL	-	-	BDL	-	-	-	-	-
Os189 (ppm)	-	BDL	BDL	-	BDL	BDL	BDL	BDL	BDL
Ir193 (ppm)	-	-	68	-	-	-	-	-	-
Pt195 (ppm)	5279	86	BDL	61	44	25	40	26	41
Au197 (ppm)	33710	111	46273	33	65	50	67	46	80
Hg202 (ppm)	17	BDL	42	0	BDL	0	BDL	0	1
Pb204 (ppm)	-	1	25864	5	3	-	8	8	36
Tl205 (ppm)	21720	1	26447	4	4	3	8	7	40
Pb206 (ppm)	20296	1	28178	5	4	2	7	8	34
Pb207 (ppm)	2661	BDL	691	0	0	BDL	0	0	-
Pb208 (ppm)	-	-	-	-	-	-	-	-	-
Bi209 (ppm)	-	-	-	-	-	-	-	-	-
Th232 (ppm)	21667	3	27501	5	4	3	8	8	36
U238 (ppm)	-	-	-	-	-	-	-	-	-
PbTotal (ppm)	-	-	-	-	-	-	-	-	-

Table D2. Trace element data for chalcopyrite continued.

Deposit	Betts Cove	Betts Cove	Betts Cove	Betts Cove	Betts Cove	Betts Cove	Betts Cove	Betts Cove	Betts Cove
Sample	KKMSC29_Cpy 12	KKMSC29_Cpy 14	KKMSC29_Cpy 22	KKMSC29_Cpy 20	KKMSC29_Cpy 19	KKMSC29_Cpy 18	KKMSC29_Cpy 17	KKMSC29_Cpy 23	KKMSC29_Cpy 16
Date	2023-11-20	2023-11-20	2023-11-20	2023-11-20	2023-11-20	2023-11-20	2023-11-20	2023-11-20	2023-11-20
Facies	Chalcopyrite-dominated	Chalcopyrite-dominated	Chalcopyrite-dominated	Chalcopyrite-dominated	Chalcopyrite-dominated	Chalcopyrite-dominated	Chalcopyrite-dominated	Chalcopyrite-dominated	Chalcopyrite-dominated
Li7 (ppm)	BDL	BDL	BDL	BDL	BDL	BDL	BDL	BDL	BDL
Be9 (ppm)	BDL	-	-	-	-	BDL	-	-	-
B11 (ppm)	BDL	BDL	BDL	BDL	BDL	BDL	BDL	BDL	BDL
Na23 (ppm)	BDL	52	BDL	BDL	BDL	BDL	BDL	BDL	BDL
Mg24 (ppm)	716	240	13	5	19	11	9	9	34
Al27 (ppm)	885	311	11	5	17	13	12	7	23
Si29 (ppm)	1638	1832	BDL	BDL	988	BDL	BDL	BDL	BDL
P31 (ppm)	BDL	BDL	BDL	BDL	BDL	BDL	BDL	BDL	BDL
S32 (ppm)	310901	330637	336011	330944	319802	278082	299891	328671	321974
K39 (ppm)	BDL	BDL	BDL	BDL	BDL	BDL	BDL	BDL	BDL
Ca44 (ppm)	BDL	BDL	BDL	BDL	BDL	BDL	BDL	BDL	BDL
Sc45 (ppm)	BDL	BDL	BDL	BDL	BDL	BDL	BDL	BDL	BDL
Ti47 (ppm)	15	7	BDL	3	BDL	BDL	BDL	BDL	-
V51 (ppm)	1	BDL	BDL	BDL	BDL	BDL	BDL	BDL	BDL
Cr52 (ppm)	BDL	BDL	BDL	BDL	BDL	BDL	BDL	BDL	BDL
Mn55 (ppm)	26	8	BDL	BDL	1	BDL	1	BDL	1
Fe57 (ppm)	241421	295259	248522	267603	263423	250156	251829	257076	248545
Co59 (ppm)	2	97	-	3	3	2	8	2	3
Ni60 (ppm)	1	-	BDL	-	BDL	BDL	-	-	-
Cu63 (ppm)	-	-	-	-	-	-	-	-	-
Zn66 (ppm)	667	750	777	726	863	821	1362	879	399
Ga71 (ppm)	0	-	-	-	-	-	-	-	-
Ge73 (ppm)	-	-	-	-	BDL	-	-	-	-
As75 (ppm)	BDL	42	2	BDL	BDL	BDL	BDL	BDL	BDL
Se77 (ppm)	2473	2557	3312	2713	3218	3248	3740	3660	3859
Rb85 (ppm)	BDL	BDL	BDL	BDL	-	BDL	BDL	BDL	BDL
Sr88 (ppm)	-	-	-	-	-	-	-	-	-
Y89 (ppm)	-	-	-	-	-	-	-	-	-
Zr90 (ppm)	BDL	BDL	BDL	-	BDL	BDL	-	BDL	BDL
Nb93 (ppm)	-	-	-	-	-	-	-	-	-
Mo95 (ppm)	-	4	-	-	-	4	-	-	4
Ru101 (ppm)	-	-	-	BDL	-	BDL	-	-	-
Rh103 (ppm)	-	-	12	-	13	11	-	-	-
Pd104 (ppm)	-	-	BDL	-	0	BDL	0	0	BDL

Pd105 (ppm)	BDL	0	1	1	1	-	-	1	1
Pd106 (ppm)	-	6	-	-	-	6	9	-	-
Ag107 (ppm)	6	5	-	-	-	8	-	-	7
Cd111 (ppm)	BDL	BDL	BDL	BDL	BDL	BDL	BDL	BDL	BDL
In115 (ppm)	-	0	0	2	1	BDL	0	0	0
Sn118 (ppm)	3	8	4	-	3	-	-	2	4
Sb121 (ppm)	BDL	BDL	BDL	BDL	BDL	BDL	BDL	BDL	BDL
Te125 (ppm)	-	-	-	-	-	-	-	-	-
Cs133 (ppm)	-	-	-	-	-	-	-	-	-
Ba137 (ppm)	-	-	-	-	-	-	-	-	-
La139 (ppm)	-	-	-	-	-	-	-	-	-
Ce140 (ppm)	-	-	-	-	-	-	-	-	-
Pr141 (ppm)	-	-	-	-	-	-	-	-	-
Nd146 (ppm)	-	-	-	-	-	-	-	BDL	-
Sm147 (ppm)	BDL	-	-	-	-	-	-	-	-
Eu153 (ppm)	-	-	-	-	-	-	-	-	-
Gd157 (ppm)	-	-	-	-	-	-	-	-	-
Tb159 (ppm)	-	-	-	-	-	-	-	-	-
Dy163 (ppm)	-	-	-	-	-	-	-	-	-
Ho165 (ppm)	-	-	-	-	-	-	-	-	-
Er166 (ppm)	-	-	-	-	-	-	-	-	-
Tm169 (ppm)	-	-	-	-	-	-	-	-	-
Yb172 (ppm)	-	-	-	-	-	-	-	-	-
Lu175 (ppm)	-	-	-	-	-	-	-	-	-
Hf178 (ppm)	BDL	BDL	BDL	-	-	BDL	BDL	-	-
Ta181 (ppm)	BDL	BDL	BDL	BDL	BDL	BDL	BDL	BDL	BDL
W182 (ppm)	1	BDL	BDL	BDL	BDL	BDL	0	BDL	BDL
Re185 (ppm)	BDL	BDL	-	-	BDL	-	BDL	-	-
Os189 (ppm)	-	BDL	BDL	BDL	-	BDL	-	BDL	BDL
Ir193 (ppm)	-	BDL	BDL	-	BDL	BDL	-	BDL	-
Pt195 (ppm)	BDL	BDL	41	32	20	33	38	46	24
Au197 (ppm)	32	46	74	62	BDL	39	69	44	46
Hg202 (ppm)	0	BDL	BDL	1	0	0	1	BDL	0
Pb204 (ppm)	-	2	4	-	7	-	27	-	-
Tl205 (ppm)	-	2	-	-	6	-	-	6	15
Pb206 (ppm)	2	2	-	21	7	5	28	6	14
Pb207 (ppm)	0	0	0	1	0	0	0	0	0
Pb208 (ppm)	-	-	-	-	-	-	-	-	-
Bi209 (ppm)	-	-	-	-	-	-	-	-	-
Th232 (ppm)	2	3	5	22	7	5	29	6	15
U238 (ppm)	-	-	-	-	-	-	-	-	-
PbTotal (ppm)	-	-	-	-	-	-	-	-	-

Table D2. Trace element data for chalcopyrite continued.

Deposit	Betts Cove	Betts Cove	Betts Cove	Betts Cove	Betts Cove	Betts Cove	Betts Cove	Betts Cove	Betts Cove
Sample	KKMSC29_Cpy 15	KKMSC29_Cpy 21	KKMSC29_Cpy 29	KKMSC29_Cpy 28	KKMSC29_Cpy 26	KKMSC29_Cpy 25	KKMSC29_Cpy 24	KKMSC29_Cpy 27	KKMSC29_Cpy 30
Date	2023-11-20	2023-11-20	2023-11-20	2023-11-20	2023-11-20	2023-11-20	2023-11-20	2023-11-20	2023-11-20
Facies	Chalcopyrite-dominated	Chalcopyrite-dominated	Chalcopyrite-dominated	Chalcopyrite-dominated	Chalcopyrite-dominated	Chalcopyrite-dominated	Chalcopyrite-dominated	Chalcopyrite-dominated	Chalcopyrite-dominated
Li7 (ppm)	BDL	3	BDL	BDL	BDL	BDL	BDL	BDL	BDL
Be9 (ppm)	-	-	BDL	-	-	BDL	-	BDL	BDL
B11 (ppm)	BDL	BDL	BDL	BDL	BDL	BDL	BDL	BDL	BDL
Na23 (ppm)	BDL	BDL	BDL	BDL	BDL	BDL	BDL	BDL	BDL
Mg24 (ppm)	31	28	8	-	54	40	331	111	27
Al27 (ppm)	34	26	8	155	30	49	459	210	30
Si29 (ppm)	BDL	BDL	1474	BDL	BDL	BDL	2355	1794	BDL
P31 (ppm)	BDL	BDL	BDL	BDL	BDL	BDL	BDL	61	BDL
S32 (ppm)	375558	350489	313197	385187	387386	372164	409807	360309	313989
K39 (ppm)	BDL	BDL	BDL	BDL	BDL	BDL	BDL	BDL	BDL
Ca44 (ppm)	BDL	BDL	BDL	BDL	BDL	BDL	343	BDL	BDL
Sc45 (ppm)	BDL	BDL	BDL	BDL	BDL	BDL	BDL	BDL	BDL
Ti47 (ppm)	BDL	BDL	-	6	BDL	10	50	-	83
V51 (ppm)	BDL	BDL	BDL	BDL	BDL	BDL	1	1	BDL
Cr52 (ppm)	BDL	BDL	BDL	BDL	BDL	BDL	21	BDL	BDL
Mn55 (ppm)	1	BDL	BDL	6	BDL	3	10	8	1
Fe57 (ppm)	281932	267072	245873	273200	258022	256675	274168	264443	240805
Co59 (ppm)	3	400	3	4	6	3	4	3	2
Ni60 (ppm)	BDL	299	-	-	1	-	6	-	1
Cu63 (ppm)	-	-	-	-	-	-	-	-	-
Zn66 (ppm)	662	1358	695	1073	972	1290	784	490	439
Ga71 (ppm)	-	BDL	-	-	-	-	-	-	BDL
Ge73 (ppm)	BDL	BDL	-	BDL	-	BDL	BDL	-	-
As75 (ppm)	BDL	BDL	BDL	BDL	BDL	BDL	BDL	BDL	BDL
Se77 (ppm)	4495	2910	3793	3459	4079	4116	4166	2657	3424
Rb85 (ppm)	BDL	BDL	BDL	BDL	BDL	BDL	BDL	BDL	BDL
Sr88 (ppm)	-	BDL	-	-	-	-	-	-	-
Y89 (ppm)	-	-	-	-	-	-	-	-	-
Zr90 (ppm)	BDL	BDL	BDL	-	-	BDL	2	BDL	BDL
Nb93 (ppm)	-	-	-	-	-	-	-	-	-
Mo95 (ppm)	-	-	-	4	4	5	-	4	-
Ru101 (ppm)	-	-	-	-	-	-	BDL	-	-
Rh103 (ppm)	-	12	12	11	-	-	-	-	10
Pd104 (ppm)	BDL	-	1	1	-	1	-	-	-

Pd105 (ppm)	1	4	2	3	1	-	1	1	0
Pd106 (ppm)	6	-	10	-	-	-	4	-	4
Ag107 (ppm)	-	-	-	10	-	-	-	-	-
Cd111 (ppm)	BDL	0	BDL	BDL	BDL	BDL	BDL	BDL	BDL
In115 (ppm)	BDL	2	0	1	0	0	0	BDL	BDL
Sn118 (ppm)	-	4	4	-	13	7	7	2	4
Sb121 (ppm)	BDL	BDL	BDL	BDL	BDL	BDL	BDL	BDL	BDL
Te125 (ppm)	-	-	-	-	-	-	-	-	-
Cs133 (ppm)	-	-	-	-	-	-	-	-	-
Ba137 (ppm)	-	-	-	-	-	-	-	-	-
La139 (ppm)	BDL	-	-	-	-	-	-	-	-
Ce140 (ppm)	-	-	-	-	-	-	-	-	-
Pr141 (ppm)	-	-	-	-	-	-	-	-	-
Nd146 (ppm)	-	-	-	-	-	-	-	-	-
Sm147 (ppm)	-	-	-	-	-	-	-	-	-
Eu153 (ppm)	-	-	-	-	-	BDL	-	-	-
Gd157 (ppm)	-	-	-	-	-	-	-	-	-
Tb159 (ppm)	-	-	-	-	-	-	-	-	-
Dy163 (ppm)	-	-	-	-	-	-	-	-	-
Ho165 (ppm)	-	-	-	-	-	-	-	-	-
Er166 (ppm)	-	-	-	-	-	-	-	-	-
Tm169 (ppm)	-	-	-	-	-	-	-	-	-
Yb172 (ppm)	-	-	-	-	-	-	-	-	-
Lu175 (ppm)	-	BDL	-	-	-	-	0	-	-
Hf178 (ppm)	-	BDL	-	-	-	-	-	-	-
Ta181 (ppm)	BDL	BDL	BDL	BDL	BDL	BDL	BDL	BDL	BDL
W182 (ppm)	BDL	BDL	BDL	BDL	BDL	BDL	1	1	BDL
Re185 (ppm)	-	-	BDL	-	-	-	-	-	BDL
Os189 (ppm)	BDL	BDL	-	-	BDL	BDL	-	-	-
Ir193 (ppm)	BDL	-	-	-	-	-	BDL	BDL	-
Pt195 (ppm)	35	25	49	35	37	37	57	BDL	31
Au197 (ppm)	45	58	119	55	56	52	41	52	55
Hg202 (ppm)	BDL	1	1	0	BDL	0	0	0	BDL
Pb204 (ppm)	-	52	-	15	22	2	4	7	10
Tl205 (ppm)	-	54	-	17	20	2	2	-	11
Pb206 (ppm)	2	54	63	-	21	2	-	7	9
Pb207 (ppm)	0	1	1	1	-	BDL	BDL	0	0
Pb208 (ppm)	-	-	-	-	-	-	-	-	-
Bi209 (ppm)	-	-	-	-	-	-	-	-	-
Th232 (ppm)	3	54	65	16	22	3	4	8	10
U238 (ppm)	-	-	-	-	-	-	-	-	-
PbTotal (ppm)	-	-	-	-	-	-	-	-	-

Table D2. Trace element data for chalcopyrite continued.

Deposit	Betts Cove	Tilt Cove	Tilt Cove	Tilt Cove	Tilt Cove	Tilt Cove	Tilt Cove	Tilt Cove	Tilt Cove
Sample	KKMSC29_Cpy 31	KKMSC63_Cpy 1	KKMSC63_Cpy 2	KKMSC63_Cpy 4	KKMSC63_Cpy 5	KKMSC63_Cpy 13	KKMSC63_Cpy 7	KKMSC63_Cpy 6	KKMSC63_Cpy 8
Date	2023-11-20	2023-11-21	2023-11-21	2023-11-21	2023-11-21	2023-11-21	2023-11-21	2023-11-21	2023-11-21
Facies	Chalcopyrite-dominated	Pyrite-dominated	Pyrite-dominated	Pyrite-dominated	Pyrite-dominated	Pyrite-dominated	Pyrite-dominated	Pyrite-dominated	Pyrite-dominated
Li7 (ppm)	BDL	50	3	BDL	BDL	BDL	BDL	BDL	BDL
Be9 (ppm)	-	-	BDL	BDL	-	BDL	BDL	BDL	-
B11 (ppm)	BDL	BDL	BDL	BDL	BDL	BDL	BDL	BDL	BDL
Na23 (ppm)	BDL	340	BDL	BDL	BDL	BDL	BDL	BDL	BDL
Mg24 (ppm)	-	10997	48514	998	29	1227	380	60	8958
Al27 (ppm)	31	4134	112	37	BDL	26	49	BDL	224
Si29 (ppm)	BDL	14918	62276	2965	1756	3691	BDL	BDL	14084
P31 (ppm)	BDL	BDL	BDL	BDL	BDL	BDL	BDL	BDL	BDL
S32 (ppm)	292361	441444	693894	458211	379792	389353	422044	352525	819582
K39 (ppm)	BDL	157	BDL	BDL	BDL	BDL	BDL	BDL	BDL
Ca44 (ppm)	BDL	2285	BDL	BDL	BDL	BDL	BDL	BDL	BDL
Sc45 (ppm)	BDL	BDL	BDL	BDL	BDL	BDL	BDL	BDL	BDL
Ti47 (ppm)	BDL	27	9	BDL	BDL	5	BDL	BDL	BDL
V51 (ppm)	BDL	21	1	4	BDL	2	BDL	BDL	2
Cr52 (ppm)	BDL	137	BDL	BDL	BDL	15	BDL	BDL	18
Mn55 (ppm)	3	365	18	4	BDL	BDL	BDL	BDL	25
Fe57 (ppm)	246463	369204	482232	301816	248543	277616	285647	268496	706087
Co59 (ppm)	3	74	1494	806	BDL	454	264	BDL	-
Ni60 (ppm)	-	-	1238	-	48	108	-	45	-
Cu63 (ppm)	-	-	-	-	-	-	-	-	-
Zn66 (ppm)	850	501	359	289	287	133	167	444	2530
Ga71 (ppm)	-	BDL	-	-	-	-	-	-	-
Ge73 (ppm)	-	BDL	-	BDL	-	-	-	-	-
As75 (ppm)	BDL	43	608	680	BDL	261	77	6	19789
Se77 (ppm)	3383	311	426	281	174	168	150	144	269
Rb85 (ppm)	BDL	BDL	BDL	BDL	BDL	BDL	BDL	BDL	BDL
Sr88 (ppm)	-	-	-	-	-	BDL	-	-	-
Y89 (ppm)	-	-	-	-	-	-	-	-	-
Zr90 (ppm)	BDL	-	-	-	-	-	-	-	-
Nb93 (ppm)	-	BDL	2	-	BDL	BDL	BDL	BDL	BDL
Mo95 (ppm)	-	-	-	BDL	-	-	-	-	-
Ru101 (ppm)	BDL	4	-	-	-	-	-	5	-
Rh103 (ppm)	-	BDL	-	-	-	BDL	-	BDL	BDL
Pd104 (ppm)	-	22	-	22	-	-	15	16	15

Pd105 (ppm)	1	-	-	BDL	BDL	-	BDL	-	1
Pd106 (ppm)	-	41	44	25	17	21	19	19	47
Ag107 (ppm)	-	3	20	11	6	-	6	-	14
Cd111 (ppm)	BDL	-	-	-	-	-	27	-	-
In115 (ppm)	0	BDL	BDL	1	1	1	2	1	1
Sn118 (ppm)	4	15	50	14	1	17	9	4	147
Sb121 (ppm)	BDL	BDL	9	2	BDL	-	BDL	BDL	-
Te125 (ppm)	-	BDL	BDL	BDL	BDL	BDL	BDL	BDL	BDL
Cs133 (ppm)	-	-	-	-	-	-	-	-	-
Ba137 (ppm)	-	-	-	-	-	-	-	-	-
La139 (ppm)	-	-	-	-	-	-	-	-	-
Ce140 (ppm)	-	-	-	-	-	-	-	-	-
Pr141 (ppm)	-	-	-	-	-	-	-	-	-
Nd146 (ppm)	-	BDL	-	-	-	-	-	-	-
Sm147 (ppm)	BDL	-	-	-	-	-	-	-	-
Eu153 (ppm)	-	-	-	-	-	-	-	-	-
Gd157 (ppm)	BDL	-	-	-	-	-	-	-	-
Tb159 (ppm)	-	-	-	-	-	-	-	-	-
Dy163 (ppm)	-	-	-	-	-	-	-	-	-
Ho165 (ppm)	-	-	-	-	-	-	-	-	-
Er166 (ppm)	-	-	-	BDL	-	-	-	-	-
Tm169 (ppm)	-	-	-	-	-	-	-	-	-
Yb172 (ppm)	-	-	-	-	-	-	-	-	-
Lu175 (ppm)	-	-	-	-	-	-	-	-	-
Hf178 (ppm)	-	-	-	-	-	-	-	-	-
Ta181 (ppm)	BDL	-	-	-	-	-	-	-	-
W182 (ppm)	BDL	BDL	BDL	BDL	BDL	BDL	BDL	BDL	BDL
Re185 (ppm)	-	2	BDL	BDL	BDL	BDL	BDL	BDL	BDL
Os189 (ppm)	BDL	BDL	-	BDL	BDL	BDL	BDL	BDL	-
Ir193 (ppm)	-	BDL	BDL	BDL	-	-	BDL	BDL	BDL
Pt195 (ppm)	28	BDL	-	-	-	-	BDL	BDL	-
Au197 (ppm)	65	214	BDL	57	BDL	56	17	BDL	46
Hg202 (ppm)	0	BDL	133	118	75	123	101	84	602
Pb204 (ppm)	-	1	2	0	BDL	1	1	0	2
Tl205 (ppm)	-	12	134	-	12	62	53	-	-
Pb206 (ppm)	23	-	-	50	-	67	52	26	534
Pb207 (ppm)	0	-	114	37	10	57	45	25	475
Pb208 (ppm)	-	BDL	2	0	BDL	0	0	0	11
Bi209 (ppm)	-	-	-	-	-	-	-	-	-
Th232 (ppm)	24	BDL	-	-	BDL	-	-	-	-
U238 (ppm)	-	13	124	42	11	61	49	27	503
PbTotal (ppm)	-	-	-	-	-	-	-	-	-

Table D2. Trace element data for chalcopyrite continued.

Deposit	Tilt Cove	Tilt Cove	Tilt Cove	Tilt Cove	Tilt Cove	Tilt Cove	Tilt Cove	Tilt Cove	Tilt Cove
Sample	KKMSC63_Cpy 15	KKMSC63_Cpy 16	KKMSC63_Cpy 19	KKMSC63_Cpy 9	KKMSC63_Cpy 10	KKMSC63_Cpy 12	KKMSC63_Cpy 11	KKMSC77_Cpy 5	KKMSC77_Cpy 7
Date	2023-11-21	2023-11-21	2023-11-21	2023-11-21	2023-11-21	2023-11-21	2023-11-21	2023-11-21	2023-11-21
Facies	Pyrite-dominated	Pyrite-dominated	Pyrite-dominated	Pyrite-dominated	Pyrite-dominated	Pyrite-dominated	Pyrite-dominated	Pyrite-dominated	Pyrite-dominated
Li7 (ppm)	BDL	BDL	BDL	BDL	BDL	BDL	BDL	BDL	BDL
Be9 (ppm)	-	-	-	BDL	-	-	-	BDL	-
B11 (ppm)	BDL	BDL	BDL	BDL	BDL	BDL	BDL	BDL	BDL
Na23 (ppm)	BDL	BDL	BDL	BDL	BDL	BDL	BDL	BDL	BDL
Mg24 (ppm)	11	250	7	108	165	656	853	5	85
Al27 (ppm)	BDL	17	BDL	29	21	137	119	BDL	12
Si29 (ppm)	BDL	1898	BDL	BDL	BDL	BDL	3159	BDL	1740
P31 (ppm)	BDL	BDL	BDL	BDL	BDL	BDL	BDL	BDL	BDL
S32 (ppm)	379001	360877	412729	373634	401468	410847	414638	402632	395387
K39 (ppm)	BDL	BDL	BDL	BDL	BDL	BDL	BDL	BDL	BDL
Ca44 (ppm)	BDL	BDL	BDL	BDL	BDL	BDL	BDL	BDL	BDL
Sc45 (ppm)	BDL	BDL	BDL	BDL	BDL	BDL	BDL	BDL	BDL
Ti47 (ppm)	-	BDL	-	BDL	BDL	BDL	8	BDL	BDL
V51 (ppm)	BDL	BDL	BDL	0	BDL	BDL	BDL	BDL	BDL
Cr52 (ppm)	BDL	BDL	BDL	BDL	BDL	10	24	BDL	BDL
Mn55 (ppm)	BDL	BDL	BDL	BDL	1	2	BDL	BDL	1
Fe57 (ppm)	269376	241572	269423	254855	277894	281311	281965	256340	290591
Co59 (ppm)	0	0	1	4	1	2	1	BDL	7
Ni60 (ppm)	-	56	44	44	-	15	36	-	-
Cu63 (ppm)	-	-	-	-	-	-	-	-	-
Zn66 (ppm)	271	128	216	141	112	125	165	1	3
Ga71 (ppm)	-	-	-	-	BDL	BDL	BDL	-	-
Ge73 (ppm)	-	-	BDL	-	BDL	-	BDL	BDL	-
As75 (ppm)	BDL	BDL	BDL	BDL	BDL	BDL	BDL	BDL	6
Se77 (ppm)	151	132	140	133	141	155	149	83	80
Rb85 (ppm)	-	BDL	BDL	BDL	BDL	BDL	BDL	BDL	-
Sr88 (ppm)	-	-	-	-	-	-	-	-	-
Y89 (ppm)	-	-	-	-	-	-	-	-	-
Zr90 (ppm)	-	-	-	-	-	-	-	-	-
Nb93 (ppm)	BDL	BDL	BDL	BDL	BDL	BDL	1	BDL	BDL
Mo95 (ppm)	-	-	-	-	-	BDL	-	-	-
Ru101 (ppm)	-	-	5	-	4	-	-	-	-
Rh103 (ppm)	-	-	BDL	-	BDL	-	-	-	BDL
Pd104 (ppm)	13	14	14	12	-	-	15	-	-

Pd105 (ppm)	BDL	-	-	-	0	BDL	BDL	-	BDL
Pd106 (ppm)	18	18	-	14	18	19	15	10	5
Ag107 (ppm)	6	6	5	3	4	-	3	BDL	BDL
Cd111 (ppm)	-	-	-	23	-	26	23	-	-
In115 (ppm)	1	1	2	1	1	BDL	1	BDL	BDL
Sn118 (ppm)	3	6	2	2	8	8	2	5	3
Sb121 (ppm)	-	-	BDL	-	BDL	BDL	-	BDL	BDL
Te125 (ppm)	BDL	BDL	BDL	BDL	BDL	BDL	BDL	BDL	BDL
Cs133 (ppm)	-	-	-	-	-	-	-	-	-
Ba137 (ppm)	-	-	-	-	-	-	-	-	-
La139 (ppm)	-	-	-	-	-	-	-	-	-
Ce140 (ppm)	-	-	-	-	-	-	-	-	-
Pr141 (ppm)	-	-	-	-	-	-	-	-	-
Nd146 (ppm)	-	-	-	-	-	-	-	-	-
Sm147 (ppm)	-	-	-	-	-	-	-	-	-
Eu153 (ppm)	-	-	-	-	-	-	-	-	-
Gd157 (ppm)	-	-	-	-	-	-	-	-	-
Tb159 (ppm)	-	-	-	-	-	-	-	-	-
Dy163 (ppm)	-	-	-	-	-	-	-	-	-
Ho165 (ppm)	-	-	-	-	-	-	-	-	-
Er166 (ppm)	-	-	-	-	-	-	-	-	-
Tm169 (ppm)	-	-	-	-	-	-	-	-	-
Yb172 (ppm)	-	-	-	-	-	-	-	-	-
Lu175 (ppm)	-	-	-	-	-	-	-	-	-
Hf178 (ppm)	-	-	-	-	-	-	BDL	-	-
Ta181 (ppm)	BDL	-	-	-	BDL	-	-	-	-
W182 (ppm)	BDL	BDL	BDL	BDL	BDL	BDL	BDL	BDL	BDL
Re185 (ppm)	BDL	BDL	BDL	BDL	BDL	BDL	BDL	BDL	BDL
Os189 (ppm)	BDL	BDL	-	BDL	BDL	-	-	-	BDL
Ir193 (ppm)	BDL	BDL	BDL	BDL	BDL	-	-	BDL	BDL
Pt195 (ppm)	BDL	BDL	-	-	-	-	BDL	BDL	-
Au197 (ppm)	42	BDL	44	43	52	51	41	43	BDL
Hg202 (ppm)	51	66	68	70	105	98	56	65	64
Pb204 (ppm)	0	0	0	BDL	1	1	BDL	BDL	BDL
Tl205 (ppm)	17	28	22	18	45	46	8	-	-
Pb206 (ppm)	-	-	-	19	42	45	9	-	14
Pb207 (ppm)	17	26	20	-	43	49	9	19	15
Pb208 (ppm)	BDL	BDL	BDL	BDL	BDL	BDL	BDL	0	0
Bi209 (ppm)	-	-	-	-	-	-	-	-	-
Th232 (ppm)	-	-	BDL	-	-	-	-	-	-
U238 (ppm)	18	27	21	20	44	48	10	19	15
PbTotal (ppm)	-	-	-	-	-	-	-	-	-

Table D2. Trace element data for chalcopyrite continued.

Deposit	Tilt Cove	Tilt Cove	Tilt Cove	Tilt Cove	Betts Cove	Betts Cove	Betts Cove	Betts Cove	Betts Cove
Sample	KKMSC77_Cpy 6	KKMSC77_Cpy 8	KKMSC77_Cpy 1	KKMSC77_Cpy 2	KKMSC32_Cpy 3	KKMSC32_Cpy 4	KKMSC32_Cpy 5	KKMSC32_Cpy 6	KKMSC32_Cpy 1
Date	2023-11-21	2023-11-21	2023-11-21	2023-11-21	2023-11-21	2023-11-21	2023-11-21	2023-11-21	2023-11-21
Facies	Pyrite-dominated	Pyrite-dominated	Pyrite-dominated	Pyrite-dominated	Sphalerite-pyrite-dominated	Sphalerite-pyrite-dominated	Sphalerite-pyrite-dominated	Sphalerite-pyrite-dominated	Sphalerite-pyrite-dominated
Li7 (ppm)	BDL	BDL	143	BDL	BDL	BDL	BDL	BDL	BDL
Be9 (ppm)	-	BDL	BDL	-	-	-	-	-	-
B11 (ppm)	BDL	BDL	165	BDL	BDL	BDL	BDL	BDL	BDL
Na23 (ppm)	102	BDL	BDL	BDL	BDL	BDL	56	BDL	BDL
Mg24 (ppm)	1542	54	207838	757	148	542	176	388	3
Al27 (ppm)	441	42	217887	518	165	661	142	350	4
Si29 (ppm)	4013	BDL	232199	BDL	BDL	2340	1759	BDL	BDL
P31 (ppm)	BDL	BDL	BDL	BDL	BDL	BDL	BDL	BDL	42
S32 (ppm)	1529853	621441	3561615	545831	310479	318805	391991	354250	359409
K39 (ppm)	BDL	BDL	BDL	BDL	BDL	BDL	BDL	BDL	BDL
Ca44 (ppm)	BDL	BDL	1931	9483	BDL	BDL	47024	BDL	BDL
Sc45 (ppm)	BDL	BDL	97	BDL	BDL	BDL	BDL	BDL	BDL
Ti47 (ppm)	18	BDL	-	20	BDL	22	6	BDL	BDL
V51 (ppm)	BDL	BDL	490	1	BDL	1	BDL	BDL	BDL
Cr52 (ppm)	14	BDL	863	BDL	BDL	8	BDL	BDL	BDL
Mn55 (ppm)	25	BDL	569	125	5	19	151	12	BDL
Fe57 (ppm)	1049505	469032	2602164	525823	243071	251198	264395	273338	251124
Co59 (ppm)	117	129	438	45	3	4	-	1	1
Ni60 (ppm)	1274	24	-	240	-	-	-	3	BDL
Cu63 (ppm)	-	-	-	-	-	-	-	-	-
Zn66 (ppm)	3	2	347	10	673	285	307	197	367
Ga71 (ppm)	BDL	-	-	-	-	-	-	-	-
Ge73 (ppm)	-	-	BDL	BDL	BDL	-	-	BDL	BDL
As75 (ppm)	834	14	189	20	BDL	BDL	BDL	BDL	BDL
Se77 (ppm)	178	49	271	61	17	24	20	19	18
Rb85 (ppm)	0	BDL	-	BDL	BDL	BDL	BDL	BDL	BDL
Sr88 (ppm)	-	-	-	-	-	-	-	-	-
Y89 (ppm)	-	-	-	-	-	-	-	-	-
Zr90 (ppm)	-	-	-	-	-	-	-	-	-
Nb93 (ppm)	1	BDL	BDL	BDL	-	BDL	-	-	BDL
Mo95 (ppm)	-	-	-	-	BDL	-	BDL	BDL	-
Ru101 (ppm)	-	-	-	16	-	-	-	-	-
Rh103 (ppm)	BDL	-	-	BDL	-	6	-	-	-
Pd104 (ppm)	15	-	-	36	-	-	-	-	-

Pd105 (ppm)	BDL	BDL	BDL	BDL	-	-	-	-	-
Pd106 (ppm)	29	8	-	70	BDL	BDL	-	-	-
Ag107 (ppm)	-	BDL	-	-	-	307	292	341	198
Cd111 (ppm)	-	7	-	-	-	-	BDL	-	BDL
In115 (ppm)	BDL	BDL	BDL	BDL	BDL	-	BDL	-	-
Sn118 (ppm)	23	15	58	86	0	BDL	BDL	1	BDL
Sb121 (ppm)	BDL	-	BDL	BDL	BDL	1	BDL	0	BDL
Te125 (ppm)	BDL	BDL	BDL	BDL	BDL	-	BDL	BDL	-
Cs133 (ppm)	-	-	-	-	BDL	BDL	BDL	BDL	BDL
Ba137 (ppm)	-	-	-	-	-	-	-	-	-
La139 (ppm)	-	-	-	-	-	-	-	-	-
Ce140 (ppm)	-	-	-	-	-	-	-	-	BDL
Pr141 (ppm)	-	-	-	-	-	-	-	-	-
Nd146 (ppm)	-	-	-	-	-	-	-	-	-
Sm147 (ppm)	-	-	BDL	-	-	-	-	-	-
Eu153 (ppm)	-	-	-	-	-	-	-	-	-
Gd157 (ppm)	-	-	-	-	-	-	BDL	-	-
Tb159 (ppm)	-	-	-	-	-	-	-	-	-
Dy163 (ppm)	-	-	-	-	-	-	-	-	-
Ho165 (ppm)	-	-	-	-	-	-	-	-	-
Er166 (ppm)	-	-	-	-	-	-	-	-	-
Tm169 (ppm)	-	-	-	-	-	-	-	-	-
Yb172 (ppm)	-	-	-	-	-	-	-	-	-
Lu175 (ppm)	-	-	-	-	-	-	-	-	-
Hf178 (ppm)	-	-	-	BDL	-	-	-	-	-
Ta181 (ppm)	-	-	-	-	BDL	-	-	-	-
W182 (ppm)	BDL	BDL	BDL	BDL	-	-	BDL	-	BDL
Re185 (ppm)	BDL	BDL	BDL	BDL	BDL	BDL	BDL	BDL	BDL
Os189 (ppm)	BDL	BDL	-	-	BDL	BDL	BDL	BDL	BDL
Ir193 (ppm)	-	BDL	-	BDL	BDL	-	-	BDL	-
Pt195 (ppm)	1	-	BDL	-	-	BDL	BDL	BDL	-
Au197 (ppm)	103	79	489	225	-	-	-	BDL	-
Hg202 (ppm)	296	108	1071	1776	BDL	BDL	BDL	BDL	BDL
Pb204 (ppm)	0	0	1	3	BDL	54	BDL	BDL	BDL
Tl205 (ppm)	197	-	1228	-	BDL	0	BDL	BDL	BDL
Pb206 (ppm)	180	54	-	1098	1	9	2	4	-
Pb207 (ppm)	202	55	1217	-	0	9	1	4	0
Pb208 (ppm)	3	1	5	5	0	9	1	4	-
Bi209 (ppm)	-	-	-	-	BDL	BDL	BDL	BDL	BDL
Th232 (ppm)	-	-	-	-	-	-	-	-	-
U238 (ppm)	197	57	1212	1053	-	-	-	-	-
PbTotal (ppm)	-	-	-	-	BDL	10	2	4	1

Table D2. Trace element data for chalcopyrite continued.

Deposit	Betts Cove	Betts Cove	Betts Cove	Betts Cove	Betts Cove	Betts Cove	Betts Cove	Betts Cove	Betts Cove
Sample	KKMSC32_Cpy 2	KKMSC35_Cpy 4	KKMSC35_Cpy 5	KKMSC35_Cpy 1	KKMSC35_Cpy 2	KKMSC35_Cpy 3	KKMSC35_Cpy 6	KKMSC35_Cpy 7	KKMSC53_Cpy 2
Date	2023-11-21	2023-11-21	2023-11-21	2023-11-21	2023-11-21	2023-11-21	2023-11-21	2023-11-21	2023-11-22
Facies	Sphalerite-pyrite-dominated	Chalcopyrite-pyrrhotite-dominated	Chalcopyrite-pyrrhotite-dominated	Chalcopyrite-pyrrhotite-dominated	Chalcopyrite-pyrrhotite-dominated	Chalcopyrite-pyrrhotite-dominated	Chalcopyrite-pyrrhotite-dominated	Chalcopyrite-pyrrhotite-dominated	Chalcopyrite-dominated
Li7 (ppm)	BDL	BDL	BDL	BDL	BDL	2	BDL	BDL	3
Be9 (ppm)	BDL	-	-	-	-	BDL	-	-	BDL
B11 (ppm)	BDL	BDL	BDL	BDL	BDL	BDL	BDL	BDL	BDL
Na23 (ppm)	BDL	BDL	BDL	BDL	BDL	BDL	BDL	BDL	BDL
Mg24 (ppm)	8	80	1363	5	18	24	7	19	25
Al27 (ppm)	4	10	2001	7	17	72	2	12	59
Si29 (ppm)	3390	BDL	14162	BDL	BDL	BDL	BDL	1635	2791
P31 (ppm)	BDL	BDL	BDL	BDL	53	88	BDL	BDL	BDL
S32 (ppm)	344441	308982	2468546	282385	371568	332187	305493	274579	447756
K39 (ppm)	BDL	BDL	139	BDL	BDL	BDL	BDL	BDL	BDL
Ca44 (ppm)	BDL	336	BDL	BDL	BDL	BDL	BDL	BDL	BDL
Sc45 (ppm)	BDL	BDL	3	BDL	BDL	BDL	BDL	BDL	BDL
Ti47 (ppm)	BDL	-	BDL	BDL	-	BDL	-	BDL	BDL
V51 (ppm)	BDL	BDL	22	BDL	BDL	BDL	BDL	BDL	BDL
Cr52 (ppm)	BDL	BDL	BDL	BDL	BDL	BDL	BDL	BDL	BDL
Mn55 (ppm)	BDL	24	169	3	5	6	BDL	2	BDL
Fe57 (ppm)	264963	285179	3407839	221887	267680	234028	232159	238699	270790
Co59 (ppm)	0	4	8937	5	6	-	10	4	2
Ni60 (ppm)	-	6	-	14	12	-	6	6	12
Cu63 (ppm)	-	-	-	-	-	-	-	-	-
Zn66 (ppm)	247	231	671	650	896	497	412	738	760
Ga71 (ppm)	-	-	-	0	-	-	-	-	-
Ge73 (ppm)	BDL	-	-	BDL	-	-	BDL	-	BDL
As75 (ppm)	BDL	6	8854	BDL	BDL	8	BDL	BDL	BDL
Se77 (ppm)	18	590	3078	1047	891	676	670	720	846
Rb85 (ppm)	BDL	BDL	BDL	BDL	BDL	BDL	BDL	BDL	BDL
Sr88 (ppm)	-	-	-	-	-	-	-	-	-
Y89 (ppm)	-	-	-	-	-	-	-	-	-
Zr90 (ppm)	-	-	-	-	-	-	-	-	-
Nb93 (ppm)	-	-	-	-	-	-	-	-	BDL
Mo95 (ppm)	BDL	BDL	32	BDL	BDL	-	BDL	BDL	BDL
Ru101 (ppm)	-	-	-	-	-	-	-	-	BDL
Rh103 (ppm)	-	-	-	-	6	-	-	-	-
Pd104 (ppm)	-	-	-	-	BDL	BDL	-	-	-

Pd105 (ppm)	-	-	-	-	-	20	-	-	-
Pd106 (ppm)	BDL	-	-	-	-	-	-	-	-
Ag107 (ppm)	178	199	4223	-	-	202	119	-	18
Cd111 (ppm)	1	4	-	7	-	-	-	8	-
In115 (ppm)	BDL	-	-	-	-	-	5	-	2
Sn118 (ppm)	1	7	9	7	9	11	7	7	1
Sb121 (ppm)	BDL	1	8	0	-	0	0	0	BDL
Te125 (ppm)	BDL	2	1368	2	-	-	BDL	BDL	-
Cs133 (ppm)	BDL	BDL	BDL	BDL	BDL	BDL	BDL	BDL	BDL
Ba137 (ppm)	-	-	-	-	-	-	-	-	-
La139 (ppm)	-	-	-	-	-	-	-	-	-
Ce140 (ppm)	-	-	-	-	-	-	-	-	-
Pr141 (ppm)	-	-	BDL	-	-	-	-	-	-
Nd146 (ppm)	-	-	-	-	-	-	-	-	-
Sm147 (ppm)	-	-	-	-	-	-	-	-	-
Eu153 (ppm)	-	-	-	-	-	-	-	-	-
Gd157 (ppm)	-	-	-	-	-	-	-	-	-
Tb159 (ppm)	-	-	-	-	-	-	-	-	-
Dy163 (ppm)	-	-	-	-	-	-	-	-	-
Ho165 (ppm)	-	-	-	BDL	-	-	-	-	-
Er166 (ppm)	-	-	-	-	-	-	-	-	-
Tm169 (ppm)	-	-	-	-	-	BDL	-	-	-
Yb172 (ppm)	-	-	-	-	-	-	-	-	-
Lu175 (ppm)	-	-	-	-	-	-	-	-	-
Hf178 (ppm)	-	-	-	-	-	-	-	-	-
Ta181 (ppm)	-	BDL	-	-	-	-	-	-	-
W182 (ppm)	-	BDL	-	-	BDL	BDL	BDL	-	-
Re185 (ppm)	BDL	BDL	2	BDL	BDL	BDL	BDL	BDL	BDL
Os189 (ppm)	BDL	BDL	BDL	BDL	BDL	BDL	BDL	BDL	BDL
Ir193 (ppm)	BDL	BDL	-	-	-	-	BDL	-	-
Pt195 (ppm)	BDL	BDL	BDL	BDL	BDL	-	BDL	-	BDL
Au197 (ppm)	-	-	-	-	-	-	-	-	-
Hg202 (ppm)	BDL	BDL	117	14	BDL	148	11	7	BDL
Pb204 (ppm)	BDL	52	2628	61	26	854	48	42	BDL
Tl205 (ppm)	BDL	1	0	BDL	BDL	1	0	0	BDL
Pb206 (ppm)	1	34	2553	17	1	44	23	18	0
Pb207 (ppm)	1	-	-	-	-	56	22	16	0
Pb208 (ppm)	1	33	2619	16	-	54	23	17	1
Bi209 (ppm)	BDL	0	15	0	0	2	0	-	BDL
Th232 (ppm)	-	-	-	-	-	-	-	-	-
U238 (ppm)	-	-	-	-	-	-	-	BDL	-
PbTotal (ppm)	1	33	2498	17	1	64	23	18	1

Table D2. Trace element data for chalcopyrite continued.

Deposit	Betts Cove	Betts Cove	Betts Cove	Betts Cove	Betts Cove	Betts Cove	Betts Cove	Betts Cove	Betts Cove
Sample	KKMSC53_Cpy 1	KKMSC53_Cpy 3	KKMSC53_Cpy 9	KKMSC53_Cpy 10	KKMSC53_Cpy 8	KKMSC53_Cpy 7	KKMSC53_Cpy 6	KKMSC53_Cpy 5	KKMSC53_Cpy 11
Date	2023-11-22	2023-11-22	2023-11-22	2023-11-22	2023-11-22	2023-11-22	2023-11-22	2023-11-22	2023-11-22
Facies	Chalcopyrite-dominated	Chalcopyrite-dominated	Chalcopyrite-dominated	Chalcopyrite-dominated	Chalcopyrite-dominated	Chalcopyrite-dominated	Chalcopyrite-dominated	Chalcopyrite-dominated	Chalcopyrite-dominated
Li7 (ppm)	5	6	2	2	BDL	BDL	BDL	BDL	38
Be9 (ppm)	-	-	-	BDL	-	-	BDL	-	-
B11 (ppm)	BDL	BDL	BDL	BDL	BDL	BDL	BDL	BDL	BDL
Na23 (ppm)	BDL	BDL	BDL	BDL	138	BDL	BDL	BDL	74
Mg24 (ppm)	35	-	68	66	6	BDL	3	15	39123
Al27 (ppm)	30	49	41	45	11	BDL	BDL	29	38548
Si29 (ppm)	BDL	BDL	2937	BDL	BDL	1840	1899	BDL	45436
P31 (ppm)	BDL	BDL	BDL	BDL	BDL	BDL	BDL	BDL	BDL
S32 (ppm)	349220	349686	361537	361098	320430	331293	332874	393204	422032
K39 (ppm)	BDL	BDL	BDL	BDL	BDL	BDL	BDL	BDL	BDL
Ca44 (ppm)	BDL	BDL	BDL	BDL	4053	BDL	BDL	179	BDL
Sc45 (ppm)	BDL	BDL	BDL	BDL	BDL	BDL	BDL	BDL	16
Ti47 (ppm)	5	BDL	BDL	BDL	BDL	-	BDL	-	15
V51 (ppm)	BDL	BDL	BDL	BDL	BDL	BDL	BDL	BDL	118
Cr52 (ppm)	BDL	BDL	BDL	BDL	BDL	BDL	BDL	BDL	691
Mn55 (ppm)	2	3	3	2	5	BDL	BDL	2	735
Fe57 (ppm)	253646	286435	274699	272405	283009	284833	255096	285152	336260
Co59 (ppm)	2	3	21	2	64	1	8	14	57
Ni60 (ppm)	6	-	391	3	-	9	-	384	-
Cu63 (ppm)	-	-	-	-	-	-	-	-	-
Zn66 (ppm)	935	374	110	703	95	926	113	120	330
Ga71 (ppm)	-	-	-	-	-	-	-	BDL	-
Ge73 (ppm)	-	BDL	BDL	BDL	BDL	-	-	-	BDL
As75 (ppm)	BDL	BDL	BDL	BDL	11	BDL	BDL	5	7
Se77 (ppm)	819	1057	598	689	669	906	887	871	1744
Rb85 (ppm)	BDL	BDL	BDL	BDL	BDL	BDL	BDL	BDL	BDL
Sr88 (ppm)	-	-	-	-	-	-	-	-	-
Y89 (ppm)	-	-	-	-	-	-	-	-	-
Zr90 (ppm)	-	-	-	-	-	-	-	-	-
Nb93 (ppm)	-	-	-	-	-	-	-	-	-
Mo95 (ppm)	BDL	1	BDL	-	BDL	BDL	BDL	-	BDL
Ru101 (ppm)	-	-	-	-	-	-	-	BDL	-
Rh103 (ppm)	-	6	-	7	-	-	6	-	6
Pd104 (ppm)	-	-	BDL	-	BDL	BDL	-	BDL	-

Pd105 (ppm)	12	-	14	-	-	-	-	-	-
Pd106 (ppm)	-	-	1	BDL	BDL	-	1	-	BDL
Ag107 (ppm)	25	20	52	-	58	18	62	63	-
Cd111 (ppm)	6	6	-	-	8	7	10	-	-
In115 (ppm)	-	1	-	2	BDL	-	-	-	-
Sn118 (ppm)	1	1	BDL	2	BDL	1	BDL	BDL	2
Sb121 (ppm)	0	2	0	1	1	0	BDL	0	-
Te125 (ppm)	5	4	2	-	-	6	-	1	456
Cs133 (ppm)	BDL	BDL	BDL	BDL	BDL	BDL	BDL	BDL	BDL
Ba137 (ppm)	-	-	-	-	-	-	-	-	-
La139 (ppm)	-	-	-	-	-	-	-	-	-
Ce140 (ppm)	-	-	-	-	-	-	-	-	-
Pr141 (ppm)	-	-	-	-	-	-	-	-	-
Nd146 (ppm)	-	-	-	-	-	-	-	-	-
Sm147 (ppm)	-	-	-	-	-	-	-	-	-
Eu153 (ppm)	-	-	-	-	-	-	-	-	-
Gd157 (ppm)	-	-	-	-	-	-	-	-	-
Tb159 (ppm)	-	-	-	-	-	-	-	-	-
Dy163 (ppm)	-	-	-	-	-	-	-	-	-
Ho165 (ppm)	-	-	-	-	-	-	-	-	-
Er166 (ppm)	-	-	-	-	-	-	BDL	-	-
Tm169 (ppm)	-	-	-	-	-	-	-	-	-
Yb172 (ppm)	-	-	-	-	-	-	-	-	BDL
Lu175 (ppm)	-	-	-	-	-	-	-	-	-
Hf178 (ppm)	-	-	-	-	-	-	-	-	-
Ta181 (ppm)	-	-	-	-	-	-	-	BDL	-
W182 (ppm)	BDL	-	-	-	-	BDL	-	-	-
Re185 (ppm)	BDL	BDL	BDL	BDL	BDL	BDL	BDL	BDL	BDL
Os189 (ppm)	BDL	BDL	BDL	BDL	BDL	BDL	BDL	BDL	BDL
Ir193 (ppm)	BDL	-	BDL	-	-	BDL	-	BDL	-
Pt195 (ppm)	BDL	BDL	BDL	BDL	-	BDL	BDL	BDL	BDL
Au197 (ppm)	-	BDL	-	-	-	BDL	0	-	-
Hg202 (ppm)	BDL	BDL	BDL	BDL	BDL	BDL	8	BDL	BDL
Pb204 (ppm)	BDL	BDL	208	BDL	179	BDL	209	195	306
Tl205 (ppm)	BDL	1	14	0	16	BDL	13	14	3
Pb206 (ppm)	-	6	-	10	169	5	197	202	-
Pb207 (ppm)	0	6	167	9	163	-	176	202	298
Pb208 (ppm)	0	7	-	9	154	5	186	202	304
Bi209 (ppm)	BDL	BDL	0	-	0	BDL	0	0	9
Th232 (ppm)	-	-	-	-	-	-	-	-	-
U238 (ppm)	-	-	-	-	-	-	-	-	-
PbTotal (ppm)	1	7	173	9	160	5	187	202	307

Table D2. Trace element data for chalcopyrite continued.

Deposit	Tilt Cove	Tilt Cove	Tilt Cove	Tilt Cove	Tilt Cove	Tilt Cove	Tilt Cove	Tilt Cove	Tilt Cove
Sample	KKMSC72_Cpy 7	KKMSC72_Cpy 8	KKMSC72_Cpy 9	KKMSC72_Cpy 4	KKMSC72_Cpy 3	KKMSC72_Cpy 2	KKMSC72_Cpy 6	KKMSC72_Cpy 12	KKMSC72_Cpy 11
Date	2023-11-22	2023-11-22	2023-11-22	2023-11-22	2023-11-22	2023-11-22	2023-11-22	2023-11-22	2023-11-22
Facies	Pyrrhotite-dominated	Pyrrhotite-dominated	Pyrrhotite-dominated	Pyrrhotite-dominated	Pyrrhotite-dominated	Pyrrhotite-dominated	Pyrrhotite-dominated	Pyrrhotite-dominated	Pyrrhotite-dominated
Li7 (ppm)	BDL	BDL	1	4	44	5	121	1	BDL
Be9 (ppm)	-	BDL	-	BDL	BDL	BDL	BDL	BDL	-
B11 (ppm)	BDL	BDL	BDL	BDL	62	BDL	BDL	BDL	BDL
Na23 (ppm)	BDL	BDL	33	141	7792	39	1415	BDL	BDL
Mg24 (ppm)	201	183	5701	133	1904007	959	5926237	43	16
Al27 (ppm)	7	22	34	37	1108	23	1730	14	5
Si29 (ppm)	BDL	BDL	8611	BDL	51787	2615	52495	BDL	BDL
P31 (ppm)	BDL	BDL	BDL	BDL	331	BDL	1747	BDL	BDL
S32 (ppm)	335213	290532	324429	364718	627161	359416	1225515	294076	302855
K39 (ppm)	BDL	BDL	BDL	BDL	340	BDL	BDL	BDL	BDL
Ca44 (ppm)	BDL	BDL	BDL	BDL	8969	BDL	16134	BDL	BDL
Sc45 (ppm)	BDL	BDL	BDL	BDL	8	BDL	24	BDL	BDL
Ti47 (ppm)	BDL	BDL	BDL	BDL	BDL	-	22	BDL	-
V51 (ppm)	BDL	0	BDL	BDL	5	BDL	3	BDL	BDL
Cr52 (ppm)	BDL	BDL	BDL	BDL	53	BDL	148	BDL	BDL
Mn55 (ppm)	3	6	6	3	62215	66	163419	2	2
Fe57 (ppm)	360382	249482	250841	259559	1684269	235392	3903936	268322	266031
Co59 (ppm)	50	1	-	4	219	-	-	1	1
Ni60 (ppm)	-	50	38	37	3582	-	-	-	42
Cu63 (ppm)	-	-	-	-	-	-	-	-	-
Zn66 (ppm)	1741	342	280	440	1206	638	641	1106	629
Ga71 (ppm)	-	-	-	-	-	-	-	-	-
Ge73 (ppm)	BDL	-	BDL	-	BDL	-	BDL	-	-
As75 (ppm)	BDL	4	BDL	BDL	17	BDL	17	BDL	BDL
Se77 (ppm)	69	49	45	74	80	67	76	65	56
Rb85 (ppm)	BDL	BDL	BDL	BDL	6	BDL	3	BDL	BDL
Sr88 (ppm)	-	-	-	-	-	-	-	-	-
Y89 (ppm)	BDL	-	-	-	-	-	-	-	-
Zr90 (ppm)	-	-	-	-	-	-	-	-	-
Nb93 (ppm)	-	-	-	-	-	-	-	-	-
Mo95 (ppm)	BDL	BDL	BDL	-	-	BDL	2	BDL	-
Ru101 (ppm)	BDL	BDL	-	-	-	-	-	-	-
Rh103 (ppm)	-	-	-	-	-	6	-	-	-
Pd104 (ppm)	-	-	-	-	-	-	BDL	BDL	BDL

Pd105 (ppm)	22	-	-	-	-	13	9	-	12
Pd106 (ppm)	-	0	0	-	-	-	-	-	-
Ag107 (ppm)	156	62	85	47	79	33	85	56	41
Cd111 (ppm)	32	4	8	-	19	6	-	-	8
In115 (ppm)	55	21	-	-	101	-	-	20	-
Sn118 (ppm)	BDL	BDL	BDL	BDL	1	1	BDL	BDL	BDL
Sb121 (ppm)	26	5	15	5	49	1	50	12	2
Te125 (ppm)	4	-	3	1	-	2	-	2	1
Cs133 (ppm)	BDL	BDL	BDL	BDL	BDL	BDL	2	BDL	BDL
Ba137 (ppm)	-	-	-	-	-	-	-	-	-
La139 (ppm)	-	-	-	-	-	-	-	-	-
Ce140 (ppm)	-	-	-	-	-	-	-	-	-
Pr141 (ppm)	-	-	-	-	-	-	-	-	-
Nd146 (ppm)	-	-	-	-	-	-	-	-	-
Sm147 (ppm)	-	-	-	-	-	-	-	-	-
Eu153 (ppm)	-	-	-	-	-	-	-	-	-
Gd157 (ppm)	-	-	-	-	-	-	-	-	-
Tb159 (ppm)	-	-	-	-	-	-	-	-	-
Dy163 (ppm)	-	-	-	-	-	-	-	-	-
Ho165 (ppm)	-	-	-	-	-	-	-	-	-
Er166 (ppm)	-	-	-	-	-	-	-	-	-
Tm169 (ppm)	-	-	-	-	-	-	-	-	-
Yb172 (ppm)	-	-	-	-	-	BDL	-	-	-
Lu175 (ppm)	-	-	-	-	-	-	-	-	-
Hf178 (ppm)	-	-	-	BDL	-	-	-	-	-
Ta181 (ppm)	-	-	-	-	-	-	-	-	-
W182 (ppm)	-	-	BDL	-	-	-	-	BDL	-
Re185 (ppm)	BDL	BDL	BDL	BDL	3	BDL	1	BDL	BDL
Os189 (ppm)	BDL	BDL	BDL	BDL	BDL	BDL	5	BDL	BDL
Ir193 (ppm)	BDL	BDL	BDL	BDL	-	-	BDL	-	BDL
Pt195 (ppm)	BDL	-	BDL	BDL	1	-	BDL	BDL	BDL
Au197 (ppm)	0	-	-	-	BDL	-	-	BDL	-
Hg202 (ppm)	13	BDL	BDL	BDL	29	8	BDL	BDL	8
Pb204 (ppm)	243	44	125	BDL	220	42	330	77	60
Tl205 (ppm)	1	0	4	BDL	10	BDL	6	1	BDL
Pb206 (ppm)	168	-	91	20	152	-	152	-	16
Pb207 (ppm)	-	27	94	19	142	-	156	53	16
Pb208 (ppm)	160	27	101	21	142	7	146	51	15
Bi209 (ppm)	1	0	1	BDL	1	0	0	0	0
Th232 (ppm)	-	-	-	-	-	-	-	-	-
U238 (ppm)	-	-	-	-	-	-	-	-	-
PbTotal (ppm)	162	27	97	20	145	8	152	52	16

Table D2. Trace element data for chalcopyrite continued.

Deposit	Tilt Cove	Betts Cove	Betts Cove	Betts Cove	Betts Cove	Betts Cove	Betts Cove	Betts Cove	Betts Cove
Sample	KKMSC72_Cpy 10	KKMSC42_Cpy 2	KKMSC42_Cpy 1	KKMSC42_Cpy 11	KKMSC42_Cpy 10	KKMSC42_Cpy 8	KKMSC42_Cpy 9	KKMSC42_Cpy 6	KKMSC42_Cpy 7
Date	2023-11-22	2023-11-22	2023-11-22	2023-11-22	2023-11-22	2023-11-22	2023-11-22	2023-11-22	2023-11-22
Facies	Pyrrhotite-dominated	Chalcopyrite-pyrrhotite-dominated	Chalcopyrite-pyrrhotite-dominated	Chalcopyrite-pyrrhotite-dominated	Chalcopyrite-pyrrhotite-dominated	Chalcopyrite-pyrrhotite-dominated	Chalcopyrite-pyrrhotite-dominated	Chalcopyrite-pyrrhotite-dominated	Chalcopyrite-pyrrhotite-dominated
Li7 (ppm)	BDL	48	40	30	5	7	BDL	8	10
Be9 (ppm)	-	BDL	-	-	-	BDL	-	-	-
B11 (ppm)	BDL	84	380	BDL	BDL	BDL	BDL	27	78
Na23 (ppm)	BDL	90	209	94	BDL	BDL	BDL	BDL	79
Mg24 (ppm)	31	22600	342	707	70	116	26	166	92
Al27 (ppm)	8	22587	296	420	50	124	10	111	127
Si29 (ppm)	BDL	70239	2604247	10490	BDL	3619	2917	3206	5195
P31 (ppm)	BDL	BDL	659	234	BDL	BDL	131	BDL	BDL
S32 (ppm)	329416	818605	1105749	563631	366164	428506	373207	414254	422628
K39 (ppm)	BDL	BDL	BDL	BDL	BDL	BDL	BDL	BDL	139
Ca44 (ppm)	BDL	4750	4149	1075	BDL	BDL	BDL	BDL	BDL
Sc45 (ppm)	BDL	9	BDL	BDL	BDL	BDL	BDL	BDL	BDL
Ti47 (ppm)	BDL	196	123	BDL	BDL	BDL	39	-	-
V51 (ppm)	BDL	46	BDL	4	BDL	BDL	3	BDL	BDL
Cr52 (ppm)	BDL	86	BDL	21	BDL	9	23	BDL	BDL
Mn55 (ppm)	1	765	22	40	5	8	BDL	10	7
Fe57 (ppm)	267767	311200	233866	294071	262499	239774	241213	263017	271398
Co59 (ppm)	3	10	2	14	-	9	10	13	18
Ni60 (ppm)	-	-	BDL	-	-	10	4	-	7
Cu63 (ppm)	-	-	-	-	-	-	-	-	-
Zn66 (ppm)	482	619	422	947	1172	754	784	799	1265
Ga71 (ppm)	-	-	-	-	-	-	-	BDL	-
Ge73 (ppm)	BDL	BDL	BDL	-	BDL	BDL	-	BDL	BDL
As75 (ppm)	BDL	60	80	BDL	11	BDL	56	23	31
Se77 (ppm)	64	2085	1692	1193	970	957	1203	1180	877
Rb85 (ppm)	BDL	BDL	-	BDL	BDL	BDL	1	BDL	BDL
Sr88 (ppm)	-	-	-	-	-	-	-	-	-
Y89 (ppm)	-	-	-	-	-	-	BDL	-	-
Zr90 (ppm)	-	-	-	-	-	-	-	-	-
Nb93 (ppm)	-	-	-	-	-	-	-	-	-
Mo95 (ppm)	-	249	BDL	BDL	-	BDL	BDL	1	-
Ru101 (ppm)	-	BDL	-	-	-	-	-	-	-
Rh103 (ppm)	6	-	1	-	-	-	-	1	2
Pd104 (ppm)	-	-	-	BDL	-	-	-	-	-

Pd105 (ppm)	12	11	-	-	-	-	-	-	21
Pd106 (ppm)	0	-	-	-	-	-	BDL	1	-
Ag107 (ppm)	50	49	12	18	19	34	28	16	27
Cd111 (ppm)	10	4	1	5	-	8	2	3	3
In115 (ppm)	-	-	-	-	20	-	28	17	-
Sn118 (ppm)	BDL	BDL	BDL	1	BDL	1	BDL	BDL	BDL
Sb121 (ppm)	8	BDL	BDL	BDL	BDL	BDL	1	0	1
Te125 (ppm)	4	348	BDL	BDL	4	8	2	-	7
Cs133 (ppm)	BDL	BDL	BDL	BDL	BDL	BDL	BDL	BDL	BDL
Ba137 (ppm)	-	-	-	-	-	-	-	-	-
La139 (ppm)	-	-	-	-	-	-	-	-	-
Ce140 (ppm)	-	-	-	-	-	-	-	-	-
Pr141 (ppm)	-	-	-	-	-	-	-	-	-
Nd146 (ppm)	-	-	-	-	-	-	-	-	-
Sm147 (ppm)	-	-	-	-	-	-	-	-	-
Eu153 (ppm)	-	-	-	-	-	-	-	-	BDL
Gd157 (ppm)	-	-	-	-	-	-	-	-	-
Tb159 (ppm)	-	-	-	-	-	-	-	-	-
Dy163 (ppm)	-	-	-	-	-	-	-	-	-
Ho165 (ppm)	-	-	-	-	-	-	-	-	-
Er166 (ppm)	-	-	-	-	-	-	-	-	-
Tm169 (ppm)	-	-	-	-	-	-	-	-	-
Yb172 (ppm)	-	BDL	-	-	-	-	-	-	-
Lu175 (ppm)	-	-	-	-	-	-	-	-	-
Hf178 (ppm)	-	-	-	-	-	-	-	-	-
Ta181 (ppm)	-	-	-	BDL	-	-	-	-	-
W182 (ppm)	-	-	BDL	-	-	-	BDL	-	-
Re185 (ppm)	BDL	2	BDL	1	BDL	BDL	2	BDL	BDL
Os189 (ppm)	BDL	BDL	BDL	BDL	BDL	BDL	BDL	BDL	BDL
Ir193 (ppm)	-	-	BDL	BDL	BDL	BDL	BDL	BDL	-
Pt195 (ppm)	BDL	BDL	BDL	BDL	BDL	BDL	BDL	-	-
Au197 (ppm)	-	-	-	-	BDL	-	-	-	BDL
Hg202 (ppm)	11	316	97	30	12	63	BDL	32	52
Pb204 (ppm)	88	937	1786	111	39	304	521	47	618
Tl205 (ppm)	0	1	0	BDL	BDL	BDL	BDL	BDL	16
Pb206 (ppm)	-	789	132	17	9	-	161	-	365
Pb207 (ppm)	62	815	156	13	8	14	195	5	360
Pb208 (ppm)	65	797	144	17	9	14	281	4	276
Bi209 (ppm)	0	45	5	1	2	2	4	0	30
Th232 (ppm)	-	-	-	-	-	-	-	-	-
U238 (ppm)	-	-	-	-	-	-	-	-	-
PbTotal (ppm)	65	813	168	17	9	18	236	5	322

Table D2. Trace element data for chalcopyrite continued.

Deposit	Tilt Cove	Tilt Cove	Tilt Cove	Tilt Cove	Tilt Cove	Tilt Cove	Tilt Cove	Tilt Cove	Tilt Cove
Sample	KKMSC70_Cpy 1	KKMSC70_Cpy 2	KKMSC70_Cpy 3	KKMSC70_Cpy 4	KKMSC70_Cpy 5	KKMSC70_Cpy 7	KKMSC70_Cpy 6	KKMSC70_Cpy 8	KKMSC70_Cpy 9
Date	2023-11-22	2023-11-22	2023-11-22	2023-11-22	2023-11-22	2023-11-22	2023-11-22	2023-11-22	2023-11-22
Facies	Chalcopyrite-pyrrhotite-dominated	Chalcopyrite-pyrrhotite-dominated	Chalcopyrite-pyrrhotite-dominated	Chalcopyrite-pyrrhotite-dominated	Chalcopyrite-pyrrhotite-dominated	Chalcopyrite-pyrrhotite-dominated	Chalcopyrite-pyrrhotite-dominated	Chalcopyrite-pyrrhotite-dominated	Chalcopyrite-pyrrhotite-dominated
Li7 (ppm)	BDL	BDL	BDL	BDL	BDL	1	BDL	BDL	BDL
Be9 (ppm)	-	-	-	-	-	-	BDL	BDL	-
B11 (ppm)	BDL	BDL	BDL	BDL	BDL	BDL	BDL	BDL	BDL
Na23 (ppm)	BDL	BDL	BDL	BDL	BDL	BDL	BDL	BDL	BDL
Mg24 (ppm)	14	352	325	324	3822	301	669	64	35
Al27 (ppm)	BDL	15	BDL	24	282	36	12	6	3
Si29 (ppm)	BDL	3008	BDL	BDL	7346	BDL	3463	BDL	BDL
P31 (ppm)	BDL	BDL	BDL	BDL	BDL	BDL	BDL	BDL	BDL
S32 (ppm)	407908	452596	444232	442308	463808	420813	413675	383677	382576
K39 (ppm)	BDL	BDL	BDL	BDL	BDL	BDL	BDL	BDL	BDL
Ca44 (ppm)	BDL	BDL	BDL	BDL	BDL	BDL	BDL	BDL	BDL
Sc45 (ppm)	BDL	BDL	BDL	BDL	BDL	BDL	BDL	BDL	BDL
Ti47 (ppm)	BDL	BDL	BDL	BDL	BDL	-	BDL	BDL	BDL
V51 (ppm)	BDL	BDL	BDL	BDL	1	BDL	BDL	BDL	BDL
Cr52 (ppm)	BDL	BDL	BDL	BDL	8	BDL	BDL	BDL	BDL
Mn55 (ppm)	BDL	BDL	3	BDL	9	3	7	BDL	BDL
Fe57 (ppm)	277395	270999	282809	282453	283402	277444	279079	286164	253239
Co59 (ppm)	1	1	1	BDL	3	1	1	1	2
Ni60 (ppm)	67	-	-	40	-	-	67	-	-
Cu63 (ppm)	-	-	-	-	-	-	-	-	-
Zn66 (ppm)	899	372	439	429	1019	380	462	576	356
Ga71 (ppm)	BDL	-	-	-	-	-	-	-	-
Ge73 (ppm)	BDL	-	BDL	-	BDL	BDL	BDL	-	BDL
As75 (ppm)	BDL	BDL	51	65	81	36	30	20	21
Se77 (ppm)	157	143	147	153	123	135	147	129	120
Rb85 (ppm)	BDL	BDL	BDL	-	BDL	BDL	BDL	BDL	BDL
Sr88 (ppm)	-	-	-	-	-	0	-	-	-
Y89 (ppm)	-	-	-	-	-	-	-	-	-
Zr90 (ppm)	-	-	-	-	BDL	-	-	-	-
Nb93 (ppm)	-	-	-	-	-	-	-	-	-
Mo95 (ppm)	BDL	-	-	BDL	BDL	1	BDL	BDL	BDL
Ru101 (ppm)	-	-	-	-	-	-	-	-	-
Rh103 (ppm)	-	-	2	-	2	-	-	-	-
Pd104 (ppm)	BDL	-	-	BDL	BDL	BDL	-	-	-

Pd105 (ppm)	-	-	17	-	-	-	16	-	16
Pd106 (ppm)	-	-	2	-	1	1	-	-	-
Ag107 (ppm)	15	16	22	22	32	20	19	22	6
Cd111 (ppm)	24	15	8	12	-	8	19	10	-
In115 (ppm)	22	-	-	-	-	-	-	-	-
Sn118 (ppm)	1	1	BDL	BDL	BDL	BDL	1	1	1
Sb121 (ppm)	0	1	1	2	6	3	1	0	-
Te125 (ppm)	7	2	3	BDL	3	BDL	-	-	1
Cs133 (ppm)	BDL	BDL	BDL	BDL	BDL	BDL	BDL	BDL	BDL
Ba137 (ppm)	-	-	-	-	-	-	-	-	-
La139 (ppm)	-	-	-	-	-	-	-	-	-
Ce140 (ppm)	-	-	-	-	-	-	-	-	-
Pr141 (ppm)	-	-	-	-	-	-	-	-	-
Nd146 (ppm)	-	-	-	-	-	-	-	-	-
Sm147 (ppm)	-	-	-	-	-	-	-	-	-
Eu153 (ppm)	-	-	-	-	-	-	-	-	-
Gd157 (ppm)	-	-	-	-	-	-	-	-	-
Tb159 (ppm)	-	-	-	-	-	-	-	-	-
Dy163 (ppm)	-	-	-	-	-	-	-	-	-
Ho165 (ppm)	-	-	-	-	-	-	-	-	-
Er166 (ppm)	-	-	-	-	-	-	-	-	-
Tm169 (ppm)	-	-	-	-	-	-	-	-	-
Yb172 (ppm)	-	-	-	-	-	-	-	-	-
Lu175 (ppm)	-	-	-	-	-	-	-	-	-
Hf178 (ppm)	-	-	-	-	-	-	-	-	-
Ta181 (ppm)	-	-	-	-	-	-	-	-	BDL
W182 (ppm)	-	BDL	-	-	-	BDL	-	-	-
Re185 (ppm)	BDL	BDL	BDL	BDL	BDL	BDL	BDL	BDL	BDL
Os189 (ppm)	BDL	BDL	BDL	BDL	BDL	BDL	BDL	BDL	BDL
Ir193 (ppm)	-	-	BDL	BDL	BDL	-	BDL	BDL	-
Pt195 (ppm)	-	BDL	-	BDL	-	-	BDL	BDL	-
Au197 (ppm)	-	-	-	-	-	-	-	BDL	-
Hg202 (ppm)	BDL	BDL	BDL	BDL	BDL	BDL	9	BDL	BDL
Pb204 (ppm)	45	BDL	51	75	BDL	60	BDL	BDL	BDL
Tl205 (ppm)	BDL	BDL	BDL	BDL	1	0	BDL	BDL	BDL
Pb206 (ppm)	12	11	14	11	67	42	-	7	13
Pb207 (ppm)	13	10	13	11	-	-	-	7	13
Pb208 (ppm)	13	11	14	11	67	43	16	7	14
Bi209 (ppm)	0	0	0	0	2	1	0	0	0
Th232 (ppm)	-	-	-	-	-	-	-	-	-
U238 (ppm)	-	-	-	-	-	-	-	-	-
PbTotal (ppm)	13	11	14	12	66	43	16	7	14

Table D2. Trace element data for chalcopyrite continued.

Deposit	Tilt Cove	Tilt Cove	Tilt Cove	Tilt Cove	Tilt Cove	Tilt Cove	Tilt Cove	Tilt Cove	Tilt Cove
Sample	KKMSC12_Cpy 26	KKMSC12_Cpy 27	KKMSC12_Cpy 12	KKMSC12_Cpy 15	KKMSC12_Cpy 16	KKMSC12_Cpy 17	KKMSC12_Cpy 18	KKMSC12_Cpy 19	KKMSC12_Cpy 10
Date	2023-11-23	2023-11-23	2023-11-23	2023-11-23	2023-11-23	2023-11-23	2023-11-23	2023-11-23	2023-11-23
Facies	Chalcopyrite-dominated	Chalcopyrite-dominated	Chalcopyrite-dominated	Chalcopyrite-dominated	Chalcopyrite-dominated	Chalcopyrite-dominated	Chalcopyrite-dominated	Chalcopyrite-dominated	Chalcopyrite-dominated
Li7 (ppm)	16	7	13	16	10	8	10	5	9
Be9 (ppm)	BDL	-	BDL	BDL	-	-	-	-	-
B11 (ppm)	BDL	BDL	BDL	BDL	50	BDL	BDL	BDL	BDL
Na23 (ppm)	BDL	BDL	BDL	BDL	BDL	BDL	BDL	BDL	BDL
Mg24 (ppm)	507	1023	812	14092	160	152	2244	1876	691
Al27 (ppm)	485	792	539	429	130	103	915	82	984
Si29 (ppm)	BDL	BDL	BDL	BDL	BDL	BDL	6843	BDL	148502
P31 (ppm)	BDL	BDL	BDL	BDL	BDL	BDL	BDL	BDL	177
S32 (ppm)	301098	280877	292455	767631	465163	368730	381249	326665	316929
K39 (ppm)	BDL	BDL	BDL	BDL	100	BDL	BDL	BDL	BDL
Ca44 (ppm)	BDL	BDL	BDL	27982	BDL	BDL	BDL	7894	667
Sc45 (ppm)	BDL	BDL	26	16	8	BDL	BDL	BDL	BDL
Ti47 (ppm)	114	BDL	-	BDL	-	BDL	53	BDL	40
V51 (ppm)	1	1	BDL	BDL	BDL	BDL	1	BDL	2
Cr52 (ppm)	BDL	BDL	BDL	BDL	BDL	BDL	BDL	BDL	BDL
Mn55 (ppm)	22	7	15	1490	3	4	19	252	17
Fe57 (ppm)	331971	230792	273591	355625	354088	337990	304649	272046	246014
Co59 (ppm)	-	10	655	4723	2	1	429	16892	11
Ni60 (ppm)	5	-	18	124	BDL	BDL	25	-	-
Cu63 (ppm)	-	-	-	-	-	-	-	-	-
Zn66 (ppm)	51	23	12	19	33	31	24	20	27
Ga71 (ppm)	BDL	-	BDL	BDL	-	-	-	-	-
Ge73 (ppm)	-	BDL	BDL	-	BDL	BDL	BDL	BDL	BDL
As75 (ppm)	73	22	1468	4275	18	36	393	35793	57
Se77 (ppm)	160	126	134	253	244	216	166	164	79
Rb85 (ppm)	BDL	BDL	BDL	BDL	BDL	BDL	BDL	BDL	BDL
Sr88 (ppm)	-	-	-	-	-	-	-	-	-
Y89 (ppm)	-	-	-	-	-	-	-	BDL	-
Zr90 (ppm)	-	-	-	-	-	-	-	-	-
Nb93 (ppm)	BDL	BDL	-	-	-	BDL	-	-	-
Mo95 (ppm)	-	BDL	-	-	-	-	-	-	-
Ru101 (ppm)	9	8	-	-	-	-	-	-	-
Rh103 (ppm)	BDL	-	BDL	1	-	-	BDL	-	1
Pd104 (ppm)	28	-	28	35	14	-	19	-	28

Pd105 (ppm)	BDL	BDL	6	-	-	BDL	BDL	BDL	0
Pd106 (ppm)	118	8	27	48	4	4	22	22	165
Ag107 (ppm)	BDL	BDL	BDL	BDL	BDL	BDL	BDL	-	BDL
Cd111 (ppm)	4	-	17	11	-	-	32	-	6
In115 (ppm)	BDL	BDL	BDL	BDL	1	1	1	BDL	1
Sn118 (ppm)	11	7	17	7	1	3	8	17	22
Sb121 (ppm)	BDL	BDL	-	7	10	BDL	BDL	56	3
Te125 (ppm)	BDL	BDL	BDL	BDL	BDL	BDL	BDL	BDL	BDL
Cs133 (ppm)	-	-	-	-	-	-	-	-	-
Ba137 (ppm)	-	-	-	-	-	-	-	-	-
La139 (ppm)	-	-	-	-	-	-	-	-	-
Ce140 (ppm)	-	-	-	-	-	BDL	-	-	-
Pr141 (ppm)	-	-	-	-	-	-	-	-	-
Nd146 (ppm)	-	-	-	-	-	-	-	-	-
Sm147 (ppm)	-	-	-	-	-	-	-	-	-
Eu153 (ppm)	-	-	-	-	-	-	-	-	-
Gd157 (ppm)	-	-	-	-	-	-	-	-	-
Tb159 (ppm)	-	-	-	-	-	-	-	-	-
Dy163 (ppm)	-	-	-	-	-	-	-	-	-
Ho165 (ppm)	-	BDL	-	-	-	-	-	-	-
Er166 (ppm)	-	-	-	-	-	-	-	-	-
Tm169 (ppm)	-	-	-	-	-	-	-	-	-
Yb172 (ppm)	-	-	-	-	-	-	BDL	-	-
Lu175 (ppm)	-	-	-	-	-	-	-	-	-
Hf178 (ppm)	-	-	-	-	-	-	-	-	-
Ta181 (ppm)	BDL	-	-	-	-	BDL	-	-	-
W182 (ppm)	BDL	BDL	BDL	BDL	BDL	BDL	BDL	BDL	BDL
Re185 (ppm)	BDL	BDL	BDL	BDL	BDL	BDL	BDL	BDL	BDL
Os189 (ppm)	-	BDL	-	-	BDL	BDL	-	BDL	-
Ir193 (ppm)	-	BDL	0	BDL	BDL	BDL	BDL	-	-
Pt195 (ppm)	-	1	-	-	BDL	-	-	-	BDL
Au197 (ppm)	BDL	65	75	179	243	112	89	82	180
Hg202 (ppm)	BDL	76	128	276	79	186	232	210	611
Pb204 (ppm)	BDL	BDL	BDL	BDL	BDL	BDL	BDL	0	0
Tl205 (ppm)	81	-	58	95	-	-	23	72	239
Pb206 (ppm)	75	14	74	76	10	-	-	41	-
Pb207 (ppm)	73	16	59	56	7	35	25	43	313
Pb208 (ppm)	1	1	2	2	0	0	1	4	2
Bi209 (ppm)	-	-	-	-	-	-	-	-	BDL
Th232 (ppm)	BDL	-	-	BDL	-	-	-	-	-
U238 (ppm)	75	16	63	73	10	30	27	52	278
PbTotal (ppm)	-	-	-	-	-	-	-	-	-

Table D2. Trace element data for chalcopyrite continued.

Deposit	Tilt Cove	Tilt Cove	Tilt Cove	Tilt Cove	Tilt Cove	Tilt Cove	Tilt Cove	Tilt Cove	Tilt Cove
Sample	KKMSC12_Cpy 9	KKMSC12_Cpy 5	KKMSC12_Cpy 6	KKMSC13_Cpy 2	KKMSC13_Cpy 3	KKMSC13_Cpy 4	KKMSC13_Cpy 6	KKMSC13_Cpy 10	KKMSC13_Cpy 9
Date	2023-11-23	2023-11-23	2023-11-23	2023-11-23	2023-11-23	2023-11-23	2023-11-23	2023-11-23	2023-11-23
Facies	Chalcopyrite-dominated	Chalcopyrite-dominated	Chalcopyrite-dominated	Pyrite-dominated	Pyrite-dominated	Pyrite-dominated	Pyrite-dominated	Pyrite-dominated	Pyrite-dominated
Li7 (ppm)	5	3	5	17	BDL	5	-	1077	19
Be9 (ppm)	-	BDL	BDL	-	-	-	BDL	-	-
B11 (ppm)	BDL	BDL	BDL	BDL	BDL	BDL	BDL	2261	BDL
Na23 (ppm)	BDL	BDL	BDL	BDL	BDL	BDL	668777	2722	738
Mg24 (ppm)	157	115	199	474	3	12541	318736	103683	29821
Al27 (ppm)	146	68	138	355	5	9754	146895	68763	24401
Si29 (ppm)	BDL	2628	BDL	5447	BDL	65427	109077968	285230	2221342
P31 (ppm)	BDL	BDL	BDL	BDL	BDL	BDL	BDL	33038	276
S32 (ppm)	277632	323156	399780	1238969	322046	432767	84446144596	38716105	666906
K39 (ppm)	BDL	BDL	BDL	123	BDL	2127	BDL	6662	9781
Ca44 (ppm)	BDL	419	BDL	BDL	BDL	1309	5985900	21767	8283
Sc45 (ppm)	BDL	BDL	BDL	BDL	BDL	6	BDL	11	37
Ti47 (ppm)	6	-	BDL	-	BDL	12	87217	5460	BDL
V51 (ppm)	0	BDL	1	1	BDL	27	BDL	6	43
Cr52 (ppm)	BDL	BDL	BDL	BDL	BDL	45	BDL	200	41
Mn55 (ppm)	3	14	27	24	1	687	85207	6683	1853
Fe57 (ppm)	239699	251876	333159	447172	251802	321329	72139144569	73341743	646828
Co59 (ppm)	5	0	4	BDL	BDL	BDL	48399	68	1
Ni60 (ppm)	BDL	-	-	4	-	BDL	1154931	-	-
Cu63 (ppm)	-	-	-	-	-	-	-	-	-
Zn66 (ppm)	38	14	112	179	117	458	112103	17867	734
Ga71 (ppm)	-	-	-	-	BDL	-	BDL	-	-
Ge73 (ppm)	-	BDL	BDL	-	BDL	-	-	-	-
As75 (ppm)	38	80	136	613	109	1003	469053341	208233395	181947
Se77 (ppm)	125	165	194	10	BDL	10	1069908	2931	13
Rb85 (ppm)	-	BDL	BDL	-	BDL	9	3356	BDL	32
Sr88 (ppm)	-	-	BDL	-	-	-	-	-	-
Y89 (ppm)	-	BDL	-	-	-	-	-	-	-
Zr90 (ppm)	-	-	-	-	-	-	-	BDL	-
Nb93 (ppm)	BDL	BDL	BDL	BDL	BDL	-	-	-	-
Mo95 (ppm)	-	-	-	-	-	-	3218	-	-
Ru101 (ppm)	-	-	-	-	-	9	-	-	-
Rh103 (ppm)	-	-	BDL	-	BDL	-	-	-	-
Pd104 (ppm)	24	17	-	-	16	-	BDL	BDL	27

Pd105 (ppm)	BDL	BDL	-	BDL	BDL	-	BDL	BDL	-
Pd106 (ppm)	3	7	17	409	16	4219	-	85175	-
Ag107 (ppm)	BDL	BDL	1	-	-	BDL	BDL	-	BDL
Cd111 (ppm)	-	8	24	1	-	-	-	-	-
In115 (ppm)	1	1	1	21	11	13	18074	79	71
Sn118 (ppm)	1	3	7	35	8	11	22612	17862	48
Sb121 (ppm)	BDL	1	1	3	-	BDL	5921	30	BDL
Te125 (ppm)	BDL	BDL	BDL	BDL	BDL	2	BDL	8	30
Cs133 (ppm)	-	-	-	-	-	-	-	-	-
Ba137 (ppm)	-	-	-	-	-	-	-	-	-
La139 (ppm)	-	-	-	-	-	-	-	-	-
Ce140 (ppm)	-	-	-	-	-	-	-	-	-
Pr141 (ppm)	-	-	-	-	-	-	-	-	-
Nd146 (ppm)	-	-	-	-	-	-	-	-	-
Sm147 (ppm)	-	-	-	-	-	-	-	-	-
Eu153 (ppm)	-	-	-	-	-	-	-	-	-
Gd157 (ppm)	-	-	-	-	-	-	-	-	-
Tb159 (ppm)	-	-	-	-	-	-	-	-	-
Dy163 (ppm)	-	-	-	-	-	-	-	-	-
Ho165 (ppm)	-	-	-	-	-	-	-	-	-
Er166 (ppm)	-	-	-	-	-	-	-	-	-
Tm169 (ppm)	-	-	-	-	-	-	-	-	-
Yb172 (ppm)	-	-	-	-	BDL	-	-	-	-
Lu175 (ppm)	-	-	-	-	-	-	-	-	-
Hf178 (ppm)	-	-	-	BDL	-	-	-	-	-
Ta181 (ppm)	-	BDL	-	BDL	-	-	-	-	-
W182 (ppm)	BDL	BDL	BDL	BDL	BDL	BDL	2757	25	BDL
Re185 (ppm)	BDL	BDL	BDL	BDL	BDL	BDL	BDL	BDL	BDL
Os189 (ppm)	BDL	BDL	BDL	BDL	-	-	1149	-	-
Ir193 (ppm)	BDL	BDL	BDL	BDL	BDL	-	BDL	BDL	BDL
Pt195 (ppm)	-	-	-	-	-	-	-	17098	391
Au197 (ppm)	42	54	70	27	BDL	BDL	1518803	BDL	53
Hg202 (ppm)	80	97	98	325	47	93	1130572	4745	728
Pb204 (ppm)	BDL	0	BDL	1	BDL	1	2675	50	28
Tl205 (ppm)	3	15	-	-	11	65	-	6339	512
Pb206 (ppm)	4	-	21	160	9	50	-	-	453
Pb207 (ppm)	4	13	21	160	9	52	26402	4799	-
Pb208 (ppm)	0	0	0	1	BDL	4	BDL	235	28
Bi209 (ppm)	-	-	-	-	-	-	-	-	-
Th232 (ppm)	-	-	-	-	-	-	-	-	-
U238 (ppm)	5	15	22	170	10	58	45378	5351	503
PbTotal (ppm)	-	-	-	-	-	-	-	-	-

Table D2. Trace element data for chalcopyrite continued.

Deposit	Tilt Cove	Tilt Cove	Tilt Cove	Tilt Cove	Tilt Cove
Sample	KKMSC13_Cpy8	KKMSC13_Cpy1	KKMSC23_Cpy2	KKMSC23_Cpy3	KKMSC23_Cpy1
Date	2023-11-23	2023-11-23	2023-11-23	2023-11-23	2023-11-23
Facies	Pyrite-dominated	Pyrite-dominated	Magnetite-dominated	Magnetite-dominated	Magnetite-dominated
Li7 (ppm)	1118	2	6	4	5
Be9 (ppm)	BDL	-	-	-	-
B11 (ppm)	BDL	BDL	BDL	BDL	BDL
Na23 (ppm)	7321	BDL	BDL	BDL	BDL
Mg24 (ppm)	9161	2201	96	73	129
Al27 (ppm)	3965	1126	172	144	765
Si29 (ppm)	2872060	13366	4681	1984	6533
P31 (ppm)	219643	702	BDL	BDL	BDL
S32 (ppm)	2945760125	367306	457200	350950	415070
K39 (ppm)	BDL	443	BDL	BDL	237
Ca44 (ppm)	BDL	1430	BDL	BDL	BDL
Sc45 (ppm)	BDL	BDL	BDL	BDL	BDL
Ti47 (ppm)	BDL	BDL	BDL	10	8
V51 (ppm)	1084	3	2	BDL	1
Cr52 (ppm)	BDL	BDL	16	BDL	BDL
Mn55 (ppm)	372	88	5	3	4
Fe57 (ppm)	2877907407	269890	270895	229772	275964
Co59 (ppm)	82669	BDL	BDL	0	1
Ni60 (ppm)	-	-	-	-	1
Cu63 (ppm)	-	-	-	-	-
Zn66 (ppm)	3100	195	18	1	8
Ga71 (ppm)	-	-	-	BDL	-
Ge73 (ppm)	574	BDL	BDL	-	BDL
As75 (ppm)	445022	109	38	43	37
Se77 (ppm)	2369	BDL	56	76	42
Rb85 (ppm)	BDL	2	BDL	BDL	BDL
Sr88 (ppm)	-	-	-	-	-
Y89 (ppm)	-	-	-	-	-
Zr90 (ppm)	-	-	-	-	-
Nb93 (ppm)	BDL	7	-	-	-
Mo95 (ppm)	-	-	-	-	-
Ru101 (ppm)	BDL	8	9	8	-
Rh103 (ppm)	BDL	-	-	-	-
Pd104 (ppm)	-	22	25	-	-
Pd105 (ppm)	-	-	BDL	BDL	-

Pd106 (ppm)	BDL	151	266	96	134
Ag107 (ppm)	BDL	BDL	BDL	BDL	BDL
Cd111 (ppm)	-	1	-	-	-
In115 (ppm)	61	36	BDL	0	BDL
Sn118 (ppm)	1525	11	1	2	2
Sb121 (ppm)	31411	BDL	BDL	BDL	BDL
Te125 (ppm)	BDL	2	BDL	BDL	0
Cs133 (ppm)	-	-	-	-	-
Ba137 (ppm)	-	-	-	-	-
La139 (ppm)	-	-	-	-	-
Ce140 (ppm)	-	-	BDL	-	-
Pr141 (ppm)	-	-	-	-	-
Nd146 (ppm)	-	-	-	-	-
Sm147 (ppm)	-	-	-	-	-
Eu153 (ppm)	-	-	-	-	-
Gd157 (ppm)	-	-	-	-	-
Tb159 (ppm)	-	-	-	-	-
Dy163 (ppm)	-	-	-	-	-
Ho165 (ppm)	-	-	-	-	-
Er166 (ppm)	-	-	-	-	-
Tm169 (ppm)	-	-	-	-	-
Yb172 (ppm)	-	-	-	-	-
Lu175 (ppm)	-	-	-	-	-
Hf178 (ppm)	-	-	BDL	-	-
Ta181 (ppm)	-	-	-	-	-
W182 (ppm)	8	BDL	BDL	BDL	BDL
Re185 (ppm)	BDL	-	BDL	BDL	BDL
Os189 (ppm)	BDL	BDL	BDL	-	BDL
Ir193 (ppm)	BDL	-	0	BDL	BDL
Pt195 (ppm)	-	1	-	-	-
Au197 (ppm)	30397	65	92	BDL	62
Hg202 (ppm)	35652	135	282	89	209
Pb204 (ppm)	BDL	1	0	0	0
Tl205 (ppm)	2488	31	-	61	-
Pb206 (ppm)	3172	25	64	44	33
Pb207 (ppm)	3785	27	54	47	33
Pb208 (ppm)	67	0	0	1	BDL
Bi209 (ppm)	-	-	-	-	-
Th232 (ppm)	-	-	BDL	-	-
U238 (ppm)	3054	30	66	51	38
PbTotal (ppm)	-	-	-	-	-

Table D3. Trace element data for pyrrhotite.

Deposit	Betts Cove	Betts Cove	Betts Cove	Betts Cove	Betts Cove	Betts Cove	Betts Cove	Betts Cove	Betts Cove
Sample	KKMSC35_Po4	KKMSC35_Po5	KKMSC35_Po6	KKMSC35_Po7	KKMSC35_Po1	KKMSC35_Po2	KKMSC35_Po3	KKMSC35_Po9	KKMSC35_Po10
Date	2023-11-21	2023-11-21	2023-11-21	2023-11-21	2023-11-21	2023-11-21	2023-11-21	2023-11-21	2023-11-21
Facies	Chalcopyrite-pyrrhotite-dominated	Chalcopyrite-pyrrhotite-dominated	Chalcopyrite-pyrrhotite-dominated	Chalcopyrite-pyrrhotite-dominated	Chalcopyrite-pyrrhotite-dominated	Chalcopyrite-pyrrhotite-dominated	Chalcopyrite-pyrrhotite-dominated	Chalcopyrite-pyrrhotite-dominated	Chalcopyrite-pyrrhotite-dominated
Li7 (ppm)	BDL	1	BDL	BDL	BDL	BDL	BDL	BDL	-
Be9 (ppm)	-	-	-	-	BDL	BDL	-	-	-
B11 (ppm)	BDL	BDL	BDL	BDL	BDL	BDL	BDL	BDL	-
Na23 (ppm)	BDL	BDL	BDL	56	BDL	BDL	BDL	BDL	-
Mg24 (ppm)	2	472	11	728	3	-	BDL	516	-
Al27 (ppm)	119	3011	208	661	5	BDL	BDL	89	-
Si29 (ppm)	BDL	6080	BDL	3446	BDL	BDL	BDL	2080	-
P31 (ppm)	BDL	104	BDL	42	BDL	BDL	BDL	BDL	-
S32 (ppm)	378020	338896	363745	368820	357770	354426	400409	371307	-
K39 (ppm)	BDL	1406	76	BDL	BDL	BDL	BDL	BDL	-
Ca44 (ppm)	BDL	2788	BDL	BDL	BDL	BDL	BDL	2733	-
Sc45 (ppm)	BDL	10	BDL	BDL	BDL	BDL	BDL	BDL	-
Ti47 (ppm)	BDL	74	BDL	BDL	BDL	BDL	BDL	-	-
V51 (ppm)	BDL	28	1	3	BDL	BDL	BDL	BDL	-
Cr52 (ppm)	BDL	BDL	BDL	BDL	BDL	BDL	BDL	7	-
Mn55 (ppm)	BDL	59	BDL	26	BDL	BDL	BDL	175	-
Fe57 (ppm)	-	-	-	-	-	-	-	-	-
Co59 (ppm)	905	902	-	736	967	959	1015	2122	-
Ni60 (ppm)	-	-	1241	560	-	-	-	-	-
Cu63 (ppm)	3	19	3	15	BDL	BDL	2	11	-
Zn66 (ppm)	12	19	BDL	12	6	BDL	4	8	-
Ga71 (ppm)	BDL	-	-	-	-	-	-	-	-
Ge73 (ppm)	-	BDL	BDL	-	BDL	BDL	BDL	-	-
As75 (ppm)	BDL	BDL	BDL	BDL	BDL	BDL	6	3962	-
Se77 (ppm)	436	464	451	418	433	454	415	479	-
Rb85 (ppm)	BDL	2	BDL	BDL	BDL	BDL	BDL	-	-
Sr88 (ppm)	-	-	-	-	BDL	-	-	-	-
Y89 (ppm)	-	-	-	-	-	-	-	-	-
Zr90 (ppm)	-	BDL	-	-	-	-	-	-	-
Nb93 (ppm)	-	-	-	-	-	-	-	-	-
Mo95 (ppm)	BDL	BDL	BDL	BDL	-	-	BDL	BDL	-
Ru101 (ppm)	-	-	-	-	-	-	-	-	-
Rh103 (ppm)	-	-	-	-	-	-	BDL	-	-
Pd104 (ppm)	-	-	-	-	-	-	-	-	-

Pd105 (ppm)	-	-	-	-	BDL	-	-	-	-
Pd106 (ppm)	BDL	-	BDL	BDL	-	BDL	BDL	-	-
Ag107 (ppm)	-	-	1	2	1	0	0	6	-
Cd111 (ppm)	-	-	BDL	BDL	BDL	-	-	0	-
In115 (ppm)	-	-	-	-	-	-	-	-	-
Sn118 (ppm)	BDL	BDL	BDL	BDL	BDL	BDL	BDL	BDL	-
Sb121 (ppm)	BDL	BDL	BDL	BDL	BDL	BDL	BDL	2	-
Te125 (ppm)	BDL	BDL	BDL	BDL	-	1	-	6	-
Cs133 (ppm)	BDL	BDL	BDL	BDL	BDL	BDL	BDL	BDL	-
Ba137 (ppm)	-	-	-	-	-	-	-	-	-
La139 (ppm)	-	-	-	-	-	-	-	-	-
Ce140 (ppm)	-	-	-	-	-	-	-	-	-
Pr141 (ppm)	-	-	-	-	-	-	-	-	-
Nd146 (ppm)	-	-	-	-	-	-	-	-	-
Sm147 (ppm)	-	-	-	-	-	-	-	-	-
Eu153 (ppm)	-	-	-	-	-	-	-	-	-
Gd157 (ppm)	-	-	-	-	-	-	-	-	-
Tb159 (ppm)	-	BDL	-	-	-	BDL	-	-	-
Dy163 (ppm)	-	-	-	-	-	-	-	-	-
Ho165 (ppm)	-	-	-	-	-	-	-	-	-
Er166 (ppm)	-	-	-	-	-	-	-	-	-
Tm169 (ppm)	-	-	-	-	-	-	-	-	-
Yb172 (ppm)	-	-	-	-	-	-	-	-	-
Lu175 (ppm)	-	-	-	-	-	-	-	-	-
Hf178 (ppm)	-	-	-	BDL	-	-	-	-	-
Ta181 (ppm)	-	-	BDL	-	-	-	-	-	-
W182 (ppm)	-	-	BDL	BDL	BDL	-	-	-	-
Re185 (ppm)	BDL	BDL	BDL	BDL	BDL	BDL	BDL	BDL	-
Os189 (ppm)	BDL	BDL	BDL	BDL	BDL	BDL	BDL	BDL	-
Ir193 (ppm)	BDL	BDL	-	BDL	BDL	BDL	BDL	BDL	-
Pt195 (ppm)	BDL	BDL	-	BDL	-	BDL	BDL	-	-
Au197 (ppm)	-	-	-	-	-	-	-	-	-
Hg202 (ppm)	25	BDL	31	20	26	29	31	25	-
Pb204 (ppm)	110	150	93	97	93	97	124	99	-
Tl205 (ppm)	BDL	0	BDL	BDL	BDL	BDL	BDL	BDL	-
Pb206 (ppm)	-	80	-	-	3	1	1	-	-
Pb207 (ppm)	0	82	-	-	3	0	1	19	-
Pb208 (ppm)	0	91	1	4	3	1	1	21	-
Bi209 (ppm)	BDL	0	BDL	BDL	0	BDL	BDL	2	-
Th232 (ppm)	-	-	-	-	-	-	-	-	-
U238 (ppm)	-	-	-	-	-	-	-	-	-
PbTotal (ppm)	2	87	2	5	5	2	3	22	-

Table D3. Trace element data for pyrrhotite continued.

Deposit	Betts Cove	Betts Cove	Betts Cove	Tilt Cove	Tilt Cove	Tilt Cove	Tilt Cove	Tilt Cove	Tilt Cove
Sample	KKMSC35_Po8	KKMSC35_Po12	KKMSC53_Po2	KKMSC72_Po13	KKMSC72_Po12	KKMSC72_Po11	KKMSC72_Po6	KKMSC72_Po5	KKMSC72_Po1
Date	2023-11-21	2023-11-21	2023-11-22	2023-11-22	2023-11-22	2023-11-22	2023-11-22	2023-11-22	2023-11-22
Facies	Chalcopyrite-pyrrhotite-dominated	Chalcopyrite-pyrrhotite-dominated	Chalcopyrite-dominated	Pyrrhotite-dominated	Pyrrhotite-dominated	Pyrrhotite-dominated	Pyrrhotite-dominated	Pyrrhotite-dominated	Pyrrhotite-dominated
Li7 (ppm)	BDL	BDL	BDL	3	4	3	BDL	BDL	4
Be9 (ppm)	-	BDL	-	-	BDL	-	-	BDL	-
B11 (ppm)	BDL	BDL	BDL	BDL	BDL	BDL	BDL	BDL	BDL
Na23 (ppm)	BDL	BDL	212	BDL	49	BDL	BDL	BDL	BDL
Mg24 (ppm)	BDL	1	113	4353	-	222	1249	80	253
Al27 (ppm)	BDL	6	73	477	121	69	48	22	58
Si29 (ppm)	BDL	BDL	BDL	9038	BDL	BDL	3942	BDL	BDL
P31 (ppm)	BDL	BDL	BDL	BDL	120	BDL	BDL	BDL	BDL
S32 (ppm)	371863	375301	465704	354212	384043	355710	417948	389898	403344
K39 (ppm)	BDL	BDL	BDL	BDL	BDL	BDL	BDL	BDL	BDL
Ca44 (ppm)	BDL	BDL	BDL	BDL	BDL	BDL	BDL	BDL	BDL
Sc45 (ppm)	BDL	BDL	BDL	BDL	BDL	BDL	BDL	BDL	BDL
Ti47 (ppm)	BDL	BDL	BDL	BDL	BDL	BDL	BDL	BDL	BDL
V51 (ppm)	BDL	BDL	BDL	BDL	1	BDL	BDL	BDL	BDL
Cr52 (ppm)	BDL	BDL	BDL	BDL	BDL	BDL	BDL	BDL	BDL
Mn55 (ppm)	BDL	BDL	3	9	10	7	10	3	7
Fe57 (ppm)	-	-	-	-	-	-	-	-	-
Co59 (ppm)	722	690	313	283	379	296	231	-	311
Ni60 (ppm)	910	661	4843	17257	-	-	15871	17737	17830
Cu63 (ppm)	3	BDL	198429	19	10	8	5	2	16
Zn66 (ppm)	BDL	BDL	69	5	5	2	BDL	BDL	3
Ga71 (ppm)	-	-	-	-	BDL	-	-	-	-
Ge73 (ppm)	-	-	BDL	BDL	BDL	BDL	BDL	BDL	-
As75 (ppm)	BDL	BDL	BDL	BDL	BDL	BDL	BDL	BDL	BDL
Se77 (ppm)	467	386	1200	70	88	65	124	168	138
Rb85 (ppm)	BDL	BDL	BDL	BDL	BDL	BDL	BDL	BDL	BDL
Sr88 (ppm)	-	-	-	-	-	-	-	-	-
Y89 (ppm)	-	-	-	-	-	-	-	BDL	-
Zr90 (ppm)	-	-	-	-	-	-	-	-	-
Nb93 (ppm)	-	-	-	-	-	BDL	-	-	-
Mo95 (ppm)	BDL	-	-	-	-	BDL	BDL	-	-
Ru101 (ppm)	-	-	-	-	-	-	BDL	-	-
Rh103 (ppm)	-	BDL	3	-	-	-	-	-	-
Pd104 (ppm)	-	-	-	-	-	-	BDL	BDL	BDL

Pd105 (ppm)	-	-	10	-	BDL	BDL	-	BDL	-
Pd106 (ppm)	-	-	BDL	BDL	BDL	-	-	BDL	-
Ag107 (ppm)	1	1	37	3	1	5	6	1	-
Cd111 (ppm)	BDL	BDL	5	BDL	BDL	BDL	-	BDL	BDL
In115 (ppm)	-	-	-	BDL	-	BDL	BDL	BDL	-
Sn118 (ppm)	BDL	BDL	BDL	BDL	BDL	BDL	BDL	BDL	BDL
Sb121 (ppm)	BDL	BDL	BDL	1	0	1	4	BDL	1
Te125 (ppm)	BDL	-	BDL	4	-	BDL	-	1	-
Cs133 (ppm)	BDL	BDL	BDL	BDL	BDL	BDL	BDL	BDL	BDL
Ba137 (ppm)	-	-	-	-	-	-	-	-	-
La139 (ppm)	-	-	-	-	-	-	-	-	-
Ce140 (ppm)	-	-	-	-	-	-	-	-	-
Pr141 (ppm)	-	-	-	-	-	-	-	-	-
Nd146 (ppm)	-	-	-	-	-	-	-	-	-
Sm147 (ppm)	-	-	-	-	-	-	-	-	-
Eu153 (ppm)	-	-	-	BDL	-	-	-	-	-
Gd157 (ppm)	-	-	-	-	-	-	-	-	-
Tb159 (ppm)	-	-	-	-	-	-	-	-	-
Dy163 (ppm)	-	-	-	-	-	-	-	-	-
Ho165 (ppm)	-	-	-	-	-	-	-	-	-
Er166 (ppm)	-	-	-	-	-	-	-	-	-
Tm169 (ppm)	-	-	-	-	-	-	-	-	-
Yb172 (ppm)	-	-	-	-	-	-	-	-	-
Lu175 (ppm)	-	-	-	-	-	-	-	-	-
Hf178 (ppm)	-	-	-	BDL	-	BDL	-	-	-
Ta181 (ppm)	BDL	-	-	-	-	BDL	-	-	-
W182 (ppm)	-	-	BDL	-	-	BDL	-	-	-
Re185 (ppm)	BDL	BDL	BDL	BDL	BDL	BDL	BDL	BDL	BDL
Os189 (ppm)	BDL	BDL	BDL	BDL	BDL	BDL	BDL	BDL	BDL
Ir193 (ppm)	-	-	BDL	BDL	BDL	BDL	BDL	-	-
Pt195 (ppm)	-	BDL	BDL	BDL	BDL	BDL	-	-	BDL
Au197 (ppm)	BDL	-	-	BDL	-	-	BDL	-	BDL
Hg202 (ppm)	26	22	BDL	BDL	18	16	19	15	18
Pb204 (ppm)	109	97	221	130	87	83	185	81	93
Tl205 (ppm)	BDL	BDL	11	BDL	BDL	BDL	BDL	BDL	BDL
Pb206 (ppm)	-	-	149	28	4	36	68	4	-
Pb207 (ppm)	-	1	163	30	7	36	67	5	38
Pb208 (ppm)	0	1	156	29	4	38	69	5	36
Bi209 (ppm)	BDL	0	0	2	0	1	1	0	1
Th232 (ppm)	-	-	-	-	-	-	-	-	-
U238 (ppm)	-	-	-	-	-	-	-	-	-
PbTotal (ppm)	2	3	157	30	6	38	69	6	37

Table D3. Trace element data for pyrrhotite continued.

Deposit	Tilt Cove	Tilt Cove	Tilt Cove	Tilt Cove	Tilt Cove	Tilt Cove	Tilt Cove	Tilt Cove	Tilt Cove
Sample	KKMSC72_Po7	KKMSC72_Po4	KKMSC72_Po3	KKMSC72_Po2	KKMSC72_Po10	KKMSC72_Po9	KKMSC72_Po8	KKMSC72_Po15	KKMSC72_Po14
Date	2023-11-22	2023-11-22	2023-11-22	2023-11-22	2023-11-22	2023-11-22	2023-11-22	2023-11-22	2023-11-22
Facies	Pyrrhotite-dominated	Pyrrhotite-dominated	Pyrrhotite-dominated	Pyrrhotite-dominated	Pyrrhotite-dominated	Pyrrhotite-dominated	Pyrrhotite-dominated	Pyrrhotite-dominated	Pyrrhotite-dominated
Li7 (ppm)	2	5	BDL	BDL	4	BDL	4	1	BDL
Be9 (ppm)	-	-	-	-	-	-	-	-	-
B11 (ppm)	BDL	BDL	BDL	BDL	BDL	BDL	BDL	BDL	19
Na23 (ppm)	BDL	BDL	BDL	BDL	BDL	BDL	BDL	BDL	BDL
Mg24 (ppm)	511	702	384	1996	166	1709	13854	10	-
Al27 (ppm)	74	158	4	8	17	11	81	7	32
Si29 (ppm)	BDL	BDL	BDL	BDL	BDL	2819	BDL	BDL	BDL
P31 (ppm)	BDL	BDL	BDL	88	BDL	BDL	BDL	BDL	BDL
S32 (ppm)	421664	399211	440506	355971	390983	362344	386625	339428	428286
K39 (ppm)	BDL	BDL	BDL	BDL	BDL	BDL	BDL	BDL	BDL
Ca44 (ppm)	BDL	BDL	BDL	BDL	275	BDL	BDL	BDL	BDL
Sc45 (ppm)	BDL	BDL	BDL	BDL	BDL	BDL	BDL	BDL	BDL
Ti47 (ppm)	9	BDL	BDL	-	BDL	-	BDL	BDL	BDL
V51 (ppm)	BDL	1	BDL	BDL	1	BDL	1	BDL	BDL
Cr52 (ppm)	BDL	9	BDL	BDL	BDL	28	BDL	BDL	BDL
Mn55 (ppm)	24	22	2	241	12	258	1463	BDL	4
Fe57 (ppm)	-	-	-	-	-	-	-	-	-
Co59 (ppm)	2962	514	206	243	309	260	655	265	-
Ni60 (ppm)	21027	17993	15756	-	16936	-	17339	-	17504
Cu63 (ppm)	111	86	40	3	17	3	160	65	56
Zn66 (ppm)	4	4	BDL	2	2	7	10	6	1143
Ga71 (ppm)	-	-	-	-	-	BDL	BDL	-	-
Ge73 (ppm)	BDL	BDL	-	BDL	BDL	-	-	BDL	-
As75 (ppm)	BDL	BDL	BDL	BDL	BDL	BDL	BDL	BDL	BDL
Se77 (ppm)	159	81	112	76	80	180	106	69	72
Rb85 (ppm)	-	BDL	BDL	BDL	BDL	BDL	-	BDL	BDL
Sr88 (ppm)	-	-	-	-	-	-	-	-	-
Y89 (ppm)	-	-	-	-	-	-	-	BDL	-
Zr90 (ppm)	-	-	-	-	-	BDL	-	-	-
Nb93 (ppm)	-	-	-	-	-	-	-	-	-
Mo95 (ppm)	-	0	-	BDL	BDL	BDL	BDL	BDL	BDL
Ru101 (ppm)	-	-	BDL	-	-	-	-	BDL	-
Rh103 (ppm)	-	-	BDL	BDL	-	-	-	-	-
Pd104 (ppm)	BDL	BDL	-	BDL	-	-	BDL	-	-

Pd105 (ppm)	-	-	-	-	-	-	BDL	-	BDL
Pd106 (ppm)	BDL	BDL	-	-	BDL	-	-	-	BDL
Ag107 (ppm)	-	3	-	1	-	1	5	2	-
Cd111 (ppm)	BDL	BDL	-	-	-	-	-	BDL	-
In115 (ppm)	-	BDL	BDL	-	-	-	-	-	-
Sn118 (ppm)	BDL	BDL	BDL	1	BDL	BDL	BDL	BDL	BDL
Sb121 (ppm)	4	1	BDL	BDL	2	BDL	2	BDL	3
Te125 (ppm)	3	BDL	1	BDL	1	2	2	BDL	-
Cs133 (ppm)	BDL	BDL	BDL	BDL	BDL	BDL	BDL	BDL	BDL
Ba137 (ppm)	-	-	-	-	-	-	-	-	-
La139 (ppm)	-	-	-	-	-	-	-	-	-
Ce140 (ppm)	-	-	-	-	-	-	-	-	-
Pr141 (ppm)	-	-	-	-	-	-	-	-	-
Nd146 (ppm)	-	-	-	-	-	-	-	-	-
Sm147 (ppm)	-	-	-	-	-	-	-	-	-
Eu153 (ppm)	-	-	-	-	-	-	-	-	-
Gd157 (ppm)	-	-	-	-	-	-	-	-	-
Tb159 (ppm)	-	-	-	-	-	-	-	-	-
Dy163 (ppm)	-	-	-	-	-	-	-	-	-
Ho165 (ppm)	-	-	-	-	-	-	-	-	-
Er166 (ppm)	-	-	BDL	-	-	-	-	-	-
Tm169 (ppm)	-	-	-	-	-	-	-	-	-
Yb172 (ppm)	-	-	-	-	-	-	-	-	-
Lu175 (ppm)	-	-	-	-	-	-	-	-	-
Hf178 (ppm)	-	-	-	-	-	-	-	-	-
Ta181 (ppm)	BDL	-	-	-	-	-	-	-	-
W182 (ppm)	-	-	-	-	BDL	BDL	-	BDL	-
Re185 (ppm)	BDL	BDL	BDL	BDL	BDL	BDL	BDL	BDL	BDL
Os189 (ppm)	BDL	BDL	BDL	BDL	BDL	BDL	BDL	BDL	BDL
Ir193 (ppm)	-	BDL	BDL	-	BDL	BDL	-	-	-
Pt195 (ppm)	BDL	BDL	BDL	BDL	BDL	BDL	-	BDL	BDL
Au197 (ppm)	BDL	-	-	-	-	BDL	-	-	-
Hg202 (ppm)	19	16	25	22	22	19	15	26	21
Pb204 (ppm)	162	108	90	94	109	81	105	86	168
Tl205 (ppm)	2	BDL	BDL	BDL	BDL	BDL	0	BDL	BDL
Pb206 (ppm)	52	33	3	-	-	8	38	8	71
Pb207 (ppm)	41	29	-	12	13	8	-	7	68
Pb208 (ppm)	56	31	3	11	13	-	35	8	72
Bi209 (ppm)	2	2	0	1	1	0	1	BDL	2
Th232 (ppm)	-	-	-	-	-	-	-	-	-
U238 (ppm)	-	-	-	-	-	BDL	-	-	-
PbTotal (ppm)	53	32	4	13	15	10	37	9	72

Table D3. Trace element data for pyrrhotite continued.

Deposit	Betts Cove	Betts Cove	Betts Cove	Betts Cove	Betts Cove	Betts Cove	Tilt Cove	Tilt Cove	Tilt Cove
Sample	KKMSC42_Po3	KKMSC42_Po2	KKMSC42_Po1	KKMSC42_Po5	KKMSC42_Po6	KKMSC42_Po4	KKMSC70_Po5	KKMSC70_Po4	KKMSC70_Po1
Date	2023-11-22	2023-11-22	2023-11-22	2023-11-22	2023-11-22	2023-11-22	2023-11-22	2023-11-22	2023-11-22
Facies	Chalcopyrite-pyrrhotite-dominated	Chalcopyrite-pyrrhotite-dominated	Chalcopyrite-pyrrhotite-dominated	Chalcopyrite-pyrrhotite-dominated	Chalcopyrite-pyrrhotite-dominated	Chalcopyrite-pyrrhotite-dominated	Chalcopyrite-pyrrhotite-dominated	Chalcopyrite-pyrrhotite-dominated	Chalcopyrite-pyrrhotite-dominated
Li7 (ppm)	BDL	BDL	5	24	BDL	6	BDL	BDL	BDL
Be9 (ppm)	BDL	-	-	-	-	-	-	-	-
B11 (ppm)	BDL	BDL	BDL	BDL	BDL	BDL	BDL	BDL	BDL
Na23 (ppm)	222	BDL	BDL	178	BDL	442	BDL	BDL	BDL
Mg24 (ppm)	BDL	BDL	564	613	52	BDL	4510	541	71
Al27 (ppm)	BDL	BDL	516	448	30	65	84	54	10
Si29 (ppm)	BDL	BDL	6308	20035	BDL	20147	8232	BDL	BDL
P31 (ppm)	BDL	BDL	BDL	BDL	BDL	138	BDL	BDL	BDL
S32 (ppm)	410089	375780	499759	970687	318054	360579	489755	449858	436277
K39 (ppm)	104	58	BDL	BDL	BDL	BDL	BDL	BDL	BDL
Ca44 (ppm)	BDL	BDL	1076	BDL	BDL	BDL	BDL	BDL	BDL
Sc45 (ppm)	BDL	BDL	BDL	BDL	BDL	12	BDL	BDL	BDL
Ti47 (ppm)	4	BDL	-	-	BDL	BDL	-	BDL	-
V51 (ppm)	BDL	BDL	2	BDL	BDL	BDL	BDL	BDL	BDL
Cr52 (ppm)	BDL	BDL	BDL	14	BDL	BDL	17	BDL	BDL
Mn55 (ppm)	BDL	BDL	18	25	BDL	7	2	BDL	BDL
Fe57 (ppm)	-	-	-	-	-	-	-	-	-
Co59 (ppm)	1343	-	1090	1809	1117	-	228	227	134
Ni60 (ppm)	-	-	1103	4227	1601	844	17712	18121	17098
Cu63 (ppm)	272	107	65	557	360	591	35	12	BDL
Zn66 (ppm)	BDL	19	13	27	15	962	5	2	BDL
Ga71 (ppm)	-	-	-	-	BDL	-	BDL	-	-
Ge73 (ppm)	-	BDL	-	-	BDL	-	BDL	BDL	BDL
As75 (ppm)	28	17	29	BDL	28	BDL	BDL	BDL	12
Se77 (ppm)	875	1020	774	790	13282	1493	127	138	137
Rb85 (ppm)	BDL	BDL	BDL	BDL	BDL	BDL	BDL	BDL	BDL
Sr88 (ppm)	-	-	-	-	-	-	-	-	-
Y89 (ppm)	-	-	-	-	-	-	-	-	-
Zr90 (ppm)	-	-	-	-	-	-	-	-	-
Nb93 (ppm)	-	-	-	-	-	-	-	-	-
Mo95 (ppm)	13	BDL	-	BDL	418	67	BDL	BDL	-
Ru101 (ppm)	-	-	-	-	-	-	-	-	-
Rh103 (ppm)	BDL	-	-	-	-	-	-	-	-
Pd104 (ppm)	-	-	-	-	-	-	-	-	-
Pd105 (ppm)	-	-	-	BDL	-	-	-	-	-

Pd106 (ppm)	BDL	-	BDL	-	BDL	-	-	-	BDL
Ag107 (ppm)	-	-	0	BDL	168	2	BDL	-	0
Cd111 (ppm)	-	-	-	-	-	2	-	-	-
In115 (ppm)	-	BDL	BDL	-	BDL	-	BDL	-	-
Sn118 (ppm)	BDL	1	BDL	BDL	2	3	BDL	BDL	1
Sb121 (ppm)	BDL	BDL	BDL	BDL	1	2	BDL	1	BDL
Te125 (ppm)	BDL	3	BDL	15	4536	23	-	2	BDL
Cs133 (ppm)	BDL	BDL	BDL	4	BDL	BDL	BDL	BDL	BDL
Ba137 (ppm)	-	-	-	-	-	-	-	-	-
La139 (ppm)	-	-	-	-	-	-	-	-	-
Ce140 (ppm)	-	-	-	-	-	-	-	-	-
Pr141 (ppm)	-	BDL	-	-	-	-	-	-	-
Nd146 (ppm)	-	-	-	-	-	-	-	-	-
Sm147 (ppm)	-	-	-	-	-	-	-	-	-
Eu153 (ppm)	-	-	-	-	-	-	-	-	-
Gd157 (ppm)	BDL	-	-	-	-	-	-	-	-
Tb159 (ppm)	-	-	-	-	-	-	-	-	-
Dy163 (ppm)	-	-	-	-	-	-	-	-	-
Ho165 (ppm)	-	-	-	-	-	-	-	-	-
Er166 (ppm)	-	-	-	-	-	-	-	-	-
Tm169 (ppm)	-	BDL	-	-	-	-	-	-	-
Yb172 (ppm)	-	-	-	-	-	-	-	-	-
Lu175 (ppm)	-	-	-	-	-	-	-	-	-
Hf178 (ppm)	-	-	-	-	-	-	-	-	-
Ta181 (ppm)	BDL	-	-	-	-	-	-	-	-
W182 (ppm)	BDL	-	BDL	-	BDL	-	BDL	-	-
Re185 (ppm)	BDL	BDL	BDL	2	45	1	BDL	BDL	BDL
Os189 (ppm)	BDL	1	BDL	BDL	BDL	6	-	BDL	BDL
Ir193 (ppm)	-	-	BDL	BDL	BDL	-	-	BDL	-
Pt195 (ppm)	-	-	BDL	BDL	-	-	BDL	-	BDL
Au197 (ppm)	-	-	-	-	BDL	BDL	BDL	-	-
Hg202 (ppm)	24	28	55	BDL	140	BDL	BDL	22	19
Pb204 (ppm)	114	135	131	BDL	101842	12712	147	105	86
Tl205 (ppm)	BDL	0	BDL	2	5	1	BDL	BDL	BDL
Pb206 (ppm)	-	72	7	294	134432	18763	4	24	3
Pb207 (ppm)	6	74	8	298	119326	-	4	23	-
Pb208 (ppm)	7	54	8	276	142686	26398	4	25	3
Bi209 (ppm)	-	0	0	31	6925	174	0	1	0
Th232 (ppm)	-	-	-	-	-	-	-	-	-
U238 (ppm)	-	-	-	-	-	-	-	-	-
PbTotal (ppm)	8	64	10	276	134927	23497	6	25	4

Table D3. Trace element data for pyrrhotite continued.

Deposit	Tilt Cove	Tilt Cove	Tilt Cove	Tilt Cove	Tilt Cove	Tilt Cove	Tilt Cove	Tilt Cove	Tilt Cove
Sample	KKMSC70_Po2	KKMSC70_Po15	KKMSC70_Po14	KKMSC70_Po3	KKMSC70_Po6	KKMSC70_Po7	KKMSC70_Po8	KKMSC70_Po10	KKMSC70_Po9
Date	2023-11-22	2023-11-22	2023-11-22	2023-11-22	2023-11-22	2023-11-22	2023-11-22	2023-11-22	2023-11-22
Facies	Chalcopyrite-pyrrhotite-dominated	Chalcopyrite-pyrrhotite-dominated	Chalcopyrite-pyrrhotite-dominated	Chalcopyrite-pyrrhotite-dominated	Chalcopyrite-pyrrhotite-dominated	Chalcopyrite-pyrrhotite-dominated	Chalcopyrite-pyrrhotite-dominated	Chalcopyrite-pyrrhotite-dominated	Chalcopyrite-pyrrhotite-dominated
Li7 (ppm)	BDL	BDL	BDL	BDL	BDL	BDL	BDL	3	2
Be9 (ppm)	-	-	-	BDL	-	-	-	-	-
B11 (ppm)	BDL	BDL	BDL	BDL	BDL	BDL	BDL	BDL	BDL
Na23 (ppm)	BDL	BDL	BDL	BDL	BDL	BDL	BDL	BDL	BDL
Mg24 (ppm)	42	484	189	670	180	2794	-	2605	442
Al27 (ppm)	5	BDL	BDL	29	30	94	328	299	50
Si29 (ppm)	BDL	BDL	BDL	BDL	BDL	BDL	13405	BDL	4957
P31 (ppm)	BDL	BDL	BDL	BDL	BDL	BDL	BDL	BDL	BDL
S32 (ppm)	447136	434177	391986	438389	449609	448179	915978	562867	472362
K39 (ppm)	BDL	BDL	BDL	BDL	BDL	BDL	BDL	BDL	BDL
Ca44 (ppm)	BDL	BDL	BDL	BDL	BDL	BDL	BDL	803	BDL
Sc45 (ppm)	BDL	BDL	BDL	BDL	BDL	BDL	BDL	BDL	BDL
Ti47 (ppm)	BDL	BDL	BDL	-	-	-	BDL	BDL	BDL
V51 (ppm)	BDL	BDL	BDL	BDL	1	BDL	BDL	1	BDL
Cr52 (ppm)	BDL	BDL	BDL	10	BDL	BDL	BDL	8	14
Mn55 (ppm)	3	15	5	BDL	BDL	BDL	11	28	7
Fe57 (ppm)	-	-	-	-	-	-	-	-	-
Co59 (ppm)	144	958	-	209	256	2083	431371	1150	180
Ni60 (ppm)	17880	35061	-	-	18518	17443	40488	49257	18243
Cu63 (ppm)	6	BDL	459	13	4	15	7855	51	16
Zn66 (ppm)	BDL	BDL	3	BDL	BDL	3	BDL	3	3
Ga71 (ppm)	-	-	-	-	-	BDL	BDL	-	BDL
Ge73 (ppm)	BDL	BDL	BDL	-	BDL	BDL	-	-	BDL
As75 (ppm)	7	BDL	13	35	35	6561	949362	58	30
Se77 (ppm)	165	128	193	130	140	152	588	173	164
Rb85 (ppm)	BDL	BDL	BDL	-	BDL	BDL	BDL	BDL	BDL
Sr88 (ppm)	-	-	-	-	-	-	-	-	-
Y89 (ppm)	-	-	-	-	-	-	-	-	-
Zr90 (ppm)	-	-	-	-	BDL	-	-	-	-
Nb93 (ppm)	-	-	-	-	-	-	-	-	-
Mo95 (ppm)	BDL	BDL	BDL	BDL	BDL	BDL	BDL	-	-
Ru101 (ppm)	-	BDL	-	-	-	-	BDL	-	-
Rh103 (ppm)	-	-	-	-	-	-	BDL	-	-
Pd104 (ppm)	-	-	-	-	-	-	BDL	BDL	-

Pd105 (ppm)	-	-	-	BDL	BDL	-	BDL	BDL	BDL
Pd106 (ppm)	-	BDL	-	-	BDL	-	-	-	-
Ag107 (ppm)	BDL	2	6	2	0	2	31	-	2
Cd111 (ppm)	1	BDL	BDL	BDL	-	-	BDL	BDL	-
In115 (ppm)	BDL	-	-	BDL	BDL	BDL	-	-	-
Sn118 (ppm)	BDL	BDL	BDL	BDL	BDL	BDL	BDL	BDL	1
Sb121 (ppm)	BDL	2	1	BDL	0	3	200	2	1
Te125 (ppm)	BDL	-	-	BDL	-	5	312	BDL	1
Cs133 (ppm)	BDL	BDL	BDL	BDL	BDL	BDL	BDL	BDL	BDL
Ba137 (ppm)	-	-	-	-	-	-	-	-	-
La139 (ppm)	-	-	-	-	-	-	-	-	-
Ce140 (ppm)	-	-	-	-	-	-	-	-	-
Pr141 (ppm)	-	-	-	-	-	-	-	-	-
Nd146 (ppm)	-	-	-	-	-	-	-	-	-
Sm147 (ppm)	-	-	-	-	-	-	-	-	-
Eu153 (ppm)	-	-	-	-	-	-	-	-	-
Gd157 (ppm)	-	-	-	-	-	-	-	-	-
Tb159 (ppm)	-	BDL	-	-	-	-	-	-	-
Dy163 (ppm)	-	-	-	-	-	-	-	-	-
Ho165 (ppm)	-	-	-	-	-	-	-	-	-
Er166 (ppm)	-	-	-	-	-	-	-	-	-
Tm169 (ppm)	-	-	-	-	-	-	-	-	-
Yb172 (ppm)	-	-	-	-	-	-	-	-	-
Lu175 (ppm)	-	-	-	-	-	-	-	-	-
Hf178 (ppm)	-	-	-	-	-	-	-	-	-
Ta181 (ppm)	-	-	-	-	BDL	-	-	-	-
W182 (ppm)	-	BDL	-	-	-	-	-	-	-
Re185 (ppm)	BDL	BDL	BDL	BDL	BDL	BDL	BDL	BDL	BDL
Os189 (ppm)	BDL	BDL	BDL	BDL	BDL	BDL	BDL	BDL	BDL
Ir193 (ppm)	-	-	-	-	-	-	-	-	BDL
Pt195 (ppm)	BDL	BDL	-	BDL	BDL	-	BDL	-	BDL
Au197 (ppm)	BDL	-	-	-	-	BDL	-	-	-
Hg202 (ppm)	BDL	25	19	25	21	21	BDL	35	25
Pb204 (ppm)	119	182	129	157	97	BDL	267	243	123
Tl205 (ppm)	BDL	1	BDL	BDL	BDL	0	3	3	0
Pb206 (ppm)	-	34	55	-	4	-	-	50	15
Pb207 (ppm)	3	-	62	8	-	-	-	49	-
Pb208 (ppm)	4	34	64	7	5	30	179	50	16
Bi209 (ppm)	0	1	4	1	1	5	115	2	1
Th232 (ppm)	-	-	-	-	-	-	-	-	-
U238 (ppm)	-	-	-	BDL	-	-	BDL	-	-
PbTotal (ppm)	5	35	62	10	6	33	186	53	17

Table D3. Trace element data for pyrrhotite continued.

Deposit	Tilt Cove	Tilt Cove	Tilt Cove	Tilt Cove	Tilt Cove
Sample	KKMSC70_Po1 1	KKMSC70_Po1 2	KKMSC13_Po1	KKMSC13_Po2	KKMSC13_Po3
Date	2023-11-22	2023-11-22	2023-11-23	2023-11-23	2023-11-23
Facies	Chalcopyrite-pyrrhotite-dominated	Chalcopyrite-pyrrhotite-dominated	Pyrite-dominated	Pyrite-dominated	Pyrite-dominated
Li7 (ppm)	BDL	BDL	6	4	2
Be9 (ppm)	-	-	-	-	-
B11 (ppm)	BDL	BDL	BDL	BDL	BDL
Na23 (ppm)	BDL	BDL	BDL	BDL	BDL
Mg24 (ppm)	229	18254	139	125	473
Al27 (ppm)	36	77	56	102	58
Si29 (ppm)	BDL	20403	1971	BDL	1229
P31 (ppm)	BDL	BDL	BDL	BDL	BDL
S32 (ppm)	537138	571867	582376	393127	554500
K39 (ppm)	BDL	BDL	BDL	BDL	BDL
Ca44 (ppm)	BDL	BDL	BDL	BDL	BDL
Sc45 (ppm)	BDL	BDL	BDL	BDL	BDL
Ti47 (ppm)	-	BDL	24	BDL	-
V51 (ppm)	BDL	BDL	1	BDL	BDL
Cr52 (ppm)	BDL	BDL	BDL	BDL	BDL
Mn55 (ppm)	3	15	2	6	202
Fe57 (ppm)	-	-	-	-	-
Co59 (ppm)	263	5275	64	BDL	0
Ni60 (ppm)	17794	-	-	21	-
Cu63 (ppm)	11	43	22	BDL	10
Zn66 (ppm)	BDL	53	9	19	234
Ga71 (ppm)	-	-	-	-	-
Ge73 (ppm)	-	BDL	BDL	-	-
As75 (ppm)	25	BDL	175	BDL	235
Se77 (ppm)	152	155	13	BDL	3
Rb85 (ppm)	BDL	-	BDL	-	BDL
Sr88 (ppm)	-	2	-	-	-
Y89 (ppm)	-	-	-	-	-
Zr90 (ppm)	-	-	-	-	-
Nb93 (ppm)	-	-	-	BDL	1
Mo95 (ppm)	BDL	15	-	-	-
Ru101 (ppm)	-	-	BDL	-	-
Rh103 (ppm)	BDL	-	-	-	-
Pd104 (ppm)	-	-	BDL	-	BDL

Pd105 (ppm)	BDL	-	BDL	BDL	-
Pd106 (ppm)	-	-	9	2	3
Ag107 (ppm)	1	4	BDL	-	1
Cd111 (ppm)	BDL	-	-	-	BDL
In115 (ppm)	-	-	BDL	BDL	BDL
Sn118 (ppm)	BDL	BDL	0	1	-
Sb121 (ppm)	0	7	BDL	1	-
Te125 (ppm)	BDL	BDL	BDL	BDL	BDL
Cs133 (ppm)	BDL	BDL	-	-	-
Ba137 (ppm)	-	-	-	-	-
La139 (ppm)	-	-	-	-	-
Ce140 (ppm)	-	-	-	-	-
Pr141 (ppm)	-	-	-	-	-
Nd146 (ppm)	-	-	-	-	-
Sm147 (ppm)	-	-	-	-	-
Eu153 (ppm)	-	-	-	-	-
Gd157 (ppm)	-	-	-	-	-
Tb159 (ppm)	-	-	-	-	-
Dy163 (ppm)	-	-	-	-	-
Ho165 (ppm)	-	-	-	-	-
Er166 (ppm)	-	-	-	-	-
Tm169 (ppm)	-	-	-	-	-
Yb172 (ppm)	-	-	-	-	-
Lu175 (ppm)	-	-	-	-	-
Hf178 (ppm)	-	-	-	-	-
Ta181 (ppm)	-	BDL	BDL	BDL	-
W182 (ppm)	BDL	-	BDL	BDL	BDL
Re185 (ppm)	BDL	BDL	BDL	BDL	BDL
Os189 (ppm)	BDL	BDL	BDL	-	-
Ir193 (ppm)	-	BDL	BDL	BDL	-
Pt195 (ppm)	BDL	BDL	BDL	-	-
Au197 (ppm)	-	-	126	36	20
Hg202 (ppm)	35	BDL	157	119	47
Pb204 (ppm)	164	108	BDL	BDL	BDL
Tl205 (ppm)	BDL	12	10	6	24
Pb206 (ppm)	13	71	11	5	23
Pb207 (ppm)	13	-	11	5	25
Pb208 (ppm)	14	70	0	BDL	0
Bi209 (ppm)	1	2	-	-	-
Th232 (ppm)	-	-	-	-	-
U238 (ppm)	BDL	-	14	6	25
PbTotal (ppm)	16	68	-	-	-

Table D4. Trace element data for sphalerite.

Deposit	Betts Cove	Betts Cove	Betts Cove	Betts Cove	Betts Cove	Betts Cove	Betts Cove	Betts Cove	Betts Cove
Sample	KKMSC05B_Sp1	KKMSC05B_Sp2	KKMSC09_Sp1	KKMSC10_Sp1	KKMSC10_Sp2	KKMSC10_Sp3	KKMSC10_Sp4	KKMSC10_Sp5	KKMSC10_Sp6
Date	2023-11-20	2023-11-20	2023-11-20	2023-11-20	2023-11-20	2023-11-20	2023-11-20	2023-11-20	2023-11-20
Facies	Chalcopyrite-dominated	Chalcopyrite-dominated	Chalcopyrite-dominated	Pyrite-dominated	Pyrite-dominated	Pyrite-dominated	Pyrite-dominated	Pyrite-dominated	Pyrite-dominated
Li7 (ppm)	BDL	BDL	BDL	BDL	BDL	BDL	BDL	BDL	BDL
Be9 (ppm)	BDL	BDL	BDL	-	-	-	BDL	-	BDL
B11 (ppm)	BDL	BDL	BDL	BDL	BDL	BDL	BDL	BDL	BDL
Na23 (ppm)	94	BDL	BDL	BDL	BDL	BDL	BDL	BDL	BDL
Mg24 (ppm)	1217	1039	BDL	BDL	296	54	190	14	6
Al27 (ppm)	1363	1080	BDL	BDL	340	52	702	43	4
Si29 (ppm)	2000	1811	BDL	BDL	848	BDL	1282	1224	1001
P31 (ppm)	BDL	BDL	BDL	BDL	34	BDL	31	61	28
S32 (ppm)	675686	361302	275319	304225	524980	350521	430995	1781287	1182848
K39 (ppm)	BDL	BDL	BDL	BDL	BDL	BDL	BDL	BDL	BDL
Ca44 (ppm)	BDL	BDL	BDL	BDL	BDL	BDL	443	BDL	BDL
Sc45 (ppm)	BDL	BDL	BDL	BDL	BDL	BDL	1	BDL	BDL
Ti47 (ppm)	3	BDL	BDL	BDL	BDL	BDL	4	3	3
V51 (ppm)	5	4	BDL	BDL	3	1	12	1	BDL
Cr52 (ppm)	BDL	4	BDL	BDL	BDL	BDL	BDL	9	BDL
Mn55 (ppm)	807	850	684	692	775	716	703	734	918
Fe57 (ppm)	217928	94837	47463	25559	182426	53020	112146	758295	519615
Co59 (ppm)	8	1	613	3	238	-	222	-	390
Ni60 (ppm)	3	1	1	BDL	6	-	-	26	38
Cu63 (ppm)	270248	44759	573	177	12569	7781	3651	1502	486
Zn66 (ppm)	-	-	-	-	-	-	-	-	-
Ga71 (ppm)	-	-	-	-	-	-	1	-	BDL
Ge73 (ppm)	BDL	BDL	BDL	-	-	BDL	-	-	-
As75 (ppm)	BDL	BDL	BDL	BDL	117	7	40	125	185
Se77 (ppm)	1010	620	335	53	170	113	115	368	151
Rb85 (ppm)	BDL	BDL	BDL	-	BDL	BDL	BDL	BDL	BDL
Sr88 (ppm)	-	0	BDL	-	-	-	-	-	BDL
Y89 (ppm)	-	BDL	-	-	-	-	-	-	-
Zr90 (ppm)	BDL	-	-	2	-	-	1	2	6
Nb93 (ppm)	BDL	-	-	-	-	-	-	-	-
Mo95 (ppm)	-	BDL	-	-	-	-	-	-	-
Ru101 (ppm)	-	-	-	-	-	-	68	-	-
Rh103 (ppm)	1	0	BDL	-	0	0	-	BDL	BDL
Pd104 (ppm)	34	31	-	76	-	89	-	-	-

Pd105 (ppm)	7	1	BDL	8	27	10	16	32	9
Pd106 (ppm)	98	76	-	1428	-	-	-	-	1742
Ag107 (ppm)	52	17	8	23	-	-	-	-	15
Cd111 (ppm)	2380	-	-	BDL	1	1	1	BDL	0
In115 (ppm)	-	62	-	0	5	2	2	14	1
Sn118 (ppm)	11	2	BDL	1	23	4	3	-	4
Sb121 (ppm)	4	2	BDL	BDL	BDL	BDL	BDL	BDL	BDL
Te125 (ppm)	3	BDL	1	-	-	-	-	-	-
Cs133 (ppm)	BDL	BDL	BDL	-	-	-	-	-	-
Ba137 (ppm)	-	-	-	-	-	-	-	-	-
La139 (ppm)	-	-	-	-	-	-	-	-	-
Ce140 (ppm)	-	-	BDL	-	-	-	-	-	-
Pr141 (ppm)	-	-	BDL	-	-	-	-	-	-
Nd146 (ppm)	BDL	-	-	-	-	-	-	-	-
Sm147 (ppm)	-	-	-	-	-	-	BDL	-	-
Eu153 (ppm)	BDL	-	-	-	-	-	-	-	-
Gd157 (ppm)	-	-	-	-	-	-	-	-	-
Tb159 (ppm)	-	-	-	-	-	-	-	-	-
Dy163 (ppm)	-	-	-	-	-	-	-	-	-
Ho165 (ppm)	-	BDL	-	-	-	-	-	-	-
Er166 (ppm)	-	-	-	-	-	-	-	-	-
Tm169 (ppm)	-	-	-	-	-	BDL	-	-	-
Yb172 (ppm)	-	BDL	-	-	-	-	-	-	-
Lu175 (ppm)	-	-	-	-	-	-	-	-	-
Hf178 (ppm)	-	-	-	BDL	-	-	-	-	-
Ta181 (ppm)	BDL	-	-	BDL	1	2	BDL	1	0
W182 (ppm)	-	-	-	BDL	BDL	BDL	BDL	BDL	BDL
Re185 (ppm)	BDL	BDL	BDL	BDL	-	-	-	BDL	-
Os189 (ppm)	BDL	BDL	BDL	BDL	BDL	BDL	BDL	0	BDL
Ir193 (ppm)	BDL	-	-	-	-	-	0	-	-
Pt195 (ppm)	-	-	-	2531	369	1404	1150	620	1188
Au197 (ppm)	BDL	-	-	3311	624	1851	1518	2427	1445
Hg202 (ppm)	1464	1703	728	BDL	0	0	BDL	0	BDL
Pb204 (ppm)	8162	9551	2400	17	160	-	-	-	36
Tl205 (ppm)	0	BDL	0	17	-	51	-	-	36
Pb206 (ppm)	46	19	81	17	155	52	39	1777	32
Pb207 (ppm)	39	18	77	0	10	5	3	42	4
Pb208 (ppm)	46	17	-	-	-	-	-	-	-
Bi209 (ppm)	3	1	-	-	-	-	-	-	-
Th232 (ppm)	-	BDL	-	73	164	81	62	1805	55
U238 (ppm)	BDL	-	-	-	-	-	-	-	-
PbTotal (ppm)	168	162	113	-	-	-	-	-	-

Table D4. Trace element data for sphalerite continued.

Deposit	Betts Cove	Betts Cove	Tilt Cove	Tilt Cove	Tilt Cove	Tilt Cove	Tilt Cove	Betts Cove	Betts Cove
Sample	KKMSC10_Sp8	KKMSC10_Sp7	KKMSC63_Sp1	KKMSC63_Sp1	KKMSC63_Sp2	KKMSC63_Sp3	KKMSC63_Sp4	KKMSC32_Sp3 1	KKMSC32_Sp3 2
Date	2023-11-20	2023-11-20	2023-11-21	2023-11-21	2023-11-21	2023-11-21	2023-11-21	2023-11-21	2023-11-21
Facies	Pyrite-dominated	Pyrite-dominated	Pyrite-dominated	Pyrite-dominated	Pyrite-dominated	Pyrite-dominated	Pyrite-dominated	Sphalerite-pyrite-dominated	Sphalerite-pyrite-dominated
Li7 (ppm)	BDL	BDL	16	6	BDL	BDL	BDL	66	49
Be9 (ppm)	-	BDL	BDL	-	BDL	-	-	-	-
B11 (ppm)	39	BDL	BDL	30	BDL	BDL	BDL	106	229
Na23 (ppm)	BDL	BDL	BDL	43	BDL	BDL	BDL	342860	421202
Mg24 (ppm)	BDL	5	2317	1409	314	8	70	91540	112098
Al27 (ppm)	4	2	576	333	17	3	22	33642	40562
Si29 (ppm)	18269	BDL	BDL	6816	886	BDL	BDL	1251258	1644373
P31 (ppm)	193	BDL	BDL	138	BDL	BDL	BDL	323	510
S32 (ppm)	8108165	392806	337967	169579	192484	182550	175308	1477749	1666947
K39 (ppm)	BDL	BDL	BDL	BDL	BDL	BDL	BDL	12370	14464
Ca44 (ppm)	BDL	BDL	634	1027	BDL	BDL	BDL	247539	289479
Sc45 (ppm)	BDL	BDL	BDL	BDL	BDL	BDL	BDL	20	14
Ti47 (ppm)	BDL	BDL	BDL	BDL	BDL	BDL	BDL	-	-
V51 (ppm)	BDL	BDL	3	4	3	BDL	BDL	21	16
Cr52 (ppm)	BDL	BDL	29	BDL	BDL	BDL	BDL	81	79
Mn55 (ppm)	457	881	143	103	24	37	23	1244	1502
Fe57 (ppm)	5136462	39863	91236	21919	22605	22643	19791	41820	50248
Co59 (ppm)	-	69	596	385	499	573	489	151	167
Ni60 (ppm)	185	-	-	-	-	3	3	52	-
Cu63 (ppm)	1592	2030	131165	610	307	78	235	73	246
Zn66 (ppm)	-	-	-	-	-	-	-	-	-
Ga71 (ppm)	-	-	-	-	-	-	-	11	-
Ge73 (ppm)	-	BDL	BDL	-	BDL	-	BDL	-	5
As75 (ppm)	3502	8	4	BDL	BDL	BDL	BDL	22	BDL
Se77 (ppm)	2103	67	236	82	87	94	92	43	164
Rb85 (ppm)	BDL	BDL	BDL	BDL	BDL	BDL	BDL	106	124
Sr88 (ppm)	-	-	-	-	-	-	-	-	-
Y89 (ppm)	-	-	-	-	-	-	-	-	-
Zr90 (ppm)	-	1	-	-	-	-	BDL	-	-
Nb93 (ppm)	BDL	-	-	BDL	-	-	BDL	-	4
Mo95 (ppm)	-	-	-	-	BDL	-	-	BDL	10
Ru101 (ppm)	-	-	1	-	BDL	BDL	BDL	BDL	-
Rh103 (ppm)	BDL	BDL	85	-	-	-	87	-	BDL
Pd104 (ppm)	-	93	-	BDL	BDL	-	-	-	-

Pd105 (ppm)	-	7	157	192	-	161	-	-	-
Pd106 (ppm)	1746	-	21	13	5	3	4	56	-
Ag107 (ppm)	-	-	2244	-	-	2033	-	-	8
Cd111 (ppm)	1	0	-	48	-	-	36	450	-
In115 (ppm)	8	1	1	BDL	BDL	BDL	BDL	-	-
Sn118 (ppm)	656	1	4	5	1	0	0	8	11
Sb121 (ppm)	BDL	BDL	BDL	8	-	BDL	-	1	0
Te125 (ppm)	-	-	BDL	0	BDL	BDL	BDL	4	BDL
Cs133 (ppm)	-	-	-	-	-	-	-	1	1
Ba137 (ppm)	-	-	-	-	-	-	-	-	-
La139 (ppm)	-	-	-	-	-	-	-	-	-
Ce140 (ppm)	-	-	-	-	-	-	-	-	-
Pr141 (ppm)	-	-	-	-	-	-	-	-	-
Nd146 (ppm)	-	-	-	-	-	-	-	-	-
Sm147 (ppm)	-	BDL	-	-	-	-	-	-	-
Eu153 (ppm)	-	-	-	-	-	-	-	-	-
Gd157 (ppm)	-	-	-	-	-	-	-	-	-
Tb159 (ppm)	-	-	-	-	-	-	-	-	-
Dy163 (ppm)	-	-	-	-	-	-	-	-	-
Ho165 (ppm)	-	-	-	-	-	-	-	-	-
Er166 (ppm)	-	-	-	-	-	-	-	-	-
Tm169 (ppm)	-	-	-	-	-	-	-	-	-
Yb172 (ppm)	-	-	-	-	-	-	-	-	-
Lu175 (ppm)	-	-	-	-	-	-	-	-	-
Hf178 (ppm)	-	-	-	-	-	-	-	-	-
Ta181 (ppm)	1	BDL	0	-	-	-	-	-	-
W182 (ppm)	BDL	BDL	BDL	0	BDL	BDL	BDL	-	3
Re185 (ppm)	-	-	BDL	BDL	BDL	BDL	BDL	BDL	BDL
Os189 (ppm)	BDL	BDL	BDL	-	BDL	BDL	-	BDL	BDL
Ir193 (ppm)	-	BDL	BDL	-	-	BDL	BDL	BDL	BDL
Pt195 (ppm)	470	1316	-	-	-	BDL	-	BDL	BDL
Au197 (ppm)	1049	1619	21924	6501	5237	5425	4919	-	-
Hg202 (ppm)	0	BDL	30309	10391	7496	7716	6931	16618	17991
Pb204 (ppm)	344	29	0	1	BDL	BDL	BDL	59384	64186
Tl205 (ppm)	341	29	-	-	10	-	8	BDL	0
Pb206 (ppm)	364	31	22	297	-	2	8	49	83
Pb207 (ppm)	47	2	17	175	8	1	6	48	65
Pb208 (ppm)	-	-	0	BDL	BDL	BDL	BDL	57	68
Bi209 (ppm)	-	-	-	-	-	-	-	0	BDL
Th232 (ppm)	364	54	-	-	-	-	-	-	-
U238 (ppm)	-	-	313	342	86	81	79	-	-
PbTotal (ppm)	-	-	-	-	-	-	-	951	1042

Table D4. Trace element data for sphalerite continued.

Deposit	Betts Cove	Betts Cove	Betts Cove	Betts Cove	Betts Cove	Betts Cove	Betts Cove	Betts Cove	Betts Cove
Sample	KKMSC32_Sp25	KKMSC32_Sp26	KKMSC32_Sp27	KKMSC32_Sp28	KKMSC32_Sp29	KKMSC32_Sp30	KKMSC32_Sp1	KKMSC32_Sp2	KKMSC32_Sp3
Date	2023-11-21	2023-11-21	2023-11-21	2023-11-21	2023-11-21	2023-11-21	2023-11-21	2023-11-21	2023-11-21
Facies	Sphalerite-pyrite-dominated	Sphalerite-pyrite-dominated	Sphalerite-pyrite-dominated	Sphalerite-pyrite-dominated	Sphalerite-pyrite-dominated	Sphalerite-pyrite-dominated	Sphalerite-pyrite-dominated	Sphalerite-pyrite-dominated	Sphalerite-pyrite-dominated
Li7 (ppm)	65	58	37	139	53	53	2	BDL	1
Be9 (ppm)	-	-	-	-	-	-	-	-	BDL
B11 (ppm)	144	69	BDL	151	54	133	BDL	BDL	BDL
Na23 (ppm)	489842	311443	233439	294862	255562	283025	BDL	BDL	BDL
Mg24 (ppm)	130020	80072	62286	-	85029	74435	-	559	61
Al27 (ppm)	46859	30559	22790	32203	37402	27144	248	615	39
Si29 (ppm)	1767549	1119137	862862	1119409	957127	1044871	1708	1101	774
P31 (ppm)	193	301	BDL	223	266	195	BDL	BDL	BDL
S32 (ppm)	1766043	1389688	1329272	1496301	1593014	1573795	647169	400430	326099
K39 (ppm)	17175	11205	8332	10546	9504	9866	BDL	BDL	BDL
Ca44 (ppm)	342266	219928	167960	208000	183802	196042	146	BDL	BDL
Sc45 (ppm)	15	14	6	4	10	13	BDL	BDL	BDL
Ti47 (ppm)	1389	908	-	-	-	-	-	3	-
V51 (ppm)	29	14	10	17	20	19	1	1	BDL
Cr52 (ppm)	83	38	29	31	55	70	BDL	BDL	BDL
Mn55 (ppm)	1343	1150	915	1175	1501	1080	662	814	729
Fe57 (ppm)	38300	44402	35111	43199	58001	37987	37044	38801	40403
Co59 (ppm)	113	127	122	-	175	121	BDL	BDL	-
Ni60 (ppm)	-	-	15	22	-	-	1	-	-
Cu63 (ppm)	95	202	497	2850	1339	864	520	61	150
Zn66 (ppm)	-	-	-	-	-	-	-	-	-
Ga71 (ppm)	-	-	-	-	-	-	-	-	-
Ge73 (ppm)	5	-	-	-	BDL	-	-	BDL	-
As75 (ppm)	BDL	21	BDL	BDL	BDL	BDL	BDL	BDL	BDL
Se77 (ppm)	143	133	72	106	108	133	15	14	20
Rb85 (ppm)	133	-	73	84	84	79	-	-	BDL
Sr88 (ppm)	-	-	-	-	-	-	-	-	-
Y89 (ppm)	-	-	-	-	-	8	-	-	-
Zr90 (ppm)	-	-	-	-	-	-	-	-	-
Nb93 (ppm)	-	-	-	-	-	-	-	-	-
Mo95 (ppm)	2	BDL	2	2	13	-	9	-	4
Ru101 (ppm)	-	-	-	-	-	BDL	-	-	-
Rh103 (ppm)	-	-	-	-	-	BDL	-	-	BDL
Pd104 (ppm)	-	-	-	-	96	-	-	-	-

Pd105 (ppm)	1	BDL	-	-	-	-	-	-	BDL
Pd106 (ppm)	-	-	55	52	-	-	-	-	69
Ag107 (ppm)	5	5	18	-	65	13	10	-	7
Cd111 (ppm)	-	470	419	435	432	421	568	-	585
In115 (ppm)	0	-	-	-	-	-	-	-	0
Sn118 (ppm)	10	9	BDL	5	4	4	BDL	BDL	0
Sb121 (ppm)	BDL	0	1	BDL	3	2	0	0	0
Te125 (ppm)	BDL	BDL	BDL	BDL	5	-	BDL	BDL	BDL
Cs133 (ppm)	1	0	0	BDL	0	0	BDL	BDL	BDL
Ba137 (ppm)	-	-	-	-	-	-	-	-	-
La139 (ppm)	-	-	-	-	-	-	-	-	-
Ce140 (ppm)	-	-	-	-	-	-	-	-	-
Pr141 (ppm)	-	-	-	-	-	-	-	-	-
Nd146 (ppm)	-	-	-	-	-	-	-	-	-
Sm147 (ppm)	-	-	-	-	-	-	-	-	-
Eu153 (ppm)	-	-	-	-	-	-	-	-	-
Gd157 (ppm)	-	-	-	-	-	-	-	-	-
Tb159 (ppm)	-	-	-	-	-	-	-	-	-
Dy163 (ppm)	-	-	-	-	-	-	-	-	-
Ho165 (ppm)	-	-	-	-	0	-	-	-	-
Er166 (ppm)	-	-	-	-	-	-	-	-	-
Tm169 (ppm)	-	-	-	-	-	-	-	-	-
Yb172 (ppm)	-	-	-	-	-	-	-	-	-
Lu175 (ppm)	-	-	-	-	-	-	-	-	-
Hf178 (ppm)	-	-	-	-	-	-	-	-	-
Ta181 (ppm)	-	-	-	-	-	-	BDL	-	-
W182 (ppm)	BDL	-	-	4	-	-	-	BDL	BDL
Re185 (ppm)	BDL	BDL	BDL	1	BDL	BDL	BDL	BDL	BDL
Os189 (ppm)	BDL	1	BDL	BDL	BDL	BDL	BDL	BDL	BDL
Ir193 (ppm)	BDL	BDL	BDL	-	BDL	-	-	BDL	-
Pt195 (ppm)	BDL	-	BDL	BDL	-	BDL	-	BDL	BDL
Au197 (ppm)	BDL	-	-	-	BDL	-	-	-	-
Hg202 (ppm)	19308	17584	16077	16394	17084	15827	1868	348	569
Pb204 (ppm)	68684	61413	56635	56717	59887	55009	6278	1187	1886
Tl205 (ppm)	0	BDL	1	1	BDL	BDL	BDL	BDL	0
Pb206 (ppm)	75	-	93	86	174	52	-	19	9
Pb207 (ppm)	-	48	94	88	181	-	16	17	-
Pb208 (ppm)	66	50	91	82	185	64	18	-	9
Bi209 (ppm)	BDL	BDL	BDL	0	0	BDL	BDL	BDL	BDL
Th232 (ppm)	-	-	-	-	-	-	-	-	-
U238 (ppm)	-	-	-	-	-	-	-	-	-
PbTotal (ppm)	1106	979	948	941	1085	895	111	35	40

Table D4. Trace element data for sphalerite continued.

Deposit	Betts Cove	Betts Cove	Betts Cove	Betts Cove	Betts Cove	Betts Cove	Betts Cove	Betts Cove	Betts Cove
Sample	KKMSC32_Sp6	KKMSC32_Sp7	KKMSC32_Sp9	KKMSC32_Sp11	KKMSC32_Sp12	KKMSC32_Sp13	KKMSC32_Sp14	KKMSC32_Sp15	KKMSC32_Sp16
Date	2023-11-21	2023-11-21	2023-11-21	2023-11-21	2023-11-21	2023-11-21	2023-11-21	2023-11-21	2023-11-21
Facies	Sphalerite-pyrite-dominated	Sphalerite-pyrite-dominated	Sphalerite-pyrite-dominated	Sphalerite-pyrite-dominated	Sphalerite-pyrite-dominated	Sphalerite-pyrite-dominated	Sphalerite-pyrite-dominated	Sphalerite-pyrite-dominated	Sphalerite-pyrite-dominated
Li7 (ppm)	BDL	BDL	BDL	BDL	BDL	BDL	BDL	BDL	BDL
Be9 (ppm)	-	-	-	-	-	BDL	-	-	-
B11 (ppm)	BDL	BDL	BDL	BDL	BDL	BDL	BDL	BDL	BDL
Na23 (ppm)	BDL	BDL	BDL	BDL	BDL	BDL	BDL	BDL	BDL
Mg24 (ppm)	3	300	230	44	BDL	42	2	238	BDL
Al27 (ppm)	3	122	12	6	1	6	2	26	BDL
Si29 (ppm)	BDL	1192	1004	678	BDL	BDL	BDL	1202	BDL
P31 (ppm)	BDL	BDL	BDL	BDL	BDL	BDL	BDL	BDL	BDL
S32 (ppm)	311896	340827	327195	303092	328062	329237	331508	299544	308842
K39 (ppm)	BDL	BDL	BDL	9	BDL	BDL	BDL	BDL	BDL
Ca44 (ppm)	BDL	139	194	BDL	BDL	BDL	BDL	205	BDL
Sc45 (ppm)	BDL	BDL	BDL	BDL	BDL	BDL	BDL	BDL	BDL
Ti47 (ppm)	-	2	BDL	2	BDL	BDL	BDL	BDL	BDL
V51 (ppm)	BDL	0	0	0	BDL	BDL	BDL	BDL	BDL
Cr52 (ppm)	BDL	2	BDL	BDL	BDL	BDL	BDL	BDL	BDL
Mn55 (ppm)	701	601	593	487	752	683	638	640	716
Fe57 (ppm)	35293	35460	34039	29432	39042	35939	37003	34057	36591
Co59 (ppm)	BDL	-	BDL	0	0	-	2	BDL	0
Ni60 (ppm)	-	-	1	0	-	-	3	-	BDL
Cu63 (ppm)	29	322	126	67	69	77	149	129	72
Zn66 (ppm)	-	-	-	-	-	-	-	-	-
Ga71 (ppm)	-	-	-	-	-	-	-	0	-
Ge73 (ppm)	BDL	BDL	BDL	BDL	-	-	BDL	-	BDL
As75 (ppm)	BDL	BDL	BDL	BDL	BDL	BDL	3	BDL	BDL
Se77 (ppm)	19	19	19	19	22	22	19	13	15
Rb85 (ppm)	BDL	BDL	BDL	BDL	-	BDL	BDL	BDL	BDL
Sr88 (ppm)	-	-	-	-	-	-	BDL	-	-
Y89 (ppm)	-	-	-	-	-	-	-	-	-
Zr90 (ppm)	-	-	-	-	-	-	-	-	-
Nb93 (ppm)	-	-	-	-	-	-	BDL	-	-
Mo95 (ppm)	4	0	0	-	BDL	-	-	BDL	BDL
Ru101 (ppm)	-	BDL	-	BDL	-	-	-	-	-
Rh103 (ppm)	BDL	-	-	BDL	-	-	BDL	BDL	BDL
Pd104 (ppm)	-	-	-	-	-	-	-	101	104

Pd105 (ppm)	-	-	-	-	-	BDL	-	-	-
Pd106 (ppm)	-	-	-	-	77	-	-	-	69
Ag107 (ppm)	3	23	16	-	4	-	15	10	-
Cd111 (ppm)	605	613	-	649	-	661	623	601	671
In115 (ppm)	-	-	-	-	-	-	-	-	-
Sn118 (ppm)	BDL	BDL	BDL	0	BDL	BDL	BDL	BDL	0
Sb121 (ppm)	0	0	0	0	0	0	0	0	BDL
Te125 (ppm)	-	1	0	BDL	BDL	BDL	1	-	BDL
Cs133 (ppm)	BDL	BDL	BDL	BDL	BDL	BDL	BDL	BDL	BDL
Ba137 (ppm)	-	-	-	-	-	-	-	-	-
La139 (ppm)	-	-	-	-	-	-	-	-	-
Ce140 (ppm)	-	-	-	-	-	-	-	BDL	-
Pr141 (ppm)	-	-	-	-	-	-	-	-	-
Nd146 (ppm)	-	-	-	-	-	-	-	-	-
Sm147 (ppm)	-	-	-	-	-	-	-	-	-
Eu153 (ppm)	-	-	-	-	-	-	-	-	-
Gd157 (ppm)	-	BDL	-	-	-	-	-	BDL	-
Tb159 (ppm)	-	-	-	-	-	-	-	-	-
Dy163 (ppm)	-	-	-	-	-	-	-	-	-
Ho165 (ppm)	-	-	-	-	-	-	-	-	-
Er166 (ppm)	-	-	-	-	-	-	-	BDL	-
Tm169 (ppm)	-	-	-	-	-	-	-	-	-
Yb172 (ppm)	-	-	-	-	-	-	-	-	-
Lu175 (ppm)	-	-	-	-	-	-	-	-	-
Hf178 (ppm)	-	-	-	-	-	-	-	-	-
Ta181 (ppm)	-	-	-	-	-	-	BDL	-	-
W182 (ppm)	-	-	BDL	BDL	BDL	-	-	BDL	-
Re185 (ppm)	BDL	-	BDL	BDL	BDL	BDL	BDL	BDL	BDL
Os189 (ppm)	BDL	BDL	BDL	BDL	BDL	BDL	BDL	BDL	BDL
Ir193 (ppm)	BDL	-	BDL	BDL	-	-	-	BDL	BDL
Pt195 (ppm)	BDL	BDL	BDL	-	BDL	BDL	BDL	BDL	-
Au197 (ppm)	-	-	-	-	-	-	-	-	-
Hg202 (ppm)	375	459	433	125	352	338	299	376	334
Pb204 (ppm)	1255	1533	1437	425	1105	1098	968	1194	1056
Tl205 (ppm)	BDL	0	0	BDL	BDL	BDL	0	BDL	BDL
Pb206 (ppm)	3	31	-	11	2	13	17	-	2
Pb207 (ppm)	3	-	34	12	2	13	17	17	-
Pb208 (ppm)	3	-	32	14	2	14	17	20	2
Bi209 (ppm)	BDL	BDL	BDL	BDL	BDL	BDL	BDL	BDL	BDL
Th232 (ppm)	-	-	-	-	-	-	-	-	-
U238 (ppm)	-	-	-	-	-	-	-	-	-
PbTotal (ppm)	22	55	54	19	19	30	33	37	18

Table D4. Trace element data for sphalerite continued.

Deposit	Betts Cove	Betts Cove	Betts Cove	Betts Cove	Betts Cove	Betts Cove	Betts Cove	Betts Cove	Betts Cove
Sample	KKMSC32_Sp17	KKMSC32_Sp18	KKMSC32_Sp19	KKMSC32_Sp20	KKMSC32_Sp21	KKMSC32_Sp22	KKMSC32_Sp23	KKMSC32_Sp24	KKMSC32_Sp34
Date	2023-11-21	2023-11-21	2023-11-21	2023-11-21	2023-11-21	2023-11-21	2023-11-21	2023-11-21	2023-11-21
Facies	Sphalerite-pyrite-dominated	Sphalerite-pyrite-dominated	Sphalerite-pyrite-dominated	Sphalerite-pyrite-dominated	Sphalerite-pyrite-dominated	Sphalerite-pyrite-dominated	Sphalerite-pyrite-dominated	Sphalerite-pyrite-dominated	Sphalerite-pyrite-dominated
Li7 (ppm)	BDL	BDL	BDL	BDL	BDL	BDL	BDL	BDL	BDL
Be9 (ppm)	-	-	-	-	-	-	-	-	-
B11 (ppm)	BDL	BDL	BDL	BDL	BDL	BDL	BDL	BDL	BDL
Na23 (ppm)	BDL	BDL	BDL	60	BDL	BDL	BDL	BDL	BDL
Mg24 (ppm)	44	1691	-	0	BDL	21	-	-	46
Al27 (ppm)	46	142	43	BDL	BDL	1	13	1	6
Si29 (ppm)	BDL	4836	1861	BDL	BDL	539	1036	BDL	BDL
P31 (ppm)	BDL	BDL	21	BDL	BDL	BDL	BDL	BDL	BDL
S32 (ppm)	340356	324085	316890	327425	316514	295090	313325	333358	389093
K39 (ppm)	BDL	BDL	BDL	BDL	BDL	BDL	BDL	BDL	BDL
Ca44 (ppm)	BDL	1607	528	BDL	BDL	BDL	165	BDL	BDL
Sc45 (ppm)	BDL	1	BDL	BDL	BDL	BDL	BDL	BDL	BDL
Ti47 (ppm)	BDL	BDL	-	BDL	BDL	-	-	-	BDL
V51 (ppm)	BDL	3	0	BDL	BDL	BDL	BDL	BDL	BDL
Cr52 (ppm)	BDL	BDL	2	BDL	BDL	BDL	BDL	BDL	BDL
Mn55 (ppm)	665	680	631	666	668	634	579	699	775
Fe57 (ppm)	37841	36033	34024	34839	37576	28371	33712	37711	38707
Co59 (ppm)	0	0	0	BDL	0	-	0	0	3
Ni60 (ppm)	2	2	-	1	-	-	1	-	1
Cu63 (ppm)	639	201	645	99	23	573	238	92	58
Zn66 (ppm)	-	-	-	-	-	-	-	-	-
Ga71 (ppm)	0	-	-	-	-	-	-	-	-
Ge73 (ppm)	BDL	-	-	BDL	-	-	-	BDL	-
As75 (ppm)	BDL	BDL	BDL	BDL	BDL	BDL	BDL	BDL	BDL
Se77 (ppm)	9	27	19	19	16	22	18	18	22
Rb85 (ppm)	BDL	-	-	BDL	-	-	BDL	BDL	BDL
Sr88 (ppm)	-	-	-	-	-	-	-	-	-
Y89 (ppm)	-	-	-	-	-	-	-	-	-
Zr90 (ppm)	-	-	-	-	-	-	-	-	-
Nb93 (ppm)	-	-	-	-	-	-	-	-	-
Mo95 (ppm)	0	1	0	1	BDL	3	3	BDL	BDL
Ru101 (ppm)	-	-	-	-	-	BDL	-	-	-
Rh103 (ppm)	-	-	-	BDL	-	BDL	-	-	BDL
Pd104 (ppm)	-	-	-	-	-	-	-	-	136

Pd105 (ppm)	BDL	BDL	BDL	-	BDL	-	-	BDL	-
Pd106 (ppm)	72	-	-	69	67	64	-	67	-
Ag107 (ppm)	8	5	13	4	2	12	11	3	-
Cd111 (ppm)	-	582	596	-	610	617	-	652	779
In115 (ppm)	-	0	-	-	-	-	-	-	-
Sn118 (ppm)	BDL	BDL	BDL	1	0	BDL	BDL	BDL	0
Sb121 (ppm)	BDL	0	0	0	BDL	0	0	-	0
Te125 (ppm)	-	-	BDL	BDL	BDL	BDL	BDL	-	BDL
Cs133 (ppm)	BDL	BDL	BDL	BDL	BDL	BDL	BDL	BDL	BDL
Ba137 (ppm)	-	-	-	-	-	-	-	-	-
La139 (ppm)	-	-	-	-	-	-	-	-	-
Ce140 (ppm)	-	-	-	-	-	-	-	-	-
Pr141 (ppm)	-	-	-	-	-	-	-	-	-
Nd146 (ppm)	-	-	-	-	-	-	-	-	-
Sm147 (ppm)	-	-	-	-	-	-	-	-	-
Eu153 (ppm)	-	-	-	-	-	-	-	-	-
Gd157 (ppm)	-	-	-	-	-	-	-	-	-
Tb159 (ppm)	-	-	-	-	-	-	-	-	-
Dy163 (ppm)	-	-	-	-	-	-	-	-	-
Ho165 (ppm)	-	-	-	-	-	-	-	-	-
Er166 (ppm)	-	-	-	-	-	-	-	-	-
Tm169 (ppm)	-	-	-	-	-	-	-	-	-
Yb172 (ppm)	-	-	-	-	-	-	-	-	-
Lu175 (ppm)	-	-	-	-	-	-	-	-	-
Hf178 (ppm)	-	-	-	-	-	-	-	-	-
Ta181 (ppm)	BDL	-	-	-	-	BDL	-	-	-
W182 (ppm)	-	-	-	BDL	-	-	BDL	-	-
Re185 (ppm)	BDL	BDL	BDL	BDL	BDL	BDL	BDL	BDL	BDL
Os189 (ppm)	BDL	BDL	BDL	BDL	BDL	BDL	BDL	BDL	BDL
Ir193 (ppm)	BDL	-	BDL	BDL	-	-	-	-	-
Pt195 (ppm)	BDL	BDL	BDL	-	BDL	BDL	BDL	-	-
Au197 (ppm)	-	-	-	-	BDL	-	-	BDL	-
Hg202 (ppm)	428	573	483	503	398	301	495	379	245
Pb204 (ppm)	1338	1662	1451	1466	1176	893	1469	1097	678
Tl205 (ppm)	BDL	BDL	BDL	BDL	BDL	0	BDL	BDL	BDL
Pb206 (ppm)	9	3	-	-	-	23	16	-	-
Pb207 (ppm)	9	4	16	5	0	22	16	-	12
Pb208 (ppm)	10	4	18	6	-	-	17	1	9
Bi209 (ppm)	BDL	BDL	BDL	BDL	BDL	BDL	BDL	BDL	BDL
Th232 (ppm)	-	-	-	-	-	-	-	-	-
U238 (ppm)	-	-	BDL	-	-	-	BDL	-	-
PbTotal (ppm)	30	29	39	28	18	36	38	18	20

Table D4. Trace element data for sphalerite continued.

Deposit	Betts Cove	Betts Cove	Betts Cove	Betts Cove	Betts Cove	Betts Cove	Betts Cove	Betts Cove	Betts Cove
Sample	KKMSC32_Sp36	KKMSC32_Sp37	KKMSC32_Sp35	KKMSC32_Sp33	KKMSC32_Sp39	KKMSC35_Sp4	KKMSC35_Sp5	KKMSC35_Sp1	KKMSC35_Sp2
Date	2023-11-21	2023-11-21	2023-11-21	2023-11-21	2023-11-21	2023-11-21	2023-11-21	2023-11-21	2023-11-21
Facies	Sphalerite-pyrite-dominated	Sphalerite-pyrite-dominated	Sphalerite-pyrite-dominated	Sphalerite-pyrite-dominated	Sphalerite-pyrite-dominated	Chalcopyrite-pyrrhotite-dominated	Chalcopyrite-pyrrhotite-dominated	Chalcopyrite-pyrrhotite-dominated	Chalcopyrite-pyrrhotite-dominated
Li7 (ppm)	BDL	BDL	BDL	BDL	BDL	BDL	BDL	BDL	BDL
Be9 (ppm)	BDL	-	-	-	BDL	-	BDL	-	-
B11 (ppm)	BDL	BDL	BDL	BDL	BDL	BDL	BDL	BDL	BDL
Na23 (ppm)	BDL	BDL	BDL	BDL	BDL	BDL	BDL	BDL	BDL
Mg24 (ppm)	2	358	BDL	134	182	10	-	16	7
Al27 (ppm)	2	33	BDL	108	90	5	39	11	2
Si29 (ppm)	BDL	1429	BDL	BDL	1003	BDL	BDL	BDL	BDL
P31 (ppm)	BDL	BDL	BDL	BDL	BDL	BDL	BDL	BDL	BDL
S32 (ppm)	333262	331272	300060	357008	338885	309950	339546	338545	319883
K39 (ppm)	BDL	BDL	BDL	BDL	BDL	BDL	13	BDL	BDL
Ca44 (ppm)	BDL	354	BDL	BDL	BDL	BDL	422	198	BDL
Sc45 (ppm)	BDL	BDL	BDL	BDL	BDL	BDL	BDL	BDL	BDL
Ti47 (ppm)	BDL	-	BDL	BDL	BDL	-	-	3	BDL
V51 (ppm)	BDL	BDL	BDL	0	BDL	BDL	BDL	BDL	BDL
Cr52 (ppm)	BDL	6	BDL	5	4	BDL	3	2	BDL
Mn55 (ppm)	659	696	678	661	618	699	950	566	578
Fe57 (ppm)	33540	33235	32192	64259	33289	47071	41277	66115	41091
Co59 (ppm)	3	-	45	48	1	247	-	263	240
Ni60 (ppm)	3	-	-	-	-	-	3	45	-
Cu63 (ppm)	521	257	167	366	149	1072	114	127	93
Zn66 (ppm)	-	-	-	-	-	-	-	-	-
Ga71 (ppm)	-	BDL	-	-	-	-	-	-	-
Ge73 (ppm)	BDL	BDL	BDL	-	-	-	-	-	-
As75 (ppm)	3	BDL	BDL	28	BDL	15	11	38	BDL
Se77 (ppm)	22	22	24	16	21	515	510	508	477
Rb85 (ppm)	BDL	BDL	BDL	BDL	BDL	BDL	BDL	BDL	BDL
Sr88 (ppm)	-	-	-	-	-	-	-	1	-
Y89 (ppm)	-	-	-	-	-	-	-	-	-
Zr90 (ppm)	-	-	-	-	-	-	-	-	-
Nb93 (ppm)	BDL	-	-	BDL	-	-	-	-	-
Mo95 (ppm)	1	-	-	0	-	BDL	BDL	BDL	BDL
Ru101 (ppm)	-	-	-	-	-	-	-	-	-
Rh103 (ppm)	BDL	-	BDL	BDL	BDL	-	-	BDL	-
Pd104 (ppm)	-	101	105	-	103	-	-	-	-

Pd105 (ppm)	-	-	-	-	-	-	-	-	BDL
Pd106 (ppm)	-	72	72	-	-	267	285	-	301
Ag107 (ppm)	11	13	-	13	-	4	-	11	13
Cd111 (ppm)	-	-	695	777	-	-	-	-	3874
In115 (ppm)	0	-	-	-	-	-	23	17	-
Sn118 (ppm)	BDL	0	BDL	BDL	BDL	4	1	1	0
Sb121 (ppm)	2	0	0	2	0	-	1	2	0
Te125 (ppm)	-	-	BDL	1	BDL	BDL	BDL	1	-
Cs133 (ppm)	BDL	BDL	BDL	BDL	BDL	BDL	BDL	BDL	BDL
Ba137 (ppm)	-	-	-	-	-	-	-	-	-
La139 (ppm)	-	-	-	-	-	-	-	-	-
Ce140 (ppm)	-	-	-	-	-	-	-	-	-
Pr141 (ppm)	-	-	-	-	-	-	-	-	-
Nd146 (ppm)	-	-	-	-	-	-	-	-	-
Sm147 (ppm)	-	-	-	-	-	-	-	-	-
Eu153 (ppm)	-	-	-	-	-	-	-	-	-
Gd157 (ppm)	-	-	-	-	-	-	BDL	-	-
Tb159 (ppm)	-	-	-	-	-	-	-	-	-
Dy163 (ppm)	-	-	-	-	-	-	-	-	-
Ho165 (ppm)	-	-	-	-	-	-	-	-	-
Er166 (ppm)	-	-	-	-	-	-	-	-	-
Tm169 (ppm)	-	-	-	-	-	-	-	-	-
Yb172 (ppm)	-	-	-	-	-	-	-	-	-
Lu175 (ppm)	-	-	-	-	-	-	-	-	-
Hf178 (ppm)	-	-	-	-	-	-	-	-	-
Ta181 (ppm)	-	BDL	BDL	-	-	-	-	-	-
W182 (ppm)	-	-	BDL	BDL	-	BDL	-	BDL	-
Re185 (ppm)	BDL	BDL	BDL	BDL	BDL	BDL	BDL	BDL	BDL
Os189 (ppm)	BDL	BDL	BDL	BDL	BDL	BDL	BDL	BDL	BDL
Ir193 (ppm)	BDL	-	BDL	BDL	BDL	-	-	-	BDL
Pt195 (ppm)	BDL	BDL	-	-	BDL	BDL	-	BDL	BDL
Au197 (ppm)	-	-	BDL	BDL	-	-	-	-	-
Hg202 (ppm)	405	470	391	255	448	151	90	204	230
Pb204 (ppm)	1200	1360	1092	734	1251	420	249	591	629
Tl205 (ppm)	0	BDL	BDL	0	BDL	0	0	0	0
Pb206 (ppm)	32	-	17	27	-	5	-	42	-
Pb207 (ppm)	33	14	17	-	-	-	-	37	29
Pb208 (ppm)	34	14	17	28	13	4	16	41	31
Bi209 (ppm)	BDL	0	BDL	BDL	BDL	BDL	0	2	1
Th232 (ppm)	-	-	-	-	-	-	-	-	-
U238 (ppm)	-	-	-	BDL	BDL	-	-	-	BDL
PbTotal (ppm)	51	35	33	37	31	10	17	48	40

Table D4. Trace element data for sphalerite continued.

Deposit	Betts Cove	Betts Cove	Betts Cove	Betts Cove	Tilt Cove	Tilt Cove	Tilt Cove	Tilt Cove	Betts Cove
Sample	KKMSC35_Sp3	KKMSC53_Sp1	KKMSC53_Sp1	KKMSC53_Sp2	KKMSC72_Sp3	KKMSC72_Sp1	KKMSC72_Sp2	KKMSC72_Sp4	KKMSC42_Sp1
Date	2023-11-21	2023-11-22	2023-11-22	2023-11-22	2023-11-22	2023-11-22	2023-11-22	2023-11-22	2023-11-22
Facies	Chalcopyrite-pyrrhotite-dominated	Chalcopyrite-dominated	Chalcopyrite-dominated	Chalcopyrite-dominated	Pyrrhotite-dominated	Pyrrhotite-dominated	Pyrrhotite-dominated	Pyrrhotite-dominated	Chalcopyrite-pyrrhotite-dominated
Li7 (ppm)	BDL	BDL	BDL	BDL	BDL	BDL	BDL	BDL	BDL
Be9 (ppm)	BDL	BDL	-	BDL	-	-	-	-	-
B11 (ppm)	BDL	BDL	BDL	BDL	BDL	BDL	BDL	BDL	BDL
Na23 (ppm)	BDL	BDL	BDL	BDL	BDL	BDL	BDL	BDL	BDL
Mg24 (ppm)	3	0	-	5	279	1758	1286	6	435
Al27 (ppm)	1	BDL	1	5	BDL	46	70	1	394
Si29 (ppm)	741	BDL	BDL	BDL	BDL	4155	2906	BDL	2320
P31 (ppm)	24	BDL	BDL	BDL	BDL	BDL	BDL	BDL	BDL
S32 (ppm)	355386	271441	243685	230731	348852	659863	287386	255676	388667
K39 (ppm)	BDL	BDL	BDL	BDL	BDL	BDL	BDL	BDL	BDL
Ca44 (ppm)	482	BDL	BDL	BDL	BDL	BDL	BDL	BDL	BDL
Sc45 (ppm)	BDL	BDL	BDL	BDL	BDL	BDL	BDL	BDL	BDL
Ti47 (ppm)	-	-	-	BDL	-	BDL	BDL	1	-
V51 (ppm)	BDL	BDL	0	BDL	BDL	BDL	BDL	0	3
Cr52 (ppm)	BDL	BDL	BDL	BDL	BDL	6	2	BDL	4
Mn55 (ppm)	778	605	475	482	52	27	48	65	988
Fe57 (ppm)	50354	54374	41785	45873	120606	458734	53026	45927	51383
Co59 (ppm)	255	667	564	-	1019	715	1137	1304	290
Ni60 (ppm)	2	0	-	37	1869	-	19	-	-
Cu63 (ppm)	23	34	53	51	4132	329	16724	7489	176
Zn66 (ppm)	-	-	-	-	-	-	-	-	-
Ga71 (ppm)	-	-	-	0	-	-	-	-	-
Ge73 (ppm)	BDL	-	BDL	BDL	-	BDL	-	-	BDL
As75 (ppm)	BDL	BDL	BDL	BDL	BDL	BDL	BDL	BDL	11
Se77 (ppm)	607	579	574	632	94	107	61	54	1006
Rb85 (ppm)	BDL	BDL	BDL	BDL	BDL	-	BDL	BDL	BDL
Sr88 (ppm)	-	-	-	-	-	0	-	-	-
Y89 (ppm)	-	-	-	-	-	-	-	-	-
Zr90 (ppm)	-	-	-	-	-	-	-	-	-
Nb93 (ppm)	-	-	-	-	-	-	-	BDL	-
Mo95 (ppm)	BDL	BDL	BDL	-	BDL	BDL	BDL	0	-
Ru101 (ppm)	-	-	-	BDL	-	-	-	-	-
Rh103 (ppm)	-	-	-	BDL	-	-	-	0	-
Pd104 (ppm)	105	-	51	-	-	68	71	63	-
Pd105 (ppm)	-	-	-	BDL	0	BDL	1	-	-

Pd106 (ppm)	-	-	132	-	259	-	214	180	-
Ag107 (ppm)	3	2	2	3	79	-	23	17	4
Cd111 (ppm)	5064	3158	-	-	-	5074	4072	3031	-
In115 (ppm)	-	5	4	-	-	-	-	-	453
Sn118 (ppm)	0	BDL	BDL	0	BDL	0	BDL	0	0
Sb121 (ppm)	0	0	0	0	12	32	6	3	0
Te125 (ppm)	BDL	0	0	-	2	1	-	0	45
Cs133 (ppm)	BDL	BDL	BDL	BDL	BDL	BDL	BDL	BDL	BDL
Ba137 (ppm)	-	-	-	-	-	-	-	-	-
La139 (ppm)	-	-	-	-	-	-	-	-	-
Ce140 (ppm)	-	-	-	-	-	-	-	-	-
Pr141 (ppm)	-	-	-	-	-	-	-	-	-
Nd146 (ppm)	-	-	-	-	-	-	-	-	-
Sm147 (ppm)	-	-	-	-	-	-	-	-	-
Eu153 (ppm)	-	-	-	-	-	-	-	-	-
Gd157 (ppm)	-	-	-	-	-	-	-	-	-
Tb159 (ppm)	-	-	-	-	-	-	-	-	-
Dy163 (ppm)	-	-	-	-	-	-	-	-	-
Ho165 (ppm)	-	-	-	-	-	-	-	-	-
Er166 (ppm)	-	-	-	-	-	-	-	-	-
Tm169 (ppm)	-	-	-	-	-	-	-	-	-
Yb172 (ppm)	-	-	-	-	-	-	-	-	-
Lu175 (ppm)	-	-	-	-	-	-	-	-	-
Hf178 (ppm)	-	-	-	-	-	-	-	-	-
Ta181 (ppm)	BDL	-	-	-	-	-	-	-	-
W182 (ppm)	BDL	BDL	BDL	-	-	-	-	-	-
Re185 (ppm)	BDL	BDL	BDL	BDL	BDL	BDL	BDL	BDL	BDL
Os189 (ppm)	BDL	BDL	BDL	BDL	BDL	BDL	BDL	BDL	BDL
Ir193 (ppm)	BDL	BDL	BDL	BDL	BDL	BDL	-	-	-
Pt195 (ppm)	BDL	BDL	BDL	-	BDL	BDL	-	BDL	BDL
Au197 (ppm)	-	-	-	-	-	3	1	-	-
Hg202 (ppm)	146	219	219	269	233	267	324	320	1278
Pb204 (ppm)	395	721	754	898	995	1205	1241	1074	4624
Tl205 (ppm)	BDL	BDL	BDL	0	0	1	0	BDL	1
Pb206 (ppm)	-	1	-	-	133	253	54	43	202
Pb207 (ppm)	12	1	6	5	-	237	-	41	-
Pb208 (ppm)	14	1	-	-	131	255	55	-	238
Bi209 (ppm)	0	BDL	-	0	1	1	1	0	8
Th232 (ppm)	-	-	-	-	-	-	-	-	-
U238 (ppm)	-	-	-	-	-	-	-	-	-
PbTotal (ppm)	19	12	17	19	144	265	72	58	302

Table D4. Trace element data for sphalerite continued.

Deposit	Betts Cove	Betts Cove	Betts Cove	Betts Cove	Tilt Cove	Tilt Cove	Tilt Cove
Sample	KKMSC42_Sp7	KKMSC42_Sp6	KKMSC42_Sp4	KKMSC42_Sp5	KKMSC13_Sp1	KKMSC13_Sp2	KKMSC13_Sp3
Date	2023-11-22	2023-11-22	2023-11-22	2023-11-22	2023-11-23	2023-11-23	2023-11-23
Facies	Chalcopyrite-pyrrhotite-dominated	Chalcopyrite-pyrrhotite-dominated	Chalcopyrite-pyrrhotite-dominated	Chalcopyrite-pyrrhotite-dominated	Pyrite-dominated	Pyrite-dominated	Pyrite-dominated
Li7 (ppm)	3	12	2	BDL	BDL	BDL	BDL
Be9 (ppm)	BDL	-	-	-	BDL	-	BDL
B11 (ppm)	BDL	BDL	BDL	BDL	BDL	BDL	BDL
Na23 (ppm)	BDL	BDL	BDL	BDL	BDL	BDL	BDL
Mg24 (ppm)	80	108	27	20	7	3	652
Al27 (ppm)	66	79	24	16	7	BDL	519
Si29 (ppm)	1140	2629	683	874	BDL	BDL	1389
P31 (ppm)	89	54	BDL	BDL	BDL	BDL	BDL
S32 (ppm)	659756	431240	293238	273515	262463	298855	280092
K39 (ppm)	BDL	BDL	BDL	BDL	BDL	BDL	BDL
Ca44 (ppm)	BDL	BDL	BDL	BDL	BDL	BDL	BDL
Sc45 (ppm)	BDL	BDL	BDL	BDL	BDL	BDL	BDL
Ti47 (ppm)	BDL	-	-	BDL	BDL	BDL	BDL
V51 (ppm)	1	1	BDL	0	BDL	BDL	2
Cr52 (ppm)	BDL	7	2	2	BDL	BDL	BDL
Mn55 (ppm)	1213	1158	1175	1333	117	148	89
Fe57 (ppm)	64846	68389	60240	59364	53896	98613	79545
Co59 (ppm)	270	263	294	-	BDL	BDL	BDL
Ni60 (ppm)	1	-	BDL	BDL	-	BDL	BDL
Cu63 (ppm)	318	300	162	76	2316	157	154
Zn66 (ppm)	-	-	-	-	-	-	-
Ga71 (ppm)	-	BDL	-	0	-	-	-
Ge73 (ppm)	-	-	-	BDL	BDL	BDL	-
As75 (ppm)	9	5	BDL	BDL	16	40	17
Se77 (ppm)	915	840	722	859	1	3	3
Rb85 (ppm)	BDL	BDL	BDL	BDL	BDL	BDL	BDL
Sr88 (ppm)	-	-	0	-	-	-	-
Y89 (ppm)	-	-	BDL	-	-	-	-
Zr90 (ppm)	-	-	-	-	-	-	-
Nb93 (ppm)	-	-	-	-	0	BDL	3
Mo95 (ppm)	BDL	BDL	59	BDL	-	-	-
Ru101 (ppm)	-	-	-	-	BDL	-	-
Rh103 (ppm)	-	-	-	BDL	86	-	89
Pd104 (ppm)	-	-	-	-	-	-	BDL
Pd105 (ppm)	BDL	-	-	-	-	82	84

Pd106 (ppm)	-	-	-	-	8	8	-
Ag107 (ppm)	-	1	3	2	1103	1119	-
Cd111 (ppm)	4985	1626	1656	2088	12	14	-
In115 (ppm)	271	-	-	-	BDL	0	1
Sn118 (ppm)	0	BDL	BDL	BDL	BDL	0	BDL
Sb121 (ppm)	BDL	BDL	-	0	BDL	BDL	BDL
Te125 (ppm)	BDL	BDL	-	BDL	BDL	BDL	BDL
Cs133 (ppm)	BDL	BDL	BDL	BDL	-	-	-
Ba137 (ppm)	-	-	-	-	-	-	-
La139 (ppm)	-	-	-	-	-	-	-
Ce140 (ppm)	-	-	-	-	-	-	-
Pr141 (ppm)	-	-	-	-	-	-	-
Nd146 (ppm)	-	-	-	-	-	-	-
Sm147 (ppm)	-	-	-	-	-	-	-
Eu153 (ppm)	-	-	-	-	-	-	-
Gd157 (ppm)	-	-	-	-	-	-	-
Tb159 (ppm)	-	-	BDL	-	-	-	-
Dy163 (ppm)	-	-	-	-	-	-	-
Ho165 (ppm)	-	-	-	-	-	-	-
Er166 (ppm)	-	-	-	-	-	-	-
Tm169 (ppm)	-	-	-	-	-	-	-
Yb172 (ppm)	-	-	-	-	-	-	-
Lu175 (ppm)	-	-	-	-	-	-	-
Hf178 (ppm)	-	-	-	-	-	-	-
Ta181 (ppm)	-	-	BDL	-	BDL	BDL	-
W182 (ppm)	-	-	BDL	BDL	BDL	BDL	BDL
Re185 (ppm)	BDL	BDL	0	BDL	BDL	BDL	BDL
Os189 (ppm)	BDL	BDL	BDL	BDL	-	BDL	-
Ir193 (ppm)	0	-	-	-	BDL	-	-
Pt195 (ppm)	BDL	-	-	BDL	BDL	BDL	-
Au197 (ppm)	-	-	-	BDL	974	372	646
Hg202 (ppm)	1144	1925	353	511	1418	558	985
Pb204 (ppm)	3110	4611	883	1189	BDL	BDL	BDL
Tl205 (ppm)	0	BDL	0	BDL	0	4	-
Pb206 (ppm)	45	2	45	13	0	3	-
Pb207 (ppm)	27	-	48	10	0	3	1
Pb208 (ppm)	28	1	46	7	BDL	0	BDL
Bi209 (ppm)	1	BDL	4	1	-	-	-
Th232 (ppm)	-	-	-	-	-	-	-
U238 (ppm)	-	-	-	-	21	11	15
PbTotal (ppm)	78	71	59	32	-	-	-

Table D5. Trace element data for cobaltite.

Deposit	Betts Cove	Betts Cove	Tilt Cove	Tilt Cove	Tilt Cove	Tilt Cove	Tilt Cove	Tilt Cove	Tilt Cove
Sample	KKMSC09_Cob 9	KKMSC09_Cob 12	KKMSC63_Cob 11	KKMSC63_Cob 5	KKMSC63_Cob 7	KKMSC70_Cob 3	KKMSC70_Cob 15	KKMSC70_Cob 14	KKMSC70_Cob 6
Date	2023-11-20	2023-11-20	2023-11-21	2023-11-21	2023-11-21	2023-11-22	2023-11-22	2023-11-22	2023-11-22
Facies	Chalcopyrite-dominated	Chalcopyrite-dominated	Pyrite-dominated	Pyrite-dominated	Pyrite-dominated	Chalcopyrite - pyrrhotite-dominated	Chalcopyrite - pyrrhotite-dominated	Chalcopyrite - pyrrhotite-dominated	Chalcopyrite - pyrrhotite-dominated
Li7 (ppm)	BDL	547	BDL	62	BDL	7	5	BDL	BDL
Be9 (ppm)	BDL	BDL	BDL	-	BDL	-	-	BDL	-
B11 (ppm)	BDL	277	BDL	BDL	BDL	BDL	BDL	BDL	BDL
Na23 (ppm)	BDL	1110	512	337	BDL	BDL	BDL	BDL	BDL
Mg24 (ppm)	14339	251571	172717	33876	58319	355336	18377	5339	11400
Al27 (ppm)	19348	324197	495	2512	15457	8324	591	161	285
Si29 (ppm)	82916	3609009	251480	137806	167888	327574	43788	7585	16468
P31 (ppm)	BDL	1927	BDL	1287	4500	246	317	BDL	BDL
S32 (ppm)	308709	14082234	2011515	12664920	56906044	2756188	2987357	264932	845180
K39 (ppm)	BDL	626	BDL	272	BDL	BDL	BDL	BDL	BDL
Ca44 (ppm)	BDL	4582	1251	1872	BDL	BDL	BDL	BDL	BDL
Sc45 (ppm)	5	130	7	7	BDL	14	BDL	BDL	BDL
Ti47 (ppm)	9	66	230	148	1946	64	BDL	BDL	BDL
V51 (ppm)	47	997	21	54	126	35	BDL	1	BDL
Cr52 (ppm)	155	1785	354	469	1840	54	19	BDL	BDL
Mn55 (ppm)	797	12383	80	255	269	345	19	19	20
Fe57 (ppm)	156175	11821998	1368036	10559345	68921371	2605964	2952565	60306	829284
Co59 (ppm)	-	-	-	-	-	-	-	-	-
Ni60 (ppm)	4542	-	51629	60777	-	89769	-	-	-
Cu63 (ppm)	63748	1226390	108970	424820	245676	10460	8393	3586	24663
Zn66 (ppm)	228	8557	8277	9285	2495	98	30	6	210
Ga71 (ppm)	-	18	-	-	-	-	BDL	-	-
Ge73 (ppm)	BDL	266	-	12	-	BDL	BDL	BDL	BDL
As75 (ppm)	657816	799167	650816	677999	234320	893412	1484193	675292	790637
Se77 (ppm)	1866	29116	3599	2772	10606	917	1388	325	569
Rb85 (ppm)	BDL	BDL	BDL	1	BDL	BDL	BDL	BDL	BDL
Sr88 (ppm)	-	-	-	-	-	-	-	BDL	-
Y89 (ppm)	1	-	-	1	-	-	-	-	-
Zr90 (ppm)	-	-	-	-	-	-	-	-	-
Nb93 (ppm)	-	-	5	79	40	BDL	-	-	BDL
Mo95 (ppm)	-	2844	-	-	-	6	BDL	3	1
Ru101 (ppm)	-	-	3	-	-	-	-	-	BDL
Rh103 (ppm)	-	-	10	-	-	-	-	-	0
Pd104 (ppm)	-	5	7	-	-	-	BDL	-	-

Pd105 (ppm)	5	26	-	3	BDL	-	-	BDL	BDL
Pd106 (ppm)	-	-	225	106	85	-	BDL	-	BDL
Ag107 (ppm)	137	-	137	39	-	93	94	-	71
Cd111 (ppm)	-	-	67	-	1910	BDL	-	BDL	4
In115 (ppm)	-	-	BDL	3	BDL	-	-	-	3
Sn118 (ppm)	BDL	44	608	855	266	BDL	BDL	BDL	BDL
Sb121 (ppm)	49	721	170	1059	-	406	302	155	194
Te125 (ppm)	-	-	BDL	1	BDL	1329	1015	403	671
Cs133 (ppm)	BDL	BDL	-	-	-	1	2	BDL	BDL
Ba137 (ppm)	-	-	-	-	-	-	-	-	-
La139 (ppm)	-	-	-	-	-	-	-	-	-
Ce140 (ppm)	-	-	-	-	-	-	-	-	-
Pr141 (ppm)	-	-	-	-	-	-	-	-	-
Nd146 (ppm)	-	-	-	-	-	-	-	-	-
Sm147 (ppm)	-	-	-	-	-	-	-	-	-
Eu153 (ppm)	-	-	-	-	-	BDL	-	-	-
Gd157 (ppm)	-	-	-	-	-	-	-	-	BDL
Tb159 (ppm)	-	-	-	-	-	-	BDL	-	-
Dy163 (ppm)	-	-	-	-	-	-	-	-	-
Ho165 (ppm)	-	-	-	-	-	-	-	-	-
Er166 (ppm)	-	-	-	-	-	-	-	-	-
Tm169 (ppm)	-	-	-	-	-	-	-	-	-
Yb172 (ppm)	-	-	-	-	-	-	-	-	-
Lu175 (ppm)	-	-	-	-	-	-	-	-	-
Hf178 (ppm)	-	-	-	-	-	-	-	-	-
Ta181 (ppm)	-	-	-	-	-	-	-	-	-
W182 (ppm)	-	-	BDL	BDL	BDL	-	-	-	-
Re185 (ppm)	3	15	BDL	7	BDL	BDL	BDL	BDL	BDL
Os189 (ppm)	BDL	BDL	-	BDL	-	BDL	3	BDL	BDL
Ir193 (ppm)	-	-	BDL	BDL	BDL	-	-	-	-
Pt195 (ppm)	BDL	BDL	-	71	-	BDL	BDL	BDL	BDL
Au197 (ppm)	-	64	65	1347	6080	13	-	-	-
Hg202 (ppm)	BDL	1374	17311	5513	8467	49	91	BDL	36
Pb204 (ppm)	2969	56899	77	22	BDL	1387	1240	121	999
Tl205 (ppm)	1	86	16098	3651	2206	39	3	1	8
Pb206 (ppm)	3173	-	16906	3596	-	1499	-	122	-
Pb207 (ppm)	-	58100	-	3551	1788	1413	-	-	952
Pb208 (ppm)	3454	55794	27	106	180	1210	524	106	-
Bi209 (ppm)	59	1664	-	-	-	418	404	113	255
Th232 (ppm)	-	-	-	-	-	-	-	-	-
U238 (ppm)	-	-	15522	3615	2011	BDL	-	-	-
PbTotal (ppm)	3356	56791	-	-	-	1403	558	111	962

Table D5. Trace element data for cobaltite continued.

Deposit	Tilt Cove	Tilt Cove	Tilt Cove	Tilt Cove	Tilt Cove	Tilt Cove	Tilt Cove	Tilt Cove	Tilt Cove
Sample	KKMSC70_Cob 7	KKMSC70_Cob 8	KKMSC12_Cob 37	KKMSC12_Cob 38	KKMSC12_Cob 40	KKMSC12_Cob 20	KKMSC12_Cob 14	KKMSC12_Cob 30	KKMSC12_Cob 31
Date	2023-11-22	2023-11-22	2023-11-23	2023-11-23	2023-11-23	2023-11-23	2023-11-23	2023-11-23	2023-11-23
Facies	Chalcopyrite - pyrrhotite-dominated	Chalcopyrite - pyrrhotite-dominated	Chalcopyrite-dominated	Chalcopyrite-dominated	Chalcopyrite-dominated	Chalcopyrite-dominated	Chalcopyrite-dominated	Chalcopyrite-dominated	Chalcopyrite-dominated
Li7 (ppm)	3	BDL	316	18	17	54	99	BDL	42
Be9 (ppm)	-	-	BDL	-	-	BDL	-	-	-
B11 (ppm)	BDL	BDL	BDL	BDL	BDL	225	BDL	BDL	BDL
Na23 (ppm)	BDL	BDL	3593	137	BDL	373	453	137	818
Mg24 (ppm)	-	23433	-	4541	1933	17442	98259	13849	26536
Al27 (ppm)	2312	738	110135	3416	1435	11327	66998	1130	10752
Si29 (ppm)	153512	29075	171695	17180	BDL	45249	126451	21946	34209
P31 (ppm)	BDL	BDL	BDL	BDL	BDL	BDL	438	369	BDL
S32 (ppm)	1037451	798111	944929	375877	334932	543493	523274	769507	513850
K39 (ppm)	BDL	BDL	174	BDL	BDL	232	514	106	BDL
Ca44 (ppm)	BDL	BDL	7282	1185	2523	BDL	23855	52976	32575
Sc45 (ppm)	3	BDL	75	BDL	BDL	15	49	20	19
Ti47 (ppm)	-	BDL	61036	85	-	46	63	86	474
V51 (ppm)	7	3	452	22	4	44	162	8	26
Cr52 (ppm)	8	BDL	899	29	BDL	127	490	59	337
Mn55 (ppm)	171	34	695	36	41	80	1614	922	1395
Fe57 (ppm)	713995	581906	300279	43038	64319	82822	185864	92499	92802
Co59 (ppm)	-	-	-	-	-	-	-	-	-
Ni60 (ppm)	37386	37058	-	3335	4413	-	5493	-	-
Cu63 (ppm)	62134	9511	36652	1169	46528	27579	1494	116	41458
Zn66 (ppm)	62	38	331	22	20	114	189	44	74
Ga71 (ppm)	-	-	18	1	-	BDL	-	-	-
Ge73 (ppm)	BDL	-	BDL	-	-	6	BDL	BDL	BDL
As75 (ppm)	1151992	971774	968059	565029	412407	800184	676633	430256	651676
Se77 (ppm)	649	600	1657	923	664	1043	967	792	787
Rb85 (ppm)	BDL	-	BDL	BDL	BDL	BDL	BDL	BDL	1
Sr88 (ppm)	-	-	-	-	BDL	-	-	-	-
Y89 (ppm)	-	-	-	-	-	-	-	-	-
Zr90 (ppm)	-	-	-	-	BDL	-	-	-	BDL
Nb93 (ppm)	-	-	BDL	-	-	BDL	-	-	-
Mo95 (ppm)	BDL	BDL	-	-	-	-	-	-	-
Ru101 (ppm)	-	-	-	-	0	-	BDL	-	-
Rh103 (ppm)	-	-	BDL	8	3	4	-	-	1
Pd104 (ppm)	-	-	2	-	6	-	5	-	7

Pd105 (ppm)	-	-	2	9	5	2	-	3	-
Pd106 (ppm)	BDL	-	133	71	16	73	68	8	456
Ag107 (ppm)	88	68	BDL	BDL	BDL	BDL	BDL	BDL	3
Cd111 (ppm)	BDL	-	-	-	2	2	-	-	-
In115 (ppm)	4	1	BDL	BDL	BDL	10	BDL	BDL	BDL
Sn118 (ppm)	BDL	BDL	355	230	137	220	256	130	159
Sb121 (ppm)	253	224	4149	1519	800	1436	2007	594	-
Te125 (ppm)	887	670	5	BDL	BDL	BDL	3	1	BDL
Cs133 (ppm)	BDL	BDL	104	-	-	-	-	-	-
Ba137 (ppm)	-	-	-	-	-	-	-	-	-
La139 (ppm)	-	-	-	-	-	-	-	-	-
Ce140 (ppm)	-	-	-	-	-	-	-	-	-
Pr141 (ppm)	-	-	-	-	-	-	-	-	-
Nd146 (ppm)	-	-	-	-	-	-	-	-	-
Sm147 (ppm)	-	-	-	-	-	-	-	-	-
Eu153 (ppm)	-	-	-	-	-	-	-	-	BDL
Gd157 (ppm)	-	-	-	-	-	-	-	-	-
Tb159 (ppm)	-	-	-	-	-	-	-	-	-
Dy163 (ppm)	-	-	-	-	-	-	-	-	-
Ho165 (ppm)	-	-	-	-	-	-	-	-	-
Er166 (ppm)	-	-	-	-	-	-	-	-	-
Tm169 (ppm)	-	-	-	-	-	-	-	-	-
Yb172 (ppm)	-	-	-	-	-	-	-	1	-
Lu175 (ppm)	-	-	-	-	-	-	-	-	-
Hf178 (ppm)	-	-	-	-	-	-	-	-	-
Ta181 (ppm)	-	-	-	BDL	-	-	-	BDL	-
W182 (ppm)	BDL	BDL	BDL	BDL	BDL	BDL	2	BDL	BDL
Re185 (ppm)	BDL	BDL	BDL	BDL	BDL	BDL	BDL	7	5
Os189 (ppm)	2	BDL	-	BDL	BDL	BDL	-	BDL	BDL
Ir193 (ppm)	-	BDL	BDL	BDL	1	BDL	BDL	BDL	BDL
Pt195 (ppm)	-	BDL	-	-	-	-	-	12	-
Au197 (ppm)	-	-	1246	132	204	607	260	BDL	425
Hg202 (ppm)	19	BDL	1772	911	358	1255	935	BDL	1058
Pb204 (ppm)	1056	595	5	BDL	BDL	0	BDL	BDL	1
Tl205 (ppm)	14	6	547	825	-	314	434	52	-
Pb206 (ppm)	-	536	584	-	-	252	474	71	456
Pb207 (ppm)	1145	-	575	532	47	329	518	67	417
Pb208 (ppm)	1129	540	142	40	13	35	62	61	38
Bi209 (ppm)	264	246	-	-	-	-	-	-	-
Th232 (ppm)	-	-	-	-	-	-	-	-	-
U238 (ppm)	-	-	588	630	53	323	494	63	424
PbTotal (ppm)	1131	546	-	-	-	-	-	-	-

Table D5. Trace element data for cobaltite continued.

Deposit	Tilt Cove	Tilt Cove	Tilt Cove	Tilt Cove	Tilt Cove	Tilt Cove	Tilt Cove	Tilt Cove	Tilt Cove
Sample	KKMSC12_Cob 32	KKMSC12_Cob 11	KKMSC12_Cob 12	KKMSC12_Cob 13	KKMSC12_Cob 1	KKMSC12_Cob 2	KKMSC12_Cob 3	KKMSC12_Cob 4	KKMSC12_Cob 6
Date	2023-11-23	2023-11-23	2023-11-23	2023-11-23	2023-11-23	2023-11-23	2023-11-23	2023-11-23	2023-11-23
Facies	Chalcopyrite-dominated	Chalcopyrite-dominated	Chalcopyrite-dominated	Chalcopyrite-dominated	Chalcopyrite-dominated	Chalcopyrite-dominated	Chalcopyrite-dominated	Chalcopyrite-dominated	Chalcopyrite-dominated
Li7 (ppm)	24	4	7	BDL	6	BDL	BDL	BDL	BDL
Be9 (ppm)	-	-	-	-	-	-	-	BDL	-
B11 (ppm)	BDL	BDL	BDL	BDL	BDL	BDL	BDL	BDL	BDL
Na23 (ppm)	374	BDL	BDL	BDL	BDL	BDL	BDL	BDL	BDL
Mg24 (ppm)	60923	266	1998	354	1352	258	116	207	127
Al27 (ppm)	13044	179	544	300	895	143	68	145	98
Si29 (ppm)	24040	4861	3195	2045	4641	1540	BDL	BDL	BDL
P31 (ppm)	BDL	BDL	BDL	BDL	BDL	BDL	BDL	BDL	BDL
S32 (ppm)	777371	274125	335358	282475	392362	295324	274174	335799	302193
K39 (ppm)	BDL	BDL	BDL	BDL	BDL	BDL	BDL	BDL	BDL
Ca44 (ppm)	85936	BDL	2071	BDL	BDL	BDL	BDL	BDL	BDL
Sc45 (ppm)	12	BDL	2	BDL	BDL	BDL	BDL	BDL	BDL
Ti47 (ppm)	39	1529	BDL	BDL	BDL	BDL	-	BDL	1557
V51 (ppm)	32	1	3	1	1	0	BDL	BDL	BDL
Cr52 (ppm)	396	BDL	11	BDL	23	BDL	BDL	BDL	BDL
Mn55 (ppm)	3660	88	123	6	10	3	1	3	60
Fe57 (ppm)	339990	45019	49448	44397	69021	49619	47118	51805	53088
Co59 (ppm)	-	-	-	-	-	-	-	-	-
Ni60 (ppm)	21940	-	2864	-	-	1327	1259	-	1252
Cu63 (ppm)	288182	4521	3183	1546	24798	6720	4469	5260	7633
Zn66 (ppm)	108	10	19	3	77	22	16	40	38
Ga71 (ppm)	-	-	-	-	-	-	-	-	-
Ge73 (ppm)	BDL	BDL	BDL	-	BDL	-	BDL	-	BDL
As75 (ppm)	745371	485413	559119	493272	633115	546917	514303	681751	601424
Se77 (ppm)	1137	598	752	706	783	787	772	975	927
Rb85 (ppm)	-	BDL	BDL	BDL	BDL	BDL	BDL	BDL	BDL
Sr88 (ppm)	-	-	-	-	-	-	-	BDL	-
Y89 (ppm)	-	-	-	-	BDL	-	-	-	BDL
Zr90 (ppm)	-	-	BDL	-	BDL	-	-	-	-
Nb93 (ppm)	-	2	-	-	BDL	-	-	1	-
Mo95 (ppm)	-	-	-	-	-	-	-	-	-
Ru101 (ppm)	8	0	BDL	BDL	-	-	-	0	-
Rh103 (ppm)	-	-	2	-	-	-	9	-	-
Pd104 (ppm)	-	-	-	-	-	14	13	-	15

Pd105 (ppm)	7	5	1	2	10	10	-	-	15
Pd106 (ppm)	192	2	3	21	7	2	1	3	6
Ag107 (ppm)	-	BDL	BDL	BDL	BDL	BDL	BDL	-	-
Cd111 (ppm)	29	-	0	-	-	1	1	-	-
In115 (ppm)	2	BDL	BDL	BDL	BDL	BDL	BDL	BDL	BDL
Sn118 (ppm)	183	142	186	202	117	133	138	209	176
Sb121 (ppm)	1515	1088	1024	1201	1213	1175	1296	1385	1751
Te125 (ppm)	BDL	BDL	BDL	BDL	BDL	BDL	BDL	BDL	BDL
Cs133 (ppm)	-	-	-	-	-	-	-	-	-
Ba137 (ppm)	-	-	-	-	-	-	-	-	-
La139 (ppm)	-	-	-	-	-	-	-	BDL	-
Ce140 (ppm)	-	-	-	-	-	-	-	-	-
Pr141 (ppm)	-	-	-	-	-	-	-	-	-
Nd146 (ppm)	-	-	-	-	-	-	-	-	-
Sm147 (ppm)	-	-	-	-	-	-	-	-	-
Eu153 (ppm)	-	-	-	-	-	-	-	-	-
Gd157 (ppm)	-	-	-	-	-	-	-	-	-
Tb159 (ppm)	-	-	-	-	-	-	-	-	-
Dy163 (ppm)	-	-	-	-	-	-	-	-	-
Ho165 (ppm)	-	-	-	-	-	-	-	-	-
Er166 (ppm)	-	-	-	-	-	-	-	-	-
Tm169 (ppm)	-	-	-	-	-	-	-	-	-
Yb172 (ppm)	-	-	-	-	-	-	-	-	-
Lu175 (ppm)	-	-	-	-	-	-	-	-	-
Hf178 (ppm)	-	BDL	BDL	-	BDL	-	BDL	-	-
Ta181 (ppm)	-	-	BDL	BDL	-	BDL	BDL	-	0
W182 (ppm)	BDL	BDL	BDL	BDL	BDL	BDL	BDL	BDL	BDL
Re185 (ppm)	BDL	BDL	BDL	BDL	BDL	BDL	BDL	BDL	BDL
Os189 (ppm)	BDL	BDL	-	BDL	-	BDL	-	-	-
Ir193 (ppm)	BDL	BDL	BDL	BDL	BDL	BDL	BDL	BDL	-
Pt195 (ppm)	10	-	2	2	-	-	-	1	-
Au197 (ppm)	228	30	50	BDL	124	BDL	BDL	BDL	BDL
Hg202 (ppm)	837	93	91	BDL	178	31	31	71	60
Pb204 (ppm)	1	0	BDL	BDL	BDL	BDL	BDL	BDL	0
Tl205 (ppm)	372	39	55	16	62	23	20	49	53
Pb206 (ppm)	358	42	73	17	64	-	19	58	-
Pb207 (ppm)	352	40	54	18	65	21	21	87	60
Pb208 (ppm)	27	5	8	5	8	4	4	4	6
Bi209 (ppm)	-	-	-	-	-	-	-	-	-
Th232 (ppm)	BDL	-	BDL	-	-	-	-	-	-
U238 (ppm)	366	41	59	17	66	22	20	71	57
PbTotal (ppm)	-	-	-	-	-	-	-	-	-

Table D5. Trace element data for cobaltite continued.

Deposit	Tilt Cove	Tilt Cove	Tilt Cove	Tilt Cove
Sample	KKMSC12_Cob7	KKMSC12_Cob8	KKMSC12_Cob9	KKMSC12_Cob10
Date	2023-11-23	2023-11-23	2023-11-23	2023-11-23
Facies	Chalcopyrite-dominated	Chalcopyrite-dominated	Chalcopyrite-dominated	Chalcopyrite-dominated
Li7 (ppm)	2	BDL	BDL	BDL
Be9 (ppm)	BDL	-	BDL	BDL
B11 (ppm)	BDL	BDL	BDL	BDL
Na23 (ppm)	BDL	BDL	BDL	BDL
Mg24 (ppm)	977	38	62	48
Al27 (ppm)	341	36	24	39
Si29 (ppm)	4348	BDL	1583	BDL
P31 (ppm)	BDL	BDL	BDL	BDL
S32 (ppm)	294214	360941	262394	177163
K39 (ppm)	BDL	BDL	BDL	BDL
Ca44 (ppm)	582	BDL	BDL	BDL
Sc45 (ppm)	BDL	BDL	BDL	BDL
Ti47 (ppm)	BDL	BDL	BDL	BDL
V51 (ppm)	1	2	0	BDL
Cr52 (ppm)	BDL	BDL	BDL	BDL
Mn55 (ppm)	39	13	BDL	1
Fe57 (ppm)	60781	87668	44371	38923
Co59 (ppm)	-	-	-	-
Ni60 (ppm)	-	-	915	928
Cu63 (ppm)	17261	180	1021	77
Zn66 (ppm)	31	BDL	BDL	BDL
Ga71 (ppm)	-	-	-	-
Ge73 (ppm)	BDL	BDL	-	-
As75 (ppm)	579186	480020	540674	443979
Se77 (ppm)	581	1243	717	461
Rb85 (ppm)	BDL	BDL	BDL	BDL
Sr88 (ppm)	-	-	-	-
Y89 (ppm)	-	-	BDL	-
Zr90 (ppm)	-	-	-	-
Nb93 (ppm)	-	-	5	3
Mo95 (ppm)	-	BDL	-	-
Ru101 (ppm)	-	-	-	-
Rh103 (ppm)	-	-	6	7
Pd104 (ppm)	7	9	10	-

Pd105 (ppm)	6	9	7	-
Pd106 (ppm)	5	-	BDL	-
Ag107 (ppm)	BDL	-	BDL	BDL
Cd111 (ppm)	-	-	0	-
In115 (ppm)	BDL	BDL	BDL	BDL
Sn118 (ppm)	88	448	147	126
Sb121 (ppm)	651	1522	1027	958
Te125 (ppm)	BDL	BDL	BDL	BDL
Cs133 (ppm)	-	-	-	-
Ba137 (ppm)	-	-	-	-
La139 (ppm)	-	-	-	-
Ce140 (ppm)	-	-	-	-
Pr141 (ppm)	BDL	-	-	-
Nd146 (ppm)	-	-	-	-
Sm147 (ppm)	-	-	-	-
Eu153 (ppm)	-	-	-	-
Gd157 (ppm)	-	-	-	-
Tb159 (ppm)	-	-	-	-
Dy163 (ppm)	-	-	-	-
Ho165 (ppm)	-	-	-	-
Er166 (ppm)	-	-	-	-
Tm169 (ppm)	-	-	-	-
Yb172 (ppm)	-	-	-	-
Lu175 (ppm)	-	-	-	-
Hf178 (ppm)	-	-	-	-
Ta181 (ppm)	-	-	-	-
W182 (ppm)	BDL	1	BDL	BDL
Re185 (ppm)	BDL	2	BDL	BDL
Os189 (ppm)	-	BDL	-	-
Ir193 (ppm)	BDL	BDL	BDL	BDL
Pt195 (ppm)	1	-	0	-
Au197 (ppm)	20	BDL	BDL	29
Hg202 (ppm)	61	145	22	BDL
Pb204 (ppm)	BDL	0	BDL	BDL
Tl205 (ppm)	25	22	7	27
Pb206 (ppm)	24	21	5	29
Pb207 (ppm)	25	22	6	48
Pb208 (ppm)	6	8	2	6
Bi209 (ppm)	-	-	-	-
Th232 (ppm)	-	-	-	-
U238 (ppm)	25	24	6	39
PbTotal (ppm)	-	-	-	-

Table D6. Trace element data for pentlandite.

Deposit	Tilt Cove	Tilt Cove	Tilt Cove	Betts Cove	Betts Cove	Betts Cove	Betts Cove	Betts Cove	Tilt Cove
Sample	KKMSC63_Pnt 1	KKMSC63_Pnt 2	KKMSC63_Pnt 6	KKMSC53_Pnt 5	KKMSC53_Pnt 7	KKMSC53_Pnt 4	KKMSC53_Pnt 2	KKMSC53_Pnt 1	KKMSC72_Pnt 22
Date	2023-11-21	2023-11-21	2023-11-21	2023-11-22	2023-11-22	2023-11-22	2023-11-22	2023-11-22	2023-11-22
Facies	Pyrite-dominated	Pyrite-dominated	Pyrite-dominated	Chalcopyrite-dominated	Chalcopyrite-dominated	Chalcopyrite-dominated	Chalcopyrite-dominated	Chalcopyrite-dominated	Pyrrhotite-dominated
Li7 (ppm)	3	6	BDL	BDL	6	2	BDL	2	BDL
Be9 (ppm)	BDL	BDL	-	-	-	-	-	-	-
B11 (ppm)	BDL	BDL	BDL	BDL	BDL	BDL	BDL	BDL	BDL
Na23 (ppm)	486	605	30	BDL	142	BDL	BDL	BDL	BDL
Mg24 (ppm)	446	4717	257	350	4836	-	430	142	670
Al27 (ppm)	165	793	24	81	2535	20	436	174	53
Si29 (ppm)	6074	6615	1700	BDL	16645	BDL	5284	3610	2807
P31 (ppm)	119	145	BDL	BDL	BDL	77	BDL	BDL	BDL
S32 (ppm)	2284290	527481	621301	1184215	1757729	1126744	1524185	1333801	1080020
K39 (ppm)	87	111	BDL	BDL	BDL	BDL	BDL	BDL	BDL
Ca44 (ppm)	391	3684	144	61137	1408	31312	735	BDL	BDL
Sc45 (ppm)	2	BDL	1	BDL	BDL	BDL	BDL	BDL	BDL
Ti47 (ppm)	BDL	7	BDL	6	BDL	-	BDL	BDL	BDL
V51 (ppm)	1	5	BDL	1	2	BDL	BDL	BDL	BDL
Cr52 (ppm)	11	36	BDL	15	BDL	BDL	BDL	BDL	BDL
Mn55 (ppm)	60	288	14	269	1165	218	45	38	37
Fe57 (ppm)	1311807	430636	396391	239438	412425	211740	353777	351491	289050
Co59 (ppm)	3777	3036	2987	-	26948	13990	16393	4259	18997
Ni60 (ppm)	-	-	-	-	-	-	-	-	-
Cu63 (ppm)	1105567	1411	47617	53679	183665	53487	179626	102687	2857
Zn66 (ppm)	1293	681	61	127	324858	152	8	12	5
Ga71 (ppm)	-	-	-	-	-	BDL	-	-	-
Ge73 (ppm)	BDL	-	BDL	-	-	BDL	BDL	-	-
As75 (ppm)	107	93	64	74	24	91	14	8	5
Se77 (ppm)	1125	263	266	2192	3428	2451	3953	3355	170
Rb85 (ppm)	BDL	BDL	BDL	BDL	BDL	BDL	BDL	0	BDL
Sr88 (ppm)	-	-	-	-	-	-	-	-	-
Y89 (ppm)	-	-	-	-	-	-	-	-	-
Zr90 (ppm)	-	-	-	-	-	-	BDL	-	-
Nb93 (ppm)	-	-	1	-	-	-	-	-	-
Mo95 (ppm)	-	1	-	-	BDL	1	BDL	-	BDL
Ru101 (ppm)	-	-	-	-	-	-	-	-	-
Rh103 (ppm)	-	2	-	-	-	-	-	2	-
Pd104 (ppm)	-	BDL	-	-	-	-	-	-	-

Pd105 (ppm)	-	BDL	0	-	-	-	-	5	BDL
Pd106 (ppm)	239	158	132	-	87	BDL	-	0	-
Ag107 (ppm)	-	6	4	320	-	150	388	240	14
Cd111 (ppm)	-	-	-	-	-	4	3	-	BDL
In115 (ppm)	21	BDL	BDL	-	-	-	-	BDL	-
Sn118 (ppm)	515	506	553	BDL	2	BDL	BDL	BDL	BDL
Sb121 (ppm)	BDL	3	2	2	4	-	0	0	10
Te125 (ppm)	BDL	BDL	BDL	6	6	4	-	-	11
Cs133 (ppm)	-	-	-	BDL	BDL	BDL	BDL	BDL	BDL
Ba137 (ppm)	-	-	-	-	-	-	-	-	-
La139 (ppm)	-	-	-	-	-	-	-	-	-
Ce140 (ppm)	-	-	-	-	-	-	-	-	-
Pr141 (ppm)	-	-	-	-	-	-	-	-	-
Nd146 (ppm)	-	-	-	-	-	-	-	-	-
Sm147 (ppm)	-	-	-	-	-	-	-	-	-
Eu153 (ppm)	-	-	-	-	-	-	-	-	-
Gd157 (ppm)	-	-	-	-	-	-	-	-	-
Tb159 (ppm)	-	-	-	-	-	-	-	-	-
Dy163 (ppm)	-	-	-	BDL	-	-	-	-	-
Ho165 (ppm)	-	-	-	-	-	-	-	-	-
Er166 (ppm)	-	-	-	-	-	-	-	-	-
Tm169 (ppm)	-	-	-	-	-	-	-	-	-
Yb172 (ppm)	-	-	-	-	-	-	-	-	-
Lu175 (ppm)	-	-	-	-	-	-	-	-	-
Hf178 (ppm)	-	-	-	-	-	-	-	-	-
Ta181 (ppm)	-	-	-	-	-	-	-	-	-
W182 (ppm)	1	BDL	BDL	-	-	BDL	-	-	-
Re185 (ppm)	BDL	BDL	BDL	BDL	BDL	BDL	BDL	BDL	BDL
Os189 (ppm)	-	BDL	-	BDL	BDL	BDL	BDL	BDL	BDL
Ir193 (ppm)	BDL	BDL	BDL	-	BDL	-	BDL	-	BDL
Pt195 (ppm)	-	-	0	BDL	-	BDL	BDL	BDL	BDL
Au197 (ppm)	84	BDL	56	-	0	-	-	-	1
Hg202 (ppm)	392	1110	944	10	28	BDL	39	38	21
Pb204 (ppm)	961	543	1146	BDL	155	75	122	99	119
Tl205 (ppm)	-	1074	992	89	45	78	66	46	78
Pb206 (ppm)	526	-	-	-	131	79	69	-	125
Pb207 (ppm)	557	1045	929	61	131	69	72	80	118
Pb208 (ppm)	-	0	0	67	137	75	69	83	139
Bi209 (ppm)	-	-	-	0	1	0	0	0	7
Th232 (ppm)	-	-	-	-	-	-	-	-	-
U238 (ppm)	570	1064	951	-	-	-	-	-	-
PbTotal (ppm)	-	-	-	66	135	75	70	84	130

Table D6. Trace element data for pentlandite continued.

Deposit	Tilt Cove	Tilt Cove	Tilt Cove	Tilt Cove	Tilt Cove	Tilt Cove	Tilt Cove	Tilt Cove	Tilt Cove
Sample	KKMSC72_Pnt 21	KKMSC72_Pnt 20	KKMSC72_Pnt 11	KKMSC72_Pnt 12	KKMSC72_Pnt 10	KKMSC72_Pnt 9	KKMSC72_Pnt 3	KKMSC72_Pnt 2	KKMSC72_Pnt 1
Date	2023-11-22	2023-11-22	2023-11-22	2023-11-22	2023-11-22	2023-11-22	2023-11-22	2023-11-22	2023-11-22
Facies	Pyrrhotite-dominated	Pyrrhotite-dominated	Pyrrhotite-dominated	Pyrrhotite-dominated	Pyrrhotite-dominated	Pyrrhotite-dominated	Pyrrhotite-dominated	Pyrrhotite-dominated	Pyrrhotite-dominated
Li7 (ppm)	BDL	7	BDL	BDL	8	BDL	BDL	BDL	BDL
Be9 (ppm)	-	BDL	-	-	BDL	BDL	BDL	-	-
B11 (ppm)	BDL	BDL	BDL	BDL	BDL	BDL	BDL	BDL	BDL
Na23 (ppm)	BDL	108	BDL	BDL	506	BDL	BDL	BDL	BDL
Mg24 (ppm)	-	-	134	1002	41667	12723	455	13458	119
Al27 (ppm)	15	208	BDL	28	1659	50	10	137	3
Si29 (ppm)	BDL	BDL	BDL	BDL	81274	2933	BDL	24168	BDL
P31 (ppm)	BDL	BDL	BDL	BDL	BDL	BDL	BDL	BDL	BDL
S32 (ppm)	1006230	1450059	1756739	1181790	7654726	1881510	1189531	1972248	1966907
K39 (ppm)	BDL	BDL	BDL	BDL	158	BDL	BDL	BDL	BDL
Ca44 (ppm)	BDL	1462	BDL	BDL	2373	BDL	BDL	BDL	BDL
Sc45 (ppm)	BDL	BDL	BDL	BDL	12	BDL	BDL	BDL	BDL
Ti47 (ppm)	BDL	-	BDL	BDL	-	-	BDL	BDL	BDL
V51 (ppm)	BDL	1	BDL	BDL	BDL	BDL	BDL	BDL	BDL
Cr52 (ppm)	BDL	17	BDL	BDL	47	BDL	BDL	BDL	BDL
Mn55 (ppm)	10	5399	8	32	396	1959	48	22	51
Fe57 (ppm)	252831	369102	136674	342689	3300140	146899	332078	150329	136929
Co59 (ppm)	17246	19510	262536	-	18939	296855	25180	320787	300561
Ni60 (ppm)	-	-	-	-	-	-	-	-	-
Cu63 (ppm)	2748	105271	26	151	305	24	4	46	36
Zn66 (ppm)	29	4031	BDL	75	127	3	7	15	2
Ga71 (ppm)	-	-	-	-	-	-	-	-	-
Ge73 (ppm)	-	BDL	BDL	-	BDL	-	-	BDL	BDL
As75 (ppm)	BDL	BDL	4	213	BDL	4	BDL	BDL	BDL
Se77 (ppm)	170	286	542	298	1759	681	274	592	649
Rb85 (ppm)	BDL	BDL	-	BDL	BDL	BDL	-	BDL	BDL
Sr88 (ppm)	-	-	-	-	-	-	-	-	-
Y89 (ppm)	-	-	-	-	-	-	-	-	-
Zr90 (ppm)	-	-	-	-	-	-	-	-	-
Nb93 (ppm)	BDL	-	-	-	-	-	-	-	-
Mo95 (ppm)	-	-	-	-	-	BDL	BDL	-	-
Ru101 (ppm)	BDL	-	-	-	-	-	-	1	-
Rh103 (ppm)	-	2	-	BDL	-	-	-	-	-
Pd104 (ppm)	1	-	-	2	-	-	-	-	1

Pd105 (ppm)	-	-	-	-	BDL	-	-	-	-
Pd106 (ppm)	BDL	2	BDL	BDL	BDL	BDL	BDL	-	BDL
Ag107 (ppm)	6	139	0	6	26	0	5	BDL	BDL
Cd111 (ppm)	BDL	39	BDL	-	BDL	-	BDL	-	BDL
In115 (ppm)	-	-	BDL	-	-	-	BDL	-	-
Sn118 (ppm)	BDL	BDL	BDL	BDL	BDL	1	BDL	BDL	BDL
Sb121 (ppm)	8	87	1	9	50	1	3	1	1
Te125 (ppm)	3	-	-	-	8	16	-	6	4
Cs133 (ppm)	BDL	BDL	BDL	BDL	BDL	BDL	BDL	BDL	BDL
Ba137 (ppm)	-	-	-	-	-	-	-	-	-
La139 (ppm)	-	-	-	-	-	-	-	-	-
Ce140 (ppm)	-	-	-	-	-	-	-	-	-
Pr141 (ppm)	-	-	-	-	-	-	-	-	-
Nd146 (ppm)	-	-	-	-	-	-	-	-	-
Sm147 (ppm)	-	-	-	-	-	-	-	-	-
Eu153 (ppm)	-	-	-	-	-	-	-	-	-
Gd157 (ppm)	-	-	-	-	-	-	BDL	-	-
Tb159 (ppm)	-	-	-	-	-	-	-	-	-
Dy163 (ppm)	-	-	-	-	-	-	-	-	-
Ho165 (ppm)	-	-	-	-	-	-	-	-	-
Er166 (ppm)	-	-	-	-	-	-	-	-	-
Tm169 (ppm)	-	-	-	-	-	-	-	-	-
Yb172 (ppm)	-	-	-	-	-	-	-	-	-
Lu175 (ppm)	-	-	-	-	-	-	-	-	-
Hf178 (ppm)	-	-	-	-	-	-	-	-	-
Ta181 (ppm)	-	BDL	-	-	-	-	-	-	-
W182 (ppm)	BDL	-	-	-	BDL	-	-	-	-
Re185 (ppm)	BDL	BDL	BDL	BDL	BDL	BDL	BDL	BDL	BDL
Os189 (ppm)	BDL	BDL	BDL	BDL	4	BDL	BDL	BDL	BDL
Ir193 (ppm)	BDL	BDL	BDL	BDL	BDL	-	-	BDL	BDL
Pt195 (ppm)	BDL	BDL	BDL	-	BDL	BDL	BDL	BDL	-
Au197 (ppm)	-	1	BDL	-	-	-	-	BDL	-
Hg202 (ppm)	BDL	BDL	42	19	234	41	BDL	40	40
Pb204 (ppm)	79	232	74	BDL	535	72	70	59	64
Tl205 (ppm)	15	20	BDL	8	86	BDL	5	BDL	BDL
Pb206 (ppm)	68	261	2	-	866	-	48	5	-
Pb207 (ppm)	65	-	-	53	-	2	-	3	2
Pb208 (ppm)	62	241	3	54	821	2	50	3	2
Bi209 (ppm)	2	4	1	3	25	1	1	3	4
Th232 (ppm)	-	-	-	-	-	-	-	-	-
U238 (ppm)	-	-	-	-	-	-	-	-	-
PbTotal (ppm)	65	248	4	53	829	3	49	5	3

Table D6. Trace element data for pentlandite continued.

Deposit	Tilt Cove	Tilt Cove	Tilt Cove	Tilt Cove	Tilt Cove	Tilt Cove	Tilt Cove	Tilt Cove	Tilt Cove
Sample	KKMSC72_Pnt 13	KKMSC72_Pnt 7	KKMSC72_Pnt 8	KKMSC72_Pnt 6	KKMSC72_Pnt 5	KKMSC72_Pnt 19	KKMSC72_Pnt 18	KKMSC72_Pnt 17	KKMSC72_Pnt 15
Date	2023-11-22	2023-11-22	2023-11-22	2023-11-22	2023-11-22	2023-11-22	2023-11-22	2023-11-22	2023-11-22
Facies	Pyrrhotite-dominated	Pyrrhotite-dominated	Pyrrhotite-dominated	Pyrrhotite-dominated	Pyrrhotite-dominated	Pyrrhotite-dominated	Pyrrhotite-dominated	Pyrrhotite-dominated	Pyrrhotite-dominated
Li7 (ppm)	BDL	BDL	3	BDL	BDL	BDL	3	3	BDL
Be9 (ppm)	-	BDL	-	-	-	-	-	-	-
B11 (ppm)	BDL	BDL	BDL	BDL	BDL	BDL	BDL	BDL	BDL
Na23 (ppm)	BDL	BDL	53	BDL	BDL	BDL	BDL	BDL	BDL
Mg24 (ppm)	60	54	563	66	46	-	-	536	221
Al27 (ppm)	3	BDL	24	7	4	16	61	112	18
Si29 (ppm)	BDL	BDL	BDL	BDL	BDL	BDL	BDL	BDL	BDL
P31 (ppm)	BDL	BDL	BDL	BDL	BDL	BDL	BDL	BDL	BDL
S32 (ppm)	1833933	1836323	1628107	1174782	1044585	1196119	1119079	1232629	1179491
K39 (ppm)	BDL	BDL	BDL	BDL	BDL	BDL	BDL	BDL	BDL
Ca44 (ppm)	BDL	BDL	BDL	BDL	BDL	BDL	BDL	BDL	BDL
Sc45 (ppm)	BDL	BDL	BDL	BDL	BDL	BDL	BDL	BDL	BDL
Ti47 (ppm)	BDL	BDL	BDL	BDL	BDL	BDL	-	BDL	-
V51 (ppm)	BDL	BDL	BDL	BDL	BDL	BDL	BDL	BDL	BDL
Cr52 (ppm)	BDL	BDL	BDL	BDL	BDL	BDL	BDL	BDL	BDL
Mn55 (ppm)	2	7	121	8	5	29	484	34	12
Fe57 (ppm)	143075	147475	589281	293629	279946	293858	274896	290056	286977
Co59 (ppm)	-	271699	-	18249	17040	19514	-	23336	23393
Ni60 (ppm)	-	-	-	-	-	-	-	-	-
Cu63 (ppm)	15	16	11	11	7	5084	33	6364	14078
Zn66 (ppm)	BDL	BDL	BDL	BDL	BDL	6	5	18	553
Ga71 (ppm)	-	-	-	-	-	BDL	-	-	-
Ge73 (ppm)	BDL	-	BDL	-	BDL	BDL	-	BDL	-
As75 (ppm)	BDL	BDL	5	BDL	BDL	BDL	BDL	BDL	BDL
Se77 (ppm)	950	603	357	222	270	417	396	429	421
Rb85 (ppm)	BDL	BDL	-	BDL	BDL	BDL	BDL	BDL	BDL
Sr88 (ppm)	-	-	-	-	-	-	-	-	-
Y89 (ppm)	-	-	-	-	-	-	-	-	-
Zr90 (ppm)	-	-	-	-	-	-	-	-	-
Nb93 (ppm)	-	-	-	-	BDL	-	-	-	-
Mo95 (ppm)	-	-	BDL	-	BDL	BDL	-	-	BDL
Ru101 (ppm)	-	-	-	-	-	-	-	-	-
Rh103 (ppm)	-	-	-	BDL	-	-	BDL	0	-
Pd104 (ppm)	-	1	-	-	1	-	-	-	-

Pd105 (ppm)	-	BDL	-	BDL	-	-	-	BDL	-
Pd106 (ppm)	BDL	BDL	-	-	-	BDL	BDL	BDL	0
Ag107 (ppm)	BDL	1	7	2	1	8	4	-	9
Cd111 (ppm)	-	BDL	-	BDL	BDL	-	BDL	-	12
In115 (ppm)	-	BDL	-	BDL	-	1	-	-	-
Sn118 (ppm)	BDL	BDL	BDL	1	BDL	BDL	BDL	BDL	BDL
Sb121 (ppm)	0	1	5	4	1	4	4	5	8
Te125 (ppm)	11	-	4	4	BDL	9	4	5	10
Cs133 (ppm)	BDL	BDL	BDL	BDL	BDL	BDL	BDL	BDL	BDL
Ba137 (ppm)	-	-	-	-	-	-	-	-	1
La139 (ppm)	-	-	-	-	-	-	-	-	-
Ce140 (ppm)	-	-	-	-	-	-	-	-	-
Pr141 (ppm)	-	-	-	-	-	-	-	-	-
Nd146 (ppm)	-	-	-	-	-	-	-	-	-
Sm147 (ppm)	-	-	-	-	-	-	-	-	-
Eu153 (ppm)	-	-	-	-	-	-	-	-	-
Gd157 (ppm)	-	-	-	-	-	-	-	-	-
Tb159 (ppm)	-	BDL	-	-	-	-	-	-	-
Dy163 (ppm)	-	-	-	-	-	-	-	-	-
Ho165 (ppm)	-	-	-	-	-	-	-	-	-
Er166 (ppm)	-	-	-	-	-	-	-	-	-
Tm169 (ppm)	-	-	-	-	-	-	-	-	-
Yb172 (ppm)	-	-	-	-	-	-	-	-	-
Lu175 (ppm)	-	-	-	-	-	-	-	-	-
Hf178 (ppm)	-	-	-	-	-	-	-	-	-
Ta181 (ppm)	-	-	-	-	-	-	-	-	-
W182 (ppm)	-	-	-	-	-	-	-	-	-
Re185 (ppm)	BDL	BDL	BDL	BDL	BDL	BDL	BDL	BDL	BDL
Os189 (ppm)	BDL	BDL	BDL	BDL	BDL	BDL	BDL	BDL	BDL
Ir193 (ppm)	-	BDL	BDL	-	BDL	BDL	BDL	-	-
Pt195 (ppm)	BDL	-	BDL	-	-	-	BDL	-	BDL
Au197 (ppm)	-	-	BDL	-	-	BDL	-	-	BDL
Hg202 (ppm)	32	41	15	17	BDL	23	15	21	11
Pb204 (ppm)	BDL	84	85	95	28	79	BDL	BDL	73
Tl205 (ppm)	BDL	BDL	3	3	1	12	10	5	9
Pb206 (ppm)	1	2	-	66	-	62	43	34	48
Pb207 (ppm)	2	2	49	56	15	68	42	-	-
Pb208 (ppm)	1	2	54	57	15	65	42	35	46
Bi209 (ppm)	2	4	4	4	0	3	1	1	3
Th232 (ppm)	-	-	-	-	-	-	-	-	-
U238 (ppm)	-	BDL	-	-	-	-	-	-	BDL
PbTotal (ppm)	2	3	52	60	15	65	43	35	46

Table D6. Trace element data for pentlandite continued.

Deposit	Tilt Cove	Tilt Cove	Tilt Cove	Tilt Cove	Tilt Cove	Tilt Cove	Tilt Cove	Tilt Cove	Tilt Cove
Sample	KKMSC70_Pnt 6	KKMSC70_Pnt 2	KKMSC70_Pnt 3	KKMSC70_Pnt 1	KKMSC70_Pnt 16	KKMSC70_Pnt 15	KKMSC70_Pnt 14	KKMSC70_Pnt 5	KKMSC70_Pnt 9
Date	2023-11-22	2023-11-22	2023-11-22	2023-11-22	2023-11-22	2023-11-22	2023-11-22	2023-11-22	2023-11-22
Facies	Chalcopyrite-pyrrhotite-dominated	Chalcopyrite-pyrrhotite-dominated	Chalcopyrite-pyrrhotite-dominated	Chalcopyrite-pyrrhotite-dominated	Chalcopyrite-pyrrhotite-dominated	Chalcopyrite-pyrrhotite-dominated	Chalcopyrite-pyrrhotite-dominated	Chalcopyrite-pyrrhotite-dominated	Chalcopyrite-pyrrhotite-dominated
Li7 (ppm)	BDL	BDL	262	BDL	BDL	BDL	BDL	BDL	BDL
Be9 (ppm)	-	BDL	-	BDL	-	BDL	-	-	-
B11 (ppm)	BDL	BDL	1758	BDL	BDL	BDL	BDL	BDL	BDL
Na23 (ppm)	BDL	BDL	5085	BDL	BDL	BDL	BDL	BDL	BDL
Mg24 (ppm)	165	211	244411	208	462	46	548	10063	8221
Al27 (ppm)	35	5	5009	BDL	23	BDL	8	87	189
Si29 (ppm)	BDL	BDL	1109855	BDL	BDL	BDL	BDL	14647	11013
P31 (ppm)	BDL	BDL	25282	BDL	BDL	BDL	BDL	BDL	BDL
S32 (ppm)	1457765	1245160	354396719	1250951	1317634	1302823	672307	1413850	1256595
K39 (ppm)	BDL	BDL	760	BDL	BDL	BDL	BDL	BDL	BDL
Ca44 (ppm)	BDL	BDL	104584	BDL	BDL	BDL	BDL	2791	BDL
Sc45 (ppm)	BDL	BDL	BDL	BDL	BDL	BDL	BDL	BDL	BDL
Ti47 (ppm)	-	BDL	-	BDL	BDL	BDL	BDL	-	BDL
V51 (ppm)	1	BDL	130	BDL	BDL	BDL	BDL	BDL	4
Cr52 (ppm)	BDL	BDL	2593	BDL	BDL	BDL	BDL	BDL	BDL
Mn55 (ppm)	4	8	1490	105	14	BDL	7	136	23
Fe57 (ppm)	299967	287798	56586488	280237	314383	275912	268725	269607	280230
Co59 (ppm)	10713	7411	7211	9677	13391	11734	15331	10921	29854
Ni60 (ppm)	-	-	-	-	-	-	-	-	-
Cu63 (ppm)	10	27	60382148	18	11	5	411	628	1396
Zn66 (ppm)	BDL	13	119659	533	3	4	7	27	14
Ga71 (ppm)	BDL	BDL	-	-	-	-	BDL	-	BDL
Ge73 (ppm)	BDL	BDL	-	-	BDL	BDL	BDL	-	-
As75 (ppm)	BDL	15	1390	11	BDL	1240	16372	782	32288
Se77 (ppm)	440	473	73873	406	361	413	409	441	619
Rb85 (ppm)	BDL	BDL	BDL	BDL	BDL	-	BDL	BDL	BDL
Sr88 (ppm)	-	-	-	-	-	-	-	-	BDL
Y89 (ppm)	-	-	-	-	-	-	-	-	-
Zr90 (ppm)	-	-	-	-	-	-	-	-	-
Nb93 (ppm)	-	BDL	-	-	BDL	-	-	-	-
Mo95 (ppm)	BDL	1	56	BDL	-	BDL	BDL	BDL	-
Ru101 (ppm)	-	-	-	-	-	-	-	-	-
Rh103 (ppm)	BDL	-	-	BDL	-	-	BDL	BDL	-
Pd104 (ppm)	-	-	BDL	-	-	-	BDL	-	-

Pd105 (ppm)	BDL	-	5098	BDL	-	BDL	-	-	-
Pd106 (ppm)	BDL	-	264	-	BDL	BDL	-	-	-
Ag107 (ppm)	BDL	BDL	-	1	-	-	3	4	5
Cd111 (ppm)	BDL	-	8647	-	BDL	-	2	-	-
In115 (ppm)	-	1	5365	-	-	-	0	-	-
Sn118 (ppm)	BDL	2	1562	BDL	BDL	BDL	1	BDL	BDL
Sb121 (ppm)	BDL	1	1053	2	4	1	12	2	18
Te125 (ppm)	7	6	282	-	12	13	64	3	66
Cs133 (ppm)	BDL	BDL	13	BDL	BDL	BDL	BDL	BDL	BDL
Ba137 (ppm)	-	-	-	-	-	-	-	-	-
La139 (ppm)	-	-	-	-	-	-	-	-	-
Ce140 (ppm)	-	-	-	-	-	-	-	-	-
Pr141 (ppm)	-	-	-	-	-	-	-	-	-
Nd146 (ppm)	-	-	-	-	-	-	-	-	-
Sm147 (ppm)	-	-	-	-	-	-	-	-	-
Eu153 (ppm)	-	-	-	-	-	-	-	-	-
Gd157 (ppm)	-	BDL	-	BDL	-	-	-	-	-
Tb159 (ppm)	-	-	-	-	-	-	-	-	-
Dy163 (ppm)	-	-	-	-	-	-	-	-	-
Ho165 (ppm)	-	-	-	-	-	-	-	-	-
Er166 (ppm)	-	-	-	-	-	-	-	-	-
Tm169 (ppm)	-	-	-	-	-	-	-	-	-
Yb172 (ppm)	-	-	-	-	-	-	-	-	-
Lu175 (ppm)	-	-	-	-	-	-	-	-	-
Hf178 (ppm)	-	-	-	-	-	BDL	-	-	-
Ta181 (ppm)	-	-	-	-	-	-	BDL	-	-
W182 (ppm)	-	-	-	BDL	-	-	BDL	-	-
Re185 (ppm)	BDL	BDL	6	BDL	BDL	BDL	BDL	BDL	BDL
Os189 (ppm)	BDL	BDL	25	BDL	BDL	BDL	BDL	BDL	BDL
Ir193 (ppm)	-	-	-	BDL	-	-	-	BDL	BDL
Pt195 (ppm)	BDL	BDL	-	BDL	BDL	BDL	BDL	-	-
Au197 (ppm)	BDL	-	-	BDL	-	BDL	-	-	BDL
Hg202 (ppm)	25	BDL	2106	25	26	19	BDL	27	44
Pb204 (ppm)	48	BDL	5167	BDL	BDL	BDL	BDL	86	69
Tl205 (ppm)	BDL	1	53	4	2	1	28	6	16
Pb206 (ppm)	-	3	6283	15	13	10	-	-	-
Pb207 (ppm)	1	4	6864	-	13	9	88	31	59
Pb208 (ppm)	1	3	6022	13	13	10	68	30	65
Bi209 (ppm)	BDL	BDL	100	1	1	1	59	3	42
Th232 (ppm)	-	-	-	-	-	-	-	-	-
U238 (ppm)	BDL	-	-	BDL	-	-	-	-	-
PbTotal (ppm)	2	4	6255	14	13	11	73	32	63

Table D6. Trace element data for pentlandite continued.

Deposit	Tilt Cove	Tilt Cove	Tilt Cove	Tilt Cove	Tilt Cove	Tilt Cove
Sample	KKMSC70_Pnt8	KKMSC70_Pnt7	KKMSC70_Pnt11	KKMSC70_Pnt10	KKMSC70_Pnt12	KKMSC70_Pnt12
Date	2023-11-22	2023-11-22	2023-11-22	2023-11-22	2023-11-22	2023-11-22
Facies	Chalcopyrite-pyrrhotite-dominated	Chalcopyrite-pyrrhotite-dominated	Chalcopyrite-pyrrhotite-dominated	Chalcopyrite-pyrrhotite-dominated	Chalcopyrite-pyrrhotite-dominated	Chalcopyrite-pyrrhotite-dominated
Li7 (ppm)	14	BDL	BDL	BDL	BDL	BDL
Be9 (ppm)	BDL	-	-	-	-	-
B11 (ppm)	BDL	BDL	BDL	BDL	BDL	BDL
Na23 (ppm)	494	BDL	BDL	BDL	BDL	BDL
Mg24 (ppm)	95885	173	160	149	482	1771
Al27 (ppm)	4034	12	10	BDL	14	17
Si29 (ppm)	228775	BDL	BDL	BDL	BDL	4494
P31 (ppm)	1332	BDL	BDL	BDL	BDL	BDL
S32 (ppm)	39329145	1225439	885002	1195521	1127933	1276961
K39 (ppm)	BDL	BDL	BDL	BDL	BDL	BDL
Ca44 (ppm)	5815	BDL	BDL	BDL	BDL	BDL
Sc45 (ppm)	BDL	BDL	BDL	BDL	BDL	BDL
Ti47 (ppm)	BDL	BDL	BDL	-	BDL	BDL
V51 (ppm)	4	BDL	BDL	BDL	BDL	BDL
Cr52 (ppm)	252	17	5	8	BDL	BDL
Mn55 (ppm)	907	6	10	8	10	12
Fe57 (ppm)	8567368	287093	283149	283468	268766	287188
Co59 (ppm)	11053	11929	6803	9345	11997	12348
Ni60 (ppm)	-	-	-	-	-	-
Cu63 (ppm)	10140351	21	60	37	11	5
Zn66 (ppm)	5795	4	9	6	10	9
Ga71 (ppm)	-	-	BDL	-	-	-
Ge73 (ppm)	BDL	BDL	BDL	BDL	BDL	BDL
As75 (ppm)	762	152	46	69	38	31
Se77 (ppm)	9161	390	374	350	359	339
Rb85 (ppm)	BDL	-	BDL	BDL	BDL	BDL
Sr88 (ppm)	-	-	0	-	-	-
Y89 (ppm)	-	-	-	-	-	-
Zr90 (ppm)	-	-	-	-	-	-
Nb93 (ppm)	-	-	-	-	-	-
Mo95 (ppm)	BDL	-	-	BDL	-	BDL
Ru101 (ppm)	BDL	-	-	-	-	-
Rh103 (ppm)	61	-	-	-	BDL	BDL
Pd104 (ppm)	BDL	-	-	-	-	-

Pd105 (ppm)	-	-	-	-	-	-
Pd106 (ppm)	-	BDL	-	-	BDL	BDL
Ag107 (ppm)	1396	BDL	-	1	-	5
Cd111 (ppm)	-	-	-	-	-	BDL
In115 (ppm)	-	0	-	0	-	BDL
Sn118 (ppm)	26	BDL	BDL	1	BDL	1
Sb121 (ppm)	357	3	5	3	1	3
Te125 (ppm)	161	8	4	3	2	6
Cs133 (ppm)	BDL	BDL	BDL	BDL	BDL	BDL
Ba137 (ppm)	-	-	-	-	-	-
La139 (ppm)	-	-	-	-	-	-
Ce140 (ppm)	-	-	-	-	-	-
Pr141 (ppm)	-	-	BDL	-	-	-
Nd146 (ppm)	-	-	-	-	-	-
Sm147 (ppm)	-	-	-	-	-	-
Eu153 (ppm)	-	-	-	-	-	-
Gd157 (ppm)	-	BDL	-	-	-	-
Tb159 (ppm)	-	-	-	-	-	-
Dy163 (ppm)	-	-	-	-	-	-
Ho165 (ppm)	-	-	-	-	-	-
Er166 (ppm)	-	-	-	-	-	-
Tm169 (ppm)	-	-	-	-	-	-
Yb172 (ppm)	-	-	-	-	-	-
Lu175 (ppm)	-	-	-	-	-	-
Hf178 (ppm)	-	-	-	-	-	-
Ta181 (ppm)	BDL	-	-	-	-	BDL
W182 (ppm)	BDL	-	-	-	BDL	-
Re185 (ppm)	BDL	BDL	BDL	BDL	BDL	BDL
Os189 (ppm)	BDL	BDL	BDL	BDL	BDL	BDL
Ir193 (ppm)	-	-	BDL	-	BDL	-
Pt195 (ppm)	BDL	-	BDL	-	BDL	BDL
Au197 (ppm)	-	-	BDL	BDL	-	-
Hg202 (ppm)	559	BDL	12	14	BDL	BDL
Pb204 (ppm)	3243	93	70	BDL	BDL	BDL
Tl205 (ppm)	67	3	13	3	3	6
Pb206 (ppm)	2166	13	57	12	18	-
Pb207 (ppm)	2013	13	54	11	-	-
Pb208 (ppm)	1989	12	54	12	14	28
Bi209 (ppm)	72	1	-	1	1	2
Th232 (ppm)	-	-	-	-	-	-
U238 (ppm)	-	-	-	-	-	-
PbTotal (ppm)	2056	13	55	12	15	29

Table D7. Trace element data for arsenopyrite.

Deposit	Tilt Cove	Tilt Cove	Tilt Cove	Tilt Cove	Tilt Cove	Tilt Cove	Tilt Cove	Tilt Cove	Tilt Cove
Sample	KKMSC13_Apy3	KKMSC13_Apy2	KKMSC13_Apy1	KKMSC13_Apy4	KKMSC13_Apy6	KKMSC13_Apy7	KKMSC13_Apy9	KKMSC13_Apy11	KKMSC13_Apy10
Date	2023-11-23	2023-11-23	2023-11-23	2023-11-23	2023-11-23	2023-11-23	2023-11-23	2023-11-23	2023-11-23
Facies	Pyrite-dominated	Pyrite-dominated	Pyrite-dominated	Pyrite-dominated	Pyrite-dominated	Pyrite-dominated	Pyrite-dominated	Pyrite-dominated	Pyrite-dominated
Li7 (ppm)	2	1	BDL	BDL	BDL	1	BDL	BDL	1
Be9 (ppm)	-	BDL	-	-	-	-	-	-	-
B11 (ppm)	BDL	BDL	BDL	BDL	BDL	BDL	BDL	BDL	BDL
Na23 (ppm)	BDL	BDL	BDL	BDL	BDL	BDL	BDL	BDL	BDL
Mg24 (ppm)	332	18	198	77	48	282	70	12	273
Al27 (ppm)	246	15	22	11	18	221	BDL	10	203
Si29 (ppm)	37213	BDL	BDL	BDL	BDL	1496	BDL	BDL	2250
P31 (ppm)	BDL	BDL	BDL	BDL	BDL	BDL	BDL	BDL	BDL
S32 (ppm)	191541	204132	168643	181128	188640	195832	194875	160133	182466
K39 (ppm)	36	BDL	BDL	BDL	BDL	61	BDL	BDL	25
Ca44 (ppm)	BDL	BDL	BDL	BDL	BDL	BDL	BDL	BDL	BDL
Sc45 (ppm)	BDL	BDL	BDL	BDL	BDL	BDL	BDL	BDL	BDL
Ti47 (ppm)	BDL	BDL	BDL	BDL	BDL	4	BDL	BDL	5
V51 (ppm)	BDL	BDL	BDL	BDL	0	1	BDL	BDL	1
Cr52 (ppm)	BDL	BDL	5	BDL	BDL	BDL	BDL	BDL	BDL
Mn55 (ppm)	36	4	15	24	BDL	33	18	BDL	19
Fe57 (ppm)	242210	267991	233554	238255	232264	255683	231718	324483	232837
Co59 (ppm)	-	BDL	BDL	BDL	BDL	-	-	BDL	0
Ni60 (ppm)	7	-	7	-	60	2	BDL	-	-
Cu63 (ppm)	21	7575	5	4	17	27	192	46	134
Zn66 (ppm)	21	111	5	1	1	152	BDL	5	64
Ga71 (ppm)	-	-	-	-	-	-	-	BDL	-
Ge73 (ppm)	BDL	BDL	-	-	-	BDL	-	-	-
As75 (ppm)	-	-	-	-	-	-	-	-	-
Se77 (ppm)	11	12	18	33	15	15	21	40	23
Rb85 (ppm)	0	BDL	BDL	BDL	BDL	0	BDL	BDL	BDL
Sr88 (ppm)	-	-	-	-	-	-	-	BDL	-
Y89 (ppm)	-	-	-	-	BDL	-	-	-	-
Zr90 (ppm)	-	-	-	-	-	-	-	-	-
Nb93 (ppm)	4	8	19	-	0	-	19	BDL	-
Mo95 (ppm)	-	-	-	-	-	-	-	-	-
Ru101 (ppm)	BDL	-	-	BDL	-	-	-	-	-
Rh103 (ppm)	-	-	-	-	BDL	-	-	BDL	-
Pd104 (ppm)	BDL	-	BDL	BDL	-	-	-	BDL	BDL

Pd105 (ppm)	-	BDL	BDL	-	-	BDL	-	-	BDL
Pd106 (ppm)	17	143	2	7	2	34	0	8	146
Ag107 (ppm)	-	1	-	-	BDL	1	BDL	BDL	-
Cd111 (ppm)	-	-	-	0	-	-	-	0	-
In115 (ppm)	1	1	BDL	BDL	BDL	BDL	BDL	BDL	0
Sn118 (ppm)	77	-	72	101	69	97	135	-	128
Sb121 (ppm)	BDL	-	BDL	26	2	BDL	4	-	8
Te125 (ppm)	0	BDL	BDL	BDL	BDL	0	BDL	BDL	BDL
Cs133 (ppm)	-	-	-	-	-	-	-	-	-
Ba137 (ppm)	-	-	-	-	-	-	-	-	-
La139 (ppm)	-	-	-	-	-	-	-	-	-
Ce140 (ppm)	-	-	-	-	-	-	-	-	-
Pr141 (ppm)	-	-	-	-	-	-	-	-	-
Nd146 (ppm)	-	-	-	-	-	-	-	-	-
Sm147 (ppm)	-	-	-	-	-	-	-	-	-
Eu153 (ppm)	-	-	-	-	-	-	-	-	-
Gd157 (ppm)	-	-	-	-	-	-	-	-	-
Tb159 (ppm)	-	-	-	-	-	-	-	-	-
Dy163 (ppm)	-	-	-	-	-	-	-	-	-
Ho165 (ppm)	-	-	-	-	-	-	-	-	-
Er166 (ppm)	-	-	BDL	-	-	-	-	-	-
Tm169 (ppm)	-	-	-	-	-	-	-	-	-
Yb172 (ppm)	-	-	-	-	-	-	-	-	-
Lu175 (ppm)	-	-	-	-	-	-	-	-	-
Hf178 (ppm)	-	-	BDL	-	-	BDL	-	-	-
Ta181 (ppm)	BDL	-	-	-	-	-	-	BDL	-
W182 (ppm)	BDL	BDL	BDL	BDL	BDL	BDL	BDL	BDL	BDL
Re185 (ppm)	BDL	BDL	BDL	BDL	BDL	BDL	BDL	BDL	BDL
Os189 (ppm)	-	-	BDL	-	-	BDL	-	-	-
Ir193 (ppm)	BDL	BDL	BDL	BDL	BDL	BDL	BDL	-	-
Pt195 (ppm)	-	-	-	-	-	-	-	-	9
Au197 (ppm)	25	BDL	BDL	BDL	BDL	BDL	BDL	BDL	BDL
Hg202 (ppm)	36	25	13	BDL	18	53	BDL	20	45
Pb204 (ppm)	0	1	BDL	BDL	BDL	BDL	BDL	BDL	0
Tl205 (ppm)	13	25	3	1	4	-	0	4	53
Pb206 (ppm)	10	-	-	1	4	33	-	3	42
Pb207 (ppm)	8	22	3	1	5	33	0	4	41
Pb208 (ppm)	0	1	0	0	0	0	0	-	-
Bi209 (ppm)	-	-	-	-	-	-	-	-	-
Th232 (ppm)	-	-	-	-	-	-	BDL	-	-
U238 (ppm)	10	22	3	1	5	35	0	4	44
PbTotal (ppm)	-	-	-	-	-	-	-	-	-

Table D7. Trace element data for arsenopyrite continued.

Deposit	Tilt Cove	Tilt Cove
Sample	KKMSC13_Apy13	KKMSC13_Apy12
Date	2023-11-23	2023-11-23
Facies	Pyrite-dominated	Pyrite-dominated
Li7 (ppm)	BDL	BDL
Be9 (ppm)	-	-
B11 (ppm)	BDL	BDL
Na23 (ppm)	BDL	BDL
Mg24 (ppm)	91	5
Al27 (ppm)	9	5
Si29 (ppm)	BDL	BDL
P31 (ppm)	BDL	BDL
S32 (ppm)	230519	195427
K39 (ppm)	BDL	BDL
Ca44 (ppm)	BDL	BDL
Sc45 (ppm)	BDL	BDL
Ti47 (ppm)	-	BDL
V51 (ppm)	0	BDL
Cr52 (ppm)	BDL	BDL
Mn55 (ppm)	25	1
Fe57 (ppm)	317759	254474
Co59 (ppm)	0	BDL
Ni60 (ppm)	-	2
Cu63 (ppm)	48	6
Zn66 (ppm)	2	1
Ga71 (ppm)	-	BDL
Ge73 (ppm)	BDL	-
As75 (ppm)	-	-
Se77 (ppm)	5	21
Rb85 (ppm)	BDL	BDL
Sr88 (ppm)	-	-
Y89 (ppm)	-	-
Zr90 (ppm)	-	BDL
Nb93 (ppm)	3	14
Mo95 (ppm)	-	-
Ru101 (ppm)	BDL	-
Rh103 (ppm)	-	-
Pd104 (ppm)	-	-
Pd105 (ppm)	BDL	BDL

Pd106 (ppm)	7	11
Ag107 (ppm)	BDL	-
Cd111 (ppm)	-	-
In115 (ppm)	BDL	BDL
Sn118 (ppm)	79	193
Sb121 (ppm)	BDL	-
Te125 (ppm)	BDL	BDL
Cs133 (ppm)	-	-
Ba137 (ppm)	-	-
La139 (ppm)	-	-
Ce140 (ppm)	-	-
Pr141 (ppm)	-	-
Nd146 (ppm)	-	-
Sm147 (ppm)	-	-
Eu153 (ppm)	-	-
Gd157 (ppm)	-	-
Tb159 (ppm)	-	-
Dy163 (ppm)	-	-
Ho165 (ppm)	-	-
Er166 (ppm)	-	-
Tm169 (ppm)	-	-
Yb172 (ppm)	-	-
Lu175 (ppm)	-	-
Hf178 (ppm)	-	-
Ta181 (ppm)	-	-
W182 (ppm)	BDL	BDL
Re185 (ppm)	BDL	BDL
Os189 (ppm)	BDL	-
Ir193 (ppm)	BDL	BDL
Pt195 (ppm)	-	-
Au197 (ppm)	BDL	BDL
Hg202 (ppm)	19	BDL
Pb204 (ppm)	BDL	BDL
Tl205 (ppm)	10	5
Pb206 (ppm)	7	-
Pb207 (ppm)	8	5
Pb208 (ppm)	0	1
Bi209 (ppm)	-	-
Th232 (ppm)	-	-
U238 (ppm)	8	5
PbTotal (ppm)	-	-

Table D8. Trace element data for bornite.

Deposit	Tilt Cove	Tilt Cove	Tilt Cove	Tilt Cove	Tilt Cove	Tilt Cove	Tilt Cove	Tilt Cove	Tilt Cove
Sample	KKMSC23_Bn2	KKMSC23_Bn3	KKMSC23_Bn3	KKMSC23_Bn4	KKMSC23_Bn5	KKMSC23_Bn6	KKMSC23_Bn10	KKMSC23_Bn11	KKMSC23_Bn7
Date	2023-11-23	2023-11-23	2023-11-23	2023-11-23	2023-11-23	2023-11-23	2023-11-23	2023-11-23	2023-11-23
Facies	Magnetite-dominated	Magnetite-dominated	Magnetite-dominated	Magnetite-dominated	Magnetite-dominated	Magnetite-dominated	Magnetite-dominated	Magnetite-dominated	Magnetite-dominated
Li7 (ppm)	2	1	BDL	BDL	3	1	2	1	2
Be9 (ppm)	-	-	BDL	-	BDL	-	-	-	-
B11 (ppm)	BDL	BDL	BDL	BDL	BDL	BDL	BDL	BDL	BDL
Na23 (ppm)	BDL	BDL	BDL	BDL	624	BDL	BDL	BDL	69
Mg24 (ppm)	1681	6	31	58	232	196	97	106	72
Al27 (ppm)	1843	7	34	55	1680	524	97	97	118
Si29 (ppm)	3806	BDL	BDL	BDL	3900	2118	2620	2314	BDL
P31 (ppm)	BDL	BDL	BDL	BDL	87	BDL	BDL	BDL	BDL
S32 (ppm)	267658	246945	239656	229910	295999	266550	260053	280723	268671
K39 (ppm)	59	BDL	BDL	BDL	29	35	BDL	BDL	37
Ca44 (ppm)	BDL	BDL	BDL	BDL	BDL	BDL	BDL	BDL	BDL
Sc45 (ppm)	BDL	BDL	BDL	BDL	BDL	BDL	BDL	BDL	BDL
Ti47 (ppm)	15	BDL	BDL	BDL	5	5	-	11	9
V51 (ppm)	5	BDL	BDL	1	1	1	BDL	0	BDL
Cr52 (ppm)	17	BDL	BDL	BDL	BDL	BDL	BDL	BDL	BDL
Mn55 (ppm)	17	BDL	BDL	BDL	7	7	4	4	2
Fe57 (ppm)	116116	111942	96900	98496	109552	105723	87249	103800	90121
Co59 (ppm)	2	-	-	BDL	2	2	BDL	BDL	BDL
Ni60 (ppm)	-	-	-	1	1	-	-	-	BDL
Cu63 (ppm)	#VALUE!	#VALUE!	#VALUE!	#VALUE!	#VALUE!	#VALUE!	#VALUE!	#VALUE!	#VALUE!
Zn66 (ppm)	65	2	4	3	41	20	9	4	2
Ga71 (ppm)	-	-	BDL	BDL	-	-	BDL	BDL	-
Ge73 (ppm)	-	-	BDL	BDL	BDL	-	BDL	-	BDL
As75 (ppm)	85	71	113	75	56	62	35	50	57
Se77 (ppm)	129	68	78	77	-	67	21	15	38
Rb85 (ppm)	0	BDL	BDL	-	BDL	BDL	BDL	BDL	BDL
Sr88 (ppm)	-	-	-	-	-	-	-	BDL	-
Y89 (ppm)	-	BDL	-	-	-	-	-	-	-
Zr90 (ppm)	-	-	-	-	-	-	-	-	-
Nb93 (ppm)	BDL	BDL	BDL	-	BDL	-	-	BDL	BDL
Mo95 (ppm)	-	-	-	-	BDL	-	-	-	-
Ru101 (ppm)	-	-	-	-	-	-	15	-	-
Rh103 (ppm)	-	BDL	-	-	BDL	-	-	-	-
Pd104 (ppm)	39	33	-	-	-	-	-	40	33

Pd105 (ppm)	-	-	-	1	0	-	-	-	BDL
Pd106 (ppm)	496	124	-	339	194	195	337	344	226
Ag107 (ppm)	1	BDL	BDL	-	11	-	1	1	-
Cd111 (ppm)	-	-	BDL	-	0	0	-	-	-
In115 (ppm)	BDL	BDL	BDL	BDL	BDL	BDL	BDL	BDL	BDL
Sn118 (ppm)	-	BDL	BDL	BDL	BDL	BDL	BDL	BDL	0
Sb121 (ppm)	-	BDL	BDL	3	1	1	BDL	BDL	BDL
Te125 (ppm)	BDL	BDL	BDL	BDL	BDL	BDL	BDL	BDL	BDL
Cs133 (ppm)	-	-	-	-	-	-	-	-	-
Ba137 (ppm)	-	-	-	-	-	-	-	-	-
La139 (ppm)	-	-	-	-	-	-	-	-	-
Ce140 (ppm)	-	-	-	-	-	-	-	-	-
Pr141 (ppm)	-	-	-	-	-	-	-	-	-
Nd146 (ppm)	-	-	-	-	-	-	-	-	-
Sm147 (ppm)	-	-	-	-	-	-	-	-	-
Eu153 (ppm)	-	-	-	-	BDL	-	-	-	-
Gd157 (ppm)	-	-	-	-	-	-	-	-	-
Tb159 (ppm)	-	-	-	-	-	-	-	-	-
Dy163 (ppm)	-	-	-	-	-	-	-	-	-
Ho165 (ppm)	-	-	-	-	-	-	-	-	-
Er166 (ppm)	-	-	-	-	-	-	-	-	-
Tm169 (ppm)	-	-	-	-	-	-	-	-	-
Yb172 (ppm)	-	-	-	-	-	-	-	-	-
Lu175 (ppm)	-	-	BDL	-	-	-	-	-	-
Hf178 (ppm)	-	-	-	BDL	-	-	-	-	-
Ta181 (ppm)	-	BDL	-	BDL	BDL	-	-	BDL	-
W182 (ppm)	BDL	BDL	BDL	BDL	BDL	BDL	BDL	BDL	BDL
Re185 (ppm)	BDL	BDL	BDL	BDL	BDL	BDL	BDL	BDL	BDL
Os189 (ppm)	-	BDL	BDL	-	-	BDL	-	BDL	BDL
Ir193 (ppm)	BDL	BDL	BDL	BDL	BDL	BDL	BDL	BDL	BDL
Pt195 (ppm)	-	-	BDL	-	-	BDL	-	-	1
Au197 (ppm)	55	43	101	140	73	54	60	53	55
Hg202 (ppm)	60	86	104	167	129	92	99	87	95
Pb204 (ppm)	BDL	BDL	BDL	BDL	BDL	BDL	BDL	BDL	BDL
Tl205 (ppm)	5	9	0	-	2	-	2	-	24
Pb206 (ppm)	-	-	0	-	-	1	2	-	20
Pb207 (ppm)	4	6	0	0	-	1	2	4	20
Pb208 (ppm)	1	1	1	2	2	2	1	2	1
Bi209 (ppm)	-	-	-	-	-	-	-	BDL	-
Th232 (ppm)	-	BDL	-	-	-	0	BDL	-	-
U238 (ppm)	5	8	2	3	3	3	4	5	22
PbTotal (ppm)	-	-	-	-	-	-	-	-	-

Table D8. Trace element data for bornite continued.

Deposit	Tilt Cove	Tilt Cove
Sample	KKMSC23_Bn8	KKMSC23_Bn9
Date	2023-11-23	2023-11-23
Facies	Magnetite-dominated	Magnetite-dominated
Li7 (ppm)	4	3
Be9 (ppm)	-	BDL
B11 (ppm)	BDL	BDL
Na23 (ppm)	35	BDL
Mg24 (ppm)	79	126
Al27 (ppm)	266	1429
Si29 (ppm)	2244	BDL
P31 (ppm)	55	377
S32 (ppm)	278929	365554
K39 (ppm)	58	222
Ca44 (ppm)	BDL	BDL
Sc45 (ppm)	BDL	BDL
Ti47 (ppm)	17	20
V51 (ppm)	BDL	5
Cr52 (ppm)	BDL	BDL
Mn55 (ppm)	4	BDL
Fe57 (ppm)	103946	97956
Co59 (ppm)	1	-
Ni60 (ppm)	BDL	BDL
Cu63 (ppm)	#VALUE!	#VALUE!
Zn66 (ppm)	5	29
Ga71 (ppm)	-	-
Ge73 (ppm)	BDL	BDL
As75 (ppm)	49	BDL
Se77 (ppm)	34	141
Rb85 (ppm)	BDL	1
Sr88 (ppm)	-	-
Y89 (ppm)	-	-
Zr90 (ppm)	-	-
Nb93 (ppm)	BDL	BDL
Mo95 (ppm)	-	-
Ru101 (ppm)	16	-
Rh103 (ppm)	-	-
Pd104 (ppm)	-	-
Pd105 (ppm)	-	-

Pd106 (ppm)	277	681
Ag107 (ppm)	1	BDL
Cd111 (ppm)	-	-
In115 (ppm)	BDL	3
Sn118 (ppm)	BDL	BDL
Sb121 (ppm)	BDL	-
Te125 (ppm)	BDL	BDL
Cs133 (ppm)	-	-
Ba137 (ppm)	-	-
La139 (ppm)	-	-
Ce140 (ppm)	-	-
Pr141 (ppm)	-	-
Nd146 (ppm)	-	-
Sm147 (ppm)	-	-
Eu153 (ppm)	-	-
Gd157 (ppm)	-	-
Tb159 (ppm)	-	-
Dy163 (ppm)	-	-
Ho165 (ppm)	-	-
Er166 (ppm)	-	-
Tm169 (ppm)	-	-
Yb172 (ppm)	-	-
Lu175 (ppm)	-	-
Hf178 (ppm)	-	-
Ta181 (ppm)	BDL	-
W182 (ppm)	BDL	BDL
Re185 (ppm)	BDL	5
Os189 (ppm)	-	-
Ir193 (ppm)	BDL	BDL
Pt195 (ppm)	2	-
Au197 (ppm)	83	BDL
Hg202 (ppm)	101	BDL
Pb204 (ppm)	BDL	BDL
Tl205 (ppm)	1	77
Pb206 (ppm)	1	79
Pb207 (ppm)	0	84
Pb208 (ppm)	1	6
Bi209 (ppm)	-	-
Th232 (ppm)	-	-
U238 (ppm)	2	53
PbTotal (ppm)	-	-

Table D9. Trace element data for magnetite.

Deposit	Tilt Cove	Tilt Cove	Tilt Cove	Tilt Cove	Tilt Cove	Tilt Cove	Tilt Cove	Tilt Cove	Tilt Cove
Sample	KKMSC63_Mag3	KKMSC63_Mag4	KKMSC63_Mag8	KKMSC63_Mag7	KKMSC63_Mag5	KKMSC63_Mag6	KKMSC63_Mag2	KKMSC63_Mag1	KKMSC63_Mag9
Date	2023-11-21	2023-11-21	2023-11-21	2023-11-21	2023-11-21	2023-11-21	2023-11-21	2023-11-21	2023-11-21
Facies	Pyrite-dominated	Pyrite-dominated	Pyrite-dominated	Pyrite-dominated	Pyrite-dominated	Pyrite-dominated	Pyrite-dominated	Pyrite-dominated	Pyrite-dominated
Li7 (ppm)	BDL	BDL	4	BDL	BDL	BDL	6	BDL	3
Be9 (ppm)	-	-	-	BDL	BDL	BDL	-	-	BDL
B11 (ppm)	BDL	77	BDL	BDL	BDL	BDL	BDL	BDL	BDL
Na23 (ppm)	BDL	BDL	3691	BDL	BDL	BDL	152	90	BDL
Mg24 (ppm)	113853	-	6691	1855	6749	17044	5319	4716	4210
Al27 (ppm)	16063	153305	822	82	459	222	264	303	185
Si29 (ppm)	106961	BDL	23222	5106	9963	25655	10068	9342	4881
P31 (ppm)	BDL	BDL	BDL	BDL	BDL	BDL	BDL	BDL	BDL
S32 (ppm)	BDL	BDL	84586	33556	BDL	22471	12091	13603	678174
K39 (ppm)	BDL	BDL	162	BDL	BDL	BDL	BDL	BDL	BDL
Ca44 (ppm)	BDL	BDL	4749	BDL	BDL	BDL	BDL	BDL	BDL
Sc45 (ppm)	36	17	18	13	17	10	14	17	5
Ti47 (ppm)	188	2663	166	112	164	153	152	143	-
V51 (ppm)	272	2224	175	198	185	201	193	190	44
Cr52 (ppm)	29526	462392	677	925	741	1270	1272	1661	921
Mn55 (ppm)	124	3103	71	16	26	33	32	21	14
Fe57 (ppm)	-	-	-	-	-	-	-	-	-
Co59 (ppm)	48	599	66	17	20	56	17	37	2416
Ni60 (ppm)	892	-	-	-	514	-	-	-	3190
Cu63 (ppm)	BDL	BDL	36811	15760	1360	3552	5141	9007	6793
Zn66 (ppm)	6988	12346	624	336	140	106	193	309	79
Ga71 (ppm)	-	-	-	-	1	-	-	-	-
Ge73 (ppm)	-	18	-	-	18	-	-	9	-
As75 (ppm)	11	12	68	8	19	55	8	47	638
Se77 (ppm)	BDL	BDL	20	BDL	BDL	BDL	BDL	BDL	101
Rb85 (ppm)	-	BDL	1	BDL	BDL	BDL	BDL	BDL	-
Sr88 (ppm)	-	-	-	-	-	-	-	-	-
Y89 (ppm)	-	-	-	-	-	-	-	-	-
Zr90 (ppm)	-	-	-	-	-	-	-	-	-
Nb93 (ppm)	-	BDL	-	BDL	-	-	BDL	-	-
Mo95 (ppm)	-	BDL	BDL	BDL	BDL	BDL	BDL	-	-
Ru101 (ppm)	-	-	-	0	-	-	BDL	-	BDL
Rh103 (ppm)	BDL	BDL	-	BDL	-	BDL	BDL	BDL	-
Pd104 (ppm)	BDL	-	BDL	-	-	-	BDL	-	BDL

Pd105 (ppm)	BDL	BDL	-	BDL	-	BDL	-	-	BDL
Pd106 (ppm)	BDL	BDL	6	-	BDL	BDL	BDL	1	4
Ag107 (ppm)	BDL	BDL	BDL	-	BDL	BDL	BDL	BDL	1
Cd111 (ppm)	-	-	4	-	-	-	1	-	-
In115 (ppm)	BDL	BDL	BDL	BDL	BDL	BDL	BDL	BDL	BDL
Sn118 (ppm)	14	1	42	27	9	-	27	18	34
Sb121 (ppm)	BDL	-	BDL	-	-	BDL	BDL	BDL	23
Te125 (ppm)	BDL	BDL	BDL	BDL	BDL	BDL	BDL	BDL	BDL
Cs133 (ppm)	-	-	-	-	-	-	-	-	-
Ba137 (ppm)	-	-	-	-	-	-	-	-	-
La139 (ppm)	-	-	-	-	-	-	-	-	-
Ce140 (ppm)	-	-	-	-	-	-	-	-	-
Pr141 (ppm)	-	-	-	-	-	-	-	-	-
Nd146 (ppm)	-	-	-	-	-	-	-	-	-
Sm147 (ppm)	-	-	-	-	-	-	-	-	-
Eu153 (ppm)	-	-	-	-	-	-	-	-	-
Gd157 (ppm)	-	-	-	-	-	-	-	-	-
Tb159 (ppm)	-	-	-	-	-	-	-	-	-
Dy163 (ppm)	-	-	-	-	-	-	-	-	-
Ho165 (ppm)	-	-	-	-	-	-	-	-	-
Er166 (ppm)	-	-	-	-	-	-	-	-	-
Tm169 (ppm)	-	-	-	-	-	-	-	-	-
Yb172 (ppm)	-	-	-	-	-	-	-	-	-
Lu175 (ppm)	-	-	-	-	-	-	BDL	-	-
Hf178 (ppm)	-	-	-	-	BDL	-	-	-	-
Ta181 (ppm)	BDL	-	BDL	-	-	-	-	-	-
W182 (ppm)	BDL	BDL	BDL	BDL	BDL	BDL	BDL	BDL	BDL
Re185 (ppm)	BDL	BDL	BDL	BDL	BDL	BDL	BDL	BDL	BDL
Os189 (ppm)	BDL	BDL	-	BDL	-	-	BDL	-	-
Ir193 (ppm)	BDL	-	BDL	BDL	BDL	BDL	-	BDL	BDL
Pt195 (ppm)	-	BDL	-	-	BDL	BDL	BDL	-	-
Au197 (ppm)	153	BDL	BDL	BDL	BDL	BDL	BDL	BDL	67
Hg202 (ppm)	255	BDL	131	BDL	BDL	BDL	BDL	BDL	157
Pb204 (ppm)	0	BDL	2	2	0	1	1	0	3
Tl205 (ppm)	8	1	56	-	-	-	-	-	-
Pb206 (ppm)	9	-	57	37	-	-	21	27	101
Pb207 (ppm)	6	1	-	32	9	24	18	23	94
Pb208 (ppm)	BDL	BDL	0	BDL	BDL	0	BDL	0	4
Bi209 (ppm)	-	-	-	-	-	-	-	-	-
Th232 (ppm)	-	BDL	-	-	-	-	-	-	-
U238 (ppm)	11	BDL	53	34	9	26	19	26	101
PbTotal (ppm)	-	-	-	-	-	-	-	-	-

Table D9. Trace element data for magnetite continued.

Deposit	Tilt Cove	Tilt Cove	Tilt Cove	Tilt Cove	Tilt Cove	Tilt Cove	Tilt Cove	Tilt Cove	Tilt Cove
Sample	KKMSC63_Mag10	KKMSC63_Mag11	KKMSC63_Mag12	KKMSC63_Mag18	KKMSC63_Mag19	KKMSC63_Mag15	KKMSC63_Mag13	KKMSC63_Mag16	KKMSC63_Mag17
Date	2023-11-21	2023-11-21	2023-11-21	2023-11-21	2023-11-21	2023-11-21	2023-11-21	2023-11-21	2023-11-21
Facies	Pyrite-dominated	Pyrite-dominated	Pyrite-dominated	Pyrite-dominated	Pyrite-dominated	Pyrite-dominated	Pyrite-dominated	Pyrite-dominated	Pyrite-dominated
Li7 (ppm)	BDL	BDL	BDL	4	11	8	9	10	BDL
Be9 (ppm)	-	BDL	BDL	-	BDL	-	BDL	-	-
B11 (ppm)	BDL	BDL	BDL	BDL	BDL	BDL	BDL	BDL	BDL
Na23 (ppm)	BDL	63	BDL	BDL	132	165	108	BDL	BDL
Mg24 (ppm)	69991	226541	12727	4960	7977	7432	-	5631	2610
Al27 (ppm)	97	226	69	1168	4905	1708	871	819	1151
Si29 (ppm)	76826	272845	18535	11621	16119	13445	34552	12496	5127
P31 (ppm)	BDL	BDL	BDL	BDL	BDL	BDL	BDL	BDL	BDL
S32 (ppm)	177561	126410	60137	BDL	5346	4838	2126	BDL	BDL
K39 (ppm)	BDL	BDL	BDL	BDL	BDL	BDL	BDL	BDL	BDL
Ca44 (ppm)	BDL	BDL	BDL	BDL	1036	950	BDL	1752	BDL
Sc45 (ppm)	5	14	10	16	18	18	13	16	5
Ti47 (ppm)	133	155	176	388	787	368	270	426	252
V51 (ppm)	126	144	157	333	172	243	273	363	313
Cr52 (ppm)	174	290	125	3663	13061	1296	3593	1256	4807
Mn55 (ppm)	23	41	19	76	225	140	71	97	50
Fe57 (ppm)	-	-	-	-	-	-	-	-	-
Co59 (ppm)	62	70	18	27	60	32	27	29	24
Ni60 (ppm)	924	-	615	417	-	-	642	-	-
Cu63 (ppm)	116257	47191	18711	25	264	351	77	42	2
Zn66 (ppm)	443	436	795	80	3426	86	74	234	150
Ga71 (ppm)	-	-	-	-	4	2	-	2	-
Ge73 (ppm)	-	11	7	-	22	-	-	-	-
As75 (ppm)	56	8	BDL	BDL	15	BDL	11	11	BDL
Se77 (ppm)	60	55	BDL	BDL	BDL	BDL	BDL	BDL	BDL
Rb85 (ppm)	BDL	BDL	BDL	BDL	BDL	BDL	BDL	BDL	BDL
Sr88 (ppm)	-	-	-	-	9	-	-	-	-
Y89 (ppm)	-	-	-	-	-	-	-	-	-
Zr90 (ppm)	-	-	-	-	-	-	-	-	-
Nb93 (ppm)	BDL	-	-	BDL	-	-	-	-	-
Mo95 (ppm)	-	-	-	-	BDL	BDL	-	BDL	BDL
Ru101 (ppm)	-	1	0	-	BDL	-	-	-	-
Rh103 (ppm)	BDL	-	BDL	-	BDL	BDL	-	BDL	-
Pd104 (ppm)	6	-	BDL	-	BDL	-	-	-	BDL

Pd105 (ppm)	-	BDL	BDL	-	BDL	BDL	BDL	BDL	-
Pd106 (ppm)	8	14	2	BDL	-	BDL	BDL	BDL	BDL
Ag107 (ppm)	2	BDL	1	BDL	-	1	-	-	-
Cd111 (ppm)	-	-	-	-	-	BDL	-	-	-
In115 (ppm)	BDL	BDL	BDL	BDL	BDL	BDL	BDL	BDL	BDL
Sn118 (ppm)	32	-	17	1	3	2	2	1	BDL
Sb121 (ppm)	BDL	BDL	BDL	-	BDL	BDL	BDL	BDL	BDL
Te125 (ppm)	BDL	BDL	BDL	BDL	BDL	BDL	BDL	BDL	BDL
Cs133 (ppm)	-	-	-	-	-	-	3	-	-
Ba137 (ppm)	-	-	-	-	-	-	-	-	-
La139 (ppm)	-	-	-	-	-	-	-	-	-
Ce140 (ppm)	-	-	-	-	-	-	-	-	-
Pr141 (ppm)	-	-	-	-	-	-	-	-	-
Nd146 (ppm)	-	-	-	-	-	-	-	-	-
Sm147 (ppm)	-	BDL	-	-	-	-	-	-	-
Eu153 (ppm)	BDL	-	-	-	-	-	-	-	-
Gd157 (ppm)	-	-	-	-	-	-	-	-	-
Tb159 (ppm)	-	-	-	-	-	-	-	-	-
Dy163 (ppm)	-	-	-	-	-	-	BDL	-	-
Ho165 (ppm)	-	-	-	-	-	-	-	-	-
Er166 (ppm)	-	-	-	-	-	-	-	-	-
Tm169 (ppm)	-	-	-	-	-	-	-	-	-
Yb172 (ppm)	-	-	-	-	-	-	-	-	-
Lu175 (ppm)	-	-	-	-	-	-	-	-	-
Hf178 (ppm)	-	-	-	-	-	-	-	-	-
Ta181 (ppm)	-	BDL	-	-	-	BDL	BDL	BDL	BDL
W182 (ppm)	BDL	BDL	BDL	BDL	BDL	BDL	BDL	BDL	BDL
Re185 (ppm)	BDL	BDL	BDL	BDL	BDL	BDL	BDL	BDL	BDL
Os189 (ppm)	BDL	BDL	BDL	-	BDL	-	-	BDL	-
Ir193 (ppm)	-	BDL	0	BDL	BDL	BDL	BDL	BDL	BDL
Pt195 (ppm)	-	-	-	-	-	-	BDL	-	BDL
Au197 (ppm)	BDL	BDL	BDL	BDL	BDL	BDL	BDL	BDL	BDL
Hg202 (ppm)	BDL	BDL	BDL	BDL	88	BDL	BDL	BDL	BDL
Pb204 (ppm)	1	4	1	1	1	2	1	1	BDL
Tl205 (ppm)	-	28	22	0	-	-	-	BDL	BDL
Pb206 (ppm)	31	26	24	-	-	1	-	-	BDL
Pb207 (ppm)	-	25	21	0	5	1	8	0	BDL
Pb208 (ppm)	0	BDL	BDL	BDL	BDL	BDL	BDL	BDL	BDL
Bi209 (ppm)	-	-	-	-	-	-	-	-	-
Th232 (ppm)	-	-	0	-	-	-	-	-	-
U238 (ppm)	30	26	22	BDL	7	BDL	8	BDL	BDL
PbTotal (ppm)	-	-	-	-	-	-	-	-	-

Table D9. Trace element data for magnetite continued.

Deposit	Tilt Cove	Tilt Cove	Tilt Cove	Tilt Cove	Tilt Cove	Tilt Cove	Tilt Cove	Tilt Cove	Tilt Cove
Sample	KKMSC72_Mag19	KKMSC72_Mag17	KKMSC72_Mag18	KKMSC72_Mag16	KKMSC72_Mag11	KKMSC72_Mag10	KKMSC72_Mag9	KKMSC72_Mag5	KKMSC72_Mag4
Date	2023-11-22	2023-11-22	2023-11-22	2023-11-22	2023-11-22	2023-11-22	2023-11-22	2023-11-22	2023-11-22
Facies	Pyrrhotite-dominated	Pyrrhotite-dominated	Pyrrhotite-dominated	Pyrrhotite-dominated	Pyrrhotite-dominated	Pyrrhotite-dominated	Pyrrhotite-dominated	Pyrrhotite-dominated	Pyrrhotite-dominated
Li7 (ppm)	6	BDL	BDL	BDL	BDL	BDL	BDL	BDL	BDL
Be9 (ppm)	-	BDL	BDL	-	-	BDL	-	BDL	BDL
B11 (ppm)	BDL	BDL	BDL	BDL	BDL	BDL	BDL	BDL	BDL
Na23 (ppm)	64	BDL	124	BDL	BDL	125	101	BDL	BDL
Mg24 (ppm)	24758	925	13502	5498	723	747	1008	440	429
Al27 (ppm)	2970	572	2987	77	35	273	102	4	5
Si29 (ppm)	22845	BDL	10751	7762	BDL	BDL	3670	BDL	BDL
P31 (ppm)	BDL	BDL	BDL	BDL	BDL	BDL	BDL	BDL	BDL
S32 (ppm)	BDL	BDL	11220	BDL	BDL	60656	BDL	BDL	BDL
K39 (ppm)	BDL	BDL	80	BDL	BDL	BDL	56	BDL	BDL
Ca44 (ppm)	BDL	BDL	BDL	BDL	BDL	BDL	BDL	BDL	BDL
Sc45 (ppm)	BDL	BDL	BDL	BDL	BDL	BDL	BDL	BDL	BDL
Ti47 (ppm)	-	119	190	157	69	35	64	12	32
V51 (ppm)	319	86	69	105	22	8	22	2	3
Cr52 (ppm)	2282	3953	2805	4339	BDL	BDL	BDL	BDL	BDL
Mn55 (ppm)	135	138	163	133	140	92	126	139	143
Fe57 (ppm)	-	-	-	-	-	-	-	-	-
Co59 (ppm)	-	33	41	33	47	41	44	46	40
Ni60 (ppm)	-	-	-	-	121	-	253	-	104
Cu63 (ppm)	20	15	119	17	7	30569	20	BDL	8000
Zn66 (ppm)	52	37	42	30	26	56	26	26	35
Ga71 (ppm)	1	-	1	0	-	-	-	1	0
Ge73 (ppm)	13	-	13	-	-	BDL	7	-	-
As75 (ppm)	BDL	BDL	12	BDL	BDL	BDL	BDL	BDL	BDL
Se77 (ppm)	BDL	BDL	BDL	BDL	BDL	11	BDL	BDL	BDL
Rb85 (ppm)	BDL	BDL	BDL	BDL	BDL	BDL	-	BDL	BDL
Sr88 (ppm)	-	-	-	-	-	-	-	-	-
Y89 (ppm)	-	-	-	-	-	-	-	-	-
Zr90 (ppm)	-	-	-	-	-	-	-	-	-
Nb93 (ppm)	-	-	-	BDL	-	BDL	-	-	-
Mo95 (ppm)	-	-	-	-	-	-	-	BDL	BDL
Ru101 (ppm)	-	-	-	BDL	-	-	-	-	-
Rh103 (ppm)	-	-	BDL	-	-	-	BDL	-	BDL
Pd104 (ppm)	BDL	-	BDL	-	BDL	BDL	-	BDL	-

Pd105 (ppm)	BDL	BDL	BDL	-	-	-	-	-	-
Pd106 (ppm)	BDL	BDL	BDL	BDL	-	-	-	BDL	-
Ag107 (ppm)	BDL	BDL	BDL	BDL	BDL	9	BDL	BDL	-
Cd111 (ppm)	BDL	BDL	4	BDL	BDL	BDL	BDL	-	-
In115 (ppm)	-	-	0	-	BDL	6	-	-	-
Sn118 (ppm)	BDL	BDL	BDL	BDL	BDL	BDL	BDL	BDL	BDL
Sb121 (ppm)	1	0	2	1	0	2	BDL	BDL	1
Te125 (ppm)	BDL	BDL	BDL	BDL	BDL	BDL	BDL	BDL	BDL
Cs133 (ppm)	BDL	BDL	BDL	BDL	BDL	BDL	BDL	BDL	BDL
Ba137 (ppm)	-	-	-	-	-	-	-	-	-
La139 (ppm)	-	-	-	-	-	-	-	-	-
Ce140 (ppm)	-	-	-	-	-	-	-	-	-
Pr141 (ppm)	-	-	-	-	-	-	-	-	-
Nd146 (ppm)	-	-	-	-	-	-	-	-	-
Sm147 (ppm)	-	-	-	-	-	-	-	-	-
Eu153 (ppm)	-	-	-	-	-	-	-	-	-
Gd157 (ppm)	-	-	-	-	-	-	-	-	-
Tb159 (ppm)	-	-	-	-	-	-	-	-	-
Dy163 (ppm)	-	-	-	-	-	-	-	-	-
Ho165 (ppm)	-	-	-	-	-	-	-	-	-
Er166 (ppm)	-	-	-	-	-	-	-	-	-
Tm169 (ppm)	-	-	-	-	-	-	-	-	-
Yb172 (ppm)	-	-	-	-	-	-	-	-	-
Lu175 (ppm)	-	-	-	-	-	-	-	-	-
Hf178 (ppm)	-	-	-	-	-	-	-	-	-
Ta181 (ppm)	-	-	-	-	BDL	-	-	-	-
W182 (ppm)	-	-	-	-	-	-	-	-	-
Re185 (ppm)	BDL	BDL	BDL	BDL	BDL	BDL	BDL	BDL	BDL
Os189 (ppm)	BDL	BDL	BDL	BDL	BDL	BDL	BDL	BDL	BDL
Ir193 (ppm)	-	-	-	BDL	BDL	-	-	-	-
Pt195 (ppm)	BDL	BDL	BDL	BDL	BDL	BDL	BDL	-	BDL
Au197 (ppm)	-	-	-	-	-	-	-	BDL	-
Hg202 (ppm)	BDL	BDL	BDL	BDL	BDL	BDL	BDL	BDL	BDL
Pb204 (ppm)	BDL	BDL	BDL	BDL	BDL	BDL	BDL	BDL	BDL
Tl205 (ppm)	BDL	BDL	BDL	BDL	BDL	1	BDL	BDL	BDL
Pb206 (ppm)	1	3	46	-	-	2	1	BDL	2
Pb207 (ppm)	1	-	28	-	-	2	1	-	2
Pb208 (ppm)	1	1	47	0	-	2	1	BDL	2
Bi209 (ppm)	BDL	BDL	BDL	BDL	BDL	BDL	BDL	BDL	BDL
Th232 (ppm)	-	-	-	-	-	-	-	-	-
U238 (ppm)	-	-	-	-	-	-	-	-	-
PbTotal (ppm)	BDL	BDL	41	BDL	BDL	2	BDL	BDL	2

Table D9. Trace element data for magnetite continued.

Deposit	Tilt Cove	Tilt Cove	Tilt Cove	Tilt Cove	Tilt Cove	Tilt Cove	Tilt Cove	Tilt Cove	Tilt Cove
Sample	KKMSC72_Mag1	KKMSC72_Mag2	KKMSC72_Mag8	KKMSC72_Mag6	KKMSC72_Mag7	KKMSC72_Mag14	KKMSC72_Mag15	KKMSC72_Mag13	KKMSC72_Mag12
Date	2023-11-22	2023-11-22	2023-11-22	2023-11-22	2023-11-22	2023-11-22	2023-11-22	2023-11-22	2023-11-22
Facies	Pyrrhotite-dominated	Pyrrhotite-dominated	Pyrrhotite-dominated	Pyrrhotite-dominated	Pyrrhotite-dominated	Pyrrhotite-dominated	Pyrrhotite-dominated	Pyrrhotite-dominated	Pyrrhotite-dominated
Li7 (ppm)	BDL	BDL	2	BDL	BDL	BDL	BDL	BDL	BDL
Be9 (ppm)	BDL	-	BDL	-	-	-	-	BDL	BDL
B11 (ppm)	91	BDL	BDL	BDL	BDL	BDL	BDL	BDL	BDL
Na23 (ppm)	BDL	BDL	65	BDL	BDL	BDL	BDL	BDL	BDL
Mg24 (ppm)	-	680	3489	454	478	331	357	369	436
Al27 (ppm)	6	24	99	17	6	5	BDL	5	10
Si29 (ppm)	11914	BDL	6225	BDL	BDL	BDL	BDL	BDL	BDL
P31 (ppm)	BDL	BDL	BDL	BDL	BDL	BDL	BDL	BDL	BDL
S32 (ppm)	BDL	BDL	15234	BDL	BDL	BDL	21017	BDL	BDL
K39 (ppm)	BDL	BDL	BDL	BDL	BDL	BDL	BDL	BDL	BDL
Ca44 (ppm)	537	BDL	BDL	BDL	BDL	BDL	BDL	BDL	BDL
Sc45 (ppm)	8	BDL	BDL	BDL	BDL	BDL	BDL	BDL	BDL
Ti47 (ppm)	105	67	34	46	-	8	79	45	69
V51 (ppm)	60	20	15	3	9	1	21	7	23
Cr52 (ppm)	47	BDL	BDL	16	BDL	BDL	BDL	BDL	BDL
Mn55 (ppm)	78	144	134	145	166	148	107	155	159
Fe57 (ppm)	-	-	-	-	-	-	-	-	-
Co59 (ppm)	47	48	41	43	43	29	28	33	35
Ni60 (ppm)	237	-	-	-	-	-	-	236	214
Cu63 (ppm)	1152	33	5322	BDL	4	51	15279	5	12
Zn66 (ppm)	33	51	128	29	26	27	500	33	40
Ga71 (ppm)	-	0	-	1	-	-	1	-	-
Ge73 (ppm)	-	-	BDL	-	-	-	-	6	BDL
As75 (ppm)	BDL	BDL	BDL	BDL	BDL	BDL	BDL	BDL	BDL
Se77 (ppm)	17	BDL	BDL	BDL	BDL	BDL	BDL	BDL	BDL
Rb85 (ppm)	1	BDL	BDL	BDL	BDL	BDL	BDL	BDL	-
Sr88 (ppm)	-	-	-	-	-	-	-	-	-
Y89 (ppm)	-	-	-	-	-	-	-	-	BDL
Zr90 (ppm)	-	-	-	-	-	-	-	-	-
Nb93 (ppm)	-	-	-	-	-	-	BDL	-	-
Mo95 (ppm)	8	-	-	BDL	BDL	BDL	-	BDL	BDL
Ru101 (ppm)	-	-	-	-	-	-	-	-	-
Rh103 (ppm)	-	-	-	-	-	BDL	0	BDL	-
Pd104 (ppm)	-	BDL	BDL	-	-	-	-	-	-

Pd105 (ppm)	-	-	BDL	-	-	BDL	-	-	BDL
Pd106 (ppm)	-	BDL	BDL	-	-	-	-	-	BDL
Ag107 (ppm)	BDL	BDL	2	BDL	BDL	BDL	1	BDL	BDL
Cd111 (ppm)	BDL	BDL	BDL	BDL	-	-	-	BDL	BDL
In115 (ppm)	-	-	-	-	-	-	-	-	-
Sn118 (ppm)	3	BDL	BDL	BDL	BDL	BDL	BDL	BDL	BDL
Sb121 (ppm)	BDL	1	5	BDL	BDL	BDL	4	0	0
Te125 (ppm)	BDL	BDL	3	BDL	-	-	-	BDL	BDL
Cs133 (ppm)	1	BDL	BDL	BDL	BDL	BDL	BDL	BDL	BDL
Ba137 (ppm)	-	-	-	-	-	-	-	-	-
La139 (ppm)	-	-	-	-	-	-	-	-	-
Ce140 (ppm)	-	-	-	-	-	-	-	-	-
Pr141 (ppm)	-	-	-	-	-	-	-	-	-
Nd146 (ppm)	BDL	-	-	-	-	-	-	-	-
Sm147 (ppm)	-	-	-	-	-	-	-	-	-
Eu153 (ppm)	-	-	-	-	-	-	-	-	-
Gd157 (ppm)	-	-	-	-	-	-	-	-	-
Tb159 (ppm)	-	-	-	-	-	-	-	-	-
Dy163 (ppm)	-	-	-	-	-	-	-	-	-
Ho165 (ppm)	-	-	-	-	-	-	-	-	-
Er166 (ppm)	-	-	-	-	-	-	-	-	-
Tm169 (ppm)	-	-	-	-	-	-	-	-	-
Yb172 (ppm)	-	-	-	-	-	-	-	-	-
Lu175 (ppm)	-	-	-	-	-	-	-	-	-
Hf178 (ppm)	-	-	-	-	-	-	-	-	-
Ta181 (ppm)	BDL	-	-	-	-	-	-	-	-
W182 (ppm)	BDL	-	-	-	-	-	2	BDL	BDL
Re185 (ppm)	BDL	BDL	BDL	BDL	BDL	BDL	BDL	BDL	BDL
Os189 (ppm)	BDL	BDL	BDL	BDL	BDL	-	BDL	BDL	BDL
Ir193 (ppm)	BDL	-	-	BDL	-	BDL	BDL	BDL	BDL
Pt195 (ppm)	BDL	BDL	BDL	BDL	BDL	-	BDL	-	-
Au197 (ppm)	-	BDL	-	-	-	-	BDL	-	-
Hg202 (ppm)	BDL	BDL	BDL	BDL	BDL	BDL	BDL	BDL	BDL
Pb204 (ppm)	368	BDL	BDL	BDL	BDL	BDL	BDL	BDL	BDL
Tl205 (ppm)	1	BDL	0	BDL	BDL	BDL	BDL	BDL	BDL
Pb206 (ppm)	59	-	30	0	BDL	BDL	2	-	BDL
Pb207 (ppm)	100	-	29	-	BDL	-	-	1	0
Pb208 (ppm)	53	0	31	0	0	-	3	0	0
Bi209 (ppm)	BDL	BDL	BDL	BDL	BDL	BDL	BDL	BDL	BDL
Th232 (ppm)	-	-	-	-	-	-	-	-	-
U238 (ppm)	-	-	-	-	-	-	BDL	-	-
PbTotal (ppm)	69	BDL	30	BDL	BDL	BDL	3	1	BDL

Table D9. Trace element data for magnetite continued.

Deposit	Tilt Cove	Tilt Cove	Tilt Cove	Tilt Cove	Tilt Cove	Tilt Cove	Tilt Cove
Sample	KKMSC13_Mag2	KKMSC13_Mag3	KKMSC13_Mag4	KKMSC23_Mag1	KKMSC23_Mag2	KKMSC23_Mag3	KKMSC23_Mag5
Date	2023-11-23	2023-11-23	2023-11-23	2023-11-23	2023-11-23	2023-11-23	2023-11-23
Facies	Pyrite-dominated	Pyrite-dominated	Pyrite-dominated	Magnetite-dominated	Magnetite-dominated	Magnetite-dominated	Magnetite-dominated
Li7 (ppm)	9	BDL	BDL	3	BDL	2	BDL
Be9 (ppm)	-	-	-	-	-	-	BDL
B11 (ppm)	BDL	BDL	BDL	BDL	BDL	BDL	BDL
Na23 (ppm)	BDL	BDL	BDL	BDL	327	BDL	BDL
Mg24 (ppm)	99439	125379	-	207	-	104	61
Al27 (ppm)	75	6	6	675	313	940	613
Si29 (ppm)	BDL	BDL	BDL	BDL	4870	BDL	BDL
P31 (ppm)	BDL	BDL	BDL	BDL	BDL	BDL	BDL
S32 (ppm)	97808	142327	203256	BDL	BDL	BDL	BDL
K39 (ppm)	BDL	BDL	BDL	86	BDL	406	139
Ca44 (ppm)	6654	5063	7451	BDL	BDL	BDL	BDL
Sc45 (ppm)	BDL	BDL	BDL	BDL	BDL	BDL	BDL
Ti47 (ppm)	-	BDL	BDL	83	-	-	-
V51 (ppm)	9	6	8	266	175	250	148
Cr52 (ppm)	BDL	BDL	BDL	193	157	75	158
Mn55 (ppm)	34752	39214	32562	107	105	106	115
Fe57 (ppm)	-	-	-	-	-	-	-
Co59 (ppm)	BDL	BDL	BDL	100	108	113	102
Ni60 (ppm)	-	15	8	23	-	-	-
Cu63 (ppm)	14	7	23	23	4583	18	12
Zn66 (ppm)	436	385	318	339	233	308	401
Ga71 (ppm)	-	-	-	-	2	-	-
Ge73 (ppm)	-	-	-	19	-	-	-
As75 (ppm)	1170	680	506	BDL	BDL	BDL	BDL
Se77 (ppm)	BDL	BDL	BDL	BDL	BDL	BDL	BDL
Rb85 (ppm)	BDL	BDL	BDL	BDL	BDL	1	1
Sr88 (ppm)	-	-	-	-	-	-	-
Y89 (ppm)	-	-	-	-	-	-	-
Zr90 (ppm)	-	-	-	-	-	-	-
Nb93 (ppm)	17	1	2	BDL	BDL	BDL	BDL
Mo95 (ppm)	-	-	-	BDL	-	-	-
Ru101 (ppm)	-	-	-	-	-	-	-
Rh103 (ppm)	-	-	-	-	-	BDL	-
Pd104 (ppm)	BDL	BDL	BDL	-	-	BDL	BDL
Pd105 (ppm)	-	BDL	-	-	BDL	BDL	-

Pd106 (ppm)	2	BDL	1	BDL	2	BDL	-
Ag107 (ppm)	-	BDL	BDL	BDL	-	BDL	BDL
Cd111 (ppm)	-	0	-	-	-	-	-
In115 (ppm)	BDL	BDL	BDL	BDL	BDL	BDL	BDL
Sn118 (ppm)	-	2	8	BDL	BDL	BDL	BDL
Sb121 (ppm)	-	BDL	BDL	BDL	BDL	BDL	BDL
Te125 (ppm)	BDL	BDL	BDL	BDL	BDL	BDL	BDL
Cs133 (ppm)	-	-	-	-	-	-	-
Ba137 (ppm)	-	-	-	-	-	-	-
La139 (ppm)	-	-	-	-	-	-	-
Ce140 (ppm)	-	-	-	-	-	-	-
Pr141 (ppm)	-	-	-	-	-	-	-
Nd146 (ppm)	-	-	-	-	-	-	-
Sm147 (ppm)	-	-	-	-	-	-	-
Eu153 (ppm)	-	-	-	-	-	-	-
Gd157 (ppm)	-	-	-	-	-	-	-
Tb159 (ppm)	2	-	-	-	-	-	-
Dy163 (ppm)	-	-	-	-	-	-	-
Ho165 (ppm)	-	-	-	-	-	-	-
Er166 (ppm)	-	-	-	-	-	-	-
Tm169 (ppm)	-	-	-	-	-	-	-
Yb172 (ppm)	-	-	-	-	-	-	-
Lu175 (ppm)	-	-	-	-	-	-	-
Hf178 (ppm)	-	-	-	-	-	-	-
Ta181 (ppm)	BDL	-	BDL	-	-	-	-
W182 (ppm)	BDL	BDL	BDL	BDL	BDL	BDL	BDL
Re185 (ppm)	BDL	BDL	BDL	BDL	BDL	BDL	BDL
Os189 (ppm)	BDL	BDL	BDL	BDL	-	BDL	BDL
Ir193 (ppm)	BDL	-	BDL	-	-	BDL	BDL
Pt195 (ppm)	BDL	-	-	-	BDL	-	BDL
Au197 (ppm)	BDL	BDL	BDL	BDL	BDL	BDL	BDL
Hg202 (ppm)	BDL	BDL	44	BDL	BDL	BDL	BDL
Pb204 (ppm)	BDL	BDL	3	BDL	BDL	BDL	BDL
Tl205 (ppm)	19	18	40	-	0	1	0
Pb206 (ppm)	18	17	-	0	1	1	0
Pb207 (ppm)	22	17	40	0	1	1	0
Pb208 (ppm)	0	0	0	BDL	BDL	BDL	BDL
Bi209 (ppm)	-	-	-	-	-	-	-
Th232 (ppm)	-	-	-	-	-	-	-
U238 (ppm)	17	17	40	BDL	BDL	BDL	BDL
PbTotal (ppm)	-	-	-	-	-	-	-

Table D10. Trace element data for chromite.

Deposit	Tilt Cove	Tilt Cove	Tilt Cove	Tilt Cove	Tilt Cove	Tilt Cove	Tilt Cove	Tilt Cove	Tilt Cove
Sample	KKMSC63_Chr 1	KKMSC63_Chr 2	KKMSC63_Chr 3	KKMSC63_Chr 4	KKMSC63_Chr 5	KKMSC63_Chr 8	KKMSC63_Chr 6	KKMSC63_Chr 9	KKMSC63_Chr 11
Date	2023-11-21	2023-11-21	2023-11-21	2023-11-21	2023-11-21	2023-11-21	2023-11-21	2023-11-21	2023-11-21
Facies	Pyrite-dominated	Pyrite-dominated	Pyrite-dominated	Pyrite-dominated	Pyrite-dominated	Pyrite-dominated	Pyrite-dominated	Pyrite-dominated	Pyrite-dominated
Li7 (ppm)	BDL	BDL	6	6	7	5	4	BDL	5
Be9 (ppm)	BDL	-	-	-	BDL	-	-	-	BDL
B11 (ppm)	106	85	BDL	90	88	65	78	BDL	BDL
Na23 (ppm)	BDL	BDL	BDL	BDL	BDL	BDL	516	BDL	229
Mg24 (ppm)	70518	69262	85432	-	79792	83482	81626	86092	87034
Al27 (ppm)	91716	93143	93174	100469	103683	100900	97754	99711	107558
Si29 (ppm)	BDL	7684	4099	BDL	BDL	BDL	BDL	3334	8812
P31 (ppm)	BDL	BDL	BDL	BDL	BDL	BDL	BDL	BDL	BDL
S32 (ppm)	BDL	BDL	BDL	BDL	BDL	BDL	BDL	BDL	BDL
K39 (ppm)	BDL	BDL	BDL	BDL	BDL	BDL	BDL	BDL	BDL
Ca44 (ppm)	BDL	BDL	BDL	BDL	BDL	BDL	BDL	BDL	BDL
Sc45 (ppm)	6	11	6	7	5	6	8	5	7
Ti47 (ppm)	2663	2758	3417	3555	3328	3524	-	3651	3673
V51 (ppm)	1882	1803	1278	1388	1490	1505	1395	1415	1510
Cr52 (ppm)	-	-	-	-	-	-	-	-	-
Mn55 (ppm)	1513	1540	1425	1447	1541	1360	1449	1358	1426
Fe57 (ppm)	185237	372379	192341	214702	222579	216988	201693	208077	219864
Co59 (ppm)	489	449	382	392	423	390	387	396	410
Ni60 (ppm)	-	652	846	874	-	-	-	-	-
Cu63 (ppm)	9	5	19	8	22	16	8	BDL	20
Zn66 (ppm)	3497	5024	1213	1388	2312	2169	1296	1425	1664
Ga71 (ppm)	-	-	-	-	-	25	-	-	-
Ge73 (ppm)	BDL	BDL	BDL	-	BDL	-	BDL	-	-
As75 (ppm)	BDL	11	BDL	BDL	BDL	BDL	BDL	BDL	BDL
Se77 (ppm)	BDL	BDL	BDL	BDL	BDL	BDL	BDL	BDL	BDL
Rb85 (ppm)	BDL	BDL	BDL	BDL	BDL	BDL	BDL	BDL	BDL
Sr88 (ppm)	BDL	-	-	-	-	-	-	-	-
Y89 (ppm)	-	-	-	-	BDL	-	-	-	-
Zr90 (ppm)	1	-	-	-	-	-	-	-	-
Nb93 (ppm)	-	BDL	BDL	-	BDL	-	-	BDL	BDL
Mo95 (ppm)	-	BDL	BDL	-	BDL	BDL	BDL	BDL	BDL
Ru101 (ppm)	BDL	BDL	BDL	-	-	BDL	-	BDL	-
Rh103 (ppm)	-	BDL	-	-	-	-	BDL	-	-
Pd104 (ppm)	BDL	-	-	-	BDL	-	-	-	BDL

Pd105 (ppm)	BDL	BDL	BDL	BDL	BDL	-	-	-	-
Pd106 (ppm)	BDL	BDL	BDL	BDL	BDL	BDL	BDL	BDL	BDL
Ag107 (ppm)	BDL	BDL	BDL	-	BDL	BDL	-	BDL	BDL
Cd111 (ppm)	BDL	BDL	BDL	BDL	-	BDL	-	-	-
In115 (ppm)	BDL	BDL	BDL	BDL	BDL	BDL	BDL	BDL	BDL
Sn118 (ppm)	BDL	10	BDL	BDL	BDL	BDL	BDL	BDL	BDL
Sb121 (ppm)	BDL	BDL	-	-	BDL	BDL	BDL	BDL	BDL
Te125 (ppm)	BDL	BDL	BDL	BDL	BDL	BDL	BDL	BDL	BDL
Cs133 (ppm)	-	-	-	-	-	-	-	-	-
Ba137 (ppm)	-	-	-	-	-	-	-	-	-
La139 (ppm)	-	-	-	-	-	-	-	-	-
Ce140 (ppm)	-	-	-	-	-	-	-	-	-
Pr141 (ppm)	-	-	-	-	-	-	-	-	-
Nd146 (ppm)	-	-	-	-	-	-	-	-	-
Sm147 (ppm)	-	-	-	-	-	-	-	-	-
Eu153 (ppm)	-	-	-	-	BDL	BDL	-	-	-
Gd157 (ppm)	-	-	-	-	-	-	-	-	-
Tb159 (ppm)	-	-	-	-	-	-	-	-	-
Dy163 (ppm)	-	-	-	-	-	-	-	-	-
Ho165 (ppm)	-	-	-	-	-	-	-	-	-
Er166 (ppm)	-	-	-	-	-	-	-	-	-
Tm169 (ppm)	-	-	-	-	-	-	-	-	-
Yb172 (ppm)	-	-	-	-	-	-	-	-	-
Lu175 (ppm)	-	-	-	-	-	-	-	-	-
Hf178 (ppm)	-	-	-	-	-	-	-	-	-
Ta181 (ppm)	-	-	BDL	BDL	BDL	-	-	BDL	-
W182 (ppm)	BDL	BDL	BDL	BDL	BDL	BDL	BDL	BDL	BDL
Re185 (ppm)	BDL	BDL	BDL	BDL	BDL	BDL	BDL	BDL	BDL
Os189 (ppm)	BDL	BDL	-	BDL	-	-	BDL	-	-
Ir193 (ppm)	BDL	BDL	BDL	BDL	-	BDL	BDL	BDL	BDL
Pt195 (ppm)	-	-	-	BDL	-	-	-	BDL	-
Au197 (ppm)	BDL	BDL	BDL	BDL	BDL	BDL	BDL	BDL	BDL
Hg202 (ppm)	BDL	BDL	BDL	BDL	BDL	BDL	BDL	BDL	BDL
Pb204 (ppm)	BDL	BDL	0	BDL	BDL	BDL	0	BDL	BDL
Tl205 (ppm)	BDL	3	BDL	-	BDL	-	-	BDL	BDL
Pb206 (ppm)	BDL	5	-	BDL	-	BDL	-	BDL	-
Pb207 (ppm)	BDL	3	BDL	0	0	BDL	BDL	BDL	0
Pb208 (ppm)	BDL	BDL	BDL	BDL	BDL	BDL	BDL	BDL	BDL
Bi209 (ppm)	-	-	-	-	-	-	-	-	-
Th232 (ppm)	-	-	-	-	-	-	-	-	-
U238 (ppm)	BDL	3	BDL	BDL	BDL	BDL	BDL	BDL	BDL
PbTotal (ppm)	-	-	-	-	-	-	-	-	-

Table D10. Trace element data for chromite continued.

Deposit	Tilt Cove	Tilt Cove	Tilt Cove	Tilt Cove
Sample	KKMSC72_Chr4	KKMSC72_Chr2	KKMSC72_Chr2	KKMSC72_Chr1
Date	2023-11-22	2023-11-22	2023-11-22	2023-11-22
Facies	Pyrrhotite-dominated	Pyrrhotite-dominated	Pyrrhotite-dominated	Pyrrhotite-dominated
Li7 (ppm)	BDL	BDL	BDL	BDL
Be9 (ppm)	-	-	-	-
B11 (ppm)	82	97	BDL	BDL
Na23 (ppm)	BDL	BDL	BDL	BDL
Mg24 (ppm)	150648	157913	-	158818
Al27 (ppm)	262553	269542	290674	264209
Si29 (ppm)	BDL	BDL	BDL	BDL
P31 (ppm)	BDL	BDL	BDL	BDL
S32 (ppm)	BDL	BDL	BDL	BDL
K39 (ppm)	BDL	BDL	BDL	BDL
Ca44 (ppm)	BDL	BDL	BDL	BDL
Sc45 (ppm)	9	BDL	BDL	BDL
Ti47 (ppm)	4738	-	5789	5457
V51 (ppm)	2616	2734	2840	2766
Cr52 (ppm)	-	-	-	-
Mn55 (ppm)	2347	2309	2472	2325
Fe57 (ppm)	217618	240481	245065	233668
Co59 (ppm)	489	540	504	475
Ni60 (ppm)	-	-	3181	3066
Cu63 (ppm)	8	BDL	BDL	BDL
Zn66 (ppm)	2696	2085	1985	1921
Ga71 (ppm)	-	-	-	-
Ge73 (ppm)	-	BDL	BDL	BDL
As75 (ppm)	BDL	BDL	BDL	BDL
Se77 (ppm)	BDL	BDL	BDL	BDL
Rb85 (ppm)	BDL	BDL	BDL	BDL
Sr88 (ppm)	-	-	-	-
Y89 (ppm)	-	-	-	-
Zr90 (ppm)	-	-	-	-
Nb93 (ppm)	-	-	-	-
Mo95 (ppm)	-	-	-	-
Ru101 (ppm)	-	-	BDL	BDL
Rh103 (ppm)	-	-	-	-
Pd104 (ppm)	-	-	BDL	-
Pd105 (ppm)	-	-	BDL	BDL

Pd106 (ppm)	BDL	-	-	BDL
Ag107 (ppm)	BDL	BDL	BDL	BDL
Cd111 (ppm)	-	-	-	BDL
In115 (ppm)	-	BDL	BDL	BDL
Sn118 (ppm)	BDL	BDL	BDL	BDL
Sb121 (ppm)	BDL	BDL	BDL	BDL
Te125 (ppm)	BDL	-	BDL	BDL
Cs133 (ppm)	BDL	BDL	BDL	BDL
Ba137 (ppm)	-	-	-	-
La139 (ppm)	-	-	-	-
Ce140 (ppm)	-	-	-	-
Pr141 (ppm)	-	-	-	-
Nd146 (ppm)	-	-	-	-
Sm147 (ppm)	-	-	-	-
Eu153 (ppm)	-	-	-	-
Gd157 (ppm)	-	-	-	-
Tb159 (ppm)	-	-	-	-
Dy163 (ppm)	-	-	-	-
Ho165 (ppm)	-	-	-	-
Er166 (ppm)	-	-	-	-
Tm169 (ppm)	-	-	-	-
Yb172 (ppm)	-	-	-	-
Lu175 (ppm)	-	-	-	-
Hf178 (ppm)	-	-	-	-
Ta181 (ppm)	-	-	-	BDL
W182 (ppm)	-	BDL	-	-
Re185 (ppm)	BDL	BDL	BDL	BDL
Os189 (ppm)	BDL	BDL	BDL	BDL
Ir193 (ppm)	BDL	-	-	-
Pt195 (ppm)	BDL	BDL	BDL	BDL
Au197 (ppm)	BDL	-	-	BDL
Hg202 (ppm)	BDL	BDL	BDL	BDL
Pb204 (ppm)	BDL	BDL	BDL	BDL
Tl205 (ppm)	BDL	BDL	BDL	BDL
Pb206 (ppm)	1	BDL	BDL	BDL
Pb207 (ppm)	1	BDL	BDL	BDL
Pb208 (ppm)	-	BDL	BDL	BDL
Bi209 (ppm)	BDL	BDL	BDL	BDL
Th232 (ppm)	-	-	-	-
U238 (ppm)	-	-	-	-
PbTotal (ppm)	BDL	BDL	BDL	BDL

Table D11. Detection limits LA-ICP-MS.

Mineral	Pyrite		Chalcopyrite		Pyrrhotite		Sphalerite		Cobaltite	
Element	LOD Min	LOD Max	LOD Min	LOD Max	LOD Min	LOD Max	LOD Min	LOD Max	LOD Min	LOD Max
Li7 (ppm)	0	1	0	10	0	2	0	1	0	44
Be9 (ppm)	0	2	0	6124	0	3	0	1	0	79
B11 (ppm)	2	32	3	65278	4	40	1	12	3	360
Na23 (ppm)	2	81	5	97919	9	52	2	16	8	1575
Mg24 (ppm)	0	15	0	9499	0	37	0	4	0	25
Al27 (ppm)	0	14	0	6642	0	4	0	1	1	53
Si29 (ppm)	130	2156	291	3882752	370	3109	120	923	323	38946
P31 (ppm)	5	65	12	137937	12	106	4	35	15	1211
S32 (ppm)	79	9591	204	6177619	468	7079	128	1993	631	27064
K39 (ppm)	3	29	3	81357	5	31	2	12	6	781
Ca44 (ppm)	16	356	38	465154	54	408	17	108	55	7912
Sc45 (ppm)	0	2	0	3402	0	2	0	1	0	33
Ti47 (ppm)	0	5	0	10813	0	5	0	2	0	62
V51 (ppm)	0	0	0	984	0	1	0	0	0	7
Cr52 (ppm)	0	4	1	8187	1	5	0	2	1	172
Mn55 (ppm)	0	1	0	2065	0	1	0	1	0	26
Fe57 (ppm)	-	-	4	31902	-	-	1	9	3	367
Co59 (ppm)	0	0	0	194	0	1	0	0	-	-
Ni60 (ppm)	0	1	0	978	0	3	0	0	0	1
Cu63 (ppm)	0	1	-	-	0	1	0	1	0	25
Zn66 (ppm)	0	2	0	2513	0	2	-	-	0	36
Ga71 (ppm)	0	0	0	281	0	0	0	0	0	0
Ge73 (ppm)	0	3	0	7	0	3	0	1	0	5
As75 (ppm)	0	10	1	97247	1	27	0	5	4	77
Se77 (ppm)	0	10	1	5197	1	21	0	2	1	46
Rb85 (ppm)	0	0	0	328	0	0	0	0	0	5
Sr88 (ppm)	0	0	0	0	0	0	0	0	0	0
Y89 (ppm)	0	0	0	0	0	0	0	0	0	0
Zr90 (ppm)	0	0	0	2	0	0	0	0	0	0
Nb93 (ppm)	0	0	0	1	0	0	0	0	0	7
Mo95 (ppm)	0	0	0	752	0	1	0	0	0	1
Ru101 (ppm)	0	0	0	2	0	0	0	0	0	0
Rh103 (ppm)	0	0	0	2	0	0	0	0	0	2
Pd104 (ppm)	0	0	0	494	0	2	0	0	0	2
Pd105 (ppm)	0	0	0	594	0	1	0	0	0	14
Pd106 (ppm)	0	0	0	2	0	0	0	0	0	7
Ag107 (ppm)	0	0	0	1150	0	0	0	0	0	1
Cd111 (ppm)	0	0	0	2	0	1	0	0	0	2

In115 (ppm)	0	0	0	846	0	0	0	0	0	18
Sn118 (ppm)	0	1	0	114	0	0	0	0	0	3
Sb121 (ppm)	0	0	0	1001	0	0	0	0	0	1
Te125 (ppm)	0	1	0	496	0	1	0	1	0	8
Cs133 (ppm)	0	0	0	1	0	0	0	0	0	1
Ba137 (ppm)	0	0	0	0	0	0	0	0	0	0
La139 (ppm)	0	0	0	0	0	0	0	0	0	0
Ce140 (ppm)	0	0	0	0	0	0	0	0	0	0
Pr141 (ppm)	0	0	0	0	0	0	0	0	0	0
Nd146 (ppm)	0	0	0	1	0	0	0	0	0	0
Sm147 (ppm)	0	0	0	0	0	0	0	0	0	0
Eu153 (ppm)	0	0	0	0	0	0	0	0	0	0
Gd157 (ppm)	0	0	0	0	0	0	0	0	0	0
Tb159 (ppm)	0	0	0	0	0	0	0	0	0	0
Dy163 (ppm)	0	0	0	0	0	0	0	0	0	0
Ho165 (ppm)	0	0	0	0	0	0	0	0	0	0
Er166 (ppm)	0	0	0	0	0	0	0	0	0	0
Tm169 (ppm)	0	0	0	0	0	0	0	0	0	0
Yb172 (ppm)	0	0	0	0	0	0	0	0	0	0
Lu175 (ppm)	0	0	0	0	0	0	0	0	0	0
Hf178 (ppm)	0	0	0	1	0	0	0	0	0	0
Ta181 (ppm)	0	0	0	1	0	0	0	0	0	0
W182 (ppm)	0	1	0	525	0	0	0	0	0	7
Re185 (ppm)	0	0	0	498	0	0	0	0	0	10
Os189 (ppm)	0	0	0	101	0	1	0	0	0	2
Ir193 (ppm)	0	0	0	640	0	0	0	0	0	4
Pt195 (ppm)	0	7	0	81	0	0	0	7	0	0
Au197 (ppm)	0	8	0	37126	0	10	0	14	0	467
Hg202 (ppm)	0	10	0	63577	2	17	0	17	2	593
Pb204 (ppm)	0	39	0	322	0	28	0	16	0	89
Tl205 (ppm)	0	0	0	0	0	0	0	0	0	2
Pb206 (ppm)	0	0	0	0	0	0	0	0	0	0
Pb207 (ppm)	0	0	0	94	0	0	0	0	0	1
Pb208 (ppm)	0	0	0	92	0	0	0	0	0	1
Bi209 (ppm)	0	0	0	0	0	0	0	0	0	0
Th232 (ppm)	0	0	0	3	0	0	0	0	0	0
U238 (ppm)	0	0	0	948	0	0	0	0	0	9
PbTotal (ppm)	0	1	0	1	0	0	0	0	0	1

Table D11. Detection limits LA-ICP-MS continued.

Mineral	Pentlandite		Arsenopyrite		Bornite		Magnetite		Chromite	
Element	LOD Min	LOD Max	LOD Min	LOD Max	LOD Min	LOD Max	LOD Min	LOD Max	LOD Min	LOD Max
Li7 (ppm)	0	2	0	0	0	0	0	2	1	2
Be9 (ppm)	0	5	0	1	0	2	5	24	0	4
B11 (ppm)	2	38	3	6	4	11	10	37	11	44
Na23 (ppm)	8	60	4	10	7	25	0	4	21	60
Mg24 (ppm)	0	49	0	2	0	9	0	3	0	11
Al27 (ppm)	0	5	0	1	1	2	605	2575	2	18
Si29 (ppm)	452	2305	216	610	445	944	25	85	905	4700
P31 (ppm)	13	130	9	30	15	37	590	6915	1	3
S32 (ppm)	540	7748	552	1460	540	2006	8	47	0	5
K39 (ppm)	6	48	3	8	7	19	71	438	0	1
Ca44 (ppm)	43	312	21	69	42	142	0	2	-	-
Sc45 (ppm)	0	3	0	1	0	1	0	4	1	2
Ti47 (ppm)	0	3	0	2	0	4	0	0	11	45
V51 (ppm)	0	1	0	0	0	0	2	7	0	0
Cr52 (ppm)	1	6	1	2	2	5	0	1	0	1
Mn55 (ppm)	0	1	0	0	0	1	-	-	1	2
Fe57 (ppm)	4	27	2	7	5	16	0	0	1	3
Co59 (ppm)	0	6	0	0	0	0	0	0	0	0
Ni60 (ppm)	-	-	0	0	0	0	0	1	0	3
Cu63 (ppm)	0	1	0	0	-	-	0	2	2	6
Zn66 (ppm)	0	2	0	0	0	1	0	0	3	11
Ga71 (ppm)	0	0	0	0	0	0	0	2	0	0
Ge73 (ppm)	0	4	0	0	0	1	1	13	0	0
As75 (ppm)	1	22	-	-	2	6	1	6	0	0
Se77 (ppm)	1	5	0	1	0	3	0	0	0	0
Rb85 (ppm)	0	0	0	0	0	0	0	0	0	0
Sr88 (ppm)	0	0	0	0	0	0	0	0	0	1
Y89 (ppm)	0	0	0	0	0	0	0	0	0	0
Zr90 (ppm)	0	0	0	0	0	0	0	0	0	1
Nb93 (ppm)	0	0	0	0	0	0	0	1	0	1
Mo95 (ppm)	0	1	0	0	0	0	0	0	0	1
Ru101 (ppm)	0	0	0	0	0	0	0	2	0	1
Rh103 (ppm)	0	0	0	0	0	0	0	1	0	0
Pd104 (ppm)	0	2	0	0	0	0	0	1	0	1
Pd105 (ppm)	0	0	0	0	0	0	0	0	0	1
Pd106 (ppm)	0	1	0	0	0	0	0	1	0	1
Ag107 (ppm)	0	0	0	0	0	0	0	1	0	1
Cd111 (ppm)	0	1	0	0	0	0	0	1	0	1

In115 (ppm)	0	0	0	0	0	0	0	0	0	0
Sn118 (ppm)	0	1	0	0	0	0	0	1	0	0
Sb121 (ppm)	0	1	0	0	0	0	0	1	0	0
Te125 (ppm)	0	1	0	0	0	0	0	0	0	0
Cs133 (ppm)	0	0	0	0	0	0	0	0	0	0
Ba137 (ppm)	0	0	0	0	0	0	0	0	0	0
La139 (ppm)	0	0	0	0	0	0	0	0	0	0
Ce140 (ppm)	0	0	0	0	0	0	0	0	0	0
Pr141 (ppm)	0	0	0	0	0	0	0	0	0	0
Nd146 (ppm)	0	0	0	0	0	0	0	0	0	0
Sm147 (ppm)	0	0	0	0	0	0	0	0	0	0
Eu153 (ppm)	0	0	0	0	0	0	0	0	0	0
Gd157 (ppm)	0	0	0	0	0	0	0	0	0	0
Tb159 (ppm)	0	0	0	0	0	0	0	0	0	0
Dy163 (ppm)	0	0	0	0	0	0	0	0	0	0
Ho165 (ppm)	0	0	0	0	0	0	0	0	0	0
Er166 (ppm)	0	0	0	0	0	0	0	0	0	0
Tm169 (ppm)	0	0	0	0	0	0	0	0	0	0
Yb172 (ppm)	0	0	0	0	0	0	0	0	0	0
Lu175 (ppm)	0	0	0	0	0	0	0	0	0	1
Hf178 (ppm)	0	0	0	0	0	0	0	0	0	1
Ta181 (ppm)	0	0	0	0	0	0	0	0	0	0
W182 (ppm)	0	0	0	0	0	0	0	1	0	0
Re185 (ppm)	0	0	0	0	0	0	0	0	0	40
Os189 (ppm)	0	1	0	0	0	0	0	0	12	51
Ir193 (ppm)	0	0	0	0	0	0	0	0	0	61
Pt195 (ppm)	0	0	0	0	0	0	0	47	0	0
Au197 (ppm)	0	15	3	5	2	9	3	47	0	0
Hg202 (ppm)	1	14	3	8	6	21	0	28	0	0
Pb204 (ppm)	0	40	0	0	0	0	0	0	0	0
Tl205 (ppm)	0	0	0	0	0	0	0	0	0	0
Pb206 (ppm)	0	0	0	0	0	0	0	0	0	0
Pb207 (ppm)	0	0	0	0	0	0	0	0	0	1
Pb208 (ppm)	0	0	0	0	0	0	0	0	1	1
Bi209 (ppm)	0	0	0	0	0	0	0	0	-	-
Th232 (ppm)	0	0	0	0	0	0	0	1	-	-
U238 (ppm)	0	0	0	0	0	0	0	0	-	-
PbTotal (ppm)	0	1	-	-	-	-	-	-	-	-

Appendix E: Secondary Ion Mass Spectrometry (SIMS) Results

Table E1. SIMS data Betts Cove.

Drill Hole	BC-21-02	BC-21-02	BC-21-02	BC-21-02	BC-21-02	BC-21-02	BC-21-02	BC-21-03	BC-21-03	BC-21-03
Sample	091Py@1	091Py@2	091Py@3	091Py@4	092Py@5	092Py@6	092Py@7	321Py@1	321Py@2	321Py@3
Mineral	Pyrite	Pyrite	Pyrite	Pyrite	Pyrite	Pyrite	Pyrite	Pyrite	Pyrite	Pyrite
Depth (m)	85.4	85.4	85.4	85.4	85.4	85.4	85.4	88	88	88
Date	2023/11/30	2023/11/30	2023/11/30	2023/11/30	2023/11/29	2023/11/29	2023/11/29	2023/11/29	2023/11/29	2023/11/29
Facies	Chalcopyrite-dominated	Chalcopyrite-dominated	Chalcopyrite-dominated	Chalcopyrite-dominated	Chalcopyrite-dominated	Chalcopyrite-dominated	Chalcopyrite-dominated	Sphalerite-pyrite-dominated	Sphalerite-pyrite-dominated	Sphalerite-pyrite-dominated
34S/32S (‰)	7.55	5.71	7.08	6.14	6.45	4.23	6.75	8.01	6.16	7.52
SEM	0.333036881	0.278192879	0.235685941	0.249376613	0.251995089	0.570015741	0.358043655	0.541950542	0.37274928	0.180232446
34S/32S (ratio)	0.043801232	0.043720866	0.043780623	0.043739639	0.043779244	0.043682681	0.043792321	0.043848009	0.04376663	0.043826184
2SD	0.000246392	0.000204437	0.000176046	0.000186008	0.000189357	0.000425343	0.000271575	0.00040635	0.000280626	0.000135925
SEM	0.032919195	0.027553403	0.023372131	0.024717871	0.024971982	0.055846099	0.035335967	0.053151203	0.036774656	0.017906236
Poisson	0.025455833	0.024632773	0.024249968	0.024262827	0.02366617	0.034009992	0.022969898	0.023218609	0.023771356	0.023721708
N	73	72	74	74	75	76	77	76	76	75

Table E1. SIMS data Betts Cove continued.

Drill Hole	BC-21-03	BC-21-03	BC-21-03	BC-21-03	BC-21-06	BC-21-06	BC-21-06	BC-21-08	BC-21-08	BC-21-08
Sample	321Py@4	322Py@5	322Py@6	322Py@7	42B1Py@1	42B1Py@2	42B1Py@3	531Py@1	531Py@2	531Py@3
Mineral	Pyrite	Pyrite	Pyrite	Pyrite	Pyrite	Pyrite	Pyrite	Pyrite	Pyrite	Pyrite
Depth (m)	88	88	88	88	106.3	106.3	106.3	28.7	28.7	28.7
Date	2023/11/29	2023/11/29	2023/11/29	2023/11/29	2023/11/30	2023/11/30	2023/11/30	2023/11/29	2023/11/29	2023/11/29
Facies	Sphalerite-pyrite-dominated	Sphalerite-pyrite-dominated	Sphalerite-pyrite-dominated	Sphalerite-pyrite-dominated	Chalcopyrite-pyrrhotite-dominated	Chalcopyrite-pyrrhotite-dominated	Chalcopyrite-pyrrhotite-dominated	Chalcopyrite-dominated	Chalcopyrite-dominated	Chalcopyrite-dominated
34S/32S (‰)	6.42	8.63	9.37	7.84	7.30	7.20	7.20	10.59	13.30	11.07
SEM	0.251497715	0.188556807	0.288513741	0.322038592	0.821394863	0.268650661	0.21701294	0.20226575	0.260452604	0.198493354
34S/32S (ratio)	0.043777921	0.043874725	0.043907231	0.043840418	0.043802557	0.043785918	0.043785696	0.043960969	0.044080022	0.043982174
2SD	0.000187741	0.000140433	0.00021715	0.000241727	0.000393565	0.000201788	0.000162223	0.000150867	0.000196999	0.000151114
SEM	0.024926303	0.018731159	0.028553692	0.031833873	0.053316085	0.026607263	0.021534419	0.020083384	0.025802425	0.019705626
Poisson	0.023651533	0.023663589	0.023354489	0.023285949	0.024995011	0.024046528	0.024238618	0.024980036	0.024856275	0.029463518
N	74	73	75	75	71	75	74	73	75	76

Table E1. SIMS data Betts Cove continued.

Drill Hole	BC-21-02	BC-21-02	BC-21-02	BC-21-02	BC-21-06	BC-21-06	BC-21-06	BC-21-06	BC-21-06	BC-21-06
Sample	091ccp@1	091ccp@2	092ccp@3	092ccp@4	42A1ccp@1	42A1ccp@2	42A1ccp@3	42A2ccp@4	42A2ccp@5	42A2ccp@6
Mineral	Chalcopyrite	Chalcopyrite	Chalcopyrite	Chalcopyrite	Chalcopyrite	Chalcopyrite	Chalcopyrite	Chalcopyrite	Chalcopyrite	Chalcopyrite
Depth (m)	85.4	85.4	85.4	85.4	106.3	106.3	106.3	106.3	106.3	106.3
Date	2023/12/01	2023/12/01	2023/12/01	2023/12/01	2023/12/01	2023/12/01	2023/12/01	2023/12/01	2023/12/01	2023/12/01
Facies	Chalcopyrite-dominated	Chalcopyrite-dominated	Chalcopyrite-dominated	Chalcopyrite-dominated	Chalcopyrite-pyrrhotite-dominated	Chalcopyrite-pyrrhotite-dominated	Chalcopyrite-pyrrhotite-dominated	Chalcopyrite-pyrrhotite-dominated	Chalcopyrite-pyrrhotite-dominated	Chalcopyrite-pyrrhotite-dominated
34S/32S (‰)	7.07	5.66	6.74	8.40	8.94	7.92	7.94	9.19	8.78	9.02
SEM	0.444135244	0.590768983	0.278340937	0.353281969	0.242055721	0.266766851	0.271853146	0.233313575	0.409853684	0.218668341
34S/32S (ratio)	0.043714157	0.04365291	0.043699733	0.043772363	0.04379592	0.043751496	0.043752343	0.043806955	0.043789116	0.04379935
2SD	0.000328848	0.000440211	0.000209939	0.000248483	0.000182022	0.000200225	0.00020401	0.000175547	0.000306349	0.00016566
SEM	0.043724684	0.057837674	0.027553566	0.034937672	0.023995551	0.026421948	0.026920878	0.02313607	0.040391419	0.021692659
Poisson	0.025281118	0.025082474	0.023337161	0.024996166	0.023541568	0.023401222	0.023392184	0.0236827	0.023569896	0.023350851
N	74	76	76	66	75	75	75	75	75	76

Table E1. SIMS data Betts Cove continued.

Drill Hole	BC-21-06	BC-21-06	BC-21-08	BC-21-08	BC-21-06	BC-21-06	BC-21-06	BC-21-06	BC-21-06	BC-21-06
Sample	42B1ccp@1	42B1ccp@2	532ccp@1	532ccp@2	42A1Po@1	42A1Po@2	42A1Po@3	42A2Po@4	42A2Po@5	42A2Po@6
Mineral	Chalcopyrite	Chalcopyrite	Chalcopyrite	Chalcopyrite	Pyrrhotite	Pyrrhotite	Pyrrhotite	Pyrrhotite	Pyrrhotite	Pyrrhotite
Depth (m)	106.3	106.3	28.7	28.7	106.3	106.3	106.3	106.3	106.3	106.3
Date	2023/12/01	2023/12/01	2023/12/01	2023/12/01	2023/12/08	2023/12/08	2023/12/08	2023/12/08	2023/12/08	2023/12/08
Facies	Chalcopyrite-pyrrhotite-dominated	Chalcopyrite-pyrrhotite-dominated	Chalcopyrite-dominated	Chalcopyrite-dominated	Chalcopyrite-pyrrhotite-dominated	Chalcopyrite-pyrrhotite-dominated	Chalcopyrite-pyrrhotite-dominated	Chalcopyrite-pyrrhotite-dominated	Chalcopyrite-pyrrhotite-dominated	Chalcopyrite-pyrrhotite-dominated
34S/32S (‰)	8.13	7.20	13.33	15.43	8.52	8.92	8.94	8.75	7.35	6.99
SEM	0.321434164	0.247240804	0.302471294	0.338504608	0.262737392	0.226765908	0.221566929	0.246817932	0.22825037	0.201721627
34S/32S (ratio)	0.043760673	0.043719919	0.043988644	0.044081019	0.043564488	0.043581842	0.043582716	0.043574516	0.043513511	0.043497687
2SD	0.000239269	0.000184345	0.000226474	0.000260268	0.000198936	0.000170892	0.000165924	0.000185838	0.000171732	0.000151862
SEM	0.031780166	0.024507945	0.029924862	0.033426567	0.026019949	0.022489529	0.021980363	0.024460496	0.022635517	0.0200238
Poisson	0.023585809	0.023746093	0.023396793	0.022841785	0.02538611	0.025491673	0.025664751	0.025963154	0.025800349	0.025736013
N	74	74	74	78	77	76	75	76	76	76

Table E1. SIMS data Betts Cove continued.

Drill Hole	BC-21-06	BC-21-06	BC-21-06	BC-21-06	BC-21-06	BC-21-06	BC-21-06	BC-21-08
Sample	42B1Po@1	42B1Po@2	42B1Po@3	42B1Po@4	42B1Po@5	42B1Po@6	42B1Po@7	532Po@1
Mineral	Pyrrhotite	Pyrrhotite	Pyrrhotite	Pyrrhotite	Pyrrhotite	Pyrrhotite	Pyrrhotite	Pyrrhotite
Depth (m)	106.3	106.3	106.3	106.3	106.3	106.3	106.3	28.7
Date	2023/12/08	2023/12/08	2023/12/08	2023/12/08	2023/12/08	2023/12/08	2023/12/08	2023/12/08
Facies	Chalcopyrite-pyrrhotite-dominated	Chalcopyrite-pyrrhotite-dominated	Chalcopyrite-pyrrhotite-dominated	Chalcopyrite-pyrrhotite-dominated	Chalcopyrite-pyrrhotite-dominated	Chalcopyrite-pyrrhotite-dominated	Chalcopyrite-pyrrhotite-dominated	Chalcopyrite-dominated
34S/32S (‰)	6.58	6.68	6.30	6.27	6.23	6.60	6.60	12.63
SEM	0.260750336	0.228593153	0.242684588	0.208225717	0.188088344	0.235192964	0.192675976	0.269790989
34S/32S (ratio)	0.043479945	0.043484408	0.043467685	0.043466443	0.043464613	0.043480995	0.043480619	0.04374387
2SD	0.000195804	0.000171873	0.000183478	0.000156609	0.000141561	0.000176779	0.000144099	0.000203756
SEM	0.025828311	0.022669218	0.024051545	0.020664581	0.018679774	0.023318166	0.019133969	0.026715103
Poisson	0.02599063	0.026242368	0.025622709	0.025907147	0.025927351	0.026113836	0.026343913	0.025843493
N	76	76	77	76	76	76	75	76

Table E2. SIMS data Tilt Cove.

Drill Hole	SZ-20-01	SZ-20-01	SZ-20-01	SZ-20-01	SZ-20-01	SZ-20-01	SZ-20-01	SZ-20-01	SZ-20-01	SZ-20-08
Sample	131Py@1	131Py@2	131Py@3	131Py@4	132Py5	132Py6	133Py@7	133Py@8	133Py@9	77A2Py@2
Mineral	Pyrite	Pyrite	Pyrite	Pyrite	Pyrite	Pyrite	Pyrite	Pyrite	Pyrite	Pyrite
Depth (m)	66.6	66.6	66.6	66.6	66.6	66.6	66.6	66.6	66.6	28.17
Date	2023/11/28	2023/11/28	2023/11/28	2023/11/28	2023/11/28	2023/11/28	2023/11/28	2023/11/28	2023/11/28	2023/11/28
Facies	Pyrite-dominated	Pyrite-dominated	Pyrite-dominated	Pyrite-dominated	Pyrite-dominated	Pyrite-dominated	Pyrite-dominated	Pyrite-dominated	Pyrite-dominated	Pyrite-dominated
34S/32S (‰)	10.72	9.94	11.02	14.05	9.58	9.87	10.91	9.32	10.30	21.62
SEM	0.387221573	0.203711551	0.214286672	0.234325028	0.405034839	0.348872276	0.459391572	0.235540337	0.245679311	0.342324526
34S/32S (ratio)	0.044122897	0.044088339	0.044136143	0.04427015	0.044073	0.044085765	0.044131441	0.04406136	0.044104558	0.044606725
2SD	0.000293743	0.000155432	0.000161482	0.000180484	0.000308669	0.000264787	0.00034322	0.000181704	0.000184801	0.000261262
SEM	0.0381827	0.020219903	0.021265966	0.023230208	0.039906664	0.034447749	0.045204217	0.023346887	0.024354275	0.033815446
Poisson	0.023016907	0.023008716	0.023360582	0.022871874	0.022819377	0.022984271	0.02332766	0.0228202	0.023566269	0.023347944
N	76	76	74	77	77	76	74	78	74	75

Table E2. SIMS data Tilt Cove continued.

Drill Hole	SZ-20-08	SZ-20-08	SZ-20-08	SZ-20-08	SZ-20-08	SZ-20-08	SZ-20-08	SZ-20-08	SZ-20-08	SZ-20-08
Sample	77A1Py@1	77B1@1	77B1@2	77B1@3	77B2@4	77B2@5	77B2@6	77A2Py@3	77A2Py@4	77A2Py@7
Mineral	Pyrite	Pyrite	Pyrite	Pyrite	Pyrite	Pyrite	Pyrite	Pyrite	Pyrite	Pyrite
Depth (m)	28.17	28.17	28.17	28.17	28.17	28.17	28.17	28.17	28.17	28.17
Date	2023/11/30	2023/11/30	2023/11/30	2023/11/30	2023/11/30	2023/11/30	2023/11/30	2023/11/28	2023/11/28	2023/11/28
Facies	Pyrite-dominated	Pyrite-dominated	Pyrite-dominated	Pyrite-dominated	Pyrite-dominated	Pyrite-dominated	Pyrite-dominated	Pyrite-dominated	Pyrite-dominated	Pyrite-dominated
34S/32S (‰)	15.84	4.63	12.80	5.60	3.42	15.49	14.61	14.59	14.22	15.56
SEM	0.262316991	0.403092128	0.316878956	0.238486382	0.19144941	0.250157873	0.362942765	0.336782774	0.233539794	0.457914926
34S/32S (ratio)	0.044165793	0.04367365	0.044031718	0.043715946	0.043620527	0.044150529	0.044111793	0.04429409	0.044277661	0.044337242
2SD	0.000197477	0.000290642	0.000234217	0.000177856	0.00014365	0.000189584	0.00026651	0.000251928	0.000174075	0.000343726
SEM	0.025988756	0.039770379	0.031344106	0.02364742	0.019013107	0.024791597	0.035850881	0.033284331	0.02316622	0.045060666
Poisson	0.02443746	0.02480244	0.024516594	0.024426762	0.024349771	0.024011203	0.024495063	0.023211535	0.023593595	0.022996088
N	74	70	72	74	75	75	71	73	72	74

Table E2. SIMS data Tilt Cove continued.

Drill Hole	SZ-20-08	SZ-20-08	SZ-20-01	SZ-20-01	SZ-20-01	SZ-20-01	SZ-20-01	SZ-20-01	SZ-20-01	SZ-20-05
Sample	77A2Py@5	77A2Py@6	131ccp@1	131ccp@3	131ccp@4	132ccp@5	132ccp@6	133ccp@8	133ccp@9	701ccpccp@1
Mineral	Pyrite	Pyrite	Chalcopyrite	Chalcopyrite	Chalcopyrite	Chalcopyrite	Chalcopyrite	Chalcopyrite	Chalcopyrite	Chalcopyrite
Depth (m)	28.17	28.17	66.6	66.6	66.6	66.6	66.6	66.6	66.6	126.45
Date	2023/11/30	2023/11/30	2023/12/04	2023/12/04	2023/12/04	2023/12/05	2023/12/05	2023/12/04	2023/12/04	2023/12/04
Facies	Pyrite-dominated	Pyrite-dominated	Pyrite-dominated	Pyrite-dominated	Pyrite-dominated	Pyrite-dominated	Pyrite-dominated	Pyrite-dominated	Pyrite-dominated	Chalcopyrite-pyrrhotite-dominated
34S/32S (‰)	23.57	14.83	10.58	12.15	10.92	2.82	11.81	11.94	10.61	16.30
SEM	0.300886103	0.435143586	0.607660892	0.869077973	0.219993458	0.386426353	0.340733893	0.301662923	0.325053226	0.304409505
34S/32S (ratio)	0.044508452	0.04412143	0.043852443	0.043922054	0.043866975	0.043565712	0.043959251	0.043911933	0.043853569	0.04410344
2SD	0.000221843	0.000327426	0.000427921	0.000629191	0.000164739	0.000285725	0.000252928	0.000222479	0.00024562	0.000223924
SEM	0.029786807	0.042845278	0.059607647	0.08441194	0.021827885	0.038120463	0.033670887	0.029854556	0.032123397	0.030127911
Poisson	0.024741627	0.023650488	0.026911492	0.066604387	0.024271382	0.029175588	0.024349269	0.024633193	0.024153202	0.025025794
N	70	75	67	72	74	74	73	72	76	71

Table E2. SIMS data Tilt Cove continued.

Drill Hole	SZ-20-05	SZ-20-05	SZ-20-05	SZ-20-05	SZ-20-05	SZ-20-08	SZ-20-08	SZ-20-08	SZ-20-08	SZ-20-08
Sample	701ccpccp@2	701ccpccp@3	702ccp@4	702ccp@5	721ccp@1	77A1ccp@1	77A1ccp@2	77A2ccp@3	77B1ccp@1	77B1ccp@2
Mineral	Chalcopyrite	Chalcopyrite	Chalcopyrite	Chalcopyrite	Chalcopyrite	Chalcopyrite	Chalcopyrite	Chalcopyrite	Chalcopyrite	Chalcopyrite
Depth (m)	126.45	126.45	126.45	126.45	143.7	28.17	28.17	28.17	28.17	28.17
Date	2023/12/04	2023/12/04	2023/12/05	2023/12/05	2023/12/04	2023/12/04	2023/12/05	2023/12/06	2023/12/05	2023/12/05
Facies	Chalcopyrite-pyrrhotite-dominated	Chalcopyrite-pyrrhotite-dominated	Chalcopyrite-pyrrhotite-dominated	Chalcopyrite-pyrrhotite-dominated	Pyrrhotite-dominated	Pyrite-dominated	Pyrite-dominated	Pyrite-dominated	Pyrite-dominated	Pyrite-dominated
34S/32S (‰)	16.78	19.23	14.76	15.09	3.42	13.67	11.13	13.71	8.18	8.96
SEM	0.286077575	0.28516758	0.43356115	0.325674931	0.5208119	0.283706959	0.371684372	0.50464372	0.31131715	0.396891665
34S/32S (ratio)	0.044124752	0.044232801	0.044089356	0.044103817	0.04359229	0.043987833	0.043876372	0.043989518	0.043799787	0.043834051
2SD	0.000212119	0.000211967	0.000319615	0.00024429	0.000388497	0.000208292	0.000278735	0.000341743	0.000235071	0.000299006
SEM	0.028326986	0.028237652	0.042716708	0.032194599	0.051114116	0.028098328	0.036677484	0.04973424	0.030781542	0.039122926
Poisson	0.024870766	0.02502263	0.024553571	0.02436854	0.023720597	0.025433478	0.025541065	0.026072084	0.024248677	0.02513989
N	72	72	72	74	76	71	75	61	76	76

Table E2. SIMS data Tilt Cove continued.

Drill Hole	SZ-20-08	SZ-20-08	SZ-20-08	SZ-20-01	SZ-20-01	SZ-20-01	SZ-20-05	SZ-20-05	SZ-20-05	SZ-20-05
Sample	77B2ccp@3	77B2ccp@3b	77B2ccp@4	133Po@1	133Po@2	133Po@2b	701Po@1	701Po@2	701Po@3	702Po@2
Mineral	Chalcopyrite	Chalcopyrite	Chalcopyrite	Pyrrhotite	Pyrrhotite	Pyrrhotite	Pyrrhotite	Pyrrhotite	Pyrrhotite	Pyrrhotite
Depth (m)	28.17	28.17	28.17	66.6	66.6	66.6	126.45	126.45	126.45	126.45
Date	2023/12/05	2023/12/05	2023/12/05	2023/12/19	2023/12/19	2023/12/19	2023/12/19	2023/12/19	2023/12/19	2023/12/19
Facies	Pyrite-dominated	Pyrite-dominated	Pyrite-dominated	Pyrite-dominated	Pyrite-dominated	Pyrite-dominated	Chalcopyrite-pyrrhotite-dominated	Chalcopyrite-pyrrhotite-dominated	Chalcopyrite-pyrrhotite-dominated	Chalcopyrite-pyrrhotite-dominated
34S/32S (‰)	7.99	7.28	9.19	13.50	13.66	11.12	15.54	15.22	15.79	16.38
SEM	0.522235939	0.532162057	0.248433169	0.252924615	0.643987509	0.319038846	0.279175056	0.192207941	0.264941174	0.240272815
34S/32S (ratio)	0.043791741	0.043760644	0.043844021	0.043782557	0.043789924	0.043678415	0.043871774	0.043857818	0.043882937	0.043908412
2SD	0.000328675	0.00038812	0.000186979	0.000190064	0.000455569	0.000235487	0.00021002	0.000144999	0.000198156	0.00017634
SEM	0.051547411	0.052262038	0.024621969	0.025063254	0.063080553	0.031550612	0.027638508	0.019087823	0.02624617	0.023831115
Poisson	0.029817667	0.026105086	0.024582774	0.025587662	0.026426959	0.026287375	0.025269992	0.025438263	0.025722487	0.026080307
N	53	72	75	75	68	73	75	75	74	71

Table E2. SIMS data Tilt Cove continued.

Drill Hole	SZ-20-05	SZ-20-05	SZ-20-05	SZ-20-05	SZ-20-01	SZ-20-02	SZ-20-03
Sample	702Po@4	721Po@1	721Po@2	721Po@3	132Arspy@1	132Arspy@2	132Arspy@3
Mineral	Pyrrhotite	Pyrrhotite	Pyrrhotite	Pyrrhotite	Arsenopyrite	Arsenopyrite	Arsenopyrite
Depth (m)	126.45	143.7	143.7	143.7	66.6	66.6	66.6
Date	2023/12/19	2023/12/19	2023/12/19	2023/12/19	2023/12/20	2023/12/20	2023/12/20
Facies	Chalcopyrite-pyrrhotite-dominated	Pyrrhotite-dominated	Pyrrhotite-dominated	Pyrrhotite-dominated	Pyrite-dominated	Pyrite-dominated	Pyrite-dominated
34S/32S (‰)	15.59	5.62	6.69	5.97	9.47	9.47	9.41
SEM	0.386818677	0.286099426	0.236273611	0.382802212	0.246879741	0.315557473	0.36930062
34S/32S (ratio)	0.043874203	0.043438521	0.043485169	0.043454239	0.043537103	0.043536833	0.043534425
2SD	0.000278384	0.000215816	0.000172944	0.000287864	0.000188106	0.000236802	0.000276594
SEM	0.03819275	0.028309623	0.023435214	0.037746794	0.024460467	0.031195527	0.036439508
Poisson	0.026298737	0.025087581	0.025971834	0.025145955	0.033388163	0.033548493	0.034039196
N	69	77	72	77	78	76	76

Appendix F: Reference Data

Table E1. QA/QC results for reference materials used for gold assays at Betts Cove.

Standard	n	Au average (g/t)	1σ	Recommended value (g/t)	%RSD	%RD
CDN-GS-10E	22	8.80	1.93	9.59	21.94	-8.27
CDN-GS-1U	4	1.05	0.01	0.97	0.79	8.73
CDN-GS-1W	19	1.08	0.04	1.06	4.02	1.44

Table E2. QA/QC results for reference materials used for gold assays at Tilt Cove.

Standard	n	Au average (g/t)	1σ	Recommended value (g/t)	%RSD	%RD
CDN-GS-10E	11	8.75	2.47	9.59	28.17	-8.72
CDN-GS-1M	2	1.09	0.01	1.07	0.46	1.40
CDN-GS-1U	1	1.11	-	0.97	-	-

Table E3. QA/QC results for reference materials used for EPMA.

Standard	SJP pyr 1-1_						
Element	Min LOD (ppm)	Max LOD (ppm)	Average (wt%) n = 53	1σ	Recommended Value	%RSD	%RD
Zn	34.39	35.87	0.01	0.00	-	79.43	-
Cu	28.67	30.23	0.00	0.00	-	98.87	-
Ni	26.63	27.96	0.00	0.00	-	71.82	-
Co	24.36	31.26	0.05	0.02	0.06	36.10	-29.86
Fe	37.57	40.35	46.72	0.23	46.37	0.49	0.75
Sb	30.10	31.59	0.01	0.01	-	82.77	-
Cd	25.57	27.36	0.01	0.01	-	72.58	-
Pb	68.49	75.62	0.12	0.04	-	37.21	-
S	10.34	28.11	53.64	0.49	54.13	0.90	-0.90
As	59.98	66.25	0.02	0.01	0.01	59.65	84.57
Se	34.68	37.45	0.01	0.01	-	70.94	-
Ag	26.21	27.58	0.01	0.01	-	78.76	-
Au	69.97	82.60	0.04	0.02	-	47.74	-

Standard	SJP ccp 1-5_						
Element	Min LOD (ppm)	Max LOD (ppm)	Average (wt%) n = 40	1σ	Recommended Value	RSD%	%RD
Zn	36.84	38.47	0.07	0.04	-	62.81	-
Cu	44.71	46.67	33.62	0.14	33.82	0.41	-0.60
Ni	28.86	30.30	0.00	0.00	-	77.54	-
Co	25.98	27.29	0.02	0.01	-	71.31	-
Fe	39.18	42.81	30.72	0.52	29.79	1.69	3.14
Sb	31.99	33.53	0.01	0.00	0.00	60.80	1346.67
Cd	27.63	29.18	0.01	0.00	-	78.88	-
Pb	66.50	71.46	0.06	0.04	-	63.64	-
S	23.62	25.76	35.51	0.14	34.49	0.40	2.95
As	58.35	64.11	0.02	0.02	0.02	69.48	34.92
Se	32.92	35.87	0.02	0.01	-	61.37	-
Ag	27.94	29.55	0.00	0.00	-	89.40	-
Au	66.88	80.75	0.03	0.02	-	51.17	-

Standard	SJP po 1-2_						
Element	Min LOD (ppm)	Max LOD (ppm)	Average (wt%) n = 22	1σ	Recommended Value	%RSD	%RD
Zn	35.28	36.78	0.01	0.00	-	62.88	-
Cu	29.37	30.51	0.01	0.00	-	54.43	-
Ni	27.37	28.56	0.25	0.05	0.09	20.87	168.37
Co	25.14	26.22	0.06	0.02	0.10	39.65	-42.29
Fe	39.04	41.79	60.03	0.57	61.25	0.95	-1.99
Sb	31.54	32.90	0.01	0.01	-	60.92	-
Cd	26.97	28.59	0.01	0.01	-	59.08	-
Pb	67.32	72.85	0.07	0.05	-	68.19	-
S	24.23	26.96	39.52	0.66	37.38	1.67	5.71
As	60.61	66.43	0.02	0.01	-	77.70	-
Se	34.20	36.07	0.01	0.01	-	57.16	-
Ag	27.80	29.52	0.01	0.00	-	57.32	-
Au	69.39	80.16	0.03	0.02	-	50.55	-

Standard	SJP sp 1-5_						
Element	Min LOD (ppm)	Max LOD (ppm)	Average (wt%) n = 37	1σ	Recommended Value	%RSD	%RD
Zn	53.24	59.32	62.89	0.36	63.23	0.58	-0.54
Cu	32.02	34.35	0.35	0.14	0.29	40.60	20.34
Ni	29.50	31.88	0.00	0.00	-	81.21	-
Co	26.17	34.41	0.01	0.00	-	73.51	-
Fe	27.53	29.87	3.43	0.22	3.29	6.55	4.11
Sb	32.64	34.49	0.01	0.01	-	74.38	-
Cd	27.96	29.48	0.15	0.01	0.15	6.47	3.25
Pb	64.72	70.11	0.07	0.03	-	47.57	-
S	21.10	28.86	32.89	1.63	32.81	4.95	0.24
As	57.83	62.63	0.03	0.01	-	55.53	-
Se	32.81	36.46	0.02	0.01	-	52.31	-
Ag	28.56	29.86	0.01	0.00	-	68.84	-
Au	65.92	80.65	0.04	0.02	-	42.96	-

Standard	SJP cob 1-13_						
Element	Min LOD (ppm)	Max LOD (ppm)	Average (wt%) n = 26	1σ	Recommended Value	%RSD	%RD
Zn	38.99	41.50	0.01	0.00	-	70.54	-
Cu	32.19	34.85	0.01	0.01	-	83.45	-
Ni	41.97	43.73	7.34	1.29	6.96	17.54	5.51
Co	39.31	42.72	20.78	1.94	21.54	9.33	-3.53
Fe	33.38	36.91	8.12	0.83	7.82	10.23	3.75
Sb	33.72	37.44	0.03	0.01	-	35.27	-
Cd	26.73	30.82	0.01	0.01	-	69.50	-
Pb	55.04	68.84	0.04	0.02	-	57.28	-
S	18.43	22.75	20.00	1.24	19.98	6.19	0.11
As	103.24	130.40	43.53	2.51	44.46	5.77	-2.08
Se	38.86	50.89	0.13	0.03	-	20.94	-
Ag	30.51	31.78	0.01	0.00	-	75.19	-
Au	67.63	82.00	0.03	0.02	-	68.17	-

Standard	SJP pnt 1-2_						
Element	Min LOD (ppm)	Max LOD (ppm)	Average (wt%) n = 20	1σ	Recommended Value	%RSD	%RD
Zn	36.64	37.68	0.01	0.01	-	71.09	-
Cu	31.36	32.49	0.01	0.01	-	50.23	-
Ni	44.71	46.33	32.88	0.46	32.64	1.39	0.73
Co	26.22	27.69	1.45	0.05	1.51	3.57	-4.41
Fe	35.90	39.95	32.51	0.38	31.93	1.16	1.83
Sb	32.78	34.02	0.01	0.01	-	55.01	-
Cd	28.00	29.36	0.01	0.00	-	60.85	-
Pb	67.78	71.17	0.04	0.03	-	77.49	-
S	24.75	27.17	33.03	0.14	33.41	0.43	-1.12
As	58.99	64.90	0.02	0.01	0.01	72.30	201.73
Se	33.96	36.16	0.02	0.01	-	79.12	-
Ag	28.78	30.06	0.01	0.01	-	83.46	-
Au	68.70	80.54	0.04	0.02	-	54.29	-

Standard	SJP asp 1-7_						
Element	Min LOD (ppm)	Max LOD (ppm)	Average (wt%) n = 5	1σ	Recommended Value	%RSD	%RD
Zn	40.38	41.04	0.01	0.01	-	66.97	-
Cu	33.44	33.89	0.01	0.00	-	52.75	-
Ni	31.52	31.85	0.00	0.00	-	48.99	-
Co	27.96	28.59	0.03	0.01	0.05	25.37	-34.26
Fe	37.39	39.56	33.84	0.10	35.15	0.28	-3.72
Sb	34.47	34.77	0.07	0.02	-	30.58	-
Cd	29.64	30.33	0.01	0.01	-	98.34	-
Pb	65.40	67.04	0.11	0.12	-	109.37	-
S	26.30	27.52	20.61	0.09	20.11	0.42	2.48
As	125.59	131.07	44.37	0.15	45.38	0.33	-2.24
Se	49.17	50.12	0.12	0.02	-	13.22	-
Ag	31.01	31.67	0.01	0.01	-	51.65	-
Au	66.71	69.82	0.02	0.01	-	52.01	-

Standard	SJP brn 1-6_						
Element	Min LOD (ppm)	Max LOD (ppm)	Average (wt%) n = 5	1σ	Recommended Value	%RSD	%RD
Zn	39.62	40.47	0.04	0.01	-	30.67	-
Cu	48.32	50.44	61.73	0.22	62.42	0.35	-1.11
Ni	31.29	31.78	0.00	0.00	-	66.73	-
Co	27.19	27.81	0.01	0.00	-	42.62	-
Fe	42.06	43.46	11.55	0.09	11.24	0.78	2.72
Sb	33.89	34.61	0.01	0.00	0.00	72.35	2033.33
Cd	29.37	29.94	0.00	0.00	-	35.32	-
Pb	65.35	68.19	0.02	0.02	-	77.52	-
S	22.80	23.66	26.33	0.14	25.65	0.52	2.64
As	60.32	62.16	0.02	0.02	0.01	97.48	69.39
Se	34.33	35.27	0.02	0.01	-	58.81	-
Ag	29.53	30.31	0.09	0.01	-	12.39	-
Au	74.65	77.45	0.03	0.02	-	51.73	-

Standard	SJP gn 1-4_						
Element	Min LOD (ppm)	Max LOD (ppm)	Average (wt%) n = 11	1σ	Recommended Value	%RSD	%RD
Zn	61.03	62.02	0.01	0.01	0.01	64.86	20.50
Cu	50.42	51.01	0.01	0.00	0.01	58.46	34.76
Ni	46.86	47.86	0.00	0.00	-	88.35	-
Co	40.06	40.98	0.01	0.01	-	80.53	-
Fe	41.54	42.84	0.02	0.01	-	40.09	-
Sb	41.73	42.36	0.01	0.01	-	46.41	-
Cd	38.77	39.61	0.01	0.01	-	58.25	-
Pb	174.47	182.01	85.89	0.39	86.55	0.45	-0.76
S	31.15	38.03	13.52	0.10	13.18	0.77	2.61
As	92.61	95.79	0.02	0.01	-	62.95	-
Se	53.42	54.91	0.02	0.02	-	108.34	-
Ag	40.74	42.16	0.14	0.01	-	7.85	-
Au	105.42	114.59	0.03	0.02	-	94.36	-

Standard	Au metal						
Element	Min LOD (ppm)	Max LOD (ppm)	Average (wt%) n = 10	1σ	Recommended Value	%RSD	%RD
Zn	65.50	66.73	0.01	0.01	-	115.94	-
Cu	53.82	55.05	0.01	0.01	-	51.20	-
Ni	50.03	50.73	0.04	0.02	-	44.90	-
Co	42.76	43.95	0.01	0.01	-	72.06	-
Fe	43.49	45.23	0.09	0.04	-	50.34	-
Sb	43.00	45.00	0.01	0.01	-	94.40	-
Cd	36.44	37.93	0.02	0.01	-	66.06	-
Pb	86.34	90.69	0.23	0.02	-	10.37	-
S	16.69	17.93	0.00	0.00	-	73.83	-
As	92.94	99.36	0.01	0.01	-	59.10	-
Se	53.94	57.45	0.02	0.01	-	64.41	-
Ag	52.74	56.34	0.02	0.01	-	55.86	-
Au	161.83	168.14	100.52	1.82	99.00	1.81	1.54

Standard	Ag metal						
Element	Min LOD (ppm)	Max LOD (ppm)	Average (wt%) n = 11	1σ	Recommended Value	%RSD	%RD
Zn	52.79	61.16	0.01	0.01	-	58.59	-
Cu	43.97	49.84	0.01	0.00	-	44.72	-
Ni	40.52	46.81	0.00	0.00	-	80.68	-
Co	34.72	40.06	0.01	0.00	-	66.70	-
Fe	35.49	41.52	0.04	0.02	-	53.94	-
Sb	38.09	41.37	0.05	0.02	-	43.15	-
Cd	38.84	47.32	0.72	0.32	-	44.94	-
Pb	77.16	125.20	14.25	31.84	-	223.53	-
S	15.90	25.69	2.18	4.85	-	222.72	-
As	80.60	93.64	0.02	0.01	-	55.58	-
Se	46.21	106.34	0.02	0.01	-	49.17	-
Te	51.32	58.36	0.62	0.45	-	72.15	-
Ag	58.17	67.82	83.16	37.15	99.00	44.67	-16.00
Au	85.31	100.89	0.01	0.01	-	49.69	-

Standard	Se metal						
Element	Min LOD (ppm)	Max LOD (ppm)	Average (wt%) n = 6	1σ	Recommended Value	%RSD	%RD
Zn	45.86	47.04	0.01	0.00	-	77.75	-
Cu	38.19	40.15	0.01	0.01	-	73.83	-
Ni	35.57	37.89	0.01	0.01	-	95.97	-
Co	31.49	32.55	0.00	0.00	-	63.89	-
Fe	34.80	36.66	0.03	0.00	-	16.65	-
Sb	36.82	38.23	0.01	0.01	-	74.33	-
Cd	29.86	32.62	0.01	0.01	-	100.41	-
Pb	74.63	91.05	0.02	0.02	-	80.96	-
S	10.63	13.82	0.00	0.00	-	70.71	-
As	137.46	147.87	0.39	0.04	-	10.12	-
Se	65.67	97.14	96.88	4.16	99.00	4.29	-2.14
Te	32.86	42.57	0.05	0.03	-	56.43	-
Ag	32.69	65.29	0.01	0.01	-	121.03	-
Au	39.81	76.97	0.04	0.02	-	58.88	-

Standard	Te metal						
Element	Min LOD (ppm)	Max LOD (ppm)	Average (wt%) n = 6	1σ	Recommended Value	%RSD	%RD
Zn	54.52	55.15	0.01	0.00	-	93.10	-
Cu	45.03	45.49	0.00	0.00	-	132.00	-
Ni	41.84	42.38	0.00	0.00	-	61.20	-
Co	35.55	36.18	0.01	0.00	-	55.48	-
Fe	36.50	37.41	0.01	0.00	-	82.21	-
Sb	49.96	50.55	0.66	0.02	-	2.62	-
Cd	39.48	40.69	0.01	0.01	-	55.24	-
Pb	74.40	77.52	0.01	0.01	-	55.18	-
S	16.13	17.31	0.01	0.00	-	30.43	-
As	109.76	124.65	0.70	0.11	-	16.31	-
Se	69.22	142.54	0.72	0.04	-	5.41	-
Te	74.49	75.70	100.66	0.16	99.00	0.16	1.68
Ag	56.41	58.48	0.01	0.00	-	60.93	-
Au	83.80	95.75	0.01	0.01	-	81.61	-

Standard	Magnetite						
Element	Min LOD (ppm)	Max LOD (ppm)	Average (wt%) n = 20	1σ	Recommended Value	%RSD	%RD
ZnO	42.01	43.65	0.03	0.07	-	237.49	-
CoO	30.97	32.41	0.10	0.01	-	9.79	-
FeO	49.37	52.51	91.57	0.36	99.00	0.39	-7.51
MnO	38.14	40.87	0.26	0.07	-	25.39	-
Cr2O3	42.63	45.80	0.01	0.00	-	64.67	-
Al2O3	38.04	39.83	0.06	0.10	-	160.87	-
V2O3	37.81	40.21	0.02	0.01	-	33.32	-
TiO2	49.80	52.87	0.08	0.07	-	93.01	-

Standard	Cr2O3						
Element	Min LOD (ppm)	Max LOD (ppm)	Average (wt%) n = 10	1σ	Recommended Value	%RSD	%RD
ZnO	39.84	41.01	0.01	0.00	-	68.18	-
CoO	27.73	28.32	0.00	0.00	-	93.82	-
FeO	27.84	31.33	0.01	0.01	-	54.04	-
MnO	36.37	38.12	0.10	0.04	-	41.64	-
Cr2O3	26.82	28.68	101.85	1.03	99.00	1.01	2.88
Al2O3	37.68	39.06	0.02	0.02	-	94.10	-
MgO	39.51	41.68	0.01	0.00	-	58.96	-
V2O3	37.41	38.53	0.01	0.01	-	37.81	-
TiO2	46.75	50.14	0.06	0.01			

Table E4. QA/QC results for reference materials used for LA-ICP-MS.

Standard	CCule						
Element	Min LOD	Max LOD	Average (ppm) n = 23	1σ	Recommended Value	%RSD	%RD
Li7	0	2	1	0	-	27	-
Be9	0	2	0	0	-	165	-
B11	3	9	7	3	-	40	-
Na23	7	61	483	88	-	18	-
Mg24	0	1	9729	4378	-	45	-
Al27	0	1	2211	623	-	28	-
Si29	191	1123	28889	3557	14648	12	97
P31	7	50	64	27	-	41	-
S32	240	2875	366724	36965	355200	10	3
K39	5	15	606	264	-	44	-
Ca44	38	112	1330	909	-	68	-
Sc45	0	1	1	1	-	45	-
Ti47	0	3	86	135	55	158	56
V51	0	0	4	2	4	34	11
Cr52	1	3	85	24	85	28	0
Mn55	0	0	97	8	96	9	1
Fe57	0	0	-	-	307000	-	-
Co59	0	0	323	70	301	22	7
Ni60	0	0	28	6	7	20	278
Cu63	0	1	241152	21092	230700	9	5
Zn66	0	1	41975	6505	30200	15	39
Ga71	0	0	3	1	3	28	-10
Ge73	0	2	5	8	1	158	417
As75	1	5	1654	769	1010	46	64
Se77	1	5	311	41	304	13	2
Rb85	0	0	1	0	-	29	-
Sr88	0	0	2	1	-	46	-
Y89	0	0	3	6	-	190	-
Zr90	0	0	3	2	0	73	1614
Nb93	0	0	1	2	16	163	-91
Mo95	0	0	6	9	0	152	81302
Ru101	0	0	3	3	0	118	-
Rh103	0	0	6	4	0	67	-
Pd104	0	0	10	5	0	46	-
Pd105	0	0	35	67	0	193	-
Pd106	0	0	92	113	205	123	-55
Ag107	0	0	198	115	74	58	167

Cd111	0	0	71	60	6	85	1084
In115	0	0	21	32	14	151	57
Sn118	0	0	50	52	104	104	-52
Sb121	0	0	119	92	62	78	92
Te125	0	1	65	77	-	118	-
Cs133	0	0	2	2	6	122	-71
Ba137	0	0	4	4	-	97	-
La139	0	0	1	0	-	56	-
Ce140	0	0	1	1	-	56	-
Pr141	0	0	0	0	-	88	-
Nd146	0	0	1	1	-	116	-
Sm147	0	0	0	0	-	53	-
Eu153	0	0	0	0	-	215	-
Gd157	0	0	0	0	-	53	-
Tb159	0	0	0	1	-	253	-
Dy163	0	0	0	0	-	77	-
Ho165	0	0	0	1	-	265	-
Er166	0	0	0	0	-	71	-
Tm169	0	0	0	0	-	278	-
Yb172	0	0	0	0	-	59	-
Lu175	0	0	0	0	-	228	-
Hf178	0	0	0	0	-	128	-
Ta181	0	0	1	2	0	287	41
W182	0	0	1	1	0	65	21782
Re185	0	0	0	0	0	59	-
Os189	0	0	0	0	0	122	-
Ir193	0	0	3	6	0	161	-
Pt195	0	7	18	18	20	104	-13
Au197	0	10	1150	2975	10	259	10958
Hg202	0	11	2482	4412	7030	178	-65
Pb204	0	22	6627	4163	3	63	245348
Tl205	0	0	3423	4440	7030	130	-51
Pb206	0	0	8888	1524	7030	17	26
Pb207	0	0	8191	3473	7030	42	17
Pb208	0	0	5621	4712	3	84	187275
Bi209	0	0	2	1	-	69	-
Th232	0	0	1140	3018	1	265	113904
U238	0	0	2693	4270	7030	159	-62
PbTotal	0	0	9132	1309	-	14	-

Standard	FeS4						
Element	Min LOD	Max LOD	Average (ppm) n = 25	1σ	Recommended Value	%RSD	%RD
Li7	0	2	0	0	-	51	-
Be9	0	2	0	0	-	150	-
B11	3	10	10	3	-	28	-
Na23	3	18	473	213	-	45	-
Mg24	0	1	111	47	-	42	-
Al27	0	1	521	165	-	32	-
Si29	255	932	4201	703	2924	17	44
P31	8	25	49	12	-	24	-
S32	181	2330	305804	26906	354985	9	-14
K39	4	13	567	650	-	115	-
Ca44	32	106	162	58	-	36	-
Sc45	0	1	1	0	-	37	-
Ti47	0	2	13	4	13	34	-2
V51	0	0	24	2	24	8	-1
Cr52	1	2	2554	440	2637	17	-3
Mn55	0	1	1203	138	1038	11	16
Fe57	0	0	-	-	510025	-	-
Co59	0	0	200	5	198	3	1
Ni60	0	0	38827	2377	37307	6	4
Cu63	0	0	91767	3462	90649	4	1
Zn66	0	1	1402	60	1384	4	1
Ga71	0	0	80	25	33	31	139
Ge73	0	1	3	7	-	222	-
As75	0	7	1926	190	1769	10	9
Se77	1	3	243	19	254	8	-5
Rb85	0	0	1	1	-	103	-
Sr88	0	0	3	2	-	59	-
Y89	0	0	9	25	-	277	-
Zr90	0	0	60	101	52	169	15
Nb93	0	0	139	118	279	85	-50
Mo95	0	0	259	130	83	50	211
Ru101	0	0	246	244	450	99	-45
Rh103	0	0	522	269	601	52	-13
Pd104	0	0	697	232	601	33	16
Pd105	0	0	560	139	601	25	-7
Pd106	0	0	444	230	237	52	87
Ag107	0	0	175	122	6	70	2637
Cd111	0	0	73	101	103	138	-29

In115	0	0	191	108	300	56	-36
Sn118	0	0	244	82	214	34	14
Sb121	0	0	160	78	90	49	78
Te125	0	1	100	27	-	27	-
Cs133	0	0	97	80	133	82	-27
Ba137	0	0	103	99	-	96	-
La139	0	0	0	0	-	79	-
Ce140	0	0	0	0	-	72	-
Pr141	0	0	0	0	-	82	-
Nd146	0	0	0	0	-	158	-
Sm147	0	0	0	0	-	78	-
Eu153	0	0	0	0	-	195	-
Gd157	0	0	0	0	-	112	-
Tb159	0	0	0	0	-	122	-
Dy163	0	0	0	0	-	65	-
Ho165	0	0	0	0	-	77	-
Er166	0	0	0	0	-	133	-
Tm169	0	0	0	0	-	132	-
Yb172	0	0	0	0	-	93	-
Lu175	0	0	0	0	-	289	-
Hf178	0	0	35	97	-	275	-
Ta181	0	0	87	116	278	132	-69
W182	0	0	292	319	235	109	24
Re185	0	0	129	55	64	43	103
Os189	0	0	111	73	181	66	-39
Ir193	0	0	166	91	201	55	-17
Pt195	0	6	354	176	259	50	37
Au197	0	6	757	907	214	120	254
Hg202	0	10	994	1338	3058	135	-68
Pb204	0	18	2507	1089	709	43	253
Tl205	0	0	1682	1150	3058	68	-45
Pb206	0	0	3123	344	3058	11	2
Pb207	0	0	2892	790	3058	27	-5
Pb208	0	0	2226	1282	1014	58	120
Bi209	0	0	692	613	-	89	-
Th232	0	0	369	1013	-	274	-
U238	0	0	984	1452	3058	148	-68
PbTotal	0	0	3167	447	-	14	-

Standard	FeS5						
Element	Min LOD	Max LOD	Average (ppm) n = 25	1σ	Recommended Value	%RSD	%RD
Li7	0	1	0	0	-	39	-
Be9	0	1	0	0	-	286	-
B11	2	8	6	2	-	38	-
Na23	4	173	330	133	-	40	-
Mg24	0	0	1070	532	-	50	-
Al27	0	3	108	40	-	37	-
Si29	255	931	2119	338	1450	16	46
P31	6	42	47	9	-	19	-
S32	215	3710	282034	29231	369370	10	-24
K39	3	15	518	556	-	107	-
Ca44	38	104	772	253	-	33	-
Sc45	0	1	0	-	-	-	-
Ti47	0	2	18	3	17	18	6
V51	0	0	23	2	22	7	2
Cr52	0	2	693	121	694	17	0
Mn55	0	0	1084	164	996	15	9
Fe57	0	0	-	-	552286	-	-
Co59	0	0	559	44	566	8	-1
Ni60	0	1	27373	1163	27315	4	0
Cu63	0	0	7724	403	8190	5	-6
Zn66	0	1	1626	213	1934	13	-16
Ga71	0	0	7	2	7	34	-5
Ge73	0	1	3	6	-	215	-
As75	0	9	18	5	17	27	8
Se77	0	3	23	3	24	13	-4
Rb85	0	0	1	1	-	103	-
Sr88	0	0	2	1	-	71	-
Y89	0	0	0	1	-	173	-
Zr90	0	0	6	12	2	186	171
Nb93	0	0	23	31	37	135	-38
Mo95	0	0	62	36	62	58	0
Ru101	0	0	116	67	98	58	18
Rh103	0	0	149	123	82	82	82
Pd104	0	0	226	141	82	62	175
Pd105	0	0	83	32	82	38	1
Pd106	0	0	58	46	3	79	1721
Ag107	0	0	3	1	4	35	-23
Cd111	0	0	13	30	1	223	1232

In115	0	0	29	44	121	149	-76
Sn118	0	0	58	42	17	72	247
Sb121	0	0	12	7	2	58	428
Te125	0	0	18	41	-	224	-
Cs133	0	0	84	70	108	84	-22
Ba137	0	0	89	84	-	95	-
La139	0	0	0	0	-	50	-
Ce140	0	0	0	0	-	68	-
Pr141	0	0	0	0	-	77	-
Nd146	0	0	0	0	-	163	-
Sm147	0	0	0	0	-	109	-
Eu153	0	0	0	0	-	184	-
Gd157	0	0	0	0	-	141	-
Tb159	0	0	0	0	-	247	-
Dy163	0	0	0	0	-	129	-
Ho165	0	0	0	0	-	229	-
Er166	0	0	0	0	-	434	-
Tm169	0	0	0	0	-	373	-
Yb172	0	0	0	0	-	282	-
Lu175	0	0	0	0	-	204	-
Hf178	0	0	2	4	-	272	-
Ta181	0	0	9	13	14	150	-40
W182	0	0	26	21	51	80	-49
Re185	0	0	47	13	35	28	37
Os189	0	0	80	38	73	48	10
Ir193	0	0	89	19	100	21	-11
Pt195	0	6	121	69	92	57	32
Au197	0	6	113	105	0	93	28228
Hg202	0	12	12	13	24	109	-51
Pb204	0	15	21	12	6	57	263
Tl205	0	0	9	5	24	56	-60
Pb206	0	0	17	3	24	18	-27
Pb207	0	0	100	234	24	233	320
Pb208	0	0	196	307	989	157	-80
Bi209	0	0	482	420	-	87	-
Th232	0	0	2	5	0	266	888
U238	0	0	5	7	24	139	-78
PbTotal	0	0	19	3	-	17	-

Standard	Mass-1						
Element	**Min LOD**	**Max LOD**	**Average (ppm) n = 24**	**1σ**	**Recommended Value**	**%RSD**	**%RD**
Li7	-	19517	1842	4820	-	262	-
Be9	0	7403	239	428	-	179	-
B11	-	498885	10480	31317	-	299	-
Na23	-	1767983	68149	79268	24481	116	178
Mg24	-	42491	4092	6696	-	164	-
Al27	-	57618	10841	17038	-	157	-
Si29	-	72848484	-20825	54534	-	-262	-
P31	-	2563204	57412	107698	-	188	-
S32	-	246464750	3821244	24347499	276000	637	1285
K39	-	755336	47043	88997	-	189	-
Ca44	-	9478725	109482	308311	-	282	-
Sc45	-	44138	1460	2054	-	141	-
Ti47	-	109902	4150	9990	-	241	-
V51	-	18249	219	375	63	171	248
Cr52	-	203513	7113	25636	37	360	19123
Mn55	-	35300	378	1265	260	334	46
Fe57	0	0	-	-	156000	-	-
Co59	-	4889	438	1208	67	275	554
Ni60	0	16360	1070	2807	97	262	1003
Cu63	-	27036	121950	61590	134000	51	-9
Zn66	-	28153	93984	78412	210000	83	-55
Ga71	0	345	54	47	50	87	7
Ge73	-	60845	2750	8020	50	292	5401
As75	-	119475	5382	14860	65	276	8180
Se77	-	125984	3823	10853	53	284	7113
Rb85	-	5949	302	859	-	285	-
Sr88	0	773	16	32	-	201	-
Y89	0	0	382	972	-	254	-
Zr90	0	0	370	603	-	163	-
Nb93	0	3375	36	88	61	247	-42
Mo95	0	13022	469	1154	-	246	-
Ru101	-	131	14	40	-	286	-
Rh103	0	2923	54	123	-	225	-
Pd104	0	3919	13	14	-	104	-
Pd105	0	14830	82	212	-	259	-
Pd106	-	6338	618	1933	67	313	822
Ag107	-	6021	597	1789	70	300	753
Cd111	0	5244	184	350	50	190	268

In115	-	2794	173	270	55	156	214
Sn118	-	14928	479	1394	55	291	771
Sb121	-	5376	320	742	15	232	2034
Te125	-	6376	1983	4564	-	230	-
Cs133	-	7272	98	197	14	201	602
Ba137	0	0	15	28	-	192	-
La139	0	0	0	2	-	369	-
Ce140	0	142	0	0	-	300	-
Pr141	0	0	0	0	-	455	-
Nd146	0	0	0	0	-	480	-
Sm147	0	0	0	0	-	469	-
Eu153	0	567	0	0	-	268	-
Gd157	-	865	96	416	-	433	-
Tb159	0	0	0	0	-	261	-
Dy163	0	124	0	0	-	469	-
Ho165	0	450	0	0	-	#DIV/0!	-
Er166	0	0	0	1	-	489	-
Tm169	0	0	0	0	-	380	-
Yb172	0	0	0	0	-	480	-
Lu175	0	0	2	8	-	315	-
Hf178	0	0	9	20	-	214	-
Ta181	0	524	36	77	20	214	80
W182	0	2515	234	603	-	257	-
Re185	-	9702	1430	2960	-	207	-
Os189	-	10973	195	271	64	139	206
Ir193	0	967	122	195	62	161	97
Pt195	-	1269	498	1133	47	227	960
Au197	0	142452	8945	26462	57	296	15592
Hg202	-	285789	12660	31027	68	245	18518
Pb204	-	1104236	51998	212700	57	409	91446
Tl205	-	2753	381	615	68	161	460
Pb206	-	941	265	194	68	73	289
Pb207	-	2573	335	651	68	194	392
Pb208	-	1119	145	242	7	168	1966
Bi209	-	1078	105	177	-	168	-
Th232	0	0	17	43	-	252	-
U238	0	3786	329	835	68	254	384
PbTotal	-	17175	1209	3533	-	292	-

Standard	PTC1b						
Element	Min LOD	Max LOD	Average (ppm) n = 25	1σ	Recommended Value	%RSD	%RD
Li7	0	3	3	1	-	22	-
Be9	0	3	0	0	-	104	-
B11	4	19	15	5	-	31	-
Na23	7	25	1756	370	-	21	-
Mg24	0	1	5924	2285	-	39	-
Al27	0	2	12174	4410	-	36	-
Si29	369	1991	30132	5041	24680	17	22
P31	13	93	137	51	-	37	-
S32	366	6324	368465	38161	299500	10	23
K39	6	25	1768	488	-	28	-
Ca44	61	175	4135	1616	-	39	-
Sc45	0	1	3	1	-	31	-
Ti47	0	4	902	371	696	41	30
V51	0	0	24	4	20	18	20
Cr52	1	6	42	6	40	14	4
Mn55	0	1	205	70	193	34	6
Fe57	0	0	-	-	367800	-	-
Co59	0	0	3444	882	3253	26	6
Ni60	0	1	123853	11740	112560	9	10
Cu63	0	2	91688	9008	79700	10	15
Zn66	0	2	3126	1005	2083	32	50
Ga71	0	0	2	1	3	36	-4
Ge73	0	3	4	9	0	224	-
As75	1	11	376	212	222	56	69
Se77	1	8	139	19	120	13	16
Rb85	0	0	7	1	-	20	-
Sr88	0	0	29	24	-	82	-
Y89	0	0	9	25	-	275	-
Zr90	0	1	6	3	1	60	293
Nb93	0	0	2	2	11	86	-78
Mo95	0	0	3	2	0	69	705
Ru101	0	0	1	1	1	99	185
Rh103	0	1	5	5	10	118	-52
Pd104	0	1	10	10	10	95	7
Pd105	0	0	16	15	10	91	71
Pd106	0	0	33	29	53	89	-38
Ag107	0	1	63	36	38	57	67
Cd111	0	0	60	50	3	83	1957

In115	0	0	43	64	120	148	-64
Sn118	0	1	86	62	6	72	1331
Sb121	0	0	17	19	30	109	-43
Te125	0	1	29	20	-	67	-
Cs133	0	0	31	60	62	195	-50
Ba137	0	0	55	52	-	94	-
La139	0	0	11	23	-	215	-
Ce140	0	0	7	5	-	66	-
Pr141	0	0	5	12	-	268	-
Nd146	0	0	5	5	-	107	-
Sm147	0	0	1	0	-	64	-
Eu153	0	0	1	2	-	263	-
Gd157	0	0	1	0	-	63	-
Tb159	0	0	1	1	-	275	-
Dy163	0	0	1	0	-	67	-
Ho165	0	0	0	1	-	168	-
Er166	0	0	0	0	-	78	-
Tm169	0	0	0	0	-	139	-
Yb172	0	0	0	0	-	78	-
Lu175	0	0	0	0	-	201	-
Hf178	0	0	0	1	-	147	-
Ta181	0	0	1	1	2	134	-75
W182	0	0	2	3	0	129	411
Re185	0	0	0	0	0	38	90
Os189	0	0	1	1	0	115	197
Ir193	0	0	1	1	7	157	-87
Pt195	0	13	6	10	2	171	192
Au197	0	16	138	353	1	256	27462
Hg202	0	16	352	510	795	145	-56
Pb204	0	35	782	500	2	64	52035
Tl205	0	0	425	523	795	123	-47
Pb206	0	0	1091	143	795	13	37
Pb207	0	0	1008	366	795	36	27
Pb208	0	0	734	546	97	74	656
Bi209	0	0	79	70	-	89	-
Th232	0	0	137	370	0	270	-
U238	0	0	341	505	795	148	-57
PbTotal	0	1	1136	158	-	14	-

Standard	NIST610						
Element	Min LOD	Max LOD	Average (ppm) n = 24	1σ	Recommended Value	%RSD	%RD
Li7	0	3	468	8	468	2	0
Be9	0	4	476	9	476	2	0
B11	7	16	350	7	350	2	0
Na23	8	432	99445	1298	99415	1	0
Mg24	0	1	648	231	432	36	50
Al27	0	22	14133	3764	10797	27	31
Si29	522	2209	327264	4247	327180	1	0
P31	18	92	413	7	413	2	0
S32	403	4929	1271	550	575	43	121
K39	6	28	466	10	464	2	0
Ca44	56	845	82378	1557	82144	2	0
Sc45	0	1	456	9	455	2	0
Ti47	0	3	612	132	452	22	35
V51	0	0	494	96	450	19	10
Cr52	1	5	398	84	408	21	-2
Mn55	0	1	469	55	444	12	6
Fe57	0	0	-	-	458	-	-
Co59	0	0	413	76	410	18	1
Ni60	0	0	495	36	459	7	8
Cu63	0	1	471	38	441	8	7
Zn66	0	1	329	54	460	16	-29
Ga71	0	0	399	107	433	27	-8
Ge73	1	5	680	843	447	124	52
As75	1	14	268	48	325	18	-18
Se77	1	5	103	27	138	27	-25
Rb85	0	0	426	8	426	2	0
Sr88	0	0	572	148	462	26	24
Y89	0	0	537	129	448	24	20
Zr90	0	0	502	82	465	16	8
Nb93	0	0	484	189	417	39	16
Mo95	0	0	319	235	-	74	-
Ru101	0	0	1	1	1	100	-38
Rh103	0	0	1	0	1	38	-6
Pd104	0	1	3	3	1	128	118
Pd105	0	0	32	74	1	227	2583
Pd106	0	0	120	136	251	114	-52
Ag107	0	0	263	70	270	27	-3
Cd111	0	0	282	174	434	62	-35

In115	0	0	470	141	430	30	9
Sn118	0	1	355	80	396	22	-10
Sb121	0	1	332	63	302	19	10
Te125	0	1	295	92	366	31	-19
Cs133	0	0	415	73	452	18	-8
Ba137	0	1	484	144	440	30	10
La139	0	0	446	13	453	3	-2
Ce140	0	0	449	14	448	3	0
Pr141	0	0	487	118	430	24	13
Nd146	0	0	560	536	453	96	24
Sm147	0	1	476	55	447	11	7
Eu153	0	0	540	156	449	29	20
Gd157	0	1	495	122	437	25	13
Tb159	0	0	484	115	437	24	11
Dy163	0	0	442	12	449	3	-1
Ho165	0	0	514	126	455	24	13
Er166	0	0	498	129	435	26	15
Tm169	0	0	439	12	450	3	-2
Yb172	0	0	510	126	439	25	16
Lu175	0	0	560	291	435	52	29
Hf178	0	0	540	190	446	35	21
Ta181	0	0	492	251	444	51	11
W182	0	0	923	1536	50	166	1750
Re185	0	0	39	21	-	55	-
Os189	0	1	1	2	-	149	-
Ir193	0	0	5	8	3	169	48
Pt195	0	9	21	29	24	135	-10
Au197	0	15	102	138	-	136	-
Hg202	0	18	302	192	426	64	-29
Pb204	0	33	287	145	60	50	382
Tl205	0	0	194	179	426	92	-54
Pb206	0	0	399	45	426	11	-6
Pb207	0	0	397	37	426	9	-7
Pb208	0	0	399	40	384	10	4
Bi209	0	0	402	61	457	15	-12
Th232	0	0	475	58	462	12	3
U238	0	0	1119	2789	426	249	163
PbTotal	0	0	394	35	-	9	-

Standard	NIST612						
Element	Min LOD	Max LOD	Average (ppm) n = 24	1σ	Recommended Value	%RSD	%RD
Li7	0	1	102	169	40	165	154
Be9	0	3	106	174	38	165	183
B11	4	15	163	119	34	73	376
Na23	11	1691	78069	30225	103858	39	-25
Mg24	0	1	177	283	68	160	160
Al27	0	70	10876	4495	11167	41	-3
Si29	322	2639	255354	100480	336061	39	-24
P31	15	79	116	153	47	132	148
S32	307	4713	3022	2863	377	95	702
K39	5	17	127	157	62	124	103
Ca44	51	381	64629	25632	85002	40	-24
Sc45	0	1	102	165	40	161	156
Ti47	0	3	133	206	44	155	201
V51	0	0	103	167	39	162	165
Cr52	1	5	91	157	36	173	149
Mn55	0	1	105	176	39	168	171
Fe57	0	0	-	-	51	-	-
Co59	0	0	91	142	36	157	155
Ni60	0	0	107	183	39	170	176
Cu63	0	1	103	163	38	159	172
Zn66	0	1	66	113	39	170	70
Ga71	0	0	89	154	37	172	142
Ge73	0	3	101	159	36	157	181
As75	1	6	59	87	36	147	65
Se77	1	7	26	33	-	127	-
Rb85	0	0	93	157	31	168	197
Sr88	0	0	177	300	38	169	363
Y89	0	0	153	282	38	184	304
Zr90	0	0	101	161	39	159	159
Nb93	0	0	113	200	37	178	202
Mo95	0	0	96	168	-	175	-
Ru101	0	0	0	0	1	91	-54
Rh103	0	1	1	1	1	64	-22
Pd104	0	0	1	1	1	62	-13
Pd105	0	0	2	3	1	146	125
Pd106	0	0	9	7	22	81	-60
Ag107	0	0	55	90	28	163	97
Cd111	0	0	50	75	39	151	28

In115	0	0	143	274	39	192	270
Sn118	0	1	78	130	35	166	125
Sb121	0	0	80	127	-	159	-
Te125	0	1	52	68	43	129	23
Cs133	0	0	90	131	39	146	128
Ba137	0	1	99	162	36	164	174
La139	0	0	100	163	38	164	159
Ce140	0	0	97	164	38	168	157
Pr141	0	0	140	267	36	191	293
Nd146	0	0	94	155	38	164	150
Sm147	0	1	99	164	36	166	177
Eu153	0	0	141	268	37	189	279
Gd157	0	0	102	162	38	159	171
Tb159	0	1	139	266	36	191	292
Dy163	0	0	94	157	38	168	145
Ho165	0	0	143	271	38	190	276
Er166	0	0	101	164	37	162	175
Tm169	0	0	93	156	39	168	138
Yb172	0	0	150	277	37	185	305
Lu175	0	1	140	264	37	188	283
Hf178	0	0	136	251	38	184	263
Ta181	0	0	104	162	38	156	173
W182	0	0	192	357	7	186	2795
Re185	0	0	14	20	-	142	-
Os189	0	1	1	1	-	113	-
Ir193	0	0	1	1	3	101	-50
Pt195	0	6	5	4	5	75	3
Au197	0	13	17	13	-	75	-
Hg202	0	13	24	26	39	111	-38
Pb204	0	42	86	139	15	161	480
Tl205	0	0	21	13	39	60	-46
Pb206	0	0	87	138	39	158	126
Pb207	0	0	86	141	39	164	122
Pb208	0	0	86	142	30	164	186
Bi209	0	0	83	129	38	156	119
Th232	0	0	103	165	37	161	175
U238	0	0	113	175	39	155	193
PbTotal	0	1	131	171	-	131	-

Standard	NIST614						
Element	Min LOD	Max LOD	Average (ppm) n = 23	1σ	Recommended Value	%RSD	%RD
Li7	0	1	1	1	2	70	-48
Be9	0	1	1	1	1	129	6
B11	2	12	80	51	1	64	5245
Na23	4	87	56196	36256	101635	65	-45
Mg24	0	0	23	16	34	73	-33
Al27	0	5	8022	6390	10797	80	-26
Si29	214	761	201648	140006	337022	69	-40
P31	9	37	31	12	11	39	172
S32	184	3334	2499	2434	291	97	759
K39	4	15	29	19	30	68	-4
Ca44	31	99	49750	35357	85049	71	-42
Sc45	0	1	3	2	1	49	325
Ti47	0	2	4	3	4	93	-1
V51	0	0	1	0	1	61	-37
Cr52	0	4	3	4	1	122	154
Mn55	0	1	1	1	1	65	-40
Fe57	0	0	-	-	19	-	-
Co59	0	0	1	0	1	92	-36
Ni60	0	0	1	1	1	107	-20
Cu63	0	1	3	2	1	51	121
Zn66	0	1	1	1	3	76	-60
Ga71	0	0	1	1	1	107	-48
Ge73	0	2	1	1	1	102	11
As75	0	6	9	19	1	203	1161
Se77	0	4	3	3	0	100	643
Rb85	0	0	1	0	1	88	-41
Sr88	0	0	23	25	1	108	2848
Y89	0	0	0	0	1	69	-48
Zr90	0	0	0	0	1	64	-52
Nb93	0	0	0	0	1	86	-54
Mo95	0	0	0	1	-	156	-
Ru101	0	0	0	1	2	156	-69
Rh103	0	0	1	1	2	62	-54
Pd104	0	0	1	1	2	81	-44
Pd105	0	0	1	1	2	76	-46
Pd106	0	0	1	1	0	86	129
Ag107	0	0	0	0	1	81	-58
Cd111	0	0	0	1	1	117	-43

In115	0	0	1	0	2	86	-66
Sn118	0	0	1	0	1	62	-16
Sb121	0	0	0	0	-	74	-
Te125	0	0	1	1	1	155	11
Cs133	0	0	1	0	3	84	-82
Ba137	0	0	1	1	1	94	93
La139	0	0	0	0	1	79	-52
Ce140	0	0	0	0	1	52	-50
Pr141	0	0	0	0	1	78	-39
Nd146	0	0	0	0	1	110	-46
Sm147	0	0	0	0	1	76	-49
Eu153	0	0	0	0	1	51	-47
Gd157	0	0	0	0	1	100	-54
Tb159	0	0	0	0	1	80	-41
Dy163	0	0	0	0	1	77	-54
Ho165	0	0	0	0	1	71	-39
Er166	0	0	0	0	1	82	-38
Tm169	0	0	0	0	1	79	-48
Yb172	0	0	0	0	1	86	-38
Lu175	0	0	1	1	1	117	-25
Hf178	0	0	1	0	1	92	-34
Ta181	0	0	0	0	1	72	-55
W182	0	0	1	0	0	67	332
Re185	0	0	0	0	-	172	-
Os189	0	0	1	2	0	155	65307
Ir193	0	0	1	1	2	180	-73
Pt195	0	9	1	1	0	93	188
Au197	0	21	3	5	-	190	-
Hg202	0	9	39	49	2	125	1580
Pb204	0	14	4	5	0	123	1518
Tl205	0	0	1	1	2	158	-73
Pb206	0	0	1	1	2	82	-47
Pb207	0	0	1	1	2	65	-57
Pb208	0	0	1	1	1	100	68
Bi209	0	0	0	0	1	70	-50
Th232	0	0	1	1	1	129	-26
U238	0	0	1	0	2	66	-69
PbTotal	0	0	1	1	-	88	-